TUEBINGEN PALEOANTHROPOLOGY BOOK SERIES –
CONTRIBUTIONS IN PALEOANTHROPOLOGY 3

HUMAN EVOLUTION AT THE CROSSROADS

EDITORS
KATERINA HARVATI AND MELANIA IOANNIDOU

TÜBINGEN
UNIVERSITY
PRESS

TUEBINGEN PALEOANTHROPOLOGY BOOK SERIES – CONTRIBUTIONS IN PALEOANTHROPOLOGY

VOLUME 03

Edited by Katerina Harvati

Human Evolution at the CROSSROADS

Katerina Harvati and Melania Ioannidou (eds.)

Human Evolution at the CROSSROADS

TÜBINGEN
UNIVERSITY
PRESS

Bibliografische Information der Deutschen Nationalbibliothek
Die Deutsche Nationalbibliothek verzeichnet diese Publikation in der Deutschen Nationalbibliografie, detaillierte bibliografische Daten sind im Internet über http://dnb.de abrufbar.

Die Online-Version des vollständigen Manuskripts dieser Publikation ist auf dem Repositorium der Universität Tübingen verfügbar unter:

Die Online-Version des vollständigen Manuskripts dieser Publikation ist auf dem Repositorium der Universität Tübingen verfügbar unter:
https://publikationen.uni-tuebingen.de/xmlui/handle/10900/163021
https://hdl.handle.net/10900/163021
https://nbn-resolving.org/urn:nbn:de:bsz:21-dspace-1630217

Tübingen University Press 2025
Universitätsbibliothek Tübingen
Wilhelmstr. 32
72074 Tübingen
tup@ub.uni-tuebingen.de
www.tuebingen-university-press.de

ISBN (Hardcover): 978-3-98945-001-1
ISBN (PDF): 978-3-98945-002-8

Satz und Umschlagsgestaltung: Cornelia True, Universität Tübingen
Umschlagbild: Artistic depiction of the interdisciplinary, multiproxy paleoenvironmental reconstruction of the Marathousa 1 site (Megalopolis, Greece), illustrating its role as a glacial refugium, investigated during CROSSROADS. All fauna depicted was recovered in excavation, while hominin presence is inferred by lithic artifacts. The vegetation is based on plant macrofossils, diatoms, pollen and stable isotope analysis of animal bones from the site. The wooden spear depicted is based on the Middle Pleistocene spears found in Schöningen (Germany).
(Vorder- und Rückseitenabbildungen von Gleiver Prieto; Copyright Katerina Harvati, Universität Tübingen)
Druck und Bindung: Druckhaus Sportflieger in der Medialis Offset GmbH
Printed in Germany

CONTENTS

INTRODUCTION TO THE VOLUME

Katerina Harvati*[1,2]

[1]*Paleoanthropology, Institute for Archaeological Sciences and Senckenberg Centre for Human Evolution and Palaeoenvironment, Department of Geosciences, Eberhard Karls University of Tübingen, Tübingen, Germany*
[2]*DFG Centre of Advanced Studies 'Words, Bones, Genes, Tools', Eberhard Karls University of Tübingen, Tübingen, Germany*
**katerina.harvati@ifu.uni-tuebingen.de*

http://dx.doi.org/10.15496/publikation-97666

THE 'CROSSROADS' PROJECT

This edited volume collects twenty eight of the contributions presented at the closing symposium of the ERC Consolidator project 'CROSSROADS', which took place in Tübingen in February 2022, shortly before the conclusion of the project. As such, it represents a large part of the work conducted under the 'CROSSROADS' research umbrella, showcasing the activities and results of the project.

'CROSSROADS' was awarded in 2016 and started its activities in April 2017. Building on the results of the previous ERC Starting Grant 'PaGE' (e.g., Harvati and Tourloukis, 2013; Harvati et al., 2018), it focused mainly on Greece with the goal of further extending the known palaeolithic record of the country through targeted, systematic fieldwork; developing a chronological and palaeoenvironmental framework for this record; and re-evaluating already existing, but understudied, fossil human remains. The 'CROSSROADS' research agenda was conducted in collaboration with multiple partners in Greece and internationally, including, most prominently, the Ephorate of Palaeoanthropology–Speleology (EPS) of the Hellenic Ministry of Culture; the Weiner Laboratory at the American School of Classical Studies at Athens (ASCSA); the Aristotle University of Thessaloniki (AUT); and the National and Kapodistrian University of Athens (NKUA). The project's extensive collaborative network in Greece and beyond is evident in the list of authors and contributions included.

In the five years of the project, the 'CROSSROADS' team conducted multiple field campaigns. These included targeted archaeological surveys: the MegaPal five year survey (2018-2022) in the Megalopolis Basin, a collaboration between the EPS and the ASCSA, under the direction of Dr. Panagopoulou, Dr. Karkanas and Prof. Harvati (e.g., Konidaris et al., 2022; chapters in this volume); the survey of the Mygdonia Basin, conducted in collaboration with the AUT and directed by Prof. Kotsakis (this volume); and our survey in Epirus, in collaboration with the NKUA under the direc-

K. Harvati: https://orcid.org/0000-0001-5998-4794

tion of Prof. Kourtessi-Philippakis (this volume). Our fieldwork also included the excavation/test excavation of several sites: the Early Pleistocene paleontological site Tsiotra Vryssi, Mygdonia Basin, in collaboration with the AUT under the direction of Profs. Koufos and Kostopoulos (e.g., Konidaris et al., 2015); the Lower Paleolithic elephant butchering site Marathousa 1, Megalopolis Basin, in collaboration with the EPS under the direction of Dr. Panagopoulou (e.g., Panagopoulou et al., 2018); and the test excavation at Morphi, Epirus, in collaboration with the NKUA under the direction of Prof. Kourtessi-Philippakis (this volume).

We conducted extensive sampling for dating and applied multiple dating methods to develop a chronological framework for our sites (e.g., Tourloukis et al., 2018; Konidaris et al., 2021; multiple chapters in this volume). We also worked on reconstructing paleoenvironments, the latter mainly focused on the extremely well-preserved record of the Megalopolis Basin, which allowed for the application of multi-proxy approaches (e.g., Bludau et al., 2021; multiple chapters in this volume) and a high-resolution reconstruction of the basin's habitat, illustrated on the cover of the volume. Additionally we were also able to collect two drill cores to analyze the Megalopolis paleoenvironment through time, a still ongoing project (this volume).

Finally, we re-examined and re-evaluated hominin fossils from Greece and beyond, including the elusive Megalopolis molar (Röding et al., 2021) and the Mugharet el'Aliya remains from Morocco (Röding et al., 2023; this volume). Most importantly, we were able to conduct a comprehensive analysis and re-dating of the human fossil remains from the Apidima cave site in Mani, Southern Greece, through our collaboration with the Museum of Anthropology of the School of Medicine of the NKUA. This important work resulted in the identification of the earliest known dispersal of early *Homo sapiens* in Eurasia, as well as other insights (Harvati et al., 2019; Harvati et al., 2021; this volume), and led to the new ERC Advanced Grant project 'FIRSTSTEPS' and the currently ongoing excavation of the Apidima site.

OVERVIEW OF THE VOLUME

Given the 'CROSSROADS' research agenda, there could be multiple ways to organise the contributions in this volume. A temporal and geographic principle, rather than thematic, was chosen, in order to best showcase related work (for example, the multiple lines of research undertaken in the Megalopolis Basin). The book is organised in three sections: section one collects six contributions from earlier periods, from the late Miocene to the early Pleistocene, represented in Northern Greece; section two is by far the largest one, presenting seventeen contributions on the Middle Pleistocene Megalopolis Basin; and section three focuses on the late Middle and Late Pleistocene, with four contributions from Greece and beyond.

SECTION 1 - THE EARLY RECORD: MYGDONIA AND NORTHERN GREECE

Section one starts with the geometric morphometric assessment of a phalanx of *Ouranopithecus macedoniensis*, one of only two postcranial elements known for this late Miocene taxon (Kunze et al., this volume). This analysis found that the phalanx most likely originates from the foot, rather than the hand, as originally considered, and shares some attributes with terrestrial primates. Chitoglou et al. (this volume) is the first of four chapters on Tsiotra Vryssi, focusing on the remains of rhinocerotids from this site. Karakosta et al. (this volume) present the canids from the same site, while Gkeme et al. (this volume) analyse the equid remains. Katsagoni et al. (this volume) present the preliminary results of the taphonomic analysis of the equids,

which suggest that the *Pachycrocuta* giant hyena may have been the agent of bone accumulation at the site. The section concludes with the chapter of Thompson et al. (this volume), presenting the results of the Mygdonia Basin archaeological survey.

SECTION TWO - THE MIDDLE PLEISTOCENE: ARCHAEOLOGICAL AND PALEOENVIRONMENTAL RESEARCH IN THE MEGALOPOLIS BASIN

Section two starts with the geological overview of the Megalopolis Basin by Kranis et al. (this volume). It continues with several contributions focusing on the Marathousa 1 site: Jacobs et al. (this volume) and Schaller et al. (this volume) present the dating results from single-grain optical dating and cosmogenic nuclide burial dating of the site, respectively. Giusti et al. (this volume) present an updated taphonomic study of the site. Guibert-Cardin (this volume) summarise the results of the use-wear analysis of the lithics from Marathousa 1, which point to use in both animal butchering and plant processing activities. Roditi et al. (this volume) present the preliminary results of the stable isotope analysis of one of the elephant individuals excavated in Marathousa 1, aiming to reconstruct the its life history, as well as paleoenvironmental conditions at the site during its lifetime. Kyrikou et al. (this volume) present the palynological analysis from Marathousa 1, while Butiseacă et al. (this volume) summarise the first results for biomarker analysis and temperature reconstruction for the same site. Vlachos et al. (this volume) summarise results from the analysis of reptiles, important paleoclimatic indicators, at the site.

The remaining chapters of section two present the results of the MegaPal survey: Karkanas et al. (this volume) offer an overview of the survey and the new sites discovered in its framework. Bludau et al. (this volume) introduce the drill cores from the Megalopolis Basin and preliminary results from ongoing analyses. Grün et al. (this volume) present the first results from U-series dating of the new sites discovered during the MegaPal survey. Athanassiou et al. (this volume) present the new large mammal fauna from Kyparissia 4, while van Kolfschoten et al. (this volume) introduce the voles from this site and their chronological implications. Perini et al. (this volume) presents the first results of the magnetostratigraphic analysis of the Kyparissia and Choremi sections. Boni et al. (this volume) focus on the molluscs from Marathousa 1, Marathousa 2 and Kyparissia 4, with the goal of reconstructing the paleoenvironment at these sites. Papadopoulou et al. (this volume) present the first analysis of ostracod remains from the site Kyparissia 4, aiming to assess the climatic conditions, including temperature and precipitation, at the site. Finally, Konidaris et al. (this volume) present the fossil macaques from Megalopolis, including new material from Kyparissia 4.

SECTION THREE - THE LATE MIDDLE AND LATE PLEISTOCENE: RESULTS FROM GREECE AND BEYOND

Section three starts with an investigation of the breakage pattern of the Apidima Cave A Middle Pleistocene crania by Beier et al. (this volume), aiming to assess potential trauma or taphonomic damage. Röding et al. (this volume) present the new analytical method of surface registration and its application to highly fragmentary fossil remains, such as those from Mugharet el'Aliya, Morocco. Tourloukis et al. (this volume) introduce the geoarchaeological and chronological results from Morphi and Popovo, Epirus. Finally, Thompson et al. (this volume) introduce the first analysis of the lithics collected during survey and test excavation at the same sites.

CONCLUSION

To conclude, I would like to thank my co-authors and long-term collaborators for their exceptional research contributions and strong team spirit which made 'CROSSROADS' such a successful and prolific project, as evidenced by the breadth and scope of the work presented here. It was a great pleasure working with you, and I hope that our collaborations continue well into the future! I warmly thank Dr. Melania Ioannidou, without whose invaluable support and contributions neither the 'CROSSROADS' closing conference, nor this volume would have been possible - thank you! I also thank Dr. William Snyder and Kim Apholz for their help in formatting and copyediting this volume, as well as Elli Baier, Karin Kiessling and Monika Doll for their organizational and administrative support. This work would not have been possible without the generous funding of the European Research Council (StG Nr. 283503; CoG Nr. 724703) and the Deutsche Forschungsgemeinschaft (DFG FOR 2237; HA 5258; Leibniz award 2021). Finally, I am immensely grateful to the University of Tübingen, the University President Bernd Engler, the late Dean Wolfgang Rosenstiel and Dean Thilo Stehle for their unwavering support through the years.

REFERENCES

Athanassiou, A., Konidaris, G.E., Tourloukis, V., Thompson, N., Giusti, D., Panagopoulou, E., Karkanas, P. and Harvati, K., this volume. The Middle Pleistocene large mammal fauna from Kyparissia (Peloponnese, S. Greece): New collected material.

Beier, J., Kouloukoussa, M., Evangelou, K., Gorgoulis, V.G., Wahl, J. and Harvati, K., this volume. A preliminary investigation of the cranial breakage patterns of the late Middle Pleistocene crania from Apidima Cave, Greece.

Bludau, I.J.E., Junginger, A., Wagner, B., Kirshcer, U., Zachow, C., Schindler, M., Tourloukis, V., Kyrikou, S., Karkanas, P., Panagopoulou, E. and Harvati, K., this volume. Overview of MAR-1A and MAR-2A drill core analysis and chronological framework.

Bludeau, I.J.E., Papadopoulou, P., Iliopoulos, G., Weiss, M., Schnabel, E., Thompson, N., Tourloukis, V., Zachow, C., Kyrikou, S., Konidaris, G.E., Karkanas, P., Panagopoulou, E., Harvati, K. and Junginger, A., 2021. Lake-Level Changes and Their Paleo-Climatic Implications at the MIS12 Lower Paleolithic (Middle Pleistocene) Site Marathousa 1, Greece. Frontiers in Earth Science, 9, 668445.

Boni, G., Syrides, G., Konidaris, G.E., Athanassiou, A., Tourloukis, V., Koukousioura, O., Panagopoulou, E., Karkanas, P. and Harvati, K., this volume. Preliminary results on the taxonomy and paleoenvironmental analysis of the mollusc fauna from Marathousa 1, Marathousa 2 and Kyparissia 4 (Middle Pleistocene, Megalopolis Basin, Greece).

Butiseacă, G.A., Vasiliev, I., Tourloukis, V., Junginger, A., Mulch, A., Karkanas, P., Panagopoulou, E. and Harvati, K., this volume. Preliminary biomarker/ paleoclimate reconstruction results from the Marathousa 1 Lower Paleolithic site (Megalopolis Basin, Greece).

Chitoglou, K., Pandolfi, L., Konidaris, G.E. and Kostopoulos, D.S., this volume. Rhinocerotidae remains from the Lower Pleistocene site of Tsiotra Vryssi, Greece: Preliminary results.

Giusti, D., Tourloukis, V., Konidaris, G.E., Thompson, N., Karkanas, P., Panagopoulou E. and Harvati, K., this volume. An updated spatial taphonomic study of the Middle Pleistocene open-air site of Marathousa 1 (Megalopolis Basin, Greece): Preliminary results.

Gkeme, A.G., Koufos, G.D., Kostopoulos, D.S. and Harvati, K., this volume. The Late Villa-

franchian equids from the locality Tsiotra Vryssi (Mygdonia Basin, Macedonia, Greece).

Grün, R., Feng, Y., Zhao, J.X., Konidaris, G.E., Athanassiou, A., Tourloukis, V., Panagopoulou, E., Karkanas, P. and Harvati, K., this volume. U-series analyses of bones from Megalopolis Basin sites.

Guibert-Cardin, J., Tourloukis, V., Panagopoulou, E., Harvati, K., Nicoud E. and Beyries, S., this volume. First traceological study of the lithic assemblage from Marathousa 1 and contextualization of the results within the European Lower Palaeolithic.

Harvati, K., Tourloukis, V., 2013. Human Evolution in the Southern Balkans. Evolutionary Anthropology, 22, pp. 43–45.

Harvati, K., Konidaris, G.E., Tourloukis, V. (Eds.), 2018. Special Issue Human Evolution at the Gates of Europe. Quaternary International Special Issue Volume, 497 Part A, pp. 1–240.

Harvati, K., Röding, C., Bosman, A., Karakostis, F.A., Grün, R., Stringer, C., Karkanas, P., Thompson, N.C., Koutoulidis, V., Moulopoulos, L.A., Gorgoulis, V.G. and Kouloukoussa, M., 2019. Apidima Cave fossils provide earliest evidence of *Homo sapiens* in Eurasia. Nature, 571, pp. 500–504.

Harvati, K., Grün, R., Duval, M., Zhao, J.X., Karakostis, A., Tourloukis, V., Gorgoulis, V. and Kouloukoussa, M., 2021. Direct U-series dating of the Apidima C human remains. Ancient connections in Eurasia. Kerns Verlag, Tübingen.

Jacobs, Z., Li, B., O'Gorman, K., Tourloukis, V., Panagopoulou, E., Karkanas, P. and Harvati, K., this volume. Single-grain optical dating of sediment samples from Marathousa 1, Southern Greece.

Karakosta, A., Konidaris, G.E., Kostopoulos, D.S., Koufos, G.D. and Harvati, K., this volume. Preliminary study of the canids from the Lower Pleistocene site of Tsiotra Vryssi (Mygdonia Basin, Greece).

Karkanas, P., Tourloukis, V., Thompson, N., Giusti, D., Tsartsidou, G., Athanassiou, T., Konidaris, G., Roditi, E., Panagopoulou, E. and Harvati, K., this volume. The Megalopolis Paleoenvironmental Project (MegaPal).

Katsagoni, A., Konidaris, G.E., Giusti, D., Koufos, G.D., Kostopoulos, D.S. and Harvati, K., this volume. Taphonomic study of the Lower Pleistocene site of Tsiotra Vryssi (Mygdonia Basin, Greece): Preliminary results on bone modifications in equid carcasses.

Konidaris, G.E., Athanassiou, A., Panagopoulou, E., Karkanas, P. and Harvati, K., this volume. Fossil macaques (Cercopithecidae, Primates) from the Middle Pleistocene of the Megalopolis Basin (Greece) with description of a new specimen from Kyparissia 4.

Konidaris, G.E., Tourloukis, V., Kostopoulos, D.S., Thompson, N., Giusti, D., Mihailidis, D., Koufos, G.D. and Harvati, K., 2015. New vertebrate localities from the Early Pleistocene of Mygdonia Basin (Macedonia, Greece): Preliminary results. Comptes Rendus Palevol., 14, pp. 353–362.

Konidaris, G.E., Kostopoulos, D.S., Maron, M., Schaller, M., Ehlers, T.A., Aidona, E., Marini, M., Tourloukis, V., Muttoni, G., Koufos, G.D. and Harvati, K., 2021. Dating of the Lower Pleistocene vertebrate site of Tsiotra Vryssi (Mygdonia Basin, Greece): biochronology, magnetostratigraphy and cosmogenic radionuclides. Quaternary, 4, 1.

Kranis, H., Skourtsos, E., Davis, G., Tourloukis, V., Panagopoulou, E., Karkanas, P. and Harvati, K., this volume. Structural control, depositional environment and geo-archaeological conditions in the Megalopolis Basin, Southern Greece.

Kunze, J., Karakostis, F.A., Ioannidou, M., Koufos, G.D. and Harvati, K., this volume. Geomet-

ric morphometric analysis of the intermediate phalanx of *Ouranopithecus macedoniensis*—a pilot study.

Kyrikou, S., Marinova, E., Bludau, I. J. E., Karkanas, P., Panagopoulou, E., Tourloukis, V., Junginger, A. and Harvati, K., this volume. The Middle Pleistocene MIS 12 palynological record from Marathousa palaeolake in Southern Greece: Highlighting favourable conditions in Marathousa 1 (MAR-1) refugial region during the severe glacial period.

Perini, S., Muttoni, G. and Tourloukis, V., this volume. Magnetostratigraphy of the Kyparissia and Choremi stratigraphic sequences (Megalopolis Basin): Preliminary results.

Panagopoulou, E., Tourloukis, V., Thompson, N., Konidaris, G., Athanassiou, A., Giusti, D., Tsartsidou, G., Karkanas, P. and Harvati, K., 2018. The Lower Palaeolithic site of Marathousa 1, Megalopolis, Greece: overview of the evidence. Quaternary International, SI Human Evolution at the Gates of Europe, 497, pp. 33–46.

Papadopoulou, P., Tsoni, M., Konidaris, G.E., Tourloukis, V., Panagopoulou, E., Karkanas, P., Harvati, K. and Iliopoulos, G., this volume. Ostracod contribution to the palaeoenvironmental study of Kyparissia-4 (Megalopolis Basin, Greece).

Roditi, E., Bocherens, H., Konidaris, G.E., Athanassiou, A., Tourloukis, V., Panagopoulou, E. and Harvati, K., this volume. First stable isotope results on the ecology of the straight-tusked elephant (*Palaeoloxodon antiquus*) from the Middle Pleistocene Marathousa 1 (Peloponnese, Greece).

Röding, C., Stringer, C., Lacruz, R.S. and Harvati, K., this volume. Mugharet el'Aliya: Adapting the method of surface registration to the hominin fossil record.

Röding, C., Zastrow, J., Scherf, H., Doukas, C. and Harvati, K., 2021. Crown outline analysis of the hominin upper third molar from the Megalopolis Basin, Peloponnese, Greece. In: H. Reyes-Centeno, K. Harvati (eds.) Ancient Connections in Eurasia. Kerns Verlag, Tübingen, pp. 13–36.

Röding, C., Stringer, C., Lacruz, R.S. and Harvati, K., 2023. Mugharet el'Aliya: affinities of an enigmatic North African Aterian maxillary fragment. American Journal of Biological Anthropology, 180, pp. 352–369.

Schaller, M., Ehlers, T.A., Tourloukis, V., Panagopoulou, E., Karkanas, P. and Harvati, K., this volume. Preliminary ages from cosmogenic nuclide burial dating of stratigraphy in the Megalopolis Basin.

Thompson, N., Kourtessi-Philippakis, G., Giusti, D., Harvati, K. and Tourloukis, V., this volume. The preliminary analysis of lithic assemblages from the archaeological survey and test-trench excavations at Popovo and Morfi, Greece.

Thompson, N., Tourloukis, V., Giusti, G., Harvati, K. and Kotsakis, K., this volume. The preliminary results of the Mygdonia Basin archaeological survey project, Greece.

Tourloukis, V., Muttoni, G., Karkanas P., Monesi, E., Scardia, G., Panagopoulou, E. and Harvati, K., 2018. Magnetostratigraphic and chronostratigraphic constraints on the Marathousa 1 Lower Palaeolithic site and the Middle Pleistocene deposits of the Megalopolis Basin, Greece. Quaternary International, SI Human Evolution at the Gates of Europe, 497, pp. 154–169.

Tourloukis, V., Kourtessi-Philippakis, G., Karkanas, P., Nomade, S., Giusti, D., Thompson, N., Varis, A., Junginger, A., Schaller, M. and Harvati, K., this volume. Geoarchaeological and geochronological investigations of Palaeolithic open-air sites in Epirus, Greece.

van Kolfschoten, T., Konidaris, G.E., Doukas, C., Athanassiou, A., Tourloukis, V., Panagopo-

ulou, E., Karkanas, P. and Harvati, K., this volume. Voles (Rodentia, Mammalia) as a proxy to date the site Kyparissia 4 (Megalopolis Basin, Greece).

VLACHOS, E., Georgalis, G.L., Konidaris, G.E., Athanassiou, A., Tourloukis, V., Thompson, N., Panagopoulou, E. and Harvati, K., this volume. Preliminary results on the reptiles from the Middle Pleistocene of Marathousa 1, Megalopolis Basin (Greece).

1 | The early record: Mygdonia and Northern Greece

1 GEOMETRIC MORPHOMETRIC ANALYSIS OF THE INTERMEDIATE PHALANX OF *OURANOPITHECUS MACEDONIENSIS*—A PILOT STUDY

Jana Kunze[1,*], Fotios Alexandros Karakostis[2], Melania Ioannidou[1], George D. Koufos[3], Katerina Harvati[1,2]

[1]*Paleoanthropology, Institute for Archaeological Sciences and Senckenberg Centre for Human Evolution and Palaeoenvironment, Department of Geosciences, Eberhard Karls University of Tübingen, Tübingen, Germany*
[2]*DFG Centre of Advanced Studies 'Words, Bones, Genes, Tools', Eberhard Karls University of Tübingen, Tübingen, Germany*
[3]*Laboratory of Geology and Palaeontology, School of Geology, Aristotle University of Thessaloniki, Thessaloniki, Greece*
**jana.kunze@outlook.com*

http://dx.doi.org/10.15496/publikation-97665

Keywords: Miocene hominoids; *Ouranopithecus*; virtual anthropology; phalangeal shape variation; geometric morphometrics

1.1 INTRODUCTION

Ravin de la Pluie (RPl) in the Axios valley, Greece, is one of the three localities where the material of the Late Miocene ape *Ouranopithecus macedoniensis* has been found to date (de Bonis et al., 1974; de Bonis and Melentis, 1978; Koufos and de Bonis, 2006; Koufos et al., 2016). The material from RPl is rich; it includes maxillary and mandibular remains, multiple isolated teeth, and just a few postcranial specimens, which to date represent the only postcranial remains associated with this species: two phalanges (proximal: RPl-86, intermediate: RPl-87).

A first analysis of the phalanges was conducted in 2014 (de Bonis and Koufos, 2014). In that study, de Bonis and Koufos followed a comparative approach, using multivariate analyses of linear measurements to assess morphological similarities to extant and fossil primates. De Bonis and Koufos concluded that both phalanges likely belong to the hand, but that an allocation to the foot cannot be excluded due to the lack of comparative material from the same species. However, since the phalanges are the only postcranial remains associated with this species so far, identifying them as either manual or pedal phalanges, as well as allocating them to a ray, is crucial. Having this information would allow for further, more detailed examinations, such as more accurate comparative analyses and reconstruction of locomotor behavior. Therefore, the goal of this study is to contribute to the identification of the intermediate phalanx RPl-87 through the application of three-dimensional (3D) geometric morphometrics (GM). Geometric morphometrics is a statistical analysis of form (shape

J. Kunze: https://orcid.org/0000-0002-4408-1362
F. A. Karakostis: https://orcid.org/0000-0003-3913-4332
M. Ioannidou: https://orcid.org/0000-0002-8199-7126
G. D. Koufos: https://orcid.org/0000-0001-9669-4884
K. Harvati: https://orcid.org/0000-0001-5998-4794

and size) in which, in contrast to traditional morphometrics, geometric information of the investigated structures can be retained throughout the analysis to provide a more detailed evaluation of shape differences (Slice, 2007). By comparing the shape of the better-preserved phalanx RPl-87 with manual and pedal intermediate phalanges of extant primates, we aim to address the following research questions:

1. Does RPl-87 belong to the foot or the hand?
2. What ray can RPl-87 be assigned to?
3. Does the specimen show morphological affinities to extant primates?

1.2 MATERIALS AND METHODS

Our comparative sample consists of scans of intermediate phalanges of *Gorilla gorilla* (n=23, 4 individuals), *Pan troglodytes* (n=24, 4 individuals), *Pongo pygmaeus* (n=24, 5 individuals), *Papio hamadryas* (n=15, 2 individuals), and *Macaca arctoides* (n=7, 1 individual) from the American Museum of Natural History Mammal Collections downloaded from MorphoSource.org. Manual and pedal phalanges from the second to fifth ray were selected for the shape analysis. Generally, it was attempted to keep the number of individuals low by including hand and foot bones from the same individual. However, this was not possible in some cases due to issues with preservation or scan quality. Moreover, a second intermediate phalanx from *G. gorilla* had to be removed as it presented as an outlier throughout the statistical analyses. Since the anatomical side of RPl-87 could not be determined so far, we analyzed bones from left and right anatomical sides together.

1.2.1. SHAPE ANALYSIS

The shape analysis was conducted in R-Studio (R version 4.1.2 for Windows; R Core Team, 2021) using the geomorph package (Adams and Otárola-Castillo, 2013). Eleven fixed landmarks were placed in geometrically corresponding positions (Table 1) together with 70 surface semilandmarks.

No	Orientation*	Descritpion*
1	Medial	Most distal point of the medial head condyle
2	Lateral	Most distal point of the lateral head condyle
3	Medial	Most palmar point of the medial head condyle
4	Lateral	Most palmar point of the lateral head condyle
5	Distal, dorsal up	Most dorsal point of the medial half of the head
6		Most dorsal point of the lateral half of the head
7	Proximal, palmar up	App. midpoint of palmar border of proximal articular surface, often most palmarly projecting point
8		App. midpoint of left border of proximal articular surface, often most medially projecting point
9		App. midpoint of right border of proximal articular surface, often most laterally projecting point
10		App. midpoint of dorsal border of proximal articular surface, often most proximally projecting point
11	Medial	Most distal point of base curvature

*Anatomical sides were pooled in the analysis, and bones were not mirrored. Therefore, to simplify landmark description, the indication of medial and lateral in this table refer to the bone as if it were right (i.e., for a bone from the left side, medial should be replaced by lateral and vice versa).

Table 1: Landmark description of the eleven fixed landmarks.

For RPl-87, the landmark placing procedure was repeated three additional times. The precision of landmark placement was calculated based on the total of four repetitions using the centroid radius approach (von Cramon-Taubadel et al., 2007).

The bones were divided into different subgroups for the analyses to address our research questions. Procrustes superimposition was performed for each group separately by rotating, centering, and scaling. The resulting Procrustes coordinates were analyzed in a principal component analysis (PCA) based on a covariance matrix. RPl-87 was not included in the original PCAs; instead, its principal component scores were calculated, and it subsequently was projected onto the PC plots. The principal components depicted in the PC plot were chosen based on what best separated the sample. To display the associated shape changes, the 'warpRefMesh' function from the package geomorph was used to create thin-plate spline grids (Bookstein, 1989). In each analysis, the specimen most similar in shape to the average sample was warped to depict the shapes at the extremes of the principal components. Additionally, a matrix including the pairwise Procrustes distances was exported from R-Studio and imported into PAST (Hammer et al., 2001), to create a neighbor joining tree.

1.3 RESULTS

1.3.1. HAND OR FOOT

The precision of landmark placement was high with a maximum error rate of 2.77%.

As our first goal was to assess whether RPl-87 belonged to the hand or the foot, the sample was divided by ray, resulting in four subgroups including both hand and foot bones.

The PC plot depicting the analysis of second intermediate phalanges (Fig. 1, top left) shows the clearest separation of hand and foot bones when PC6 (2.76% of variance) is plotted against PC1 (65.88% of variance). RPl-87 plots inside the convex hull of foot bones extending mainly towards PC1 negative, whereas the hand bones are concentrated more towards PC1 positive and PC6 positive. It should be noted that the variation on PC6 appears to be mainly driven by one *Gorilla* specimen. In the neighbor joining tree (Fig. 1, top right), RPl-87 is closest to some *Gorilla* and *Pan* foot bones, as well as *Papio* foot bones. This is also reflected in the Procrustes distance values (not shown), as the *Ouranopithecus* phalanx shows the least mean distance to the *Papio* species.

In the analysis of the third ray (not shown), in which the best separation was achieved through a combination of PC1 (63.24% of variance) and PC4 (4.56% of variance), the *Ouranopithecus* specimen shows a distinctively higher negative loading on PC1 than the rest of the sample, placing it outside the convex hulls of either hand or foot bones. Nonetheless, it is closer to the majority of foot bones, in particular those of *Gorilla* and *Pan*, than to hand bones, which plot more towards PC1 positive and PC4 negative. The neighbor joining tree shows RPl-87 positioned at its bottom with two *Pan* foot bones in the closest proximity. As in the PC plot, the majority of hand bones are positioned further away from the *Ouranopithecus* bone, indicating that the bone is more similar to the foot bones in the sample. The species means of Procrustes distances place RPl-87 closest to *Gorilla* and *Papio*, whereas the similarity to *Pan*, as indicated by the neighbor joining tree, is limited to the two foot bones.

The shape analysis of the fourth ray (not shown) consistently showed poor separation of hand and foot bones, irrespective of the combination of principal components. Therefore, it was decided to focus on the PC axes reflecting the highest amount of variance: PC1 (62.07%) and PC2 (10.33%). As

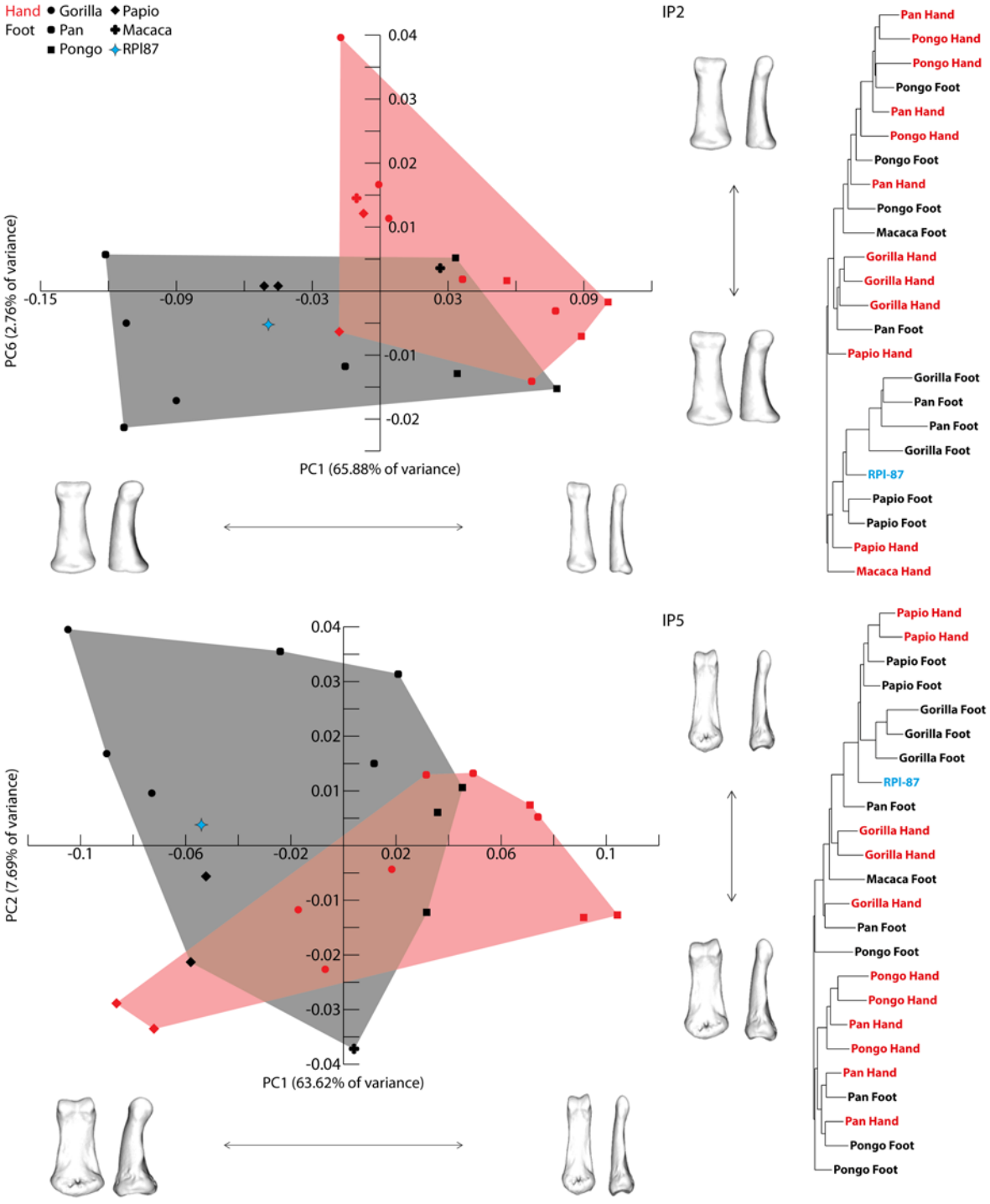

Figure 1: Top: PCA of Procrustes superimposed landmarks of the second intermediate phalanx without a priori group association. PC1 compared to PC6. Shape changes along PC1 and PC6 are illustrated below and to the right of the plot respectively. The neighbor joining tree based on the Procrustes distances is depicted on the right.
Bottom: PCA of Procrustes superimposed landmarks of the fifth intermediate phalanx without a priori group association. PC1 compared to PC2. Shape changes along PC1 and 2 are illustrated below and to the right of the plot respectively. The neighbor joining tree based on the Procrustes distances is depicted on the right. Coloration and symbology follow the legend in the top image.

in the analysis of the third intermediate phalanx, RPl-87 plots outside the range of either hand or foot bones. On PC1, it is most similar to a *Papio* hand bone that differs from the remaining hand bones in the sample by its high negative loading on that axis. When considering both PC1 and PC2, two *Gorilla* foot bones on the margin of the foot bone convex hull are slightly closer to the *Ouranopithecus* bone. On the neighbor joining tree, the *Papio* hand bone is situated on a sister branch to RPl-87 and three *Gorilla* foot bones are located on branches in the proximity. This is also reflected in the Procrustes distance values, as RPl-87 is closest to the *Papio* and *Gorilla* species. As in the PC plot, the separation of hand and foot bones is poor in the tree due to the high amount of overlap. However, there is a higher concentration of foot bones towards the bottom of the tree and in the proximity of RPl-87, while most hand bones, particularly those of *Pan* and *Pongo*, are located further away from the fossil.

Finally, when analyzing the intermediate phalanges of the fifth ray (Fig. 1, bottom left), the best separation was achieved by plotting PC1 (63.62% of variance) and PC2 (7.69% of variance). RPl-87 plots inside the shape variation of foot bones, closest to a *Papio* and a *Gorilla* specimen. The neighbor joining tree (Fig. 1, bottom right) shows the *Ouranopithecus* specimen situated close to a *Pan* and three *Gorilla* foot bones, but also in the proximity of *Papio* bones of both hand and foot. The latter is also reflected in the Procrustes distance values, as the mean distance is smaller from RPl-87 to *Papio* than to *Gorilla*.

Correlation analyses of PC1 and centroid size show that there is a moderate correlation (Pearson's r=0.55-0.66, assumptions are met) between these variables. However, this correlation does not appear to be related to size differences among species, but rather to differences in size among hand and foot bones, the latter being typically larger than the former.

1.3.2. RAY ALLOCATION AND AFFINITIES TO EXTANT PRIMATES

As the previous analyses have generally placed RPl-87 closer to foot bones than to hand bones, the latter were removed from the sample. In order to determine the ray RPl-87 belongs to, the foot bones of all rays were analyzed together in the subsequent analyses.

The plot of PC1 (60.9% of variance) and PC2 (9.08% of variance) shows substantial overlap between the different rays (Fig. 2, top left). The shape changes along PC1 appear to be mostly related to length-to-width proportions, with longer and more slender bones on PC1 positive and shorter and broader bones on PC1 negative. Shape changes on PC2 can be attributed to bone robusticity, particularly at the head and base, asymmetry in distal extension of the head condyles and the degree of proximal extension of the palmar area of the base. While the overlap among rays is particularly visible around the center of PC1, some degree of separation of the different rays is apparent at the extremes of this axis. The convex hulls of the second and fifth intermediate phalanx extend towards PC1 negative, while PC1 positive shows a higher concentration of bones from the third and fourth ray. With its negative PC1 loading, RPl-87 plots inside the range of variation of both second and fifth intermediate phalanges. The neighbor joining tree also reflects the overlap among rays (Fig. 2, top right), although the branches in the proximity of RPl-87 are mainly associated with bones from the second and fifth ray, with the only exception of a *Gorilla* fourth intermediate phalanx. In terms of Procrustes distances, this *Gorilla* bone appears to be closest to the fossil specimen. Nonetheless, when calculating the mean distance of each ray, RPl-87 shows the least distance to fifth intermediate phalanges, followed by bones of the second ray.

An improved separation is achieved when the phalanges are grouped by species instead of ray

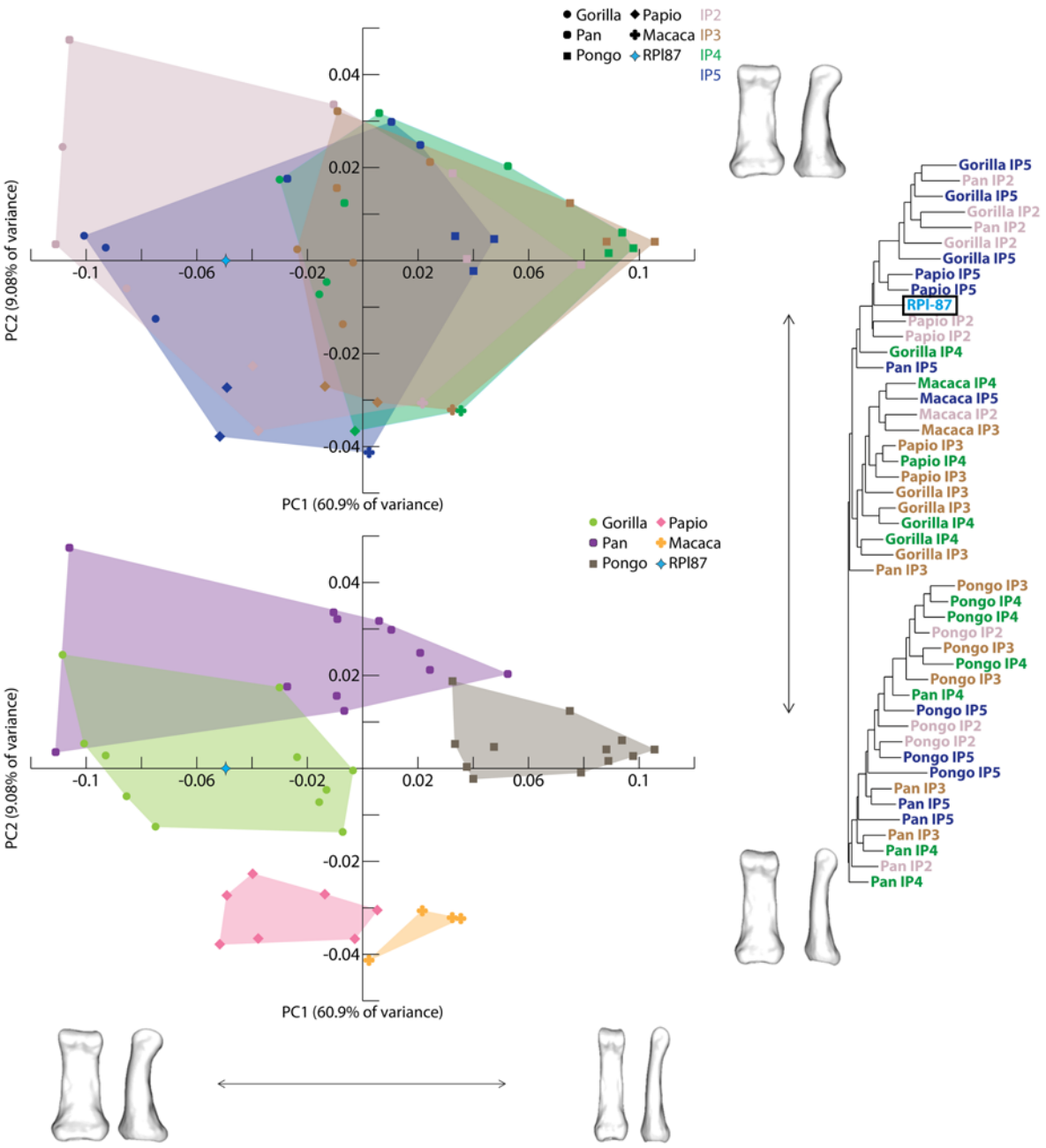

Figure 2: PCA of Procrustes superimposed landmarks of the pedal phalanges without a priori group association. PC1 compared to PC2. The upper plot depicts grouping by ray while the lower plot depicts grouping by species. Since the two plots represent the same analysis, the shape changes along PC1 and 2, illustrated below and to the right of the plots, respectively, apply for both plots. The neighbor joining tree based on the Procrustes distances is depicted on the right with coloration based on the different rays.

(Fig. 2, bottom left). This suggests that the variation driving the principal component analysis is not related to the differences in shape among rays, but to the differences among species. With its longer and more slender foot bones, *Pongo* is located at the extreme of PC1 positive. In contrast, *Gorilla* plots towards PC1 negative, together with two *Pan* foot bones. The majority of *Pan* bones, however, are clustered around the center of PC1 and towards PC2 positive. *Papio* and *Macaca* have

a similar loading on PC2 as they both fall on the negative extreme of this component, with *Papio* on PC1 negative and *Macaca* on PC1 positive. RPl-87 plots in the center of the *Gorilla* convex hull, indicating a possible similarity in shape to that species. Interestingly, in the neighbor joining tree, as well as in Procrustes distance values, the *Ouranopithecus* bone is more similar to the *Papio* foot bones. These contradictory results can be explained by that the PC plot focuses only on two axes of shape variance, whereas the Procrustes distances cover the entire shape variation in the sample.

PC1 of this analysis is again moderately correlated with centroid size (Pearson's r=0.52, assumptions are met). In this case, however, this correlation appears to be driven by size differences among the rays (ray 2 and 5 compared to ray 3 and 4) instead of species-related size differences, as the two species with the overall largest phalanges (*Gorilla* and *Pongo*) are represented on both extremes of PC1.

To further localize the ray RPl-87 belongs to, an analysis was conducted including only pedal intermediate phalanges of the second and fifth ray (not shown). However, the overlap between bones of the two rays is too extensive both in the PC plot and the neighbor joining tree to draw meaningful conclusions. Procrustes distance values indicate that RPl-87 is slightly more similar to fifth intermediate phalanges than to those of the second ray, but only by a small margin (0.085 as compared to 0.087).

1.4 DISCUSSION

This pilot study was an attempt at identifying the intermediate phalanx RPl-87, one of the only two postcranial elements so far associated with *Ouranopithecus macedoniensis,* through the application of 3D geometric morphometrics. According to the results of the principal component analyses and the neighbor joining trees, the shape of RPl-87 more closely resembles the shape of foot bones in our comparative sample. It differs from most hand bones analyzed here. This would suggest that, in contrast to a previous assessment of this specimen (de Bonis and Koufos, 2014), RPl-87 can likely be attributed to the foot. Additionally, the fact that the fossil plots outside the shape variation of both hand and foot bones of the third and fourth ray suggests that its shape diverges notably from the bones of these rays. This is supported by our analysis including foot bones only, which focused on ray identification. Despite the overlap among rays, the PC plot indicates a similarity in shape of RPl-87 and intermediate phalanges of the second and fifth ray. These results are in accordance with those by de Bonis and Koufos (2014), who suggested that the specimen represents a paramedian digit (two and five). Unfortunately, it was not possible to further specify the ray in this pilot study, as the overlap in shape of these two rays is too great. This could possibly be due to the fact that our sample includes bones from both the right and left side. The two paramedian digits are asymmetric in their morphology, especially of the head condyles, but in the opposite direction (i.e., a more distally extending head condyle can usually be observed on the lateral side of the second and the medial side of the fifth intermediate phalanx). Therefore, for a clearer identification, it would be necessary to identify the anatomical side of RPl-87. If this is not possible without first identifying the ray, the second option is to analyze a larger sample with balanced proportions of left and right phalanges to better observe and interpret potential patterns. While our analyses have identified a moderate correlation between the respective PC1s and size, this does not appear to be associated with species-related size differences, but rather with differences in size among hands, feet, and rays. Therefore, we propose that the variance on the first PCs is mainly

driven by variation in shape, whereas their correlation with size is likely an ancillary effect.

Our results additionally suggest RPl-87 to be most similar in shape to *Gorilla* and *Papio* foot bones. While reconstructing individual behavior from overall bone shape can be misleading (e.g., see Wallace et al., 2020), the fact that RPl-87 is more similar in shape to the terrestrial species than it is to *Pongo*—the most arboreal species in our sample—could suggest that *Ouranopithecus macedoniensis* was a terrestrial primate as well. A comparable conclusion has been drawn by de Bonis and Koufos (2014), as they have found similar morphological affinities in their analysis. Further support can be found in reconstructions of the paleoenvironment at Ravin de la Pluie, indicating an open and dry environment in this area (Koufos, 2006), and in the results of the microwear analysis on teeth of other fossils attributed to *O. macedoniensis* (Ungar, 1996; Merceron et al., 2005).

1.5 CONCLUSION AND OUTLOOK

The analysis of the overall bone shape of the intermediate phalanx RPl-87 has shown that the specimen can likely be attributed to the second or fifth ray of the foot. Additionally, its morphology appears to be most similar to intermediate phalanges of *Gorilla gorilla* and *Papio hamadryas*. While this study succeeded in showing the great potential of using 3D geometric morphometric analysis to identify the intermediate phalanx RPl-87, it also presented some issues that impede drawing secure conclusions. To corroborate and specify the results of this pilot study, future analyses of this bone should increase the size of the comparative sample. Not only should the number of individuals of the species analyzed here be increased, but future studies ideally should also include additional species of extant and—more crucially—fossil primates. Another important step is to apply a more detailed and specialized landmark configuration. RPl-87 shows some distinctive morphological traits such as the subtle curvature of its bone shaft and the faint development of its flexor sheath ridges. These traits could be captured with more specific landmark placement or with curve semilandmarks.

Finally, the shape analysis should be extended to the proximal phalanx RPl-86. As the two specimens represent a proximal and an intermediate phalanx, respectively, thorough analyses of not only the overall shapes of the bones, but also of their articular surfaces specifically, could shed light on whether these bones are from the same individual, the same foot or even from the same ray.

ACKNOWLEDGMENTS

This research was supported by the ERC Consolidator Grant ERC-CoG-724703 (“CROSSROADS”) and the ERC Advanced Grant ERC-AdG-101019659 (“FIRSTSTEPS”), both awarded to K.H. We are grateful to the American Museum of Natural History Mammal collection (S. Almécija, D. Boyer, E. Delson) for making the 3D models of great ape hand remains available online at MorphoSource.org (Duke University). Finally, we thank our reviewers, A. Bosman and E. Delson, whose comments helped improve and clarify this manuscript.

REFERENCES

Adams, D.C. and Otárola-Castillo, E., 2013. Geomorph: an R package for the collection and analysis of geometric morphometric shape data. Methods in Ecology and Evolution, 4(4), pp. 393–399.

de Bonis, L. and Melentis, J., 1978. Les Primates hominoïdes du Miocène supérieur de Macédoine–Étude de la mâchoire supérieure.

In Annales de Paléontologie (vertébres), 64, pp. 185–202.

de Bonis, L. and Koufos, G.D., 2014. First discovery of postcranial bones of *Ouranopithecus macedoniensis* (Primates, Hominoidea) from the late Miocene of Macedonia (Greece). Journal of Human Evolution, 74, pp. 21–36.

de Bonis, L., Bouvrain, G., Geraads, D. and Melentis, J., 1974. Première découverte d'un primates hominoïde dans le Miocène supérieur de Macédonie (Grèce). Comptes rendus de l'Académie des Sciences, Paris, série D, 278, pp. 3063–3066.

Bookstein, F.L., 1989. Principal Warps: Thin-Plate Splines and the Decomposition of Deformations. IEEE Transactions on Pattern Analysis and Machine Intelligence, 11(6), pp. 567–585.

Cramon-Taubadel, N. von, Frazier, B.C. and Lahr, M.M., 2007. The Problem of Assessing Landmark Error in Geometric Morphometrics: Theory, Methods, and Modifications. American Journal Physical Anthropolology, 134(1), pp. 24–35.

Hammer, Ø., Harper, D.A.T. and Ryan, P.D., 2001. PAST: Paleontological Statistics Software Package for Education and Data Analysis. Paleontologia Electronica, 4(1), pp. 1–9.

Koufos, G.D., 2006. Palaeoecology and chronology of the Vallesian (late Miocene) in the Eastern Mediterranean region. Palaeogeography, Palaeoclimatology, Palaeoecology, 234(2-4), pp. 127–145.

Koufos, G.D. and de Bonis, L., 2006. New material of *Ouranopithecus macedoniensis* from late Miocene of Macedonia (Greece) and study of its dental attrition. Geobios, 39(2), pp. 223–243.

Koufos, G.D., de Bonis, L. and Kugiumtzis, D., 2016. New material of the hominoid *Ouranopithecus macedoniensis* from the Late Miocene of the Axios Valley (Macedonia, Greece) with some remarks on its sexual dimorphism. Folia Primatologica, 87(2), pp. 94–122.

Merceron, G., Blondel, C., de Bonis, L., Koufos, G.D. and Viriot, L., 2005. A New Method of Dental Microwear Analysis: Application to Extant Primates and *Ouranopithecus macedoniensis* (Late Miocene of Greece). Palaios, 20(6), pp. 551–561.

R Core Team, 2021. R: A language and environment for statistical computing. R Foundation for Statistical Computing, Vienna.

Slice, D.E., 2007. Geometric morphometrics. Annual Review of Anthropology, 36, pp. 261–281.

Ungar, P.S., 1996. Dental microwear of European Miocene catarrhines: evidence for diets and tooth use. Journal of Human Evolution, 31(4), pp. 335–366.

Wallace, I.J., Burgess, M.L. and Patel, B.A., 2020. Phalangeal curvature in a chimpanzee raised like a human: Implications for inferring arboreality in fossil hominins. PNAS, 117(21), pp. 11223–11225.

2 RHINOCEROTIDAE REMAINS FROM THE LOWER PLEISTOCENE SITE OF TSIOTRA VRYSSI, GREECE: PRELIMINARY RESULTS

Krystalia Chitoglou[1,*], Luca Pandolfi[2], George E. Konidaris[3], Dimitris S. Kostopoulos[1]

[1]*Laboratory of Geology and Palaeontology, School of Geology, Aristotle University of Thessaloniki, Greece*
[2]*Dipartimento di Scienze Università degli Studi della Basilicata, Via dell'Ateneo Lucano, 10, 85100 Potenza, Italy*
[3]*Paleoanthropology, Institute for Archaeological Sciences and Senckenberg Centre for Human Evolution and Palaeoenvironment, Department of Geosciences, Eberhard Karls University of Tübingen, Tübingen, Germany*
**krystal.chito@gmail.com*

http://dx.doi.org/10.15496/publikation-97664

Keywords: *Stephanorhinus*; Late Villafranchian; Pleistocene; Mygdonia Basin; Greece

2.1 INTRODUCTION

Pleistocene rhinocerotids are poorly investigated in Greece, compared to the Miocene ones. The limited systematic studies, as well as the scanty and fragmentary material allow only partial classifications, frequently at the genus level, i.e., *Stephanorhinus* sp. Based on the recent review by Giaourtsakis (2022), during the Pleistocene, rhinocerotids were represented by two genera in Greece; *Coelodonta* and *Stephanorhinus*. The most common representative of the genus Stephanorhinus is *S. etruscus*, which has been reported more or less certainly from the Early Pleistocene (middle Villafranchian to Epivillafranchian) faunas of Kalamoto 1 and 2, Krimni, Livakos, Molykrio, Psychiko, Richea, Aivaliki, Tourkovounia 3-5 and Vatera DS. The Middle–Late Pleistocene species, *S. hemitoechus*, is recorded in the localities of Penios and Petralona (Athanassiou, 2011; Symeonidis et al., 2006; Tsoukala, 2018; Giaourtsakis, 2022), whereas *S. jeanvireti* is present in some Pliocene localities, such as Angelochori, Milia and Saint George Priporos (Guérin and Tsoukala, 2013; Tsoukala, 2018).

This contribution presents the preliminary results of the study of the Rhinocerotidae remains from the fossiliferous site of Tsiotra Vryssi (TSR) in the Mygdonia Basin (Northern Greece). The site, discovered in 2014, belongs to the upper parts of the Gerakarou Formation and yielded a late Villafranchian vertebrate fauna dated between 1.78 Ma and ~1.5 Ma (Konidaris et al., 2021). Among the mammalian remains, Rhinocerotidae are represented by numerous specimens, and their study aims to contribute to the taxonomy of the Greek Pleistocene rhinoceroses as well as to the biochronological and biogeographical distribution of the genus *Stephanorhinus* in Europe.

K. Chitoglou: https://orcid.org/0009-0005-0009-4742
D. S. Kostopoulos: https://orcid.org/0000-0001-5074-9050
G. E. Konidaris: https://orcid.org/0000-0002-7041-233X
L. Pandolfi: https://orcid.org/0000-0002-4186-4126

2.1.1. MATERIALS AND METHODS

The TSR Rhinocerotidae assemblage includes 61 dental and postcranial specimens, the most complete of which are preliminarily presented here. No adequately preserved or informative cranial specimens have been discovered so far. The specimens were measured using a digital caliper based on a combination of methods proposed by Guérin (1980), Mazza (1988), Fortelius et al. (1993) and Lacombat (2005). The material was compared morphologically and metrically with known Eurasian *Stephanorhinus* specimens based both on direct observations and on published literature. The TSR material is stored at the Museum of Geology, Palaeontology and Palaeoanthropology of the Aristotle University of Thessaloniki (LGPUT).

2.1.2. SYSTEMATIC PALEONTOLOGY

The morphological and metrical comparison of TSR rhinoceros remains points to the distinction of two taxa.

Cranial, dental and fragmented material (Fig. 1 A–D) (n=41 specimens) were ascribed to *Stephanorhinus* sp., because of their poor preservation and/or the advanced stage of dental wear that resulted in lacking distinctive characters. Yet, lower teeth can be distinguished in two groups according to their size. The same applies to the vertebrae and the fragmentary postcranial material, where no confident attribution at specific level is possible.

The rest of the material is attributed to two morphotypes, A and B. Smaller in size specimens, referred to the Morphotype A (n=13 specimens),

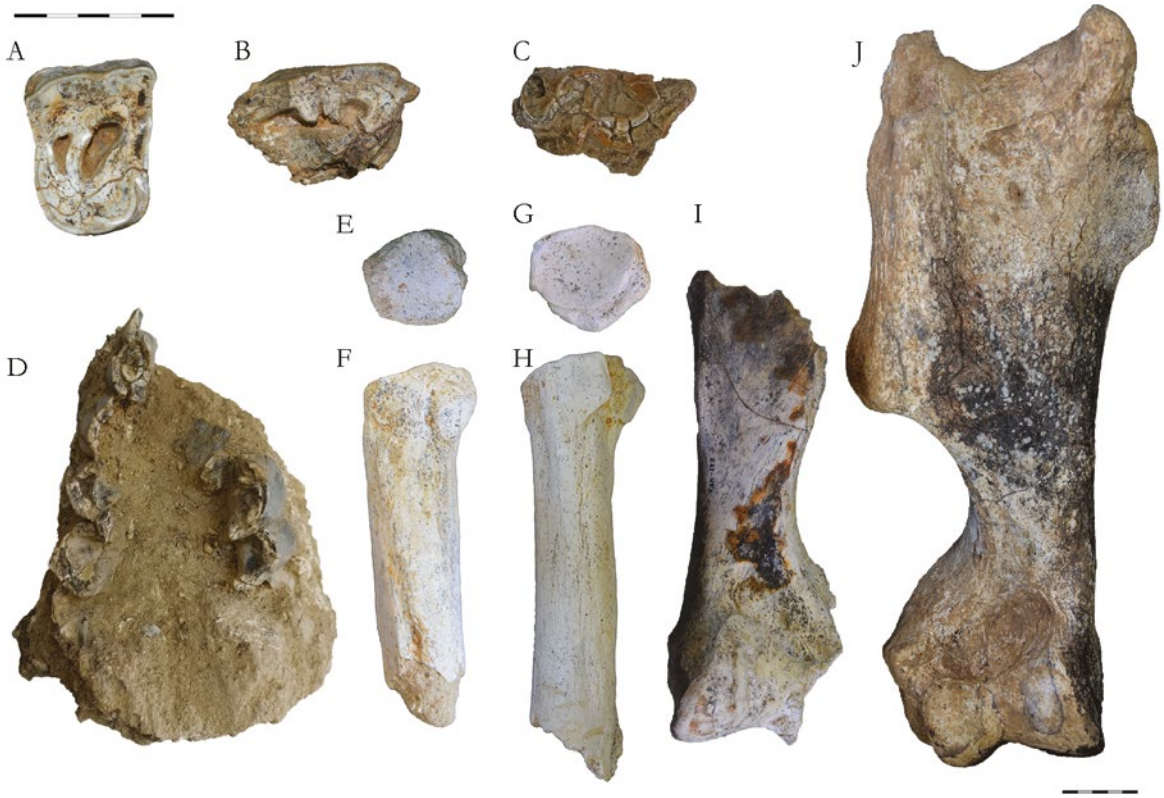

Figure 1: Selected rhinocerotid material from TSR. *Stephanorhinus* sp.: A, right P4. TSR-F14-19; B, right M3, TSR-E19-10; C, right lower molar, TSR-G21-29; D. mandibular fragment preserving the left p2–p4 and right p4, TSR-D18-24. Morphotype A: E–F, MtIV, TSR-F18-64a; I, humerus, TSR-133. Morphotype B: G–H, MtIV, TSR-G16-41; and J, humerus, TSR-G19-13. –Left scale bar for A–H and right for IJ, 50 mm.

are the distal part of a left humerus TSR-133 (Fig. 1I); a proximal part of a left ulna, TSR-G21-73; two proximal parts of left radii, TSR-G21-72 and TSR-C17-7; a tibia, TSR-50; and the articulated tarsals and metatarsals TSR-F18-64 (Fig. 1 E–F). Specimens larger in size, ascribed to the Morphotype B (n=7 specimens), include a complete right humerus, TSR-G19-13 (Fig. 1J); a proximal epiphysis of a left fourth metacarpal (McIV), TSR-F18-64; an almost complete femur, TSR-F18-56; femoral diaphyses TSR-G20-50, TSR-D16-27 and TSR-F22-3; and a fourth metatarsal (MtIV), TSR-G16-41 (Fig. 1G–H).

The two morphotypes can be clearly distinguished based on the biometrical comparison of the humeri, (Fig. 2A), where TSR-133 falls close to the range of the small-sized rhinoceros *S. etruscus*, whereas TSR-G19-13 is much larger, greater than

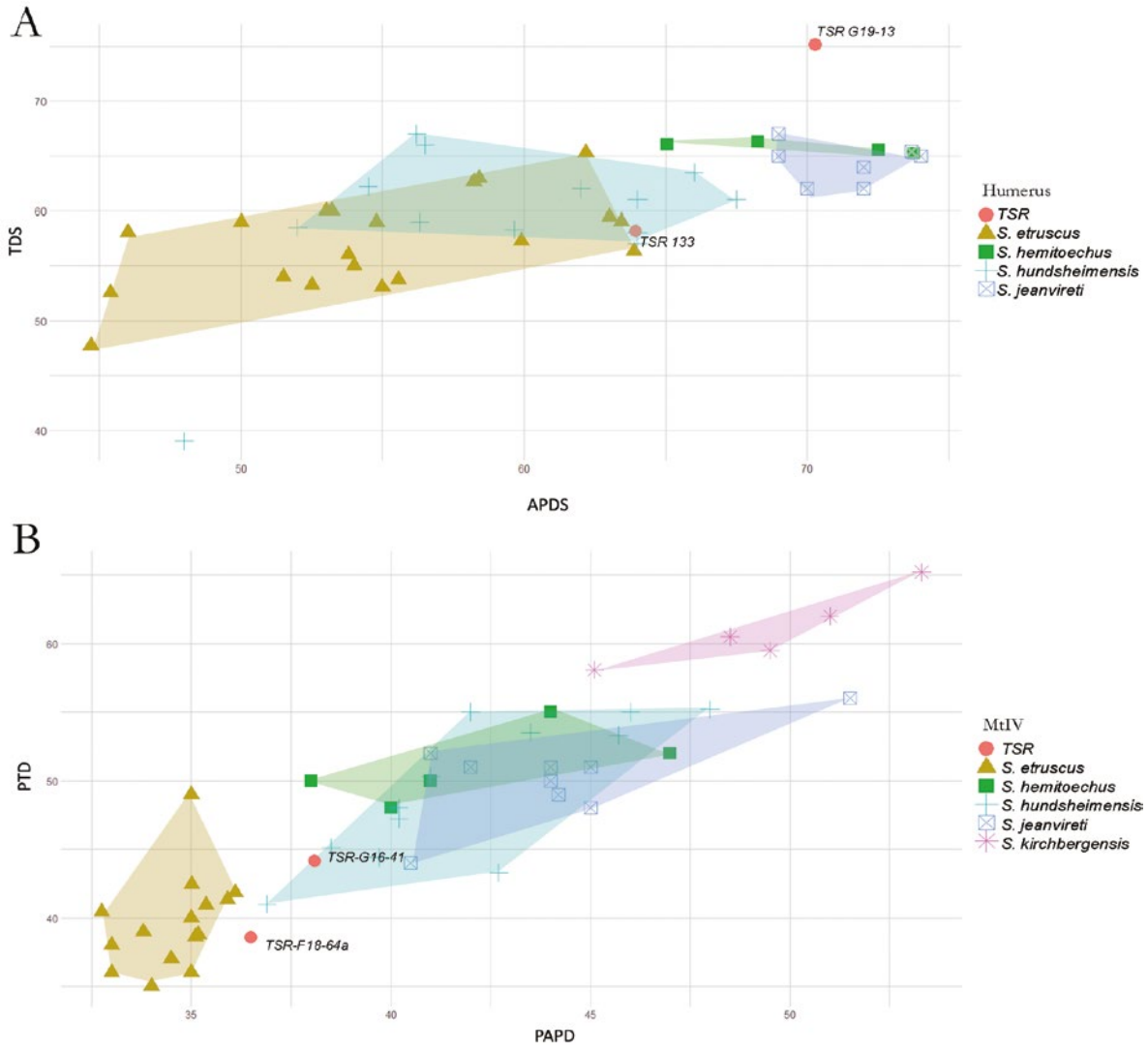

Figure 2: A: Scatter plot of transversal diameter (TDS) and anteroposterior diameter (APDS) of the humeral diaphysis from Tsiotra Vryssi, Morphotype A-TSR-133 and Morphotype B-TSR-G19-13, in mm. Data from: Guérin and Heintz (1971); Guérin (1972, 2004); Mazza (1988); Fortelius et al. (1993); Mazza et al. (1993); Kahlke (2001); Lacombat and Moulle (2005); Pandolfi (2011); Pandolfi and Tagliacozzo (2015); Pandolfi et al. (2017). B: Scatter plot of the proximal transversal diameter (PTD) and proximal anteroposterior diameter (PAPD) of MtIV specimens from Tsiotra Vryssi, Morphotype A-TSR-F18-64a, Morphotype B-TSR-G16-41, in mm. Data from Guérin (1972); Mazza (1988); Fortelius et al. (1993); Kahlke (2001); Lacombat (2005); Guérin and Tsoukala (2013); Pandolfi et al. (2017).

S. hemitoechus and *S. jeanvireti.* However, diaphyseal *Stephanorhinus* measurements show remarkable intraspecific variability, also affected by the ontogenetic age of the individual. Therefore, future analyses will focus on the articular surfaces of the distal epiphysis. Regardless of the poor preservation of TSR-133, which preserves only the medial part of the distal epiphysis and part of the diaphysis, these two specimens differ in morphological features as well. TSR-133 has a much slenderer diaphysis and a flatter medial part of the proximal border of the trochlear medial lip than TSR-G19-13. Accordingly, metrical and morphological distinction is evident in the two preserved MtIV: the much larger TSR-G16-41 and the smaller TSR-F18-56a. The scatter plot of the transversal diameter of the proximal epiphysis against its anteroposterior diameter shows that TSR-G16-41 falls into the range of *S. hundsheimensis,* whereas the specimen TSR-F18-64a is close to the range of *S. etruscus* (Fig. 2B). Additionally, the MtIV TSR-G16-41 differs from TSR-F18-64a in the more transversally elongated proximal articular surface in proximal view. In medial view, the anterior articular surface for the MtIII of TSR-F18-64a has a round shape, whereas the same surface in TSR-G16-41 has almost double the size and is square-shaped. Furthermore, in the same view, the posterior articular surface in TSR-G16-41 is in contact with the lateral tuberosity, resulting in a posterior extension.

2.1.3. DISCUSSION AND CONCLUSIONS

Morphological and biometrical comparisons of the TSR rhinocerotid material with Eurasian specimens indicate the presence of two morphotypes, likely representing two distinct species of *Stephanorhinus.* The co-existence of two or more *Stephanorhinus* species at the same locality has already been documented elsewhere, e.g., at the late Middle Pleistocene site of Ponte Molle (Italy) where the probable mixed-feeder *S.* cf. *hemitoechus* coexisted with the browser *S. kirchbergensis* (Pandolfi, 2013; Pandolfi and Marra, 2015) or the fauna of Montopoli (Italy), at the Plio-Pleistocene boundary, where the browsers *S. etruscus* and *S. jeanvireti* co-occurred (Pandolfi, 2013). *Stephanorhinus etruscus* and *S. hundsheimensis* are also documented as probably coexisting in the late Early Pleistocene fauna of Pietrafitta (Italy), but the material may come from different fossiliferous levels (Cirilli et al., 2020), and in the Middle Pleistocene site of Castellana (Italy) where reworking of the material is, however, mentioned (Mazza and Varola, 1999).

The presence of two morphotypes in a single site has also been reported at Dmanisi (Georgia), where this co-existence was interpreted as either a niche partitioning between rhinoceroses with different feeding habits (browse-dominated and grass-dominated mixed feeders) or as the occurrence of two ecomorphotypes of the same rhinoceros' species (Pandolfi et al., 2021). In the latter hypothesis, the TSR rhinocerotid may represent a single species, which differentiated from the typical *S. etruscus,* perhaps showing affinities towards *S. hundsheimensis,* or as a transitional local population.

Further material and thorough study of the TSR rhinoceroses will possibly allow the confirmation of the coexistence of two species during the late Early Pleistocene in Eurasia. Furthermore, in combination with their taxonomic identification at the species level, this will probably lead to significant conclusions regarding the chrono-spatial distribution of European rhinoceroses during the Early Pleistocene.

ACKNOWLEDGMENTS

Excavation at TSR was supported by the ERC Consolidator Grant ERC-CoG-724703 ("CROSSROADS") and the ERC Starting Grant ERC-StG-283503 ("PaGE"), both awarded to K.H. We also thank the two reviewers, I. Giaourtsakis and A. Athanassiou, for their useful comments.

REFERENCES

Athanassiou, A., 2011. The late Pleistocene fauna of Peneiós valley (Lárissa, Thessaly, Greece): new collected material. 9th Annual Meeting of the European Association of Vertebrate Palaeontologists, Heraklion, Crete, Greece (Vol. 14).

Cirilli, O., Pandolfi, L. and Bernor, R.L., 2020. The Villafranchian perissodactyls of Italy: knowledge of the fossil record and future research perspectives. Geobios, 63, pp.1–21.

Fortelius, M., Mazza, P. and Sala, B., 1993. *Stephanorhinus* (Mammalia: Rhinocerotidae) of western European Pleistocene, with a revision of *S. etruscus* (Falconer, 1868). Palaeontographia italica, 80(6) , pp. 63–155.

Giaourtsakis, I.X., 2022. The fossil record of rhinocerotids (Mammalia: Perissodactyla: Rhinocerotidae) in Greece, in: Vlachos, E. (Ed.), in: Fossil Vertebrates of Greece, Volume 2: Laurasiatherians, Artiodactyles, Perissodactyles, Carnivorans, and Island Endemics. Springer, Cham, pp. 409–500.

Guérin, C., 1972. Une nouvelle espèce de rhinocéros (Mammalia, Perissodactyla) à Vialette (Haute-Loire, France) et dans d'autres gisements du Villafranchien inférieur européen: Dicerorhinus jeanvireti n. sp. Travaux et Documents des Laboratoires de Géologie de la Faculté des Sciences de Lyon, 49, pp. 53–150.

Guérin, C. 1980. Les rhinoceros (Mammalia, Perissodactyla) du Miocene terminal au Pleistocene superieur en Europe occidentale: comparison avec les especes actuelles. Documents du Laboratoire de Géologie de la Faculté des Sciences de Lyon, 79, pp. 1–1182.

Guérin, C., 2004. Les rhinocéros (Mammalia, Perissodactyla) du gisement villafranchien moyen de Saint-Vallier (Drôme). Geobios, 37, pp. 259–278.

Guérin, C., Heintz, E., 1971. *Dicerorhinus etruscus* (Falconer, 1859), Rhinocerotidae, Mammalia, du Villafranchien de la Puebla de Valverde (Teruel, Espagne). Bulletin du museum Naturelle d'histoire Nat., 3.

Guérin, C., Tsoukala, E., 2013. The Tapiridae, Rhinocerotidae and Suidae (Mammalia) of the Early Villafranchian site of Milia (Grevena, Macedonia, Greece). Geodiversitas, 35(2), pp. 447–489.

Kahlke, H. D., 2001. Die Rhinocerotiden-Reste aus dem Unterpleistozän von Untermaßfeld, in: Kahlke, R.-D. (Ed.), Das Pleistozän von Untermaßfeld bei Meiningen (Thüringen), Teil 2. Habelt, Mainz, pp. 501–555.

Konidaris, G.E., Kostopoulos, D.S., Maron, M., Schaller, M., Ehlers, T.A., Aidona, E., Marini, M., Tourloukis, V., Muttoni, G., Koufos, G.D. and Harvati, K., 2021. Dating of the Lower Pleistocene vertebrate site of Tsiotra Vryssi (Mygdonia Basin, Greece): Biochronology, magnetostratigraphy, and cosmogenic radionuclides. Quaternary, 4(1), 1.

Lacombat, F., 2005. Les rhinocéros fossiles des sites préhistoriques de l'Europe méditerranéenne et du Massif Central. Paléontologie et implications bio-chronologiques. BAR International Series, 1419. Oxford Archaeopress.

Lacombat, F., Moullé, P.-E., 2005. Description paléontologique du *Stephanorhinus hundsheimensis* (Toula, 1902) Pléistocène Inférieur de la Tour de Grimaldi (Ligurie, Italie). Bulletin du Museé d'Athropologie préhistorique de Monaco, 44, pp. 33–38.

Mazza, P., 1988. The Tuscan Early Pleistocene rhinoceros *Dicerorhinus etruscus*. Palaeontographia Italica, 75, pp. 1–87.

Mazza, P., Sala, B. and Fortelius, M., 1993. A small latest Villafranchian (late Early Pleistocene) rhinoceros from Pietrafitta (Perugia, Umbria, Central Italy) with notes on the Pirro and Westerhoven rhinoceroses. Palaeontographia Italica, 80, pp. 25–50.

Mazza, P., Varola, A., 1999. Revision of the Middle Pleistocene rhinoceros remains from Contrada Monticelli (Castellana, Bari, Southern Italy). II Quaternario, 12(1), pp. 99–104.

Pandolfi, L., 2011. *Stephanorhinus kirchbergensis* (Jäger, 1839) from the Middle Pleistocene deposit of Riano (Rome, Central Italy). Alpine and Mediterranean Quaternary, 24(1), pp. 103–112.

Pandolfi, L., 2013. Rhinocerotidae (Mammalia, Perissodactyla) from the Middle Pleistocene site of Ponte Milvio, Central Italy. Bollettino della Società Paleontologica Italiana, 52, pp. 219–229.

Pandolfi, L. and Marra, F., 2015. Rhinocerotidae (Mammalia, Perissodactyla) from the chrono-stratigraphically constrained Pleistocene deposits of the urban area of Rome (Central Italy). Geobios, 48, pp. 147–167.

Pandolfi, L. and Tagliacozzo, A., 2015. *Stephanorhinus hemitoechus* (Mammalia, Rhinocerotidae) from the Late Pleistocene of Valle Radice (Sora, Central Italy) and re-evaluation of the morphometric variability of the species in Europe. Geobios, 48, pp. 169–191.

Pandolfi, L., Cerdeño, E., Codrea, V. and Kotsakis, T., 2017. Biogeography and chronology of the Eurasian extinct rhinoceros *Stephanorhinus etruscus* (Mammalia, Rhinocerotidae). Comptes Rendus Palevol, 16, pp. 762–773.

Pandolfi, L., Bartolini-Lucenti, S., Cirilli, O., Bukhsianidze, M., Lordkipanidze, D. and Rook, L., 2021. Paleoecology, biochronology, and paleobiogeography of Eurasian Rhinocerotidae during the Early Pleistocene: The contribution of the fossil material from Dmanisi (Georgia, Southern Caucasus). Journal of Human Evolution, 156, p. 103013.

Symeonidis, N.K., Giaourtsakis, I.X., Seemann, R. and Giannopoulos, V.I., 2006. Aivaliki, a new locality with fossil rhinoceroses near Alistrati (Serres, Greece). Beiträge zur Paläontologie, 30, pp. 437–451.

Tsoukala, E., 2018. Rhinocerotidae from the Late Miocene and Late Pliocene of Macedonia, Greece. A revision of the Neogene–Quaternary Rhinocerotidae of Greece. Revenue de Paléobiologie, 37, pp. 609–630.

3 PRELIMINARY STUDY OF THE CANIDS FROM THE LOWER PLEISTOCENE SITE OF TSIOTRA VRYSSI (MYGDONIA BASIN, GREECE)

Anastasia Karakosta[1,*], George E. Konidaris[2], Dimitris S. Kostopoulos[1], George D. Koufos[1], Katerina Harvati[2]

[1]*Laboratory of Geology and Palaeontology, School of Geology, Aristotle University of Thessaloniki, Thessaloniki, Greece*
[2]*Paleoanthropology, Institute for Archaeological Sciences and Senckenberg Centre for Human Evolution and Palaeoenvironment, Department of Geosciences, Eberhard Karls University of Tübingen, Tübingen, Germany*
**ankarak95@gmail.com*

http://dx.doi.org/10.15496/publikation-97663

Keywords: *Canis*; Lower Pleistocene; Villafranchian; Tsiotra Vryssi; Mygdonia Basin

3.1 INTRODUCTION

The Lower Pleistocene site of Tsiotra Vryssi (TSR), discovered in 2014, is located in the south-eastern part of the Mygdonia Basin (northern Greece) and belongs to the upper part of the Gerakarou Formation (Konidaris et al., 2015). The site has revealed a rich late Villafranchian fauna, which is dated between 1.78 and ~1.5 Ma (Konidaris et al., 2021). Among the faunal assemblage, canids are well-represented and their cranial, mandibular and dental material consists of 17 specimens (excavation seasons 2014–2019) stored at the Museum of Geology, Palaeontology and Palaeoanthropology of the Aristotle University of Thessaloniki (LGPUT). The aim of the present study is to provide preliminary results on their taxonomy based on their morphological and metrical comparison with Early Pleistocene European taxa known from the literature.

The TSR material comprises medium- and large-sized canids, which are consistent morphologically and metrically with an attribution to *Canis*. Several *Canis* species are documented in Europe during the late Villafranchian. *Canis etruscus* and *C. arnensis* were possibly already present slightly before the beginning of the late Villafranchian, and they are best recorded in several Italian localities dated to 2.0–1.8 Ma (e.g., Cherin et al., 2014; Bartolini Lucenti and Rook, 2016). *Canis etruscus* in particular is suggested as the possible ancestor of the more advanced *C. mosbachensis* and subsequently of the modern wolf (e.g., Sotnikova and Rook, 2010). *Canis accitanus* from Fonelas-P1 (~2.0 Ma, Spain), is a debated taxon; Brugal and Boudadi-Maligne (2011) suggest that it rather belongs to *C. arnensis*, whereas Martínez-Navarro et al. (2021) propose that it could be part of the intraspecific variability of *C. etruscus*, which is also present at the site.

Recent discoveries have furthermore revealed

 http://dx.doi.org/10.15496/publikation-97663

A. Karakosta: https://orcid.org/0009-0000-8054-8380
G. E. Konidaris: https://orcid.org/0000-0002-7041-233X
D. S. Kostopoulos: https://orcid.org/0000-0001-5074-9050
G. D. Koufos: https://orcid.org/0000-0001-9669-4884
K. Harvati: https://orcid.org/0000-0001-5998-4794

new species. *Canis borjgali* from Dmanisi (~1.8 Ma, Georgia) shares morphological features with *C. mosbachensis*, therefore this species was proposed as a closer ancestor of the *C. lupus* lineage instead of the more primitive *C. etruscus* (Bartolini Lucenti et al., 2020). *Canis orcencis* from Venta Micena (~1.6 Ma, Spain) resembles *C. mosbachensis* and *C. apolloniensis* from Apollonia-1 (~1.3–1.0 Ma, Greece; Koufos, 2018), but shows some distinct morphological traits (Martínez-Navarro et al., 2021). According to Madurell-Malapeira et al. (2022), *C. orcencis* and *C. apolloniensis* could be ascribed to *C. mosbachensis*, which successfully dispersed in Europe during the late Early–Middle Pleistocene, until the appearance of *C. lupus*.

Regarding the large-sized European canids, the hypercarnivorous *Canis* (*Xenocyon*) *falconeri* is best recorded in Upper Valdarno (Italy) and Fonelas-P1, while recent findings reveal an earlier record in the middle Villafranchian (Bartolini Lucenti and Spassov, 2022). This taxon was replaced by the more advanced *Canis* (*Xenocyon*) *lycaonoides*, which is found in many European localities (e.g., Dmanisi, Pirro Nord, Apollonia-1), usually along with a medium-sized *Canis* (e.g., Bartoloni Lucenti et al., 2021).

3.2 RESULTS AND DISCUSSION

Morphological and metric data of the cranial, mandibular and dental material of TSR indicate the presence of two medium-sized canids (of which one is smaller- and the other larger-sized) and of one large-sized canid.

The larger medium-sized canid is recognized as *Canis* sp. (morphotype A). Its study is based on the specimen TSR-D17-37, which is a complete cranium associated with the mandible (Fig. 1a), and additional isolated specimens. *Canis* sp. (morphotype A) shares many morphological and metric features with both *C. borjgali* and *C. apolloniensis* (Fig. 2), thus a firm attribution to one of these two species is uncertain at the moment.

The smaller medium-sized canid is identified as *Canis* sp. (morphotype B) based on the specimen TSR-G20-11, which is a complete cranium with a right hemimandible and three associated but isolated teeth, all belonging to the same individual (Fig. 1b). This morphotype is generally similar in morphology to *Canis* sp. (morphotype A) but differs metrically (Fig. 2), as well as in some morphological traits such as the blunter outline of the nuchal crest of the cranium in dorsal view

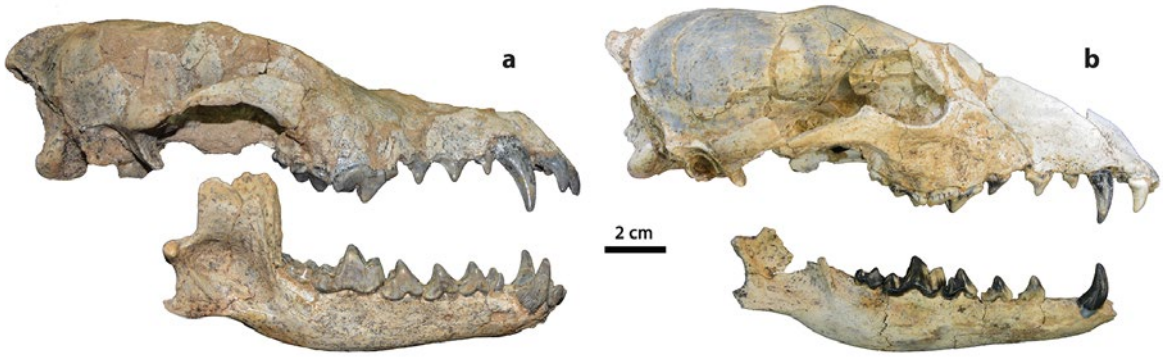

Figure 1: Right lateral view of crania and mandibles of the medium-sized canids from TSR. a, *Canis* sp. (morphotype A) (TSR-D17-37a, b); b, *Canis* sp. (morphotype B) (TSR-G20-11a, b).

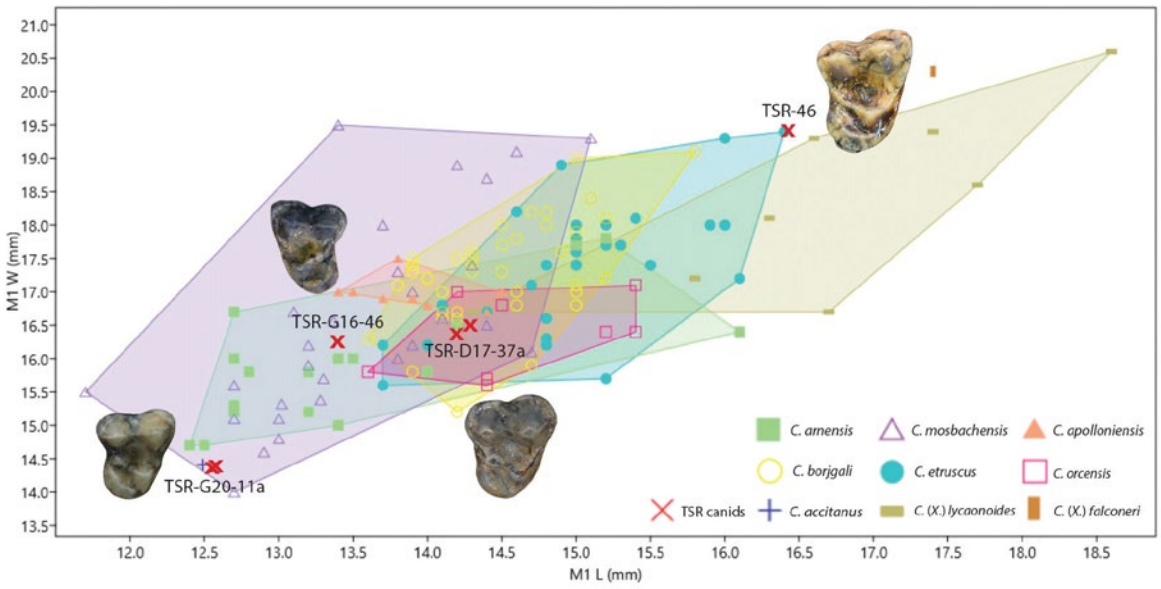

Figure 2: Scatter plot of length/width of the upper M1 of the TSR canids in comparison to several European ones. *Canis* sp. (morphotype A) (TSR-D17-37a; TSR-G16-46), *Canis* sp. (morphotype B) (TSR-G20-11a) and *Canis* (*Xenocyon*) sp. (TSR-46).

instead of triangular on TSR-D17-37a; and the smaller and not so mesially placed P4 protocone. However, several dissimilarities may be part of the unknown intraspecific variability, and thus both morphotypes could belong to a single species. *Canis* sp. (morphotype B) also portrays an overall slenderer cranial and dental morphology, that could be perhaps attributed to sexual dimorphism. Sex-related differences are already mentioned for *C. mosbachensis* (Sotnikova, 2001) and modern wolves (e.g., Trbojević and Ćirović, 2016). Although *Canis* sp. (morphotype B) displays metric similarities with *C. accitanus* and *C. arnensis* (Fig. 2), clear morphological differences preclude an attribution to any of these species.

Canis sp. (morphotype A) and *Canis* sp. (morphotype B) differ from *C. etruscus* and *C. arnensis* in many dental characters, e.g., the M1 trigon basin is deeper than the talon one; the p3 alveolus lays lower in the mandible than those of the adjacent teeth; the mesial margin of the paraconid of m1 is distally inclined (e.g., Bartolini Lucenti et. al., 2020). Overall, their morphology seems to mostly resemble that of taxa related to the *C. mosbachensis* lineage such as *C. borjgali*, *C. apolloniensis* and *C. orcensis.*

The large-sized canid of TSR is attributed to *Canis* (*Xenocyon*) sp., based on the study of the isolated upper first molar (M1) TSR-46, which was originally ascribed to *C. etruscus* (Konidaris et al., 2015) and subsequently to *Canis* sp. (Konidaris et al., 2021). The proportions of the tooth (Fig. 2) are indeed very similar to the lectotype of *C. etruscus*; yet, unlike *C. etruscus*, the trigon basin of the tooth is deeper, while the talon one is shallower. Metrically, it is larger than the rest of the TSR *Canis* morphotypes (Fig. 2). It is also distinct in the crest-like morphology of the metaconule, which is commonly observed in the hypercarnivorous forms (e.g., Martínez-Navarro et al., 2021). In general, the morphology of the tooth is similar to that of the holotype of *C.* (*Xenocyon*) *lycaonoides* from Gombasek (Slovakia; Kretzoi, 1938: Tafel 3, Fig. 4), but is not so robust and triangular in shape as in *C.* (*Xenocyon*) *lycaonoides* from Apollonia-1 (Koufos, 2018: Fig. 8c).

3.3 CONCLUSIONS

Two medium-sized canids were recognized at TSR, *Canis* sp. (morphotype A) and *Canis* sp. (morphotype B), both showing notable resemblance with the taxa related to the *Canis mosbachensis* lineage; however, their relationships (i.e., two distinct species *vs* intra-specific variants related to sexual dimorphism) remain currently unclear and require further examination. The large-sized canid is attributed to *Canis* (*Xenocyon*) sp. and represents the oldest record of the taxon in Mygdonia Basin, and perhaps also in Greece.

The recent discoveries of new material in several European sites and the erection of new species have modified the old established taxonomy of the *Canis* representatives. Tsiotra Vryssi is dated to a critical period for the *Canis* intrageneric speciation, and as such the rich and well-preserved canid material from the site may shed light into the evolutionary history of the lineage during the European Pleistocene. Therefore, future research will focus on the comprehensive study and comparison of all available material (cranial and postcranial, plus recently discovered new material), aiming to illuminate the status and relationships of the two identified medium-sized morphotypes, and thus to contribute to the better understanding of the Early Pleistocene European canids.

ACKNOWLEDGMENTS

Excavation at TSR was supported by the ERC Consolidator Grant ERC-CoG-724703 ("CROSSROADS") and the ERC Starting Grant ERC-StG-283503 ("PaGE"), both awarded to K.H. K.H. is also supported by the ERC Advanced Grant ERC-AdG-101019659 ("FIRSTSTEPS"). The authors kindly thank A. Athanassiou and S. Roussiakis for their valuable comments which improved the manuscript.

REFERENCES

Bartolini Lucenti, S., Rook, L., 2016. A review on the Late Villafranchian medium-sized canid *Canis arnensis* based on the evidence from Poggio Rosso (Tuscany, Italy). Quaternary Science Reviews, 151, pp. 58–71.

Bartolini Lucenti, S., Spassov, N., 2022. Cave canem! The earliest *Canis* (*Xenocyon*) (Canidae, Mammalia) of Europe: Taxonomic affinities and paleoecology of the fossil wild dogs. Quaternary Science Reviews, 276, p. 107315.

Bartolini Lucenti, S., Bukhsianidze, M., Martínez-Navarro and B., Lordkipanidze, D., 2020. The wolf from Dmanisi and augmented reality: review, implications, and opportunities. Frontiers in Earth Science, 8, 131.

Bartolini Lucenti, S., Madurell-Malapeira, J., Martínez-Navarro, B., Palmqvist, P., Lordkipanidze, D. and Rook, L., 2021. The early hunting dog from Dmanisi with comments on the social behaviour in Canidae and hominins. Scientific Reports, 11, 13501.

Brugal, J. P., Boudadi-Maligne, M., 2011. Quaternary small to large canids in Europe: Taxonomic status and biochronological contribution. Quaternary International, 243, pp. 171–182.

Cherin, M., Bertè, D.F., Rook, L. and Sardella, R., 2014. Re-defining *Canis etruscus* (Canidae, Mammalia): A new look into the evolutionary history of Early Pleistocene dogs resulting from the outstanding fossil record from Pantalla (Italy). Journal of Mammal Evolution, 21, pp. 95–110.

Konidaris, G.E., Tourloukis, V., Kostopoulos, D.S., Thompson, N., Giusti, D., Michailidis, D., Koufos, G.D. and Harvati, K., 2015. Two new vertebrate localities from the Early Pleistocene of Mygdonia Basin (Macedonia, Greece): Preliminary results. Comptes Rendus Palevol, 14, pp. 353–362.

Konidaris, G.E., Kostopoulos, D.S., Maron, M., Schaller, M., Ehlers, T.A., Aidona, E., Marini, M., Tourloukis, V., Muttoni, G., Koufos, G.D. and Harvati, K., 2021. Dating of the Lower Pleistocene vertebrate site of Tsiotra Vryssi (Mygdonia Basin, Greece): biochronology, magnetostratigraphy, and cosmogenic radionuclides. Quaternary, 4(1), 1.

Koufos, G., 2018. New material and revision of the Carnivora, Mammalia from the Lower Pleistocene locality Apollonia 1, Greece. Quaternary, 1(1), p. 6.

Kretzoi, M., 1938. Die Raubtiere von Gombaszög nebst einer Übersicht der Gesamtfauna (Ein Beitrag zur Stratigraphie des Altquartärs). Annales Musei Nationalis Hungarici, 31, pp. 88–157.

Madurell-Malapeira, J., Bartolini Lucenti, S., Prat-Vericat, M., Sorbelli, L., Blasetti, A., Ferretti, M.P., Goro, A. and Cherin, M., 2022. Jaramillo-aged carnivorans from Collecurti (Colfiorito Basin, Italy). Historical Biology, 34(10), pp. 1928–1940.

Martínez-Navarro, B., Lucenti, S.B., Palmqvist, P., Ros-Montoya, S., Madurell-Malapeira, J. and Espigares, M.P., 2021. A new species of dog from the Early Pleistocene site of Venta Micena (Orce, Baza Basin, Spain). Comptes Rendus Palevol, 20, pp. 297–314.

Sotnikova, M.V., 2001. Remains of Canidae from the Lower Pleistocene site of Untermassfeld, in: Kahlke, R.D. (Ed.), Das Pleistozän von Untermassfeld bei Meiningen (Thüringen) Teil. 2. Habelt, Bonn, pp. 607–632.

Sotnikova, M., Rook, L., 2010. Dispersal of the Canini (Mammalia, Canidae: Caninae) across Eurasia during the Late Miocene to Early Pleistocene. Quaternary International, 212(2), pp. 86–97.

Trbojević, I., Ćirović, D., 2016. Sexual dimorphism and population differentiation of the wolf (*Canis lupus*) based on morphometry in the Central Balkans. North-Western Journal of Zoology, 12, pp. 349–355.

4 THE LATE VILLAFRANCHIAN EQUIDS FROM THE LOCALITY TSIOTRA VRYSSI (MYGDONIA BASIN, MACEDONIA, GREECE)

Anastasia G. Gkeme[1,*], George D. Koufos[1], Dimitris S. Kostopoulos[1], Katerina Harvati[2,3]

1Laboratory of Geology and Palaeontology, School of Geology, Aristotle University of Thessaloniki, Thessaloniki, Greece
[2]Paleoanthropology, Institute for Archaeological Sciences and Senckenberg Centre for Human Evolution and Palaeoenvironment, Department of Geosciences, Eberhard Karls University of Tübingen, Tübingen, Germany
[3]DFG Centre for Advanced Studies 'Words, Bones, Genes, Tools', Eberhard Karls University of Tübingen, Tübingen, Germany
**gkemeanasta@geo.auth.gr*

http://dx.doi.org/10.15496/publikation-97668

Keywords: Mammalia; Equidae; late Villafranchian; Greece; Tsiotra Vryssi

4.1 INTRODUCTION

The genus *Equus* arrived from North America to Eurasia at the beginning of Pleistocene (2.58 Ma) (Lindsay et al., 1980; Azzaroli, 1983; Bernor et al., 2019; Rook and Martínez-Navarro, 2010; Rook et al., 2019) with its first occurrence marking a faunal turnover and significant environmental changes from humid-warm ecosystems to colder-drier conditions. During the Early Pleistocene, *Equus* had been already significantly radiated in Eurasia, providing several lineages, some of them surviving till recent times.

In Greece, the *Equus* datum is possibly traced in Damatria (Rhodes Island; van der Meulen and van Kolfschoten, 1986). Equids are the most common element in the Pleistocene Greek faunal assemblages, often exceeding 50% of the local finds in number of specimens. Most of the Greek *Equus* remains come from the middle–late Villafranchian and Epivillafranchian. Mygdonia Basin (Central Macedonia, Greece), being at the crossroads of three continents, becomes an important path for faunal dispersals and a gateway for faunas coming from Asia Minor to South-Western Europe and vice versa. Several mammal fossiliferous sites have been discovered in this basin by the Laboratory of Geology and Palaeontology, Aristotle University of Thessaloniki (LGPUT) and many fossils have been unearthed, providing important palaeontological and biochronological data for Greece and beyond (Koufos and Kostopoulos, 2016 and references therein). Tsiotra Vryssi (TSR), a fossiliferous locality in Mygdonia Basin, dated between 1.78–1.5 Ma (Konidaris et al., 2021), provided a rich sample of fossil equids. Konidaris et al. (2015) preliminarily reported two species of *Equus* based on their size.

4.2 MATERIALS AND METHODS

More than 440 equid remains have been unearthed from Tsiotra Vryssi and they are stored at the LGPUT. The sample is represented mainly by man-

A. G. Gkeme: https://orcid.org/0000-0002-7807-2675
G. D. Koufos: https://orcid.org/0000-0001-9669-4884
D. S. Kostopoulos: https://orcid.org/0000-0002-5475-5666
K. Harvati: https://orcid.org/0000-0001-5998-4794

Figure 1: Equid remains from Tsiotra Vryssi (TSR): (a) Articulated left hind limb (at the TSR site) preserving all elements from the distal part of tibia to the third phalanx; (b) Left third metacarpal in articulation with the phalanges, TSR-F18-53 (medium-sized); (c) Fragmentary right mandibular body with p2–m2, TSR-F20-15 (medium-sized); (d) Left third metatarsal, TSR-179 (large-sized); (e, f) Third metatarsals, TSR-F17-31d (left), and TSR-F17-12 (right) respectively (medium-sized).

dibular fragments, dental remains and postcranial elements, many of which are articulated (Fig. 1). There is also an extremely fragmentary cranium (TSR-162) belonging to a juvenile individual less than 1 year old based on Levine's (1982) tooth aging tables (with DP1-DP4 and M1 erupting).

The systematics of TSR equids is mainly based on third metacarpals and third metatarsals. We compare them with Eurasian Pleistocene *Equus* species. In particular, the studied material was compared with equids from several Greek and European localities dating from the middle Villafranchian to Epivillafranchian (data from literature are indicated in the parentheses only in the cases where we did not use our personal datasets): *E. stenonis* from Dafnero (Western Macedonia, Greece), Sésklo (Magnesia, Greece), Volax (Drama Basin, Greece), Saint-Vallier (France), Chilhac (France), La Puebla de Valverde (Spain; Eisenmann, 1979), Matassino (Italy), Terranova (Italy), Upper Valdarno (Italy); *E. altidens* (=*E. stenonis mygdoniensis* Koufos, 1992) from Gerakarou and Libakos; *E. altidens* from Krimni-3 (Mygdonia Basin, Greece); *E. altidens* from Dmanisi (Georgia; Bernor et al., 2021), Pirro Nord (Italy), Selvella-Gioiella (Italy; Alberdi and Palombo, 2013); *E. altidens granatensis* from Venta Micena (Eisenmann, 2011); *E. apolloniensis* from Apollonia (Mygdonia Basin, Greece). We used principal component analysis (PCA) in PAST 4.05. Missing values were treated by applying iter-

ative imputation. The nomenclature and measurements follow the recommendations of Eisenmann et al. (1988).

4.3 ANALYSIS AND RESULTS

As originally stated by Konidaris et al. (2015) and recently by Gkeme (2023), two species of *Equus* have been recognized in TSR material based on their size and metapodial slenderness: a medium-sized and a relatively large-sized *Equus*. The medium-sized equid has typically stenonoid cheek teeth (Fig. 1c) with a V-shaped linguaflexid, shallow ectoflexid on premolars and always deep on molars, and relatively long and slender metapodials (Fig. 1b, e, f). The large-sized equid has larger teeth (V-shaped linguaflexid, deep ectoflexid on molars and occasionally on premolars, rounded and often elongated metaconids, lingually pointed metastylids), and the metapodials are longer and more robust (Fig. 1d).

Figure 2 (a, b) exhibits the PCA results for (a) third metacarpals (MCIII) and (b) third metatarsals (MTIII). The PC1 and PC2, for the third metacarpals, account for most of the variance with 87.4 % (PC1=60.63%; PC2=26.8%), and for the third metatarsals, with 93.6% (PC1=74.7%; PC2=18.9%). The PC1 indicates a progressively slenderer morphology from positive to negative values, whereas PC2 separates species by the maximum length (M1) with more to less elongated metapodials (from positive to negative values) (Fig. 2a, b). The third metacarpals of the medium-sized species from TSR, overlap with the equids from Libakos and Krimni-3, and as it seems, they are slightly longer than those from Gerakarou (Fig. 2a, 2c1). Furthermore, the MCIII from TSR overlaps with *E. altidens* from Pirro Nord and mostly from Venta Micena. Generally, the equids from the Greek localities Tsiotra Vryssi, Krimni-3, Gerakarou and Libakos overlap with the European *E. altidens* samples, and they all differentiated from the various *E. stenonis* Greek (Dafnero, Sésklo, Volax) and the rest of the European (Saint-Vallier, Olivola, Upper Valdarno, Chilhac) samples because of their slenderness (Fig. 1a).

The third metatarsals of the TSR medium-sized species overlap with Gerakarou and Libakos, while Krimni-3 shows slightly longer metatarsals as it is shown in the PCA analysis (Fig. 2b). Here too, the equids from these localities overlap with the samples of *E. altidens*, and they are distinguished from *E. stenonis* based on their slenderness. There are two specimens, TSR-179 (Fig. 2b) and TSR-D16-41 (large-sized species) that plot outside the convex hull of *E. altidens* and within the variation of *E. stenonis* and *E. apolloniensis*. These third metatarsals are relatively long, but more robust than those of the medium-sized species. The slenderness index, minimal breadth at the middle of the diaphysis (M3) / maximal length (M1) % (Alberdi et al., 1998; Eisenmann, 2002) is 11.8 and 13 for TSR-179 and TSR-D16-41, respectively, versus 11.4 (n=11; min=10.9, max=11.9) for the medium-sized species.

4.4 DISCUSSION

The taxonomy of the slender late Villafranchian European equids is still a matter of debate (Koufos 1992; Alberdi et al. 1998; Forstén 1999; Eisenmann 2010; Gkeme et al. 2017; Bernor et al. 2021; Cirilli et al. 2021; Gkeme 2023 among others). The TSR equids provide some new insights into the late Villafranchian equid faunal assemblages of Greece and southwestern Europe. The presence of a medium-sized equid in the TSR fauna similar in size and slenderness to *E. altidens* (=*E. stenonis mygdoniensis* Koufos, 1992) from Gerakarou and Krimni-1, 3 (see Koufos et. al. 2022; Gkeme 2023) and the other European samples of *E. altidens* (including *E. a. granatensis* from Venta Micena) may

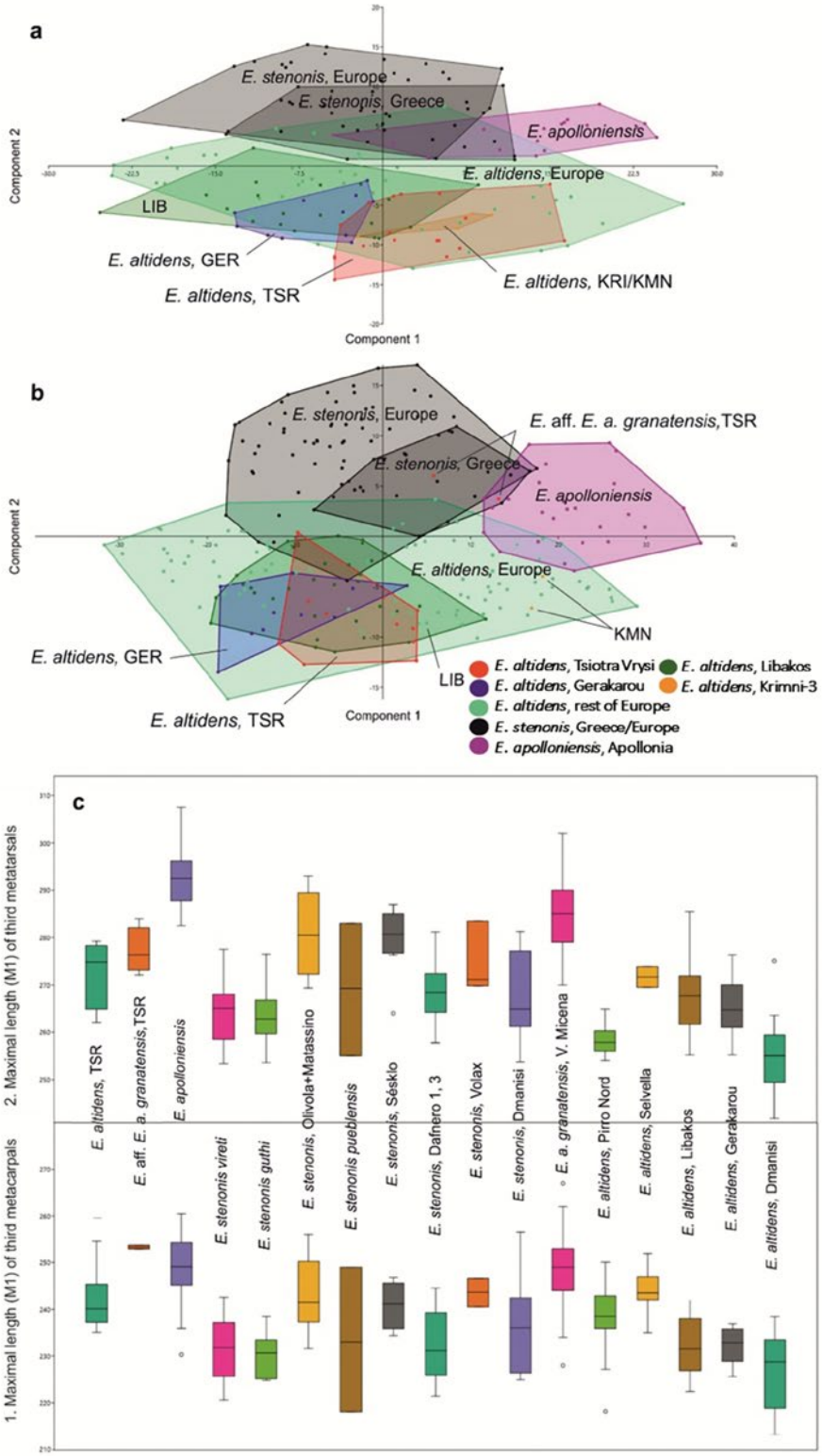

Figure 2: (a, b) PCA of the third metacarpals and third metatarsals, respectively, from Tsiotra Vryssi (TSR) in comparison with those from various Greek and other European localities; (c) Boxplots comparing the maximum length of the third metapodials from TSR with other Greek and European samples. Boxplots include minimum, median and maximum values with first and third quartile of each sample and outliers.

give some new information about the systematic position of this taxon. The equid from Gerakarou (including the equid from Krimni 1) was originally described by Koufos (1992) as a distinct subspecies of *E. stenonis* (*E. stenonis mygdoniensis*) despite its much slenderer built and smaller overall size. Forstén (1999) and Gkeme et al. (2017) referred the equid from Libakos to *E. altidens*, an equid identical to the one from Gerakarou, suggesting that they both belong to *E. altidens*. However, Eisenmann (2017) considered '*E. s. mygdoniensis*' as a valid taxon and raised it at the species level (*Allohippus mygdoniensis*), while she suggested the cautious use of the name *E. altidens*, because the erection of this species was mainly based on teeth. Recently, Cirilli et al. (2021), Bernor et. al. (2021) and Gkeme (2023) considered '*E. s. mygdoniensis*' as a junior synonym of *E. altidens*, thus favoring the preliminary work of Gkeme et al. (2017) and the recent review of the Early Pleistocene slender equids from Greece by Koufos et al. (2022). The presence of *E. altidens* at TSR possibly validates this theory, since the variability reported by the European *E. stenonis* populations seems to be similar in Gerakarou, Libakos, Tsiotra Vryssi, Krimni and the European *E. altidens* samples.

The large-sized *Equus* from TSR is less abundant, at least in number of identified specimens (less than 20). Some of the dental remains (belonging to the larger species) exhibit peculiar features like those described by Eisenmann (2010) as common features of the *Sussemionus* subgenus and in particular those from Venta Micena (see Gkeme, 2023). Furthermore, according to Gkeme (2023: fig.5.40a), the third metacarpals from TSR exhibit the same morphology and morphometry as those of *E. altidens granatensis* from Venta Micena. However, the metatarsals resemble both *E. stenonis* and *E. apolloniensis* based on their slenderness and size. For this reason, the large-sized *Equus* is pulled under the name *Equus* aff. *E. a. granatensis* following Gkeme's (2023) commendation. The presence of two species of *Equus* in the TSR fauna validates its young age (slightly younger than Gerakarou and older than Apollonia) marking an important faunal turnover at the late Early Pleistocene: slender equids (eg. *E. altidens*) replaced the more robust and archaic ones (*E. stenonis*).

ACKNOWLEDGMENTS

Excavation at TSR was supported by the ERC Consolidator Grant ERC-CoG-724703 ("CROSSROADS") and the ERC Starting Grant ERC-StG-283503 ("PaGe"), both awarded to K.H. K.H. is also supported by the ERC Advanced Grant ERC-AdG-101019659 ("FIRSTSTEPS"). A.G.G. is co-financed by Greece and the European Union (European Social Fund—ESF) through the Operational Program "Human Resources Development, Education and Lifelong Learning" in the context of the Project "Strengthening Human Resources Research Potential via Doctorate Research" (MIS-5000432), implemented by the State Scholarships Foundation (IKY). We are grateful to all the field members for their valuable contribution, and those who helped with the preparation of the material at the LGPUT. A.G.G. would also like to thank E. Cioppi and L. Bellucci (Museo di Storia Naturale dell'Univerisità degli Studi di Firenze, sezione di Geologia e Paleontologia, Florence), E. Robert (Université Claude Bernard - 1, Lyon), D. Berthet (Musée des Confluences, Lyon), C. Banassat and V. Brissaud (Musée de Paléontologie Christian Guth de Chilhac, Chilhac) and L. Costeur (Natural History Museum Basel, Basel) for providing access to the fossil *Equus* collections at their disposal. The authors wish to thank the two reviewers, A. Athanassiou (Ministry of Culture, Ephorate of Palaeoanthropology-Speleology) and S. Roussiakis (National and Kapodistrian University of Athens), for their useful comments which have improved the quality of this manuscript.

REFERENCES

Alberdi, M.T., Ortiz-Jaureguizar, E. and Prado, J.L., 1998. A quantitative review of European stenonoid horses. Journal of Paleontology, 72(2), pp. 371–387.

Alberdi, M.T. and Palombo, M.R., 2013. The late Early to early Middle Pleistocene stenonoid horses from Italy. Quaternary International, 288, pp. 25–44.

Azzaroli, A., 1983. Quaternary mammals and the "end-Villafranchian" dispersal event-a turning point in the history of Eurasia. Palaeogeography, Palaeoclimatology, Palaeoecology, 44, pp. 117–139.

Bernor, R.L., Cirilli, O., Bukhsianidze, M., Lordkipanidze, D. and Rook, L., 2021. The Dmanisi *Equus*: Systematics, biogeography, and paleoecology. Journal of Human Evolution, 158, e103051.

Bernor, R.L., Cirilli, O., Jukar, A.M., Potts, R., Buskianidze, M. and Rook, L., 2019. Evolution of early *Equus* in Italy, Georgia, the Indian Subcontinent, East Africa, and the origins of African zebras. Frontiers in Ecology and Evolution, 7, p.e166.

Cirilli, O. Saarinen, J., Pandolfi, L., Rook, L. and Bernor, R.L., 2021. An updated review on *Equus stenonis* (Mammalia, Equidae): new implications for the European Early Pleistocene *Equus* taxonomy and paleoecology, and remarks on the Old World *Equus* evolution. Quaternary Science Reviews, 269, p.e107155.

Eisenmann, V., 2002. The primitive horses of the Vatera Formation (Lesbos, Greece), Proceedings of the 1st International Workshop "On Late Plio/Pleistocene Extinction and Evolution in the Palearctic. The Vatera site". Annales Géologiques des Pays Helléniques, 39(A), pp. 131–153.

Eisenmann, V., 2010. Sussemionus, a new subgenus of *Equus* (Perissodactyla, Mammalia). Comptes Rendus. Biologies, 333(3), pp. 235-240.

Eisenmann, V., 2011. Venta Micena and *Equus granatensis*. https://vera-eisenmann.com/. Accessed on December 10, 2020.

Eisenmann, V., 2017. The Senèze text. https://vera-eisenmann.com/. Accessed on December 15, 2020.

Eisenmann, V., Alberdi, M.T., De Giuli, C. and Staesche, U., 1988. Methodology, in: Woodburne, M. and Sondaar, P.Y. (Eds.), Studying Fossil Horses. EJ Brill Press, Leiden, pp. 1–71.

Forstén, A., 1999. A review of *Equus stenonis* Cocchi (Perissodactyla, Equidae) and related forms. Quaternary Science Reviews, 18(12), pp. 1373–1408.

Gkeme, A.G., 2023. Study of the Quaternary equids of Greece: systematics, biostratigraphy, phylogeny, palaeoecology. Ph.D. Thesis, School of Geology, Aristotle University of Thessaloniki, Annex Number of Scientific Annals of the School of Geology No 236, 289 pp.

Gkeme, A.G., Koufos, G.D. and Kostopoulos, D.S., 2017. The Early Pleistocene stenonoid horse from Libakos and Polylakkos (Western Macedonia, Greece): biochronological and palaeoecological implications and dispersal events. 15th RCMNS Congress, Athens, Greece, 67.

Konidaris, G.E., Tourloukis, V., Kostopoulos, D.S., Thompson, N., Giusti, D., Michailidis, D., Koufos, G.D. and Harvati, K., 2015. Two new vertebrate localities from the Early Pleistocene of Mygdonia Basin (Macedonia, Greece): preliminary results. Comptes Rendus Palevol, 14(5), pp. 353–362.

Konidaris, G.E., Kostopoulos, D.S., Maron, M., Schaller, M., Ehlers, T.A., Aidona, E., Marini, M., Tourloukis, V., Muttoni, G., Koufos, G.D. and Harvati, K., 2021. Dating of the Lower Pleistocene vertebrate site of Tsiotra Vr-

yssi (Mygdonia Basin, Greece): Biochronology, magnetostratigraphy, and cosmogenic radionuclides. Quaternary, 4(1), 1.

Koufos, G.D., 1992. Early Pleistocene equids from Mygdonia Basin (Macedonia, Greece). Palaeontographia Italica, 79, pp. 167–199.

Koufos, G.D. and Kostopoulos, D.S., 2016. The Plio-Pleistocene large mammal record of Greece: implications for early human dispersals into Europe, in: Harvati, K. and Roksandic, M. (Eds.), Paleoanthropology of the Balkans and Anatolia: Human Evolution and Its Context. Springer, Dordrecht, pp. 269–280.

Koufos, G.D., Vlachou, T.D. and Gkeme, A.G., 2022. The fossil record of equids (Mammalia: Perissodactyla: Equidae) in Greece, in: Vlachos, E. (Eds.), Fossil Vertebrates of Greece Volume 2: Laurasiatherians, Artiodactyles, Perissodactyles, Carnivorans, and Island Endemics. Springer, Cham, pp. 351–401.

Levine, M., 1982. The use of crown height measurements and eruption-wear sequences to age horse teeth, in: Wilson, B., Grigson, C. and Payne, S. (Eds.), Ageing and sexing of animal bones from archaeological sites. British Archaeological Reports, British Series, 109, pp. 223–250.

Lindsay, E.H., Opdyke, N.D. and Johnson, N.M., 1980. Pliocene dispersal of the horse *Equus* and Late Cenozoic mammalian dispersal events. Nature, 287(5778), pp. 135–138.

Rook, L. and Martínez-Navarro B., 2010. Villafranchian: the long story of a Plio-Pleistocene European large mammal biochronologic unit. Quaternary International, 219, pp. 134–144.

Rook, L., Bernor, R.L., Avilla, L.S., Cirilli, O., Flynn, L., Jukar, A.M., Sanders, W., Scott, E. and Wang, X., 2019. Mammal biochronology (Land Mammal Ages) around the world from Late Miocene to Middle Pleistocene and major events in horse evolutionary history. Frontiers in Ecology and Evolution, 7, e278.

van der Meulen, A.J. and van Kolfschoten, T., 1986. Review of the Late Turolian to Early Biharian mammal faunas from Greece and Turkey. Memorie della Società Geologica Italiana, 31, pp. 201–211.

5 TAPHONOMIC STUDY OF THE LOWER PLEISTOCENE SITE OF TSIOTRA VRYSSI (MYGDONIA BASIN, GREECE): PRELIMINARY RESULTS ON BONE MODIFICATIONS IN EQUID CARCASSES

Anastasia Katsagoni[1,*], George E. Konidaris[2], Domenico Giusti[2], George D. Koufos[1], Dimitris S. Kostopoulos[1], Katerina Harvati[2,3]

[1]*Laboratory of Geology and Palaeontology, School of Geology, Aristotle University of Thessaloniki, Thessaloniki, Greece*
[2]*Paleoanthropology, Institute for Archaeological Sciences and Senckenberg Centre for Human Evolution and Palaeoenvironment, Department of Geosciences, Eberhard Karls University of Tübingen, Tübingen, Germany*
[3]*DFG Centre for Advanced Studies 'Words, Bones, Genes, Tools', Eberhard Karls University of Tübingen, Tübingen, Germany*
**anastasiakat221@gmail.com*

http://dx.doi.org/10.15496/publikation-97671

Keywords: taphonomy; tooth marks; *Equus*; late Villafranchian; carnivores

5.1 INTRODUCTION

The fossiliferous site of Tsiotra Vryssi (TSR; Mygdonia Basin, Greece) is dated to the Lower Pleistocene, between 1.78 and 1.5 Ma, and has yielded a rich late Villafranchian vertebrate fauna, including diverse medium- to very large-sized herbivores (equids, bovids, cervids, giraffids, rhinocerotids, elephantids) and several large carnivorans (hyaenids, canids, ursids, felids) (Konidaris et al., 2015, 2021). Previous spatial taphonomic research has investigated the distribution of the TSR fossils and suggested multiple dispersion events and recurrent spatial rearrangement of a lag, (peri)autochthonous assemblage within a fluvial system (Giusti et al., 2019). Herein, we present preliminary results of our ongoing taphonomic study on carnivore modifications, and we focus on equid postcranial bones, which comprise the bulk of the TSR vertebrate assemblage. For the analysis, we perform a set of standard taphonomic analyses, following the "physical attribute approach" of Domínguez-Rodrigo et al. (2007, 2015a), in which the alterations in the physical attributes of skeletal elements constitute the major component for the interpretation of the taphonomic history of the assemblage. Therefore, besides the skeletal part representation, we focus here on bone surface modifications and bone damage patterns aiming to reveal the main biotic agent responsible for the modification of bones.

5.2 MATERIALS AND METHODS

The studied material comprises all postcranial elements from TSR attributed to the genus *Equus*, which were collected during the excavation seasons of 2014–2019. All specimens are stored at the Mu-

A. Katsagoni: https://orcid.org/0000-0002-8510-6941
G. E. Konidaris: https://orcid.org/0000-0002-7041-233X
D. Giusti: https://orcid.org/0000-0003-1438-4036
G. D. Koufos: https://orcid.org/0000-0001-9669-4884
D. S. Kostopoulos: https://orcid.org/0000-0002-5475-5666
K. Harvati: https://orcid.org/0000-0001-5998-4794

seum of Geology, Palaeontology and Palaeoanthropology of the Aristotle University of Thessaloniki (LGPUT).

Equus is represented at TSR by two species, one of medium and one of large size (Konidaris et al., 2015; Gkeme et al., this volume). Body mass estimations were conducted separately for the medium- and the large-sized species, following the methodology of Eisenmann and Sondaar (1998). For this, we considered only metapodials belonging to articulated limbs that could be confidently classified either as subadult juvenile or adult individuals. This classification was based on the sequence of epiphyseal fusion in modern horses, and in particular, the fusion of the distal epiphysis in the radius (for metacarpals), and the distal epiphysis in the tibia (for metatarsals), which fuse towards the end of the epiphyseal bone fusing sequence (Budras et al., 2011) and are abundant in the articulated elements of the assemblage.

Skeletal part representation was examined by calculating the number of identified specimens (NISP), the minimum number of elements (MNE), and the minimum animal units (MAU). MNE calculations take into consideration anatomical overlap of fragments, size, and ontogenetic age. The minimum number of individuals (MNI) was calculated as well.

The nature of fractures was studied following the methodology of Villa and Mahieu (1991), where fracture angle, outline, and edge are considered. Fresh fractures are generally characterized by oblique angles, curved outlines, and smooth edges, whereas dry fractures generally have right angles, transverse outlines, and jagged edges.

Bone damage patterns are quantified using the classification of long limb bones into "taphotypes" (Domínguez-Rodrigo et al., 2015b: Fig. 1). Each long limb bone is classified into one of the 16 taphotypes (0–15), depending on its preserved portion. Additionally, regression analysis was used to study the correlation of epiphyses abundance with marrow cavity volume and bone density (as in Palmqvist and Arribas, 2001). The data for marrow cavity volume and bone density concerns modern horses and is taken from Outram and Rowley-Conwy (1998) and Lam et al. (1999), respectively.

Carnivore tooth marks were classified into pits, punctures, scores, and furrows, following the criteria set by Pobiner (2007); recorded carnivore damage also includes notches and furrowing (deletion of cancellous bone). Identified tooth marks were measured with a digital caliper to the nearest 1/100 of a millimeter, directly onto the bone surface, under strong light and magnification. The measurements taken are length (maximum dimension) and breadth (maximum dimension transversal to length).

5.3 RESULTS

The mean body mass is calculated at 257 kg for the medium-sized, and 343 kg for the large-sized *Equus* species. They both fall within the size group 4 (150–350 kg) of Palombo (2010), and therefore their skeletal elements are treated here collectively regardless of species attribution. NISP, MNE, and MAU values are given in Table 1. NISP values reveal a greater abundance of limb bones over other elements, while MNE and MAU values show a clear over-representation of tibiae and metapodials, and an under-representation of axial elements and femora. The minimum number of individuals (MNI) is 15.

Fracture variables suggest that most studied fractures occurred when the bones were still in a fresh state. Specifically, curved outlines appear in 67.9% of fractures, smooth edges in 69.8%, and oblique angles in 45.3%. Intermediate outlines and mixed angles are also relatively common (24.5 and 37.7%, respectively).

	NISP	MNE	MAU
Atlas	4	4	4
Axis	3	3	3
3th-7th cervical	14	14	3
Sacrum	1	1	1
Scapula	11	11	6
Pelvis	2	2	2
Humerus	11	11	6
Radius	11	10	5
Ulna	3	3	2
Metacarpal	25	25	13
Femur	7	7	4
Tibia	26	25	13
Metatarsal	23	22	11
Lateral metapodial	53	53	—
Carpals	61	61	—
Astragalus	14	14	7
Calcaneus	13	13	7
Other tarsals	39	39	—
Proximal phalanx	23	23	6
Intermediate phalanx	17	17	4
Distal phalanx	23	23	6
Sesamoids	47	47	—
Metapodial	6	—	—
Total	437	—	—

Table 1: NISP, MNE, and MAU values of *Equus* specimens in TSR.

The implementation of taphotypes (Domínguez-Rodrigo et al. 2015b: Fig. 1) allowes us to quantify the degree and pattern of bone damage in an assemblage. Metapodials from TSR usually belong to taphotype 1, i.e., complete bones (80.0% for metacarpals; 82.6% for metatarsals). On the contrary, taphotype 15, i.e., cylinder, is frequent in humeri (36.4%) and femora (42.9%). The radius frequently lacks the proximal epiphysis and part of the diaphysis (taphotypes 4 and 5; 27.3% and 18.2%, respectively), while complete radii are also relatively abundant (27.3%). Tibiae are rarely preserved complete, with the majority retaining only the distal half, or part of it (26.9% for taphotypes 4 and 5 each). Such a deletion of epiphyses appears to be non-random, rather it shows a degree of selectivity. This pattern is further supported by the regression analysis of abundance of epiphyses with bone marrow content and bone density. There appears to be a statistically significant inverse relationship between abundance of epiphyses and bone marrow content (Fig. 1A), i.e., high-nutritional value epiphyses are missing, and conversely less nutritious epiphyses are preserved. Accordingly, the abundance of epiphyses displays a strong positive correlation with bone mineral density (R^2=0.80),

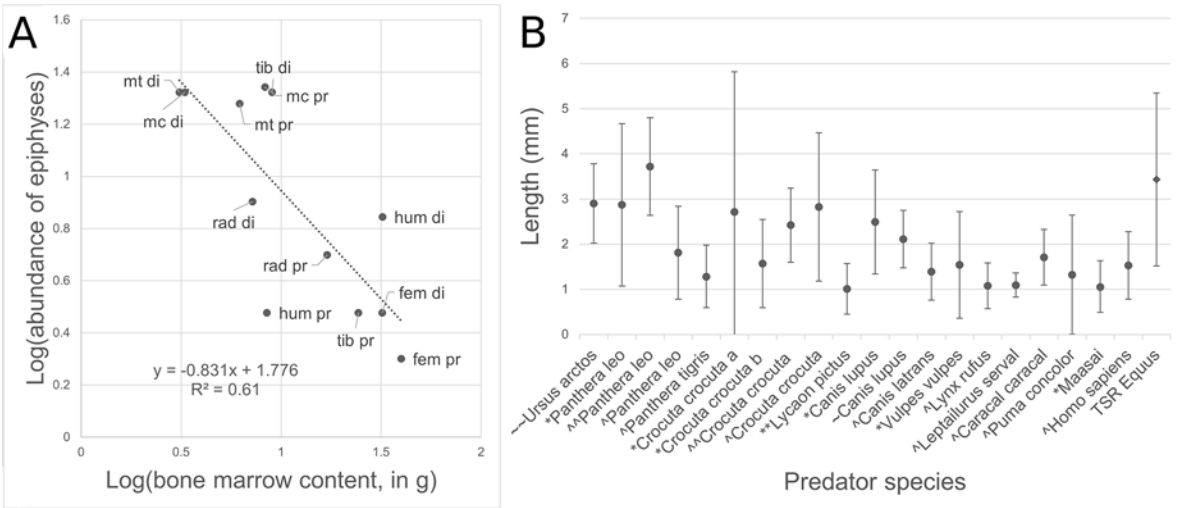

Figure 1: A, Regression analysis between abundance of epiphyses in the *Equus* specimens from TSR and bone marrow content in modern horses (data from Outram and Rowley-Conwy, 1998). B, Mean values and standard deviation intervals of pit length on the diaphysis. Data from: ~~ Domínguez-Rodrigo and Piqueras (2003), * Andrés et al. (2012), ^^ Sala et al. (2012), ^ Delaney-Rivera (2009), ** Yravedra et al. (2014) and ~ Sala et al. (2014), in comparison with *Equus* from TSR.

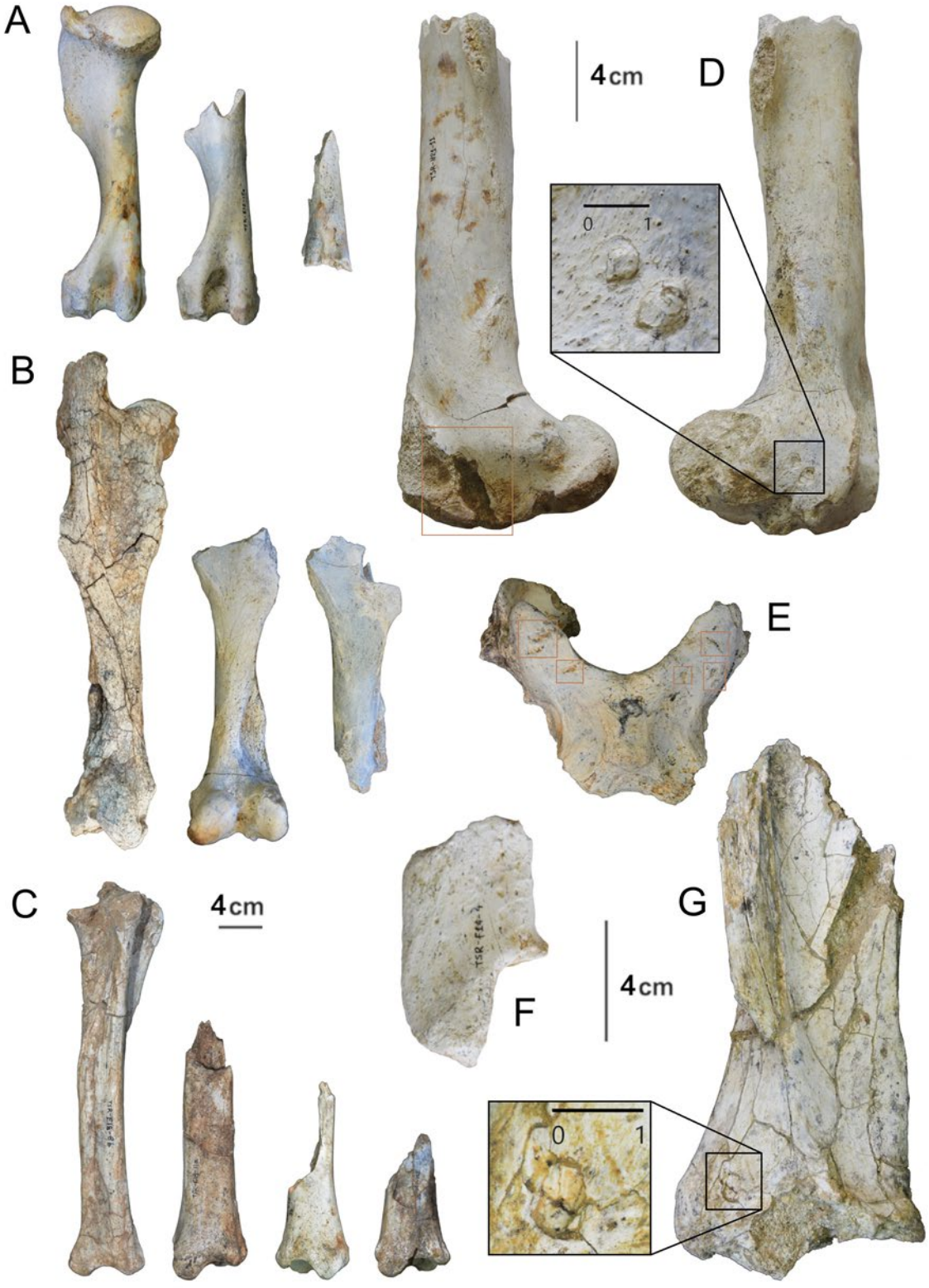

Figure 2: Left: Bone consumption sequence in humerus (A), femur (B), and tibia (C) in the TSR equid assemblage. Right: Examples of carnivore modifications in equid bones: Femur with furrowing and punctures (D), atlas with furrowing, scores, and pits (E), calcanei with furrowing (F), and scapula with jagged edges with a crenulated outline, and puncture (G).

i.e., epiphyses with high mineral density are over-represented.

Carnivore modifications are frequent in the assemblage (Fig. 2), usually in the form of tooth marks, as well as furrowing and notches. The higher percentages of modified elements, displaying any type of carnivore alteration, are recorded in femora (85.7%) and humeri (72.7%); most tibiae (69.2%) are modified as well. Among long limb bones, the least modified elements are metacarpals (16.0%), while metatarsals and radio-ulnae also display relatively low percentages of modification (30.4 and 36.4%, respectively).

Regarding tooth marks, 475 pits, 201 scores, and 12 punctures were recorded. In Figure 1B the mean and standard deviation values of pit length on the diaphysis from TSR are plotted along data from studies conducted with extant predators. The TSR values are comparable to those of some of the largest modern carnivorans, such as lions, hyaenas, and grey wolves. Additionally, a relatively wide range is observed, with the upper limit surpassing that of almost all modern species.

5.4 DISCUSSION

The bone damage patterns in the studied material reveal a significant involvement of carnivorans in the modification of the *Equus* remains from the TSR accumulation. There appears to be preferential deletion of nutrient-dense (with high marrow yield) elements, such as the upper limb bones and axial elements, as well as bone portions, i.e., proximal epiphysis in the humerus, tibia, and radius, and both epiphyses in the femur. Moreover, most fractures are green indicating that the deletion of the aforementioned portions occurred when bones were still fresh and not later during the diagenetic process. Carnivore modification is frequent, especially in the upper limb bones, the majority of which bear tooth marks. The most frequent tooth marks are pits, and their dimensions suggest that they were inflicted by a large-sized carnivoran (Fig. 1B).

Several large carnivorans have been found to date at TSR: the ursid *Ursus etruscus*, the hyaenid *Pachycrocuta brevirostris*, the felid *Megantereon* sp., and several *Canis* sp. morphotypes (two medium- and one large-sized) (Konidaris et al., 2015, 2021; Koufos et al., 2018, Karakosta et al., this volume), while the large carnivoran late Villafranchian fauna of the Mygdonia Basin additionally includes the felids *Panthera gombaszoegensis* and *Homotherium latidens* (Koufos, 2014, 2018). *Ursus etruscus* is regarded an omnivorous carnivoran that consumed both plant and vertebrate matter, the latter possibly consisting mainly of fish (Medin et al., 2017); therefore, it can be rather safely excluded as a candidate for inflicting the heavy bone modifications observed at TSR. Additionally, the level of epiphyseal furrowing and bone deletion (including diaphyseal fragmentation) at TSR is incompatible with a predominantly felid modification. Extant pantherine felids cause generally limited and targeted furrowing in medium/large carcasses, while they usually produce minor/moderate bone deletion (e.g., Pobiner and Blumenschine, 2003; Domínguez-Rodrigo et al., 2012; Rodríguez-Alba et al., 2019; Pobiner et al., 2020), and the same can be hypothesized for the large felids present at TSR. Specifically regarding sabre-tooths, it is suggested that their dental morphology would not allow them to thoroughly exploit carcasses, and therefore cause significant bone modifications (e.g., Valkenburgh and Ruff, 1987; Palmqvist et al., 2011, and references cited therein); but see Marean and Ehrhardt (1995) for *Homotherium* tooth-marking. Modern wolves have the capacity to fracture ungulate bones; however, in wild populations, significant deletion of bone portions is rare in large-sized carcasses and is mainly observed in small-sized prey and medium-sized juvenile carcasses (Haynes, 1982; Yravedra et al., 2011). On the contrary, the

African wild dog is a flesh specialist that causes limited to moderate bone alteration, in particular in terms of bone deletion (Yravedra et al., 2014). Modern hyaenas are by far the most destructive of the extant carnivorans. Hyaena modified assemblages are characterized by an under-representation of axial elements (Binford, 1981; Capaldo, 1998), and high levels of fragmentation of limb bones (Haynes, 1983; Hill, 1989; Domínguez-Rodrigo et al., 2015b). Remarkably, the giant hyaena *Pachycrocuta brevirostris* possessed craniodental adaptations that reveal even greater bone cracking capabilities (Palmqvist et al., 2011). In Venta Micena (Spain; Lower Pleistocene), regarded as a bone accumulation site of *Pachycrocuta*, a preferential deletion of epiphyses in relation to their marrow/fat content and mineral density has been observed, reflected in the consumption sequence of limb elements (Palmqvist et al., 2011, and references cited therein). Specifically, the sequence of consumption is proximodistal in the humerus and tibia, distoproximal in metapodials, and without a clear direction in the femur and radius, but involving the deletion of both epiphyses (Palmqvist et al., 2011). Such a sequence of bone portion consumption, in addition to the degree of bone deletion (Palmqvist and Arribas, 2001: Fig. 2) are common attributes between Venta Micena and TSR.

5.5 CONCLUSIONS

The preliminary taphonomic study on the bone modifications in equid postcranial bones from TSR reveals high levels of gross bone damage and tooth marking, indicating that the main biotic taphonomic signal of the assemblage reflects the action of a large carnivoran that engaged in the intensive exploitation of large ungulate carcasses, similarly to modern hyaenas. Therefore, the study points towards the hyaena *Pachycrocuta brevirostris* (identified at the site) as the primary biotic agent of bone modifications at TSR. This is further corroborated by the similarities with the *Pachycrocuta* bone accumulation site Venta Micena in terms of the preferential deletion of epiphyses with high nutrient content, the degree of bone deletion, and the sequence of bone portion consumption. However, the involvement, even to a minor degree, of other contemporaneous large carnivorans in the alternation of bones cannot be completely ruled out. In order to achieve a more conclusive interpretation of the taphonomic history of TSR, future study directions will focus on the inclusion of the other ungulate size groups, the consideration of additional parameters (e.g., levels of articulation, tooth mark spatial distribution, notches), the investigation of the ontogenetic age profiles, and the examination of the coprolites found at the site.

ACKNOWLEDGMENTS

Excavation at TSR was supported by the ERC Consolidator Grant ERC-CoG-724703 (“CROSSROADS”) and the ERC Starting Grant ERC-StG-283503 (“PaGE”), both awarded to K.H. G.E.K. and K.H. are supported by the Deutsche Forschungsgemeinschaft (DFG Project no. 463225251, “MEGALOPOLIS”). K.H. is also supported by the ERC Advanced Grant ERC-AdG-101019659 (“FIRSTSTEPS”). Research of A.K. at the University of Tübingen was supported by the Erasmus+ exchange program. We thank the reviewers, E. Tsoukala and G. Iliopoulos, for their comments and suggestions.

REFERENCES

Andrés, M., Gidna, A.O., Yravedra, J. and Domínguez-Rodrigo, M., 2012. A study of dimensional differences of tooth marks (pits

and scores) on bones modified by small and large carnivores. Archaeological and Anthropological Sciences, 4, pp. 209–219.

Binford, L.R., 1981. Bones: Ancient Men and Modern Myths. Academic Press, New York.

Budras, K.D., Sack, W.O. and Röck, S., 2011. Anatomy of the Horse. Schlütersche, Hannover.

Capaldo, S.D., 1998. Simulating the formation of dual-patterned archaeofaunal assemblages with experimental control samples. Journal of Archaeological Science, 25(4), pp. 311–330.

Delaney-Rivera, C., Plummer, T.W., Hodgson, J.A., Forrest, F., Hertel, F. and Oliver, J.S., 2009. Pits and pitfalls: taxonomic variability and patterning in tooth mark dimensions. Journal of Archaeological Science, 36(11), pp. 2597–2608.

Domínguez-Rodrigo, M., Piqueras, A., 2003. The use of tooth pits to identify carnivore taxa in tooth-marked archaeofaunas and their relevance to reconstruct hominid carcass processing behaviours. Journal of Archaeological Science, 30(11), pp. 1385–1391.

Domínguez-Rodrigo, M., Egido, R.B. and Egeland, C.P., 2007. Deconstructing Olduvai: A Taphonomic Study of the Bed I Sites. Springer, Dordrecht.

Domínguez-Rodrigo, M., Gidna, A.O., Yravedra, J. and Musiba, C., 2012. A comparative neo-taphonomic study of felids, hyaenids and canids: an analogical framework based on long bone modification patterns. Journal of Taphonomy, 10, pp. 151–169.

Domínguez-Rodrigo, M., Barba, R., Soto, E., Sesé, C., Santonja, M., Pérez-González, A., Yravedra and J., Galán, A.B., 2015a. Another window to the subsistence of Middle Pleistocene hominins in Europe: A taphonomic study of Cuesta de la Bajada (Teruel, Spain). Quaternary Science Reviews, 126, pp. 67–95

Domínguez-Rodrigo, M., Yravedra, J., Organista, E., Gidna, A., Fourvel, J.B. and Baquedano, E., 2015b. A new methodological approach to the taphonomic study of paleontological and archaeological faunal assemblages: a preliminary case study from Olduvai Gorge (Tanzania). Journal of Archaeological Science, 59, pp. 35–53.

Eisenmann, V., Sondaar, P., 1998. Pliocene vertebrate locality of Çalta, Ankara, Turkey. 7. *Hipparion*. Geodiversitas, 20, pp. 409–439.

Giusti, D., Konidaris, G.E., Tourloukis, V., Marini, M., Maron, M., Zerboni, A., Thompson, N., Koufos, G.D., Kostopoulos, D.S. and Harvati, K., 2019. Recursive anisotropy: a spatial taphonomic study of the Early Pleistocene vertebrate assemblage of Tsiotra Vryssi, Mygdonia Basin, Greece. Boreas, 48(3), pp. 713–730.

Gkeme, A.G., Koufos, G.D., Kostopoulos, D.S. and Harvati, K., this volume. The Late Villafranchian equids from the locality Tsiotra Vryssi (Mygdonia Basin, Macedonia, Greece).

Haynes, G., 1982. Utilization and skeletal disturbances of North American prey carcasses. ARCTIC, 35, pp. 266–281.

Haynes, G., 1983. A guide for differentiating mammalian carnivore taxa responsible for gnaw damage to herbivore limb bones. Paleobiology, 9(2), pp. 164–172.

Hill, A., 1989. Bone modification by modem spotted hyenas, in: Bonnichsen, R., Sorg, M.H. (Eds.), Bone Modification. Center for the Study of the First Americans, Orono, Maine, pp. 169–178.

Karakosta, A., Konidaris, G.E., Kostopoulos, D.S., Koufos, G.D. and Harvati, K., this volume. Preliminary study of the canids from the Lower Pleistocene site of Tsiotra Vryssi (Mygdonia Basin, Greece).

Konidaris, G.E., Tourloukis, V., Kostopoulos, D.S., Thompson, N., Giusti, D., Michailidis, D., Koufos, G.D. and Harvati, K., 2015. Two new vertebrate localities from the Early Pleistocene of Mygdonia Basin (Macedonia,

Greece): Preliminary results. Comptes Rendus Palevol, 14(5), pp. 353–362.

Konidaris, G.E., Kostopoulos, D.S., Maron, M., Schaller, M., Ehlers, T.A., Aidona, E., Marini, M., Tourloukis, V., Muttoni, G., Koufos, G.D. and Harvati, K., 2021. Dating of the Lower Pleistocene vertebrate site of Tsiotra Vryssi (Mygdonia Basin, Greece): biochronology, magnetostratigraphy, and cosmogenic radionuclides. Quaternary, 4(1), pp. 1–18.

Koufos, G.D., 2014. The Villafranchian carnivoran guild of Greece: implications for the fauna, biochronology and paleoecology. Integrative Zoology, 9(4), pp. 444–460.

Koufos, G.D., 2018. New material and revision of the Carnivora, Mammalia from the Lower Pleistocene locality Apollonia 1, Greece. Quaternary, 1(6), pp. 1–38.

Koufos, G.D., Konidaris, G.E. and Harvati, K., 2018. Revisiting *Ursus etruscus* (Carnivora, Mammalia) from the Early Pleistocene of Greece with description of new material. Quaternary International, 497, pp. 222–239.

Lam, Y.M., Chen, X. and Pearson, O.M., 1999. Intertaxonomic variability in patterns of bone density and the differential representation of bovid, cervid, and equid elements in the archaeological record. American Antiquity, 64(2), pp. 343–362.

Marean, C.W., Ehrhardt, C.L., 1995. Paleoanthropological and paleoecological implications of the taphonomy of a sabertooth's den. Journal of Human Evolution, 29(6), pp. 515–547.

Medin, T., Martínez-Navarro, B., Rivals, F., Madurell-Malapeira, J., Ros-Montoya, S., Espigares, M.P., Figueirido, B., Rook, L. and Palmqvist, P., 2017. Late Villafranchian *Ursus etruscus* and other large carnivorans from the Orce sites (Guadix-Baza basin, Andalusia, southern Spain): Taxonomy, biochronology, paleobiology, and ecogeographical context. Quaternary International, 431, pp. 20–41.

Outram, A., Rowley-Conwy, P., 1998. Meat and marrow utility indices for horse (*Equus*). Journal of Archaeological Science, 25(9), pp. 839–849.

Palmqvist, P., Arribas, A., 2001. Taphonomic decoding of the paleobiological information locked in a lower Pleistocene assemblage of large mammals. Paleobiology, 27(3), pp. 512–530.

Palmqvist, P., Martínez-Navarro, B., Pérez-Claros, J.A., Torregrosa, V., Figueirido, B., Jiménez-Arenas, J.M., Espigares, M.P., Ros-Montoya, S. and De Renzi, M., 2011. The giant hyena *Pachycrocuta brevirostris*: Modelling the bone-cracking behavior of an extinct carnivore. Quaternary International, 243(1), pp. 61–79.

Palombo, M.R., 2010. A scenario of human dispersal in the northwestern Mediterranean throughout the Early to Middle Pleistocene. Quaternary International, 223–224, pp. 179–194.

Pobiner, B.L., 2007. Hominin-carnivore interactions: Evidence from modern carnivore bone modification and Early Pleistocene archaeofaunas (Koobi Fora, Kenya; Olduvai Gorge, Tanzania). Rutgers University, New Brunswick.

Pobiner, B.L., Blumenschine, R.J., 2003. A taphonomic perspective on Oldowan hominid encroachment on the carnivoran paleoguild. Journal of Taphonomy, 1(2), pp. 115–141.

Pobiner, B., Dumouchel, L. and Parkinson, J., 2020. A new semi-quantitative method for coding carnivore chewing damage with an application to modern African lion-damaged bones. Palaios, 35(7), pp. 302–315.

Rodríguez-Alba, J.J., Linares-Matás, G. and Yravedra, J., 2019. First assessments of the taphonomic behaviour of jaguar (*Panthera onca*). Quaternary International, 517, pp. 88–96.

Sala, N., Algaba, M., Arsuaga, J., Aranburu, A.

and Pantoja-Pérez, A., 2012. A taphonomic study of the Búho and Zarzamora caves. Hyenas and humans in the Iberian Plateau (Segovia, Spain) during the Late Pleistocene. Journal of Taphonomy, 10(3–4), pp. 477–497.

Sala, N., Arsuaga, J.L., Haynes, G., 2014. Taphonomic comparison of bone modifications caused by wild and captive wolves (*Canis lupus*). Quaternary International, 330, pp. 126–135.

van Valkenburgh, B., Ruff, C.B., 1987. Canine tooth strength and killing behaviour in large carnivores. Journal of Zoology, 212(3), pp. 379–397.

Villa, P., Mahieu, E., 1991. Breakage patterns of human long bones. Journal of Human Evolution, 21(1), pp. 27–4.

Yravedra, J., Lagos, L. and Bárcena, F., 2011. A taphonomic study of wild wolf (*Canis lupus*) modification of horse bones in Northwestern Spain. Journal of Taphonomy, 9(1), pp. 37–65.

Yravedra, J., Andrés, M. and Domínguez-Rodrigo, M., 2014. A taphonomic study of the African wild dog (*Lycaon pictus*). Archaeological and Anthropological Sciences, 6, pp. 113–124.

6 THE PRELIMINARY RESULTS OF THE MYGDONIA BASIN ARCHAEOLOGICAL SURVEY PROJECT, GREECE

Nicholas Thompson[1,*], Vangelis Tourloukis[1,2], Domenico Giusti[1], Katerina Harvati[1,3], Kostas Kotsakis[4]

[1]*Paleoanthropology, Institute for Archaeological Sciences and Senckenberg Centre for Human Evolution and Palaeoenvironment, Department of Geosciences, Eberhard Karls University of Tübingen, Tübingen, Germany*
[2]*Department of History and Archaeology, School of Philosophy, University of Ioannina, Ioannina, Greece*
[3]*DFG Centre for Advanced Studies 'Words, Bones, Genes, Tools', Eberhard Karls University of Tübingen, Tübingen, Germany*
[4]*Department of Archaeology, Aristotle University of Thessaloniki, Thessaloniki, Greece*
**nikothompso@yahoo.com*

http://dx.doi.org/10.15496/publikation-97662

Keywords: Lower Palaeolithic; Pleistocene; Mygdonia Basin; target-oriented survey

6.1 INTRODUCTION

During the past 2 million years, mass dispersal events of mammals from Africa into Eurasia possibly triggered the arrival of early hominins (Bar-Yosef and Belfer-Cohen, 2001; Abbate and Sagri, 2012; Koufos and Kostopoulos, 2016; Muttoni et al., 2018). At Early Pleistocene sites, where rich fauna complements the presence of carnivore and hominin activity, important taphonomic processes further complicate the recovery and interpretation of early human behaviors and remains. Evidence of hominins from this period is sparse and is found at only a handful of locations outside of Africa (Garcia et al., 2013). Even though an obvious gap continues to exist in Greece and the Balkans, this region of Europe is located in the direct path of human migrations out of Africa and Asia. For the Middle Pleistocene, the paleoanthropological, archaeological, and paleontological records of Greece are currently improving, in large part through the efforts of the ERC projects PaGE and CROSSROADS and the associated MegaPal survey (e.g., Panagopoulou et al., 2015; Harvati et al., 2018; Karkanas et al., this volume; Tourloukis et al., this volume; Athanassiou et al., this volume; Konidaris et al., this volume; Thompson et al., this volume), therefore starting to fill this research gap of Eastern Europe during this crucial period of hominin migrations.

CROSSROADS aimed to continue to fill this gap in the Early to Middle Pleistocene record by conducting multidisciplinary systematic fieldwork to locate stratified dateable contexts that promote the construction of a chronostratigraphic framework for this region of Eurasia. The Mygdonian Basin archaeological survey was therefore part of this effort and was conducted in 2019, 2021 and

N. Thompson: https://orcid.org/0009-0003-4770-1744
V. Tourloukis: https://orcid.org/0000-0002-9527-2708
D. Giusti: https://orcid.org/0000-0003-1438-4036
K. Harvati: https://orcid.org/0000-0001-5998-4794
K. Kotsakis: https://orcid.org/0000-0003-2918-2955

2022 by the Aristotle University of Thessaloniki, in collaboration with the University of Tübingen Paleoanthropology team, in the framework of CROSSROADS. The survey was a direct target-oriented double-intensive archaeological investigation of Pleistocene sediments, aiming to identify traces of human activity by systematically surveying exposed section profiles and by collecting lithic artifacts from stratified dateable contexts.

6.2 PREVIOUS RESEARCH

Whereas the Mygdonia Basin of Central Macedonia and Chalkidiki is well-known for its fossiliferous localities, such as Apollonia (Koufos et al., 1992, 1997; Kostopoulos, 1997; Konidaris et al., 2020; Gkeme et al., 2021), Tsiotra Vryssi (Konidaris et al., 2015, 2021; Koufos et al., 2018; Giusti et al., 2019), and Kalamoto (Tsoukala and Chatzopoulou, 2005) to name a few, the archaeology of the basin is less known, even though the Petralona cranium, discovered in the early 1960s in Chalkidiki, is probably one of the most famous and best-preserved Middle Pleistocene paleoanthropological findings from Greece (see Harvati et al., 2009; Harvati, 2022). The Petralona cave, located circa 30 km to the southeast of our project area is where speleothems surrounding the cranium were dated by U-series and revised Electron Spin Resonance analyses to 150–250 ka (Grün, 1996). Study of the Petralona cranium, e.g., as conducted by Harvati (2009), has determined the remains to represent *Homo heidelbergensis*, considered ancestral to Neanderthals. Nevertheless, the original stratigraphic position of the cranium is unknown, and it cannot be correlated with any geological layers, lithics or fauna; furthermore, the artifactual status of the published lithic material has been questioned (Harvati et al., 2009; Tourloukis and Harvati, 2018).

The lithics from the cave, according to Darlas (1995), consist mainly of quartz and occasionally bauxite, with rare pebble tools and no handaxes. Instead, side scrapers, notches and denticulates are frequent (Darlas, 1995), whereas the poor choices in raw materials is due to the lack of flint from this region of Macedonia (see Litsios, 2012, for sources of flint to the west of the Axios river valley).

The Langadas Archaeological Survey Project was the first systematic archaeological research conducted in the Mygdonia Basin, by Kotsakis and colleagues who identified Middle Palaeolithic surface lithic scatters at Zagliveri, Doumbia and Sarakina (Andreou and Kotsakis, 1994; Papagianni, 2000). To date, those Palaeolithic results remain unpublished (see Andreou and Kotsakis, 1999; Kotsakis and Koliopoulos, 2007; for results from later periods). Whereas that project was a diachronic multi-period survey, our more recent research instead focused mainly on the Early to Middle Pleistocene sediments and aimed to locate lithic artifacts from stratified contexts.

6.3 GEOLOGY

The Neogene to Quaternary sedimentary sequence of the basin consists of the Mygdonian and Premygdonian Group (Koufos et al., 1995). The oldest Chryssavgi Formation (Fm) dates to the Middle Miocene and overlies the basement of the basin. Of interest to us were the Early Pleistocene Gerakarou and Platanochori Fm's and the Pleistocene sediments of the Mygdonian Group. Because the deposition of the basin occurred over a period of 2 million years, this is an ideal region to locate the earliest presence of hominins from this part of Europe. The Gerakarou Fm (over 100 m thick) is represented by red-bed sediments consisting of unconsolidated gravels, sand, silt, and clay, accumulated in a fluvio-torrential environment (Koufos et al., 1995). The overlying Platanochori Fm is 10–20 m thick and formed in a fluvial, fluvio-la-

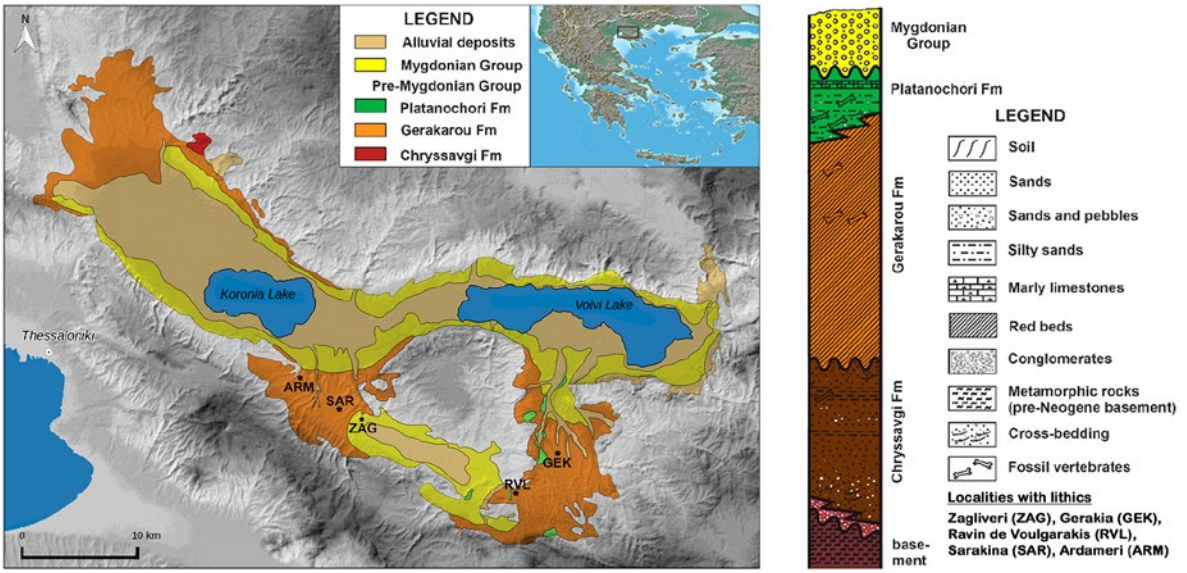

Figure 1: Geological map of the Neogene and Quaternary lithostratigraphic units of the Mygdonia Basin with composite stratigraphic column and the localities with lithic finds (modified from Koufos et al., 1995 and Konidaris et al., 2015). The name for the locality of Ravin de Voulgarakis is adapted from the palaeontological site (Kostopoulos and Koufos, 2007) because there are no toponyms available for this region of the basin.

custrine depositional environment. It represents the transition between the Gerakarou Fm and the overlying lacustrine sediments of the Mygdonian Group that was deposited during the Middle Pleistocene to Holocene (Koufos et al., 1995; Maravelis et al., 2022). On the geological map of the region (Fig. 1), the localities where lithics have been recovered are designated accordingly.

6.4 SURVEY METHODS

The survey areas were designated by locality and survey unit (SU) number. A SU is an arbitrary unit of observation developed to record and document archaeological phenomena on a dynamic landscape (Tourloukis et al., 2016; Thompson et al., 2018). Because our survey is target-oriented or otherwise referred to as deposit-centered (see Holcomb et al., 2020 for a recent review of this survey approach in Greece), the two main groups targeted for survey are stratigraphic profiles (vertical exposures) and fields (horizontal exposures). For stratigraphic profiles, intact stratified lithic remains can be potentially placed in a chronostratigraphic sequence, and therefore constitute the main targeted group of this survey. At exposed section profiles even though there is typically better preservation of artifacts, there were also limitations of survey, such as restricted access due to the size of the section profiles, difficult terrain, and occasional disturbances like slope wash and slumping. As for fields, some benefits include easy access to large survey areas of exposed ancient sediments, typically with good seasonal visibility, but also with mixed assemblages that are exposed to weathering and possible plow damage or trampling.

Therefore, proper field documentation was essential to verify the geological context, especially for the low-density lithic scatters that are associated with the sandy fluvial depositional contexts. Consequently, finds were either recorded as 'surface' or 'stratified', photographs were taken both close up and at a distance to record the context, and field forms were employed to document not only the survey areas, but to also record essential geoarchaeological phenomena such as geomorphological setting, disturbances, surface visibility, and

GIS spatial data (Tourloukis et al., 2016; Thompson et al., 2018).

6.5 RESULTS

The survey area encompassed Early–Late Pleistocene sediments of the Mygdonia Basin, northern Greece, where the total area surveyed was 52.3 ha (Table 1), representing 17 SUs from 9 localities (11 targets inspected were section profiles, and 8 fields). In total, more than 200 lithics were recovered from 10 SUs (lithic counts are preliminary as the analysis is on-going; 1 SU with lithic artifacts collected from stratified contexts and 9 SUs with lithics recovered as isolated surface finds or from lithic scatters).

In general, the survey focused on inspecting the exposed section profiles to the south of Lake Volvi and Lake Koronia because this is where the major drainage systems of the region occur. This gently sloping, incised region of the basin stands in stark contrast to the northern part of the basin that is affected more extensively by tectonics, uplift and alluviation from present-day rivers. To the west, near the Lagkadikia drainage system, are the localities of the Gerakarou Fm. These SUs occurred at the localities of Lagkadikia, Sarakina and Ardameri (a fossiliferous locality also known as Vassiloudi; Koufos et al., 1995), whereas the SU of Zagliveri is located in Pleistocene gravel deposits of the Mygdonian Group (I.G.M.R. 1978, Mountrakis et al., 1996). At the Megalo Rema drainage system to the east, are the localities of Ravin de Voulgarakis located in the Platanochori Fm, whereas Gerakia, Krimni and Riza consisted mainly of the Gerakarou Fm with limited exposures of the Platanochori Fm (Mountrakis et al., 1996) that were typically inaccessible due to the steep landscape and the position of this Fm in the uppermost part of the section profiles. Overall, the Platanochori Fm is patchier on the landscape, while the older red-

		SU area		Lithics		Elevation	
Sites	SUs	(hectares)	Target	strat.	surface	masl	Geological Fm
Zagliveri	1	0,3	section	3	16	196	Pleistocene gravels
Sarakina	1, 2	4,1	field	0	169	212	Gerakarou

		SU area		Lithics		Elevation	
Localities/ Findspots	SUs	(hectares)	Target	strat.	surface	masl	Geological Fm
Ravin de Voulgarakis	1-3	5,8	field	0	7	182	Platanochori
Riza	1, 2	1,6	section	0	0	350	Platanochori, Gerakarou
Gerakia	1, 2	3,3	section	0	0	135	Gerakarou
Krimni	2	0,8	section	0	6	180	Gerakarou
Megalo Rema	7	21,5	section, field	0	5	194	Gerakarou
Ardameri	1-4	14,3	section, field	0	4	203	Gerakarou
Lagkadikia	1	0,6	section	0	0	120	Gerakarou

Table 1: List of sites and findspots by locality and SU number.

bed sediments of the Gerakarou Fm are the most obvious of the survey area, due to the thickness of this formation and by the distinctive runnels that form on the section profiles from erosion and exposure to the elements. The systematic study of the collected lithics is ongoing; therefore, any mention hereafter is based on observations that were made in the field. In total, 188 lithics were recovered from sites and 22 from findspots.

6.6 FINDSPOTS

The four localities with findspots are Ravin de Voulgarakis, Krimni, Megalo Rema and Ardameri, where lithics were identified either as isolated surface finds, or low-density lithic scatters (Tab. 1).

At Ravin de Voulgarakis we conducted three SUs, all in fields, where calcareous calcitic nodules resembling marl from the fluvio-lacustrine Platanochori Fm produced a white chalky texture and color that was visible on the ground surface. At this locality, lithics were collected as surface finds and consisted of undiagnostic quartz artifacts of unknown age, with the exception of a possibly Middle Palaeolithic quartz core from SU 2. Overall, the findspots consisted of low-density lithic scatters, none of which have been found in direct association with the fossiliferous site of Ravin de Voulgarakis.

To the east of Megalo Rema, we conducted one SU in fields located above the floodplain, bordered by large, steep, and occasionally heavily eroded section profiles ranging in height from 8 to 40 m of Gerakarou and Platanochori Fm's. In the foothills above the drainage to the east of these sections, four quartz lithics were collected on the surface of a plowed field, including a possible core. On the geotectonic map of Langadhas (Mountrakis et al., 1996), the sediment from this area is designated as Gerakarou Fm, although the red colored sediment of the field where lithics were found appears to be a possible paleosol that caps the Gerakarou Fm. Lastly, a Middle Paleolithic heavily rolled and battered radiolarite lateral scraper was found in the modern Megalo Rema riverbed during reconnaissance.

Near the known fossil locality of Krimni, a SU was conducted along a dirt road where exposed sections 1-4 meters in height were inspected. The

Figure 2: Pedestrian surface survey in field of more recent sediments capping the thick Gerakarou Fm at Ardameri SU 3. Note the density and various sizes of quartz visible on the ground surface, ranging from boulders to pebbles in size (for scale, the hammer is 30 cm in length). In the image to the right, a quartz flake was recovered on the section profile. Insets of the lithic on the right as recovered and on the left in dorsal, right lateral, ventral, and left lateral views.

sediments of this SU consisted mainly of the Gerakarou Fm, with an isolated section of possibly more recent Pleistocene sediments, located near the top of a hill. To the north of the uppermost road, ~40 m from the edge of a field near the end of the SU, five possible flakes and a core were found on the surface near a possible reddish paleosol about a meter thick located on the western edge of the road cut. All finds were recovered in a 15 m area, either close to the low-lying section, or in a gully of the dirt road. All finds are of quartz, whereas one large, isolated flake of limestone or andesite was also recovered on the surface of a gully to the southeast of the quartz lithics.

At the locality of Ardameri where numerous section profiles of the Gerakarou Fm were surveyed, we conducted four SUs and collected quartz lithic artifacts from the surface of fields and section profiles at SUs 1, 2 and 3. Unfortunately, even though artifacts were recovered on the section profiles, they were not found in-situ. Therefore, when steep vertical section profiles are overlain by younger sediments, it is important to be particularly cautious when designating finds as stratified (Fig. 2). Also, because stratified artifacts from this survey have so far been recovered from sandy fluvial depositional contexts, where the finds tend to be low in density, hence the importance of being overcritical of context when trying to correctly identify paleosols or remnants of intact ancient terraces that may preserve in-situ remains.

6.7 SITES

As a general rule of our survey approach, sites were designated when surface lithic scatters with a find density of >10 lithics per 10 sq. m were identified or when lithic artifacts were recovered from stratified contexts (Tourloukis et al., 2016). In total, two localities were designated as sites. At Zagliveri, the lithics were recovered from both stratified and surface contexts, and at Sarakina, the finds were collected from dense surface lithic scatters (Tab. 1).

At the locality of Sarakina, two SUs were conducted, both in fields. In total, 169 lithics were recovered at both SUs. This locality is by far the densest scatter of artifacts in the project area with mainly quartz lithics, a possible radiolarite flake and two patinated pieces of flint. In general, the finds appear to be a mix of older and younger remains possibly spanning from the Palaeolithic to the Mesolithic, with diagnostic tools such as possible scrapers, perforators, and microliths. Overall,

Figure 3: The site of Zagliveri looking to the northeast. The inset shows a stratified quartz lithic artifact and the location in the gravels where it was discovered.

even though only two SUs were conducted in this region, the area is vast and, in all likelihood, contains additional lithic surface remains.

At Zagliveri (Fig. 2), we conducted one SU at a large section profile exposed as a road-cut where a mix of surface and stratified finds were recovered from a gravel layer mapped as Middle–Late Pleistocene sediments of the Mygdonian Group (Mountrakis et al., 1996). Three stratified lithics were recovered from the lowermost gravel layer of the section profile and 16 lithics from the surface. All finds were made of quartz.

6.8 CONCLUDING REMARKS

In conclusion, after three field seasons of survey, sporadic stratified quartz artifacts were collected from gravel deposits at Zagliveri. However, the predominance of surface finds complicates assigning temporal periods to the artifacts based solely on typology. The study of the collected assemblage is ongoing, and we anticipate that it will facilitate a better understanding of the core and flake technology from the Early–Middle Pleistocene including information on younger periods that has until recently gone unnoticed from this region of Greece.

ACKNOWLEDGMENTS

This research was supported by the ERC Consolidator Grant ERC-CoG-724703 ("CROSSROADS") and the ERC Advanced Grant ERC-AdG-101019659 ("FIRSTSTEPS"), both awarded to K.H. K.H. is also supported by the ERC Advanced Grant ERC-AdG-101019659 ("FIRSTSTEPS"). We would like to thank the Ephorate of Antiquities of the Thessaloniki Prefecture and the Faculty of History and Archaeology of the Aristotle University of Thessaloniki. Part of the study involved in this research was carried out at the Laboratory for Interdisciplinary Research in Archaeology (EDAE/LIRA), Department of Archaeology, School of History and Archaeology, Aristotle University of Thessaloniki. Also, we thank M. Ntinou and G. Konidaris for their critical comments and assessment of this manuscript during the review process.

REFERENCES

Abbate, E., Sagri, M., 2012. Early to Middle Pleistocene *Homo* dispersals from Africa to Eurasia: Geological, climatic and environmental constraints. Quaternary International, 267, pp. 3–19.

Andreou, S., Kotsakis, K., 1994. Prehistoric rural communities in perspective: the Langadas survey project. Collection de l'Institut des Sciences et Techniques de l'Antiquité, 508(1), pp. 17–26.

Andreou, S., Kotsakis, K., 1999. Counting people in an artifact poor landscape: The Langadas case, Macedonia, Greece. Reconstructing Past Population Trends in Mediterranean Europe (3000 BC–AD 1800), pp. 35–43.

Athanassiou, A., Konidaris, G.E., Tourloukis, V., Thompson, N., Giusti, D., Panagopoulou, E., Karkanas, P. and Harvati, K., this volume. The Middle Pleistocene large mammal fauna from Kyparissia (Peloponnese, S. Greece): New collected material.

Bar-Yosef, O., Belfer-Cohen, A., 2001. From Africa to Eurasia—early dispersals. Quaternary International, 75(1), pp. 19–28.

Darlas, A., 1995. 3 The earliest occupation of Europe: the Balkans, in: Analecta Praehistorica Leidensia 27: The earliest occupation of Europe: Proceedings of the European science foundation workshop at Tautavel (France), 1993 Volume 27. Leiden University Press, pp. 51–59.

Garcia, J., Martínez, K. and Carbonell, E., 2013. The early Pleistocene stone tools from Vallparadís (Barcelona, Spain): rethinking the European mode 1. Quaternary International, 316, pp. 94–114.

Giusti, D., Konidaris, G.E., Tourloukis, V., Marini, M., Maron, M., Zerboni, A., Thompson, N., Koufos, G.D., Kostopoulos, D.S. and Harvati, K., 2019. Recursive anisotropy: a spatial taphonomic study of the Early Pleistocene vertebrate assemblage of Tsiotra Vryssi, Mygdonia Basin, Greece. Boreas, 48(3), pp. 713–730.

Gkeme, A.G., Koufos, G.D. and Kostopoulos, D.S., 2021. Reconsidering the equids from the Early Pleistocene fauna of Apollonia 1 (Mygdonia Basin, Greece). Quaternary, 4(2), p. 12.

Grün, R., 1996. A re-analysis of electron spin resonance dating results associated with the Petralona hominid. Journal of Human Evolution, 30(3), pp. 227–241.

Harvati, K., 2009. Petralona: link between Africa and Europe? Hesperia Supplements, 43, pp. 31–47.

Harvati, K., 2022. The Hominin Fossil Record from Greece, in: Fossil Vertebrates of Greece Volume 1. Springer Cham, pp. 669–688.

Harvati, K., Panagopoulou, E. and Runnels, C., 2009. The paleoanthropology of Greece. Evolutionary Anthropology: Issues, News, and Reviews: Issues, News, and Reviews, 18(4), pp. 131–143.

Holcomb, J.A., Runnels, C. and Wegmann, K.W., 2020. Deposit-centered archaeological survey and the search for the Aegean Palaeolithic: A geoarchaeological perspective. Quaternary International, 550, pp. 169–183.

I.G.M.R., 1978. Geological Map of Greece, Zangliverion sheet, Scale 1:50,000. Institute of Geological and Mining Research.

Karkanas, P., Tourloukis, V., Thompson, N., Giusti, D., Tsartsidou, G., Athanassiou, T., Konidaris, G., Roditi, E., Panagopoulou, E. and Harvati, K., this volume. The Megalopolis Paleoenvironmental Project (MegaPal).

Konidaris, G.E., Tourloukis, V., Kostopoulos, D.S., Thompson, N., Giusti, D., Michailidis, D., Koufos, G.D. and Harvati, K., 2015. Two new vertebrate localities from the Early Pleistocene of Mygdonia Basin (Macedonia, Greece): preliminary results. Comptes Rendus Palevol, 14(5), pp. 353–362.

Konidaris, G.E., Kostopoulos, D.S. and Koufos, G.D., 2020. *Mammuthus meridionalis* (Nesti, 1825) from Apollonia-1 (Mygdonia Basin, Northern Greece) and its importance within the Early Pleistocene mammoth evolution in Europe. Geodiversitas, 42(6), pp. 69–91.

Konidaris, G.E., Kostopoulos, D.S., Maron, M., Schaller, M., Ehlers, T.A., Aidona, E., Marini, M., Tourloukis, V., Muttoni, G., Koufos, G.D. and Harvati, K., 2021. Dating of the Lower Pleistocene vertebrate site of Tsiotra Vryssi (Mygdonia Basin, Greece): Biochronology, magnetostratigraphy, and cosmogenic radionuclides. Quaternary, 4(1), p. 1.

Konidaris, G.E., Athanassiou, A., Panagopoulou, E., Karkanas, P. and Harvati, K., this volume. Fossil macaques (Cercopithecidae, Primates) from the Middle Pleistocene of the Megalopolis Basin (Greece) with description of a new specimen from Kyparissia 4.

Kostopoulos, D.S., 1997. The Plio-Pleistocene artiodactyls (Vertebrata, Mammalia) of Macedonia 1. The fossiliferous site "Apollonia-1", Mygdonia Basin of Greece. Geodiversitas, 19(4), pp. 845–875.

Κωστοπουλος, Δ., Κουφός, Γ.Δ., 2007. Similarity relationships among Greek middle miocene to early-Middle pleistocene mammal assemblages. *Δελτίον της Ελληνικής Γεωλογικής Εταιρίας, 40*(1), pp. 134–141.

Kotsakis, K., Koliopoulos, I., 2007. Prehistoric Macedonia, in: Koliopoulos, I. (Ed.), The History of Macedonia, pp. 1–22.

Koufos, G.D., Kostopoulos, D.S., 2016. The Plio-Pleistocene large mammal record of Greece: Implications for early human dispersals into Europe, in: Harvati, K., Roksandic, M. (Eds.), Paleoanthropology of the Balkans and Anatolia. Springer Dordrecht, pp. 269–280.

Koufos, G.D., Konidaris, G.E. and Harvati, K., 2018. Revisiting *Ursus etruscus* (Carnivora, Mammalia) from the Early Pleistocene of Greece with description of new material. Quaternary International, 497, pp. 222–239.

Koufos, G., Kostopoulos, D., Koliadimou, K. and Syridis, G., 1992. Apollonia, a New Vertebrate Site in the Pleistocene of the Mygdonia Basin (Macedonia, Greece)-the 1st Fossil Fresh-Water Mollusks in the Area. Comptes Rendus Académie des Sciences Paris, 315, pp. 1041–1046.

Koufos, G.D., Syrides, G.E., Kostopoulos, D.S. and Koliadimou, K.K., 1995. Preliminary results about the stratigraphy and the palaeoenvironment of Mygdonia Basin, Macedonia, Greece. Geobios, 28, pp. 243–249.

Koufos, G.D., Kostopulos, D.S. and Sylvestrou, I., 1997. *Equus apolloniensis* n. sp. (Mammalia, Equidae) from the latest Villafranchian locality of Apollonia, Macedonia, Greece. Paleontologia i Evolució, 30, pp. 49–76.

Litsios, P., 2012. The chipped stone tools from the open-air palaeolithic sites of the Axios valley and the basin of Langadas (Macedonia, Greece). Master of Arts thesis (in Greek), Aristotle University of Thessaloniki, Thessaloniki.

Maravelis, A.G., Bourli, N., Vlachos, E. and Zelilidis, A., 2022. The Sedimentary Basins from the Miocene to the Present in Greece: Examples for the Most Studied Basins from North Greece, in: Vlachos, E. (Ed.), Fossil Vertebrates of Greece Volume 1. Springer Cham, pp. 13–31.

Mountrakis, D., Kilias, A., Pavlides, S., Sotiriadis, L., Psilovikos, A., Astaras, Th. Vavliakis, E., Koufos, G., Dimopoulos, G., oulios, G., Chistaras, V., Skordilis, M., Tranos, M., Spyropoulos, N., Patras, D., Syrides, G., Lambrinos, N., and Laggalis, T., 1996. Neotectonic map of Greece, Langadhas sheet. Earthquake Planning and Protection

Organisation and European Center on Prevention and Forecasting of Earthquakes, scale 1:100,000.

Muttoni, G., Scardia, G. and Kent, D.V., 2018. Early hominins in Europe: The Galerian migration hypothesis. Quaternary Science Reviews, 180, pp. 1–29.

Panagopoulou, E., Tourloukis, V., Thompson, N., Athanassiou, A., Tsartsidou, G., Konidaris, G.E., Giusti, D., Karkanas, P. and Harvati, K., 2015. Marathousa 1: a new Middle Pleistocene archaeological site from Greece. Antiquity, 343, pp.1–8.

Papagianni, D., 2000. Middle Palaeolithic occupation and technology in northwestern Greece: the evidence from open-air sites British Archaeological Reports 882, Oxford.

Thompson, N., Tourloukis, V., Panagopoulou, E. and Harvati, K., 2018. In search of Pleistocene remains at the Gates of Europe: Directed surface survey of the Megalopolis Basin (Greece). Quaternary international, 497, pp. 22–32.

Thompson, N., Kourtessi-Philippakis, G., Giusti, D., Harvati, K. and Tourloukis, V., this volume. The preliminary analysis of lithic assemblages from the archaeological survey and test-trench excavations at Popovo and Morfi, Greece.

Tourloukis, V., Harvati, K., 2018. The Palaeolithic record of Greece: A synthesis of the evidence and a research agenda for the future. Quaternary International, 466, pp. 48–65.

Tourloukis, V., Kourtessi-Philippakis, G., Karkanas, P., Nomade, S., Giusti, D., Thompson, N., Varis, A., Junginger, A., Schaller, M. and

Harvati, K., this volume. Geoarchaeological and geochronological investigations of Palaeolithic open-air sites in Epirus, Greece.

Tourloukis, V., Thompson, N., Garefalakis, C., Karkanas, P., Konidaris, G.E., Panagopoulou, E. and Harvati, K., 2016. New Middle Palaeolithic sites from the Mani peninsula, southern Greece. Journal of Field Archaeology, 41(1), pp. 68–83.

Tsoukala, E., Chatzopoulou, K., 2005. A new Early Pleistocene (latest Villafranchian) site with mammals in Kalamotó (Mygdonia Basin, Macedonia, Greece)–preliminary report. Mitteilungen der Kommission für Quartärforschung der Österreichischen Akademie der Wissenschaften, 14, pp. 213–233.

2 | The Middle Pleistocene: archaeological and paleoenvironmental research in the Megalopolis Basin

7 STRUCTURAL CONTROL, DEPOSITIONAL ENVIRONMENT AND GEO-ARCHAEOLOGICAL CONDITIONS IN THE MEGALOPOLIS BASIN, SOUTHERN GREECE

Haralambos Kranis[1,*], Emmanuel Skourtsos[1], George Davis[2], Vangelis Tourloukis[3,4], Eleni Panagopoulou[5], Panagiotis Karkanas[6], Katerina Harvati[3]

[1]*Department of Geology and Geoenvironment, National and Kapodistrian University of Athens, Athens, Greece*
[2]*Department of Geosciences, University of Arizona, Tucson, AZ, USA*
[3]*Paleoanthropology, Institute for Archaeological Sciences and Senckenberg Centre for Human Evolution and Palaeoenvironment, Department of Geosciences, Eberhard Karls University of Tübingen, Tübingen, Germany*
[4]*Department of History and Archaeology, School of Philosophy, University of Ioannina, Ioannina, Greece*
[5]*Hellenic Ministry of Culture, Ephorate of Palaeoanthropology–Speleology, Athens, Greece*
[6]*M.H. Wiener Laboratory for Archaeological Science, American School of Classical Studies at Athens, Athens, Greece*
**hkranis@geol.uoa.gr*

http://dx.doi.org/10.15496/publikation-97672

Keywords: geoarchaeology; neotectonics; basin evolution

7.1 INTRODUCTION

The Megalopolis Basin (MB) is an intra-montane basin, located in the actively extending domain of the Hellenic Arc, in the central Peloponnese (Fig 1). Its sedimentary fill includes an initial deposition of Pliocene lacustrine marly sands and marls, succeeded by Pleistocene fluvial and lacustrine, lignite-bearing sediments and Late Quaternary fluvial terraces of the Alfeios river (Lüttig and Marinos, 1962; Vinken, 1965). The paleogeographic setting and depositional environment(s) of the MB were controlled by the interplay between tectonic activity and climatic fluctuations throughout the Quaternary, two controlling factors that function at different time scales.

7.2 BASIN FILL AND STRUCTURAL CONTROLS ON SEDIMENTATION

The post-Pliocene basin fill of the MB includes the Megalopolis and Apiditsa formations (fm) and the Marathousa member. Megalopolis fm represents a fluvial depositional environment and includes metamorphic clasts (quartzites and schists). Non-systematic paleoflow measurements indicate that it was sourced from the E-ESE; however, within the present-day catchment of the Alfeios drainage basin, no metamorphic outcrops are present (Fig. 1). Thus, the occurrence of metamorphic clasts within the Megalopolis fm can be explained by a stream piracy that must have occurred during the late stages of deposition, which cut off the ba-

H. Kranis: https://orcid.org/0000-0002-3626-7300
E. Skourtsos: https://orcid.org/0000-0003-2742-6733
V. Tourloukis: https://orcid.org/0000-0002-9527-2708
E. Panagopoulou: https://orcid.org/0000-0002-4268-6157
P. Karkanas: https://orcid.org/0000-0002-7156-671X
K. Harvati: https://orcid.org/0000-0001-5998-4794

sin portion that fed the basin with metamorphic clasts. Such an event is believed to be the result of the NNW-ward propagation of the Sparta fault system and the uplift of the Leontari horst at the southern extremity of the MB.

Apiditsa fm was sourced from the W/WSW and contains no metamorphic clasts. Its source area lies in the bedrock outcrops (Pindos Unit) that border the MB from the west. It is a formation whose deposition lasted throughout the evolution of the MB and is mapped as chronostratigraphically equivalent to the Megalopolis fm; from the re-evaluation of borehole data and field reconnaissance it is found to mostly overlie the Megalopolis fm at its basal part. However, towards the top it appears to be partly overlain by it. The deposition of the Apiditsa fm is believed to be controlled by the tectonic activity on the western boundary of the MB, through the NNW-SSE, east-throwing Ellinitsa Fault and (possibly) the Lykaion Fault System. The lignite-bearing Marathousa member is regarded to be the distal equivalent to the Megalopolis and Apiditsa fm. It interfingers stratigraphically both with the Megalopolis fm in the east and with the Apiditsa fm in the west and its sedimentological characteristics show a gradual change from purely limnic to transitional to fluvial from east to west.

Moreover, the configuration of the pre-Pliocene basement of the MB appears to also have played a part in the evolution of the basin, which presents a fault-controlled bedrock salient between Kyparissia and Marathousa villages (Fig. 1), with the alpine bedrock cropping out at the former location and a basement horst (Leontari) located at the southern part of the MB (Fig. 1). Some of these faults, which had formed a fault-controlled paleorelief, were transgressively covered by the ba-

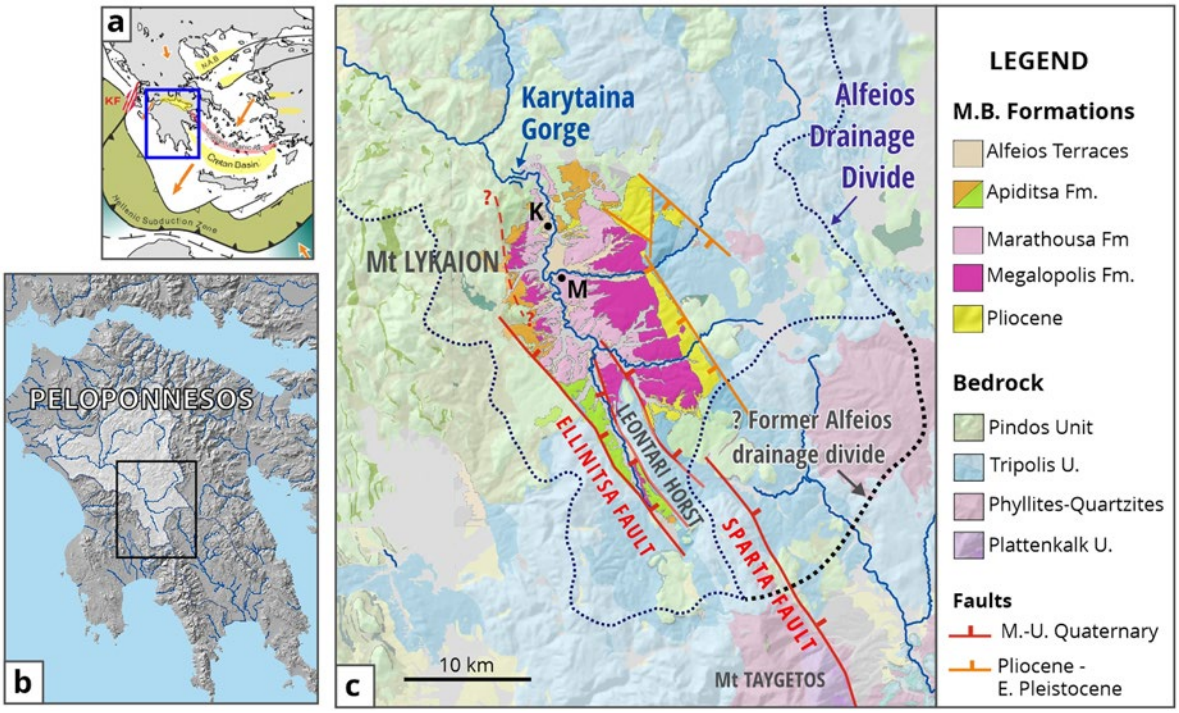

Figure 1: (a) General location map. Yellow shading denotes active extensional domains. Orange arrows denote GPS velocity vectors: KF: Kefallonia Fault; NAB: North Aegean Basin. (b) Shaded relief map of the Peloponnesos; highlighted is the drainage basin of the Alfeios River. (c) Generalized geological map of the Megalopolis Basin (MB). Fault ticks on downthrown block. K and M stand for the locations of Kyparissia and Marathousa villages, respectively.

sin deposits, remained active at least during the early stages of sedimentation in the basin (Kranis et al., 2020).

The last stage in the evolution of the MB is characterized by the establishment of the modern Alfeios drainage, initially depositing floodplain sediments, subsequently cutting into them and form terraces, following episodic(?) drops of its base-level, owing to alternating climatic conditions and/or surges of fault activity. Finally, the breaching of the basement salient in the NNW (Karytaina gorge), led to the establishment of the present-day base level, with Alfeios cutting into its more recent deposits.

7.3 GEO-ARCHAEOLOGICAL IMPLICATIONS

We suggest that prehistoric human habitation was governed not only by climatic and societal conditions, but also by local geological and tectonic factors. The Megalopolis Basin provides such examples: hominins exercised their activities at locations where the geological conditions were favorable: (i.e., avoiding marshy, swampy ground), while being close to freshwater (i.e., river- or lakeside). Such conditions can be provided by suitable geological formations, which can be either 'stable' basin sediments or bedrock outcrops. The former can be represented by the Apiditsa and Megalopolis formations, while the latter are the carbonate outcrops of the Pindos Unit. The findings at the Marathousa 1 and Kyparissia sites (Panagopoulou et al., 2018; Athanassiou et al., this volume; Karkanas et al., this volume) are located at the flanks of a basement salient within the MB, which is controlled by intra-basinal NNW-SSE and ENE-SSW faults.

Thus, the interplay between tectonics, climate and sedimentation provides the necessary conceptual framework in the process of geo-archaeological and paleoanthropological investigations.

ACKNOWLEDGMENTS

This research was conducted under a permit granted to the Ephorate of Palaeoanthropology-Speleology, Hellenic Ministry of Culture, and the American School of Classical Studies at Athens. It was supported by the ERC Consolidator Grant ERC-CoG-724703 ("CROSSROADS") and the ERC Starting Grant ERC-StG-283503 ("PaGE"), both awarded to K.H. K.H. is also supported by the ERC Advanced Grant ERC-AdG-101019659 ("FIRSTSTEPS"). We would also like to thank A. Athanassiou and S. Mavroulis for their constructive comments and suggestions on an earlier version of the manuscript.

REFERENCES

Athanassiou, A., Konidaris, G.E., Tourloukis, V., Thompson, N., Giusti, D., Panagopoulou, E., Karkanas, P. and Harvati, K., this volume. The Middle Pleistocene large mammal fauna from Kyparissia (Peloponnese, S. Greece): New collected material.

Karkanas, P., Tourloukis, V., Thompson, N., Giusti, D., Tsartsidou, G., Athanassiou, A., Konidaris, G.E., Roditi, E., Panagopoulou, E. and Harvati, K., this volume. The Megalopolis Paleoenvironmental Project (MegaPal).

Kranis, H., Skourtsos, E., Davis, G., Karkanas, P., Tourloukis, V., Panagopoulou, E. and Harvati, K., 2020. Switch-on, switch-off: Plio-Quaternary evolution of the Megalopolis Basin (Southern Greece), through structural overprinting, interaction and fault migration. EGU General Assembly 2020,

Online, 4–8 May 2020, EGU2020-19950.

Lüttig, G.W., Marinos, G., 1962. Zur Geologie des neuen Griechischen Braunkohlen-Lagerstätte von Megalopolis. Braunkohle, 14, pp. 222–231.

Panagopoulou, E., Tourloukis, V., Thompson, N., Konidaris, G., Athanassiou, A., Giusti, D., Tsartsidou, G., Karkanas, P and Harvati, K., 2018. The Lower Palaeolithic site of Marathousa 1, Megalopolis, Greece: Overview of the evidence. Quaternary International, 497, pp. 33–46.

Vinken, R., 1965. Stratigraphie und Tektonik des Beckens von Megalopolis (Peloponnes, Griechenland). Geologisches Jahrbuch, 83, pp. 97–148.

8 SINGLE-GRAIN OPTICAL DATING OF SEDIMENT SAMPLES FROM MARATHOUSA 1, SOUTHERN GREECE

Zenobia Jacobs[1,2]*, Bo Li[1,2], Kieran O'Gorman[1], Vangelis Tourloukis[3,4], Eleni Panagopoulou[5], Panagiotis Karkanas[6], Katerina Harvati[3]

[1]*Centre for Archaeological Science, School of Earth, Atmospheric and Life Sciences, University of Wollongong, Wollongong, Australia*
[2]*Australian Research Council Centre of Excellence for Australian Biodiversity and Heritage (CABAH), University of Wollongong, Wollongong, Australia*
[3]*Paleoanthropology, Institute for Archaeological Sciences and Senckenberg Centre for Human Evolution and Palaeoenvironment, Department of Geosciences, Eberhard Karls University of Tübingen, Tübingen, Germany*
[4]*Department of History and Archaeology, School of Philosophy, University of Ioannina, Ioannina, Greece*
[5]*Hellenic Ministry of Culture, Ephorate of Palaeoanthropology–Speleology, Athens, Greece*
[6]*M. H. Wiener Laboratory for Archaeological Science, American School of Classical Studies at Athens, Athens, Greece*
**zenobia@uow.edu.au*

http://dx.doi.org/10.15496/publikation-97661

Keywords: feldspar; middle Pleistocene; single grains; pIRIR; standardized growth curve

8.1 INTRODUCTION

Previous optical dating of sediment samples from Marathousa-1 used a multi-aliquot multi-grain procedure for feldspar mineral grains to obtain the equivalent dose (Jacobs et al., 2018). This was the best procedure available at the time for measurement of feldspar grains close to the upper limit of the technique (Li et al., 2017). A range of statistically consistent, but imprecise, age estimates were reported for 8 samples from two excavation areas at Marathousa 1 that suggested deposition of the clastic sediment package between lignite seams II and III during MIS 12 (478–424 ka; Lisiecki & Raymo, 2005). A measurement procedure for individual grains of feldspar has since been developed (e.g., Jacobs et al., 2019) as well as a procedure for direct measurement of the internal potassium content of individual grains (O'Gorman et al., 2021). Here, we present the updated multi-grain aliquot ages using a revised internal beta dose rate as well as single-grain age estimates for the same set of samples. The single grain D_e distributions suggest that the feldspar mineral grains in the lacustrine facies are well-bleached and that the age estimates are reliable.

8.2 MATERIALS AND METHODS

Eight sediment samples were collected from two excavation areas (A and B) at Marathousa 1 from the clastic sediment package between lignite seams II and III. Details about the location of samples,

Z. Jacobs: https://orcid.org/0000-0001-5424-5837
B. Li: https://orcid.org/0000-0003-4186-4828
K. O´Gorman: https://orcid.org/0000-0002-2231-2457
V. Tourloukis: https://orcid.org/0000-0002-9527-2708
E. Panagopoulou: https://orcid.org/0000-0002-4268-6157
P. Karkanas: https://orcid.org/0000-0002-7156-671X
K. Harvati: https://orcid.org/0000-0001-5998-4794

sample collection, preparation and estimation of the environmental dose rate for all samples are provided in Jacobs et al. (2018).

For D_e determination, we applied a single aliquot regenerative-dose (SAR) pIRIR procedure for individual K-feldspar grains (Blegen et al., 2015; Thomsen et al., 2008), in which the single-grain pIRIR signal was measured at 275 °C for 2 s using the IR laser after a prior-IR stimulation at a high stimulation temperature (200 °C) for 200 s (Li and Li, 2012). A preheat of 320°C for 60 s was applied prior to measurement of the natural (L_n), regenerative (L_x) and test dose (T_n, T_x) signals and an IR bleaching step at 325°C for 100 s was used at the end of each measurement cycle.

Luminescence measurements were made on an automated Risø TL-DA-20 reader. Infrared stimulation of individual K-feldspar grains was achieved using a focused laser beam (830 nm) (Bøtter-Jensen et al., 2003). Individual K-feldspar grains were mounted onto standard Risø single grain discs (Bøtter-Jensen et al., 2000). The IRSL emissions were detected using an Electron Tubes Ltd 9235B photomultiplier tube fitted with Schott BG-39 and Corning 7-59 filters to transmit wavelengths of 320–480 nm.

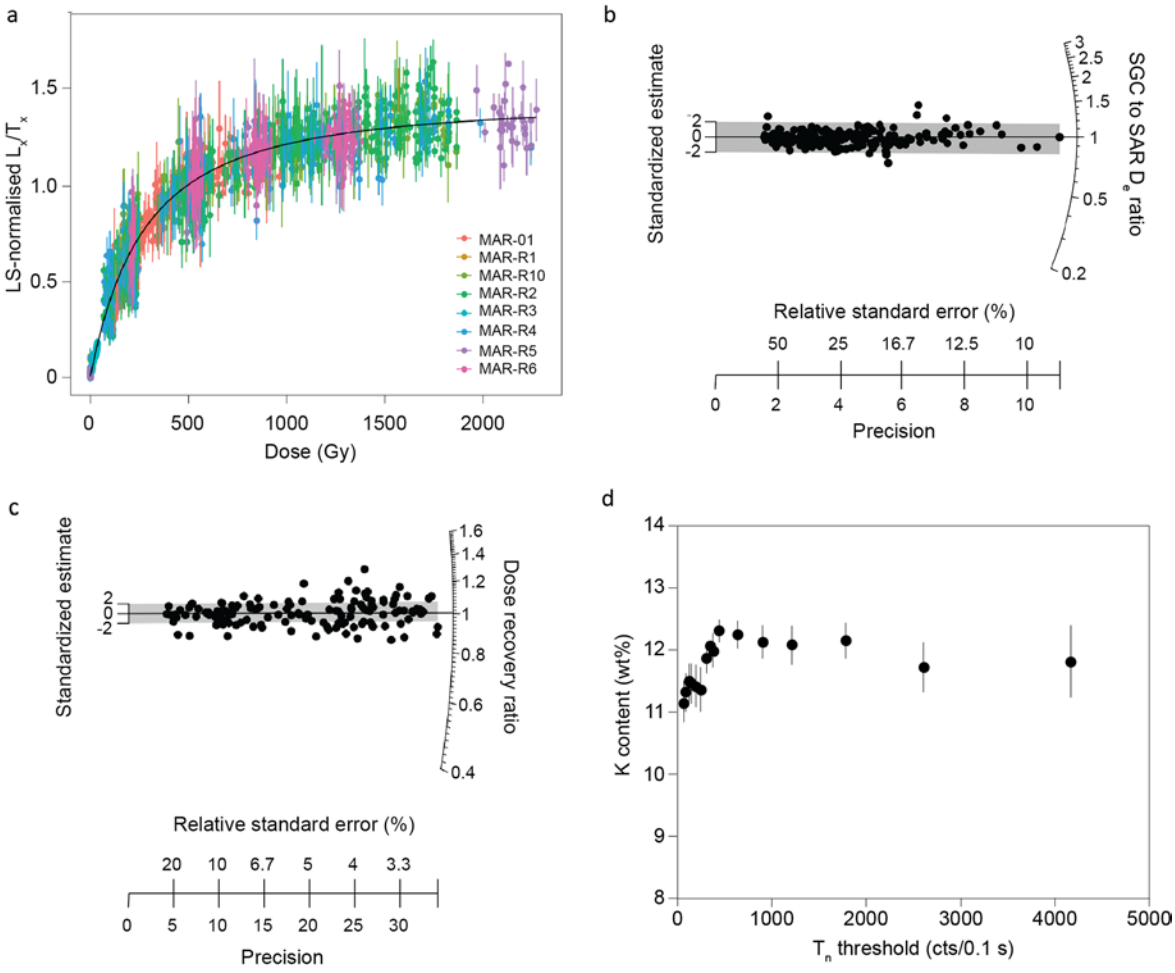

Figure 1: a, LS-normalised L_x/T_x data and best-fit SGC. b, Ratio of SAR D_e and SGC D_e values shown as a radial plot; the grey bar is centred on unity (ratio of 1). c. Measured-to-given dose ratios for individual grains shown as a radial plot; the grey bar is centred on unity (ratio of 1). d. Whole-of-grain average K concentrations (wt%) plotted as a function of T_n-sensitivity.

To estimate the D_e, a combined standardized growth curve (SGC) and L_nT_n method (Li et al., 2015b, 2017, 2020) were adopted. To establish the SGC, a total of 2700 grains from different samples were measured with a full SAR pIRIR procedure. The following criteria were used to reject grains with unsuitable behaviors or poor dose response curves (DRCs): 1) the initial T_n signal is less than 3σ above of the corresponding background count, or the relative standard error on T_n is >25%; 2) the ratio of the L_x/T_x zero-dose value to the maximum regenerative-dose L_x/T_x value is >5%; 3) the L_x/T_x data points are too scattered, i.e., they have large figure-of-merit (FOM) and reduced-chi-square (RCS) values higher than 10% and 5, respectively. This resulted in a total of 457 grains accepted for SGC establishment. We adopted the least-square normalization (LS-normalization) procedure (Li et al., 2016) to normalize the L_x/T_x data and used a general-order kinetics (GOK) function (Guralnik et al., 2015) to fit the normalized data. The LS-normalized data and the corresponding SGC are displayed in Fig. 1a (n = 2560), showing that different grains share the same dose response pattern that can be well described by the SGC.

We validated the SGC by comparing SGC-derived D_e values against D_e values obtained for the same grains using their individual full SAR dose response curves; 96.7% of grains have SGC and SAR D_e values that were indistinguishable from each other at 2σ (Fig. 1b). We further tested the suitability of the approach using a dose recovery test (given dose = ~600 Gy; measured-to-given dose ratio = 1.01 ± 0.01; n = 135; Fig. 1c), and a residual dose test after bleaching in a solar simulator for 8 hours (10 ± 1 Gy; n = 68). Both tests gave satisfactory results. Given the old ages of our samples, we did not apply any residual dose correction. No fading correction was applied according to the lack of fading observed from single aliquots (Jacobs et al., 2018).

All luminescence data, including curve fitting, equivalent dose estimation, error estimation, age model analysis and graphic display were analyzed using the R packages *numOSL* (Peng et al., 2013; Peng and Li, 2017) and *Luminescence* (Kreutzer et al., 2012).

Whole-of-grain average potassium (K) concentrations of individual grains (n = 86) from two samples from the Megalopolis Basin—ELS1 and TRP5—were measured using qualitative evaluation of minerals using energy dispersive spectroscopy (QEM-EDS). Measurement and analysis of grains followed the procedure presented in O'Gorman et al. (2021). Only grains that had a luminescence signal and that were accepted for D_e determination were included.

8.3 RESULTS

The distributions of the SGC-normalized L_n/T_n values for the accepted grains from 7 of 8 samples are shown in Fig. 2a–g (left panels). Not enough data was obtained for sample MAR-R9. All other samples show D_e distributions that are dominated by a single population, but with the presence of a small proportion of outliers (shown as open circles). Outliers were identified based on the normalised median absolute deviation (nMAD) (Rousseeuw et al., 2006); any log L_n/T_n ratio that has a nMAD value greater than 2 was rejected.

The 'T_n threshold' procedure was also applied to test whether there is any dependence of D_e on brightness (e.g., Jacobs et al., 2019). The results are shown in Fig. 2a–g (right panels). The final D_e values were determined from only those grains in the plateau region (dashed lines). The final D_e value for each sample, the weighted mean L_n/T_n value after applying nMAD, was calculated using the central age model (Galbraith et al., 1999) and then projected onto the SGC.

The QEM-EDS results show that the internal K content of the measured feldspar grains are cor-

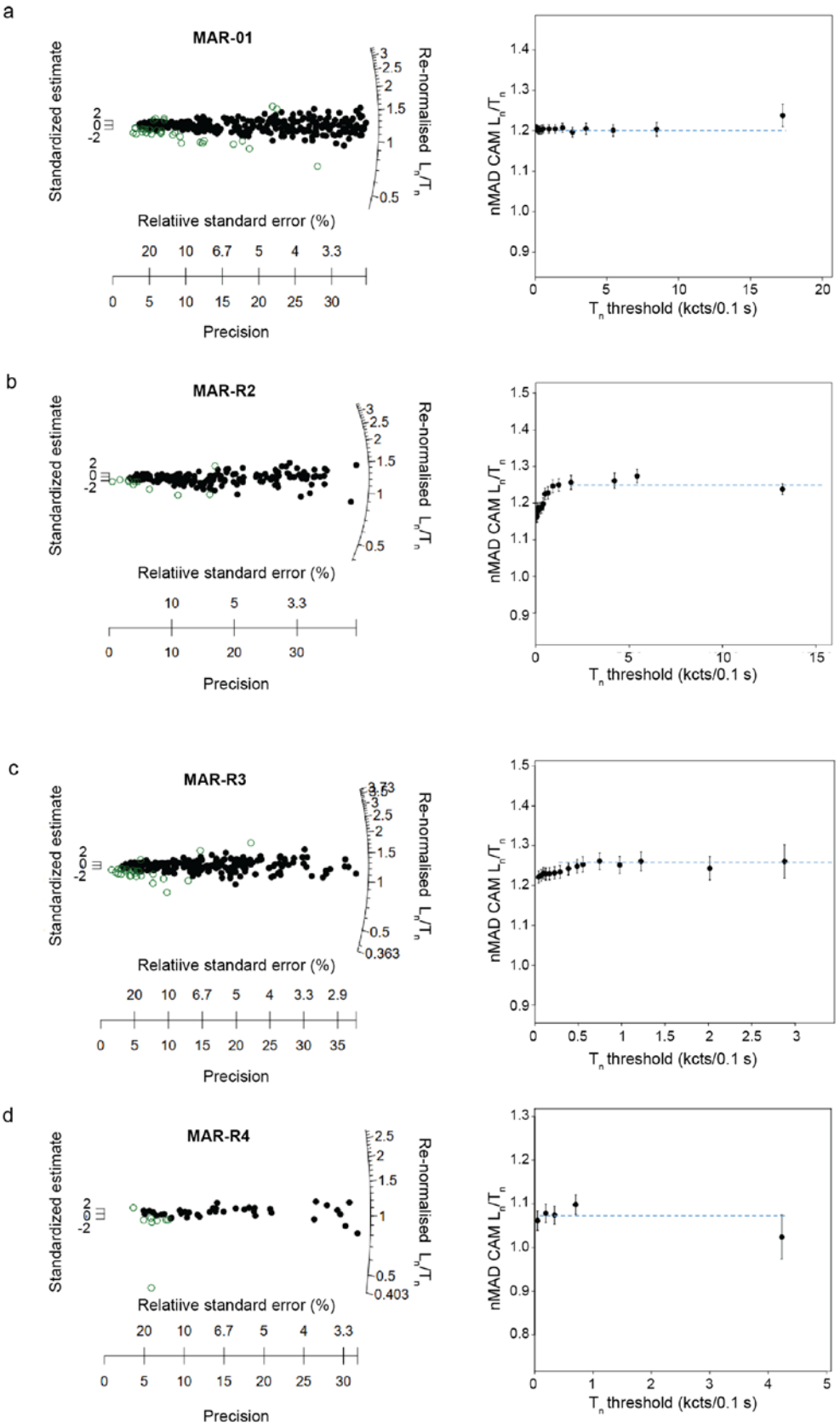
a
MAR-01
Standardized estimate
Re-normalised L_n/T_n
Relatiive standard error (%)
20 10 6.7 5 4 3.3
Precision
0 5 10 15 20 25 30
nMAD CAM L_n/T_n
T_n threshold (kcts/0.1 s)
b
MAR-R2
Relatiive standard error (%)
10 5 3.3
c
MAR-R3
0.363
20 10 6.7 5 4 3.3 2.9
d
MAR-R4
0.403

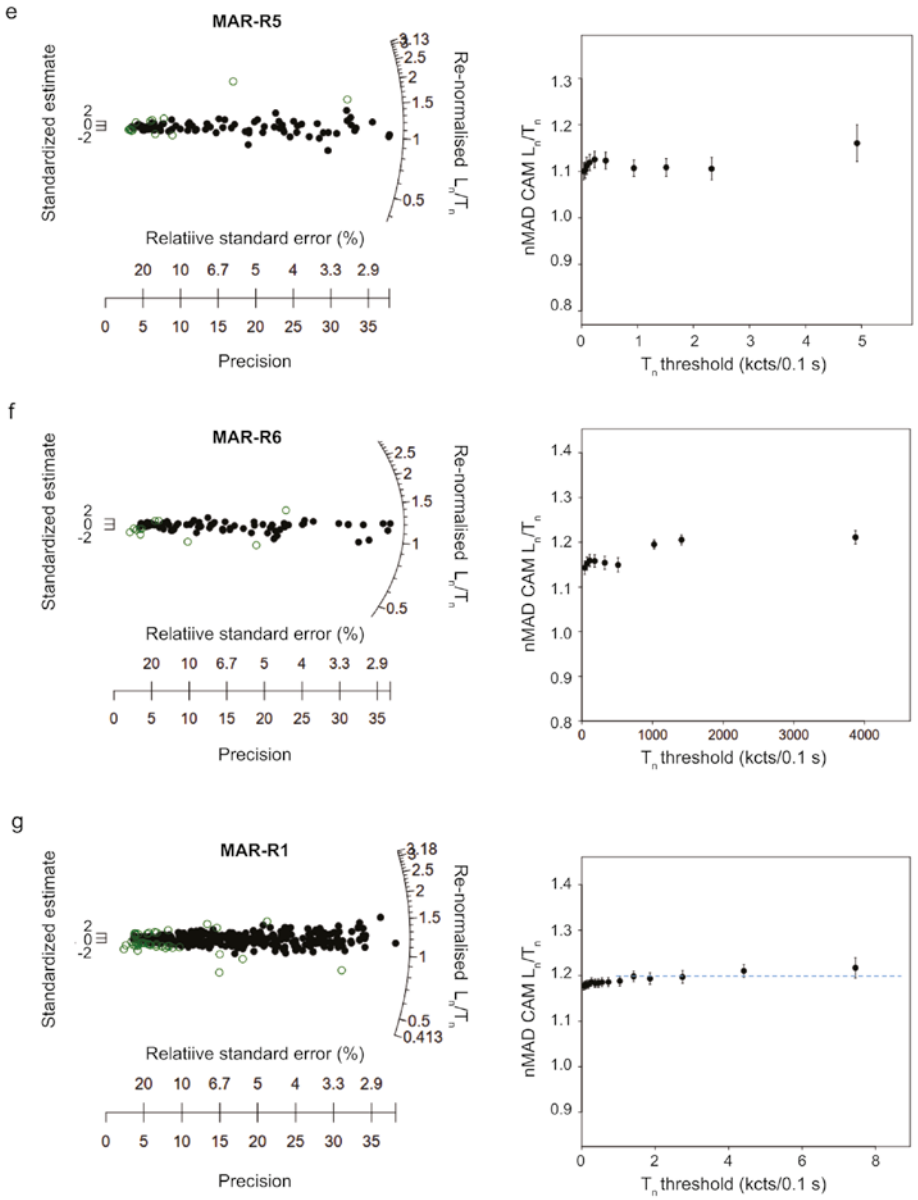

Figure 2: The radial plots on the left panel show the distributions of re-normalized L_n/T_n ratios for K-feldspar grains. The open circles are outliers identified by nMAD. The right panel shows the nMAD CAM re-normalized L_n/T_n ratios plotted as a function of T_n threshold each sample. The blue lines represent the plateau region of the re-normalized L_n/T_n ratio.

related with sensitivity when T_n is less than ~500 counts per 0.1 s of stimulation time; the latter was measured as the intensity of the test dose signal for the natural dose (T_n). We calculated the mean K content by filtering the grains using a series of T_n thresholds (Fig. 1d), which shows that the mean K content increases with T_n threshold. This is similar to the pattern shown for the L_n/T_n results (Fig. 2). The T_n-weighted mean internal K concentrations of grains from ELS1 and TRP5 are 11.9 ± 0.4 and 11.7 ± 0.7 wt%, respectively. When combined, an overall mean of 11.8 ± 0.4 wt% K is calculated, resulting in an internal beta dose rate of 0.827 ± 0.048 Gy/ka (assuming a Rb concentration of 400 ± 100 µg/g; Huntley and Hancock (2001)) for 200 µm-diameter grains. This is consistent with the previously assumed 0.829 ± 0.099 Gy/ka (Jacobs et al., 2018). Based on the new QEM-EDS results,

Sample	Water content (%)	External dose rate (Gy/ka)		Internal dose rate (Gy/ka)[A]	Total dose rate (Gy/ka)	Equivalent dose				Age ± 2σ (ka)
		Beta	Gamma			D_e (Gy)[B]	Method	N[C]	OD (%)[D]	
MAR-R4	75	0.52 ± 0.05	0.49 ± 0.05	0.478 ± 0.053	1.49 ± 0.10	622 ± 55	MAR			418 ± 93
						629^{+89}_{-73}	SG	31/37	9 ± 2	422^{+82}_{-75}
MAR-R9	64	0.72 ± 0.07	0.60 ± 0.05	0.846 ± 0.075	2.17 ± 0.11	816 ± 88	MAR			392 ± 96
MAR-R10	57	0.82 ± 0.07	0.59 ±0.05	0.846 ± 0.075	2.26 ± 0.13	884 ± 74	MAR			392 ± 80
						910^{+75}_{-66}	SG	309/343	14 ± 1	403^{+57}_{-55}
MAR-01	57	0.84 ± 0.07	0.68 ± 0.07	0.846 ± 0.075	2.39 ± 0.14	1124 ± 58	MAR			471 ± 74
						992^{+83}_{-73}	SG	120/126	14 ± 1	416^{+60}_{-58}
MAR-R2	50	0.65 ± 0.06	0.55 ± 0.04	0.846 ± 0.075	2.08 ± 0.12	940 ± 56	MAR			453 ± 75
						1070^{+179}_{-187}	SG	86/98	14 ± 1	516^{+105}_{-89}
MAR-R3	50	0.73 ± 0.06	0.63 ± 0.04	0.660 ± 0.090	2.02 ± 0.12	959 ± 35	MAR			474 ± 35
		0.69 ± 0.06		0.846 ± 0.075	2.17 ± 0.11	115^{+190}_{-145}	SG	137/146	17 ± 1	515^{+105}_{-88}
MAR-R5	53	0.47 ± 0.04	0.45 ± 0.04	0.846 ± 0.075	1.77 ± 0.11	887 ± 44	MAR			422 ± 80
						732^{+98}_{-81}	SG	52/58	12 ± 1	415^{+76}_{-69}
MAR-R6	53	0.56 ± 0.05	0.57 ± 0.05	0.846 ± 0.075	1.97 ± 0.12	855 ± 50	MAR			433 ± 73
						943^{+81}_{-70}	SG	20/28	10 ± 1	477^{+71}_{-68}

[a] Grain size for MAR and SG De values for MAR-R3 is 90-125 μm in diameter, for the MAR age for MAR-R3 is 125-180 μm in diameter and for the rest it is 180-212 μm in diameter.

[b] The error on the MAR D_e is at 1σ, whereas the errors on the SG estimates are at 2σ.

[c] N = number. The numbers shown are before and after rejection of outliers and passing the T_n threshold.

[d] OD were obtained after removing outliers.

Table 1: Equivalent dose (D_e) and environmental dose rates for multi-grains (MAR) and single-grain (SG) age estimates for samples from Marathousa 1.

we, therefore, have assumed a K concentration of 12 ± 1 wt%, with a larger uncertainty assumed to allow larger variation among different samples.

The revised total dose rates and multi-grain age estimates are reported in Table 1, together with the new single-grain ages presented here for the first time. Ages are presented in stratigraphic order. Uncertainties on the single-grain D_e values and age estimates are presented at 2σ to reflect the asymmetry of the estimates as a result of working along the saturated part of the dose response curve.

The multi- and single-grain ages are statistically consistent, suggesting that both methods are reliable for estimation of burial dose for the sediments at Marathousa. Our preferred age estimates are, however, those obtained by single grains as these represent the smallest meaningful unit of measurement (e.g., Jacobs and Roberts, 2007). The single-grain ages range from 403^{+57}_{-55} ka at 2σ for MAR-R10 in UB5a above the hiatus in the top part of the sequence to 516^{+105}_{-89} ka for MAR-R2 in UB7 at the base of the sequence. All ages from all units are statistically consistent and there is no clear stratigraphic trend; the resolution of the chronology is too coarse. The ages for all samples from between lignite seems II and III are consistent with deposition during MIS 12.

ACKNOWLEDGMENTS

This research was conducted under a permit granted to the Ephorare of Palaeoanthropology-Speleology, Hellenic Ministry of Culture, and the American School of Classical Studies at Athens. It was supported by the ERC Consolidator Grant ERC-CoG-724703 ("CROSSROADS") and the ERC Starting Grant ERC-StG-283503 ("PaGE"), both awarded to K.H. K.H. is also supported by the ERC Advanced Grant ERC-AdG-101019659 ("FIRSTSTEPS"). We thank T. Lachlan and L. Yu for valuable help in the Optical Dating Facility at the University of Wollongong and the reviewers for constructive and useful feedback.

REFERENCES

Blegen, N., Tryon, C.A., Faith, J.T., Peppe, D.J., Beverly, E.J., Li, B. and Jacobs, Z., 2015. Distal tephras of the eastern Lake Victoria basin, equatorial East Africa: correlations, chronology and a context for early modern humans. Quaternary Science Reviews, 122, pp. 89–111.

Bøtter-Jensen, L., Andersen, C.E., Duller, G.A.T. and Murray, A.S., 2003. Developments in radiation, stimulation and observation facilities in luminescence measurements. Radiation Measurements, 37, pp. 535–541.

Bøtter-Jensen, L., Bulur, E., Duller, G.A.T. and Murray, A.S., 2000. Advances in luminescence instrument systems. Radiation Measurements, 32, pp. 523–528.

Galbraith, R.F., Roberts, R.G., Laslett, G.M., Yoshida, H. and Olley, J.M., 1999. Optical dating of single and multiple grains of quartz from Jinmium rock shelter, northern Australia, part 1, Experimental design and statistical models. Archaeometry, 41, pp. 339–364.

Guralnik, B., Li, B., Jain, M., Chen, R., Paris, R.B., Murray, A.S., Li, S.H., Pagonis, V., Valla, P.G. and Herman, F., 2015. Radiation-induced growth and isothermal decay of infrared-stimulated luminescence from feldspar. Radiation Measurements, 81, pp. 224–231.

Huntley, D.J., Baril, M.R., 1997. The K content of the K-feldspars being measured in optical dating or in thermoluminescence dating. Ancient T, 15, pp. 11–13.

Huntley, D.J., Hancock, R.G.V., 2001. The Rb contents of the K-feldspar grains being measured in optical dating. Ancient TL, 19, pp. 43–46.

Jacobs, Z., Roberts, R.G., 2007. Advances in

optically stimulated luminescence dating of individual grains of quartz from archaeological deposits. Evolutionary Anthropology 16, 210–223.

Jacobs, Z., Li, B., Karkanas, P., Tourloukis, V., Thompson, N., Panagopoulou, E. and Harvati, K., 2018. Optical dating of K-feldspar grains from Middle Pleistocene lacustrine sediment at Marathousa 1 (Greece). Quaternary International, 497, pp. 170–177.

Jacobs, Z., Li, B., Shunkov, M.V., Kozlikin, M.B., Bolikhovskaya, N.S., Agadjanian, A.K., Uliyanov, V.A., Vasiliev, S.K., O'Gorman, K., Derevianko, A.P. and Roberts, R.G., 2019. Timing of archaic hominin occupation of Denisova Cave in southern Siberia. Nature, 565, pp. 594–599.

Kreutzer, S., Schmidt, C., Fuchs, M.C., Dietze, M., Fischer, M. and Fuchs, M., 2012. Introducing an R package for luminescence dating analysis. Ancient TL, 30, pp. 1–8.

Li, B., Li, S.H., 2012. A reply to the comments by Thomsen et al. on "Luminescence dating of K-feldspar from sediments: A protocol without anomalous fading correction". Quaternary Geochronology, 8, pp. 49–51.

Li, B., Roberts, R.G., Jacobs, Z., Li, S.H. and Guo, Y.J., 2015. Construction of a 'global standardised growth curve' (gSGC) for infrared stimulated luminescence dating of K-feldspar. Quaternary Geochronology, 27, pp. 119–130.

Li, B., Jacobs, Z., Roberts, R.G., 2016. Investigation of the applicability of standardised growth curves for OSL dating of quartz from Haua Fteah cave, Libya. Quaternary Geochronology, 35, pp. 1–15.

Li, B., Jacobs, Z., Roberts, R.G., Galbraith, R. and Peng, J., 2017. Variability in quartz OSL signals caused by measurement uncertainties: Problems and solutions. Quaternary Geochronology, 41, pp. 11–25.

Li, B., Jacobs, Z., Roberts, R.G., 2020. Validation of the LnTn method for De determination in optical dating of K-feldspar and quartz. Quaternary Geochronology, 58, 101066.

Lisiecki, L.E., Raymo, M.E., 2005. A Pliocene-Pleistocene stack of 57 globally distributed benthic δ18O records. Paleoceanography, 20, PA1003.

O'Gorman, K., Brink, F., Tanner, D., Li, B. and Jacobs, Z., 2021. Calibration of a QEM-EDS system for rapid determination of potassium concentrations of feldspar grains used in optical dating. Quaternary Geochronology, 61, 101123.

Peng, J., Dong, Z., Han, F., Long, H. and Liu, X., 2013. R package numOSL: numeric routines for optically stimulated luminescence dating. Ancient TL, 31, pp. 41–48.

Peng, J., Li, B., 2017. Single-aliquot regenerative-dose (SAR) and standardised growth curve (SGC) equivalent dose determination in a batch model using the R Package 'numOSL'. Ancient TL, 35, pp. 32–53.

Rousseeuw, P.J., Debruyne, M., Engelen, S. and Hubert, M., 2006. Robustness and Outlier Detection in Chemometrics. Critical Reviews in Analytical Chemistry, 36, pp. 221–242.

Thomsen, K.J., Murray, A.S., Jain, M. and Botter-Jensen, L., 2008. Laboratory fading rates of various luminescence signals from feldspar-rich sediment extracts. Radiation Measurements, 43, pp. 1474–1486.

9 PRELIMINARY AGES FROM COSMOGENIC NUCLIDE BURIAL DATING OF STRATIGRAPHY IN THE MEGALOPOLIS BASIN

Mirjam Schaller[1,2,*], Todd A. Ehlers[2], Vangelis Tourloukis[3,4], Eleni Panagopoulou[5], Panagiotis Karkanas[6], Katerina Harvati[3]

[1]*Department of Geosciences, Eberhard Karls University of Tübingen, Tübingen, Germany*
[2]*School of Geographical and Earth Sciences, University of Glasgow, Glasgow, United Kingdom*
[3]*Paleoanthropology, Institute of Archaeological Sciences and Senckenberg Centre for Human Evolution and Palaeoenvironment, Department of Geosciences, Eberhard Karls University of Tübingen, Tübingen, Germany*
[4]*Department of History and Archaeology, School of Philosophy, University of Ioannina, Ioannina, Greece*
[5]*Hellenic Ministry of Culture, Ephorate of Paleoanthropology–Speleology, Athens, Greece*
[6]*M.H. Wiener Laboratory for Archaeological Science, American School of Classical Studies at Athens, Athens, Greece*
**mirjam.schaller@glasgow.ac.uk*

http://dx.doi.org/10.15496/publikation-97660

Keywords: Megalopolis Basin; burial dating; cosmogenic nuclides

9.1 INTRODUCTION

The Megalopolis Basin, an intra-mountain depression in the Central Peloponnese (Greece), consists of Pliocene–Pleistocene lacustrine and fluvial sediments. The Choremi Formation, which contains several archaeological sites of interest (e.g., Panagopoulou et al., 2018), dates to the Early and Middle Pleistocene (van Vugt et al., 2000). However, numerical dating of Middle Pleistocene lacustrine and fluvial sediments is challenging (Rixhon et al., 2017). Commonly used dating methods have a limited age range (e.g., ^{14}C dating) or are restricted due to a paucity of datable material (e.g., teeth). An intensively studied and numerically dated archaeological site in the Megalopolis Basin is Marathousa-1 (Fig. 1). Relative correlations of Marathousa-1 put the sedimentary deposits into glacial Marine Isotope Stages (MIS). Possible scenarios from relative correlations suggest sediment deposition during MIS 16 (Van Vugt et al., 2000) as well as MIS 14, or possibly MIS 12 (Okuda et al., 2002; Tourloukis et al., 2018). Numerical age dating of the sediment with pIRIR on K-Feldspar reflects a deposition during MIS 12 (Jacobs et al., 2018), although these samples are near, or at, a saturation of this technique and could represent minimum ages. In contrast, a cervid molar from the artifact- and fossil-bearing unit dated with ESR indicates a deposition age during MIS 13 and a maximum age during MIS 16 (Blackwell et al., 2018). Neither relative nor numerical dating give a conclusive answer of the depositional age for archaeological findings at the Marathousa-1 site.

M. Schaller: https://orcid.org/0000-0003-2722-9537
T. A. Ehlers: https://orcid.org/0000-0001-9436-0303
V. Tourloukis: https://orcid.org/0000-0002-9527-2708
E. Panagopoulou: https://orcid.org/0000-0002-4268-6157
P. Karkanas: https://orcid.org/0000-0002-7156-671X
K. Harvati: https://orcid.org/0000-0001-5998-4794

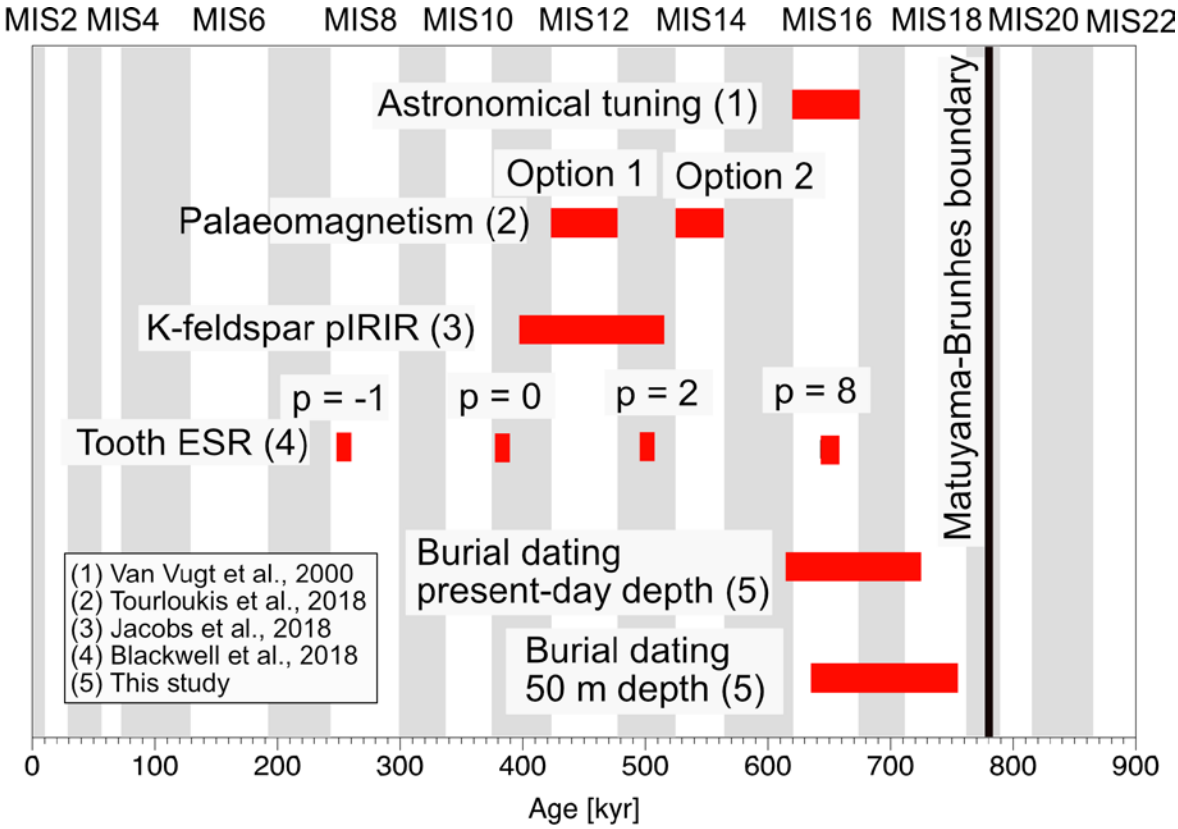

Figure 1: Compilation of relative and numerical deposition age ranges for Marathousa-1 (red blocks). In addition, the age of the Brunhes-Matuyama boundary and the ages of the different Marine Isotope Stages MIS are indicated. Glacial and interglacial MIS are in white and gray, respectively.

In this study, numerical ages of sediment deposits are addressed with the method of burial daring with a pair of in situ-produced cosmogenic nuclides (e.g., Granger, 2014). Some studies refer to this technique as 'simple' burial dating, in contrast to the isochron burial dating technique. The cosmogenic nuclides used here are ^{26}Al and ^{10}Be in situ-produced in quartz. The method makes use of the fact that ^{26}Al decays faster than ^{10}Be. The production rate ratio of ^{26}Al/^{10}Be in quartz during sediment production is known. Hence the measured ratio in quartz material from sediment deposits can be used to monitor the time since sediment production. Under the assumption that sediment transport time is short in comparison to burial time, the sediment deposition age can be determined. Four samples from Marathousa-1 and three from Tripotamos-4 were analyzed and deposition ages were calculated.

9.2 STUDY AREAS AND SAMPLING LOCATIONS

The Megalopolis Basin formed during the Late Miocene–Pliocene times and contains Pliocene–Pleistocene lacustrine and fluvial deposits of more than 250 m thickness (Vinken, 1965). These deposits have previously been divided into six formations, of which the Choremi formation is of interest. In the deposits of this formation, the archaeological sites Marathousa-1 and Tripotamos-4 were investigated with in situ-produced cosmogenic nuclides.

9.2.1. MARATHOUSA-1

The Lower Palaeolithic site Marathousa-1 is located at ~350 m above mean sea level and is exposed inside one of the lignite mines (also called Marathousa Mine) at the center-west part of the basin. Paleoanthropological material was found in lacustrine deposits with clay, silt, and sand, which are sandwiched between the lignite seam II and III. The detrital sediments were sampled for cosmogenic nuclide analysis at Martahousa-1A in the stratigraphic layer UA3b (Table 1) directly overlying the artifact-bearing horizon (UA3c/UA4, see Karkanas et al., 2018). In Marathousa-1B, two samples were collected from the stratigraphic layer UB4a and in the lowermost part of UB9. Samples from the stratigraphic layers UA3b and UB4a were very clay-rich. Only a small amount and fine-grained quartz was recovered, making the application of cosmogenic nuclide burial dating difficult. In contrast, more and coarser-grained quartz was separated from the stratigraphical layer UB9.

9.2.2. TRIPOTAMOS-4

The archaeological site of Tripotamos-4 was found in the area east of the village of Tripotamos. Two survey units (4 and 5) were examined more closely in 2020. The deposits are stratigraphically placed into, but most likely lie above, the lignite seam III (Löhnert and Nowack, 1965). At this location, lacustrine, bluish grey clayey deposits, poor in organic material, are laterally interfingered with fluvial/fluvio-lacustrine deposits of yellow sandy silts and intercalated layers of coarser grained sands and gravels. Sediment samples from survey unit 4 were collected from a layer of yellow sands of terrestrial origin for dating with in situ-produced cosmogenic nuclides.

Stratigraphic layer	Sample ID	Location (WGS 84)		Altitude	Excavation square	Present-day Overburden		
		°N Latitude	°E Longitude	m			m	
Marathousa-1								
UA3b	CN-UA3b-1	37,40833	22,09147	349.51	940/671	30	±	3
UA3b	CN-UA3b-2	37,40833	22,09147	349.51	940/669	30	±	3
UB4a	CN-UB4a-1	37,40833	22,09147	350.85-350.65	934/610	30	±	3
UB9, lowermost part	CN-UB9-1	37,40833	22,09147		East Section	30	±	3
Tripotamos-4								
	TRP Cosmo 1	37,3589	22,10722	394,8		7	±	1
	TRP Cosmo 2	37,3589	22,10722	394,8		7	±	1
	TRP Cosmo 3	37,3589	22,10722	394,8		7	±	1

Table 1: Sample location and information.

9.3 BURIAL DATING METHOD

Pairs of in situ-produced cosmogenic nuclides analyzed in quartz sediment can be used for burial dating based on different decay rates of two isotopes measured in the same sample material (e.g., Granger et al., 1997; Granger and Muzikar, 2001). Age determination of sediment deposition in the two study areas makes use of minimum and maximum burial ages with in situ-produced ^{26}Al and ^{10}Be concentrations in quartz (e.g., Granger, 2014). A minimum burial age is calculated based on the sample specific ^{26}Al/^{10}Be ratio and the assumption of no post-burial irradiation due to deep burial (e.g., 50 m). In contrast, using the present-day sample depth will result in a maximum burial age. As sediment overburden may have diminished over time (e.g., due to post-depositional erosion), the "real" age of the sediment deposit is bracketed by the minimum and maximum ages.

Samples from Marathousa-1A and 1B were collected from different depths, whereas samples collected in Tripotamos-4 were from the same stratigraphic depth. After washing and sieving the samples, quartz was separated and cleaned to reach Al-concentrations in quartz as low as possible (goal <100 ppm). Al and Be were extracted according to protocols outlined in Schaller et al. (2016). ^{26}Al/^{27}Al and ^{10}Be/^{9}Be ratios of samples, blanks, and standards were measured at the AMS facility of Cologne (Dewald et al., 2013). ^{26}Al and ^{10}Be concentrations of samples were corrected for chemistry blanks (Table 2). ^{27}Al concentrations were measured with standard addition on an ICP-OES at the University of Tübingen.

Minimum and maximum burial ages were determined with a MatLab script modified from Schaller et al. (2016). Decay constants used for ^{26}Al and ^{10}Be were (9.830 ± 0.250) x10^{-7} (see Norris et al., 1983) and (4.997 ± 0.043) x10^{-7} (Chmeleff et al., 2010; Korschinek et al., 2010). Sea level-high latitude (SLHL) production rates for ^{26}Al are 28.54, 0.84, and 0.081 atoms/(g(qtz) yr) for nucleonic, stopped muonic, and fast muonic production, respectively (Borchers et al., 2016; Braucher et al., 2011). The SLHL production rates are 3.92, 0.012, and 0.039 atoms/(g(qtz) yr) for nucleonic, stopped muonic, and fast muonic ^{10}Be production, respectively (Borchers et al., 2016; Braucher et al., 2011). The ^{26}Al/^{10}Be ratio of production at SLHL is ~7.4. SLHL production rates are scaled to the sample location with the online calculator of Marrero et al. (2016) using the scaling procedure "SA" based on Lifton et al. (2014). Production rates at the sampling depths were calculated based on nucleonic, stopped muonic, and fast muonic adsorption lengths, which are 157, 1500, and 4320 g/cm^2, respectively (Braucher et al., 2011). The density of the overburden was assumed to be constant over time with a value of 2.0 ± 0.1 g/cm^3. As the production rates of the sediment source in the past cannot be determined, the values of the production rates at the sample location were used for age calculation. This assumption results in a maximum burial age. The minimum overburden for Tripotamos-4 assumed to be 7 m and results in a maximum burial age. The original amount of sediment deposited in the study areas, as well as post-depositional erosion of sediments, are both unknown. Given this uncertainty, a second burial age was calculated with the assumption of an initial (depositional) overburden of 50 m, that would have been eroded post-depositional in the recent past. This second approach (50 m of original overburden) provides the sensitivity of the burial ages reported here to changing depositional conditions.

Table 2: Cosmogenic nuclide information.

Stratigraphic layer	Sample ID	Grain size µm	Qtz dissolved g	Qtz ^{27}Al conc. ppm	^{26}Al/^{27}Al	Error %	^{26}Al conc. 10^4 atoms/g(qtz)			m(^{9}Be) mg	^{10}Be/^{9}Be	Error %	^{10}Be conc. 10^4 atoms/g(qtz)			^{26}Al/^{10}Be			Burial dating present-day depth kyr			Burial dating 50 m depth kyr		
Marathousa-1 [a]																			(30 m depth)			(50 m depth)		
UA3b	CN-UA3b-1	125-250	68,47	374	4,03E-14	7,45	33,62	±	2,51	0,29	2,29E-13	4,30	6,36	±	0,28	5,28	±	0,46	642	±	98	674	±	100
UA3b	CN-UA3b-2	125-250	72,43	389	3,85E-14	6,81	33,40	±	2,28	0,29	2,50E-13	4,08	6,59	±	0,27	5,07	±	0,40	725	±	92	758	±	94
UB4a	CN-UB4a-1	125-1000	11,34	515	4,85E-14	6,59	55,40	±	3,68	0,29	6,21E-14	4,64	10,20	±	0,50	5,43	±	0,45	609	±	96	627	±	98
UB9, lowermost part	CN-UB9-1	250-500	75,93	156	1,44E-13	4,20	50,08	±	2,11	0,29	3,83E-13	3,45	9,64	±	0,33	5,20	±	0,28	702	±	66	723	±	68
																mean ± stdev			670	±	53	696	±	57
Tripotamos-4 [b]																			(7 m depth)			(50 m depth)		
Unit4	TRP Cosmo 1	250-500	39,72	108	1,74E-13	4,57	41,87	±	2,73	0,34	1,33E-13	3,8	7,64	±	0,32	5,48	±	0,43	1180	±	238	611	±	95
Unit4	TRP Cosmo 2	250-500	39,83	122	1,67E-13	4,73	45,41	±	2,84	0,34	1,23E-13	3,9	7,05	±	0,30	6,44	±	0,49	467	±	173	278	±	90
Unit4	TRP Cosmo 3	250-500	39,58	111	1,68E-13	4,49	41,57	±	2,64	0,34	1,28E-13	3,8	7,36	±	0,31	5,65	±	0,43	1046	±	225	548	±	93
																mean ± stdev			898	±	379	479	±	177

[a] The ^{26}Al and ^{10}Be concentrations are corrected with a chemistry blank of 44129 ±8045 atoms and 35521 ±11511 atoms, respectively.

The nucleonic, stopped and fast muonic production rates at sample location for ^{26}Al are 25.211 atoms/(g(qtz)*yr), 0.799 atoms/(g(qtz)*yr), and 0.077 atoms/(g(qtz)*yr), respectively.

The nucleonic, stopped and fast muonic production rates at sample location for ^{10}Be are 3.518 atoms/(g(qtz)*yr), 0.011 atoms/(g(qtz)*yr), and 0.037 atoms/(g(qtz)*yr), respectively.

[b] For the ^{26}Al concentrations there is no chemistry blank detected. The ^{10}Be concentrations were corrected with 23017 ±15063 atoms, respectively.

The nucleonic, stopped and fast muonic production rates at sample location for ^{26}Al are 26.152 atoms/(g(qtz)*yr), 0.819 atoms/(g(qtz)*yr), and 0.079 atoms/(g(qtz)*yr), respectively.

The nucleonic, stopped and fast muonic production rates at sample location for ^{10}Be are 3.651 atoms/(g(qtz)*yr), 0.012 atoms/(g(qtz)*yr), and 0.038 atoms/(g(qtz)*yr), respectively.

9.4 RESULTS

9.4.1. MARATHOUSA-1

In situ-produced cosmogenic nuclide concentrations of ^{26}Al and ^{10}Be for the replicate samples from Marathousa-1A are (33.62 ±2.51) and (33.40 ±2.28) x10^4 atoms/g(qtz) and (6.36 ±0.28) and (6.59 ±0.27) x10^4 atoms/g(qtz), respectively (Table 2). $^{26}Al/^{10}Be$ ratios are 5.28 ±0.46 and 5.07 ±0.40 for the two replicate samples. Based on the present-day sample depth of 30 m, these ratios result in burial ages of 642 ±98 kyr and 725 ±92 kyr.

Two samples from Marathousa-1B collected from a different sample location show in situ-produced cosmogenic nuclide concentrations of ^{26}Al and ^{10}Be of (55.40 ±3.68) and (55.08 ±2.11) x10^4 atoms/g(qtz) and (10.20 ±0.50) and (9.64 ±0.33) x10^4 atoms/g(qtz), respectively (Table 2). The two samples have $^{26}Al/^{10}Be$ ratios of 5.43 ±0.45 and 5.20 ±0.28. The burial ages based on the present-day sampling depth of 30 m are 609 ±96 kyr and 702 ±67 kyr.

9.4.2. TRIPOTAMOS-4

In situ-produced cosmogenic nuclide concentrations of ^{26}Al and ^{10}Be for the three samples range from (41.57 ±2.64) to (45.41 ±2.84) x10^4 atoms/g(qtz) and (7.05 ±0.30) to (7.64 ±0.32) x10^4 atoms/g(qtz), respectively (Table 2). $^{26}Al/^{10}Be$ ratios are 5.48 ±0.43, 6.44 ±0.49, and 5.65 ±0.43 for the three samples from the same stratigraphic layer. Based on the sampling depth of 7 m below the present-day surface, these ratios result in burial ages of 1180 ±238 kyr, 467 ±173 kyr, and 1046 ±225 kyr. Based on a constant burial depth of 50 m, the ages are 611 ±95 kyr, 278 ±90 kyr, and 548 ±93 kyr, respectively.

9.5 DISCUSSION

9.5.1. MARATHOUSA-1 AND TRIPOTAMOS-4

The four analyzed samples from Marathousa-1 resulted in burial ages ranging from 609 ±96 kyr to 725 ±92 kyr. The large errors in the ages result from uncertainties in the cosmogenic nuclide concentrations as well as the propagation of these errors in the age calculation. Additional analytical problems were caused by the restricted sample amount as well as the cleanness of the quartz (e.g., ^{27}Al concentration). Nevertheless, the four samples report minimum burial ages that agree with each other within error (Table 2). The resulting mean minimum burial age is 670 ±53 kyr putting the sediment layer between lignite seam II and III within MIS 16 (Fig. 1). An assumption made and influencing the burial age is the cosmogenic production rate in the sediment production area. A best guess of a value for this production rate is the production rate of the sample location. As this production rate is a minimum value, the resulting age is a maximum burial age. Unfortunately, neither the production rates in the sediment source nor the burial depth over time can be completely evaluated. Therefore, the herein reported burial age is considered a best estimate possible with this technique.

The Tripotamos-4 location has similar uncertainties with the calculated burial ages. Even though there was enough and well-cleaned sample material available, the calculated ages from the three samples collected at 7 m depth are highly variable. One sample does not even agree within error with the other two samples. In addition, the sampling depth of 7 m is insufficient to avoid post-depositional irradiation and nuclide production. Due to this, the burial age based on 7 m of overburden should be considered as the maximum age because if (as is likely) additional overburden

was present in the past, then the age would be younger than this 7 m overburden estimate. Assuming that the samples were covered with 50 m overburden over most of the time, the mean burial age is 479 ±177 ky. However, the sediment deposit cannot be attributed to a MIS, only the relative stratigraphy is maintained, and the numerical age of the archaeological site Tripotamos-4 remains vague.

9.6 CONCLUSIONS

The archaeological site of Marathousa-1 has been attributed with relative and numerical dating techniques to MIS12. However, the cosmogenic nuclide-based new mean burial age from Marathousa-1 of 670 ±53 kyr suggests that the site could belong to MIS16. Unfortunately, such an age determination does not match well with the rest of the chronological evidence based on both site- and basin-scale chronostratigraphic constraints (Tourloukis et al., 2018 and references therein). Samples from Tripotamos-4 could not be used to date the deposit above lignite seam III. The mean burial age based on the three samples and assuming a constant overburden of 50 m resulted in an age of 479 ±177 kyr showing a large error due to highly variable age constraints. Therefore, considering the error margin of this assessment, the attribution of Tripotamos-4 to a MIS is not possible based on the available data.

ACKNOWLEDGMENTS

This research was conducted under a permit granted to the Ephorate of Palaeoanthropology-Speleology, Hellenic Ministry of Culture. It was supported by the ERC Consolidator Grant ERC-CoG-724703 (“CROSSROADS”) and the ERC Starting Grant ERC-StG-283503 (“PaGE”), both awarded to K.H. K.H. is also supported by the ERC Advanced Grant ERC-AdG-101019659 (“FIRSTSTEPS”). We would like to thank G. Rixhon and an anonymous reviewer for their input and improvement of the extended abstract.

REFERENCES

Blackwell B.A.B., Sakhrani, N., Singh, I.K., Gopalkrishne, K.K., Tourloukis, V., Panagopoulou, E., Karkanas, P., Blickstein, J.I.B., Skinner, A.R., Florentin, J.A. and Harvati, K. 2018. ESR Dating Ungulate Teeth and Molluscs from the Paleolithic Site Marathousa 1, Megalopolis Basin, Greece, Quaternary, 1, 22.

Borchers, B., Marrero, S., Balco, G., Caffee, M., Goehring, B., Lifton, N., Nishiizumi, K., Phillips, F., Schaefer, J. and Stone, J., 2016. Geological calibration of spallation production rates in the CRONUS-Earth project. Quaternary Geochronology, 31, pp. 188–198.

Braucher, R., Merchel, S., Borgomano, J. and Bourlès, D.L., 2011. Production of cosmogenic radionuclides at great depth: A multi element approach. Earth and Planetary Science Letters, 309, pp. 1–9.

Chmeleff, J., von Blanckenburg, F., Kossert, K. and Jakob, D., 2010. Determination of the 10Be half-life by multicollector ICP-MS and liquid scintillation counting. Nuclear Instruments and Methods in Physics Research Section B: Beam Interactions with Materials and Atoms, 268, pp. 192–199.

Dewald, A., Heinze, S., Jolie, J., Zilges, A., Dunai, T., Rethemeyer, J., Melles, M., Staubwasser, M., Kuczewski, B., Richter, J., Radtke, U., von Blanckenburg, F. and Klein, M., 2013. Cologne AMS, a dedicated center for accelerator mass spectrometry in Germany. Nuclear Instruments and Methods in Physics Research Section B: Beam Interactions with Materials

and Atoms, 294, pp. 18–23.

Granger, D.E., 2014. Cosmogenic Nuclide Burial Dating in Archaeology and Paleoanthropology. Treatise on Geochemistry, 14, pp. 81–97.

Granger, D.E. and Muzikar, P.F., 2001. Dating sediment burial with in situ-produced cosmogenic nuclides: Theory, techniques, and limitations. Earth and Planetary Science Letters, 188, pp. 269–281.

Granger, D.E., Kirchner, J.W. and Finkel, R.C., 1997. Quaternary downcutting rate of the New River, Virginia, measured from differential decay of cosmogenic 26Al and 10Be in cave-deposited alluvium. Geology, 25 (2), pp. 107–110.

Jacobs, Z., Li, B., Karkanas, P., Tourloukis, V., Thompson, N., Panagopoulou, E. and Harvati, K., 2018. Optical dating of K-feldspar grains from Middle Pleistocene lacustrine sediment at Marathousa 1 (Greece), Quaternary International, 497, pp. 170–177.

Karkanas, P., Tourloukis, V., Thompson, N., Giusi, D., Panagopoulou, E. and Harvati, K., 2018. Sedimentology and micromorphology of the Lower Palaeolithic lakeshore site Marathousa 1, Megalopolis Basin, Greece. Quaternary International, 497, pp. 123–136.

Korschinek, G., Bergmaier, A., Faestermann, T., Gerstmann, U.C., Knie, K., Rugel, G., Wallner, A., Dillmann, I., Dollinger, G., von Gostomski, C.L., Kossert, K., Maiti, M., Poutivtsev, M. and Remmert, A., 2010. A new value for the half-life of 10Be by Heavy-Ion Elastic Recoil Detection and liquid scintillation counting. Nuclear Instruments and Methods in Physics Research Section B: Beam Interactions with Materials and Atoms, 268, pp. 187–191.

Lifton, N., Sato, T., Dunai, T., 2014. Scaling in situ cosmogenic nuclide production rates using analytical approximations to atmospheric cosmic-ray fluxes. Earth and Planetary Science Letters, 386, pp. 149–160.

Löhnert, E. and Nowak, H., 1965. Die Braunkohlenlagerstätte von Khoremi im Becken von Megalopolis. Peloponnes. Geologisches Jahrbuch, 82, pp. 84-–868.

Marrero, S.M., Phillips, F.M., Borchers, B., Lifton, N., Aumer, R. and Balco, G., 2016. Cosmogenic nuclide systematics and the CRONUScalc program. Quaternary Geochronology, 31, pp. 160–187.

Norris, T.L., Gancarz, A.J., Rokop, D.J. and Thomas, K.W., 1983. Half-life of 26A1. Lunar Planet. Sci. Conf., Journal of Geophysical Research, 88, B331–B333.

Okuda, M., van Vugt, N., Nakagawa, T., Ikeya, M., Hayashida, A., Yusada, Y. and Setoguchi, T., 2002. Palynological evidence for the astronomical origin of lignite-detritus sequences in the Middle Pleistocene Marathousa Member, Megalopolis, SW Greece. Earth and Planetary Science Letters, 201, pp. 143–157.

Panagopoulou, E., Tourloukis, V., Thompson, N., Konidaris, G., Athanassiou, A., Giusti, D., Tsartsidou, G., Karkanas, P. and Harvati, K., 2018. The Lower Palaeolithic site of Marathousa 1, Megalopolis, Greece: Overview of the evidence. Quaternary International, 497, pp. 33–46.

Rixhon, G., Briant, R., Cordier, S., Duval, M., Jones, A. and Scholz, D., 2017. Revealing the pace of river landscape evolution during the Quaternary: Recent developments in numerical dating methods. Quaternary Science Reviews, 166, pp. 91–113.

Schaller, M., Ehlers, T. A., Stor, T., Torrent, J., Lobato, L., Christl, M. and Vockenhuber, C., 2016. Timing of European fluvial terrace formation and incision rates constrained by cosmogenic nuclide dating. Earth and Planetary Science Letters, 451, pp. 221–231.

Tourloukis, V., Muttoni, G., Karkanas, P., Monesi E., Scardia, G., Panagopoulou, E. and

Harvati, K., 2018. Magnetostratigraphic and chronostratigraphic constraints on the Marathousa 1 Lower Palaeolithic site and the Middle Pleistocene deposits of the Megalopolis Basin, Greece, Quaternary International, 497, pp. 154–169.

Van Vugt, N., de Bruijn, H., van Kolfschoten, M. and Langereis, C.G., 2000. Magneto- and cyclostratigraphy and mammal-fauna's of the Pleistocene lacustrine Megalopolis Basin, Peloponnesos, Greece, Geologica Ultraiectina, 189, pp. 69–92.

Vinken, R., 1965. Stratigraphie und Tektonik des Beckens von Megalopolis (Peloponnes, Griechenland). Geol. Jahrb., 83, pp. 97–148.

10 AN UPDATED SPATIAL TAPHONOMIC STUDY OF THE MIDDLE PLEISTOCENE OPEN-AIR SITE OF MARATHOUSA 1 (MEGALOPOLIS BASIN, GREECE): PRELIMINARY RESULTS

Domenico Giusti[1,*], Vangelis Tourloukis[1,2], George E. Konidaris[1], Nicholas Thompson[1], Panagiotis Karkanas[3], Eleni Panagopoulou[4], Katerina Harvati[1,5]

[1]*Paleoanthropology, Institute for Archaeological Sciences and Senckenberg Centre for Human Evolution and Palaeoenvironment, Department of Geosciences, Eberhard Karls University of Tübingen, Tübingen, Germany*
[2]*Department of History and Archaeology, School of Philosophy, University of Ioannina, Ioannina, Greece*
[3]*M.H. Wiener Laboratory for Archaeological Science, American School of Classical Studies at Athens, Athens, Greece*
[4]*Hellenic Ministry of Culture, Ephorate of Palaeoanthropology–Speleology, Athens, Greece*
[5]*DFG Centre for Advanced Studies 'Words, Bones, Genes, Tools', Eberhard Karls University of Tübingen, Tübingen, Germany*
**domenico.giusti@uni-tuebingen.de*

http://dx.doi.org/10.15496/publikation-97659

Keywords: site formation processes; spatial analysis; Middle Pleistocene; open-air site; Greece

10.1 INTRODUCTION

In recent years, a growing number of Middle Pleistocene sites in Europe yielding evidence of elephant exploitation has further fed the long-lasting debate over past human-elephant interactions (Konidaris et al., 2021). Viewed in the broader context of past human-carnivore-megafauna interactions, evidence of elephant exploitation provides further insights into past human behaviors, diet and subsistence strategies. However, modeling past human behaviors is not straightforward: direct types of evidence for repetitive elephant exploitation (i.e., cut-marks, bone tools or breakages for brain/marrow extraction, embedded lithic tools) are rather rare, whereas indirect types of evidence—such as spatial association, or tool use-wear and residues patterns—are significantly more common, although often questionable (Giusti, 2021; Konidaris and Tourloukis, 2021). Spatial association, for instance, does not necessarily imply causation: spatial associations of lithics and modified fauna are not direct evidence of a cultural accumulation, because syn- and post-depositional processes may equally produce spatial associations. Therefore, in spite of the growing archaeological record, the mode of acquisition and processing of the elephant carcass, the degree of exploitation of the carcass, its timing relative to, eventually, carnivore scavenging and to the carcass decomposition are, more often than not, inadequately understood.

The open-air site of Marathousa 1 (MAR-1), Megalopolis Basin, Greece, offers important insights into the understanding of the Middle Pleistocene mega-fauna exploitation in Europe. The site, dated to ca. 400–500 ka (Marine Isotope Stage 12; Blackwell et al., 2018; Doukas et al., 2018; Jacobs

D. Giusti: https://orcid.org/0000-0003-1438-4036
V. Tourloukis: https://orcid.org/0000-0002-9527-2708
G. E. Konidaris: https://orcid.org/0000-0002-7041-233X
N. Thompson: https://orcid.org/0009-0003-4770-1744
P. Karkanas: https://orcid.org/0000-0002-7156-671X
E. Panagopoulou: https://orcid.org/0000-0002-4268-6157
K. Harvati: https://orcid.org/0000-0001-5998-4794

et al., 2018; Tourloukis et al., 2018a; Konidaris et al., 2018), yielded strong evidence (cut-marks) of elephant exploitation by Middle Pleistocene hominins. Since the site's discovery in 2013, two excavation areas were systematically investigated until 2019: Area A (Fig. 1a) where a partial skeleton of a single individual of *Palaeoloxodon antiquus* was unearthed, together with a relatively small number of lithic artifacts and other faunal remains; and Area B (Fig. 1b), about 60 m to the south of Area A, where the lithic assemblage is significantly richer and occurs in association with elephant remains of another individual, as well as remains of other mammal taxa. As yet, evidence of butchering (cut-marks) has been identified on two of the elephant bones from Area A, as well as on one elephant bone (accompanied by peeling) and other mammal bones from Area B (Konidaris et al., 2018). Additionally, a bone diaphysis fragment that most likely also belongs to an elephant, has been provisionally identified as a percussor, as it preserves percussion marks, as well as a flake scar and cut-marks (Tourloukis et al., 2018b). However, despite multiple types of evidence pointing to a multi-carcass butchering site, it is of primary importance to evaluate the taphonomy and degree of site integrity, before reliably deducing behavioral inferences from the material record.

The site occurs at the margin of a paleolake of the Megalopolis Basin. The sedimentary sequences of both areas include lacustrine and fluviolacustrine clastic deposits sandwiched between two lignite seams. A clear and well-documented hiatus divides both sequences in two parts: a lower subaqueous sequence of bedded sands and silts and an organic rich upper sequence partially subaerial. The hiatus is attributed to the exposure of a lake shore surface and subsequent erosion by a gravity flow process, such as a mud- or hyperconcentrated-flow (Karkanas et al., 2018). Indeed, the sequence above the hiatus is characterized by a series of erosional-bounded depositional units, attributed to mudflows (i.e., UA3–UA2, UB5–UB2; Fig. 2). The hiatus correlates the main find-bearing units of both areas, namely UA3c and UB4c (Fig. 2). Specifically, in Area A the elephant remains lie at the contact of UA3c/4 and are covered by UA3c (Fig. 2a); while in Area B, most of the remains were collected

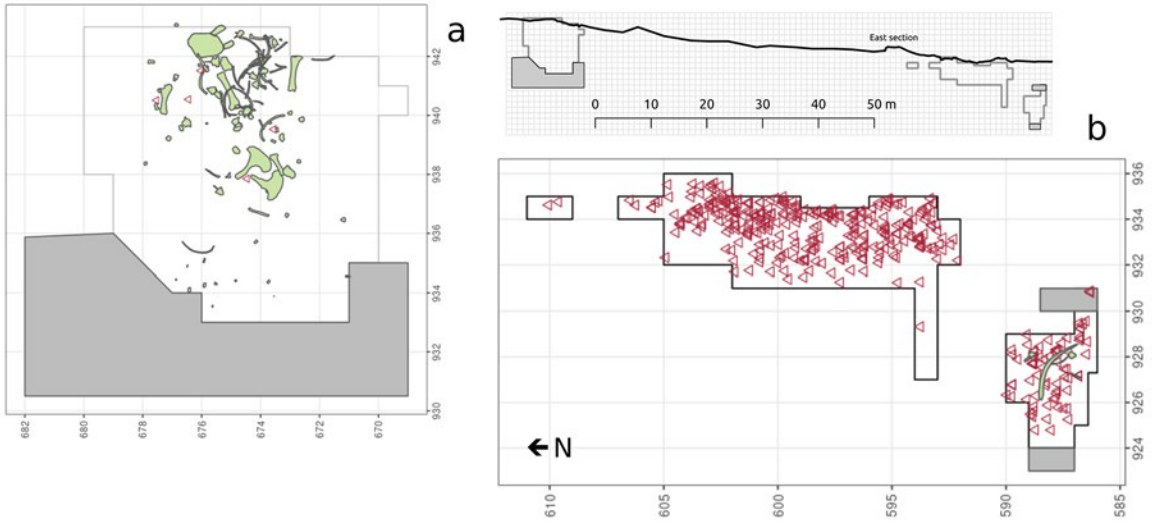

Figure 1: Distribution maps of the plotted remains from a) areas A (units UA3c and UA4) and b) B (units UB4c and UB5a), collected until 2019. Due to their high number, lithic debris/chips are not plotted. Grey zones mark the 2019 trench extensions. Area B is located 60 m to the South.

from unit UB4c and mostly close to the contact with the underlying unit (Fig. 2b).

In order to decipher the depositional nature of the main find horizons, an initial spatial taphonomic study was conducted in order to evaluate the degree and reliability of the spatial association of the lithic artifacts with the elephant and the other faunal remains from both areas (Giusti et al., 2018). From different spatial perspectives, and in agreement with preliminary taphonomic observations of the archaeological and paleontological material (Konidaris et al., 2018; Tourloukis et al., 2018b), the results all supported an autochthonous origin of the lithic and faunal assemblages, subject to minor post-depositional reworking. Thus, the results of Giusti et al. (2018) were in agreement with the current interpretation of MAR-1 as a butchering site. Giusti et al. (2018) analyzed material collected from 2013 to 2016, during systematic excavations of the site. Systematic investigation of the site continued until 2019, allowing us to significantly extend the excavation areas and collect more data.

The present study builds upon the previous preliminary results and incorporates new data, allowing us to test our former conclusions and refine our initial inferences. Specifically, as regards the spatial taphonomy of the site, the main research question is whether we are still looking at an autochthonous assemblage (subject to minor post-depositional reworking), or not.

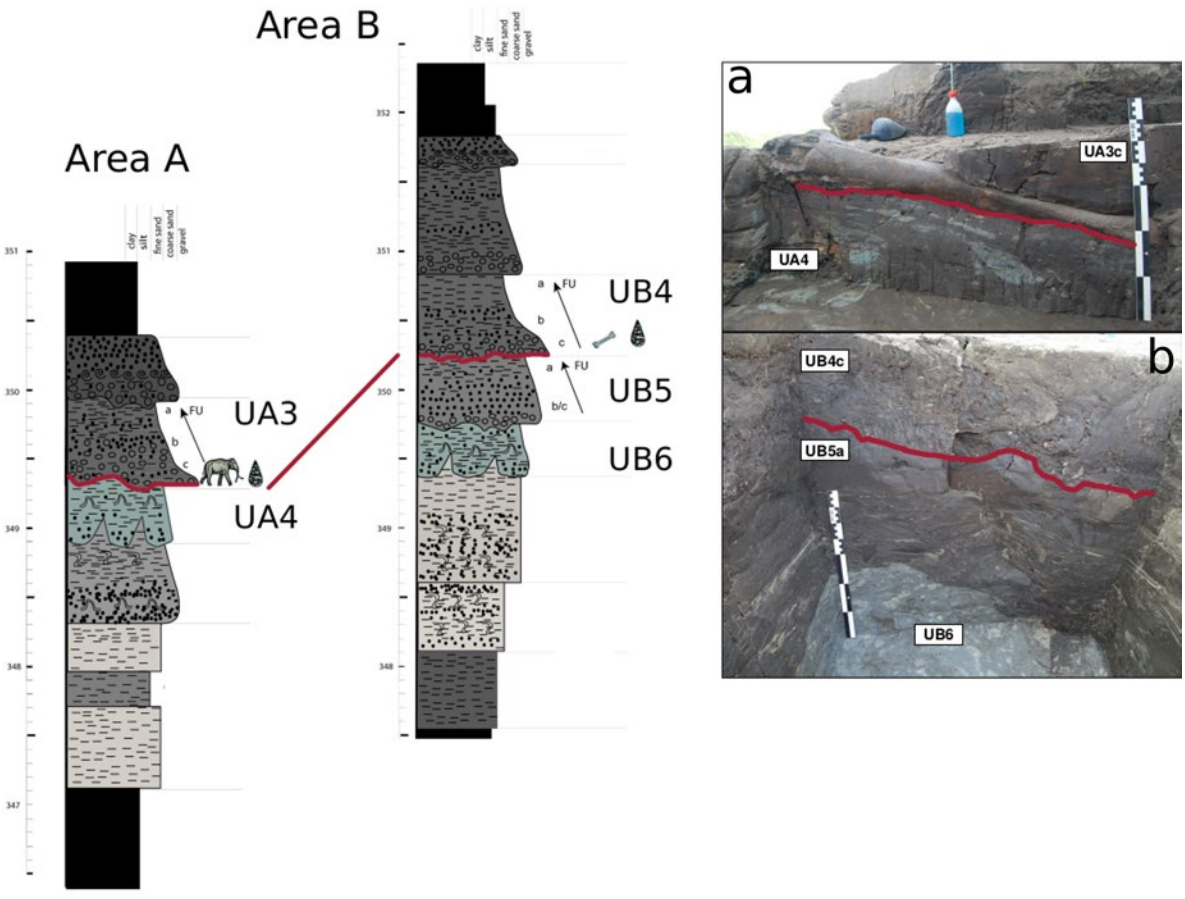

Figure 2: Stratigraphic setting of the Marathousa 1 site, modified after Karkanas et al. (2018). Absolute elevations in m a.s.l. Photograph (2017) of the left femur of the *Palaeoloxodon antiquus* skeleton, lying at the UA3c/4 contact and covered by unit UA3c (a). West profile (2014) of the excavation Area B (square 932/603), exposing the UB4c/5a (black solid line) and the UB5/6 erosional contacts (b).

10.2 MATERIALS AND METHODS

From 2013 to 2019, systematic investigation of the Marathousa 1 site were carried out by a joint team from the Ephorate of Palaeoanthropology-Speleology (Hellenic Ministry of Culture) and the University of Tübingen. High-resolution techniques were used to document the archaeological process as completely as possible, allowing us to acquire a large dataset. A total station was used to record the three-dimensional position of finds (i.e., all the lithic artifacts, teeth and diagnostic bones; bones and organic material with length equal to and greater than 20 mm), samples, collected spits of sediment (of 5 and 10 cm thickness, in Area B and A respectively) and geological features, such as exposed erosional surfaces. The dimensions (length, width and thickness) of plotted finds were measured on-site with a millimeter accuracy. The orientation (plunge and bearing) of elongated finds was recorded with a compass and inclinometer with a 1-degree accuracy.

The present study analyzes material recovered from the more extensively excavated stratigraphic units, namely UA3c and UA4 in Area A, UB4c and UB5a in Area B (Table 1). In order to consistently use the same sampling strategy as in the first study, the regions of investigation are limited in Areas A and B to the square units excavated respectively until 2016 (28 m^2) and 2019 (74 m^2). In contrast to Area B, many sediment bags from the last excavation campaigns in Area A are yet to be screened or sorted. Including sieved material is especially important in Area A, since the number of lithics (mostly debris, but also tool-resharpening chips) collected over the years from sieved sediment substantially exceeded the number of finds plotted in the field. Nevertheless, whilst the Area A sample is only slightly bigger (×1.2), the Area B sample is definitely larger (×1.9) with respect to our previous dataset.

Similar to what was presented in Giusti et al. (2018), two contrasting hypotheses of depositional scenarios are here tested. The allochthonous model implies significant transport of the material by the mud-flow from the original locus of deposition to the site; in this scenario, the lithics and fauna cannot be shown to belong to the same depositional event. In contrast, the autochthonous model assumes that the flow event eroded an exposed surface where the elephant and the archaeological material were already lying. The latter model implies the loss of any original, pristine spatial relations between remains, but minor transport from the primary depositional locus. We are here interested in investigating the vertical distribution of the finds from both areas, with respect to the erosional surfaces between UA3c/4 and UB4c/5. Our assumption is that a statistically significant concentration of unsorted finds in the proximity of the erosional surfaces would suggest an autochthonous origin of the assemblage, whereas a homogeneous vertical distribution of finds in UA3c or UB4c would support the allochthonous hypothesis. Indeed, gravity flow processes such as hyperconcentrated flows are highly erosive and show rather chaotic structures,

		Lithic				Bone tool	Fauna	
Sample	n	Debris	Flake	Tool	Core		Mammalia	AAPR
UA3c (2013-2016)	343	56	2	1			86	198
UA4 (2013-2016)	72	7	2				22	41
UB4c (2013-2019)	2324	1391	296	72	23	2	396	144
UB5a (2013-2019)	181	101	23	5	3		37	12

Table 1: List of sampled observations for the vertical distribution analysis. The Mammalia sample includes large and small mammals. However, it does not include specimens of the order Proboscidea, to be sampled for further specific analysis. AAPR: Amphibia, Aves, Pisces, Reptilia.

which might result in normal or inverse grading (Benvenuti and Martini, 2002; Pierson, 2005).

By applying an IDW (Inverse Distance Weighting) interpolation of recorded random three-dimensional points of the UA3c/4 and UB4c/5 stratigraphic hiatus, we were able to build geostatistical models of the erosional surfaces. Thus, we measured the minimum orthogonal distance (*d*) of each find to the interpolated erosional surface of the respective area (Giusti et al. 2018). The distribution of the distances *d* is finally estimated by means of histograms and density functions.

10.3 PRELIMINARY RESULTS AND DISCUSSION

Fig. 3 shows the distribution of the minimum orthogonal distances (*d*) of the UA3c and UA4 finds to the UA3c/4 surface; and the distribution of the distance *d* of the UB4c and UB5a finds to the UB-4c/5a surface. With regards to the units above the erosional surfaces (i.e., UA3c and UB4c), both distributions clearly skew to the right, with mean values between 0.1 and 0.2 m from the stratigraphic contact with the underlying units UA4 and UB5a. The density functions show that different classes of lithic artifacts and faunal remains have similar distributions, thus suggesting the absence of any sort of grading. Hence, most of the material from units UA3c and UB4c indistinctly occurs in proximity to the erosional surfaces, within the first 10-20 cm, whereas the rest is gradually dispersed towards the upper part of the units, up to about 50 cm. Such a distribution is consistent with the hypothesis of an autochthonous assemblage. Conversely, we would expect a normal distribution in the case of a homogeneous vertical distribution, and eventually inverse grading, or a continuously aggrading bed (Benvenuti and Martini, 2002).

As for the units below the erosional surfaces (i.e., UA4 and UB5a), both distributions skew to the left with much shorter tails. Indeed, both distributions are compressed within 20-30 cm below surface, with mean values around 10 cm. The density functions of the UB5a sample show similar distributions for different classes of lithic artifacts and faunal remains, thus suggesting no size sorting.

The occurrence of material very close to, or at the contact with the erosional surfaces, supports

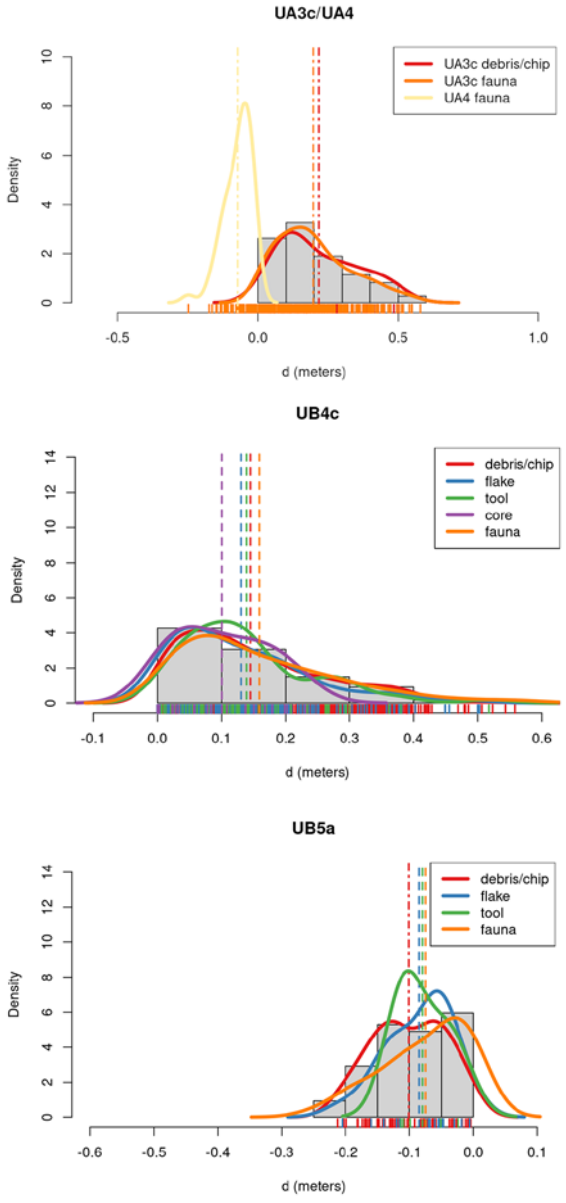

Figure 3: Distribution of minimum orthogonal distances (*d*) to the UA3c/4 and UB4c/5a surfaces. The histogram represents the total distribution; the curves express density functions for each class of find (UA3c fauna plots on the x-axis with negative *d* values); dashed lines indicate mean values.

again our working hypothesis that the primary deposition of the archaeological assemblage occurred *in situ*, and a subsequent gravity flow event eroded it. Thus, according to our autochthonous hypothesis, the material would have been only locally reworked in both areas. The exceptional preservation and number of mint-to-sharp lithic artifacts, as well as the rather good state of the bone preservation would support this hypothesis, suggesting limited, if any, transport over a short distance and/or for a short time span, and a common taphonomic history for both lithics and fauna. A further indication that the lithic and fauna assemblages have not undergone substantial reworking would come from the currently in progress refitting analyses. To date, 5 bone refits have been found from unit UB4c, and 1 between two mammal bone fragments from units UB4c and UB5a. Similarly, a limestone flake from unit UB4c has been found to refit a core from the same unit, and a radiolarite flake from UB4b has been found to refit a core from UB4c. Nonetheless, the original, pristine spatial extension and relationship between items would have been lost, precluding any further high-resolution investigation of the spatial dimension of past human behaviors. Whereas the erosional event represents a snapshot of a relatively short time-frame, little is known about the duration and intensity of the human activities before the depositional event that capped and preserved the archaeological record. We might argue that, considering the high rate of bone fragmentation and the density of lithic debris/chips, it is likely that the assemblage represents a palimpsest of repeated events of hunting/scavenging and exploitation of lake shore resources, similar to what Schlanger (1992) refers to as a persistent place. However, little is known about the intensity of human activities preserved after the UA3/UB4 mud-flow. The sedimentary sequence above the main hiatus is characterized by a series of erosional-bounded depositional units all attributed to mud- or hyperconcentrated-flows (i.e., UA3–UA2, UB5–UB2; Fig. 2) and a relatively small number of lithic artifacts and faunal remains were recovered from most of those units; nevertheless, the small amount of scattered finds from those units does not allow for hypothesis testing – it only indicates human presence, with an intensity that at the present cannot be assessed.

Therefore, although we can reliably conclude that hominin exploitation of elephant carcasses and other mammals occurred at MAR-1, inferences about the mode of acquisition and processing of the carcasses (hunting or active/passive scavenging), as well as the degree of exploitation (partial or complete) are speculative in light of the current information. Furthermore, despite the relatively high rate of cut-marks (2 out of 2 elephant individuals with cut-marks), the temporal resolution of the archaeological record is too low to allow for testable assumptions about the intensity of occupation and degree of exploitation (systematic or occasional) of elephants by humans. A better understanding of the frequency of past human-elephant interactions has major implications for the broader debate about the role of meat consumption in the biological and cultural evolution of hominins.

ACKNOWLEDGMENTS

Excavation at Marathousa 1 was conducted under a permit granted to the Ephorate of Palaeoanthropology-Speleology, Hellenic Ministry of Culture. It was supported by the ERC Consolidator Grant ERC-CoG-24703 (“CROSSROADS”) and the ERC Starting Grant ERC-StG-83503 (“PaGE”), both awarded to K.H. V.T., G.E.K. and K.H. are also supported by the Deutsche Forschungsgemeinschaft (DFG Project no. 463225251, “MEGALOPOLIS”). K.H. is also supported by the ERC Advanced Grant ERC-AdG-101019659 (“FIRSTSTEPS”). We are grateful to all the participants in the excavation campaigns in Marathousa

1 for their essential collaboration. We would also like to thank E. Discamps and the anonymous reviewer for their comments and suggestions.

REFERENCES

Benvenuti, M., Martini, I.P., 2002. Analysis of terrestrial hyperconcentrated flows and their deposit, in: Martini, I.P., Baker, V.R., Garzón, G. (Eds.), Flood and Megaflood Processes and Deposits. Vol. 32 of Special Publication of the International Association of Sedimentologists. Blackwell Publishing Ltd., pp. 167–193.

Blackwell, B.A.B., Sakhrani, N., Singh, I.K., Gopalkrishna, K.K., Tourloukis, V., Panagopoulou, E., Karkanas, P., Blickstein, J.I.B., Skinner, A.R., Florentin, J.A., Harvati, K., 2018. ESR Dating Ungulate Teeth and Molluscs from the Paleolithic Site Marathousa 1, Megalopolis Basin, Greece. Quaternary, 1(3), 22.

Doukas, C., van Kolfschoten, T., Papayianni, K., Panagopoulou, E., Harvati, K., 2018. The small mammal fauna from the palaeolithic site Marathousa 1 (Greece). Quaternary International, 497, pp. 95–107.

Giusti, D., Tourloukis, V., Konidaris, G.E., Thompson, N., Karkanas, P., Panagopoulou, E. and Harvati, K., 2018. Beyond maps: Patterns of formation processes at the Middle Pleistocene open-air site of Marathousa 1, Megalopolis Basin, Greece. Quaternary International, 497, pp. 137–153.

Giusti, D., 2021. Investigating the spatio-temporal dimension of past human-elephant interactions: a spatial taphonomic approach, in Konidaris, G. E., Barkai, R., Tourloukis, V., Harvati, K. (Eds.), Human-elephant interactions: from past to present. Tübingen University Press, pp. 261–285.

Jacobs, Z., Li, B., Karkanas, P., Tourloukis, V., Thompson, N., Panagopoulou, E., Harvati, K., 2018. Optical dating of K-feldspar grains from Middle Pleistocene lacustrine sediment at Marathousa 1 (Greece). Quaternary International, 497, pp. 170–177.

Karkanas, P., Tourloukis, V., Thompson, N., Giusti, D., Panagopoulou, E. and Harvati, K., 2018. Sedimentology and micromorphology of the Lower Palaeolithic lakeshore site Marathousa 1, Megalopolis Basin, Greece. Quaternary International, 497, pp. 123–136.

Konidaris, G.E., Barkai, R., Tourloukis, V. and Harvati, K., 2021. Human-elephant interactions: from past to present. Tübingen University Press, Tübingen.

Konidaris, G.E., Tourloukis, V., 2021. Proboscidea-*Homo* interactions in open-air localities during the Early and Middle Pleistocene of western Eurasia: a palaeontological and archaeological perspective, in: Konidaris, G. E., Barkai, R., Tourloukis, V., Harvati, K. (Eds.), Human-elephant interactions: from past to present. Tübingen University Press, pp. 67–104.

Konidaris, G., Athanassiou, A., Tourloukis, V., Thompson, N., Giusti, D., Panagopoulou, E., Harvati, K., 2018. The skeleton of a straight-tusked elephant (*Palaeoloxodon antiquus*) and other large mammals from the Middle Pleistocene butchering locality Marathousa 1 (Megalopolis Basin, Greece): preliminary results. Quaternary International, 497, pp. 65–84.

Pierson, T.C., 2005. Distinguishing between Debris Flows and Floods from Field Evidence in Small Watersheds (USGS Numbered Series, U.S. Geological Survey).

Schlanger, S.H., 1992. Recognizing persistent places in Anasazi settlement systems, in: Rossignol, J., Wandsnider, L. (Eds.), Space, time, and archaeological landscapes. Springer, pp. 91–112.

Tourloukis, V., Muttoni, G., Karkanas, P., Monesi, E., Scardia, G., Panagopoulou, E., Harvati, K., 2018a. Magnetostratigraphic and chronos-

tratigraphic constraints on the Marathousa 1 Lower Palaeolithic site and the Middle Pleistocene deposits of the Megalopolis Basin, Greece. Quaternary International, 497, pp. 154–169.

Tourloukis, V., Thompson, N., Panagopoulou, E., Giusti, D., Konidaris, G. E., Karkanas, P., Harvati, K., 2018b. Lithic artifacts and bone tools from the Lower Palaeolithic site Marathousa 1, Megalopolis, Greece: Preliminary results. Quaternary International, 497, pp. 47–64.

11 FIRST TRACEOLOGICAL STUDY OF THE LITHIC ASSEMBLAGE FROM MARATHOUSA 1 AND CONTEXTUALIZATION OF THE RESULTS WITHIN THE EUROPEAN LOWER PALAEOLITHIC

Juliette Guibert–Cardin[1,*], Vangelis Tourloukis[1,2], Eleni Panagopoulou[3], Katerina Harvati[1,4], Elisa Nicoud[5], Sylvie Beyries[5]

[1]*Paleoanthropology, Institute for Archaeological Sciences and Senckenberg Centre for Human Evolution and Palaeoenvironment, Department of Geosciences, Eberhard Karls University of Tübingen, Tübingen, Germany*
[2]*Department of History and Archaeology, School of Philosophy, University of Ioannina, Ioannina, Greece*
[3]*Hellenic Ministry of Culture, Ephorate of Palaeoanthropology–Speleology, Athens, Greece*
[4]*DFG Centre for Advanced Studies 'Words, Bones, Genes, Tools', Eberhard Karls University of Tübingen, Tübingen, Germany*
[5]*Université Côte d'Azur, CNRS, CEPAM, Nice, France*
** juliette.guibert-cardin@cepam.cnrs.fr*

http://dx.doi.org/10.15496/publikation-97669

Keywords: Lower Palaeolithic; small tools; Taphonomy; Use-wear analysis; Techno-morpho-functional analysis

11.1 INTRODUCTION

The European Lower Palaeolithic demonstrates a wide range of human settlements and various lithic production techniques. This variability is still poorly understood, hindering the assessment of hominin techno-economical choices. Recent studies on lithic variability of the Middle Pleistocene investigated whether differences in assemblage composition is related to cultural or temporal trends, site function, or availability of raw materials.

Here we focus on small flakes which constitute important blanks in many lithic assemblages of the Lower Palaeolithic (Rocca et al., 2016). They are present both in Africa and Eurasia from ≥1 Ma to 300 ka (Burdukiewicz and Ronen, 2003; Derevianko, 2006; Lemorini, 2018). Although the origin of such assemblage diversity is still debated, it is proposed to be related to the age of assemblages, to the unique preservation of sites, or to specialized activities or durations. In order to better understand how small lithics were utilized, we conduct techno-morpho-functional and traceological analyses. The combined approach provides the opportunity to further assess the *chaîne opératoire* from the production of tools to their use and curation through the analysis of their final morphology before discard.

We report the preliminary results from a traceological study of lithics from Marathousa 1 (Megalopolis, Greece). The site is located in the Megalopolis Basin which periodically hosted an

J. Guilbert-Cardin: https://orcid.org/0000-0002-1767-6328
V. Tourloukis: https://orcid.org/0000-0002-9527-2708
E. Panagopoulou: https://orcid.org/0000-0002-4268-6157
K. Harvati: https://orcid.org/0000-0001-5998-4794
S. Beyries: https://orcid.org/0000-0003-4798-701X

ancient lake (Panagopoulou et al., 2018; Bludau et al. 2021). The archaeological layer is attributed to Marine Isotope Stage 12 (Tourloukis et al., 2018a). The archaeological remains are at the contact of sedimentary units UA3-UA4 and UB4-UB5 (Karkanas et al., 2018). The excavation took place in two sections, approximately 60 m apart, areas A and B. Area A exhibits numerous elephant bones from a largely complete single individual with anthropogenic cut-marks and a low density of lithic finds (Konidaris et al., 2018). Area B has yielded a higher density of lithics, but also additional elephant remains and other bones with cut-marks and anthropogenic modifications. The lithic assemblage is composed of 2058 artifacts. The raw materials of local origin are radiolarite, flint, limestone and quartz, collected in close proximity to the site (Tourloukis et al., 2018b). The lithic assemblage is composed of exhausted cores, flakes, and tools and belongs to a flake-based industry. Blank types are varied. The aim of the debitage is to produce blanks with sharp and durable edges. Technological studies provide numerous data on technological behaviors but questions remain about tool use and site function.

11.2 METHODS

The objective of this pilot study is to assess the potential for use-wear analysis on a sample of 250 lithic artifacts from Areas A and B. The sample is representative of the whole assemblage (Table 1). The analysis was carried out in two stages: a taphonomic analysis of the flint and radiolarite artifacts to determine the nature of post-depositional processes; and then a functional analysis of the 250 artefacts in the sample. This last part of the work is in progress: 13 pieces have been analyzed so far and are presented here.

The taphonomical study was founded on the methodological approach developed by petroarchaeologists (Fernandes, 2012; Fernandes and Raynal, 2005). The aim of this methodology is to identify the post-depositional processes within the archaeological site.

Lithic type	Radiolarite	Flint	Limestone	Quartz	Sandstone	Total
Unretouched blanks	148	21	15	10	1	195
Cores/Core fragments	7	0	5	2	0	14
Flakes >15 mm	96	12	8	4	1	121
Chips <15 mm	38	7	0	3	0	48
Debris	7	2	2	1	0	12
Retouched blanks	47	7	1	0	0	55
Backed pieces	9	2	1	0	0	12
Notched pieces	10	2	0	0	0	12
Denticulates	7	0	0	0	0	7
Scrapers	6	1	0	0	0	7
Core tools	7	0	0	0	0	7
Retouched pieces	4	1	0	0	0	5
Composite tools	3	1	0	0	0	4
Pointed pieces	1	0	0	0	0	1
Total	**195**	**28**	**16**	**10**	**1**	**250**

Table 1: Sample details.

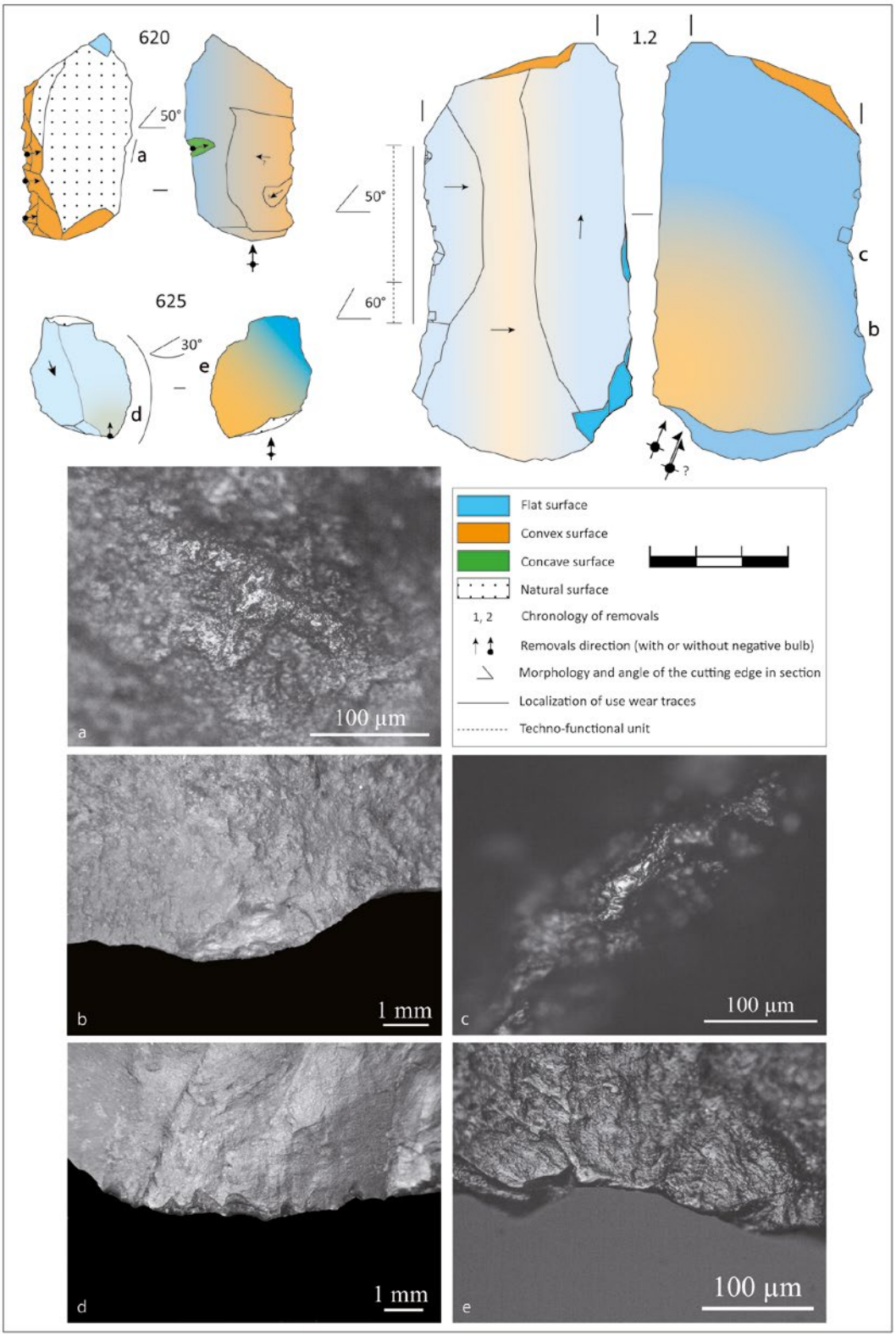

Figure 1: Diacritical sketches of lithics with use-wear traces and photos of traces. a. functional spot polish from flake 620 (used in a longitudinal motion possibly for butchering activities); b. and c. crushing and smooth spot polish visible on the cutting edge of flake 1.2 (used to process hard material in a longitudinal motion); d. and e. angular scars oblique to the edge, smooth spot polish and striations oblique to the edge of flake 625 (used in a longitudinal motion for butchering activities).

The techno-morpho-functional approach, conceived by M. Lepot (1993) and E. Boëda (1997) is occasionally combined with use-wear analysis to better characterize lithic assemblages from the Lower and Middle Paleolithic (Bonilauri, 2010; Claud, 2008; Guibert-Cardin et al., 2021). First, the functional analysis of lithics was conducted at both low and high magnifications to identify active parts and modes of tool use. Lastly, an analysis of the dorsal-scar pattern and the succession of each removal in the manufacturing of tools with use-wear traces was conducted. We seek to understand the existing relationships between the production of blanks for tools, morphology, retouch and use.

11.3 RESULTS

The pieces analyzed for the taphonomical study are exceptionally well preserved: the overwhelming majority of the pieces examined exhibit slight alterations, providing the opportunity to conduct use-wear analysis at both low and high magnifications. Post-depositional surface modifications are mainly of chemical origin; however, some mechanical alterations attest to slight movement of the lithics after deposition. This observation reinforces the interpretation of minor reworking of the find layers according to Giusti et al. (2018).

Currently, 13 lithics were analyzed for use-wear with a stereomicroscope and a metallographic microscope. Five in total show use wear traces and one exhibits technological traces (for the detailed results and comparisons with the experimental use-wear traces see Guibert-Cardin et al., 2022). The remaining seven lithics do not exhibit use-wear traces. However, this does not necessarily imply that the latter were not utilized.

MAR1 1.2 (Fig. 1) is a flint flake with a backing. The opposite edge is unretouched and bears bifacial and oblique scars and striations parallel to the working edge indicating a longitudinal motion. The processed material is hard because crushing and smooth polish are present and scars are large and overlap. The active edge is unretouched and is opposite to a back.

MAR1 620 (Fig. 1) is a radiolarite backed knife. The back is created by abrupt retouch and is opposite an unretouched edge bearing spots of smooth polish and short and isolated striations. These use-wear traces are similar to those produced during butchering activities. Striations are oblique to the edge indicating a longitudinal motion.

MAR1 625 (Fig. 1) is an unretouched radiolarite tool. One edge exhibits bifacial scars, striations oblique to the edge and a symmetrical rounding resulting from a longitudinal motion. The scar characteristics are the same as those one would expect from butchering activities, namely with a triangular shape and bending and cone initiations. MAR1 605 (Fig. 2) is an unretouched radiolarite flake with a short back. The secant cutting edge exhibits dissymmetric use-wear traces indicating a transversal motion. The scars have circular and elongated forms, and the polish is domed and smooth. These characteristics are indicative of plant processing.

MAR1 637 (Fig. 2) is a thick radiolarite chunk with a convergent spine created by retouching. Use-wear traces are located on this spine. The scars are bifacial and the striations are perpendicular to the edge, implying a transversal bidirectional motion. The material processed is semi-hard because polish and striations are on high areas and the scars are infrequent. Rounding and numerous striations are indicative of an abrasive material. These traces are possibly related to the hammerstone, although they could also indicate the processing of a semi-hard and abrasive material.

MAR1 1132 (Fig. 2) is a thick flake with a cortical back opposite a retouched edge. On the face opposite to the retouch, the edge exhibits a band of polish and associated striations strictly parallel to each other indicating that they come from the

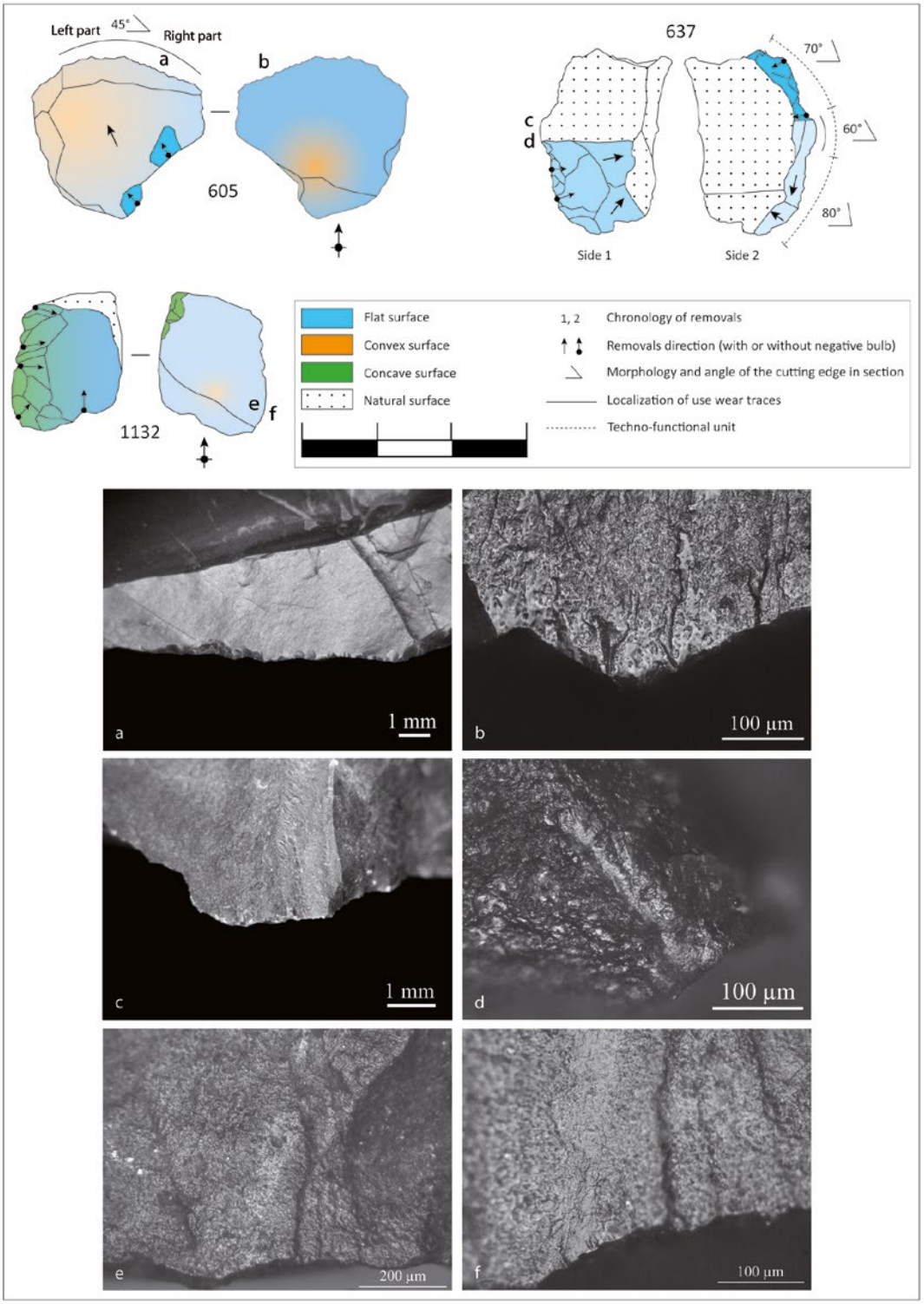

Figure 2: Diacritical sketches of lithics with functional and technological traces and photos of traces. a. and b. circular and elongated small scars opposite to a smooth domed polish on the cutting edge of flake 605 (used to process plant in a transversal unidirectional motion); c. and d. small irregular scars opposite to a rough to smooth polish on a slightly rounded arris with long striations perpendicular to the edge of flake 637 (related to technological traces or utilized on a semi hard material in a transversal bidirectional motion); e. and f. large band of polish in the center of a crescent-shaped crack and numerous organized striations on the ventral surface opposite the retouch scars of flake 1132 (technological traces).

same event. These traces are associated with an impact mark and this combination of traces probably has a technological origin.

In summary, motions and material processed are varied. Tools exhibiting use-wear traces include unretouched and retouched flakes that frequently display a back opposite to the active edge, maybe to facilitate gripping.

	Isotopic stage	Nr. subjected to functional analysis	Nr. with use wear traces	Motion				Material processed							Prehension/ hafting	Other	
				Long.	Transv.	Both	Und.	Animal	Vegetal	Hard	Semi hard	Soft	Und.	Residues			
Evron Quarry, Israel	19	?	?													Impact traces	Chazan, 2013
Isernia la Pineta, Italy	15	C. 1230	>261	x	x		x	x	1?				x			Short activity	Longo et al., 1997 Minelli et al., 2004
Ficoncella, Italy	13	129	13	x	x						x	x				Short activity	Lemorini, 2018
Revadim, Israel	13-12	283	109	80	16	8	5	5		53 ....22.... .....3.....		21	5	Animal	Prehension	Short activity. One flake = one activity	Venditti et al., 2019a Venditti et al., 2019b
Marathousa 1, Greece	12-11	14	5	3	2			1	1	2	1						Guibert--Cardin et al., in press, 2022
Fontana Ranuccio, Italy	11	?	?	x	x						x						Marinelli et al., 2019
Aridos 1 and 2, Spain	11 or 9	77	33	31	2	5	2	38	2								Ollé, 2003
Qesem cave, Israel	11-8	743	231	155	31	42	3	83	19	1	12 25 .....91....			Various	Wrapping?	Short activity	Venditti, 2019 Lemorini, 2015
Schöningen, Germany	9	13	3	2			1	1	2			1		Animal, vegetal	Prehension		Rots et al., 2015
La Polledrara di Cecanibbio, Italy	9	155	20	x	x			x	x						Prehension		Lemorini, 2018

Table 2: Use-wear data on small flakes from Lower Palaeolithic sites in Europe and the Levant.

11.4 DISCUSSION

This study confirms the exceptional state of preservation of the site. Moreover, it confirms that butchering activities took place at both excavation areas and demonstrates that plants were exploited. The activities carried out at Marathousa 1 involved a broader range of activities than originally hypothesized. Tools with use-wear traces do not show any significant standardization in terms of blank shape or form, except for the recurrent presence of an active edge opposite a natural or retouched back (Guibert-Cardin et al., 2022). These first functional results from Marathousa 1 are part of the current discussions on the function of small flakes in the Lower Palaeolithic.

Use-wear analyses on small blanks and tools have been performed on assemblages from fewer than ten sites in total (Table 2). Small tools are mainly used to process soft and semi-hard materials and when worked materials can be identified, they primarily involve butchering activities and to a lesser extent, vegetal materials (Lemorini, 2018; Venditti, 2019; Guibert-Cardin et al., 2022). It is frequently suggested that small tools are used in the final stages of the butchering process (Longo et al., 1997; Venditti et al., 2019b). Our preliminary results suggest that small tools were used for different tasks as also seen in the Italian sites of La Ficoncella and La Polledrara di Cecanibbio (Aureli et al., 2016; Lemorini, 2018). One of the most recurring questions about small tools is the mode of prehension. Small flakes from Revadim, La Polledrara di Cecanibbio and Schöningen exhibit prehension traces, whereas at Qesem Cave, they were possibly wrapped (Lemorini, 2018; Rots et al., 2015; Venditti, 2019; Venditti et al., 2019a). With the current functional data on tools from Marathousa 1, there is no evidence to determine the mode of prehension. However, the presence of a back or an unsharpened edge opposite or adjacent to the active part, as well as the lack of standardization of the tools, suggests hand use rather than hafting. Experimental reproductions of small tools demonstrate that backing opposite to a sharp edge provides a superior grip and promotes the application of force and precision (Chazan, 2013; Jones, 1980; Starkovich et al., 2021).

This preliminary study enriches the sparse functional data available on small tools and more generally on Lower Palaeolithic tools. Use-wear analyses are rare on Lower Palaeolithic assemblages because of taphonomic problems. However, by coupling techno-morpho-functional and use-wear analysis, it is possible to access the techno-economic choices of human groups. The pursuit of the functional analysis of lithics from Marathousa 1 will contribute to better qualify, quantify and understand tool structure, function and activities carried out.

ACKNOWLEDGMENTS

Excavation at Marathousa 1 was conducted under a permit granted to the Ephorate of Palaeoanthropology-Speleology, Hellenic Ministry of Culture. It was supported by the ERC Consolidator Grant ERC-CoG-724703 (“CROSSROADS”) and the ERC Starting Grant ERC-StG-283503 (“PaGE”), both awarded to K.H. J.G.C., V.T. and K.H. are also supported by the Deutsche Forschungsgemeinschaft (DFG Project no. 463225251, “MEGALOPOLIS”). K.H. is also supported by the ERC Advanced Grant ERC-AdG-101019659 (“FIRSTSTEPS”). J.G.C. was also supported by the CEPAM, UMR 7264, and the French government through the “Université Côte d’Azur UCA-JEDI Investments in the Future” project managed by the National Research Agency (ANR) with the reference number ANR-15-IDEX-01. We thank

the two reviewers for their constructive comments, which helped improve the manuscript.

REFERENCES

Aureli, D., Rocca, R., Lemorini, C., Modesti, V., Scaramucci, S., Milli, S., Giaccio, B., Marani, F., Palombo, M.R. and Contardi, A., 2016. Mode 1 or mode 2? "Small tools" in the technical variability of the European Lower Palaeolithic: The site of Ficoncella (Tarquinia, Lazio, central Italy). Quaternary International, 393, pp. 169–184.

Bludau, I.J.E., Papadopoulou, P., Iliopoulos, G., Weiss, M., Schnabel, E., Thompson, N., Tourloukis, V., Zachow, C., Kyrikou, S., Konidaris, G.E., Karkanas, P., Panagopoulou, E., Harvati, K. and Junginger, A., 2021. Lake-Level Changes and Their Paleo-Climatic Implications at the MIS12 Lower Paleolithic (Middle Pleistocene) Site Marathousa 1, Greece. Frontiers in Earth Science, 9, 668445.

Boëda, E., 1997. Technogénèse de systèmes de production lithique au Paléolithique inférieur et moyen en Europe occidentale et au Proche-Orient. HDR, University of Paris X - Nanterre, Paris.

Bonilauri, S., 2010. Les outils du Paléolithique moyen, une mémoire technique oubliée ? Approche techno-fonctionnelle appliquée à un assemblage lithique de conception Levallois provenant du site d'Umm el Tlel (Syrie centrale). Doctoral dissertation, University of Paris X - Nanterre, Paris.

Burdukiewicz, J.M., Ronen, A., 2003. Lower Palaeolithic small tools in Europe and the Levant. BAR International Series. Archeopress, Oxford.

Chazan, M., 2013. Butchering with small tools: the implications of the Evron Quarry assemblage for the behaviour of *Homo erectus*. Antiquity, 87, pp. 350–367.

Claud, E., 2008. Le statut fonctionnel des bifaces au Paléolithique moyen récent dans le Sud-Ouest de la France. Etude tracéologique intégrée des outillages des sites de La Graulet, La Conne de Bergerac, Combe de Brune 2, Fonseigner et Chez-Pinaud/Jonzac. Doctoral dissertation, University of Bordeaux I, Bordeaux.

Derevianko, A.P., 2006. The Lower Paleolithic small tool industry in Eurasia: migration or convergent evolution? Archaeology, Ethnology & Anthropology of Eurasia, 1, pp. 2–32.

Fernandes, P., 2012. Itinéraires et transformations du silex: une pétroarchéologie refondée, application au Paléolithique moyen. Doctoral dissertation, University of Bordeaux I, Bordeaux.

Fernandes, P., Raynal, J. P., 2005. Pétroarchéologie du silex: un retour aux sources. Comptes Rendus Palevol, 5, pp. 829–837.

Giusti, D., Tourloukis, V., Konidaris, G., Thompson, N., Karkanas, P., Panagopoulou, E. and Harvati, K., 2018. Beyond maps: Patterns of formation processes at the Middle Pleistocene open-air site of Marathousa 1, Megalopolis Basin, Greece. Quaternary International, 497, pp. 137–153.

Guibert-Cardin, J., Capellari, F., Lhomme, V., Connet, N., Nicoud, E. and Beyries, S., 2021. Lower Palaeolithic stone tools: a techno-functional study of the Soucy 3P assemblage (France), in: Beyries, S., Hamon, C., Maigrot, Y. (Eds.), Beyond use-wear traces: going from tools to people by means of archaeological wear and residue analyses. Sidestone Press, Nice, pp. 101–115.

Guibert-Cardin, J., Tourloukis, V., Thompson, N., Panagopoulou, E., Harvati, K., Nicoud, E. and Beyries, S., 2022. The function of small tools in Europe during the Middle Pleistocene: the case of Marathousa 1 (Megalopolis, Greece). Journal of Lithic Studies 9(1).

Jones, P., 1980. Experimental butchery with

modern stone tools and its relevance for Palaeolithic archaeology. World Archaeology, 12, pp. 153–165.

Karkanas, P., Tourloukis, V., Thompson, N., Giusti, D., Panagopoulou, E. and Harvati, K. 2018. Sedimentology and micromorphology of the Lower Palaeolithic lakeshore site Marathousa 1, Megalopolis Basin, Greece. Quaternary International, 497, pp. 123–136.

Konidaris, G., Athanassiou, A., Tourloukis, V., Thompson, N., Giusti, D., Panagopoulou, E. and Harvati, K., 2018. The skeleton of a straight-tusked elephant (*Palaeoloxodon antiquus*) and other large mammals from the Middle Pleistocene butchering locality Marathousa 1 (Megalopolis Basin, Greece): preliminary results. Quaternary International, 497, pp. 65–84.

Lemorini, C., 2018. Small tools and the *Palaeoloxodon - Homo* interaction in the Lower Palaeolithic. The contribution of use-wear analysis, in: Borgia, V., Cristiani, E. (Eds.), Palaeolithic Italy. Advanced studies on early human adaptations in the Apennine peninsula. Sidestone Press, pp. 27–35.

Lepot, M., 1993. Approche techno-fonctionnelle de l'outillage lithique moustérien: essai de classification des parties actives en termes d'efficacité technique : application à la couche M2e sagittale du Grand abri de la Ferrassie (fouille Henri Delporte). Master dissertation, University of Paris X – Nanterre, Paris.

Longo, L., Peretto, C., Sozzi, M., Vannucci, S., 1997. Artefacts, outils ou supports épuisés ? Une nouvelle approche pour l'étude des industries du Paléolithique ancien : le cas d'Isernia la Pineta (Molise, Italie centrale). L'Anthropologie, 101, pp. 579–596.

Marinelli, F., Lemorini, C. and Zampetti, D., 2019. La funzione degli "small tools" nell'ambito delle industrie litiche scheggiate acheuleane della Penisola Italiana: il caso studio del sito laziale di Fontana Ranuccio. IpoTESI di Preistoria, 11, pp. 57–72.

Minelli, A., Arzarello, M., Longo, L., Ollé, A., Vergès, J.M. and Peretto, C., 2004. New data on the lithic industry of Isernia La Pineta: typology, technology and functional analysis, in: Le Secrétariat du Congrès (Eds.), Human Origins and the Lower Palaeolithic - XIVth UISPP Congress. BAR International Series, Liège, pp. 59–68.

Ollé, A., 2003. Variabilitat i patrons functionals en els sistemes tèchnics de Mode 2. Anàlisi de les deformacions d'ùs en els conjunts litics del Riparo Esterno de Grotta Paglicci (Rignano Garcanico, Foggia), Aridos (Arganda, Madrid) i Galeria-TN (Sierra de Atapuerca, Burgos). Doctoral dissertation, University of Tarragona - Rovira i Virgila, Tarragona.

Panagopoulou, E., Tourloukis, V., Thompson, N., Konidaris, G., Athanassiou, A., Giusti, D., Tsartsidou, G., Karkanas, P. and Harvati, K., 2018. The Lower Palaeolithic site of Marathousa 1, Megalopolis, Greece: Overview of the evidence. Quaternary International, 497, pp. 33–46.

Rocca, R., Abruzzese, C. and Aureli, D., 2016. Europeans Acheuleans: Critical perspectives from the East. Quaternary International, 411, pp. 402–411.

Rots, V., Hardy, B., Serangeli, J. and Conard, N., 2015. Residue and microwear analyses of the stone artifacts from Schöningen. Journal of Human Evolution, 89, pp. 298–308.

Starkovich, B., Cuthbertson, P., Kitagawa, K., Thompson, N., Konidaris, G., Rots, V., Münzel, S.C., Giusti, D., Schmid, V.C., Blanco-Lapaz, A., Lepers, C. and Tourloukis, V., 2021. Minimal tools, maximum meat: A pilot experiment to butcher an elephant foot and make elephant bone tools using Lower Paleolithic stone tool technology. Ethnoarchaeology, 12, pp. 118–147.

Tourloukis, V., Muttoni, G., Karkanas, P., Monesi, E., Scardia, G., Panagopoulou, E. and Harvati, K., 2018a. Magnetostratigraphic and chronostratigraphic constraints on the Marathousa 1 Lower Palaeolithic site and the Middle Pleistocene deposits of the Megalopolis Basin, Greece. Quaternary International, 497, pp. 154–169.

Tourloukis, V., Thompson, N., Panagopoulou, E., Giusti, D., Konidaris, G., Karkanas, P. and Harvati, K., 2018b. Lithic artifacts and bone tools from the Lower Palaeolithic site Marathousa 1, Megalopolis, Greece: Preliminary results. Quaternary International, 497, pp. 47–64.

Venditti, F., 2019. Understanding lithic recycling at the Late Lower Palaeolithic Qesem Cave, Israël. A functional and chemical investigation of small flakes. Archaeopress Archaeology, Oxford.

Venditti, F., Agam, A. and Barkai, R., 2019a. Techno-functional analysis of small recycled flakes from Late Acheulian Revadim (Israel) demonstrates a link between morphology and function. Journal of Archaeological Science: Reports, 28.

Venditti, F. Cristiani, E., Nunziante-Cesaro, S., Agam, A., Lemorini, C. and Barkai, R., 2019b. Animal residues found on tiny Lower Paleolithic tools reveal their use in butchery. Scientific reports, 9, 13031.

12 FIRST STABLE ISOTOPE RESULTS ON THE ECOLOGY OF THE STRAIGHT-TUSKED ELEPHANT (*PALAEOLOXODON ANTIQUUS*) FROM THE MIDDLE PLEISTOCENE MARATHOUSA 1 (PELOPONNESE, GREECE)

Effrosyni Roditi[1,*], Hervé Bocherens[2], George E. Konidaris[1], Athanassios Athanassiou[3], Vangelis Tourloukis[1,4], Eleni Panagopoulou[3], Katerina Harvati[1,5]

[1]*Paleoanthropology, Institute for Archaeological Sciences and Senckenberg Centre for Human Evolution and Palaeoenvironment, Department of Geosciences, Eberhard Karls University of Tübingen, Tübingen, Germany*
[2]*Biogeology, Department of Geosciences and Senckenberg Centre for Human Evolution and Palaeoenvironment, Eberhard Karls University of Tübingen, Tübingen, Germany*
[3]*Hellenic Ministry of Culture, Ephorate of Paleoanthropology–Speleology, Athens, Greece*
[4]*Department of History and Archaeology, School of Philosophy, University of Ioannina, Ioannina, Greece*
[5]*DFG Centre for Advanced Studies 'Words, Bones, Genes, Tools', Eberhard Karls University of Tübingen, Tübingen, Germany*
**effrosyni.roditi@uni-tuebingen.de*

http://dx.doi.org/10.15496/publikation-97670

Keywords: Stable isotopes; paleoecology; Middle Pleistocene; *Palaeoloxodon*; Megalopolis Basin

12.1 INTRODUCTION

Carbon and oxygen stable isotope analysis of mammalian carbonate bioapatite is, nowadays, a well-established and widely used approach for past ecological investigations and paleoenvironmental reconstructions. Carbon is incorporated into mammalian tissues through their dietary intake. In this regard, the ratios of stable carbon isotopes in the tissues of primary consumers—hereafter expressed using the delta (δ) notation, wherein $\delta^{13}C=[(^{13}C/^{12}C)_{sample}/(^{13}C/^{12}C)_{standard} - 1] \times 1000$—reflect the isotopic composition of the ingested plant matter (DeNiro and Epstein, 1978), enriched by ~14.1 ± 0.5‰ in tooth enamel carbonate of large herbivores (Cerling and Harris, 1999; Passey et al., 2005), due to physiological and metabolic processes. In terrestrial ecosystems, variation in the isotopic signature of plant carbon permits a distinction between the two main photosynthetic pathways, i.e., C_4 and C_3 (Ehleringer and Monson, 1993), with the former group consisting of warm growth season grasses and forbs, which demonstrate higher average $\delta^{13}C$ value (~–13‰), and the latter incorporating trees, shrubs, and cool growth season grasses and sedges with a modern aver-

E. Roditi: https://orcid.org/0000-0002-1917-7645
H. Bocherens: https://orcid.org/0000-0002-0494-0126
G. E. Konidaris: https://orcid.org/0000-0002-7041-233X
A. Athanassiou: https://orcid.org/0000-0002-9140-7011
V. Tourloukis: https://orcid.org/0000-0002-9527-2708
E. Panagopoulou https://orcid.org/0000-0002-4268-6157
K. Harvati: https://orcid.org/0000-0001-5998-4794

age $\delta^{13}C$ value of ~–27‰ (Bender, 1971; Kohn, 2010). Within plant communities utilizing the C_3 photosynthetic pathway, additional environmentally controlled fractionation occurs, which is governed by multiple factors, such as degree of canopy closure, water availability, temperature, irradiance, or atmospheric CO_2 diffusion (van der Merwe and Medina, 1991; Heaton, 1999; Hofman-Kamińska et al., 2018). The interplay of these factors enables further habitat distinctions within the wide range of $\delta^{13}C$ values documented in C_3-dominated ecosystems, since carbon isotopic ratios of herbivores feeding under closed canopy conditions, i.e., dense forests, tend to be lower than for herbivores foraging in open woodlands, open parklands and grasslands, or at the top of the canopy (Drucker et al., 2008; Bocherens and Drucker, 2013).

Oxygen stable isotopic ratios in the skeletal tissues of large mammals essentially reflect those of ingested water. Variation in the isotopic composition of the latter occurs as a result of several geospatial, climatic, and environmental parameters, for instance degree of continentality, altitudinal differences, amount of precipitation, temperature, as well as differences in the hydrological processes of water bodies (for a detailed overview see Pederzani and Britton, 2019). In organisms that acquire water predominantly from drinking, i.e., obligate drinkers, oxygen stable isotopes track primarily the isotopic composition of the local meteoric water (Kohn and Cerling, 2002). In middle and high latitudes, the $\delta^{18}O$— provided by the equation $[(^{18}O/^{16}O)_{sample}/(^{18}O/^{16}O)_{standard} - 1] \times 1000$ —of meteoric water is considered to be mainly associated with surface temperature and local precipitation (Fricke and O'Neil, 1996), where higher $\delta^{18}O$ values are observed in warmer and drier environments but lower values indicate colder or more humid periods (Bocherens and Drucker, 2013; Pederzani and Britton, 2019).

Figure 1: Map showing the location of European sites with available stable isotope data for *Palaeoloxodon antiquus* (made with Natural Earth, naturalearthdata.com).

Systematic excavations at the Middle Pleistocene open-air site Marathousa 1 (MAR-1) in the Megalopolis Basin (Peloponnese, Greece) revealed the partial skeleton of a straight-tusked elephant (*Palaeoloxodon antiquus*). The elephant was found at the base of the find-bearing sedimentary Unit 3 in Area A and is stratigraphically and spatially associated with lithic artefacts, and faunal (ostracods, molluscs, fishes, amphibians, reptiles, birds, mammals) and floral remains (see Harvati et al., 2018; Panagopoulou et al., 2018). The archaeological deposits are dated to ca. 450 ka and are correlated to the glacial Marine Isotope Stage 12 (Doukas et al., 2018; Jacobs et al., 2018; Karkanas et al., 2018; Tourloukis et al., 2018). The elephant skeleton belongs to a male individual with an estimated upper limit of its ontogenetic age between 64–71 years based on the tooth wear of the preserved upper third molars, which is also consistent with the extent of epiphyseal fusion of the skeletal elements (Konidaris et al., 2018). Additionally, the taphonomic study of the elephant's remains revealed cutmarks on some of the skeletal elements, indicating hominin exploitation of the carcass (Konidaris et al., 2018), while the traceological analysis of stone-tools further confirms that they were used in butchering activities (Guibert-Cardin et al., 2022).

In this study, we employ stable isotope analysis on enamel carbonates in order to reconstruct the average diet, and, subsequently, the preferred foraging habitat of the MAR-1 elephant. Since evidence of butchering directly associates the specimen with hominin activity, the resulting paleoenvironmental data can be used to infer the conditions surrounding hominin presence in the Megalopolis Basin. Because only one individual was available for analysis, we compared our results with published isotopic data for *Palaeoloxodon antiquus* from other European Middle Pleistocene localities, namely La Polledrara di Cecanibbio, Casal de' Pazzi (Palombo et al., 2005), and Poggetti Vecchi (Capalbo, 2018) in Italy; Neumark-Nord 1 (Grube et al., 2010), Steinheim an der Murr, and Mauer (Pushkina et al., 2014) in Germany (Fig. 1).

12.2 MATERIALS AND METHODS

We sampled the second distalmost lamella of the right upper third molar. The sample's surface was mechanically cleaned with a diamond-tipped handheld rotary tool to remove cementum and expose the enamel. Subsequently, the first few millimeters of the enamel layer were also removed to avoid contamination (Koch et al., 1997). Multiple samples were drilled perpendicularly across the tooth-growth axis, each yielding approximately 15 mg of enamel powder. Here, we present the average value obtained by analyzing the individual samples, to simulate a bulk-sampling strategy for the sake of comparison with other published records.

Following the pretreatment protocol described by Bocherens et al. (1994) and Koch et al. (1997), 1.35 ml of 2.5% sodium hypochlorite (NaOCl) was added to the sample vials, homogenized with high-speed vibration, and left to react for 24 hours to remove organic matter. Subsequently, the samples were centrifuged at 35000 rounds/minute for 3 minutes, the solution was removed, and the contents were rinsed repeatedly with MilliQ water. Next, a 1M Acetic Acid Buffer solution was added and left to react with the samples for 24 hours, to remove nonstructural carbonates. After the acetic acid buffer was extracted, the samples were rinsed three times with MilliQ H_2O and dried at 35°C for 72 hours. This process produced approximately 3 mg of purified biogenic apatite, which was reacted with concentrated orthophosphoric acid (H_3PO_4) to release CO_2. Stable isotope ratios were then obtained by analyzing the gaseous CO_2 with continuous multi-flow isotope ratio mass spectrometry (IRMS) at the University of Tübingen. Two international standards, IAEA-603 (Interna-

tional Atomic Energy Agency) and NBS-18 (National Bureau of Standards, now National Institute

$$\delta^{j}X = \frac{(^{j}X/^{i}X)_{sample}}{(^{j}X/^{i}X)_{standard}} - 1$$

of Standards and Technology or NIST), as well as three in-house standards were used for calibration. Results are expressed using the standard δ notation:

where ^{j}X is the heavier isotope and ^{i}X is the lighter isotope (Bond and Hobson, 2012). Measured ratios refer to $^{13}C/^{12}C_{VPDB}$ or $^{18}O/^{16}O_{VSMOW}$, wherein VPDB is Vienna Peedee Belemnite and VSMOW is Vienna Standard Mean Ocean Water.

12.3 RESULTS AND DISCUSSION

The mean $\delta^{13}C$ of the structural carbonate from the enamel of the straight-tusked elephant from MAR-1 is –11.2‰ (VPDB). The value falls within the expected range for a diet consisting purely of C_3 vegetation (–19.5‰ – –8.0‰ VPDB) after applying an enrichment factor of 1.5‰ (Koch et al., 2004; Tipple et al., 2010) to account for the difference in Pleistocene atmospheric CO_2 values relative to present day, due to the effects of fossil fuel burning. Furthermore, a mesic habitat consisting of open woodland can be deduced, considering that, in temperate environments, $\delta^{13}C$ values of Pleistocene herbivores lower than ~–14‰ indicate foraging under closed canopy forests, whereas values between –14‰ and –8‰ suggest more open landscapes (Farquhar et al., 1989; Ehleringer and Monson, 1993; Bocherens, 2003; Domingo et al., 2017; Metcalfe, 2021).

Similar results were obtained from the carbon stable isotope analysis of a *Palaeoloxodon antiquus* individual from the Middle Pleistocene site of Poggetti Vecchi (Italy, MIS 7), which yielded an average $\delta^{13}C$ value of –11.05‰ VPDB (Capalbo, 2018). Additionally, the $\delta^{13}C$ value of the MAR-1 specimen falls within the range of $\delta^{13}C$ values (from –13.7‰ to –9.9‰ VPDB) obtained for the straight-tusked elephant population of Casal de' Pazzi (Italy, MIS 7; Palombo et al., 2005). In contrast, results from La Polledrara di Cecanibbio (Italy, MIS 9) demonstrated higher $\delta^{13}C$ values (from –9‰ to –10.9‰ VPDB) (Palombo et al., 2005), suggesting that this population was feeding in a drier environment with more open C_3 vegetation compared to the MAR-1 elephant, and the majority of the specimens from Italy correlated with MIS 7. The $\delta^{13}C$ values of *P. antiquus* specimens from three sites in Germany, namely Neumark-Nord 1 (MIS 5; Grube et al., 2010), Steinheim an der Murr (MIS 11; Pushkina et al., 2014), and Mauer (MIS 15; Pushkina et al., 2014), appear to be lower than those of the MAR-1 specimen (Fig. 2), suggesting more forested and humid environments for the German localities.

With respect to oxygen isotope ratios, the average $\delta^{18}O$ value of the enamel bioapatite for the MAR-1 elephant (+23.5‰ VSMOW) plots lower than those of the Italian *P. antiquus* specimens correlated with MIS 7 and MIS 9, with values ranging between +24.8‰ and +27.6‰ VSMOW (Fig. 2). Higher oxygen isotopic values (+25.5‰ – +28.0‰ VSMOW) were also obtained for the specimens of Neumark-Nord 1 in Germany during MIS 5. However, in juxtaposition with the results obtained for the elephants of Steinheim an der Murr and Mauer, the MAR-1 elephant demonstrates a higher $\delta^{18}O$ value. This likely indicates that the interglacial specimens from La Polledrara, Casal de' Pazzi, and Poggetti Vecchi in Italy, as well as those of Neumark-Nord 1, experienced warmer or more arid climatic conditions compared to the MAR-1 elephant, whereas cooler or more humid conditions characterize the environment of the interglacial populations from Steinheim an der Murr and Mauer in Germany. The influence of continentality may have also contributed in part to this pattern, specifically concerning the comparison of

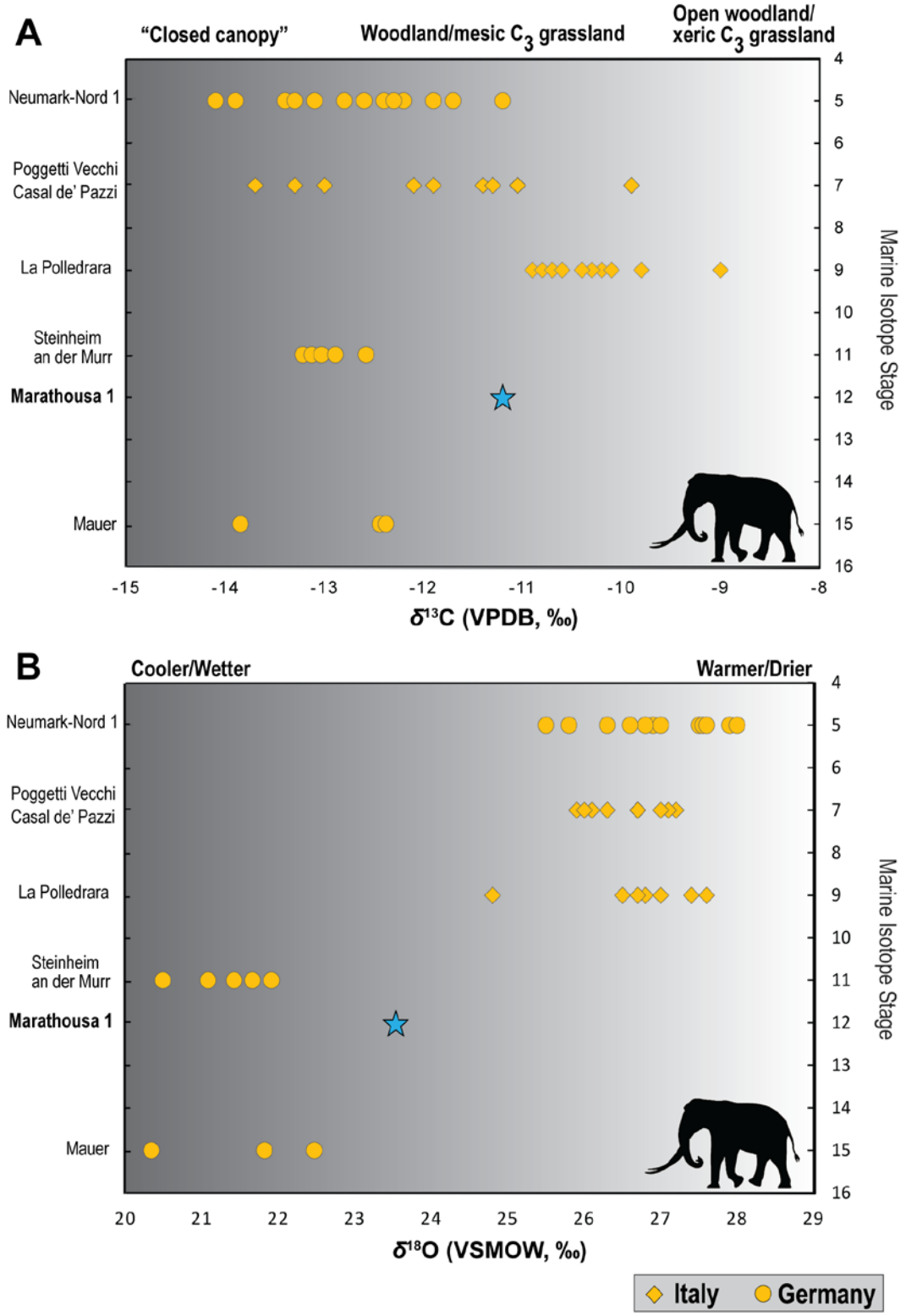

Figure 2: A, mean $\delta^{13}C$ values and B, mean $\delta^{18}O$ values for the straight-tusked elephant (*Palaeoloxodon antiquus*) of Marathousa 1 (MAR-1) compared to published *Palaeoloxodon* isotopic data from other European Middle Pleistocene localities. Marathousa 1 is the single locality correlated with a glacial stage.

the Mediterranean sites with data from Germany, wherein values are expected to become more ^{18}O-depleted as distance from the coast increases.

Overall, the results are compatible with the correlation of the archaeological sequence from MAR-1 with a glacial stage (MIS 12; see also Boni et al., this volume; Butiseacă et al., this volume; Kyrikou et al., this volume), reflecting colder conditions in the eastern European peri-Mediterranean region during glacial stages. Nevertheless, the carbon and oxygen isotopic composition of the studied elephant individual suggests that moderately humid conditions likely persisted in the Megalopolis Basin, which, in turn, supported abundant C_3 vegetation cover. This indicates that the effects of the glaciation in the area were less severe, creating conditions that provided essential subsistence resources to both fauna and hominins, therefore aiding their survival.

CONCLUSIONS

The preliminary results of the stable isotope study on the *Palaeoloxodon antiquus* from the Middle Pleistocene of Marathousa 1 highlight the significance of the method in obtaining important palaeoecological insights from an individual organism with the prospect of addressing broader paleoenvironmental concepts. The present study provides additional support to the hypothesis that the region acted as a refugium for fauna and hominins through the palaeoecological characterization of the individual. Future research will focus on the investigation of intra-tooth isotopic profiles with the aim to obtain temporally high-resolution palaeoecological data and investigate in greater detail potential sources of variation in the isotopic composition of the individual, such as possible seasonal fluctuations in resource availability.

ACKNOWLEDGMENTS

Excavation at Marathousa 1 was conducted under a permit granted to the Ephorate of Palaeoanthropology–Speleology, Hellenic Ministry of Culture. It was supported by the ERC Consolidator Grant ERC-CoG-724703 (“CROSSROADS”) and the ERC Starting Grant ERC-StG-283503 (“PaGE”), both awarded to K.H. G.E.K., V.T. and K.H. are also supported by the Deutsche Forschungsgemeinschaft (DFG Project no. 463225251, “MEGALOPOLIS”). E.R. and K.H. are also supported by the ERC Advanced Grant ERC-AdG-101019659 (“FIRSTSTEPS”). The authors are grateful to the two reviewers, A. Junginger and D. Pushkina, for their insightful comments and suggestions.

REFERENCES

Bender, M.M., 1971. Variations in the $^{13}C/^{12}C$ ratios of plants in relation to the pathway of photosynthetic carbon dioxide fixation. Phytochemistry, 10(6), pp. 1239–1244.

Bocherens, H., 2003. Isotopic biogeochemistry and the palaeoecology of the mammoth steppe fauna. Deinsea, 9(1), pp. 57–76.

Bocherens, H., Fizet, M. and Mariotti, A., 1994. Diet, physiology and ecology of fossil mammals as inferred from stable carbon and nitrogen isotope biogeochemistry: implications for Pleistocene bears. Palaeogeography, Palaeoclimatology, Palaeoecology, 107(3-4), pp. 213–225.

Bocherens, H., Drucker, D.G., 2013. Carbonate stable isotopes | Terrestrial teeth and bones, in: Elias, S. A. and Mock, C. J.(Eds.), Encyclopedia of Quaternary Science (Second Edition). Amsterdam: Elsevier.

Bond, A. L., Hobson, K. A., 2012. Reporting sta-

ble-isotope ratios in ecology: Recommended terminology, guidelines and best practices. Waterbirds, 35(2), pp. 324–331.

Boni, G., Syrides, G., Konidaris, G.E., Athanassiou, A., Tourloukis, V., Koukousioura, O., Panagopoulou, E., Karkanas, P. and Harvati, K., this volume. Preliminary results on the taxonomy and paleoenvironmental analysis of the mollusc fauna from Marathousa 1, Marathousa 2 and Kyparissia 4 (Middle Pleistocene, Megalopolis Basin, Greece).

Butiseacă, G.A., Vaseliev, I., Tourloukis, V., Jungінger, A., Mulch, A., Karkanas, P., Panagopoulou, E. and Harvati, K., this volume. Preliminary biomarker/paleoclimate reconstruction results from the Marathousa 1 Lower Paleolithic site (Megalopolis Basin, Greece).

Capalbo, C., 2018. Multiproxy-based reconstruction of the feeding habits from the late Middle Pleistocene straight-tusked elephant population of Poggetti Vecchi (Southern Tuscany, Italy). Alpine and Mediterranean Quaternary, 31, pp. 113–119.

Cerling, T.E., Harris, J. M., 1999. Carbon isotope fractionation between diet and bioapatite in ungulate mammals and implications for ecological and paleoecological studies. Oecologia, 120, pp. 347–363.

DeNiro, M.J., Epstein, S., 1978. Influence of diet on the distribution of carbon isotopes in animals. Geochimica et Cosmochimica Acta, 42(5), pp. 495–506.

Domingo, L., Rodríguez-Gómez, G., Libano, I. and Gómez-Olivencia, A., 2017. New insights into the Middle Pleistocene paleoecology and paleoenvironment of the Northern Iberian Peninsula (Punta Lucero Quarry site, Biscay): A combined approach using mammalian stable isotope analysis and trophic resource availability modeling. Quaternary Science Reviews, 169, pp. 243–262.

Doukas, C., van Kolfschoten, T., Papayianni, K., Panagopoulou, E. and Harvati, K., 2018. The small mammal fauna from the Palaeolithic site Marathousa 1 (Greece). Quaternary International, 497, pp. 95–107.

Drucker, D. G., Bridault, A., Hobson, K. A., Szuma, E. and Bocherens, H., 2008. Can carbon-13 in large herbivores reflect the canopy effect in temperate and boreal ecosystems? Evidence from modern and ancient ungulates. Palaeogeography, Palaeoclimatology, Palaeoecology, 266(1-2), pp. 69-82.

Ehleringer, J.R., Monson, R.K., 1993. Evolutionary and ecological aspects of photosynthetic pathway variation. Annual Review of Ecology and Systematics, 24, pp. 411–439.

Farquhar, G.D., Ehleringer, J. R. and Hubick, K. T., 1989. Carbon isotope discrimination and photosynthesis. Annual Review of Plant Biology, 40, pp. 503–537.

Fricke, H.C., O'Neil, J. R., 1996. Inter- and intra-tooth variation in the oxygen isotope composition of mammalian tooth enamel phosphate: implications for palaeoclimatological and palaeobiological research. Palaeogeography, Palaeoclimatology, Palaeoecology, 126(1-2), pp. 91–99.

Grube, R., Palombo, M., Iacumin, P. and Di Matteo, A., 2010. What did the fossil elephants from Neumark-Nord eat?, in: Meller H. (Ed.), Elefantenreich. Eine Fossilwelt in Europa. Halle: Landesamt für Denkmalpflege und Archäologie Sachsen-Anhalt, pp. 253–272.

Guibert-Cardin, J., Tourloukis, V., Thompson, N., Panagopoulou, E., Harvati, K., Nicoud, E. and Beyries, S., 2022. The function of small tools in Europe during the Middle Pleistocene: The case of Marathousa 1 (Megalopolis, Greece). Journal of Lithic Studies, 9.

Harvati K., Konidaris G. and Tourloukis V., 2018. Human Evolution at the Gates of Europe, Quaternary International Special Issue, 497, pp. 1–240.

Heaton, T. H., 1999. Spatial, species, and temporal variations in the $^{13}C/^{12}C$ ratios of C_3 plants: implications for palaeodiet studies. Journal of Archaeological Science, 26(6), pp. 637–649.

Hofman-Kamińska, E., Bocherens, H., Borowik, T., Drucker, D. G. and Kowalczyk, R., 2018. Stable isotope signatures of large herbivore foraging habitats across Europe. PLoS ONE, 13, p. e0190723.

Jacobs, Z., Li, B., Karkanas, P., Tourloukis, V., Thompson, N., Panagopoulou, E. and Harvati, K., 2018. Optical dating of K-feldspar grains from Middle Pleistocene lacustrine sediment at Marathousa 1 (Greece). Quaternary International, 497, pp. 170–177.

Karkanas, P., Tourloukis, V., Thompson, N., Giusti, D., Panagopoulou, E. and Harvati, K., 2018. Sedimentology and micromorphology of the Lower Palaeolithic lakeshore site Marathousa 1, Megalopolis Basin, Greece. Quaternary International, 497, pp. 123–136.

Koch, P. L., Tuross, N. and Fogel, M.L., 1997. The effects of sample treatment and diagenesis on the isotopic integrity of carbonate in biogenic hydroxylapatite. Journal of Archaeological Science, 24(5), pp. 417–429.

Koch, P.L., Diffenbaugh, N. S. and Hoppe, K. A., 2004. The effects of late Quaternary climate and pCO_2 change on C_4 plant abundance in the south-central United States. Palaeogeography, Palaeoclimatology, Palaeoecology, 207(3-4), pp. 331–357.

Kohn, M.J., 2010. Carbon isotope compositions of terrestrial C_3 plants as indicators of (paleo) ecology and (paleo)climate. Proceedings of the National Academy of Sciences, 107(46), pp. 19691–19695.

Kohn, M.J., Cerling, T. E., 2002. Stable isotope compositions of biological apatite. Reviews in Mineralogy and Geochemistry, 48(1), pp. 455–488.

Konidaris, G.E., Athanassiou, A., Tourloukis, V., Thompson, N., Giusti, D., Panagopoulou, E. and Harvati, K., 2018. The skeleton of a straight-tusked elephant (*Palaeoloxodon antiquus*) and other large mammals from the Middle Pleistocene butchering locality Marathousa 1 (Megalopolis Basin, Greece): preliminary results. Quaternary International, 497, pp. 65–84.

Kyrikou, S., Marinova, E., Bludau, I. J. E., Karkanas, P., Panagopoulou, E., Tourloukis, V., Junginger, A. and Harvati, K., this volume. The Middle Pleistocene MIS 12 palynological record from Marathousa palaeolake in Southern Greece: Highlighting favourable conditions in Marathousa 1 (MAR-1) refugial region during the severe glacial period.

Metcalfe, J.Z., 2021. C_3 plant isotopic variability in a boreal mixed woodland: implications for bison and other herbivores. PeerJ, 9, p. e12167.

Palombo, M.R., Filippi, M.L., Iacumin, P., Longinelli, A., Barbieri, M. and Maras, A., 2005. Coupling tooth microwear and stable isotope analyses for palaeodiet reconstruction: the case study of late Middle Pleistocene *Elephas* (*Palaeoloxodon*) *antiquus* teeth from Central Italy (Rome area). Quaternary International, 126, pp. 153–170.

Panagopoulou, E., Tourloukis, V., Thompson, N., Konidaris, G., Athanassiou, A., Giusti, D., Tsartsidou, G., Karkanas, P. and Harvati, K., 2018. The Lower Palaeolithic site of Marathousa 1, Megalopolis, Greece: overview of the evidence. Quaternary International, 497, pp. 33–46.

Passey, B.H., Robinson, T.F., Ayliffe, L.K., Cerling, T.E., Sponheimer, M., Dearing, M.D., Roeder, B.L. and Ehleringer, J. R., 2005. Car-

bon isotope fractionation between diet, breath CO_2, and bioapatite in different mammals. Journal of Archaeological Science, 32(10), pp. 1459–1470.

Pederzani, S., Britton, K., 2019. Oxygen isotopes in bioarchaeology: Principles and applications, challenges and opportunities. Earth-Science Reviews, 188, pp. 77–107.

Pushkina, D., Bocherens, H. and Ziegler, R., 2014. Unexpected palaeoecological features of the Middle and Late Pleistocene large herbivores in southwestern Germany revealed by stable isotopic abundances in tooth enamel. Quaternary International, 339–340, pp. 164–178.

Tipple, B.J., Meyers, S.R. and Pagani, M., 2010. Carbon isotope ratio of Cenozoic CO_2: A comparative evaluation of available geochemical proxies. Paleoceanography, 25(3), pp. PA3202.

Tourloukis, V., Muttoni, G., Karkanas, P., Monesi, E., Scardia, G., Panagopoulou, E. and Harvati, K., 2018. Magnetostratigraphic and chronostratigraphic constraints on the Marathousa 1 Lower Palaeolithic site and the Middle Pleistocene deposits of the Megalopolis Basin, Greece. Quaternary International, 497, pp. 154–169.

van der Merwe, N.J., Medina, E., 1991. The canopy effect, carbon isotope ratios and foodwebs in Amazonia. Journal of Archaeological Science, 18(3), pp. 249–259.

13 THE MIDDLE PLEISTOCENE MIS 12 PALYNOLOGICAL RECORD FROM MARATHOUSA PALAEOLAKE IN SOUTHERN GREECE: HIGHLIGHTING FAVOURABLE CONDITIONS IN MARATHOUSA 1 (MAR-1) REFUGIAL REGION DURING THE SEVERE GLACIAL PERIOD

Styliani Kyrikou[1,2,*], Elena Marinova[3], Ines J. E. Bludau[2,4], Panagiotis Karkanas[6], Eleni Panagopoulou[7], Vangelis Tourloukis[1,8], Annett Junginger[2,4], Katerina Harvati[1,2,4,5]

[1]*Paleoanthropology, Institute for Archaeological Sciences, Eberhard Karls University of Tübingen, Tübingen, Germany*
[2]*Department of Geosciences, Eberhard Karls University of Tübingen, Tübingen, Germany*
[3]*Laboratory for Archaeobotany Baden-Württemberg State Office for Cultural Heritage, Hemmenhofen, Germany*
[4]*Senckenberg Centre for Human Evolution and Palaeoenvironment, Tübingen, Germany*
[5]*DFG Centre for Advanced Studies 'Words, Bones, Genes, Tools', Eberhard Karls University of Tübingen, Tübingen, German*
[6]*M.H. Wiener Laboratory for Archaeological Science, American School of Classical Studies at Athens, Athens, Greece*
[7]*Hellenic Ministry of Culture, Ephorate of Paleoanthropology–Speleology, Athens, Greece*
[8]*Department of History and Archaeology, University of Ioannina, Ioannina, Greece*

**styliani.kyrikou@uni-tuebingen.de*

http://dx.doi.org/10.15496/publikation-97658

Keywords: palynological analysis; southern Greece; Megalopolis Basin; MIS 12; Middle Pleistocene

13.1 INTRODUCTION

Regarded as one of the refugial regions of the Mediterranean basin during the glacial periods of the Quaternary in terms of the long-term persistence of plants (e.g., Médail and Diadema 2009; Tzedakis et al., 2006), Greece would have provided the needed ecological conditions to sustain high biodiversity of plants and animals, and thus abundant resources for human populations. Furthermore, the geographic position of Greece lies directly on a major dispersal route connecting Eurasia and Africa (e.g., Harvati et al., 2009; Harvati, 2016; 2022; Tourloukis and Karkanas, 2012). These geographic and ecological conditions suggest a long and continuous presence of early humans in the region (e.g., Harvati and Tourloukis, 2013; Harvati and Roksandic, 2016). Although the paleoanthropological record is relatively poor due to historical research biases —focusing on later archaeological periods— recent work has begun to uncover important new evidence on the early human presence in Greece.

The stratified Middle Pleistocene site Mar-

S. Kyrikou: https://orcid.org/0009-0000-8199-1317
E. Marinova: https://orcid.org/0000-0003-3793-3317
I. Bludau: https://orcid.org/0000-0002-0876-9012
P. Karkanas: https://orcid.org/0000-0002-7156-671X
E. Panagopoulou: https://orcid.org/0000-0002-4268-6157
V. Tourloukis: https://orcid.org/0000-0002-9527-2708
A. Junginger: https://orcid.org/0000-0003-3486-0888
K. Harvati: https://orcid.org/0000-0001-5998-4794

athousa 1 (hereafter MAR-1) was discovered by a joint team from the Ephorate of Paleoanthropology and Speleology (EPS), Hellenic Ministry of Culture, and the Paleoanthropology working group of the University of Tübingen during the 2013 paleoanthropological survey of the PaGE project (‚Paleoanthropology at the Gates of Europe') in the Megalopolis Basin (Peloponnese, southern Greece; Thompson et al., 2018). The site was subsequently excavated from 2014 to 2019 under the auspices of the EPS in the framework of the ERC projects PaGE and CROSSROADS. It has yielded >1000 stratified lithic artifacts (Tourloukis et al., 2018b), some of them preserving use-wear associated with butchering activities (Guibert-Cardin et al., this volume), associated with large mammal bones, including cut-marked specimens (Konidaris et al., 2018, 2022) and other faunal (Doukas et al., 2018; Michailidis et al., 2018; Vlachos et al., this volume) and paleobotanical remains (Field et al., 2018). These rich finds indicate human activities at MAR-1 during the Middle Pleistocene period spanning the glacial period that corresponds to the Marine Isotope Stage (MIS) 12 (Jacobs et al., 2018; Jacobs et al., this volume; Tourloukis et al., 2018a).

So far, the limited evidence concerning the vegetation and climatically forced plant population changes (Field et al., 2018; Nickel et al., 1996; Okuda et al., 2002) at the time of deposition of the excavated MAR-1 assemblages constrains our knowledge of the paleoenvironmental setting that sustained the Megalopolis ecosystem during the course of one of the most severe glacials (MIS 12) of the Quaternary (e.g., Koutsodendris et al., 2019; McManus et al., 1999; Naafs et al., 2014). Pollen records are considered a powerful tool for recognizing and studying refugial sites (e.g., Keppel et al., 2012 and references therein), allowing the inference of the diachronic shifts in past environmental conditions and biodiversity. Their analysis can potentially furnish a continuous record of the vegetation components (pollen species/taxa) within a specific geographic area. The long-term persistence of plant taxa (over millennia) under unstable climate conditions shows *in situ* refugia (e.g., Keppel et al., 2012; Médail and Diadema, 2009). A previously published, high-resolution pollen record from western Greece demonstrates the continuous presence of temperate tree taxa withstanding recurrent glacials through the Quaternary (Tzedakis et al., 2002). Under this perspective, the Quaternary pollen data from our study area (MAR-1) in southern Greece can furnish important insights concerning the continuous persistence or diminishing of temperate tree populations during the course of MIS 12, thereby indicating the potential for their survival (or not), as well as for other organisms related to their ecosystem at that time.

To better understand the mechanisms of MAR-1´s dynamic paleoenvironment (e.g., Bludau et al., 2021; Karkanas et al., 2018), we performed a detailed palynological analysis of a profile from the excavated Area B at the MAR-1 site, covering the lithological units from UB9 to 1 and spanning approximately the period from ~480 to ~420 ka (according to the age model proposed by Tourloukis et al., 2018a). The scope of this study is to highlight first-order trends of the plant communities within the Megalopolis catchment as well as vegetation responses to short-term climatic oscillations, with a particular emphasis on the fossiliferous and archeological horizon shortly before, during the course and after the hominin activity within the area. The palynological analysis, in conjunction with lake level reconstruction and sedimentological interpretations, can shed light on the local paleoenvironmental conditions that shaped the Megalopolis ecosystem, thus making an important contribution to the study of the site.

13.2 STUDY AREA

The sedimentary sequence (MAR-1) is situated in the northwest part of the Marathousa coal mine (37° 24' 31.6"N, 22° 05' 29.01"E at 350 m a.s.l.; Thompson et al., 2018) within the Megalopolis Basin, located in central Peloponnese, Southern Greece (Fig. 1). The studied profile is 7 m long and subdivided into ten lithological units (hereafter UB) (Karkanas et al., 2018). It is bounded by two lignite seams (LG), i.e., LGII (UB10) and LGIII (UB1), while the rest units from UB9 to 2 consist of lacustrine and fluviolacustrine clastic deposits (silts, sands, clays and lignitic clays) (e.g., Bludau et al., 2021; Karkanas et al., 2018). In the middle part of the sequence, the unit UB6 appears to be eroded laterally in some parts of the site. The sedimentological analysis attributes this erosional event most possibly to a localized character (Karkanas et al., 2018).

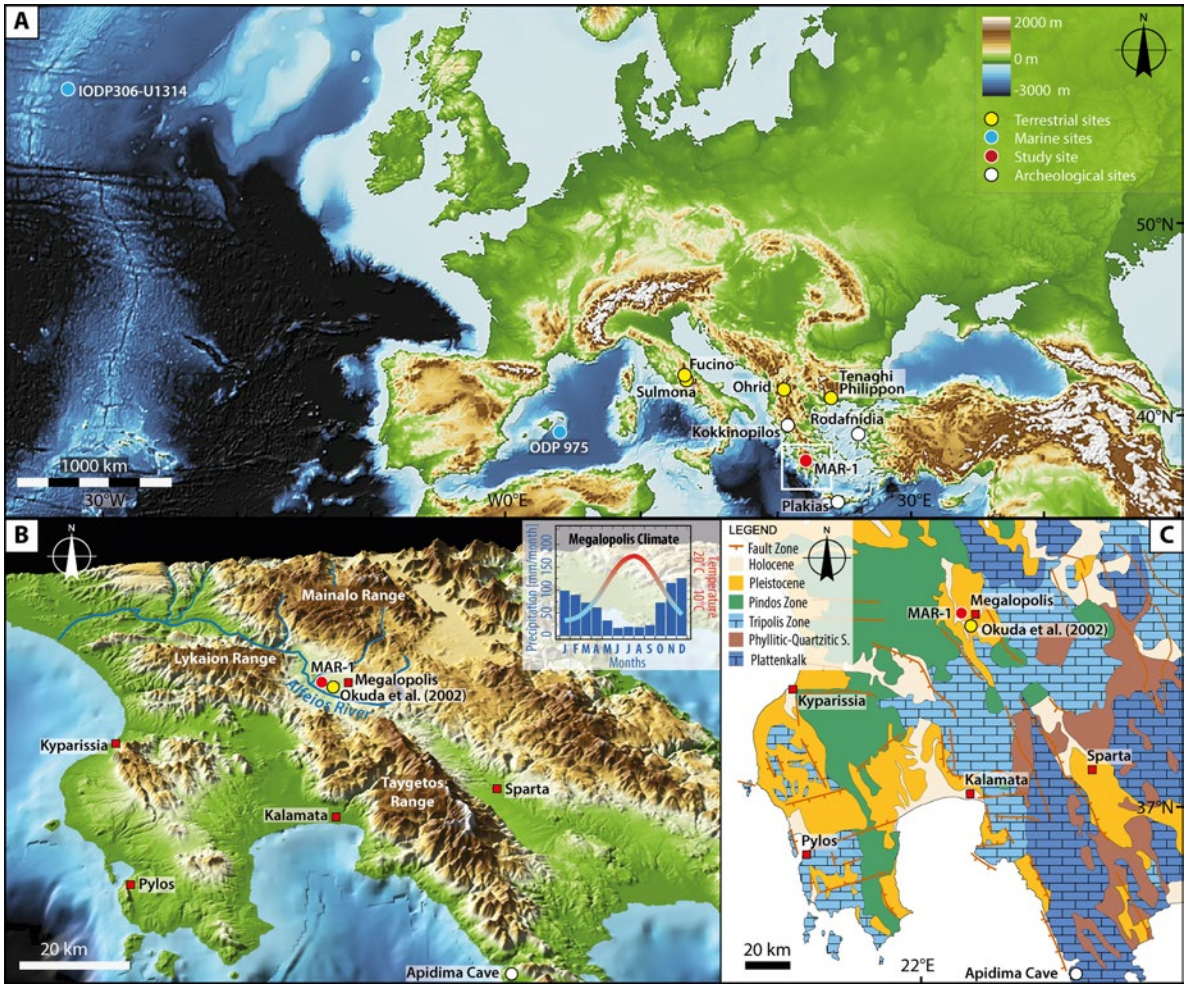

Figure 1: Geographical and geological position of the Megalopolis Basin and Marathousa 1 (MAR-1) site [modified from Bludau et al. (2021)]. (A) Overview map of Europe and North Atlantic with references sites from the Mediterranean region and North Atlantic (Bludau et al., 2021 and references therein). Red dot shows the location of MAR-1. (B) Geographical map of SW Peloponnese showing the location of the Megalopolis Basin (red square), different coring sites of MAR-1 (red dot, present study) and Okuda et al. (2002) (yellow dot) within the basin, and surrounding area. Megalopolis is an intramontane basin surrounded by the mountains Lykaion to the west (1421 m a.s.l.), Mainalo (1981 m a.s.l.) to the east and the mountain range of Taygetos to the south (2404 m a.s.l.). (C) Geological map of SW Peloponnese. Megalopolis is a half-graben basin NNW-SSE oriented by Pleistocene secondary faults. It was formed on a Mesozoic-Palaeogene basement of the central Peloponnese and filled with Pliocene-Pleistocene fluvial and lacustrine sediments (Karkanas et al., 2018 and references therein).

The modern climate of the site is typically Mediterranean, characterized by hot and dry summers, while winters are wetter and milder. The mean annual precipitation rates range between 750–1000 mm (Okuda et al., 2002). The present-day flora of Peloponnese at low and mid altitudes (0-1200 m) comprises Mediterranean vegetation with *Pinus halepensis* forming stands near the sea. Further inland, the vegetation is characterized by maquis ecosystems, which mainly consist of evergreen shrubs and trees (such as *Olea, Ceratonia, Juniperus phoenica, Quercus coccifera, Q. ilex, Pinus halepensis, Phillyrea latifolia, Pistacia terebinthus, P. lentiscus, Calicotome villosa, Myrtus communis,* etc.) and mixed deciduous forests (e.g., *Carpinus orientalis, Ostrya carpinifolia, Quercus pubescens, Celtis australis, Acer, Sorbus domestica*) situated on the higher altitudes within this zone. At higher elevations (>~ 900 to 1800 m), the dominant Greek silver fir (*Abies cephalonica*) forms montane forests, while the lower slopes (~1300-1600 m) are covered by dense forests of the Black Pine (*Pinus nigra* subsp. *pallasiana*) (Polunin, 1980).

13.3 MATERIALS AND METHODS

A 7-meter profile was obtained three meters north of Area B at the MAR-1 site during the field seasons in 2017 and 2018 (see Karkanas et al., 2018 for further details). For the scope of the study, 56 pollen samples were analyzed with a sampling resolution ranging from 5 to 15 cm. For palynological analysis, 3 grams of dry sediment mass were processed for each sample. The processing was carried out using the standard pollen analytical methods modified by Fægri and Iversen (1989). The steps included adding of two tablets of *Lycopodium* spores (Batch No.1031/20484 spores/tablet) in each sample, chemical treatment with cold HCL (10%), KOH (10%) and cold HF (40%), acetolysis, and sieving through 250 μm and 10 μm sieves. Residues were stored and mounted in glycerin jelly.

Microscopic analysis was performed using a transmitted-light microscope at x400 magnification. Pollen and spore identifications were based on Beug (2004), Reille (1992), Chester and Raine (2001), and the Northwest European Pollen Flora (Blackmore et al., 2003; Clarke et al., 1991; Punt et al., 1991; 2009; van Benthem et al., 1984), while the identification of non-pollen palynomorphs (NPPs) was based on van Geel et al. (1981). Concerning the identification of the highly local (aquatic) vegetation, Poaceae pollen is assembled into two groups according to the grains' size (Beug, 2004; Joly et al., 2007); namely the former group, i.e., Wild Grasses encompasses all grains having a diameter greater than 37 μm, whereas grains smaller than that are assigned into the group of *Phragmites australis*. *Typha* species (*T. angustifolia* and *T. latifolia*) and *Sparganium* were identified according to the roundness and diameter of pollen grains (Beug, 2004; Finkelstein, 2003).

Palynomorphs and NPPs were examined in each pollen slide, and a minimum of 500 pollen grains were registered per sample. The relative abundances of pollen taxa were calculated based on the total pollen sum (PS), excluding spores and aquatic taxa. The percentages of aquatic pollen taxa (see Fig. 2, groups of emergent, submerged, and floating-leaved) were calculated on the basis of the total pollen sum (PS) plus the sum of aquatic pollen taxa (AS), (PS+AS). For the pollen percentage diagram, data were plotted using the TILIA 2.4 software (Grimm, 1992). Pollen assemblage zones are supported via stratigraphically constrained cluster analysis using the CONISS software (Grimm, 1987); the zones are labelled with the prefix MARPZ (MARathousa Palynological Zone) and numbered from the bottom to the top of the sequence.

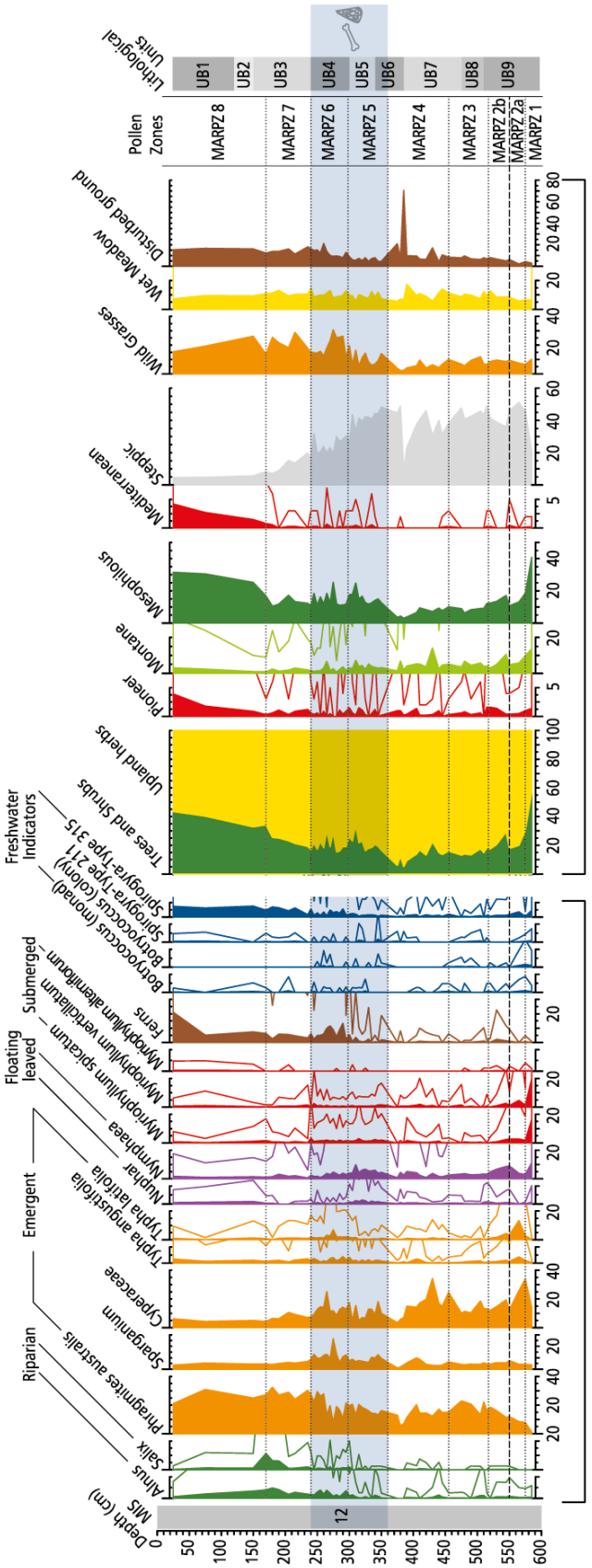

Figure 2: Percentage (%) pollen diagram, plotted against depth (cm). The horizontal dotted lines separate the diagram into zones based on the pollen assemblages. The pollen assemblage zones are numbered from the bottom to the top with the prefix MARPZ, and next to them are shown the corresponding lithological units with the prefix UB. The horizontal dashed line at the bottom of the diagram separates MARPZ 2 into two subzones. The light blue band indicates the archeological horizon. The left-hand side of the diagram shows the local (aquatic) vegetation of the MAR-1 site; the pollen taxa are grouped according to their habitat: Riparian (shown in green color), Emergent (orange color), Floating-leaved (purple color), Submerged (red color); the NPPs group Freshwater indicators (shown in blue color). On the right-hand side, the diagram illustrates selected ecological groups of the broader catchment: Pioneer (*Juniperus, Hippophae ramnoides, Ephedra fragilis, Ephedra distahya*, Ericaceae, *Corylus*), Montane (*Abies, Betula*), Mesophilous (*Quercus robur, Quercus cerris, Ulmus, Zelkova, Humulus, Tilia, Carpinus betulus, Acer, Ostrya, Sorbus-Type, Liquidambar*), Mediterranean (*Olea, Phillyrea, Pistacia lentiscus, Quercus ilex*), Steppic (*Artemisia*, Amaranthaceae, Caryophyllaceae), Wild Grasses (Poaceae), Wet meadow (*Mentha-Type*, Scrophulariaceae, *Filipendula, Lythrum-Type*, Fabaceae, *Papaver rhoeas, Potentilla, Gallium, Anthemis, Valeriana officinalis, Lysimachia vulgaris*), Disturbed Ground (*Polygonum aviculare, Ranunculus acris-Type, Plantago lanceolata, Plantago coronopus, Cirsium, Rumex-Type, Urtica doica, Urtica pilulifera*).

13.4 RESULTS

Pollen preservation in the clastic sequence (mainly UB8–UB6) was moderate, with ample grains appearing to a higher deterioration degree, albeit without inhibiting their identification; the preservation in organic-rich layers (UB9, UB5–UB1) was overall good.

The results of the palynological analysis of the MAR-1 pollen record are presented in Figure 2. Overall, the pollen assemblages document the predominance of open vegetation in the catchment area of Megalopolis for most of the studied interval, corresponding to MIS 12 (Bludau et al., 2021; Tourloukis et al., 2018a). More specifically, pollen abundances show three long-term vegetation changes: a) in MARPZ 1 (lower half of UB9) arboreal pollen (AP) accounts for over 50% of the total terrestrial taxa (mainly represented by mesophilous and montane taxa exhibiting mean values of ~30% and ~12%, respectively); this documents the presence of woodlands in the surroundings of the Megalopolis Basin, next b) in-between MARPZ 2 and MARPZ 7 (upper half of UB9–lower half of UB3) the tree-pollen taxa range from 35% to 13%, reflecting the development of open vegetation communities; specifically, steppic taxa predominate the assemblages in-between MARPZ 2–MARPZ 5, reaching a mean of ~40%, whereas from MARPZ 6 upwards, they become replaced mainly by poaceous taxa (i.e., Wild grasses, ~21%), and c) at the uppermost part of the sequence, in MARPZ 8 (upper half of UB3–UB1,) AP values reach over 40% in total; these tree-pollen abundances indicate a moderate expansion of open woodlands in the surroundings of the basin. The most common tree taxa of MARPZ 8 comprise mesophilous taxa (~26% mean); Mediterranean and pioneer taxa slightly increase by 2.5% and ~2% on average, respectively, compared to the underlying pollen assemblages. Superimposed on the long-term vegetation changes, three short-term positive shifts of tree-pollen taxa are recorded throughout the clastic unit, with the first having been recorded in MARPZ 2b (upper half of UB9) and the other two shifts falling within the archeological horizon in MARPZ 5 and MARPZ 6, respectively, each representing ~30% (on average) of the total terrestrial vegetation (Fig. 2).

Concerning the local (aquatic) vegetation, the highest abundances of aquatic-pollen taxa (i.e., emergent, floating-leaved, and submerged) (~70% max) are documented at the lowermost part of the sequence in MARPZ 1. The most thriving taxon in this assemblage constitutes *Myriophyllum* (i.e., submerged taxa; Fig. 2), with its species *M. verticillatum* and *M. spicatum* reaching their highest abundances in the entire sequence, while they considerably drop in the overlying lithological units (upper half of UB9–UB1). The emergent taxa dominate the aquatic pollen assemblages from MARPZ 2 to MARPZ 8, with Cyperaceae pollen holding its higher abundances in-between MARPZ 2 and MARPZ 4 (upper half of UB9–UB6). In contrast, *Phragmites australis* becomes the thriving species from MARPZ 6 upwards. The assemblages falling within the archeological horizon (i.e., MARPZ 5–MARPZ 6) are marked by a short-term increase in the abundances of floating-leaved taxa, mainly of *Nymphaea* that exhibits ~10% on average, followed by a slight increase of *Nuphar* (Fig. 2). The submerged taxa appear also increased, albeit reaching lower abundances compared to MARPZ 1. Regarding emergent taxa, *Phragmites australis* and Cyperaceae comprise the most common taxa among them; the abundances of *Typha* spp. and *Sparganium* show a slight increase.

13.5 DISCUSSION

Overall, the long-term vegetation pattern of the MAR-1 pollen record reflects an open plant landscape dominated by drought-tolerant herb com-

munities (steppic taxa; Fig. 2), with limited forest cover represented by few scattered mesophilous trees growing in the surrounding of the Megalopolis Basin. This vegetation composition indicates dry and cold conditions during the studied interval (MIS 12), particularly between MARPZ 2 and MARPZ 7 (upper half of UB9–lower half of UB3). Previous investigations conducted on the fossil record and sediments from MAR-1 confirm harsh climatic conditions during the deposition of the corresponding lithological units (UB9–UB3) of the sequence (e.g., Bludau et al., 2021; Field et al., 2018; Karkanas et al., 2018). However, at the same time, when open vegetation formations (mainly xerophytic grasslands) predominated the plant landscape, the vegetation was also influenced by short-term positive climate shifts during the glacial period of MIS 12 (see §13.4). Moderate enhancements of mesophilous tree taxa —with the most prominent documented within the archeological horizon (MARPZ 5, Fig. 2)— evidence open deciduous woodlands occurring at low and mid-elevations around the basin. These temporal changes in tree cover suggest a climate variability during the deposition of UB5 and UB4, with a shift towards milder (i.e., increased temperatures) and wetter (i.e., sufficient moisture availability for tree growth) conditions within the basin. In addition, the replacement of steppe/xerophytic elements (*Artemisia*, Amaranthaceae, Caryophyllaceae) by wild grasses and other mesic non-woody taxa (e.g., Poaceae, *Mentha*, *Filipendula*, *Lythrum*-Type, Fabaceae, *Gallium*, *Plantago lanceolata*, *P. coronopus*) in MARPZ 6 (UB4; Fig. 2) confirms climate improvement (increasing humidity) at the area during that period. This palynological evidence is supported by paleobotanical and element data from the MAR-1 sequence. Specifically, warm conditions are inferred by the increased presence of phytoliths from Chloridoids grasses —known for growing in warm, open grasslands— in the corresponding sediments (Field et al., 2018). Moreover, a short-lived increase of Rb/Sr ratios —a geochemical proxy which is regarded as a precipitation proxy in MAR-1's sediments (Bludau et al., 2021)— recorded in UB5 implies wet conditions, and, thus further corroborating our evidence for a humid climate at that period.

Shortly before the deposition of the archeological horizon, an abrupt decrease in the abundances of all pollen taxa, spores, and NPPs is documented towards the top of MARPZ 4 (boundary between UB7 and UB6). An exception is the concurrent, sharp increase in the values of disturbed ground pollen taxa (Fig. 2). This evidence suggests that the dramatic drop of the proxies is rather associated with the depositional regime of the MAR-1 sequence (see for further details in §13.2; and Karkanas et al., 2018) than climate change. The hypothesis for a variable environment during the deposition of UB7 and UB6 is also argued by Bludau et al. (2021), who documented a sharp drop in the values of all geochemical and biological proxies.

From MARPZ 8 upwards (upper half of UB3–UB1), the steady increase of mesophilous tree taxa is accompanied by a slight rise of thermophilous Mediterranean ones, reflecting the gradual development of open mixed deciduous woodlands growing at low and mid-altitudes in the Megalopolis catchment. This evidence implies climate amelioration with a shift towards warmer conditions. Such prevailing climate is also argued by Field et al. (2018), who infer warm conditions based on phytolith data, specifically the Chloridoids short grasses documented in UB2 and the upper lignite unit UB1 of the MAR-1 sequence.

Focusing on the strongly local vegetation of MAR-1, the so-called azonal vegetation, the wetland plants —known as reeds, sedges, and cattails (emergent group, Fig. 2)— are constantly present throughout the pollen record, indicating the presence of marshes along the paleolake shoreline. *Phragmites australis*, the common reed, consti-

tutes the most prominent element of the marshy vegetation, particularly from MARPZ 6 upwards (UB4–UB1). Furthermore, an enhanced abundance of floating-leaved and submerged taxa (e.g., *Nymphaea*, *Myriophyllum* spp.) documented between MARPZ 5 and MARPZ 6 (archeological horizon, UB6–UB4, Fig. 2) shows the existence of a stagnant, shallow water environment, with a water depth reaching up to 2 meters (Dimopoulos et al., 2005) and possibly having been unaffected by high-energy flows. In addition to this, relative meso- to eutrophic conditions are also implied for MAR-1 paleolake owing to the increasing abundance of green algae *Spirogyra*-Type 315 (van Geel et al., 1981) and *Botryococcus* (e.g., Shumilovskikh et al., 2021). Such paleoenvironmental conditions agree with previously published studies conducted on the MAR-1 sedimentary sequence (Bludau et al., 2021; Field et al., 2018), suggesting the presence of a shallow freshwater lake/pond environment with low suspended sediment in Marathousa 1 at that time.

Towards the boundary between MARPZ 7 and MARPZ 8 (upper half of UB3), a prominent increase of riparian trees, mainly of willows (*Salix*), points to wetter conditions at the site, given that moist soils are a prerequisite for their growth. Damp ground is also implied by the synchronous rise of alders (*Alnus*). Wetter conditions are further supported by increased Rb/Sr ratios recorded in the corresponding sediments (Bludau et al., 2021). In contrast, a shift in the floristic composition of MAR-1's azonal vegetation is documented in the uppermost palynological assemblage (MARPZ 8/ upper half of UB3–UB1). More specifically, the previous alluvial woodland has turned into an open area where sparse patches of riparian trees grow adjacent to the reed marsh in the littoral zone of the paleolake. This vegetation change was influenced to a certain extent by dry conditions (decreased Rb/Sr ratios, Bludau et al., 2021). Furthermore, the floating-leaved and submerged vegetation appears to have decreased from MARPZ 7 upwards (UB3–UB1). Nonetheless, in this case, this decrease was likely affected by the lake-water environment. Indeed, increasing abundances of freshwater indicators (i.e., Spirogyra-Type 315; Fig. 2) have been recorded since MARPZ 6 (UB4), reflecting the growth of algal blooms in MAR-1 paleolake. This evidence implies eutrophic conditions in the water, which are known for negatively affecting the vegetation growing inside the water (e.g., Dong et al., 2014). The hypothesis of eutrophication in the lake-water environment is strengthened by geochemical and biological data from the MAR-1 sequence. Specifically, anoxic conditions deduced by decreased Mn/Fe ratios (a proxy of oxygenation in MAR-1's sediments) as well as the absence of aquatic microfossils in the respecting deposits (Bludau et al., 2021) corroborate the notion of eutrophic waters at that time.

13.6 CONCLUSIONS

This study presents the first palynological record of the Lower Palaeolithic Marathousa 1 site, spanning the glacial period of MIS 12. It provides a concise overview of the vegetation development and the climatically forced population changes within the basin during one of the most intense glaciations of the Quaternary. Overall, our pollen dataset shows an open plant landscape in the surroundings of the Megalopolis Basin dominated by herbaceous vegetation. Woodlands dramatically decrease already from the lowermost part of the sequence (boundary MARPZ 1–MARPZ 2/UB9) and become replaced by xerophytic grasslands predominating the landscape until MARPZ 5 (middle part of MAR-1 sequence; UB5–UB6), indicating cold and dry conditions at that period. Short-term positive shifts of tree populations are also recorded within the same sedimentary deposits (i.e., upper half of UB9–UB4; MARPZ 2–MARPZ 6), implying

temporarily milder and wetter conditions. Towards the uppermost part of the record (MARPZ 8), the slow but steady redevelopment of open woodlands in the surroundings of the basin was possibly favored by a climatic amelioration, mainly warmer conditions.

During the time of the deposition of the fossiliferous and archeological layers (i.e., UB5–UB4/ MARPZ 5–MARPZ 6), the pollen assemblages indicate favorable environmental and climate conditions supporting the survival of diverse ecosystems during MIS 12. Notably, three main vegetation formations are documented in these deposits. Initially, rich marshy vegetation was locally developed on the periphery of the paleolake, and swampy vegetation alongside small streams near the lake. Xeric (MARPZ 5) to mesic (MARPZ 6) grasslands represent the second vegetation formation, and the third one consists of open mixed deciduous woodlands, which temporarily occurred at the low and mid altitudes of the Megalopolis Basin. This floristic composition —encompassing various ecosystems within the archaeological horizon (i.e., aquatic, semi-aquatic and terrestrial) (Fig. 2)— would have provided a variety of food sources for living organisms. In addition, the mosaic distribution of the vegetation could have furnished suitable habitats for the survival of diverse wildlife species and hominins, thus rendering MAR-1 an attractive location for organisms to survive during a period that was marked by one of the most extensive glacial phases of the Pleistocene recorded in Southern Greece (Pope et al., 2017).

ACKNOWLEDGMENTS

Excavation at Marathousa 1 was conducted under a permit granted to the Ephorate of Palaeoanthropology-Speleology, Hellenic Ministry of Culture. It was supported by the ERC Consolidator Grant ERC-CoG-724703 (“CROSSROADS”) and the ERC Starting Grant ERC-StG-283503 (“PaGE”), both awarded to K.H. V.T. and K.H. are also supported by the Deutsche Forschungsgemeinschaft (DFG Project no. 463225251, “MEGALOPOLIS”). K.H. is also supported by the ERC Advanced Grant ERC-AdG-101019659 (“FIRST-STEPS”). We thank the two anonymous reviewers for their constructive comments.

REFERENCES

Beug, H.J., 2004. Leitfaden der Pollenbestimmung für Mitteleuropa und angrenzende Gebiete (Guide to the Pollen Analysis for Central Europe and the Adjacent Areas). Pfeil, München.

Blackmore, S., Steinmann, J.A.J., Hoen, P.P. and Punt, W., 2003. Betulaceae and Corylaceae. In The Northwest European Pollen Flora, 65 (ed. by W. Punt & S. Blackmore), pp. 71–98. Elsevier, Amsterdam. (Review of Palaeobotany and Palynology 123).

Bludau, I.J.E., Papadopoulou, P., Iliopoulos, G., Weiss, M., Schnabel, E., Thompson, N., Tourloukis, V., Zachow, C., Kyrikou, S., Konidaris, G.E., Karkanas, P., Panagopoulou, E., Harvati, K. and Junginger, A., 2021. Lake-Level Changes and Their Paleo-Climatic Implications at the MIS12 Lower Paleolithic (Middle Pleistocene) Site Marathousa 1, Greece. Frontiers in Earth Science, 9, 668445.

Chester, P., Raine, J., 2001. Pollen and spore keys for Quaternary deposits in the northern Pindos Mountains, Greece. Grana, 40, pp. 299–387.

Clarke, G.C.S., Punt, W. and Hoen, P.P., 1991. Ranunculaceae. In The north-west European pollen flora VI (ed. by W. Punt & S. Blackmore), pp. 117–271. Elsevier, Amsterdam. (Review of Palaeobotany and Palynology 69).

Dimopoulos, P., Sýkora, K.V., Gilissen, C., Wiecherink, D. and Georgiadis, T., 2005. Vegetation ecology of Kalodiki Fen (NW Greece).

Biologia Bratislava 60, pp. 69-82.

Dong, J., Yang, K., Li, S., Li, G. and Song, L., 2014. Submerged vegetation removal promotes shift of dominant phytoplankton functional groups in a eutrophic lake. Journal of Environmental Sciences, 26 (8), pp. 1699-1707.

Doukas, C., van Kolfschoten, T., Papayianni, K., Panagopoulou, E. and Harvati, K., 2018. The Small Mammal Fauna from the Palaeolithic Site Marathousa 1 (Greece). Quaternary International, 497, pp. 95–107.

Fægri, K., Iversen, J., 1989. Textbook of pollen analysis, (fourth edition). In: Fægri, K., Kaland, P.E., and Krzywinski, K. (Eds.). John Wiley and Sons, Chichester, pp. 328.

Field, M. H., Ntinou, M., Tsartsidou, G., van Berge Henegouwen, D., Risberg, J., Tourloukis, V., Thompson, N., Karkanas, P., Panagopoulou, E. and Harvati, K., 2018. A Palaeoenvironmental Reconstruction (Based on Palaeobotanical Data and Diatoms) of the Middle Pleistocene Elephant (*Palaeoloxodon antiquus*) Butchery Site at Marathousa, Megalopolis, Greece. Quaternary International, 497, pp. 108–122.

Finkelstein, S.A., 2003. Identifying pollen grains of *Typha* latifolia, *Typha* angustifolia, and *Typha* ×glauca. Canadian Journal of Botany, 81, pp. 985–990.

Grimm, E.C., 1987. CONS: a FORTRAN 77 program for stratigraphically constrained cluster analysis by the method of incremental sum of squares. Computers & Geosciences, 13, pp. 13–35.

Grimm, E.C., 1992. TILIA 1.12/TILIAGRAPH 1.18 (software). Illinois State Museum, Spring.

Guibert-Cardin, J., Tourloukis, V., Panagopoulou, E., Harvati, K., Nicoud E. and Beyries, S., this volume. First traceological study of the lithic assemblage from Marathousa 1 and contextualization of the results within the European Lower Palaeolithic.

Harvati, K., 2016. Paleoanthropology in Greece: Recent Findings and Interpretations, in Paleoanthropology of the Balkans and Anatolia: Human Evolution and its Context. Vertebrate Paleobiology and Paleoanthropology Series. Springer, pp. 3–14.

Harvati, K., 2022. The Hominin Fossil Record from Greece. The Fossil Vertebrates of Greece Vol. 1 – Basal Vertebrates, Basal Tetrapods, Afrotherians, Glires, and Primates. Springer – Nature Publishing Group, 18.

Harvati, K., Panagopoulou, E. and Runnels, C., 2009. The Paleoanthropology of Greece. Evolutionary Anthropology,18, pp. 131–143.

Harvati K., Tourloukis V., 2013. Human Evolution in the Southern Balkans. Evolutionary Anthropology, 22, pp. 43–45.

Harvati K, Roksandic, M. (Eds.), 2016. Paleoanthropology of the Balkans and Anatolia: Human Evolution and its Context. Vertebrate Paleobiology and Paleoanthropology Series, Springer: Dordrecht.

Jacobs, Z., Li, B., Karkanas, P., Tourloukis, V., Thompson, N., Panagopoulou, E. and Harvati, K., 2018. Optical Dating of K-Feldspar Grains from Middle Pleistocene Lacustrine Sediment at Marathousa 1 (Greece). Quaternary International, 497, pp. 170–177.

Jacobs, Z., Li, B., O'Gorman, K., Tourloukis, V., Panagopoulou, E., Karkanas, P. and Harvati, K., this volume. Single-grain optical dating of sediment samples from Marathousa 1, Southern Greece.

Joly, C., Laurent, B., Barreau, M., Mancheron, A. and Visset, L., 2007. Grain and annulus diameter as criteria for distinguishing pollen grains of cereals from wild grasses. Review of Palaeobotany and Palynology, 146, pp. 221–233.

Karkanas, P., Tourloukis, V., Thompson, N., Giusti, D., Panagopoulou, E., and Harvati, K., 2018. Sedimentology and Micromorphology of the Lower Palaeolithic Lakeshore Site Mara-

thousa 1, Megalopolis Basin, Greece. Quaternary International, 497, pp. 123–136.

Keppel, G., Van Niel, K. P., Wardell-Johnson, G.W., Yates, C.J., Byrne, M., Mucina L., Schut, A. G.T., Hopper, S.D. and Franklin, S.E., 2012. Refugia: identifying and understanding safe havens for biodiversity under climate change. Global Ecology and Biogeography, 21, pp. 393–404.

Konidaris, G.E., Athanassiou, A., Tourloukis, V., Thompson, N., Giusti, D., Panagopoulou, E. and Harvati K., 2018. The Skeleton of a Straight-Tusked Elephant (*Palaeoloxodon antiquus*) and Other Large Mammals from the Middle Pleistocene Butchering Locality Marathousa 1 (Megalopolis Basin, Greece): Preliminary Results. Quaternary International, 497, pp. 65–84.

Konidaris, G., Athanassiou A., Panagopoulou E. and Harvati K., 2022. First record of *Macaca* (Cercopithecidae, Primates) in the Middle Pleistocene of Greece. Journal of Human Evolution, 162, 103104.

Koutsodendris, A., Kousis, I., Peyron, O., Wagner, B. and Pross, J., 2019. The Marine Isotope Stage 12 pollen record from Lake Ohrid (SE Europe): Investigating short-term climate change under extreme glacial conditions. Quaternary Science Reviews.

McManus, J.F., Oppo, D.W. and Cullen, J.L., 1999. A 0.5-million-year record of millennial-scale climate variability in the North Atlantic. Science, 283, pp. 971–975.

Médail, F., Diadema, K., 2009. Glacial Refugia Influence Plant Diversity Patterns in the Mediterranean Basin. Journal of Biogeography, 36, pp. 1333–1345.

Michailidis, D., Konidaris, G.E., Athanassiou, A., Panagopoulou, E., and Harvati, K., 2018. The Ornithological Remains from Marathousa 1 (Middle Pleistocene; Megalopolis Basin, Greece). Quaternary International, 497, pp. 85–94.

Naafs, B.D.A., Hefter, J. and Stein, R., 2014. Dansgaard-Oeschger forcing of sea surface temperature variability in the midlatitude North Atlantic between 500 and 400 ka (MIS 12). Paleoceanography 29, pp. 1024–1030.

Nickel, B., Riegel, W., Schoenherr, T. and Velitzelos, E., 1996. Environments of coal formation in the Pleistocene lignite at Megalopolis, Peloponnesus (Greece)-reconstructions from palynological and petrological investigations. Neues Jahrbuch Geologie und Paläontologie Abhandlungen Band 200, pp. 201–220.

Okuda, M., van Vugt, N., Nakagawa, T., Ikeya, M., Hayashida, A., Yasuda, Y. and Setoguchi T., 2002. Palynological Evidence for the Astronomical Origin of lignite-detritus Sequence in the Middle Pleistocene Marathousa Member, Megalopolis, SW Greece. Earth and Planetary Science Letters, 201, pp. 143–157.

Polunin, O., 1980. Flowers of Greece and the Balkans, a field guide. Oxford University Press, pp. 28–83.

Pope, R.J., Hughes, P.D. and Skourtsos, E., 2017. Glacial history of Mount Chelmos, Peloponnesus, Greece. Geological Society, London, Special Publications, pp. 211–236.

Punt, W., Bos, J.A.A. and Hoen, P.P., 1991. Oleaceae. In The north-west European pollen flora VI (ed. by W. Punt & S. Blackmore), pp. 23–47. Elsevier, Amsterdam (Review of Palaeobotany and Palynology 69).

Punt, W., Hoen, P.P., 2009. Asteraceae – Asteroideae. In The Northwest European Pollen Flora, 70 (ed. by W. Punt & S. Blackmore), pp. 22–183. Elsevier, Amsterdam (Review of Palaeobotany and Palynology 157).

Reille, M., 1992. Pollen et spores d'europe et d'afrique du nord (Pollen and Spores of Europe and North Africa). Laboratoire de Botanique historique et Palynologie, Marseille.

Shumilovskikh, L., O'Keefe, J. and Marret, F., 2021. An overview of the taxonomic groups of

NPPs. In: Marret, F., O'Keefe, J., Osterloff, P., Pound, M. and Shumilovskikh, L. (Eds.), Applications of Non-Pollen Palynomorphs: from Palaeoenvironmental Reconstructions to Biostratigraphy. Geological Society of London, Special Publications 511, pp. 13-61.

Thompson, N., Tourloukis, V., Panagopoulou, E. and Harvati, K., 2018. In Search of Pleistocene Remains at the Gates of Europe: Directed Surface Survey of the Megalopolis Basin (Greece). Quaternary International, 497, pp. 22–32.

Tourloukis, V., Karkanas, P., 2012. The Middle Pleistocene Archaeological Record of Greece and the Role of the Aegean in Hominin Dispersals: New Data and Interpretations. Quaternary Science Reviews, 43, pp. 1–15.

Tourloukis, V., Muttoni, G., Karkanas, P., Monesi, E., Scardia, G., Panagopoulou, E. and Harvati, K., 2018a. 136. STYLIANI KYRIKOU ET AL. Magnetostratigraphic and Chronostratigraphic Constraints on the Marathousa 1 Lower Palaeolithic Site and the Middle Pleistocene Deposits of the Megalopolis Basin, Greece. Quaternary International, 497, pp. 154–169.

Tourloukis, V., Thompson, N., Panagopoulou, E., Giusti, D., Konidaris, G. E., Karkanas, P. and Harvati, K., 2018b. Lithic Artifacts and Bone Tools from the Lower Palaeolithic Site Marathousa 1, Megalopolis, Greece: Preliminary Results. Quaternary International, 497, pp. 47–64.

Tzedakis, P.C., Lawson, I.T., Frogley, M.R., Hewitt, G.M. and Preece, R.C., 2002. Buffered Tree Population Changes in a Quaternary Refugium: Evolutionary Implications. Science, 297, pp. 2044–2047.

Tzedakis, C., Hooghiemstra, H. and Pälike, H., 2006. The last 1.35 million years at Tenaghi Philippon: revised chronostratigraphy and long-term vegetation trends. Quaternary Science Reviews, 25, pp. 3416–3430.

van Benthem, F., Clarke, G.C.S. and Punt, W., 1984. The Northwest European Pollen Flora, 33. Review of Palaeobotany and Palynology 42, pp. 87–110.

van Geel, B., Bohncke, S.J.P. and Dee, H., 1981. A palaeoecological study of an upper Late Glacial and Holocene sequence from 'De Borchert' (The Netherlands). Review of Palaeobotany and Palynology 31, pp. 367-448.

Vlachos, E., Georgalis, G.L., Konidaris, G.E., Athanassiou, A., Tourloukis, V., Thompson, N., Panagopoulou, E. and Harvati, K., this volume. Preliminary results on the reptiles from the Middle Pleistocene of Marathousa 1, Megalopolis Basin (Greece).

14 PRELIMINARY BIOMARKER/PALEOCLIMATE RECONSTRUCTION RESULTS FROM THE MARATHOUSA 1 LOWER PALEOLITHIC SITE (MEGALOPOLIS BASIN, GREECE)

Geanina-Adriana Butiseacă*[,1], Iuliana Vasiliev[2], Vangelis Tourloukis [1,3,4,5], Annett Junginger[3,4], Andreas Mulch[2,6], Panagiotis Karkanas[7], Eleni Panagopoulou[8], Katerina Harvati [1,3,4]

[1]*Paleoanthropology, Institute for Archaeological Sciences, Eberhard Karls University of Tübingen, Tübingen, Germany*
[2]*Senckenberg Biodiversity and Climate Research Centre (BiK-F), Frankfurt am Main, Germany*
[3]*Senckenberg Centre for Human Evolution and Palaeoenvironment, Tübingen, Germany*
[4]*Department of Geosciences, Eberhard Karls Universität Tübingen, Tübingen, Germany*
[5]*Department of History and Archaeology, School of Philosophy, University of Ioannina, Ioannina, Greece*
[6]*Institute of Geosciences, Goethe University, Frankfurt am Main, Germany*
[7]*M.H. Wiener Laboratory for Archaeological Science, American School of Classical Studies at Athens, Athens, Greece*
[8]*Hellenic Ministry of Culture, Ephorate of Palaeoanthropology–Speleology, Athens, Greece*
**butiseacageanina.@gmail.com*

http://dx.doi.org/10.15496/publikation-97655

Keywords: Lower Palaeolithic; southern Greece; biomarkers; hominin presence; cooling

14.1 INTRODUCTION

The Marathousa 1 (MAR-1) site is located in central Peloponnese, Greece (Fig. 1A), and was discovered in 2013 as part of a targeted, systematic survey in the Megalopolis Basin by a joint team from the Ephorate of Paleoanthropology and Speleology (Hellenic Ministry of Culture) and the Paleoanthropology group of the University of Tübingen (see Panagopoulou et al., 2015, 2018; Harvati et al., 2018). It is one of the few Lower Paleolithic sites in Greece and has been chronologically assigned to the glacial period of Marine Isotope Stage 12 (MIS 12) (Tourloukis et al., 2018b; Jacobs et al., 2018; Blackwell et al., 2018; Bludau et al., 2021). Even if paleoenvironmental suggestions were made by Bludau et al. (2021), the paleoclimatic conditions in the area are not properly constrained yet, making it difficult to assess the MAR-1 evidence in the context of hominin presence in mainland Greece during glacial periods. Here, we perform biomarker analysis to identify changes in the mean air annual temperature (MAAT), paleo-soil pH and organic matter input. Preliminary results from the Marathousa 1 Area B profile (Fig. 1B) indicate major changes affecting southern Greece during the time of hominin presence. Our data show an important cooling episode between ~447 and 444 ka (± 20 ka) (reported dates are based on the age model of Bludau et al., 2021; see Table 1), during the deposition of the clastic sequence, which ends at the stratigraphic level of the

G. Butiseaca: https://orcid.org/0000-0002-1579-1998
I. Vasiliev: https://orcid.org/0000-0002-1024-6966
V. Tourloukis: https://orcid.org/0000-0002-9527-2708
A. Junginger: https://orcid.org/0000-0002-7112-8584
A. Mulch: https://orcid.org/0000-0002-9141-7535
P. Karkanas: https://orcid.org/0000-0002-7156-671X
E. Panagopoulou: https://orcid.org/0000-0002-4268-6157
K. Harvati: https://orcid.org/0000-0001-5998-4794

archaeological horizon (350.25 cm, Table 1), with mean air annual temperatures as low as 4.5 °C. The lowest registered temperature coinciding with the human presence indicates a direct link between the environmental conditions and the hominin presence in Peloponnese. This evidence supports the hypothesis that the local climatic conditions at Marathousa 1 favored the survival of hominins and other animal species during glacial intervals, acting as a climatic and geographic refugium.

14.2 MATERIALS AND METHODS

14.2.1. LIPID EXTRACTION, FRACTIONATION AND ANALYSIS

Thirty-six sedimentary rock samples were collected from the Area B profile, spanning the stratigraphic units UB10-UB1. The samples were dried, weighed and ground using agate mortar and pestle. Lipids were further extracted using a Soxhlet apparatus with a mixture of dichloromethane and methanol 7.5:1 (*v:v*) and pre-extracted cellulose thimbles. Extracts were evaporated to near dryness under N_2 flow using a TurboVap LV. Subsequently elemental sulfur was removed from the total lipid extracts (TLE) using Cu shreds activated using 10% HCl. The vials containing TLE, activated Cu and magnetic rods were placed on a rotary table for >16 hours. Afterwards, the TLEs were filtered over a Na_2SO_4 column. The remaining solvents were evaporated using N_2. The desulphurization step was repeated until no reaction with the Cu was observed. Up to 50% of the TLE was archived while the rest was further separated into fractions containing different lipids using Al_2O_3 column chromatography. The polar fraction containing glycerol dialkyl glycerol tetraether lipids (GDGTs) was dis-

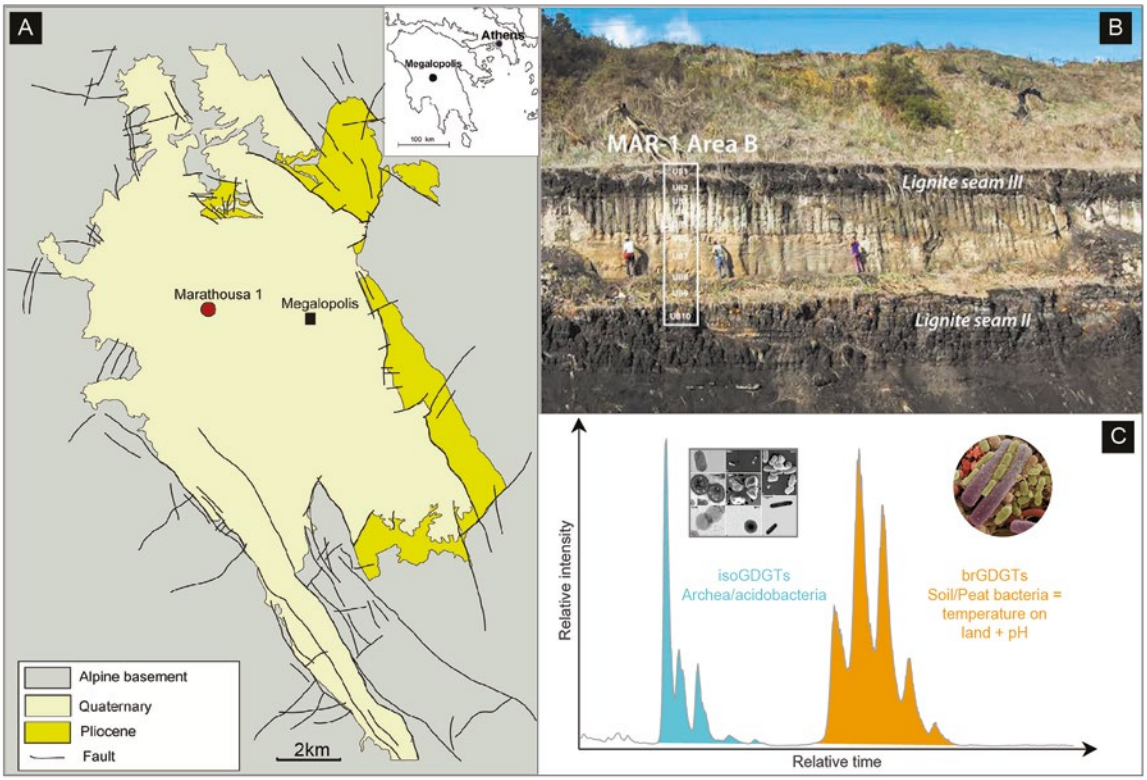

Figure 1: A) Location of the site, after Karkanas et al. (2018); B) Marathousa 1 Area B profile. Modified after Bludau et al. (2021); C) example of a chromatogram with the main glycerol dialkyl glycerol tetraethers (GDGTs) groups.

solved in a 1 mL mixture of *n*-hexane (*n*-hex)/isopropanol (IPA)-(99:1, *v:v*) and slightly dispersed using an ultrasonic bath (~ 30s per sample) and filtered over a 0.45-mm PTFE filter using a 1mL syringe. The polar fraction was measured using an HPLC Shimadzu, UFLC performance, double column; eluents *n*-hex (A) and IPA (B) coupled with an ABSciex 3200 QTrap chemical ionization mass spectrometer (HPLC/APCIeMS) at the Senckenberg Biodiversity and Climate Research Centre (SBiK-F) in Frankfurt am Main, Germany. For each sample, we used a 5 mL injection volume, and GDGTs detection was achieved through single-ion monitoring. Both isoprenoid and branched GDGTs (isoGDGTs and brGDGTs, respectively) were analyzed within a single acquisition run for each sample. Quantification was performed using the Analyst software and the peaks were integrated manually for each sample up to five times, depending on the sample, with a final average value.

14.2.2. MEAN AIR ANNUAL TEMPERATURE CALCULATION (MAAT) AND PALEO- SOIL PH

The continental mean air annual temperature estimations are based on the relative distribution of brGDGT membrane lipids originating in the Megalopolis catchment area (Fig. 1C). For MAAT and soil pH calculation, we used the calibration of de Jonge et al. (2014), where:

MAAT' = 7.17 + (17.8 × GDGT Ia) + (25.9 × GDHT Ib) + (34.4 × GDGT Ic) – (28.6 × GDGT IIa)

pH = 7.15 + 1.59 × CBT'

CBT' (Cyclisation ratio of Branched Tetraethers) is expressed as:

CBT= log10 ((GDGT Ic + GDGT IIa' + GDGT IIb' + GDGT IIc' + GDGT IIIa' + GDGT IIIb' + GDGT IIIc') / (GDGT Ia + GDGT IIa + GDGT IIIa))

where *GDGT I – GDGT III* are brGDGTs.

Root Mean Square Error (RMSE) of the biomarker-based MAAT is ~4.6 °C.

14.2.3. BIT INDEX

The BIT (Branched and Isoprenoid Tetraethers) index defines the terrigenous versus aquatic components of organic input into the basin. The BIT index is the ratio of the three major brGDGTs (mostly terrigenous) to isoGDGT crenarchaeol (aquatic) (Hopmans et al., 2004):

BIT= [(GDGT-I) + (GDGT-II) + (GDGT-III)] /

[(crenarchaeol) + (GDGT-I) + (GDGT-II) + (GDGT-III)]

Crenarchaeol is a compound derived from Thaumarchaeota (Sinninghe Damsté et al., 2002) and is abundant mostly in the water column, although in small percentages it can also occur in soils (Weijers et al., 2007). BrGDGTs occur in high abundances in terrestrial settings, including soils and peats (Hopmans et al., 2004; Peterse et al., 2012). BIT values close to 1 indicate a predominantly terrigenous source, while low values (close to 0) indicate a strong aquatic source of the organic matter (Schouten et al., 2013).

14.3 RESULTS

14.3.1. MAAT ESTIMATES BASED ON brGDGTs

Measured MAAT values from Marathousa 1 Area B range from 4.5 °C to ~10 °C (± 4.6 °C) (Fig. 2A, Table 1) with a mean value of 6.8 °C. The temperature decreases gradually from the base of the section (UB10, ~7.5 °C) until the middle (UB6) when it attains the minimum registered. This cooling interval is punctuated by two small warming events, one in UB8 (BC_145 sample,

MAAT equation error is 4.6 ºC.					
Ages after Bludau et al. (2021) computed age model.					
Sample Name	**Age (ka)**	**Str. level (cm)**	**MAAT (ºC) (de Jonge et al., 2014)**	**pH (de Jonge et al., 2014)**	**BIT (Hopmans, 2004)**
Top25	428,86	353,05	6,71	6,65	0,99
Top50	430,31	352,80	8,88	6,68	0,99
Top100	433,09	352,30	8,39	6,75	0,99
Top115	433,91	352,15	9,14	6,62	0,99
Top125	434,36	352,05	9,97	6,73	0,98
Top150	435,86	351,80	9,18	6,45	0,97
Top170	437,10	351,60	6,36	6,23	0,99
351_30	438,90	351,30	7,35	6,57	0,99
351_15	439,81	351,15	7,62	6,58	0,99
350_95	440,98	350,95	6,90	6,66	0,99
350_85	441,59	350,85	6,89	6,50	0,99
350_70	442,50	350,70	7,02	6,42	0,99
350_65	442,79	350,65	6,97	6,57	0,99
350_55	443,40	350,55	8,59	6,42	0,99
350_40	444,30	350,40	6,80	6,51	0,99
350_25	444,63	350,25	5,17	6,56	0,99
350_20	444,91	350,20	5,93	6,58	0,99
350_15	445,22	350,15	5,08	6,47	0,99
350_05	445,22	350,05	4,95	6,44	0,99
350_00	445,22	350,00	5,50	6,83	1,00
349_95	445,22	349,95	5,24	6,41	0,99
349_85	445,71	349,85	4,64	6,37	0,99
349_75	446,35	349,75	4,54	6,30	0,99
349_70	446,68	349,70	5,35	6,85	1,00
BC_0	447,01	349,65	7,95	6,86	0,75
BC_15	448,01	349,50	7,52	6,44	0,96
BC_30	448,90	349,35	5,62	6,34	0,99
BC_55	450,65	349,10	5,12	6,36	0,98
BC_60	451,05	349,05	5,07	6,29	0,98
BC_90	453,13	348,75	5,96	6,43	0,99
BC_125	455,49	348,40	6,42	6,38	0,97
BC_145	457,01	348,20	8,40	6,48	0,89
BC_160	458,19	348,05	6,64	6,47	0,99
BC_190	459,77	347,75	5,97	6,66	0,98
BC_240	463,00	347,10	7,46	6,64	1,00
BC_320	464,00	347,06	7,57	6,92	1,00

Table 1: MAAT, paleo-pH and BIT data obtained from GDGTs.

8.4 °C) and another one peaking at the UB7-UB6 transition (BC_0 sample, 8.0 °C). The interval between UB6 and the base of UB4 is marked by a sustained cooling episode with an average MAAT value of 5.2 °C, corresponding to the glacial maximum (at ~440–450 ka). After this interval, MAAT follows an overall warming trend towards the top, to reach the overall maximum in the section (in the top of UB2). Temperatures remain high (average value of 9.1 °C) over the entire UB1 unit deposition, when another cooling seems to start at the very top of the section (Top25 sample, 6.7 °C).

14.3.2. SOIL pH ESTIMATES BASED ON brGDGTs

Paleo-soil pH values from Marathousa 1 somewhat follow the general MAAT trend, with values corresponding to mildly acidic and neutral soils (from 6.2 to 6.9, with an average value of 6.5; Fig. 2B; Table 1). Values decrease gradually from UB10 (6.9, sample BC_320) to UB6 (6.3, sample 349_75), punctuated by a short interval with more neutral values at the UB6–UB5 contact (up to 6.9, sample BC_0). From UB6 until the top of the section, the pH values are increasing in a stepwise manner, with the most striking change in the UB3–UB2 transition, where values increase by 0.5, from 6.2 to 6.7, after a sharp previous decrease from ~6.5. The values maintain close to neutral values until the top of the section, with an average value of 6.7.

14.3.3. BIT INDEX

Compared with the other proxies, the BIT index values are rather constant, with an average value of 0.98 (Fig. 2C, Table 1). The only lower values in the section are corresponding to the samples BC_145 (0.89) and BC_0 (0.75), the last one attaining the minimum value.

14.4 DISCUSSION

Quaternary glaciations have strongly shaped the European continent due to the large extent of mountain glaciers and ice caps built up during this time interval. MIS 12 (478–424 ka; Lisieki and Raymo, 2005) is the correspondent of Mindel glaciation in the Alpine domain and Elster in Northern Europe, overall representing a strong global event. While most paleoclimatic records derive from the marine domain (e.g., Alonso-Garcia et al., 2011; Wang et al., 2010; Lisieki and Raymo, 2005; Zachos et al., 2008), continental archives are scarce due to the lack of extended depositional sequences. The only available records of similar age are from Ohrid Lake (Albania, Northern Macedonia; Koutsodendris et al., 2019), Tenaghi Philippon (Northern Greece; Tzedakis et al., 2006) and Sulmona Basin (Italy; Regattieri et al., 2016), all on the northern margin of the Mediterranean Sea.

There is an increasing effort in the Mediterranean area to understand and quantify these glacial events and the potential of isolated areas to function as refugia, in order to understand the presence of hominins and other mammals within the Mediterranean and southern European space during glacial intervals. The Lower Paleolithic site Marathousa 1 (~465–425 ka; Bludau et al., 2021) is particularly important in this discussion due to the presence of an archaeological level, which currently holds the earliest known radiometrically dated evidence of human presence in the region (Tourloukis and Harvati, 2018; Harvati et al., 2018). Therefore, in the current work, we will focus on the archaeological horizon.

14.4.1. HOW COLD WAS CENTRAL PELOPONNESE DURING MIS 12?

The presence of glaciers in the Peloponnesian mountains (Leontaritis et al., 2020) opened a new

question of how and if the glacial signal would be expressed at lower elevations. Marathousa 1 Area B provides the first MAAT record for MIS 12 in Greece, with temperatures as low as 4.5 °C (Fig. 2A), supporting the presence of glacial conditions in the Megalopolis Basin during this time interval. The minimum temperature (glacial maximum) is registered in the UB6–UB5 units, until the contact with UB4, between ~450–440 ka. The drop in temperature recorded at Marathousa 1 correlates with a significant decrease in tree pollen in the Megalopolis Basin (Kyrikou et al., this volume) and the presence of levels with mud cracks in the sedimentological record (i.e., UB6–UB5, UB5–UB4 contacts; Karkanas et al., 2018), indicating that the intense cooling event was associated with evaporative conditions. An overall decrease in precipitation in the Mediterranean domain

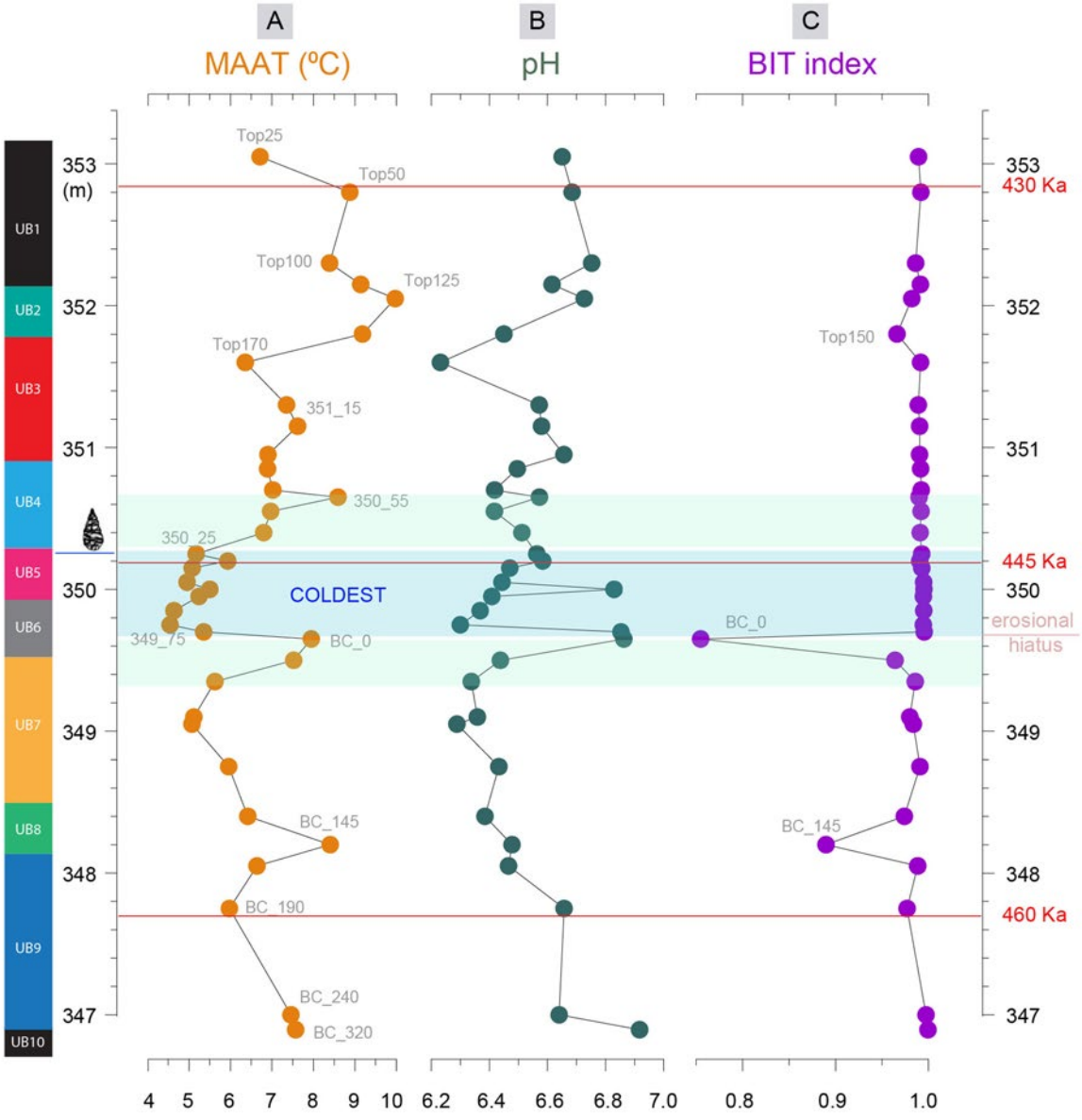

Figure 2: Biomarker results from Marathousa 1 Area B site: A. MAAT; B. paleo-soil pH; C. BIT index. The stratigraphic units are represented on the left side. The tool symbol marks the archaeological horizon. Red lines depict time lines based on the Bludau et al., 2021 age model.

during this period is suggested by Wagner et al. (2019) from the Lake Ohrid record. Interestingly, the paleo-soil pH values (Fig. 2B) are more neutral (~6.7–6.9) for these specific levels with mud cracks, indicating less levigated soils, while for the rest of the interval (within UB6–UB5 units) pH values are more acidic (up to 6.3), indicating more humid soils. This fact can be a consequence of the local landscape change (Bludau et al., 2021), with a lake mudflat migrating due to a climate and/or tectonically-driven fluctuating lake level (Karkanas et al., 2018). Thus, soils remain more hydrated due to the river presence and meltwater inputs from higher elevations (Bludau et al., 2021) even if the temperatures in the basin are low. The presence of the lake in the center of the basin and of smaller ponds in the side mudflat could have further influenced the local climate, as water has a higher heat sequestration capacity (i.e., it needs more solar energy to warm up). It is possible that the existence of a long-term water source in the basin could have elevated the temperature locally because the heat trapped in the lake water during summer is released slowly in the cold season, while running water (i.e., the drainage system flowing into the lake) has a lower freezing point. These factors, as well as the sheltered position of Megalopolis Basin, result in relatively favorable conditions, which allowed it to act as a refugium for faunal as well as Paleolithic human communities.

14.4.2. HOMININ PRESENCE AT MARATHOUSA 1 IN THE CLIMATIC CONTEXT

Marathousa 1 was excavated systematically from 2014 to 2019 by a joint team from the Ephorate of Paleoanthropology and Speleology (Hellenic Ministry of Culture), and the Paleoanthropology group, University of Tübingen, in the context of the ERC projects PaGE and CROSSROADS (e.g., Panagopoulou et al., 2015; Harvati, 2016; Harvati et al., 2018 and references therein). Human activity is attested by >2000 lithic and bone artefacts (Tourloukis et al., 2018a), as well as numerous faunal remains with evidence of processing by humans (Konidaris et al., 2018), recovered during excavations from both excavation areas (Area A and B). In our samples, the archaeological horizon lies at the base of UB4 unit (Area B), (Tourloukis et al., 2018a), at the UB4–UB5 erosional contact (Giusti et al., 2018). In area A, the archaeological horizon is found at the UA3–UA4 erosional contact, which is the equivalent of the UB5–UB6 contact of Area B, suggesting that hominins were present in the area during the whole interval of UB6–UB4 (Giusti et al., 2018; Karkanas et al., 2018; Konidaris et al., 2018; Tourloukis et al., 2018a).

Remarkably, the archaeological horizon lies within the very cold interval registered at Marathousa 1, where MAAT vary from 5.9 to 4.5 °C (Fig. 2A). The association of archaeological artefacts with this interval indicates that hominins were present at Marathousa 1 during the glacial maximum, confirming the hypothesis that Megalopolis acted as a glacial refugium (e.g., Bludau et al., 2021; Tourloukis and Harvati, 2018). The presence of a rich flora (Field et al., 2018) and fauna at the site, including large and small mammals (Konidaris et al., 2018, 2022; Doukas et al., 2018), birds (Michailidis et al., 2018), as well as reptiles and amphibians (Vlachos and Delfino, 2016; Vlachos et al., this volume), reinforce this conclusion, suggesting a continuous faunal presence in the basin during MIS 12.

The Marathousa 1 MAAT record exhibits a general cooling trend (Fig. 2A), from the base of the section up to UB4 unit base. The ~4 °C cooling is interrupted by two short warming peaks, the first at BC_145 sample (UB8) and the second at BC_0 (UB7–UB6). The minimum calculated temperature is registered at the base of UB6, close to UB7 contact, immediately after the warming peak (Fig. 2A). This peak is truncated by an erosional surface,

part of an event that affects other proxies too (i.e., chemical and physical components; Bludau et al., 2021), not only the biomarker record. Except the temperature curve truncation, our data indicate a major change also in the pH and BIT index (Fig. 2B, C). At this specific level, BIT value is decreasing dramatically from 0.96 to 0.73. Since lower values such as (0.73) appear usually in proximal marine environments (Hopmans et al., 2004), this anomaly could be induced by enhanced evaporation. Karkanas et al. (2018) document the presence of drying cracks, as well as carbonate nodules/concretions within this interval, highlighting the onset of arid conditions. Taking into consideration the above, we conclude that hominin presence at Marathousa 1 took place in the context of intensification of glacial conditions in the Peloponnese, confirming the potential of the Megalopolis Basin to have acted as a refugium during MIS 12.

14.5 CONCLUSIONS

The biomarker data from Marathousa 1 indicate an overall cooling for the lower half of the section, peaking between ~450–440 ka (stratigraphic units UB6 to UB4). Our data confirms for the first time the presence of glacial conditions in the Megalopolis Basin and brings new insight into the MIS 12 expression in Peloponnese. The interval with the lowest registered temperatures overlaps with the presence of hominins in the area, supporting the potential of Megalopolis to have acted as a refugium for hominins, as well as animal and plant communities.

ACKNOWLEDGEMENTS

Excavation at Marathousa 1 was conducted under a permit granted to the Ephorate of Palaeoanthropology-Speleology, Hellenic Ministry of Culture. It was supported by the ERC Consolidator Grant ERC-CoG- 24703 ("CROSSROADS") and the ERC Starting Grant ERC-StG-83503 ("PaGE"), both awarded to K.H. V.T. and K.H. are also supported by the Deutsche Forschungsgemeinschaft (DFG Project no. 463225251, "MEGALOPOLIS"). K.H. is also supported by the ERC Advanced Grant ERC-AdG-101019659 ("FIRST-STEPS"). G.A.B. is supported with funds from the DFG (2021 Gottfried Wilhelm Leibniz Prize awarded to K.H.). G.A.B. thanks U. Treffert for the help in the laboratory and all reviewers for the useful comments and suggestions.

REFERENCES

Alonso-Garcia, M., Sierro, F. J. and Flores, J. A., 2011. Arctic Front Shifts in the Subpolar North Atlantic during the Mid-pleistocene (800-400ka) and Their Implications for Ocean Circulation. Palaeogeography, Palaeoclimatology, Palaeoecology 311(3–4), pp. 268–280.

Blackwell, B., Sakhrani, N., Singh, I., Gopalkrishna, K.K., Tourloukis, V., Panagopoulou, E., Karkanas, P., Blickstein, J.I.B., Skinner, A.R., Florentin, J. and Harvati, K., 2018. ESR dating ungulate teeth and molluscs from Marathousa 1, Greece. Quaternary, 1(3), 22.

Bludau, I.J.E., Papadopoulou, P., Iliopoulos, G., Weiss, M., Schnabel., E., Thompson, N., Tourloukis, V., Zachow, C., Kyrikou, S., Konidaris, G. E., Karkanas., P., Panagopoulou, E., Harvati, K. and Junginger, A., 2021. Lake-Level Changes and Their Paleo-Climatic Implications at the MIS12 Lower Paleolithic (Middle Pleistocene) Site Marathousa 1, Greece. Frontiers in Earth Science, 9, 668445.

De Jonge, C., Hopmans, E.C., Zell, C.I., Kim, J.-H., Schouten, S. and Sinninghe Damsté, J.S., 2014. Occurrence and abundance of 6-methyl branched glycerol dialkyl glycerol tetra-

ethers in soils: Implications for palaeoclimate reconstruction. Geochimica et Cosmochimica Acta, 141, pp. 97–112.

Doukas, C., van Kolfschoten, T., Papayianni, K., Panagopoulou, E. and Harvati, K., 2018. The Small Mammal Fauna from the Palaeolithic Site Marathousa 1 (Greece). Quaternary International, 497, pp. 95–107.

Field, M.H., Ntinou, M., Tsartsidou, G., van Berge Henegowuen, D., Tourloukis, V.,Thompson, N., Karkanas, P., Panagopoulou, E. and Harvati, K., 2018. A palaeoenvironmental reconstruction (based on palaeobotanical data and diatoms) of the Middle Pleistocene elephant (*Palaeoloxodon antiquus*) butchery site at Marathousa, Megalopolis, Greece. Quaternary International, 497, pp. 108–122.

Giusti, D., Tourloukis, V., Konidaris, G., Thompson, N., Karkanas, P., Panagopoulou, E. and Harvati, K., 2018. Beyond Maps: Patterns of Formation Processes at the Middle Pleistocene Open-Air Site of Marathousa 1, Megalopolis Basin, Greece. Quaternary International, 497, pp. 137–153.

Harvati, K., 2016. Paleoanthropology in Greece: Recent Findings and Interpretations, in: Harvati, K., Roksandic, M. (Eds.), Paleoanthropology of the Balkans and Anatolia: Human Evolution and its Context. Vertebrate Paleobiology and Paleoanthropology Series. Springer, Dordrecht, pp. 3–14.

Harvati, K., Konidaris, G. and Tourloukis, V., 2018. Special issue human evolution at the gates of Europe. Quaternary International, 497, pp. 1–240.

Hopmans, E.C., Weijers, J.W.H., Schefuss, E., Herfort, L., Sinninghe Damsté, J.S. and Schouten, S., 2004. A novel proxy for terrestrial organic matter in sediments based on branched and isoprenoid tetraether lipids. Earth and Planetary Science Letters, 224, pp. 107–116.

Jacobs, Z., Li, B., Karkanas, P., Tourloukis, V., Thomson, N., Panagopoulou, E. and Harvati, K., 2018. Dating the Middle Pleistocene Marathousa 1 (Greece) lacustrine sediment using multiple-aliquot pre-dose multi-elevated-temperature post-infrared infrared stimulated luminescence (MET-Pirir). Quaternary International, 497, pp. 170–177.

Karkanas, P., Tourloukis, V., Thompson, N., Giusti, D., Panagopoulou, E. and Harvati, K., 2018. Sedimentology and micromorphology of the Lower Palaeolithic lakeshore site Marathousa 1, Megalopolis Basin, Greece. Quaternary International, 497, pp. 123–136.

Konidaris, G.E., Athanassiou, A., Tourloukis, V., Thompson, N., Giusti, D., Panagopoulou, E. and Harvati, K., 2018. The Skeleton of a Straight-Tusked Elephant (*Palaeoloxodon antiquus*) and Other Large Mammals from the Middle Pleistocene Butchering Locality Marathousa 1 (Megalopolis Basin, Greece): Preliminary Results. Quaternary International, 497, pp. 65–84.

Konidaris, G.E., Athanassiou, A., Panagopoulou, E. and Harvati, K., 2022. First record of *Macaca* (Cercopithecidae, Primates) in the Middle Pleistocene of Greece. Journal of Human Evolution, 162, 103104.

Koutsodendris, A., Kousis, I., Peyron, O., Wagner, B. and Pross, J., 2019. The Marine Isotope Stage 12 Pollen Record from Lake Ohrid (SE Europe): Investigating Short-Term Climate Change under Extreme Glacial Conditions. Quaternary Science Reviews, 221, 105873.

Kyrikou, S., Marinova, E., Bludau, I. J. E., Karkanas, P., Panagopoulou, E., Tourloukis, V., Junginger, A. and Harvati, K., this volume. The Middle Pleistocene MIS 12 palynological record from Marathousa palaeolake in Southern Greece: Highlighting favourable conditions in Marathousa 1 (MAR-1) refugial region during the severe glacial period.

Leontaritis, A.D., Kouli, K. and Pavlopoulos, K., 2020. The Glacial History of Greece: a Comprehensive Review. Mediterranean Geoscience Reviews, 2 (2), pp. 65–90.

Lisiecki, L.E. and Raymo, M.E., 2005. A Pliocene-Pleistocene Stack of 57 Globally Distributed Benthic $\delta^{18}O$ Records. Paleoceanography, 20, a–n.

Michailidis, D., Konidaris, G.E., Athanassiou, A., Panagopoulou, E. and Harvati, K., 2018. The ornithological remains from Marathousa 1 (Middle Pleistocene; Megalopolis Basin, Greece). Quaternary International, 497, pp. 85–94.

Panagopoulou, E., Tourloukis, V., Thompson, N., Athanassiou, A., Tsartsidou, G., Konidaris, G.E., Giusti, D., Karkanas, P. and Harvati, K., 2015. Marathousa 1: a New Middle Pleistocene Archaeological Site from Greece. Antiquity, 343, pp. 1–8.

Panagopoulou, E., Tourloukis, V., Thompson, N., Konidaris, G.E., Athanassiou, A., Giusti, D., Tsarsidou, G., Karkanas, P. and Harvati, K., 2018. The lower Palaeolithic site of Marathousa 1, Megalopolis, Greece: overview of the evidence. Quaternary International, 497, pp. 33–46.

Peterse, F., van der Meer, J., Schouten, S., Weijers, J.W.H., Fierer, N., Jacckson, R.B., Kim, J.-H. and Sinninghe Damsté, J.S., 2012. Revised calibration of the MBT-CBT paleotemperature proxy based on branched tetraether membrane lipids in surface soils. Geochimica et Cosmochimica Acta, 96, pp. 215–229.

Regattieri, E., Giaccio, B., Galli, P., Nomade, S., Peronace, E., Messina, P., Sposato, A., Boschi, C. and Gemelli, M., 2016. A Multi-Proxy Record of MIS 11-12 Deglaciation and Glacial MIS 12 Instability from the Sulmona Basin (central Italy). Quaternary Science Reviews, 132, pp. 129–145.

Schouten, S., Hopmans, E.C. and Sinninghe Damsté, J.S., 2013. The organic geochemistry of glycerol dialkyl glycerol tetraether lipids: A review. Organic Geochemistry, 54, pp. 19–61.

Sinninghe Damsté, J.S., Schouten, S., Hopmans, E.C., van Duin, A.C.T. and Geenevasen, J.A.J., 2002. Crenarchaeol: the characteristic core glycerol dibiphytanyl glycerol tetraether membrane lipid of cosmopolitan pelagic crenarchaeota. Journal of Lipid Research, 43(10).

Tourloukis, V. and Harvati, K., 2018. The Palaeolithic Record of Greece: A Synthesis of the Evidence and a Research Agenda for the Future. Quaternary International, 466, pp. 48–65.

Tourloukis, V., Thomson, N., Panagopoulou, E., Giusti, D., Konidaris, G.E., Karkanas, P. and Harvati, K., 2018a. Lithic artifacts and bone tools from the Lower Palaeolithic site Marathousa 1, Megalopolis, Greece: Preliminary results. Quaternary International, 497, pp. 47–64.

Tourloukis, V., Muttoni, G., Karkanas, P., Monesi, E., Scardia, G., Panagopoulou, E. and Harvati, K., 2018b. Magnetostratigraphic and chronostratigraphic constraints on the Marathousa 1 Lower Palaeolithic site and the Middle Pleistocene deposits of the Megalopolis Basin, Greece. Quaternary International, 497, pp. 154–169.

Tzedakis, P. C., Hooghiemstra, H. and Pälike, H., 2006. The Last 1.35 Million Years at Tenaghi Philippon: Revised Chronostratigraphy and Long-Term Vegetation Trends. Quaternary Science Reviews, 25(23–24), pp. 3416–3430.

Vlachos, D. and Delfino, M., 2016. Food for thought: Sub-fossil and fossil chelonian remains from Franchthi Cave and Megalopolis confirm a glacial refuge for *Emys orbicularis* in Peloponnesus (S. Greece). Quaternary Science Reviews, 150, pp. 158–171.

Vlachos, E., Georgalis, G.L., Konidaris, G.E., Athanassiou, A., Tourloukis, V., Thompson, N., Panagopoulou, E. and Harvati, K., this volume. The reptiles from the Middle Pleistocene of Marathousa 1, Megalopolis Basin (Greece).

Wagner, B., Vogel, H., Francke, A., Friedrich, T., Donders, T., Lacey, J. H., Leng, M.J., Regattieri, E., Sadori, L., Wilke, T., Zanchetta, G., Albrecht, C., Bertini, A., Combourieu-Nebout, N., Cvetkoska, A., Giaccio, B., Grazhdani, A., Hauffe, T., Holtvoeth, J., Joannin, S., Jovanovska, E., Just, J., Kouli, K., Kousis, I., Koutsodendris, A., Krastel, S., Lagos, M., Leicher, N., Levkov, Z., Lindhorst, K., Masi, A., Melles, M., Mercuri, A.M., Nomade, S., Nowaczyk, N., Panagiotopoulos, K., Peyron, O., Reed, J.M., Sagnotti, L., Sinopoli, G., Stelbrink, B., Sulpizio, R., Timmermann, A., Tofilovska, S., Torri, P., Wagner-Cremer, F., Wonik, T. and Zhang, X., 2019. Mediterranean winter Rainfall in Phase with African Monsoons during the Past 1.36 Million Years. Nature, 573(7773), pp. 256–260.

Wang, P., Tian, J. and Lourens, L. J., 2010. Obscuring of Long Eccentricity Cyclicity in Pleistocene Oceanic Carbon Isotope Records. Earth Planet. Scientific Letters, 290(3-4), pp. 319–330.

Weijers, J.W.H., Schouten, S., van der Donker, J., Hopmans E.C. and Sinninghe Damsté, J., 2007. Environmental controls on bacterial tetraether membrane lipid distribution in soils. Geochimica et Cosmochimica Acta, 71, pp. 703–713.

Zachos, J.C., Dickens, G.R. and Zeebe R.E., 2008. An early Cenozoic perspective on greenhouse warming and carbon-cycle dynamics. Nature, 451, pp. 279–283.

15 PRELIMINARY RESULTS ON THE REPTILES FROM THE MIDDLE PLEISTOCENE OF MARATHOUSA 1, MEGALOPOLIS BASIN (GREECE)

Evangelos Vlachos[1]*, Georgios L. Georgalis[2], George E. Konidaris[3], Athanassios Athanassiou[4], Vangelis Tourloukis[3,5], Nicholas Thompson[3], Eleni Panagopoulou[4], Katerina Harvati[3,6]

[1]*CONICET and Museo Paleontológico Egidio Feruglio, Chubut, Argentina*
[2]*Institute of Systematics and Evolution of Animals, Polish Academy of Sciences, Kraków, Poland*
[3]*Paleoanthropology, Institute for Archaeological Sciences and Senckenberg Centre for Human Evolution and Palaeoenvironment, Department of Geosciences, Eberhard Karls University of Tübingen, Tübingen, Germany*
[4]*Hellenic Ministry of Culture, Ephorate of Palaeoanthropology–Speleology, Athens, Greece*
[5]*Department of History and Archaeology, School of Philosophy, University of Ioannina, Ioannina, Greece*
[6]*DFG Centre for Advanced Studies 'Words, Bones, Genes, Tools', Eberhard Karls University of Tübingen, Tübingen, Germany*
**evlacho@mef.org.ar*

http://dx.doi.org/10.15496/publikation-97650

Keywords: lizards; snakes; Squamata; Testudines; turtles

15.1 INTRODUCTION

Marathousa 1 (MAR-1) is a Middle Pleistocene (Lower Palaeolithic) locality situated in the Megalopolis Basin (Arcadia, Peloponnese), an area known since the early 20th century for its mammalian fossils. It was discovered in 2013 during a targeted Palaeolithic survey within the lacustrine sediments of the basin, and excavated from 2013 to 2019 in two large pits, dubbed 'Area A' and 'Area B' (Panagopoulou et al., 2018). MAR-1 yielded important archaeological and paleontological finds, including a partial elephant skeleton and other vertebrate fossils in close stratigraphic association with evidence of human activity (lithic and bone artifacts, cut and percussion marks on bones) (Konidaris et al., 2018; Tourloukis et al., 2018). The identified macromammalian fauna consists of *Macaca sylvanus* cf. *pliocena* (macaque), *Palaeoloxodon antiquus* (straight-tusked elephant), *Castor fiber* (beaver), *Vulpes* sp. (fox), *Canis* sp. (wolf-sized canid), *Mustela* sp. (weasel), *Lutra simplicidens* (otter), *Felis* sp. (wildcat), *Hippopotamus antiquus* (hippo), *Bison* sp. (bison), *Dama* sp. (fallow deer), and *Cervus elaphus* (red deer) (Konidaris et al., 2018, 2022). Moreover, the locality produced abundant fossils of plants, insects, ostracods, molluscs, fishes, amphibians, reptiles, birds, and micromammals, which offer valuable evidence about the locality's paleoenvironment and biochronology (Doukas et al., 2018; Field et al., 2018; Michailidis et al., 2018; Bludau et al., 2021; Boni et al., this volume). MAR-1 is radiometrically, magnetostratigraphically and biochronologically dated to

E. Vlachos: https://orcid.org/0000-0002-1980-7109
G. L. Georgalis: https://orcid.org/0000-0001-7759-6146
G. E. Konidaris: https://orcid.org/0000-0002-7041-233X
A. Athanassiou: https://orcid.org/0000-0002-9140-7011
V. Tourloukis: https://orcid.org/0000-0002-9527-2708
N. Thompson: https://orcid.org/0009-0003-4770-1744
E. Panagopoulou: https://orcid.org/0000-0002-4268-6157
K. Harvati: https://orcid.org/0000-0001-5998-4794

500–400 ka, and is correlated to the glacial Marine Isotope Stage MIS 12 (Panagopoulou et al. 2018, and references therein).

Until recently, our knowledge of the fossil record of squamates and turtles in Greece has been limited to isolated findings. However, focused research during the last decade has led to a complete re-evaluation of the known fossils, as well as to numerous new discoveries, new occurrences, and even new taxa (summarized in Georgalis and Delfino, 2022, and Vlachos, 2022; and references therein). In the Megalopolis Basin, turtle fossils are

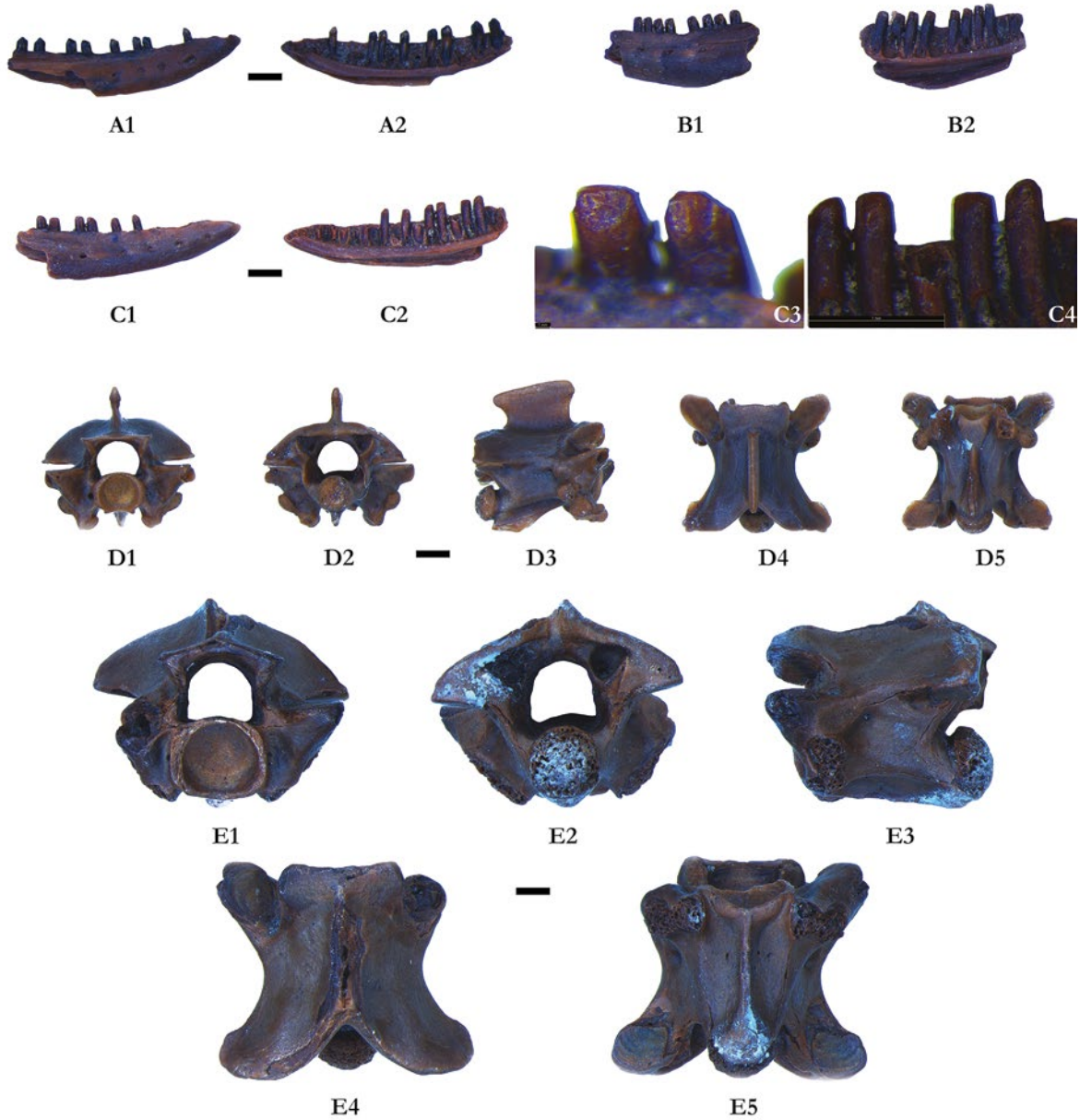

Figure 1: Selected specimens of lizards and snakes from Marathousa 1. A) Right dentary (937.677 5a) of Lacertidae indet. (morphotype A) in labial (A1) and lingual (A2) views. B) Left dentary (939.671 13a) of Lacertidae indet. (morphotype B) in labial (B1) and lingual (B2) views. C) Right dentary (936.671 2m) of Lacertidae indet. (morphotype A) in labial (C1) and lingual (C2) views and close up photographs of the teeth in labial (C3) and lingual (C4) views. D) Trunk vertebra (940.671 8a) of *Natrix natrix* in anterior (D1), posterior (D2), right lateral (D3), dorsal (D4), and ventral (D5) views. E) Mid-trunk vertebra (941.671 15a) of *Malpolon insignitus* in anterior (E1), posterior (E2), left lateral (E3), dorsal (E4), and ventral (E5) views.

known from historical collections in Megalopolis (Melentis, 1966; Vlachos and Delfino, 2016), as well as from the more recent systematic investigations in the Kyparissia localities (Athanassiou et al., 2018). The purpose of this communication is to present our preliminary results of the study of the squamate and turtle specimens recovered in the Marathousa 1 locality.

15.2 LIZARDS

Lizards are relatively rare, represented by isolated teeth and fragmentary dentaries, bearing elements pertaining to indeterminate Lacertidae (Fig. 1A-C).

The best preserved lacertid specimens are dentaries that bear teeth with pleurodont dentition, with typical bicuspid or tricuspid teeth, and an open Meckel's groove (Fig. 1A-B) (Čerňanský and Syromyatnikova, 2019; Villa and Delfino, 2019). In some of the lacertid dentaries, the tooth crowns are heavily worn, and the cusps cannot be clearly discerned (Fig. 1C). A more precise identification is not possible due to the fragmentary nature of the specimens and the inadequate knowledge of the skeletal anatomy of extant lacertids. Nevertheless, it seems that the MAR-1 fossil material corresponds to two different lacertid species, judging from differences in the tooth morphology and the degree of slenderness of the dentaries (Fig. 1A and 1C vs. 1B), but this could only be ascertained upon more complete material.

Several different lacertids occur today in Peloponnese.

15.3 SNAKES

Snakes are by far the most abundant squamates, represented by numerous isolated trunk and caudal vertebrae (Fig. 1D-E). Almost all pertain to the natricid *Natrix natrix* (common grass snake). The absence of colubrids (which are the dominant snake group today) and viperids is notorious, but still a number of rather fragmentary vertebrae can only be referred to as Colubriformes indet. and therefore, some of them could pertain to these families.

Natrix natrix is by far the most abundant squamate in Marathousa 1; perhaps, even more than 90% of the identified specimens pertain to this species (Fig. 1D). Its taxonomic identification is confirmed by several characters: hypapophyses are present throughout the trunk vertebrae, being sigmoid and with a rounded tip; a moderately depressed neural arch; a neural spine that is overhanging both anteriorly and posteriorly; prezygapophyseal accessory processes that are moderately long; parapophyseal processes that are directed anteriorly; and an elongated centrum (see Szyndlar, 1984, 1991; Georgalis et al., 2019).

Additional fragmentary *Natrix* vertebrae occur in the sample, not preserving their hypapophyses and/or neural spines. Although most likely they too pertain to *Natrix natrix*, the missing relevant diagnostic structures cannot exclude a referral to the other species of the genus that occurs in modern Greek herpetofaunas, i.e., *Natrix tessellata*. They are treated here as *Natrix* sp.

Natrix natrix is a clear indicator of some nearby water habitat, although the species can also occur relatively far from water. *Natrix* is also a common inhabitant of the extant herpetofauna of the area (both *N. natrix* and *N. tessellata* occur today in Peloponnese) and has also a relatively widespread and relatively continuous fossil record in Greece, spanning since the Miocene (Georgalis and Delfino, 2022). The other snakes and lizards from MAR-1 could probably pertain to taxa already present in the broader area today but this cannot be securely asserted with the available fossil material.

A single large vertebra can be tentatively referred to the psammophiid *Malpolon insignitus* (Eastern Montpellier snake) (Fig. 1E) based on its

large size and sharp haemal keel (see Georgalis and Szyndlar, 2022). However, there are some differences with other known *Malpolon* specimens, most importantly the very low ratio of centrum length (CL) to neural arch width (NAW) (CL/NAW less than 1.1), while this value is usually slightly higher in extant *Malpolon* specimens (CL/NAW above 1.3). Unfortunately, important features, such as the length of the prezygapophyseal accessory processes and the height of the neural spine, cannot be observed in this specimen due to its preservational status.

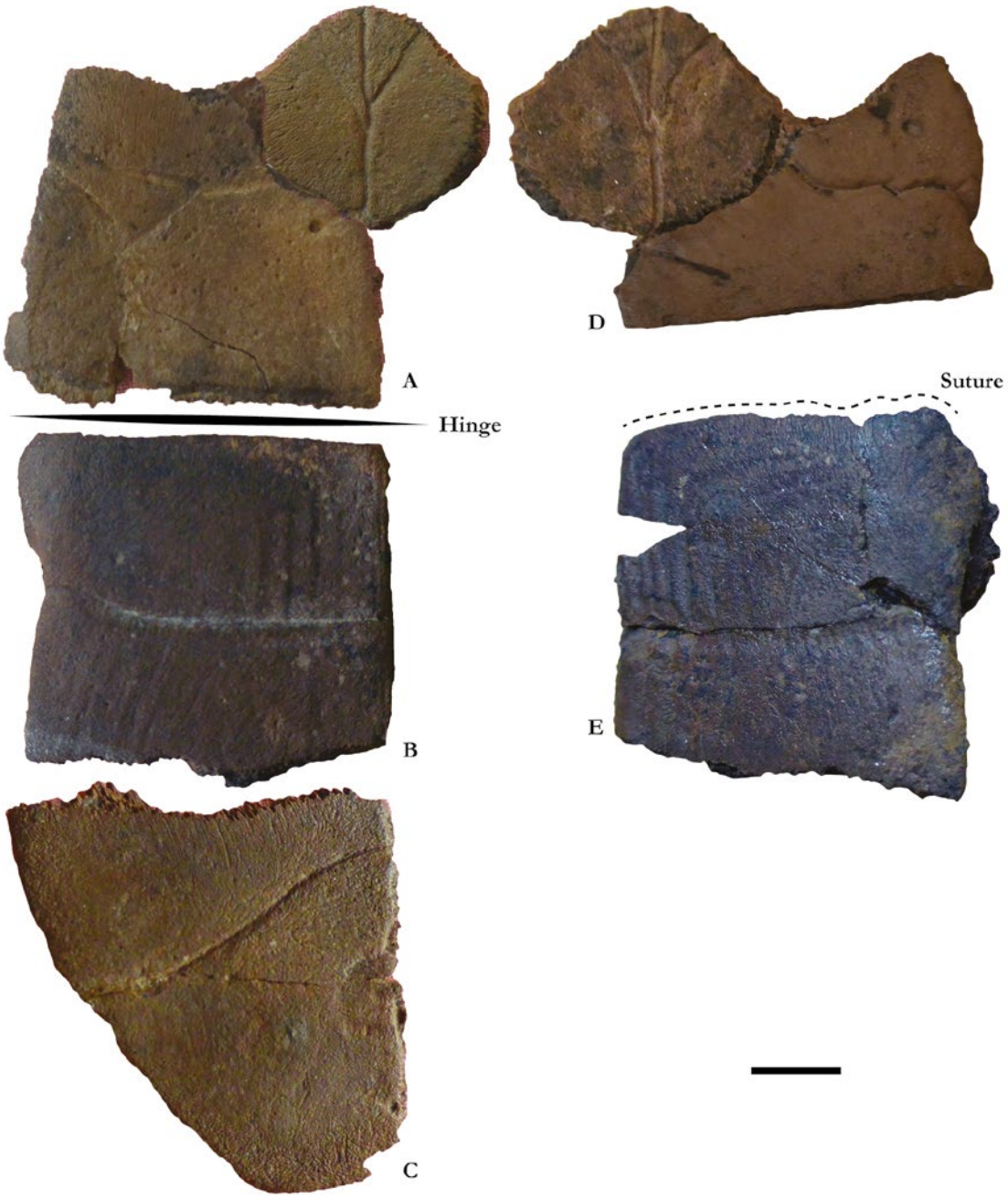

Figure 2: Selected plastral elements of the turtles from Marathousa 1. A–C, *Emys orbicularis*: A, associated entoplastron and right hyoplastron; B, right hypoplastron; C, right xiphiplastron. D–E, *Mauremys rivulata*: D, associated entoplastron and left hyoplastron; E, left xiphiplastron. Scale bar equals 1 cm.

15.4 TURTLES

Turtles are the most abundant reptile fossils in MAR-1, being more abundant in Area A with at least 750 specimens, compared to the approximately 100 specimens in Area B. They comprise, mostly, isolated elements of the carapace and plastron found dispersed, without any anatomical association (Fig. 2). Nevertheless, a few elements are found in articulation, including successive neural plates, suprapygal/pygal area, successive peripherals, and parts of the plastron. Additionally, some appendicular elements are identified, including fragmented humeri, parts of the pelvis, a complete tibia, and a phalanx. Their preservation is quite good, allowing taxonomic identification of many diagnostic elements of the turtle shell.

Although the extant herpetofauna and the fossil record in Peloponnesus include both aquatic and terrestrial testudine taxa, all studied specimens in Marathousa 1 clearly belong to the freshwater species that currently inhabit the area: the European pond turtle *Emys orbicularis* (Testudinoidea: Emydidae) and the Balkan terrapin *Mauremys rivulata* (Testudinoidea: Geoemydidae). Although the shells of these taxa are similar in many aspects, the presence of a movable hinge between the hyoplastra and the hypoplastra, the connection of the carapace and plastron with connective tissues, and the absence of a medially-directed pivoting process on the fifth peripheral bone (see Joyce and Bell, 2004) in *Emys orbicularis* allow a clear distinction of many isolated fragments of the plastra of these species (Fig. 2).

Additional characters allow to further identify the European pond turtle in the isolated fragments of the Marathousa 1 turtle material: several of the entoplastra are hexagonal and longer than wide, the xiphiplastra show a rounded end with a small anal notch, anal scutes are much longer medially compared to the femorals, and the expansion of the vertebral 5 to the pygal (see more in Vlachos and Delfino 2016). However, some comparable elements show characters that are more compatible with the anatomy of the Balkan terrapin. In particular, an associated wider than long entoplastron and hyoplastron show a humero-pectoral sulcus that crosses the posterior part of the entoplastron, several hypoplastra show a clear suture with the bridge, the presence of keels in some isolated neurals, and minute differences in the morphology and orientation of the suture between the epiplastra and the hyoplastra are characters that are typically and consistently found in *Mauremys*.

The plastral elements of turtles are ideal for providing some initial estimations on the skeletal element representation and taxonomic abundance, because plastra have—compared to the carapace—fewer and clearly identifiable elements both in terms of side and position. Based on the initial identifications of the Marathousa 1 material in both Areas A and B, xiphiplastra prove to be the most abundant element for *Emys*, whereas the entoplastron is the most abundant element for *Mauremys*. This allows us to estimate the presence of at least 15 *Emys* and 4 *Mauremys* in Area A, and 7 *Emys* and 2 *Mauremys* in Area B (based on the Minimum Number of Individuals, MNI). Not only is *Emys* always more abundant compared to *Mauremys*, but their relative abundances are similar in both Areas and overall: the European pond turtle represents at least two-thirds of the turtle material in Marathousa 1.

Based on all the above, we can safely identify the presence of two aquatic (freshwater) turtles, which indicate the presence of important and permanent water bodies in the area, both rivers and ponds. Their presence also indicates that during winter the average temperature should be above freezing, whereas average summer temperatures should be high enough to allow the sexual differentiation based on temperature. In fact, Peloponnesus has been considered as a glacial refuge of *Emys orbicularis* in the Balkans (see Vlachos and Delfino,

2016, and references therein). Both aquatic turtle species identified in Marathousa 1 are known in the extant and extinct herpetofauna of the region (Vlachos and Delfino, 2016; Athanassiou et al., 2018; Vlachos, 2022). Finally, and as these two species can be adapted to different environmental conditions including different pollution and salinity levels, some degree of niche differentiation can be hypothesized for Marathousa 1. Further niche differentiation could be speculated geographically and/or temporally in the region, compared to the nearby, but stratigraphically lower Kyparissia localities, collectively and preliminarily dated to the early Middle Pleistocene (see Athanassiou et al., 2018). Besides the common presence of the European pond turtle, Kyparissia material does not contain any *Mauremys* specimens, but it does contain elements of a terrestrial species, the tortoise *Testudo marginata* that is so far missing from Marathousa 1.

15.5 CONCLUSIONS

The preliminary analysis of the MAR-1 reptiles identified the presence of lizards, snakes, and turtles. Lizards are represented by Lacertidae indet. (possibly two species), snakes by *Natrix natrix* and *Malpolon insignitus*, and turtles by *Emys orbicularis* and *Mauremys rivulata*. In particular, the presence and abundance of *Natrix natrix*, *Emys orbicularis* and *Mauremys rivulata* support the existence of a nearby and permanent water source throughout the year, and altogether highlight the importance of the paleolake system, in agreement with the existing paleoenvironmental reconstruction of the locality. All identified reptile species are recorded in today's Peloponnese, but the precise chronostratigraphic and paleoenvironmental context of Marathousa 1 allows more detailed analyses. Therefore, future research will focus on the comprehensive analysis of the MAR-1 reptiles, including detailed descriptions, paleoecology, as well as the horizontal and vertical distribution of the specimens at the site.

ACKNOWLEDGMENTS

Excavation at Marathousa 1 was conducted under a permit granted to the Ephorate of Palaeoanthropology–Speleology, Hellenic Ministry of Culture. It was supported by the ERC Consolidator Grant ERC-CoG-724703 ("CROSSROADS") and the ERC Starting Grant ERC-StG-283503 ("PaGE"), both awarded to K.H. K.H. is also supported by the ERC Advanced Grant ERC-AdG-101019659 ("FIRSTSTEPS"). G.L.G. acknowledges funding from the Ulam Program of the Polish National Agency for Academic Exchange (PPN/ULM/2020/1/00022/U/00001). G.E.K., V.T. K.H. are also supported by the Deutsche Forschungsgemeinschaft (DFG Project no. 463225251, "MEGALOPOLIS"). We thank all field team members, and especially those that participated in the washing and sorting of the sediment in the field and the lab. We would like to deeply thank the reviewers for helpful comments that helped improving this manuscript and the editorial team for the editorial and production tasks.

REFERENCES

Athanassiou, A., Michailidis, D., Vlachos, E., Tourloukis, V., Thompson, N. and Harvati, K. 2018. Pleistocene vertebrates from the Kyparíssia lignite mine, Megalopolis Basin, S. Greece: Testudines, Aves, Suiformes. Quaternary International, 497, pp. 178–197.

Bludau, I.J.E., Papadopoulou, P., Iliopoulos, G., Weiss, M., Schnabel, E., Thompson, N., Tourloukis, V., Zachow, C., Kyrikou, S., Konidaris, G.E., Karkanas, P., Panagopoulou, E., Harvati, K. and Junginger, A., 2021. Lake-level chang-

es and their paleoclimatic implications at the MIS12 Lower Paleolithic (Middle Pleistocene) site Marathousa 1, Greece. Frontiers in Earth Science, 9, p. 668445.

Boni, G., Syrides, G., Konidaris, G.E., Athanassiou, A., Tourloukis, V., Koukousioura, O., Panagopoulou, E., Karkanas, P. and Harvati, K., this volume. Preliminary results on the taxonomy and paleoenvironmental analysis of the mollusc fauna from Marathousa 1, Marathousa 2 and Kyparissia 4 (Middle Pleistocene, Megalopolis Basin, Greece).

Čerňanský, A., Syromyatnikova, E.V. 2019. The first Miocene fossils of *Lacerta* cf. *trilineata* (Squamata, Lacertidae) with a comparative study of the main cranial osteological differences in green lizards and their relatives. PLoS ONE 14(8), p. e0216191.

Doukas, C., van Kolfschoten, T., Papayianni, K., Panagopoulou, E. and Harvati, K., 2018. The small mammal fauna from the palaeolithic site Marathousa 1 (Greece). Quaternary International, 497, pp. 95–107.

Field, M.H., Ntinou, M., Tsartsidou, G., van Berge Henegouwen, D., Risberg, J., Tourloukis, V., Thompson, N., Karkanas, P., Panagopoulou, E. and Harvati, K., 2018. A palaeoenvironmental reconstruction (based on palaeobotanical data and diatoms) of the Middle Pleistocene elephant (*Palaeoloxodon antiquus*) butchery site at Marathousa, Megalopolis, Greece. Quaternary International, 497, pp. 108–122.

Georgalis, G.L., Delfino, M., 2022. The fossil record of lizards and snakes (Reptilia: Squamata) in Greece, in: Vlachos, E. (Ed.), Fossil vertebrates of Greece Volume 1: Basal Vertebrates, Amphibians, Reptiles, Afrotherians, Glires, and Primates. Springer Nature, pp. 205–235.

Georgalis, G.L., Szyndlar, Z., 2022. First occurrence of *Psammophis* (Serpentes) from Europe witnesses another Messinian herpetofaunal dispersal from Africa – biogeographic implications and a discussion of the vertebral morphology of psammophiid snakes. The Anatomical Record, 305(11), pp. 3263–3282.

Georgalis, G.L., Villa, A., Ivanov, M., Vasilyan, D. and Delfino, M. 2019. Fossil amphibians and reptiles from the Neogene locality of Maramena (Greece), the most diverse European herpetofauna at the Miocene/Pliocene transition boundary. Palaeontologia Electronica, 22.3.68, pp. 1–99.

Joyce, W.G., Bell, C.J., 2004. A review of the comparative morphology of extant testudinoid turtles (Reptilia: Testudines). Asiatic Herpetological Research, 10, pp. 53–109.

Konidaris, G.E., Athanassiou, A., Tourloukis, V., Thompson, N., Giusti, D., Panagopoulou, E. and Harvati, K., 2018. The skeleton of a straight-tusked elephant (*Palaeoloxodon antiquus*) and other large mammals from the Middle Pleistocene butchering locality Marathousa 1 (Megalopolis Basin, Greece): preliminary results. Quaternary International, 497, pp. 65–84.

Konidaris, G.E., Athanassiou, A., Panagopoulou, E. and Harvati, K., 2022. First record of *Macaca* (Cercopithecidae, Primates) in the Middle Pleistocene of Greece. Journal of Human Evolution, 162, p. 103104.

Melentis, J.K., 1966. *Clemmys caspica* aus dem Pleistozän des Beckens von Megalopolis im Peloponnes (Griechenland). Annales Géologiques des Pays Helléniques, 17, pp. 169–181.

Michailidis, D., Konidaris, G.E., Athanassiou, A., Panagopoulou, E. and Harvati, K., 2018. The ornithological remains from Marathousa 1 (Middle Pleistocene; Megalopolis Basin, Greece). Quaternary International, 497, pp. 85–94

Panagopoulou, E., Tourloukis, V., Thompson, N., Konidaris, G., Athanassiou, A., Giusti,

D., Tsartsidou, G., Karkanas, P. and Harvati, K., 2018. The Lower Palaeolithic site of Marathousa 1, Megalopolis, Greece: Overview of the evidence. Quaternary International, 497, pp. 33–46.

Szyndlar, Z., 1984. Fossil snakes from Poland. Acta Zoologica Cracoviensia, 28, pp. 1–156.

Szyndlar, Z., 1991. A review of Neogene and Quaternary snakes of Central and Eastern Europe. Part II: Natricinae, Elapidae, Viperidae. Estudios Geológicos, 47, pp. 237–266.

Tourloukis, V., Thompson, N., Panagopoulou, E., Giusti, D., Konidaris, G.E., Karkanas, P. and Harvati, K., 2018. Lithic artifacts and bone tools from the Lower Palaeolithic site Marathousa 1, Megalopolis, Greece: preliminary results. Quaternary International, 497, pp. 47–64.

Villa, A., M. Delfino, 2019. A comparative atlas of the skull osteology of European lizards (Reptilia: Squamata). Zoological Journal of the Linnean Society 187(3), pp. 828–928.

Vlachos, E., Delfino, M., 2016. Food for thought: sub-fossil and fossil chelonian remains from Franchthi Cave and Megalopolis confirm a glacial refuge for *Emys orbicularis* in Peloponnesus (S. Greece). Quaternary Science Reviews, 150, pp. 158–171.

Vlachos, E. 2022. The fossil record of turtles and tortoises (Reptilia: Testudines) in Greece, in: Vlachos, E. (Ed.), Fossil vertebrates of Greece Volume 1: Basal Vertebrates, Amphibians, Reptiles, Afrotherians, Glires, and Primates. Springer Nature, pp. 245–281.

16 THE MEGALOPOLIS PALEOENVIRONMENTAL PROJECT (MEGAPAL)

Panagiotis Karkanas[1]*, Vangelis Tourloukis[2,3], Nicholas Thompson[2], Domenico Giusti[2], Georgia Tsartsidou[4], Athanassios Athanassiou[4], George E. Konidaris[2], Effrosyni Roditi[2], Eleni Panagopoulou[4], Katerina Harvati[2,5]

[1]*M.H. Wiener Laboratory for Archaeological Science, American School of Classical Studies at Athens, Greece*
[2]*Paleoanthropology, Institute for Archaeological Sciences and Senckenberg Center for Human Evolution and Palaeoenvironment, Department of Geosciences, Eberhard Karls Universität Tübingen, Germany*
[3]*Department of History and Archaeology, School of Philosophy, University of Ioannina, Ioannina, Greece*
[4]*Hellenic Ministry of Culture, Ephorate of Palaeoanthropology–Speleology, Athens, Greece*
[5]*DFG Centre of Advanced Studies 'Words, Bones, Genes, Tools' ,Eberhard Karls University of Tübingen, Tübingen, Germany*
**tkarkanas@ascsa.edu.gr*

http://dx.doi.org/10.15496/publikation-97646

Keywords: Lower Palaeolithic; Pleistocene; Megalopolis Basin; survey

16.1 INTRODUCTION

The Lower Paleolithic record of Greece remains poorly known, even though the Greek Peninsula lies on one of the likeliest dispersal roots between Africa, Western Asia and Europe (Harvati et al., 2009; Tourloukis and Karkanas, 2012). Furthermore, the Balkans is one of the three major southern European refugia for fauna, flora, and possibly human populations during glacial periods, and therefore should have been among those parts of the continent that were relatively continuously occupied (e.g., Tzedakis et al., 2002; Harvati, 2016, 2022). Notwithstanding its importance, paleoanthropological research in the region has until recently been sparse, mainly owing to research priorities focused on later periods. The scanty evidence at hand chiefly consists of sites and findspots lacking a paleoenvironmental and chronological context (Tourloukis and Karkanas, 2012; Harvati, 2016, 2022; Tourloukis and Harvati, 2018). This type of evidence is therefore difficult to interpret and offers a fragmentary and ambiguous, yet highly intriguing, picture.

The recently discovered Lower Paleolithic site of Marathousa 1 (Panagopoulou et al., 2018; Harvati et al., 2018, and references therein) highlights the potential importance of the broader region in human evolution research. Located in the Megalopolis Basin, Marathousa 1 dates to ca. 400–500 ka and as such, it is one of the oldest archaeological sites in Greece and the only known elephant-butchering open-air site in the Balkans. The open-cast lignite mines in the basin have exposed the geological sequence of a paleo-lake, which was active from ca. 900–300 ka (though frequently interrupt-

 http://dx.doi.org/10.15496/publikation-97646

P. Karkanas: https://orcid.org/0000-0002-7156-671X
V. Tourloukis: https://orcid.org/0000-0002-9527-2708
N. Thompson: https://orcid.org/0009-0003-4770-1744
D. Giusti: https://orcid.org/0000-0003-1438-4036
G. Tsartsidou: https://orcid.org/0000-0003-3379-1681
A. Athanassiou: https://orcid.org/0000-0002-9140-7011
G. E. Konidaris: https://orcid.org/0000-0002-7041-233X
E. Roditi: https://orcid.org/0000-0002-1917-7645
E. Panagopoulou: https://orcid.org/0000-0002-4268-6157
K. Harvati: https://orcid.org/0000-0001-5998-4794

ed by fluvial sedimentary regimes) (van Vugt et al., 2000), hosting a rich fauna and serving as an ideal habitat for hominin populations (see, e.g., Konidaris et al., 2018; Athanassiou et al., 2018; Michailidis et al., 2018; Doukas et al., 2018). In addition to a long and continuous geological sequence, the near-shore and lacustrine conditions under which the Megalopolis sediments were deposited (Karkanas et al., 2018) enabled the excellent preservation of organic materials: these include not only mammalian fauna, but also paleobotanical and microfaunal material (Field et al., 2018), and even minuscule and fragile remains such as wood, seeds, molluscs, rodents, birds, reptiles, eggshells, fish and insects (Panagopoulou et al., 2018). Therefore, the Megalopolis Basin offers an ideal setting to locate evidence of human presence during the earliest phases of human dispersal to Europe, as well as to pursue a detailed understanding of the paleoenvironmental conditions and their impact on human habitation and adaptation over time.

Built upon the targeted systematic survey for stratified remains in 2012-13 (Thompson et al., 2018); and the subsequent discovery (2013) and excavation (2013-19) of Marathousa 1 (Panagopoulou et al., 2018) by our joint team in the context of the ERC projects PaGE and CROSSROADS, a new five-year project was initiated in 2018: the Megalopolis Paleoenvironmental Project (MegaPal). MegaPal is a collaboration between the Hellenic Ministry of Culture and the American School of Classical Studies at Athens (ASCSA). Dr. P. Karkanas from ASCSA in collaboration with Prof. Katerina Harvati from Tübingen University and Dr. Eleni Panagopoulou from the Ministry of Culture are leading the project, in the framework of the ERC grant CROSSROADS awarded to Prof. Harvati. MegaPal is a multifaceted interdisciplinary project with many other institutes participating in its implementation.

The project has three main objectives largely overlapping with the broader research goals of CROSSROADS:

1. to survey exposed section profiles throughout the Megalopolis Basin, focusing on the lowest components of the geological sequence to locate archaeological evidence older than, or contemporary with, the chronology of Marathousa 1 (ca. 450 ka: Jacobs et al., 2018). This goal addresses the question of whether southeast Europe was occupied already in the Early or early Middle Pleistocene, as is the case in the southwestern and northern parts of the continent;
2. to help develop for the first time a regional chronological framework of the Lower Paleolithic in Greece and the Balkans in general. This goal will assess whether a gap existed between the earliest arrival of humans and the subsequent human activity in the Megalopolis Basin, or instead to determine whether hominin habitation was relatively continuous, as expected for areas with a refugium status;
3. to provide a palaeoecological framework within which to interpret the archaeological record of existing (Marathousa 1) and future sites with human activity in the Megalopolis Basin. This aim addresses the question of how behavioral and biological changes are related to environmental conditions, climatic fluctuations and landscape use.

16.2 METHODOLOGY

Field investigations were conducted by a small team of specialists (geologists, Palaeolithic archaeologists, paleontologists) who systematically examined the longitudinal profiles of sedimentary exposures. The project tests in the field a predictive model for locating early hominin sites, which has been conceptualized based on the sedimentological and stratigraphic study of the Marathousa

1 site (Karkanas et al., 2018). According to the model, the high probability areas of the geological sequence are those that confirm sedimentary evidence of shallow lake levels, terrestrial erosional surfaces and subaerial exposures. This type of sedimentary facies occurs mainly as relatively thin horizons or erosional contacts within sedimentary units, which directly underlie or overlie lignite seams thereby denoting also depositional environments that indicate transitional conditions from colder to warmer climatic stages and vice versa.

The survey focused on examining the part of the sequence between Lignite Units I and III. Survey areas were designated as "Survey Units" (SUs), which are arbitrary units of observation delineated by stratigraphic or artificial boundaries, such as the start/end of a tier inside the mine (Thompson et al., 2018). A large number of survey units were investigated, which were located inside the mines of Kyparissia, Marathousa and Choremi.

In addition to field survey, an extensive sampling program is in progress including a plethora of techniques. Several dating methods are employed including cosmogenic nuclides, paleomagnetism, electron spin resonance, U-Th series, and luminescence. An extensive micromorphological and sedimentological analysis of strata is conducted, as well as novel soil biochemistry analyses also including several palaeoenvironmental proxies (e.g., diatoms, sponge spicules, pollen, phytoliths, charcoal, wood, and seed).

Two boreholes from the Marathousa mine are also studied. The first one took place at the western part of the Marathousa mine and close to the Paleolithic site of Marathousa 1, reaching a total depth of 103 m. The other drill site was located at the northeastern part of the same mine next to the site of Marathousa 2 and reached a depth of 123 m. The goal of this ongoing study, currently underway at the University of Tübingen (see Bludau

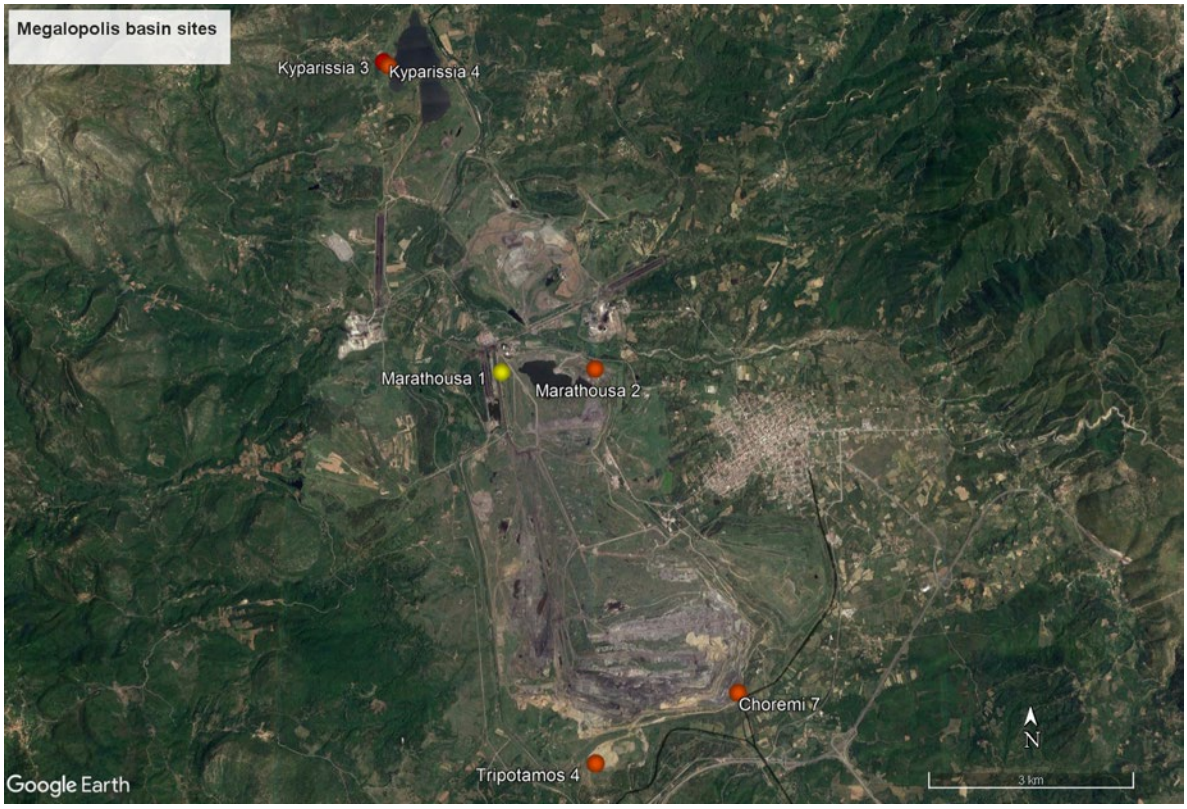

Figure 1: Location of the archaeological and paleontological sites mentioned in the text.

et al., this volume), is to retrieve and analyze environmental and biological proxies, such as micro-faunal and micro-fossil remains (e.g., insects, molluscs, ostracods, diatoms), plant micro- and macro-remains (pollen, phytoliths, gyrogonites, oospores, wood, fruit, seeds, spores, stamens, buds, scales), as well as geochemical and mineralogical data, which will altogether allow us to pursue a paleoenvironmental reconstruction of the paleo-lake system and its evolution through time.

Finally, a tectonosedimentary analysis of the basin is in progress with the aim to synthesize and analyze the geometry and sedimentary architecture of the entire basin and produce a complete history of the sedimentary fill (Kranis et al., 2020; this volume). The analysis of these diverse proxies, in combination with a well-constrained age model, will lead to a sophisticated, high-resolution reconstruction of the evolution of the paleoenvironment of the Megalopolis Basin. This reconstruction will put in context the highly significant archaeological findings already recovered. Importantly, however, it will also provide a detailed framework for understanding the interaction between early humans and their environment, with the ultimate goal of elucidating human adaptation in the Pleistocene, as well as of establishing a predictive model for identifying new Lower Palaeolithic sites in the area and in wetland environments in general.

16.3 RESULTS

During the five field campaigns of the project, MegaPal has identified five archaeological sites, one every field season, an exceptional rate of discovery (Fig. 1). In addition, numerous paleontological sites have been identified. The most important to be mentioned here is the oldest one, Choremi 6 (CHO-6), which is located under lignite seam Ia and therefore predates the Brunhes/Matuyama boundary (Tourloukis et al., 2018a). CHO-6 includes dental and post-cranial remains of hippopotamus, most likely belonging to a single individual. The fossils were found stratified at the contact between a lignite seam and the underlying deposit of grey clays, at an elevation of 291 m above sea level (masl). Oxidation features and rhizoliths indicate the presence of a paleo-surface that was subaerially exposed and was later covered by a swamp.

The first site discovered, Marathousa 2 (MAR-2), was found during the first year of the project, in 2018, and is located in a stratigraphic position similar to that of Marathousa 1, but on the eastern side of the mine (Fig. 1). MAR-2 is located above lignite seam IIb and below lignite seam IIIa, at an elevation of 355 masl (Fig. 2a). The site produced mainly paleontological findings, but with clear evidence of human modification of the fauna in the form of cut marks, which indicate butchering activities in the area (Konidaris et al., 2019, 2023). A lithic artifact was discovered during the last field season in the same stratigraphic unit as the hippopotamus bones with cut marks, thereby confirming the presence of human activities in the eastern part of the Marathousa mine (Konidaris et al., 2023).

The second site identified is Kyparissia 4 (KYP-4; Fig. 1). This was an already well-known paleontological locality found and studied by Athanassiou (2018) and Athanassiou et al., (2018). During a subsequent inspection of the area, lithic remains were discovered that could represent the earliest currently known evidence of human presence in Greece. The site lies on top of a weathered limestone protrusion of the Alpine basement in the north-westernmost edge of the former Pleistocene lake at Megalopolis. The sedimentary sequence comprises mainly silts and organic-rich muds occasionally rich in mollusc shells (Fig. 2b) that suggest a shoreline environment in the proximity of a carbonate spring (Boni et al., this volume; Papadopoulou et al., this volume). Based on the lignite

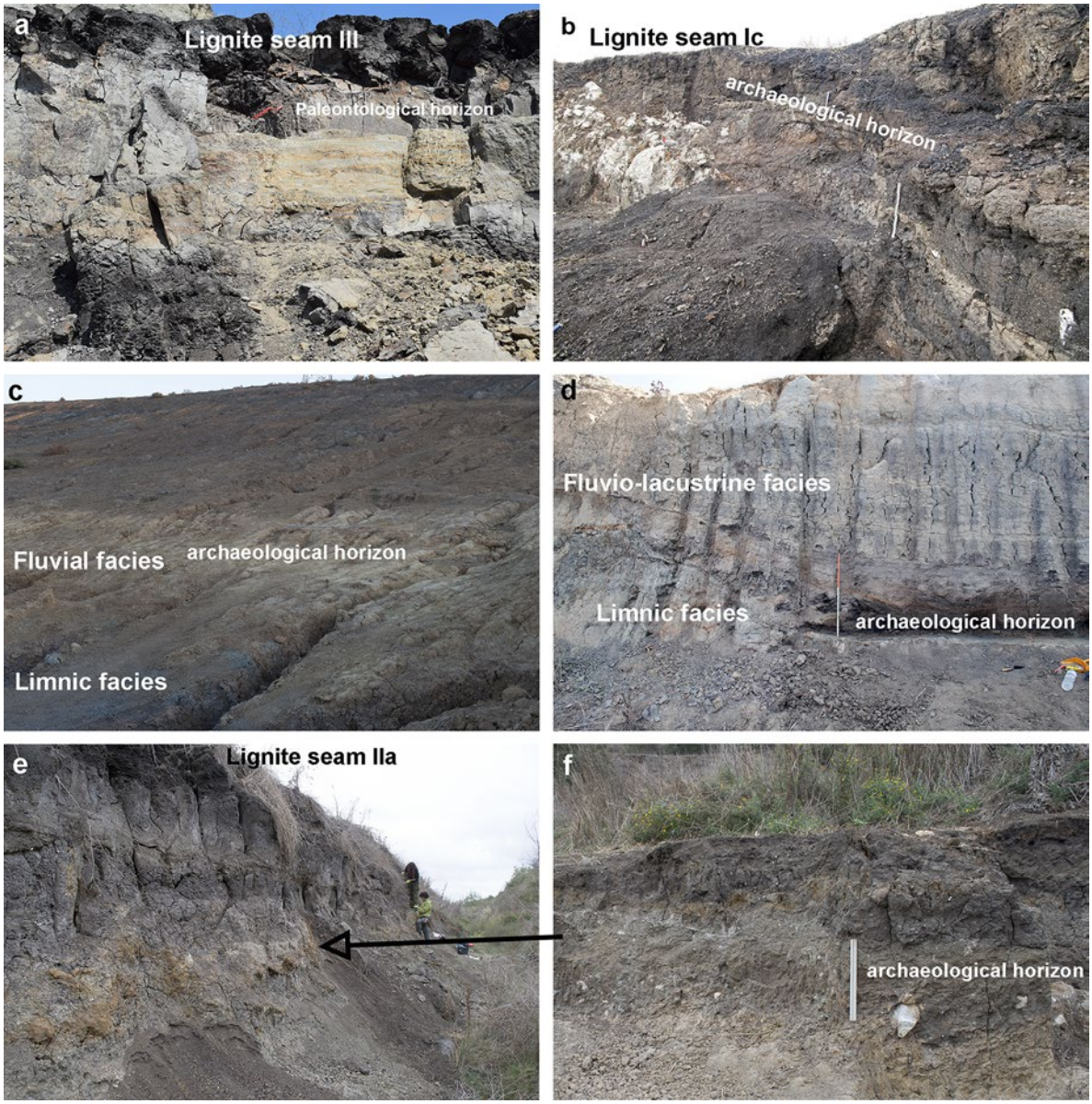

Figure 2: a) Marathousa 2 site; b) Kyparissia 4 site; c) Tripotamos 4 site; d) Choremi 7 site; e) and f) Kyparissia 3 site.

stratigraphy of the area, KYP-4 should be located close to the top of lignite seam I, at an elevation of 330 masl and therefore is stratigraphically much older than Marathousa 1.

KYP-4 is characterized by a typical Galerian fauna of an early Middle Pleistocene age (Athanassiou et al., this volume; van Kolfschoten et al., this volume). It comprises mainly artiodactyls (cervids, hippopotamids, bovids, suids), followed by rhinoceroses, few carnivorans, rodents, birds and turtles. Additionally, a primate tooth belongs to the macaque *Macaca sylvanus* documenting the second evidence for the presence of monkeys in the basin (Konidaris et al., this volume). Whereas the faunal remains suggest an older age than that of Marathousa 1, the lithic assemblage (N=53) is similar to the one of Marathousa 1 (Tourloukis et al., 2018b) with predominately small-sized debitage products and few retouched tools.

The site of Tripotamos 4 (TRP-4) was found in 2020 and it is located at the southwestern edge of the basin (Fig. 1). Archaeological and faunal re-

mains are concentrated along a light-colored silty-sand layer. The findings are found at the contact between bluish lacustrine muds and coarser clastic sediments deposited in a terrestrial environment with clear evidence of exposure in the form of iron-rich crusts (Fig. 2c). These sediments probably represent the first evidence of the transition of the limnic Marathousa Member to the fluvial Megalopolis Member at the western margin of the basin. In the lignite stratigraphy, TPR4 is most likely located stratigraphically above lignite seam IIIa at an elevation of about 390 masl. Therefore, the site is stratigraphically younger than Marathousa 1.

TRP-4 is very rich in archaeological finds, particularly lithics. The lithic assemblage (N=206) consists of flakes and flake fragments, cores, debris and retouched tools, and there is no evidence of bifacial knapping. Overall, when compared to the assemblages from Marathousa 1 and Kyparissia 4, the lithic toolkit from TRP-4 shows affinities with the older material from MAR-1 and KYP-4, but it also presents potentially noteworthy differences in aspects of core management and core exploitation. Due to the more terrestrial environment of deposition, the faunal material is less well preserved, comprising mostly long-bone fragments, but also a cervid antler and elephantid lamellar fragments.

During the fourth field season the new site of Choremi 7 (CHO-7) was discovered. The site is found at the eastern margin of the mine at an elevation of 384 masl, at a similar elevation to TRP-4 (Fig. 1). Archaeological remains were identified at an erosional contact between bluish lacustrine muds of the Marathousa Member and an overlying underwater channel of silts and sands of the Megalopolis fluvial member (Fig. 2d). In contrast to what was observed in the case of TRP-4, CHO-7 is located above the entire lignite sequence of seam III, and specifically above the last lignite seam IIIc. Therefore, although both sites are located in a similar depositional environment at the contact of Marathousa limnic with Megalopolis fluvial sediment, CHO-7 appears to be stratigraphically much younger than TRP-4. This is also confirmed by the rich lithic assemblage that was discovered (N=116), which shows evidence of Middle Palaeolithic affinities and includes tools shaped by bifacial knapping and preferential treatment of raw materials that differs from the other sites. The fauna is relatively rich, consisting mainly of shaft fragments of cervids, a few remains of birds, and several bones with cut-marks. Several wood fragments and well-preserved pinecones were also found. CHO-7 is the youngest site of the sequence, and it demarcates the end of the lacustrine phase of the Megalopolis Basin at the eastern margin of the basin and the beginning of the establishment of the modern drainage system of the Alpheios River.

Finally, the fifth site identified is Kyparissia 3 (KYP-3) (Fig. 1). This was also an already known paleontological locality found and studied by Athanassiou (2018) and Athanassiou et al., (2018). KYP-3 is located above KYP-4 site at an elevation of 346 masl. Stratigraphically, it is placed in the upper parts of the clastic unit underlying Lignitic Seam II (Fig. 2e and f), and is therefore younger than Kyparissia 4, but older than Marathousa 1. During a reinvestigation of the area, skeletal remains of elephant and other large mammals were found in direct spatial and stratigraphic association with lithic artifacts (N=19). The newly collected faunal material of the site is dominated by elephant skeletal elements (a molar and several bones, mainly ribs), but also includes artiodactyls (Hippopotamidae, Cervidae, Suidae), as well as turtles and birds. The lithic artifacts consist of simple flakes, flake fragments and debris from core reduction, as well as a few possible tools or tool fragments with evidence of retouch, all of which are made of radiolarite.

16.4 CONCLUDING REMARKS

The five-year program of surface and geoarchaeological investigations resulted in the identification of five new and important Palaeolithic sites in the Megalopolis Basin, all dating to the Middle Pleistocene. The sites preserve cultural and faunal remains in stratigraphic contexts and offer a unique opportunity to investigate human behavior over time, for an important period in the history of human evolution and in an area that had been thus far little investigated. There are a lot of studies to be conducted, but the preliminary palaeoenvironmental indications obtained through the Megalopolis geological sequence demonstrate the presence of humans in the basin during multiple periods within the Middle Pleistocene and a likely refugium status of the area.

ACKNOWLEDGMENTS

The 2018-2021 Field survey in the Megalopolis Basin was conducted in the framework of the Megalopolis Paleoenvironmental Project (MegaPal) under a permit granted to the Ephorate of Paleoanthropology–Speleology, Hellenic Ministry of Culture, and the American School of Classical Studies at Athens. Fieldwork was supported by the ERC Consolidator Grant ERC-CoG-724703 ("CROSSROADS"), awarded to K.H. G.E.K., V.T. and K.H. are also supported by the Deutsche Forschungsgemeinschaft (DFG Project no. 463225251, "MEGALOPOLIS"). K.H. is also supported by the ERC Advanced Grant ERC-AdG-101019659 ("FIRSTSTEPS"). We would like to thank our reviewers G. Syrides and P. Elefanti for their constructive comments and suggestions.

REFERENCES

Athanassiou, A., 2018. Pleistocene vertebrates from the Kyparíssia lignite mine, Megalopolis Basin, S. Greece: Rodentia, Carnivora, Proboscidea, Perissodactyla, Ruminantia. Quaternary International, 497, pp. 198–221.

Athanassiou, A., Konidaris, G.E., Tourloukis, V., Thompson, N., Giusti, D., Karkanas, P. and Harvati, K., this volume. The Middle Pleistocene large mammal fauna from Kyparissia (Peloponnese, S. Greece): New collected material.

Athanassiou, A., Michailidis, D., Vlachos, E., Tourloukis, V., Thompson, N. and Harvati, K., 2018. Pleistocene vertebrates from the Kyparíssia lignite mine, Megalopolis Basin, S. Greece: Testudines, Aves, Suiformes. Quaternary International, 497, pp. 178–197.

Bludau, I.J.E., Junginger, A., Wagner, B., Kirscher, U., Zachow, C., Schindler, M., Tourloukis, V., Kyrikou, S., Karkanas, P., Panagopoulou, E. and Harvati, K., this volume. Overview of MAR-1A and MAR-2A drill core analysis and chronological framework.

Boni, G., Syrides, G., Konidaris, G.E., Athanassiou, A., Tourloukis, V., Koukousioura, O., Panagopoulou, E., Karkanas, P. and Harvati, K., this volume. Preliminary results on the taxonomy and paleoenvironmental analysis of the mollusc fauna from Marathousa 1, Marathousa 2 and Kyparissia 4 (Middle Pleistocene, Megalopolis Basin, Greece).

Doukas, C., van Kolfschoten, T., Papayianni, K., Panagopoulou, E. and Harvati, K., 2018. The small mammal fauna from the palaeolithic site Marathousa 1 (Greece). Quaternary International, 497, pp. 95–107.

Field, M.H., Ntinou, M., Tsartsidou, G., van Berge Henegouwen, D., Tourloukis, V., Thompson, N., Karkanas, P., Panagopoulou, E. and Harvati, K., 2018. A palaeoenvironmental recon-

struction (based on palaeobotanical data and diatoms) of the Middle Pleistocene elephant (*Palaeoloxodon antiquus*) butchery site at Marathousa, Megalopolis, Greece. Quaternary International, 497, pp. 108–122.

Harvati, K., 2016. Paleoanthropology in Greece: recent findings and interpretations, in Harvati, K. and Roksandic, M. (Eds.), Paleoanthropology of the Balkans and Anatolia: Human Evolution and its Context. Vertebrate Paleobiology and Paleoanthropology Series, pp. 3–14. Springer, Dordrecht.

Harvati, K., 2022. The hominin fossil record from Greece, in: Vlachos, E. (Ed.), Fossil Vertebrates of Greece Vol. 1 – Basal vertebrates, amphibians, reptiles, afrotherians, glires, and primates. Springer – Nature Publishing Group, Cham, pp. 669–688.

Harvati, K., Panagopoulou, E. and Runnels, C., 2009. The paleoanthropology of Greece. Evolutionary Anthropology, 18, pp. 31–43.

Harvati, K., Konidaris, G. and Tourloukis, E. (Eds.), 2018. Human Evolution at the Gates of Europe. Quaternary International, 497.

Jacobs, Z., Li, B., Karkanas, P., Tourloukis, ppV., Thompson, N., Panagopoulou, E. and Harvati, K., 2018. Beyond maps: Optical dating of K-feldspar grains from Middle Pleistocene lacustrine sediment at Marathousa 1 (Greece). Quaternary International, 497, pp. 170–177.

Karkanas, P., Tourloukis, V., Thompson, N., Giusti, D., Panagopoulou, E. and Harvati, K., 2018. Sedimentology and micromorphology of the Lower Palaeolithic lakeshore site Marathousa 1, Megalopolis Basin, Greece. Quaternary International, 497, pp. 123–136.

Konidaris, G.E., Athanassiou, A., Panagopoulou, E., Karkanas, P. and Harvati, K., this volume. Fossil macaques (Cercopithecidae, Primates) from the Middle Pleistocene of the Megalopolis Basin (Greece) with description of a new specimen from Kyparissia 4.

Konidaris, G.E., Athanassiou, A., Tourloukis, V., Thompson, N., Giusti, D., Panagopoulou, E. and Harvati, K., 2018. The skeleton of a straight-tusked elephant (*Palaeoloxodon antiquus*) and other large mammals from the Middle Pleistocene butchering locality Marathousa 1 (Megalopolis Basin, Greece): preliminary results. Quaternary International, 497, pp. 65–84.

Konidaris, G., Tourloukis, V., Athanassiou, A., Giusti, D., Thompson, N., Panagopoulou, E., Karkanas, P. and Harvati, K., 2019. Marathousa 2: A new Middle Pleistocene locality in Megalopolis Basin (Greece) with evidence of human modifications on faunal remains. Proceedings of the European Society for the study of Human Evolution, 8, 82.

Konidaris, G., Tourloukis, V., Boni, G., Athanassiou, A., Giusti, D., Thompson, Syrides, G., N., Panagopoulou, E., Karkanas, P. and Harvati, K., 2023. Marathousa 2: A new Middle Pleistocene locality in Megalopolis Basin (Greece) with evidence of human exploitation and megafauna (*Hippopotamus*). PaleoAnthropology 2023, pp. 34-55.

Kranis, H., Skourtsos, E., Davis, G., Karkanas, P., Tourloukis, V., Panagopoulou, E. and Harvati, K., 2020. Switch-on, switch-off: Plio-Quaternary evolution of the Megalopolis Basin (Southern Greece), through structural overprinting, interaction and fault migration, European Geoscience Union – EGU General Assembly 2020, Online, 4–8 May 2020.

Michailidis, D., Konidaris, G.E., Athanassiou, A., Panagopoulou, E. and Harvati, K., 2018. The ornithological remains from Marathousa 1 (Middle Pleistocene; Megalopolis Basin, Greece). Quaternary International, 497, pp. 85–94.

Panagopoulou, E., Tourloukis, V., Thompson, N., Konidaris, G., Athanassiou, A., Giusti, D., Tsartsidou, G., Karkanas, P. and Harvati,

K., 2018. The Lower Palaeolithic site of Marathousa 1, Megalopolis, Greece: Overview of the evidence. Quaternary International, 497, pp. 33–46.

Papadopoulou, P., Tsoni, M., Konidaris, G.E., Tourloukis, V., Panagopoulou, E., Karkanas, P., Harvati, K. and Iliopoulos, G., this volume. Ostracod contribution to the palaeoenvironmental study of Kyparissia-4 (Megalopolis Basin, Greece).

Thompson, N., Tourloukis, V., Panagopoulou, E. and Harvati, K., 2018. In search of Pleistocene remains at the Gates of Europe: Directed surface survey of the Megalopolis Basin (Greece). Quaternary International, 497, pp. 22–32.

Tourloukis, V., Karkanas, P., 2012. The Middle Pleistocene record of Greece and the role of the Aegean in hominin dispersals: new data and interpretations. Quaternary Science Reviews 43, pp. 1-15.

Tourloukis V., Harvati K. 2018. The Palaeolithic record of Greece: a synthesis of the evidence and a research agenda for the future. Quaternary International, SI Filling the Geographic Gaps in the Human Evolutionary Story, 466, 48–65.

Tourloukis, V., Muttoni, G., Karkanas, P., Mones, E., Scardia, G., Panagopoulou, E. and Harvati, K., 2018a. Magnetostratigraphic and chronostratigraphic constraints on the Marathousa 1 Lower Palaeolithic site and the Middle Pleistocene deposits of the Megalopolis Basin, Greece. Quaternary International, 497, pp. 47–64.

Tourloukis, V., Thompson, N., Panagopoulou, E., Giusti, D., Konidaris, G., E., Karkanas, P. and Harvati, K., 2018b. Lithic artifacts and bone tools from the Lower Palaeolithic site Marathousa 1, Megalopolis, Greece: Preliminary results. Quaternary International, 497, pp. 47–64.

Tzedakis, P.C., Lawson, I.T., Frogley, M.R., Hewitt, G.M. and Preece, R.C., 2002.Buffered tree population changes in a Quaternary refugium: Evolutionary implications. Science, 297, pp. 2044–2047.

van Kolfschoten, T., Konidaris, G.E., Doukas, C., Athanassiou, A., Tourloukis, V., Panagopoulou, E., Karkanas, P. and Harvati, K., this volume. Voles (Rodentia, Mammalia) as a proxy to date the site Kyparissia 4 (Megalopolis Basin, Greece).

van Vugt, N., de Bruijn, H., van Kolfschoten, T. and Langereis, C.G., 2000. Magneto- and cyclostratigraphy and mammal-fauna's of the Pleistocene lacustrine Megalopolis Basin, Peloponnesos, Greece. Geologica Ultrajectina, 189, pp. 69–92.

17 OVERVIEW OF MAR18-1A AND MAR18-2A DRILL CORE ANALYSIS AND CHRONOLOGICAL FRAMEWORK

Ines J. E. Bludau[1,2]*, Annett Junginger[1,2]*, Bernd Wagner[3], Uwe Kirscher[1], Charlotte Zachow[1], Maria Schindler[1], Vangelis Tourloukis[1,4,5], Styliani Kyrikou[1,4], Panagiotis Karkanas[6], Eleni Panagopoulou[7], Katerina Harvati[1,2,4,8]

[1]*Department of Geosciences, Eberhard Karls University of Tübingen, Tübingen, Germany*
[2]*Senckenberg Centre for Human Evolution and Palaeoenvironment, Tübingen, Germany*
[3]*Institute of Geology and Mineralogy, University of Cologne, Cologne, Germany*
[4]*Paleoanthropology, Institute for Archaeological Sciences, Eberhard Karls University of Tübingen, Tübingen, Germany*
[5]*Department of History and Archaeology, School of Philosophy, University of Ioannina, Ioannina, Greece*
[6]*M.H. Wiener Laboratory for Archaeological Science, American School of Classical Studies at Athens, Athens, Greece*
[7]*Hellenic Ministry of Culture, Ephorate of Palaeoanthropology-Speleology, Athens, Greece*
[8]*DFG Centre for Advanced Studies 'Words, Bones, Genes, Tools', Eberhard Karls University of Tübingen, Tübingen, Germany*
**ines.bludau@uni-tuebingen.de, annett.junginger@uni-tuebingen.de*

http://dx.doi.org/10.15496/publikation-97673

Keywords: Megalopolis Basin; Early Mid Pleistocene Transition; μ-XRF; stratigraphy; Brunhes-Matuyama Boundary

17.1 INTRODUCTION

Greece, with its position between continental Europe, Africa and Asia, is an important crossroad for the hominin migration into Europe (e.g., Harvati et al., 2009; Tourloukis and Karkanas, 2012; Harvati, 2016; Harvati et al., 2018). Its significance as a glacial refuge or simply as a transit region is still heavily debated due to the scarcity of archaeological evidence from the Paleolithic (Agustí et al., 2009; Harvati, 2016; Muttoni et al., 2013; Reyes-Centeno et al., 2017; Stewart and Stringer, 2012; Tsakanikou et al., 2021). The archaeological site Marathousa (MAR-1), located in the Megalopolis Basin on the central Peloponnese, is one of only four Lower Paleolithic sites identified in the country until recently (Tourloukis and Harvati, 2018). Its preservation and chronological framework are optimal for investigating the significance of the region as a glacial refugium or simply a transit region. The Megalopolis Basin consists mainly of lignite-bearing fluvio-lacustrine sediments. The basin filling was drilled and cored in 2018, retrieving two complete cores (MAR18-1A and MAR18-2A) and first results are presented here.

Preceding studies of the archaeological site MAR-1 revealed sediments indicative of a paleo-lake shoreline environment. The sediments contain various fossils (e.g., mammalian bones, seeds, leaves and wood pieces), as well as lithic tools, indicating hominin activities (Field et al., 2018; Konidaris et al., 2018; Tourloukis et al.,

I. Bludau: https://orcid.org/0000-0002-0876-9012
A. Junginger: https://orcid.org/0000-0003-3486-0888
B. Wagner: https://orcid.org/0000-0002-1369-7893
U. Kirscher: https://orcid.org/0000-0003-4203-1430
Ch. Zachow: https://orcid.org/0009-0006-4735-4131
V. Tourloukis: https://orcid.org/0000-0002-9527-2708
S. Kyrikou: https://orcid.org/0009-0000-8199-1317
P. Karkanas: https://orcid.org/0000-0002-7156-671X
K. Harvati: https://orcid.org/0000-0001-5998-4794
E. Panagopoulou: https://orcid.org/0000-0002-4268-6157

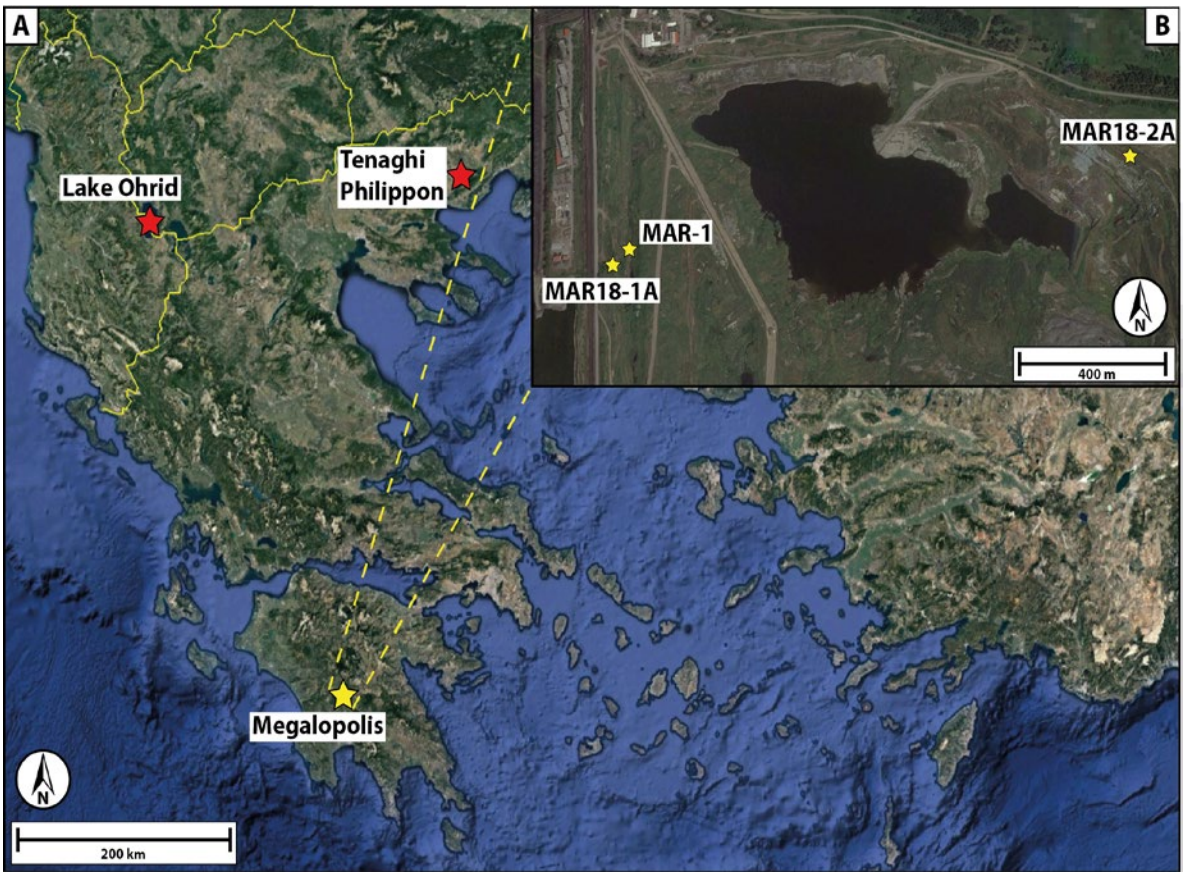

Figure 1: A) Overview of the drill location (yellow star) on the Peloponnese peninsula and sites (red stars) mentioned in the text. B) Drill locations of MAR18-1A and MAR18-2A (Google Earth image).

2018b). Remarkable is a large assortment of lithic tools in spatial and stratigraphic association with the bones of a straight-tusked elephant *Palaeoloxodon antiquus* that show cut marks, being evidence for butchering activities of hominins (Konidaris et al., 2018; Tourloukis et al., 2018b). MAR-1 was dated to ~450 ka, corresponding with Marine Isotope Stage (MIS) 12. Paleoenvironmental reconstructions conducted at the 6-m profile of MAR-1 revealed the presence of seasonal ponds and the potential of the basin as a refuge for hominins and other animals during the tentatively harsh, glacial climate conditions (Bludau et al., 2021; Tourloukis et al., 2018a).

The 6-m long sedimentary succession of MAR-1 is part of the ca. 135 m thick Marathousa Member, deposited during the Pleistocene (Van Vugt et al., 2001). The sediment succession is characterized by alternating layers of clastics (clays, sands and silts) and lignites (Vinken, 1965) and covers the period ~800–400 ka (Tourloukis et al., 2018a; van Vugt et al., 2001). Over the past years, additional archaeological localities within the Marathousa Member have been identified (Konidaris et al., 2023; Karkanas et al., this volume). In order to provide a temporally well-constrained paleoenvironmental framework, two sediment cores, MAR18-1A and MAR18-2A, have been drilled through the entire Marathousa Member in 2018 (Figs. 1; 2). Here, an overview of the ongoing analysis is presented. The deposition of the cored sediments occurred during the middle and end phase of the Early-Middle Pleistocene Transition (EMPT), with the Brunhes-Matuyama Boundary (B-M Boundary, 780 ka) located at ~83 m core depth in MAR18-1A (Fig. 2; see preliminary re-

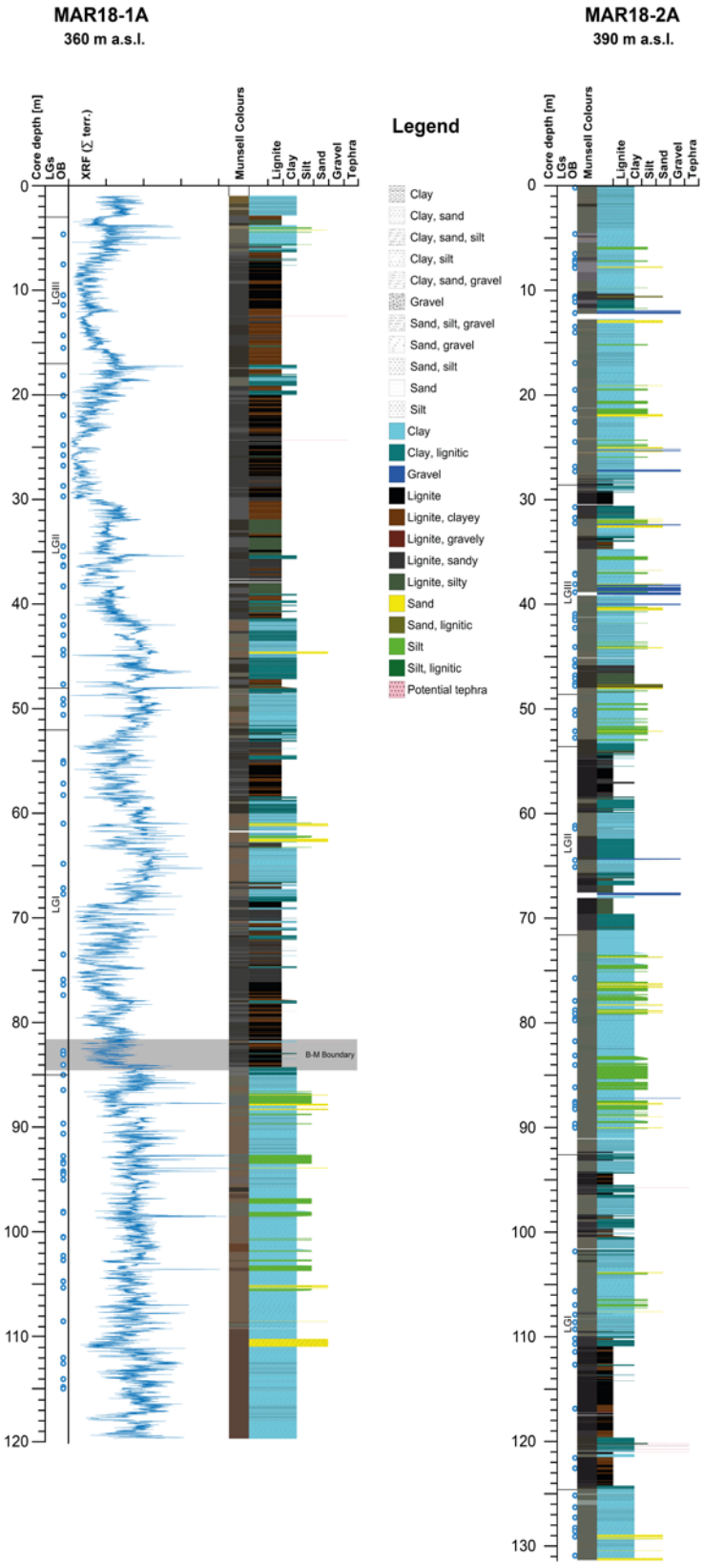

Figure 2: Stratigraphy of cores MAR18-1A and MAR18-2A with first µ-XRF results showing the sum of terrestrial elements (Al, Fe, K, Rb, Si, Ti), as well as the inferred depth of the Brunhes-Matuyama Boundary (B-M Boundary).

sults) and with MAR-1, representing ~450 ka, at ~15–17 m core depth. The EMPT is a major global climate transition from ~41 ka to ~100 ka glacial-interglacial periodicity, which lasted in total from 1.4 to 0.4 Ma, ending with the Mid-Brunhes Event (Head and Gibbard, 2015). Besides the scarcity of terrestrial proxy-records in the Mediterranean realm covering large parts of the EMPT, these cores, together with the number of new archaeological sites in the basin, bear a high potential for understanding how environmental changes may have influenced the behavior of hominins in Greece over time.

17.2 DATA AND METHODS

Two sediment cores were retrieved in 2018, MAR18-1A (N 37.408387°, E 22.090907°) ~20 m north to the archeological site MAR-1, and MAR18-2A (N 37.410291°, E 22.108264°) located 1.5 km east of MAR-1 (Fig. 1) with a drill depth of 103 m and 123 m, respectively. In 2019, additional outcrop descriptions at the MAR18-2A site have been conducted (MAR19-2AP) in order to correlate the lithologies with the drill cores. The drilling was carried out without liners due to the high abundance of lignites, with each drill run being 3 m. The cores were cut into 1 m long sections and stored in wooden boxes for transport. In the laboratory, the cores were transferred into plastic liners and cut into two halves lengthwise, with an archive half for non-destructive analyses, and a working half for destructive analyses. After core opening, a detailed core description was performed, followed by non-destructive μ-XRF core analysis at the Geoscience department at Cologne University. Core logging was performed using the Corelyzer and Psicat software.

The core analysis is complemented by ongoing grain-size analysis, CNS, TOC, micro-tephra, as well as paleomagnetic measurements. In order to provide an age model for the drilled cores, different age modelling approaches are currently tested for their robustness focusing on the uppermost 87 m of the MAR18-1A core. The study utilizes and compares three different age modelling approaches: a) a classical statistical model with a static bandpass filter (Duesing et al., 2021; Grant et al., 2017; Hays et al., 1976); b) the multiband wavelet model (MUBAWA) with adaptive bandpass filters (Duesing et al., 2021), both tuning the dataset to orbital parameters; c) a hiatus model that constructs an age model based on dating and statistical properties of the sediments and their depositional behavior (Trauth, 2014). At 87 m depth, a drastic shift in sedimentology pattern (dark lignites and clays to grey and brown clays) indicates the presence of a considerable hiatus. Consequently, the study is restricted to the uppermost 87 m. The hiatus occurs just below the approximate depth of the B-M Boundary, which is tentatively at ~83 m, and is considered to indicate that either the Early Pleistocene or the Pliocene sediments (clays, sands and gravels) of the underlying Trilofon Formation have been reached.

17.3 PRELIMINARY RESULTS

17.3.1. STRATIGRAPHY AND μ-XRF

While the drilled core depths were 103 m (MAR18-1A) and 123 m (MAR18-2A), the described material encompasses ~119 m and ~131 m, respectively. The differences in lengths can be caused by the open-core-drilling technique, where clays can stretch and lignites expand, by gas (CH_4) expansion or sediment lengthening during core lifting from the borehole. Both cores consist of alternately deposited clastic material (clay, silt and sand) and lignites, with the occurrence of more clastic material in the lower parts (Fig. 2). Due to the irregular

Section	Section Depth	Core Depth	Tephra
MAR18-1A 08-1	0.57—0.58	13.06—13.07	—
MAR18-1A 12-1	0.10—0.11	25.15—25.16	+
MAR18-1A 12-2	0.08—0.09	26.00—26.01	+
MAR18-1A 12-2	0.15—0.16	26.07—26.08	+
MAR18-1A 12-3	0.05—0.06	27.03—27.04	+
MAR18-1A 13-4	0.34—0.35	31.20—31.21	—
MAR18-1A 14-2	0.18—0.19	32.00—32.01	—
MAR18-1A 22-3	0.70—0.71	51.55—51.56	—
MAR18-1A 26-2	0.24—0.25	62.51—62.52	—
MAR18-1A 26-2	0.49—0.50	62.76—62.77	—
MAR18-1A 26-2	0.58—0.59	62.85—62.86	—
MAR18-1A 26-2	0.86—0.87	63.13—63.14	—
MAR18-1A 29-4	0.08—0.09	72.80—72.81	—
MAR18-1A 29-4	0.25—0.26	72.97—72.98	—
MAR18-1A 29-4	0.40—0.41	73.12—73.13	—
MAR18-1A 29-4	0.50—0.51	73.22—73.23	—

Table 1: Overview of analyzed µ-tephra samples in core sections and with total core depth.

behavior of lignites and their different composition in general, lignite seams in the cores can only tentatively be assigned to the three (LGI/Elias, LGII/Otto, LGIII/Panagiotis) known lignite seams from outcrop observations. The correlations place LGI in MAR18-1A between depths ~87–52 m, LGII to ~48–20 m and LGIII to 17–3 m. Respective lignite seams are found in MAR18-2A core at ~124–92 m (LGI), ~71–53 m (LGII) and ~48–28 m (LGIII) depths.

Core Depth (m)	Age (ka)	Error (ka)	Method
12.95	415	46	Post-infrared infrared stimulated luminescence (Jacobs et al., 2018)
13.05	420	10	Age modelling (Tourloukis et al., 2018)
18.05	451	35	Post-infrared infrared stimulated luminescence (Jacobs et al., 2018)
19.45	457	40	Post-infrared infrared stimulated luminescence (Jacobs et al., 2018)
19.55	468	34	Post-infrared infrared stimulated luminescence (Jacobs et al., 2018)
20.00	480	10	Age modelling (Tourloukis et al., 2018)
83.00	780	10	Paleomagnetic measurements

Table 2: Overview of dating methods, ages and errors used in the age modelling.

An important change in MAR18-1A core lithology takes place at a depth of ~87 m (Fig. 2). Massive yellowish brown silty and sandy clays occasionally interrupted by olive-grey clays (below) sharply transition to black and grey lignites that are intercalated with layers of reddish, brown and grey clays, silts and sands (above). While iron oxide and carbonate nodules often appear in the clastic layers, their number is markedly higher in the lower part of the core. Shell fragments can often be found in the lignites and lignitic clays. Compared to MAR18-1A, MAR18-2A contains significantly less black and grey lignites and rather dark greenish-grey, as well as olive-grey, clastic material. The clastics comprise clays, silts and sands, and often contain iron and carbonate nodules. Shell fragments were encountered especially in the lower lignites and in some thin layers of the upper clastics. The differences in the thickness and sedimentology of the two cores are attributed to their location relative to the former lake. MAR18-1A is located at the western, shallower margin of the basin, where-

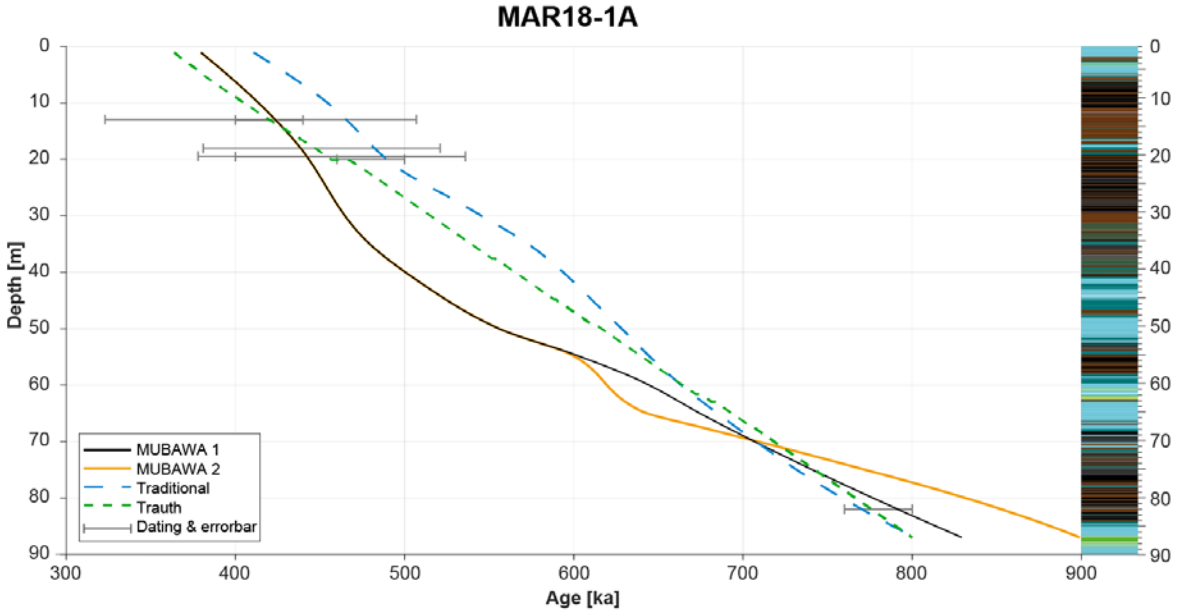

Figure 3: Summary of different age modelling approaches of core MAR18-1A with MUBAWA 1 being the preferred age model at this stage of the analysis.

as MAR18-2A is placed in the eastern, deeper part of the former lake (Vinken, 1965).

The µ-XRF analysis reveals high counts of terrestrial elements (e.g., Al, Ti, K, Fe, Rb, Si) typically observed in the clastic sediments, while low counts mirror the organic rich lignites.

17.3.2. CHRONOLOGY

The first results of the paleomagnetic analyses of MAR18-1A reveal the presence of the B-M Boundary located between ~81.5–84.5 m core depth. The tentative depth of the archaeological site MAR-1 sediments in the core MAR18-1A, that is dated to ~450 ka, most likely at 14–16 m core depth. Consequently, the sedimentary sequence between the lowermost and uppermost lignite seam in the core must encompass at least the time period between ~780–450 ka.

For micro-tephra analysis, horizons were selected where odd peaks in the in the µ-XRF record occurred. While tephra shards could be identified in several samples (Tab. 1), it was not enough for a more detailed analysis.

On the basis of the existing and preliminary ages (Tab. 2), the different age models (Trauth, Classic, MUBAWA) yield a rough general depositional time period of MAR18-1A between ~350–800 ka, ~410–800 ka and ~375–900 ka, respectively, with high internal depositional variations (Fig. 3). Of those, the age model generated with the MUBAWA code is considered the best fitting one. This highly statistical approach does not overly rely on input ages, it utilizes them only as control feature to evaluate the precision of various generated models, and compensates for post depositional diagenetic changes like compaction.

17.4 FUTURE PERSPECTIVE

The cores MAR18-1A and MAR18-2A are remarkable due to their length and continuity in sedimentation which is unparalleled in this region so far. Combining the results of the cores MAR18-1A and MAR18-2A with the two contemporaneous climate archives of Tenaghi Philippon (Tzedakis et al., 2006) and Lake Ohrid (Wagner et al., 2019), grants the opportunity to provide a region-

al paleo-climate gradient map of the EMPT and its potential impact on hominin migrations. The insights gained by performing a paleoenvironmental reconstruction from the cores using a multiproxy approach including pollen, biomarker, geochemistry and aquatic microfossils will help to identify why and when the Megalopolis Basin has served as a refuge region. Furthermore, potential forcing mechanisms that may have triggered hominin migrations could be identified, increasing the understanding of potential migration routes. Finally, it will be possible to clarify why hominins choose to settle in certain areas, which in turn might aid in identifying other archeological sites.

ACKNOWLEDGMENTS

Excavation at Marathousa 1 and research in Marathousa 2 were conducted under a permit granted to the Ephorate of Palaeoanthropology-Speleology, Hellenic Ministry of Culture, and the American School of Classical Studies at Athens. They were supported by the ERC Consolidator Grant ERC-CoG-724703 ("CROSSROADS") and the ERC Starting Grant ERC-StG-283503 ("PaGE"), both awarded to K.H. K.H. is also supported by the ERC Advanced Grant ERC-AdG-101019659 ("FIRSTSTEPS"). We would also like to thank the two reviewers who took the time to review the manuscript and greatly appreciate their constructive comments, which helped to improve the quality of the manuscript.

REFERENCES

Agustí, J., Blain, H.A., Cuenca-Bescós, G. and Bailon, S., 2009. Climate forcing of first hominid dispersal in Western Europe. Journal of Human Evolution, 57, pp. 815–821.

Bludau, I.J.E., Papadopoulou, P., Iliopoulos, G., Weiss, M., Schnabel, E., Thompson, N., Tourloukis, V., Zachow, C., Kyrikou, S., Konidaris, G.E., Karkanas, P., Panagopoulou, E., Harvati, K. and Junginger, A., 2021. Lake-Level Changes and Their Paleo-Climatic Implications at the MIS 12 Lower Paleolithic (Middle Pleistocene) Site Marathousa 1, Greece. Frontiers in Earth Science, 9, pp. 1–26.

Duesing, W., Berner, N., Deino, A.L., Foerster, V., Kraemer, K.H., Marwan, N. and Trauth, M.H., 2021. Multiband Wavelet Age Modeling for a ~293 m (~600 kyr) Sediment Core From Chew Bahir Basin, Southern Ethiopian Rift. Frontiers in Earth Science, 9, pp. 1–15.

Field, M.H.H., Ntinou, M., Tsartsidou, G., van Berge Henegouwen, D., Risberg, J., Tourloukis, V., Thompson, N., Karkanas, P., Panagopoulou, E. and Harvati, K., 2018. A palaeoenvironmental reconstruction (based on palaeobotanical data and diatoms) of the Middle Pleistocene elephant (*Palaeoloxodon antiquus*) butchery site at Marathousa, Megalopolis, Greece. Quaternary International, 497, pp. 108–122.

Grant, K.M., Rohling, E.J., Westerhold, T., Zabel, M., Heslop, D., Konijnendijk, T. and Lourens, L., 2017. A 3 million year index for North African humidity/aridity and the implication of potential pan-African Humid periods. Quaternary Science Reviews, 171, pp. 100–118.

Harvati, K., 2016. Paleoanthropology of the Balkans and Anatolia, Paleoanthropology of the Balkans and Anatolia, Vertebrate Paleobiology and Paleoanthropology. Springer Netherlands, Dordrecht.

Harvati, K., 2009. Petralona: link between Africa and Europe? Hesperia Supplements, 43, pp. 31–47.

Harvati, K., Konidaris, G., Tourloukis, V., 2018. Special Issue Human Evolution at the Gates of Europe. Quaternary International, 497, 1–240.

Hays, J.D., Imbrie, J., Shackleton, N.J., 1976. Variations in the earth's orbit: Pacemaker of the ice ages. Science, 194, pp. 1121–1132.

Head, M.J. and Gibbard, P.L., 2015. Early-Middle Pleistocene transitions: Linking terrestrial and marine realms. Quaternary International, 389, pp. 7–46.

Karkanas, P., Tourloukis, V., Thompson, N., Giusti, D., Tsartsidou, G., Athanassiou, A., Konidaris, G.E., Roditi, E., Panagopoulou, E. and Harvati, K., this volume. The Megalopolis Paleoenvironmental Project (MegaPal).

Konidaris, G., Tourloukis, V., Boni, G., Athanassiou, A., Giusti, D., Thompson, N., Syrides, G., Panagopoulou, E., Karkanas, P. and Harvati, K., 2023. Marathousa 2: A New Middle Pleistocene Locality in the Megalopolis Basin (Greece) With Evidence of Hominin Exploitation of Megafauna (*Hippopotamus*). PaleoAnthropology, Vol. 2023:1, pp. 34–55.

Konidaris, G.E., Athanassiou, A., Tourloukis, V., Thompson, N., Giusti, D., Panagopoulou, E. and Harvati, K., 2018. The skeleton of a straight-tusked elephant (*Palaeoloxodon antiquus*) and other large mammals from the Middle Pleistocene butchering locality Marathousa 1 (Megalopolis Basin, Greece): preliminary results. Quaternary International, 497, pp. 65–84.

Muttoni, G., Scardia, G., Kent, D.V., 2013. A critique of evidence for human occupation of Europe older than the Jaramillo subchron (~1Ma): Comment on "The oldest human fossil in Europe from Orce (Spain)" by Toro-Moyano et al. (2013). Journal of Human Evolution, 65, pp. 746–749.

Reyes-Centeno, H., Rathmann, H., Hanihara, T. and Harvati, K., 2017. Testing modern human out-of-Africa dispersal models using dental nonmetric data. Current Anthropology, 58, pp. S406–S417.

Stewart, J.R., Stringer, C.B., 2012. Human evolution out of Africa: The role of refugia and climate change. Science, 335, pp. 1317–1321.

Tourloukis, V., Harvati, K., 2018. The Palaeolithic record of Greece: A synthesis of the evidence and a research agenda for the future. Quaternary International, 466, pp. 48–65.

Tourloukis, V., Karkanas, P., 2012. The Middle Pleistocene archaeological record of Greece and the role of the Aegean in hominin dispersals: New data and interpretations. Quaternary Science Reviews, 43, pp. 1–15.

Tourloukis, V., Muttoni, G., Karkanas, P., Monesi, E., Scardia, G., Panagopoulou, E. and Harvati, K., 2018a. Magnetostratigraphic and chronostratigraphic constraints on the Marathousa 1 Lower Palaeolithic site and the Middle Pleistocene deposits of the Megalopolis Basin, Greece. Quaternary International, 497, pp. 154–169.

Tourloukis, V., Thompson, N., Panagopoulou, E., Giusti, D., Konidaris, G.E., Karkanas, P. and Harvati, K., 2018b. Lithic artifacts and bone tools from the Lower Palaeolithic site Marathousa 1, Megalopolis, Greece: Preliminary results. Quaternary International, 497, pp. 47–64.

Trauth, M.H., 2014. A new probabilistic technique to build an age model for complex stratigraphic sequences. Quaternary Geochronology, 22, pp. 65–71.

Tsakanikou, P., Galanidou, N., Sakellariou, D., 2021. Lower Palaeolithic archaeology and submerged landscapes in Greece: The current state of the art. Quaternary International, 584, pp. 171–181.

Tzedakis, P.C., Hooghiemstra, H., Pälike, H., 2006. The last 1.35 million years at Tenaghi Philippon: revised chronostratigraphy and long-term vegetation trends. Quaternary Science Reviews, 25, pp. 3416–3430.

Van Vugt, N., Langereis, C.G. and Hilgen, F.J., 2001. Orbital forcing in Pliocene - Pleistocene

Mediterranean lacustrine deposits: Dominant expression of eccentricity versus precession. Palaeogeography, Palaeoclimatology, Palaeoecology, 172, pp. 193–205.

Vinken, R., 1965. Stratigraphie und Tektonik des Beckens von Megalopolis (Peloponnes, Griechenland). Geologisches Jahrbuch, 83, pp. 97–148.

Wagner, B., Vogel, H., Francke, A., Friedrich, T., Donders, T., Lacey, J.H., Leng, M.J., Regattieri, E., Sadori, L., Wilke, T., Zanchetta, G., Albrecht, C., Bertini, A., Combourieu-Nebout, N., Cvetkoska, A., Giaccio, B., Grazhdani, A., Hauffe, T., Holtvoeth, J., Joannin, S., Jovanovska, E., Just, J., Kouli, K., Kousis, I., Koutsodendris, A., Krastel, S., Lagos, M., Leicher, N., Levkov, Z., Lindhorst, K., Masi, A., Melles, M., Mercuri, A.M., Nomade, S., Nowaczyk, N., Panagiotopoulos, K., Peyron, O., Reed, J.M., Sagnotti, L., Sinopoli, G., Stelbrink, B., Sulpizio, R., Timmermann, A., Tofilovska, S., Torri, P., Wagner-Cremer, F., Wonik, T. and Zhang, X., 2019. Mediterranean winter rainfall in phase with African monsoons during the past 1.36 million years. Nature, 573, pp. 256–260.

18 U-SERIES ANALYSES OF BONES FROM MEGALOPOLIS BASIN SITES

Rainer Grün[1,2,3], Yuexing Feng[2], Jian-Xin Zhao[2], George E. Konidaris[4], Athanassios Athanassiou[5], Vangelis Tourloukis[4,6], Eleni Panagopoulou[5], Panagiotis Karkanas[7], Katerina Harvati[3,4]

[1]*Research School of Earth Sciences, The Australian National University, Canberra, Australia*
[2]*School of Earth and Environmental Sciences, University of Queensland, Queensland, Australia*
[3]*DFG Centre for Advanced Studies 'Words, Bones, Genes, Tools', Eberhard Karls University of Tübingen, Tübingen, Germany*
[4]*Paleoanthropology, Institute for Archaeological Sciences and Senckenberg Centre for Human Evolution and Palaeoenvironment, Department of Geosciences, Eberhard Karls University of Tübingen, Tübingen, Germany*
[5]*Hellenic Ministry of Culture, Ephorate of Palaeoanthropology–Speleology, Athens, Greece*
[6]*Department of History and Archaeology, School of Philosophy, University of Ioannina, Ioannina, Greece*
[7]*M.H. Wiener Laboratory for Archaeological Science, American School of Classical Studies at Athens, Athens, Greece*
**rwgruen@gmail.com*

http://dx.doi.org/10.15496/publikation-97644

Keywords: U-series analysis; U-diffusion into bones; minimum age estimates

18.1 INTRODUCTION

The Megalopolis Basin (Peleponnese, Greece) hosted a large lake during the Pleistocene. Its sequence consists of fluviolacustrine deposits containing lignite seams. The paleolake sequence commences at ~900 ka and continued to ~150 ka, covering the late Early Pleistocene and the entire Middle Pleistocene (Tourloukis et al., 2018 and references therein). It offers the unique opportunity to investigate human activity in the basin and its environmental context through time, the goal of the MEGAPAL survey and CROSSROADS project (Harvati, this volume; Karkanas et al., this volume).

In order to shed light on the chronological framework of human activity and paleoenvironmental change in the Megalopolis Basin, we applied U-series analyses on bone samples from a series of archaeological and paleontological sites in the basin. Bone fragments of macro-mammals (37 specimens in total) were sampled from stratified contexts from four sites: Kyparissia-3 (8 specimens) and Kyparissia-4 (19 specimens) are located at the eastern part of the Kyparissia mine, and both yielded a rich vertebrate fauna (including mainly cervids, hippopotamuses and elephants), while Kyparissia-T (5 specimens), located in the southern part of the mine, represents mainly an accumulation of hippopotamus bones (Athanassiou et al., 2018). The previously known Kyparissia-4 paleontological locality was recently revisited by the CROSSROADS team, resulting not only in an expansion of its known faunal assemblage (Athanassiou, et al., this volume), but importantly in the identi-

R. Grün: https://orcid.org/0000-0003-1366-3674
J. Zhao: https://orcid.org/0000-0002-2413-6178
G. E. Konidaris: https://orcid.org/0000-0002-7041-233X
A. Athanassiou: https://orcid.org/0000-0002-9140-7011
V. Tourloukis: https://orcid.org/0000-0002-9527-2708
E. Panagopoulou: https://orcid.org/0000-0002-4268-6157
P. Karkanas: https://orcid.org/0000-0002-7156-671X
K. Harvati: https://orcid.org/0000-0001-5998-4794

fication of associated lithic artifacts (Karkanas et al., this volume). The fourth site, Tripotamos-4 (5 specimens), a newly discovered locality, is located at the southeastern corner of the Choremi mine and yielded a rich lithic assemblage together with some faunal remains, belonging mainly to cervids and bovids (Karkanas et al., this volume).

18.2 MATERIALS AND METHODS

18.2.1. U-SERIES DATING

The U-series results show a complex mixture of overprinting U-diffusion processes, which require a basic introduction to U-series analyses of bones. The bones of living organisms are virtually free of uranium, which helps to keep mutation rates down. Any uranium that is measured in fossil bones migrated into the bone after it was buried. If the U-uptake was a fast process, occurring shortly after burial, the calculated closed system U-series age is close to the burial age. However, if the diffusion process is ongoing or delayed, the calculated closed system U-series results underestimate the burial age by an unknown amount. Delayed strong U-uptake is often associated with hydrological changes, e.g., river incisions leading to an activation of the ground water circulation or changes in the precipitation regime. The calculated U-series results must therefore be regarded as minimum age estimates for the burial of the bone and actually indicate the timing of a U-uptake event. On top of this, U-leaching may occur, which complicates the interpretation of the results even further.

The basic principles of U-series measurements using laser ablation mass spectrometry and the interpretation of the results from bones were described by Grün et al. (2014). U-series dating is based on the fact that uranium (U^{6+}) is water soluble while thorium is not. Minerals precipitated from water contain U, but no Th. Within the ^{238}U decay chain, the activity ratio of ^{230}Th over ^{234}U is zero to start with. In addition, most waters contain an excess of ^{234}U over ^{238}U. With time the $^{230}Th/^{234}U$ activity ratio will increase until it reaches equilibrium ($^{230}Th/^{234}U=1$) after about 600 ka. Similarly, the $^{234}U/^{238}U$ ratio will decline until it reaches equilibrium ($^{234}U/^{238}U=1$). There is no straight algorithm for solving the age equation, this is done by iterations in a computer program. Graphically, it can be shown in an isotope evolution diagram (lower most panels of the Figures). The measured $^{230}Th/^{234}U$ and $^{234}U/^{238}U$ values are plotted into the diagram. The curved horizontal lines show the development of the $^{234}U/^{238}U$ ratio over time and the vertical lines give the age. Following the $^{234}U/^{238}U$ lines to the Y-axis yields the initial $^{234}U/^{238}U$ ratio ($^{234}U/^{238}U_0$) that was present in the U-source.

18.2.2. DIFFUSION ADSORPTION AND DIFFUSION ADSORPTION DECAY MODELS

Two models were developed for describing U-diffusion into bone: diffusion adsorption (DA; for details see Pike et al., 2002) and diffusion adsorption decay (DAD; Sambridge et al., 2012). Both treat bone as a homogeneous medium, thus are only applicable to dense bones. Looking at a cross section of a bone, the DA model predicts constant $^{234}U/^{238}U$ ratios and u-shaped U-concentration and age profiles. The model assumes that after an unspecified, but relatively short time after burial the system becomes closed (Pike, 2000). Thus, the afore-mentioned u-shaped age profiles will flatten out with time. If older samples are plotted in an isotope evolution diagram, they will form a cluster (see e.g., Fig. 2D). The DAD model assumes continuing U-diffusion. The U-concentration and age profiles are similar to those of the DA model, however, the $^{234}U/^{238}U$ ratios would also show a

u-shaped profile and the u-shaped age profiles are maintained over time, similar to Figs. 6F and G. In the isotope evolution diagram, the data would cross the $^{234}U/^{238}U$ evolution lines, as shown in Fig. 6H.

Leaching can be recognised by increasing ages towards the outside of the bone combined with decreasing U-concentrations. Data points that lie to the right of the $^{234}U/^{238}U$ lines in the isotope evolution diagram must have experienced U-leaching (e.g., Fig. 7D). Secondary overprints are characterised by lower ages at the outside (e.g., Fig. 2G). If the U-source of a secondary overprint has a different $^{234}U/^{238}U_0$ composition, these show up in the $^{234}U/^{238}U$ cross sections (e.g., Fig. 1B) and isotope evolution diagrams (e.g., Fig. 1D).

The samples were measured at the Radioisotope Laboratory at the School of Earth and Environmental Sciences, University of Queensland following the procedures described by Grün et al. (2014). All isotopes were measured simultaneously. The figures show examples of the various U-diffusion processes. All errors are 2-σ. Averaged ages from a bone sequence were calculated from the integrated analytical results before converting them into a single age. No ^{232}Th corrections were carried out as all analyses had elemental U/Th ratios well in excess of 1000.

All samples from Kyparissia-T were from spongy bones and were not analyzed. The other three sites are discussed by their relative age according to their stratigraphical position (youngest to oldest).

18.3 RESULTS

18.3.1. TRIPOTAMOS-4

Figs. 1 and 2 show the results from four of the five bones from the site. TRP4-F29 (Figs. 1A to D) shows two distinct U-diffusion processes. Towards the outside, the $^{234}U/^{238}U$ ratios and U-concentrations increase while the $^{230}Th/^{234}U$ ratios and resulting ages decrease (Figs. 1B, C), indicating a secondary U-overprint. The process is clearly demonstrated in the isotope evolution diagram (Fig. 1D). The central data points cluster around 180 ka, but it cannot be ascertained whether these were also partly affected by the secondary overprint. Thus, it is not certain that this cluster presents the timing of an earlier distinct U-diffusion event. Note that the secondary overprint is very recent (Holocene). TRP4-F24 (Figs. 1E to H) shows an older section with higher $^{234}U/^{238}U$ ratios, lowering towards the outside (Figs. 1F). These regions are associated with increasing $^{230}Th/^{234}U$ ratios and decreasing U-concentrations (Figs. 1F, G), both signs of leaching. This is further demonstrated in the isotope evolution diagram with two data points in the leaching zone (Figs. 1H). The central data cluster has an average age of 206±11 ka.

Samples TRP4-F20 and F31 (Fig. 2) behave significantly different to the previous two. TRP4-F20 (Fig. 2A to D) is the best-behaved sample of the whole data set. As there is no structure in the isotope ratio and age cross sections (Figs. 2B and C), continuous diffusion can be ruled out. The cluster in Fig. 2D represents a single diffusion event at 362±43 ka. TRP4-F31 (Fig. 2E to H) shows a secondary overprint at the outside from a U-source with higher $^{234}U/^{238}U_0$ ratios. The rest of the data form a cluster at 466±110 ka. A third sample (TRP4-F23), behaving similarly to F-31, contains a cluster at 368±46 ka. The weighted mean of the three samples points to a U-mobilisation event at 365±31 ka.

At Tripotamos-4 three distinct U-uptake events are recorded: the last during the Holocene (overprint in TRP4-F29), an earlier during MIS 7 (191 to 243 ka, MIS boundaries from Lisiecki and Raymo, 2005). The three older clusters may be the result of two uptake phases, one during MIS 9 (300 to 337 ka), the other during MIS 11 (374 to

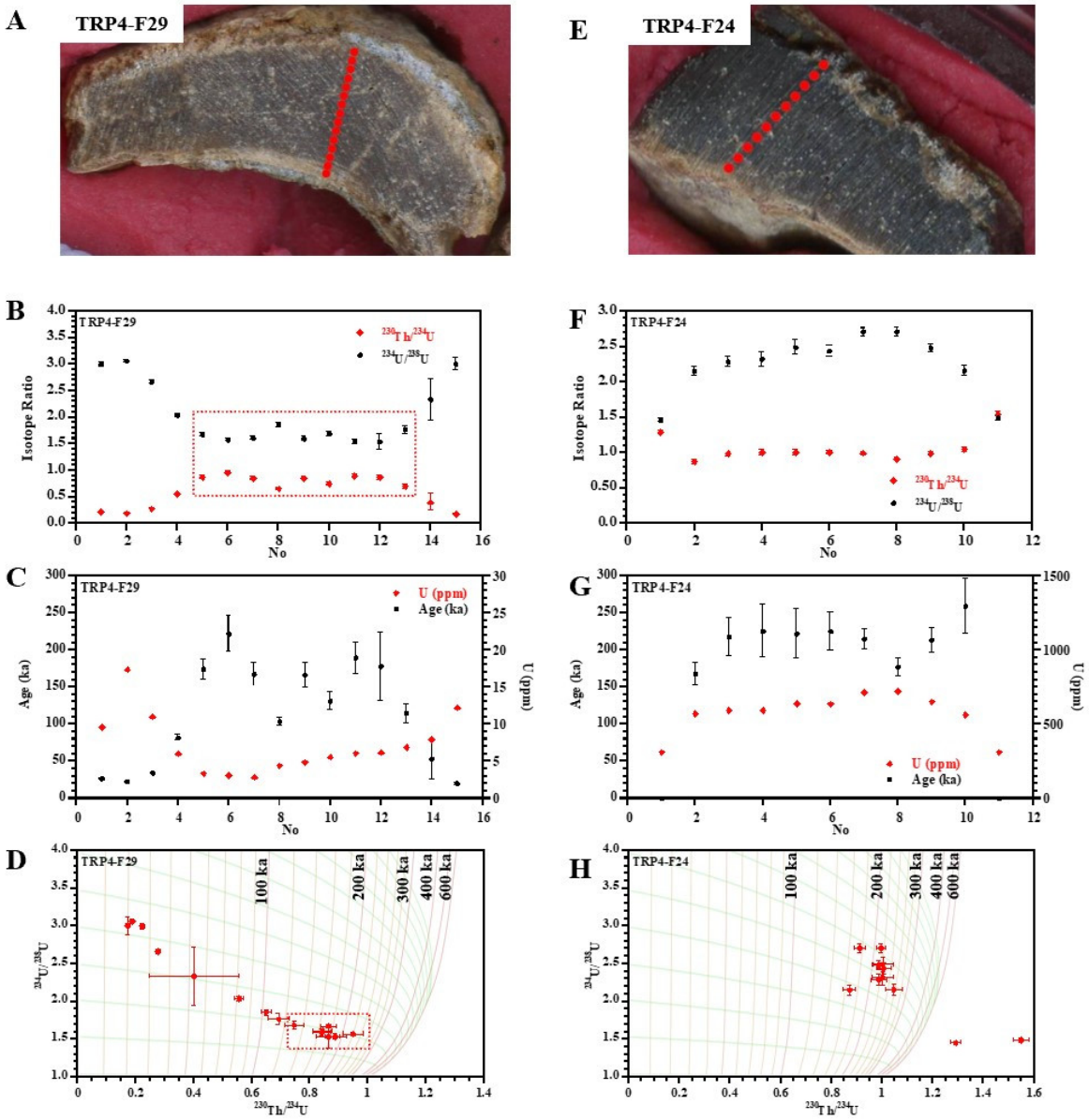

Figure 1: Results of TRP4-F29 and TRP4-F24 from Tripotamos-4. A, E: photos of the bone and location of the individual laser spot analyses; B, F: Plot of the measured $^{230}Th/^{234}U$ and $^{234}U/^{238}U$ ratios; C, G: calculated ages (left scale) and U-concentrations (right scale); D, H: isotope evolution diagrams.

424 ka), however, the data are not precise enough to make this distinction. The weighted mean is closer to MIS 11 but does not exclude MIS 9.

18.3.2. KYPARISSIA-3

Probably the most interesting sample from this site is KYP-901. It contains virtually no uranium: 0.25 ppm at the first data point and 0.09±0.04 ppm for all others. This means that there are areas where no U-mobilisation took place for more than 400 ka. The presence of the lignite bands may be responsible for the complex U-history of the bones. The lignite redox reduces U^{6+} to U^{4+}, which is water insolvable. If waters run through a high redox area before reaching a bone, it may well be free of any uranium (as perhaps demonstrated by KYP-901).

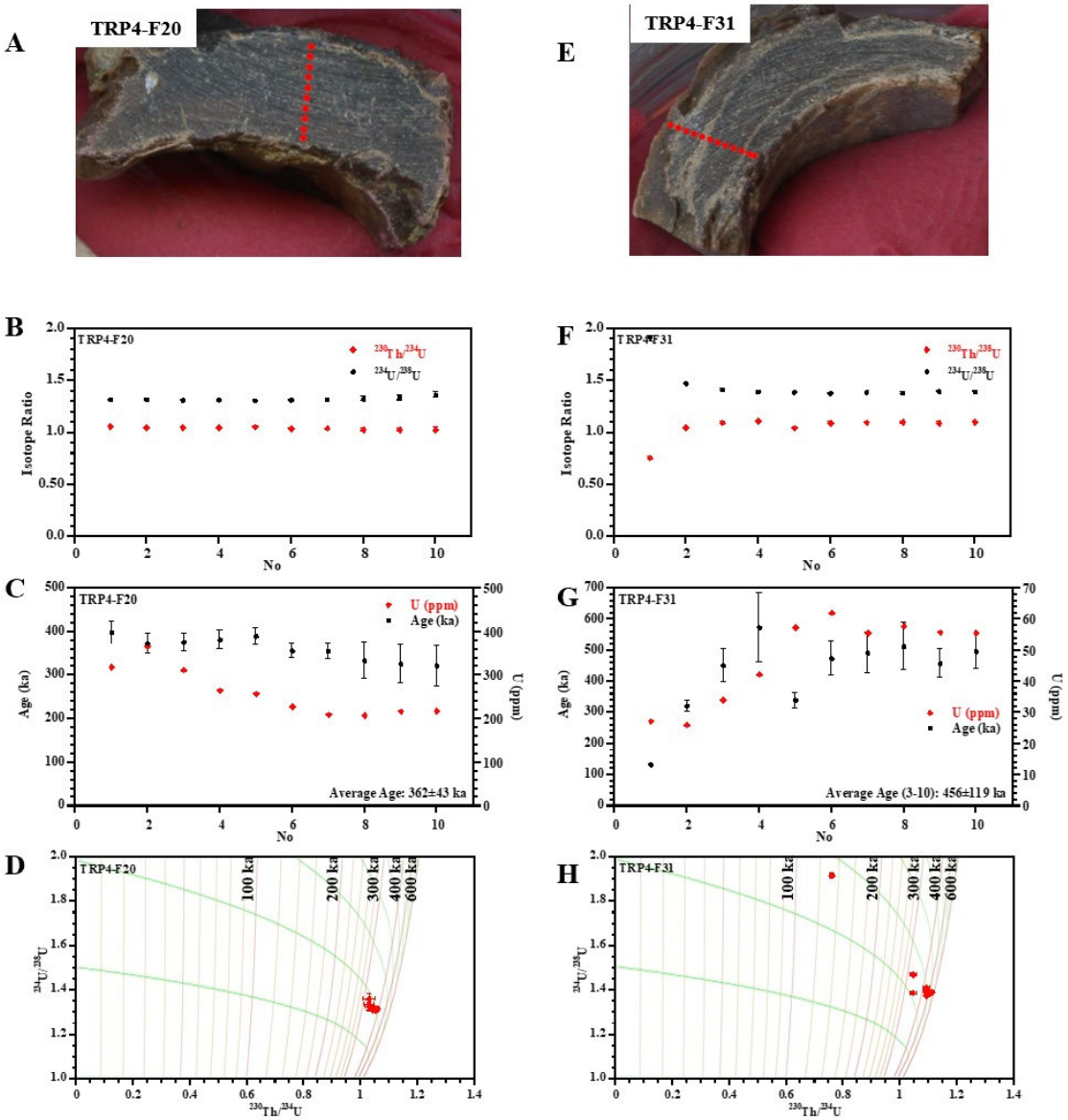

Figure 2: Results of TRP4-F20 and TRP4-F31 from Tripotamos-4. A, E: photos of the bone and location of the individual laser spot analyses; B, F: Plot of the measured 230Th/234U and 234U/238U ratios; C, G: calculated ages (left scale) and U-concentrations (right scale); D, H: isotope evolution diagrams.

KYP-131 (Figs. 3A to D) shows a secondary overprint at the outside. The rest clusters around 466±121 ka, some of the scatter is probably due to uranium micro-migration within the bone (e.g., Duval et al., 2011). The data of KYP-18 (Figs. 3A to D) are in the same isotope range as KYP-131 but scatter more (compare Figs. 3D and H).

Sample KYP-94 (Fig. 4A to D) shows a secondary overprint at the outside with average ages of 204±12 ka. The data further inside have large uncertainties because of the low U-concentrations, they average at 346±89 ka. KYP-85 (Fig. 4E to H) shows the same overprint at the outside as KYP-94 at 205±11 ka.

The remaining data have large uncertainties because of the low U-concentrations. The sample also shows a significant amount of leaching (Fig. 4H). Samples KYP-14A and B (Fig. 5) are from

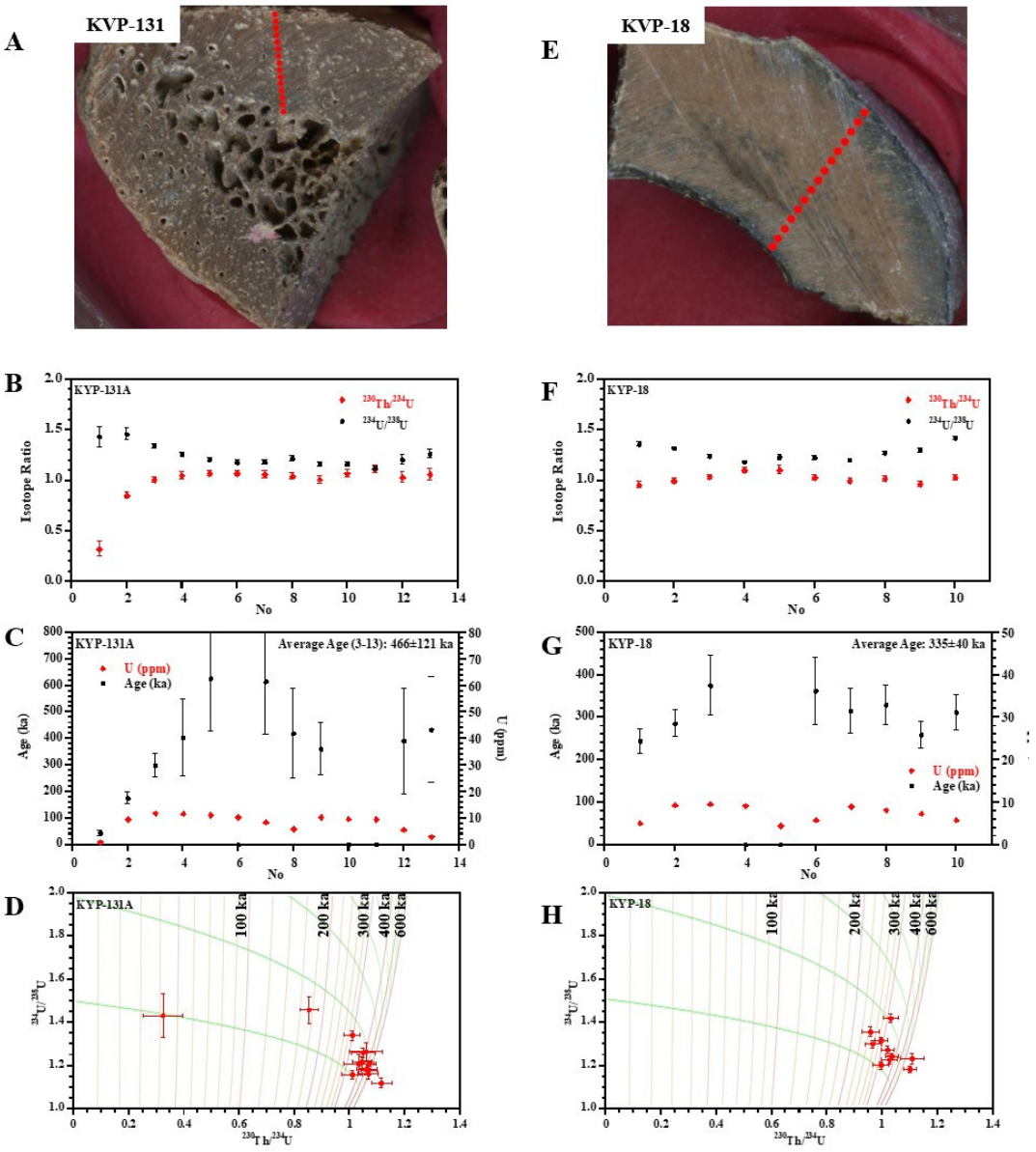

Figure 3: Results of KYP-131 and KYP-18 from Kyparissia-3. A, E: photos of the bone and location of the individual laser spot analyses; B, F: Plot of the measured 230Th/234U and 234U/238U ratios; C, G: calculated ages (left scale) and U-concentrations (right scale); D, H: isotope evolution diagrams.

the same bone. The data of KYP-14A (Fig. 5A to D) cluster tightly at 110±4 ka with only the outer data point indicating a later overprint. The inner data points of sample KYP-14B (Fig. 5E to H) cluster around 114±4 ka, relating to the same uptake event indicated in KYP-14A. The outer, older data points may relate to an earlier U-uptake event that diffused only into the outer section of the bone. This may be related to the 200 ka event observed in KYP-85 and 94, but the apparent ages are somewhat younger because of mixing with the later U-diffusion.

The bones from Kyparissia-3 document three distinct U-uptake events at 110±4 ka, 205±8 ka and 347±35 ka. The first two can be clearly associated with the interglacials of MIS 5 and MIS 7, while the one at 347±35 ka may relate to MIS 9 (300 to 337 ka) or MIS 11 (374-424 ka).

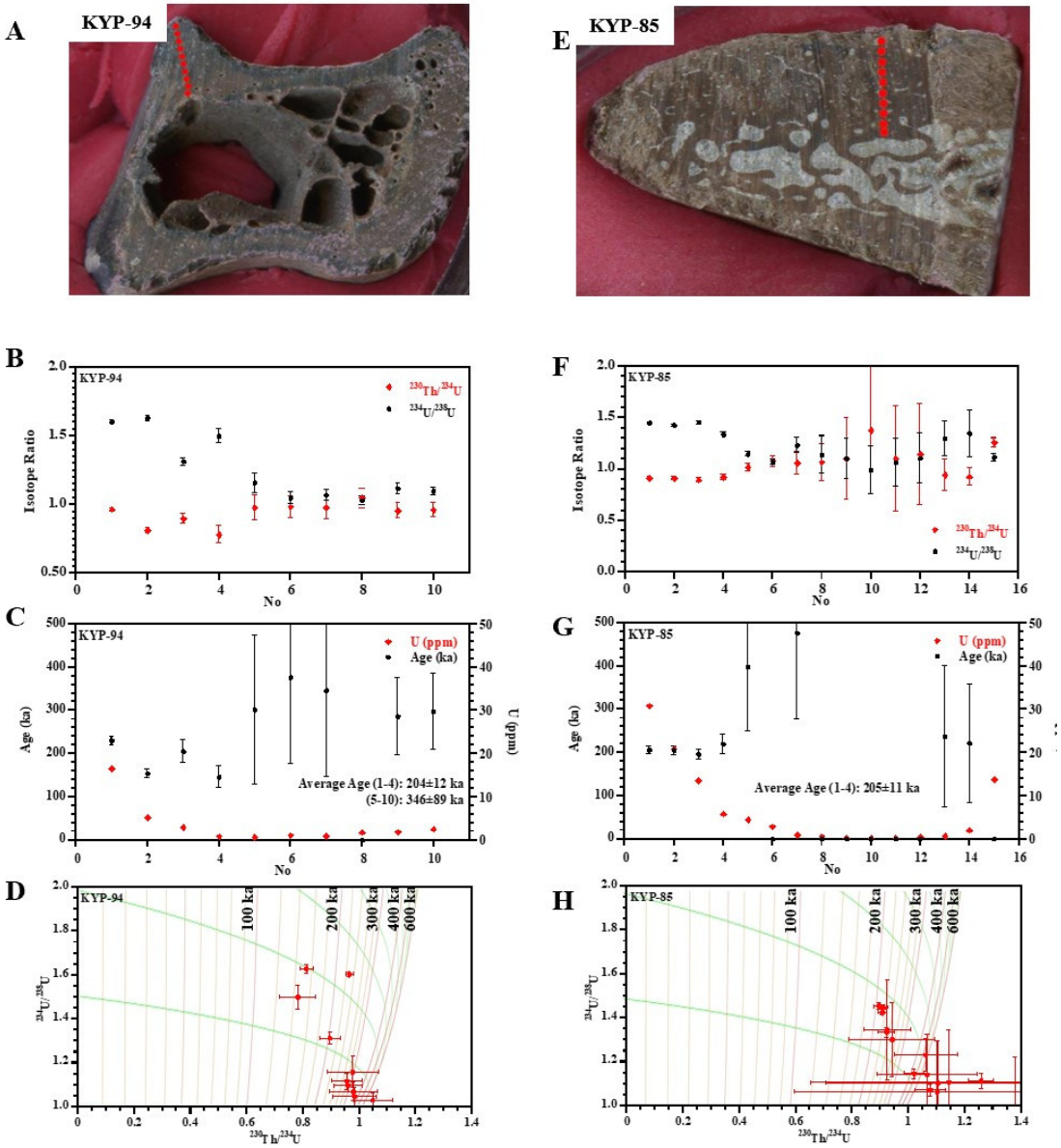

Figure 4: Results of KYP-94 and KYP-85 from Kyparissia-3. A, E: photos of the bone and location of the individual laser spot analyses; B, F: Plot of the measured $^{230}Th/^{234}U$ and $^{234}U/^{238}U$ ratios; C, G: calculated ages (left scale) and U-concentrations (right scale); D, H: isotope evolution diagrams.

18.3.3. KYPARISSIA-4

This is stratigraphically the oldest site. Virtually all samples show leaching. KYP4A-F125 (Fig. 6A to D) shows leaching at the inside surface, but also within the sample. The remaining data points cannot be explained by a simple diffusion process. It seems that two U-sources were operating with slightly different $^{234}U/^{238}U$ ratios, one slightly above the $^{234}U/^{238}U_0$ evolution line and one slightly below (Fig. 6D). However, such sequences of data cannot be produced by diffusion in direction of the analysed transect (the data according to the DA model would cluster, according to the DAD model it would follow the direction of the blue data points in Fig. 6H). It could be explained by continuing diffusion into separate individual vol-

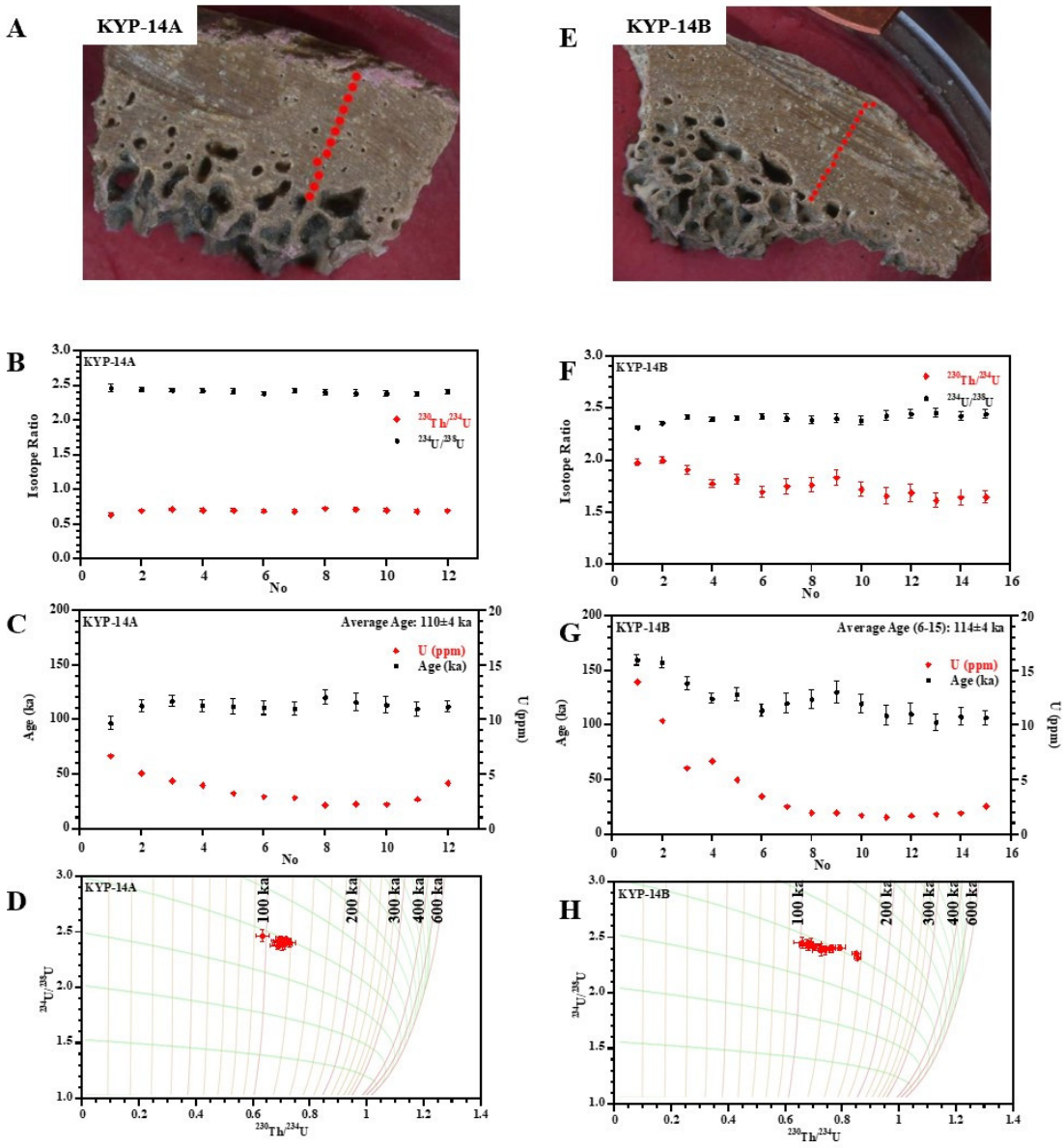

Figure 5: Results of KYP-14A and KYP-14B from Kyparissia-3. A, E: photos of the bone and location of the individual laser spot analyses; B, F: Plot of the measured $^{230}Th/^{234}U$ and $^{234}U/^{238}U$ ratios; C, G: calculated ages (left scale) and U-concentrations (right scale); D, H: isotope evolution diagrams.

umes, e.g., diffusion proceeding at a right angle to the transect. But this is speculative.

18.4 DISCUSSION

14 samples behaved similarly to KYP4A-F78 (Fig. 6E to H). At first glance, the samples show isotope distributions that are expected from the DAD model: both the $^{234}U/^{238}U$ and $^{230}Th/^{234}U$ ratios show u-shaped profiles (Fig. 6F), the calculated ages and U-concentrations are also u-shaped. However, all samples have the highest U-concentrations at the outside and all samples show leaching (Fig. 6H). The relationship of increasing the $^{234}U/^{238}U$ ratios with increasing $^{230}Th/^{234}U$ ratios is the direct result of a continuing U-diffusion process (as postulated by the DAD model). The blue

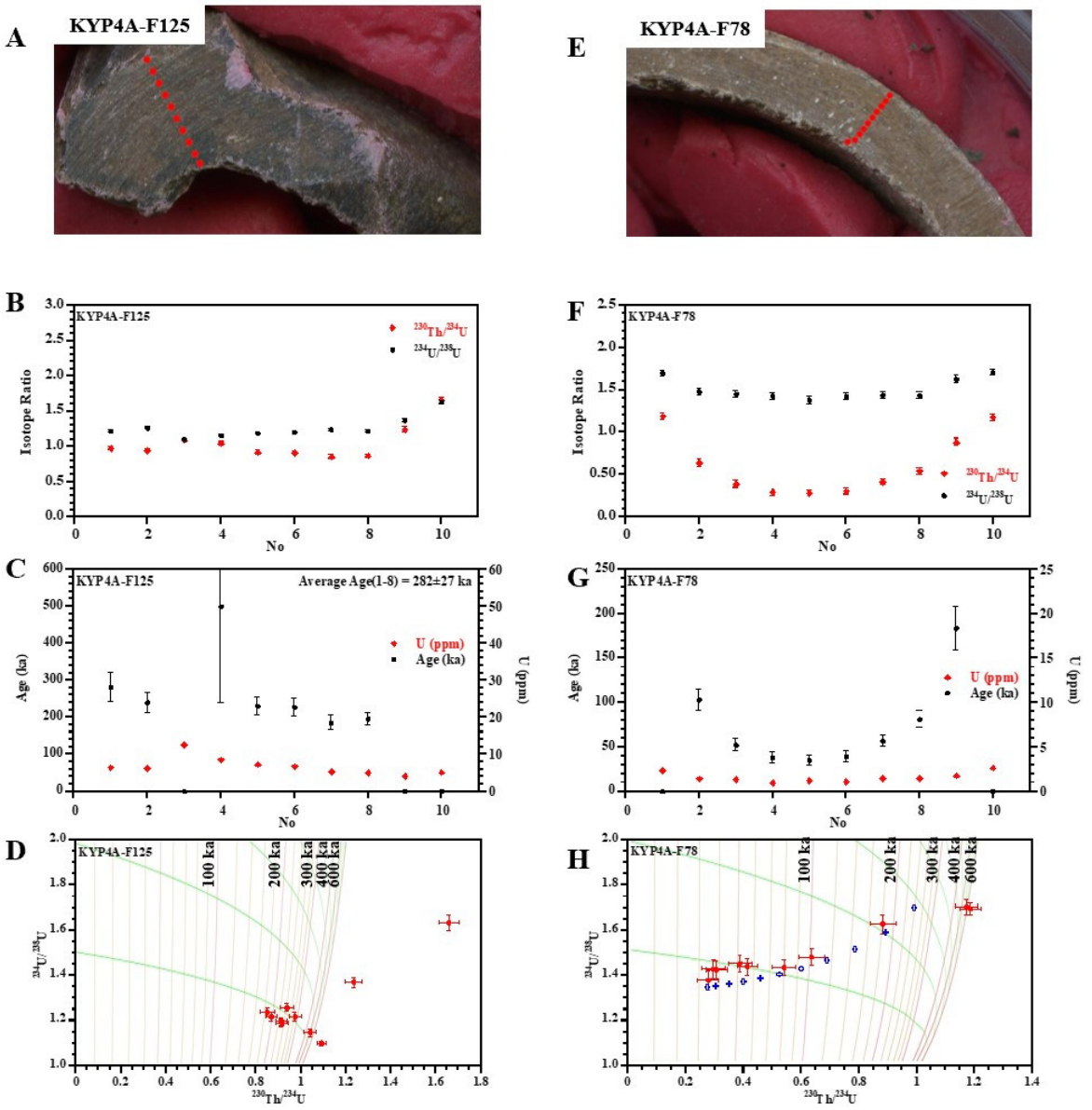

Figure 6: Results of KYP4A-F125 and KYP4A-F78 from Kyparissia-4. A, E: photos of the bone and location of the individual laser spot analyses; B, F: Plot of the measured $^{230}Th/^{234}U$ and $^{234}U/^{238}U$ ratios; C, G: calculated ages (left scale) and U-concentrations (right scale); D, H: isotope evolution diagrams. The blue data points in Figure 6H are from a model calculation using the DAD diffusion model and data from Grün et al. (2014), their Figure 4.

data points in Fig. 6H result from a theoretical calculation of a 280 ka old sample using the data from Grün et al. (2014, their Fig. 4D). However, the analytical data of the bones from Kyparissia-4 cannot be fitted by the DAD model as the extrapolation of the $^{234}U/^{238}U$ ratios towards the surfaces of the bone would require very large, unrealistic values. Fitting the central data points with the DAD model results in ages around 150 ka, with very large uncertainties (the result for KYP4A-F78 was 154±25 ka). It seems that the samples have undergone at least three U-diffusion stages: firstly, an uptake leaving u-shaped diffusion isotope and U-concentration profiles, then leaching, then a later overprint. The u-shaped isotope profiles may be the result of the mixing of the first uptake and a later overprint (this was also observed for an old sample from Melka Kunture, Grün et al. (2014),

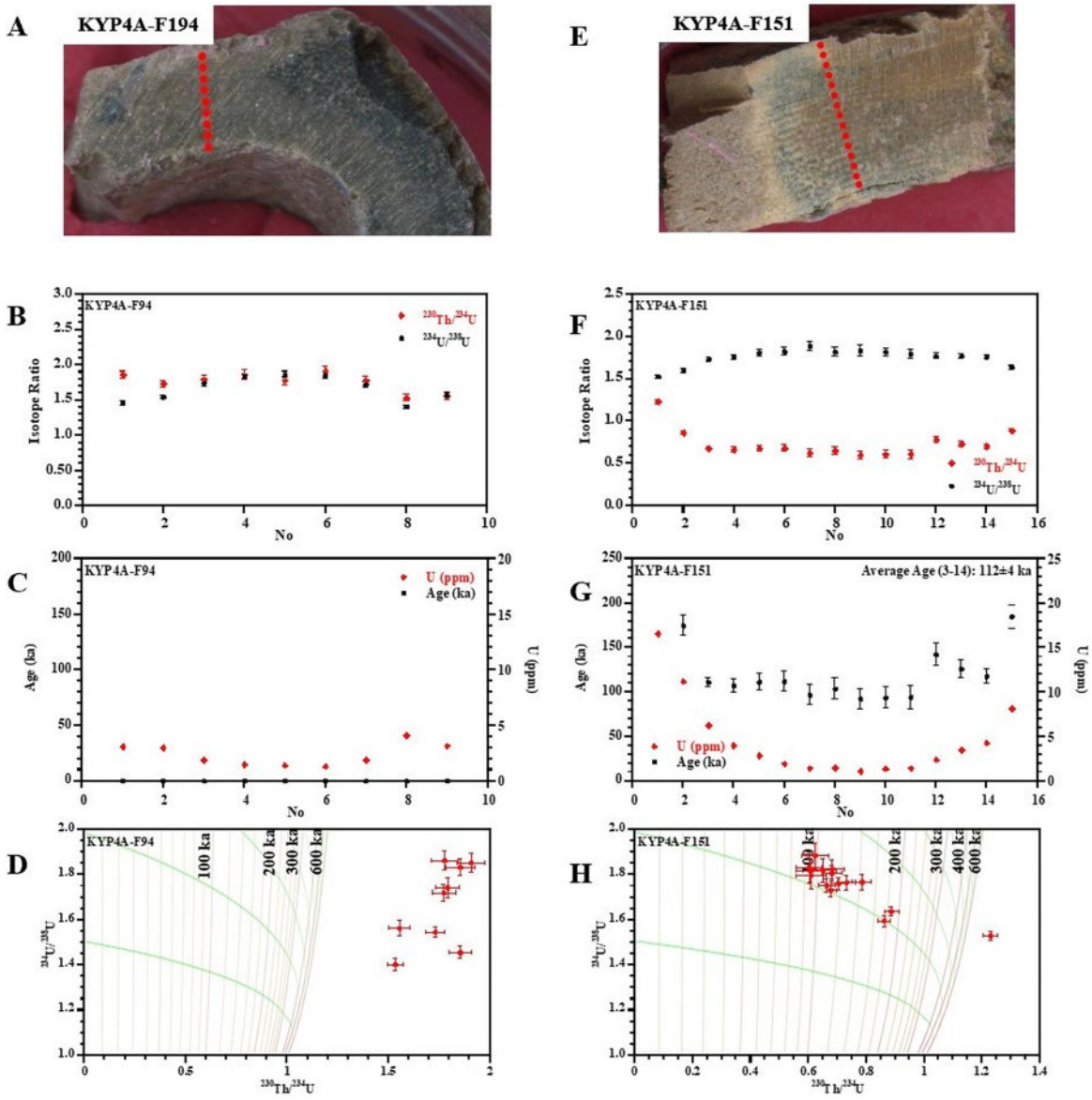

Figure 7: Results of KYP4A-F194 and KYP4A-F151 from Kyparissia-4. A, E: photos of the bone and location of the individual laser spot analyses; B, F: Plot of the measured $^{230}Th/^{234}U$ and $^{234}U/^{238}U$ ratios; C, G: calculated ages (left scale) and U-concentrations (right scale); D, H: isotope evolution diagrams.

their Fig. 18). It is not possible to speculate when these processes took place.

Two samples showed massive leaching as shown by KYP4A-F194 (Fig. 7A to D). Note that the U-concentration profile is still u-shaped (Fig. 7C). Two other samples behaved like KYP4A-F151 (Fig. 7E to H) showing clusters around 100 ka and leaching towards the outside of the sample. The cluster of KYP4A-F151 has an average age of 112±4 ka, that of the other sample (KYP4A-F106) was too scattered. The DA model predicts that the U-concentrations would decrease towards the outside as a result of leaching, but this is clearly not the case (Fig. 7G).

The bones from Kyparissia-4 show a complex history of U-uptake and leaching processes. As frustrating as it is, only one sample allows the identification of a distinct uptake phase at 112±4

ka. While it is clear that earlier continuing uptake processes took place, it is not possible to derive any age information from the data.

CONCLUSIONS

The U-series results on the bone samples from the Megalopolis Basin allow the identification of three distinct U-uptake phases corresponding to MIS 1, 5 and 7. Whether one or two distinct older uptake phases took place cannot be decided because of the large errors for the older data. The mean age of the older phases falls into the glacial of MIS 10 (337 to 374 ka). However, assuming that the U-diffusion events processes took place during an interglacial (as did the three later ones), the older U-accumulations took place either in MIS 9 or MIS 11, or both. The results give a minimum age of 365±31 ka for Tripotamos-4 and 347±35 ka for Kyparissia-3. The only tangible date of 112±4 ka for Kyparissia-4 is not particularly helpful to tie down the age of this site. A combination of U-series and ESR dating on teeth could contribute to provide finite age estimates (Grün et al., 1988).

ACKNOWLEDGMENTS

This research was conducted under a permit granted to the Ephorate of Palaeoanthropology–Speleology, Hellenic Ministry of Culture, and the American School of Classical Studies at Athens. Fieldwork was supported by the ERC Consolidator Grant ERC-CoG-724703 ("CROSSROADS") and the ERC Advanced Grant ERC-AdG-101019659 ("FIRSTSTEPS"), both awarded to K.H. We thank Q. Shao, College of Geography Science, Nanjing Normal University, for some IDAD calculations. We thank the anonymous reviewers for their constructive comments.

REFERENCES

Athanassiou, A., Michailidis, D., Vlachos, E., Tourloukis, V., Thompson, N. and Harvati, K., 2018. Pleistocene vertebrates from the Kyparíssia lignite mine, Megalopolis Basin, S. Greece: Testudines, Aves, Suiformes. Quaternary International, 497, pp. 178–197.

Athanassiou, A., Konidaris, G., Tourloukis, V., Thompson, N., Giusti, D., Karkanas, P. and Harvati, K., this volume. The middle Pleistocene large mammal fauna from Kyparissia (Peloponnese, S. Greece): New collected material.

Duval, M., Aubert, M., Hellstrom, J. and Grün, R., 2011. High resolution, LA-ICP-MS mapping of U and Th isotopes in an Early Pleistocene equid tooth from Fuente Nueva-3 (Orce, Andalusia, Spain). Quarternary Geochronology, 6, pp. 458–467.

Grün, R., Schwarcz, H.P. and Chadam, J.M., 1988. ESR dating of tooth enamel: Coupled correction for U-uptake and U-series disequilibrium. Nuclear Tracks and Radiation Measurements, 14, pp. 237–241.

Grün, R., Eggins, S., Kinsley, L., Mosely, H. and Sambridge, M., 2014. Laser ablation U-series analysis of fossil bones and teeth. Palaeogeography, Palaeoclimatology, Palaeoecology, 416, pp. 150–167.

Harvati, K., this volume. Introduction to the volume.

Karkanas, P., Tourloukis, V., Thompson, N., Giusti, D., Tsartsidou, G., Athanassiou, A., Konidaris, G., Roditi, E., Panagopoulou, E. and Harvati, K., this volume. The Megalopolis Paleoenvironmental Project (MegaPal).

Lisiecki, L.E., Raymo, M.E., 2005. A Pliocene – Pleistocene stack of 57 globally distributed benthic $\delta^{18}O$ records. Paleoceanography, 20(1).

Pike, A.W.G., 2000. Uranium series dating of archaeological bone by thermal ionization mass

spectrometry. Doctoral dissertation, University of Oxford, UK.

Pike, A.W.G., Hedges, R.E.M. and Van Calsteren, P., 2002. U-series dating of bone using the diffusion-adsorption model. Geochimica et Cosmochimica Acta, 66, pp. 4273–4286.

Sambridge, M., Grün, R. and Eggins, S., 2012. U-series dating of bone in an open system: The diffusion-adsorption decay model. Quarternary Geochronology, 9, pp. 42–53.

Tourloukis, V., Muttoni, G., Karkanas, P., Monesi, E., Scardia, G., Panagopoulou, E. and Harvati, K., 2018. Magnetostratigraphic and chronostratigraphic constraints on the Marathousa 1 Lower Palaeolithic site and the Middle Pleistocene deposits of the Megalopolis Basin, Greece. Quarternary International, 497, pp. 154–169.

19 THE MIDDLE PLEISTOCENE LARGE MAMMAL FAUNA FROM KYPARISSIA (PELOPONNESE, S. GREECE): NEW COLLECTED MATERIAL

Athanassios Athanassiou[1,*], George E. Konidaris[2], Vangelis Tourloukis[2,3], Nicholas Thompson[2], Domenico Giusti[2], Eleni Panagopoulou[1], Panagiotis Karkanas[4], Katerina Harvati[2,5]

[1]*Hellenic Ministry of Culture, Ephorate of Palaeoanthropology–Speleology, Athens, Greece*
[2]*Paleoanthropology, Institute for Archaeological Sciences and Senckenberg Centre for Human Evolution and Palaeoenvironment, Department of Geosciences, Eberhard Karls University of Tübingen, Tübingen, Germany*
[3]*Department of History and Archaeology, School of Philosophy, University of Ioannina, Ioannina, Greece*
[4]*M.H. Wiener Laboratory for Archaeological Science, American School of Classical Studies at Athens, Athens, Greece*
[5]*DFG Centre of Advanced Studies 'Words, Bones, Genes, Tools', Eberhard Karls University of Tübingen, Tübingen, Germany*
**aathanas@geol.uoa.gr*

http://dx.doi.org/10.15496/publikation-97642

Keywords: Greece; Megalopolis Basin; Middle Pleistocene; large mammals

19.1 INTRODUCTION

Kyparíssia is a fossil vertebrate locality of Middle Pleistocene age, situated at the NW margin of the Megalopolis Basin (central Peloponnese, Greece), within the homonymous lignite mine. The Megalopolis area, an intramontane basin filled mainly with Pleistocene fluvial and lacustrine sediments, is well known since the dawn of the 20th century for its palaeontological wealth, particularly regarding fossils of mammalian megaherbivores (see Athanassiou, 2018; Athanassiou et al., 2018; Konidaris et al., 2018; and references therein). The development of extensive open-cast mines since 1970 provided access to long and deep stratigraphic sections, facilitating the discovery of new sites. The Kyparíssia mine is the northernmost in the basin and was in full operation until 2006. The mine area is filled with lacustrine deposits, dominated by thick lignite layers, which are covered unconformably by fluvial and alluvial fan sediments.

The first fossils in the area of the mine came to light in October 2004, when a large part of a section collapsed, exposing elements of an elephant skeleton among the rubble. Subsequent fieldwork during the following years resulted in the discovery of five sites (KYP1–KYP4, KYPT), mainly along the western margin of the mine (Athanassiou, 2018: Fig. 1). According to our current understanding of the locality's stratigraphy, the finds come from two main fossiliferous levels with an altitude difference of about 15 m, which are not expected to differ significantly, at least concerning the large mammal association. The fauna was pub-

A. Athanassiou: https://orcid.org/0000-0002-9140-7011
G. E. Konidaris: https://orcid.org/0000-0002-7041-233X
V. Tourloukis: https://orcid.org/0000-0002-9527-2708
N. Thompson: https://orcid.org/0009-0003-4770-1744
D. Giusti: https://orcid.org/0000-0003-1438-4036
E. Panagopoulou: https://orcid.org/0000-0002-4268-6157
P. Karkanas: https://orcid.org/0000-0002-7156-671X
K. Harvati: https://orcid.org/0000-0001-5998-4794

lished by Athanassiou (2018) and Athanassiou et al. (2018), who described the following taxa (collectively from all KYP sites): turtles (*Emys orbicularis, Testudo marginata*), birds (*Anas crecca*, *Anas platyrhynchos*, *Cygnus olor*, *Mareca strepera*, *Spatula clypeata*, *Spatula querquedula*, *Fulica atra*, *Anhinga* sp.), a rodent (*Castor fiber*), carnivorans (*Canis* sp., Hyaenidae indet., *Felis* sp., *Panthera* sp.), a proboscidean (*Palaeoloxodon antiquus*), perissodactyles (*Stephanorhinus* sp., *Equus* sp.) and artiodactyles (*Sus scrofa, Hippopotamus antiquus*, *Praemegaceros verticornis*, *Cervus elaphus*, *Dama* sp., *'Cervus' peloponnesiacus*, Cervidae indet., and *Bison* sp.).

This diverse fauna indicated the great potential of the locality. Thus, a new 3-year field research program was initiated at Kyparíssia in 2019, as part of the Megalopolis Palaeoenvironmental Project (MegaPal), in order to further investigate its palaeontological content, stratigraphy, and possible human presence (Karkanas et al., this volume). The new research focused mainly on the KYP4 site, an area with dense fossil content, discovered in 2007. A significant new discovery is the recovery of several lithic artifacts at KYP4 in direct stratigraphic and spatial association with fossils. Moreover, a new site, named Kyparíssia-5 (KYP5), was discovered in 2021, ~200 m NNE of KYP4. In general, finds from other locations within the mine are scarce. Both sites, KYP4 and KYP5, are situated very close to a basement outcrop (limestones of the Pindos geotectonic zone) and correspond to a depositional environment very close to the lake shore. They both belong to the lower fossiliferous level of the locality. At KYP4 two main areas of interest were designated, Area A (corresponding to the fossiliferous findspot in Athanassiou, 2018) and Area B, to the east of Area A, which represents one exposed section profile along the current lake shore; in addition, a third findspot in between these areas yielded few fossils and was designated as Area C. The main vertebrate-bearing layers generally consist of dark grey sandy muds, rich in organic remains, mud clasts and mollusc shells.

Below, we present a brief preliminary description of the most important new large mammal finds and an update on the locality's faunal content. The studied specimens were numbered sequentially for the entire locality, but each number is preceded by the abbreviation of the corresponding site. The specimen numbers of unstratified finds are preceded by the locality abbreviation (KYP). The tooth positions are indicated as: P/p, upper/lower premolar; M/m, upper/lower molar. All measurements are in mm. The use of parentheses denotes an inaccurate or estimated measurement. Measurement abbreviations: L, length; W, width (p, proximal; d, distal; a, articular); H, height. All fossils presented herein are stored in the collections of the Ephorate of Palaeoanthropology–Speleology (Hellenic Ministry of Culture, Athens, Greece).

19.2 SYSTEMATICS

19.2.1. RODENTIA

A large-sized rodent of castorid morphology is present in KYP4, represented in the recently collected material by a left hemimandible (Fig. 1a). The specimen preserves the complete cheek tooth row (p4–m3), as well as the incisor, which extends through the entire ventral part of the mandible (> 90 mm, along its labial side), but is broken supralveolarly. The incisor is triangular in cross section and has a smooth and flat enamel band on its labial side, excluding an attribution to *Trogontherium cuvieri* and pointing to the extant Eurasian species *Castor fiber* (Fostowicz-Frelik, 2008). The cheek teeth are very hypsodont with very deep striids, in accordance with the morphology of *Castor fiber*. This is the first occurrence of this species in KYP4.

19.2.2. CARNIVORA

This order is represented in the new KYP collection by a partial skull of a fox (*Vulpes* sp.) from KYP4, and a partial ursid mandible (*Ursus* sp.; surface find). The former preserves the left rostral part of the skull with P4–M2 (KYP4-1160; Fig. 1b). Dimensionally, the teeth are small (P4: 12.2×5.7, M1: 9.0×10.3, M2: 5.7×7.3 mm), being comparable to those of *Vulpes alopecoides* and the small-

Figure 1: Rodentia, Carnivora, Perissodactyla and Artiodactyla from Kyparíssia: a, *Castor fiber*, left mandible (KYP4-1163) in dorsal (a1) and lingual (a2) view; b, *Vulpes* sp. (KYP4-1160), partial skull in left lateral (b1) and ventral (b2) view; c, *Ursus* sp. (KYP-1161), partial mandible in dorsal (c1) and lingual (c2) view; d, *Hippopotamus antiquus* (KYP4-1004), left maxilla in ventral (occlusal) view; e, *Hippopotamus antiquus* (KYP4-1006), partial right mandible in occlusal (e1) and right lateral (e2) view; f, *Equus* sp. (KYP4-1151), m1/2 in occlusal view; g, *Stephanorhinus* sp. (KYP4-1197), left P3/4 in occlusal view; h, *Stephanorhinus* sp. (KYP4-1195), left astragalus in dorsal view. Graphical scale equals 5 cm (a–c, f–h) and 10 cm (d, e).

est individuals of *Vulpes vulpes* (Bartolini Lucenti and Madurell-Malapeira, 2020: Fig. 9). The ursid mandible (KYP-1161; Fig. 1c) preserves only the first molar, whose dimensions (L = 26.7 mm, W = 11.9 mm) indicate a large individual, comparable to *Ursus deningeri* or a very large *Ursus arctos* (Rossi and Santi, 2011: Fig. 12). Both *Vulpes* and *Ursus* are new to Kyparíssia, while *Ursus* is a new element for the entire Megalopolis Basin.

19.2.3. PERISSODACTYLA

Rhinoceroses and horses are rare faunal elements in the Megalopolis Basin. Rhinoceros finds from this region have been historically referred to multiple species, but they are currently considered as *Stephanorhinus* sp. (Giaourtsakis, 2022 and references therein). New finds from Kyparíssia include two cheek teeth, cervical vertebrae, and some other postcranial bones. The teeth (KYP4-1196, KYP4-1197; Fig. 1g) are almost totally worn and may belong to the same individual, as they were also found in spatial proximity. Their proportions indicate that they are probably premolars (P3/4). The postcranial elements (carpals, tarsals, metapodials) indicate a rather small-sized species, such as *Stephanorhinus hemitoechus* (see Guérin, 1980), but they do not provide any diagnostic character for a species-level determination. The horses (*Equus* sp.) are represented by just one isolated lower tooth (KYP4-1151), a little-worn right molar (m1 or m2; Fig. 1f) (L=28.0, W=(14), H=66 mm). Both perissodactyl taxa are new for KYP4.

19.2.4. HIPPOPOTAMIDAE

Hippopotamus antiquus is a frequent taxon in Kyparíssia (Athanassiou et al., 2018). The recently collected material includes a fragmentary skull preserving parts of the maxillae and the occipital region, as well as the left P4–M3 row (KYP4-1004; Fig. 1d), a right partial mandible with the complete molar row (surface find, KYP4-1006; Fig. 1e), isolated teeth, and several postcranial elements of the axial and appendicular skeleton. All three areas of KYP4 have yielded hippopotamus finds. Those from Area B (nine vertebrae, more than eleven ribs, scapular fragments, a partial humerus, a cuneiform) probably belong to a single individual.

The preserved dental row of the skull KYP4-1004 has a molar-series length of 168 mm. The M1 is almost worn out, the P4 and M2 exhibit medium wear, while the M3 is almost unworn and not fully erupted. A separately found, large-sized upper canine (surface find at KYP4B; maximal diameter: 59.5 mm) has the characteristic pisiform cross section. A fragmentary lower canine is similarly robust (maximal diameter: 68.0 mm). The mandible KYP4-1006 belongs to a young adult individual with a moderately worn m1, a slightly worn m2, and an unworn and still-erupting m3.

A right third metacarpal (KYP4-1007) (L=168.7 mm, Wpa=67.0 mm, Wda=60.6 mm) compares with the largest specimens of *Hippopotamus antiquus* given by Kahlke (1997) and Mazza (1995). On the contrary, a right second metatarsal (KYP4-1008) is small, similar to the smallest specimens of the same species.

Figure 2: Cervidae from Kyparíssia: a, *Praemegaceros verticornis* (KYP4-1050), right metacarpal III-IV in dorsal view; b, *Praemegaceros verticornis* (KYP4-1048), right metatarsal III-IV in dorsal view; c, *Dama* sp. (KYP-1090), right metacarpal III-IV in dorsal view; d, *Dama* sp. (KYP4-1093), right metatarsal III-IV in dorsal view; e, *Praemegaceros verticornis* (KYP4-1067), skull in dorsal (e1) and ventral (e2) view; f, *Cervus elaphus* (KYP5-1194), right antler in lateral view; g, *Praemegaceros verticornis* (KYP4-1069), left mandible with p2–m3 in lateral view; h, cervid metapodial scatter diagrams comparing *Dama* sp. (blue dots) and *Praemegaceros verticornis* (green dots) from KYP4 to recent *Dama dama* (orange open dots), *Dama clactoniana* (yellow open dots), *Cervus elaphus* from Mosbach (black open dots), *Praemegaceros verticornis* from Voigtstedt (green open dot) and Bilshausen (green open triangle). Green lines represent the ranges of female and male *Dama dama geiselana*, respectively; black lines the range of recent *Cervus elaphus* from Italy. The Mt III-IV plot includes two *Praemegaceros* specimens (KYP4-301 and KYP4-302) published by Athanassiou (2018). Comparative data from Kahlke (1965), Leonardi and Petronio (1976), Pfeiffer (1998, 2002), Di Stefano et al. (2015) and Stefaniak (2015). Graphical scale equals 10 cm (a–d) and 20 cm (e–g).

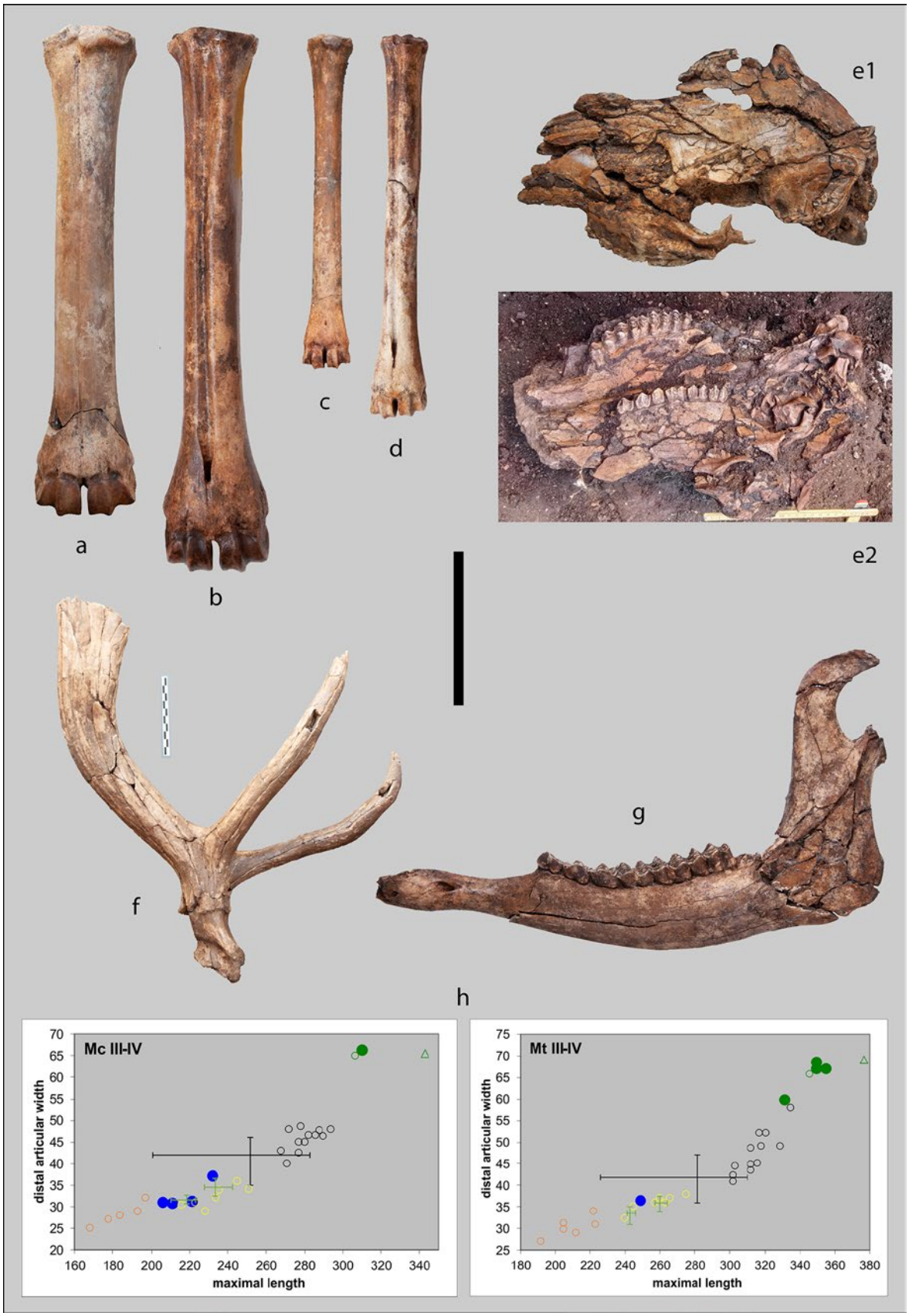
a
b
c
d
e1
e2
f
g
h
Mc III-IV
distal articular width
maximal length
Mt III-IV
distal articular width
maximal length

19.2.5. CERVIDAE

Three size-groups of Cervidae have been identified in the new material, dimensionally corresponding to fallow deer, red deer, and giant deer. Both cranial and postcranial specimens are available. Fallow deer-sized material (*Dama* sp.) comprises isolated teeth and postcranial elements, most notably six complete metapodials (Fig. 2c, d). These belong to a fairly large fallow deer, similar in size to the Middle Pleistocene *Dama clactoniana* and the Eemian *D. dama geiselana* (Fig. 2h), but smaller than *Dama roberti* (see Breda, 2015).

The red deer, *Cervus elaphus*, is best represented in KYP5, where a partially preserved, unshed right antler has been collected. This specimen (KYP5-1194; Fig. 2f) is large-sized, and preserves part of the pedicel, the burr, the proximal part of the beam (up to a height of 45 cm, following its caudal face), as well as the two first tines. No new dental or postcranial specimens from KYP4 can be securely referred to this species.

On the contrary, the giant deer *Praemegaceros verticornis* is well represented at KYP4 by a skull (KYP4-1067; Fig. 2e), two left hemimandibles (KYP4-1068 and KYP4-1069; Fig. 2g) and several postcranial bones (Fig. 2a, b). The skull is very fragmentary because it has suffered a severe, probably syndepositional, dorsoventral compression. It lacks antlers, so it belongs to a female individual. Both dental rows are preserved. Their size (LPM=134 mm, LP=57–61 mm, LM=81 mm) is very similar to KYP4-633 (Athanassiou, 2018: Table 5) and the sample from Voigtstedt, Germany (Kahlke, 1965), but smaller than KYP2-345 (Athanassiou, 2018: Table 5), West Runton, Great Britain (Azzaroli, 1953: p. 61) and Süßenborn, Germany (Kahlke, 1969: p. 573).

The mandibles are not particularly pachygnathic. The lower dentition features a semimolarized p4 and a non-molarized p3. Dimensionally, the lower dentitions are slightly (~5%) larger than their conspecifics from Mosbach and Süßenborn, Germany (Kahlke, 1960, 1969) and very similar to those from Voigtstedt (Kahlke, 1965). The postcranial elements are robust and very similar dimensionally to those from Voigtstedt, as well. A metrical comparison of the metapodials is given in Fig. 2h.

19.2.6. SCARCELY REPRESENTED TAXA

A distal part of a left femur collected at KYP3, as well as a left metatarsal IV (surface find south of KYP1) belong to an elephantid, and are consistent with an attribution to *Palaeoloxodon antiquus*, a species previously documented in the locality (Athanassiou, 2018). A suid upper canine (surface find at KYP4A) is referred to a male *Sus scrofa*. In addition, a primate upper molar, collected at KYP4 (KYP4-1075) and referred to *Macaca sylvanus*, is described in a separate report (Konidaris et al., this volume) and is a new faunal element for Kyparíssia.

19.3 BIOCHRONOLOGY–PALAEOECOLOGY

Most of the taxa represented in the Kyparíssia fauna have rather wide biostratigraphic ranges. Most characteristic is the cervid *Praemegaceros verticornis*, which appeared at about 0.8 Ma and became extinct at 0.4 Ma (Croitor, 2006). The absence of this taxon from Marathousa 1, dated to 0.42–0.48 Ma (Konidaris et al., 2018; Tourloukis et al., 2018), if not accidental, may indicate an earlier local extinction and an earlier date for Kyparíssia. The study of micromammals is more informative in terms of biochronology, since van Kolfschoten et al. (this volume) document the presence of *Mimomys* spp. and *Microtus (Microtus)* in KYP4, thus constraining its age to 0.6–0.8 Ma.

Palaeoecologically, the recently collected material corroborates our understanding of the Middle Pleistocene environment of Kyparíssia as a vegetation-rich lacustrine habitat, surrounded by mixed deciduous forests and woodlands, which, as a permanent body of water, attracted animals from the wider area (Athanassiou, 2018; Athanassiou et al., 2018). Concerning the new reported faunal elements from Kyparíssia, the presence of the beaver, which uses trunks and branches to build dams, further supports the existence of extended forested lake shores, while *Macaca* (see Konidaris et al., this volume), *Vulpes* and *Ursus* are also taxa that thrive in forested environments. The scarce presence of the horse, and to a lesser degree of the rhinoceros, is the only indication of more open stretches of land, though possibly at a certain distance from the lake area. Further palaeoenvironmental indications for KYP4 are provided in Boni et al. (this volume) and Papadopoulou et al. (this volume).

19.4 CONCLUSIONS

Renewed research at Kyparíssia, carried out during the years 2019–2021 has added new material, new taxa and an additional site to the already published ones. The fossils collected from KYP4 corroborate the abundance of *Hippopotamus* (including a partial skeleton) and cervids in the fauna, particularly those of the genus *Praemegaceros*. A close stratigraphic association of the fossils with lithic

Order	Family	Taxon	KYP	KYP1	KYP2	KYP3	KYP4	KYP5	KYPT
Rodentia	Castoridae	*Castor fiber*	●				●		
Primates	Cercopithecidae	*Macaca sylvanus*					●		
Carnivora	Ursidae	*Ursus* sp.	●						
	Canidae	*Canis* sp.	●						
		Vulpes sp.					●		
	Hyaenidae	Hyaenidae indet.	●			●			
	Felidae	*Panthera* sp.				●			
		Felis sp.				●			
Proboscidea	Elephantidae	*Palaeoloxodon antiquus*	●	●		●	●		
Perissodactyla	Rhinocerotidae	*Stephanorhinus* sp.	●				●		
	Equidae	*Equus* sp.	●	●			●		
Artiodactyla	Suidae	*Sus scrofa*	●			●	●		
	Hippopotamidae	*Hippopotamus antiquus*	●	●		●	●		●
	Cervidae	*Praemegaceros verticornis*	●	●	●	●	●		
		Cervus elaphus	●	●		●	●	●	
		Dama sp.	●	●		●	●		
		´Cervus´ peloponnesiacus	●	?		?	?		
		Cervidae indet.	●	?		?	?		●
	Bovidae	*Bison* sp.	●	●			●		

Table 1: Comprehensive list of large fossil mammals from Kyparíssia, indicating the faunal content of each site (KYP1–KYP5, KYPT), as well as unstratified material (KYP). Combined data from Athanassiou (2018), Athanassiou et al. (2018) and the present study. Documented presence is indicated by '●', possible presence by '?'.

artefacts was also documented for the first time, underlining the archaeological significance of the site (Karkanas et al., this volume). Several taxa are recorded for the first time at KYP4: *Castor fiber*, *Stephanorhinus* sp., *Equus* sp., *Sus scrofa*, *Vulpes* sp. and *Macaca sylvanus*. *Ursus* sp., found south of KYP4, was so far unknown from any locality within the Megalopolis Basin. Finally, a new site, KYP5, was discovered. The new faunal list of Kyparíssia (Table 1) is compatible with the previously proposed early Middle Pleistocene age of the locality (Athanassiou, 2018).

ACKNOWLEDGMENTS

Field survey in the Megalopolis Basin was conducted in the framework of the Megalopolis Paleoenvironmental Project (MegaPal) under a permit granted to the Ephorate of Palaeoanthropology–Speleology, Hellenic Ministry of Culture, and the American School of Classical Studies at Athens. Fieldwork was supported by the ERC Consolidator Grant ERC-CoG-724703 ("CROSSROADS"), awarded to K.H. G.E.K., V.T. and K.H. are also supported by the Deutsche Forschungsgemeinschaft (DFG Project no. 463225251, "MEGALOPOLIS"). K.H. is also supported by the ERC Advanced Grant ERC-AdG-101019659 ("FIRSTSTEPS"). We thank all team members who have participated in the fieldwork, as well as the reviewers D. Kostopoulos and G. Iliopoulos, for their comments and suggestions.

REFERENCES

Athanassiou, A., 2018. Pleistocene vertebrates from the Kyparíssia lignite mine, Megalopolis Basin, S. Greece: Rodentia, Carnivora, Proboscidea, Perissodactyla, Ruminantia. Quaternary International, 497, pp. 198–221.

Athanassiou, A., Michailidis, D., Vlachos, E., Tourloukis, V., Thompson, N. and Harvati, K., 2018. Pleistocene vertebrates from the Kyparíssia lignite mine, Megalopolis Basin, S. Greece: Testudines, Aves, Suiformes. Quaternary International, 497, pp. 178–197.

Azzaroli, A., 1953. The deer of the Weybourn Crag and Forest Bed of Norfolk. Bulletin of the British Museum (Natural History), 2(1), pp. 1–96.

Bartolini Lucenti, S., Madurell-Malapeira, J., 2020. Unravelling the fossil record of foxes: An updated review on the Plio-Pleistocene *Vulpes* spp. from Europe. Quaternary Science Reviews, 236, 106296.

Boni, G., Syrides, G., Konidaris, G.E., Athanassiou, A., Tourloukis, V., Koukousioura, O., Panagopoulou, E., Karkanas, P. and Harvati, K., this volume. Preliminary results on the taxonomy and paleoenvironmental analysis of the mollusc fauna from Marathousa 1, Marathousa 2 and Kyparissia 4 (Middle Pleistocene, Megalopolis Basin, Greece).

Breda, M., 2015. The early Middle Pleistocene fallow deer *Dama roberti*: new insight on species morphology from a complete postcranial skeleton from Valdemino (northwestern Italy). Geological Journal, 50(3), pp. 257–270.

Di Stefano, G., Pandolfi, L., Petronio, C. and Salari, L., 2015. The morphometry and the occurrence of *Cervus elaphus* (Mammalia, Cervidae) from the Late Pleistocene of the Italian Peninsula. Rivista Italiana di Paleontologia e Stratigrafia, 121(1), pp. 103–120.

Fostowicz-Frelik, Ł., 2008. First record of *Trogontherium cuvieri* (Mammalia, Rodentia) from the middle Pleistocene of Poland and review of the species. Geodiversitas, 30(4), pp. 765–778.

Giaourtsakis, I.X., 2022. The fossil record of rhinocerotids (Mammalia: Perissodactyla: Rhinocerotidae) in Greece, in: Vlachos, E. (Ed.),

Fossil Vertebrates of Greece, vol. 2: Laurasiatherians, Artiodactyles, Perissodactyles, Carnivorans, and Island Endemics. Springer, Cham, pp. 409–500.

Guérin, C., 1980. Les rhinocéros (Mammalia, Perissodactyla) du Miocène terminal au Pléistocène supérieur en Europe occidentale: comparaison avec les espèces actuelles. Documents des Laboratoires de Géologie Lyon, 79(1–3), pp. 1–1185.

Kahlke, H.D., 1960. Die Cervidenreste aus den Altpleistozänen Sanden von Mosbach (Biebrich-Wiesbaden). Abhandlungen der Deutschen Akademie der Wissenschaften zu Berlin, 1959(7), pp. 1–75.

Kahlke, H.D., 1965. Die Cerviden-Reste aus den Tonen von Voigtstedt in Thüringen. Paläontologische Abhandlungen, 2(2/3), pp. 379–426.

Kahlke, H.D., 1969. Die Cerviden-Reste aus den Kiesen von Süßenborn bei Weimar. Paläontologische Abhandlungen, 3(3/4), pp. 547–610.

Kahlke, R.D., 1997. Die *Hippopotamus*-Reste aus dem Unterpleistozän von Untermaßfeld, in: Kahlke, R.D. (Ed.), Das Pleistozän von Untermaßfeld bei Meiningen (Thüringen), Teil 1. Habelt, Mainz, pp. 277–374.

Karkanas, P., Tourloukis, V., Thompson, N., Giusti, D., Tsartsidou, G., Athanassiou, A., Konidaris, Roditi, E., Panagopoulou, E., Karkanas, P. and Harvati, K., this volume. The Megalopolis Paleoenvironmental Project (MegaPal).

Konidaris, G.E., Athanassiou, A., Panagopoulou, E., Karkanas, P. and Harvati, K., this volume. Fossil macaques (Cercopithecidae, Primates) from the Middle Pleistocene of the Megalopolis Basin (Greece) with description of a new specimen from Kyparissia 4.

Konidaris, G.E., Athanassiou, A., Tourloukis, V., Thompson, N., Giusti, D., Panagopoulou, E. and Harvati, K., 2018. The skeleton of a straight-tusked elephant (*Palaeoloxodon antiquus*) and other large mammals from the Middle Pleistocene butchering locality Marathousa 1 (Megalopolis Basin, Greece): preliminary results. Quaternary International, 497, pp. 65–84.

Leonardi, G., Petronio, C., 1976. The fallow deer of European Pleistocene. Geologica Romana, 15, pp. 1–67.

Mazza, P., 1995. New evidence on the Pleistocene hippopotamuses of Western Europe. Geologica Romana, 31, pp. 61–241.

Papadopoulou, P., Tsoni, M., Konidaris, G.E., Tourloukis, V., Panagopoulou, E., Karkanas, P., Harvati, K. and Iliopoulos, G., this volume. Ostracod contribution to the palaeoenvironmental study of Kyparissia-4 (Megalopolis Basin, Greece).

Pfeiffer, T., 1998. Die fossilen Damhirsche von Neumark-Nord (Sachsen-Anhalt) — *D. dama geiselana* n. ssp. Eiszeitalter und Gegenwart, 48, pp. 72–86.

Pfeiffer, T., 2002. The first complete skeleton of *Megaloceros verticornis* (Dawkins, 1868), Cervidae, Mammalia, from Bilshausen (Lower Saxony, Germany): description and phylogenetic implications. Mitteilungen aus dem Museum für Naturkunde in Berlin, Geowissenschaftliche Reihe, 5, pp. 289–308.

Rossi, M., Santi, G., 2011. *Ursus deningeri–spelaeus* group from Cerè Cave (Veneto, North Italy) in the new evolutionary frame of the cave bear. Part one: skulls and mandibles. Annalen des Naturhistorischen Museums in Wien, 113A, pp. 567–590.

Stefaniak, K., 2015. Neogene and Quaternary Cervidae from Poland. Institute of Systematics and Evolution of Animals of the Polish Academy of Sciences, Kraków.

Tourloukis, V., Muttoni, G., Karkanas, P., Monesi, E., Scardia, G., Panagopoulou, E. and Harvati, K., 2018. Magnetostratigraphic and chronostratigraphic constraints on the Marathousa 1 Lower Palaeolithic site and the Mid-

dle Pleistocene deposits of the Megalopolis Basin, Greece. Quaternary International, 497, pp. 154–169.

van Kolfschoten, T., Konidaris, G.E., Doukas, C., Athanassiou, A., Tourloukis, V., Panagopoulou, E., Karkanas, P. and Harvati, K., this volume. Voles (Rodentia, Mammalia) as a proxy to date the site Kyparissia 4 (Megalopolis Basin, Greece).

20 VOLES (RODENTIA, MAMMALIA) AS A PROXY TO DATE THE SITE KYPARISSIA 4 (MEGALOPOLIS BASIN, GREECE)

Thijs van Kolfschoten[1,2*], George E. Konidaris[3], Constantin Doukas[4], Athanassios Athanassiou[5], Vangelis Tourloukis[3,6], Eleni Panagopoulou[5], Panagiotis Karkanas[7], Katerina Harvati[3]

[1]*Faculty of Archaeology, Leiden University, the Netherlands*
[2]*Joint International Research Laboratory of Environmental and Social Archaeology, Shandong University, Qingdao, China*
[3]*Paleoanthropology, Institute for Archaeological Sciences and Senckenberg Centre for Human Evolution and Palaeoenvironment, Department of Geosciences, Eberhard Karls University of Tübingen, Tübingen, Germany*
[4]*Faculty of Geology and Geoenvironment, National and Kapodistrian University of Athens, Athens, Greece*
[5]*Hellenic Ministry of Culture, Ephorate of Palaeoanthropology–Speleology, Athens, Greece*
[6]*Department of History and Archaeology, School of Philosophy, University of Ioannina, Ioannina, Greece*
[7]*M.H. Wiener Laboratory for Archaeological Science, American School of Classical Studies at Athens, Athens, Greece*
[*]*T.van.Kolfschoten@arch.leidenuniv.nl*

http://dx.doi.org/10.15496/publikation-97667

Keywords: mammalian biostratigraphy; *Mimomys*; *Microtus*; Pleistocene; Quaternary

20.1 INTRODUCTION

The Palaeolithic record provides us insights into the hominin migration patterns and into the way hominins adapted to the changing climatic conditions, as well as how they evolved both physically and culturally. In order to make such interpretations, the age of a Palaeolithic site is of pivotal importance; however, dating of deposits with Palaeolithic finds is often a great challenge. Absolute dating methods, such as radiocarbon, luminescence (TL as well as OSL), potassium-argon or U/Th dating, are possible options to apply. Nonetheless, besides their assets, they also have specific limitations, and the application of absolute dating methods does not always yield reliable ages. An alternative way to estimate the age of a site is the so-called relative dating method. A classic example of the relative dating is the application of the biostratigraphical evidence. Biochronological dating is based on the fact that the fossil record changes through time due to the migration, evolution and extinction of species, and the detailed knowledge of these changes can be applied to provide relative age estimations for a site. The Quaternary mammalian fossil record yields detailed biostratigraphical data. The climatic fluctuations that characterize the Quaternary, resulted in major mammalian migration/dispersal events and rapid evolution of specific species/lineages. The Quaternary fossil record shows an increase of crown height in the molars of different taxa (e.g., mammoth, rhinoceros, voles), a phenomenon that is regarded as an adaptation to the incorporation of more abrasive

T. Kolfschoten: https://orcid.org/0000-0003-1716-3394
G. E. Konidaris: https://orcid.org/0000-0002-7041-233X
A. Athanassiou: https://orcid.org/0000-0002-9140-7011
V. Tourloukis: https://orcid.org/0000-0002-9527-2708
E. Panagopoulou: https://orcid.org/0000-0002-4268-6157
P. Karkanas: https://orcid.org/0000-0002-7156-671X
K. Harvati: https://orcid.org/0000-0001-5998-4794

foods into the diet. Changes in the rodent fauna constitute the base for the biostratigraphical subdivision of the Quaternary into Villanyian, Biharian and Thoringian.

A relatively rapid evolution can be observed in the dental record of fossil voles (Rodentia, Arvicolidae). Different lineages show successively, but not simultaneously, an increase of crown height in the molars, the formation of crown cementum, the development of rootless molars, changes in enamel structure and in the differentiation of the enamel thickness, and the formation of additional enamel in the upper M3 and the lower m1 that results in an increase of complexity of the occlusal surface of both molars. Voles of the genus *Mimomys* are very abundant in the fossil record. The appearance of *Mimomys* species, which have molars with crown cementum, such as *M. minor* and *M. hajnackensis*, mark the beginning of the Villanyian during the Pliocene (van der Meulen and van Kolfschoten, 1986). The appearance of the genus *Microtus* in the European fossil record is regarded as the marker of the Villanyian/Biharian boundary (Fejfar and Heinrich, 1990). Voles of the genus *Microtus*, characterized by unrooted molars, are well-represented and often a dominant taxon in the micro-mammalian fauna since their Early Pleistocene appearance ca. 2 million years ago (Tesakov, 1998). The evolutionary changes in the water vole lineage resulted in the replacement of *Mimomys savini* (a species with rooted molars) by *Arvicola cantiana* (with unrooted molars), which marks the Biharian/Toringian transition with an age of ca. 0.5 Ma.

20.2 FOSSIL VOLES FROM THE MEGALOPOLIS BASIN

The occurrence of mammalian fossils in the Pleistocene deposits of the Megalopolis Basin is well-known since the beginning of the 20th century (Skouphos, 1905), and since then several studies have described the large mammalian remains (e.g., Melentis, 1961, 1965; Sickenberg, 1975; Athanassiou, 2018; Konidaris et al., 2018). In the last decades, several systematic studies of the Megalopolis Basin's small mammals have been conducted (see also Doukas and Papayianni, 2016), particularly focusing on the late Early–Middle Pleistocene Marathousa Member. The Marathousa Member (Choremi Formation) consists mainly of clastic deposits of fluvio-lacustrine origin, intercalated by lignite seams; the latter are distinguished into three main lignite packages, namely Lignite Seams I, II and III (from the lower to the upper one) (Vinken, 1965). Below is a summary of the studies conducted so far on the micromammals originating from these deposits.

20.2.1. THOKNIA

Benda et al. (1987) published the small mammal assemblage collected from the lower lignite bed exposed in the Thoknia lignite mine (Fig. 1a). They identified only two taxa, *Mimomys* (*Kislangia*) *rex* and *Pliomys* cf. *bolkia*, and they state that the presence of *Mimomys rex* and the absence of *Microtus* (even though the assemblage is small) allows for a correlation to the upper part of the Villanyian.

20.2.2. CHOREMIOU SECTION

In order to contribute to the discussion on the stratigraphical position of the Marathousa Member, a team of Greek and Dutch paleontologists sampled at the Choremiou section (Choremi lignite mine; Fig. 1a) four different levels with mammalian remains: CHO 1 and CHO 2 are from Lignite I, CHO 3 is from the base of Lignite II, and CHO 4 is from deposits that were originally

assigned to Lignite III. However, the study of the small mammals from Marathousa 1 (see below) and the recent research in the basin (Karkanas et al., this volume), which shows extensive faulting in the Choremi mine, indicate that the CHO 4 fauna originates from a lower lignite seam.

All four CHO samples yielded vertebrate remains: Reptilia are well represented in CHO 2, CHO 3 and CHO 4, while mammalian remains are most abundant in CHO 3 and CHO 4, with 68 and 94 identifiable specimens, representing ten and seven species, respectively (van Vugt et al., 2000). The Choremiou faunal assemblages include three different voles: *Pliomys* aff. *episcopalis*, *Mimomys* aff. *savini* and *Mimomys* sp. The large vole, *Mimomys* aff. *savini*, with hypsodont molars with crown cementum in the re-entrant angles, is by far the most abundant species. The majority of the larger lower m1 molars show an occlusal pattern that resembles *Mimomys savini*; the pattern of only a few larger lower m1 molars resembles that of the molars from Thoknia assigned to *Mimomys rex* by Benda et al. (1987). Both CHO 2 and CHO 4 yielded in addition a rooted molar with a *Mimomys* pattern and crown cementum in the re-entrant angles, that are too small to be assigned to *Mimomys* aff. *savini*. These two molars are therefore listed as *Mimomys* sp.

Mimomys aff. *savini*, the species that is well represented in the four Choremiou assemblages, does not show any difference in morphology and size among the different levels. This observation suggests that the four faunas do not differ much in age and, as a consequence, it indicates that there is no major stratigraphical hiatus in that particular part of the Choremiou sequence.

Remarkable is the absence of the genus *Microtus* in the Choremiou faunal assemblages. Benda et al. (1987) assumed a late Villanyian age of the Marathousa Member because of the absence of the genus *Microtus* in the Thoknia small mammal assemblage. However, a taphonomic/ecological explanation seems to be more applicable (van Vugt et al., 2000). The complete absence of terrestrial molluscs in the fauna CHO 2, CHO 3 and CHO 4 combined with the dominance of aquatic taxa in the herpetofauna, indicate specific paleoenvironmental conditions that are unfavorable for the accumulation of terrestrial voles, such as *Microtus*. Hence, the absence of *Microtus* in the Choremiou assemblages does not necessarily contradict the late Early Pleistocene age of the CHO 1 and CHO 2 faunal assemblages, and the early Middle Pleistocene age of the assemblages CHO 3 and CHO 4.

20.2.3. MARATHOUSA 1

A more recent small mammal assemblage has been collected from lacustrine deposits intercalated between Lignite Seams II and III, exposed at the Middle Pleistocene (Lower Palaeolithic) site Marathousa 1 (MAR-1), located in the Marathousa mine (Fig. 1a; Panagopoulou et al., 2018). The small mammal assemblage is diverse and includes *Crocidura* sp., *Arvicola mosbachensis*, *Microtus* sp. (cf. *M. arvalis*), *Apodemus sylvaticus* vel *A. flavicollis* and ?*Alactaga* indet., but it is dominated by the voles *Arvicola* and *Microtus* (Doukas et al., 2018). The molars of the larger water vole do not have roots. This indicates that the faunal assemblage is younger than the Choremiou section assemblages, where *Mimomys*, the predecessor of the genus *Arvicola*, is the predominant arvicolid. The unrooted *Arvicola* molars show a positive '*Mimomys*' enamel differentiation with a mean SDQ (Schmelzband-Differenzierung-Quotient; Heinrich, 1982) value of 122, which indicates a late Middle Pleistocene age (ca. 400 ka.; Marine Isotope Stages-MIS 12/11) for the lacustrine deposits, in broad agreement with the radiometric and magnetostratigraphic dating (Blackwell et al., 2018; Jacobs et al., 2018; Tourloukis et al., 2018).

Marathousa Lignite Seam III, which is overlying the deposits that yielded the MAR-1 small mammal assemblage, must therefore be of late Middle Pleistocene age or younger.

20.2.4. KYPARISSIA 4

A fourth site in the Megalopolis Basin that yielded fossil micromammals is Kyparissia 4 (KYP-4) in the Kyparissia mine (Fig. 1a, b). KYP-4 was discovered in 2007 and has yielded a rich and diverse assemblage of large mammals (Athanassiou, 2018; Athanassiou et al., 2018). In 2019, KYP-4 was revisited during a systematic and targeted field survey in the framework of the Megalopolis Paleoenvironmental Project (MegaPal) and the CROSSROADS ERC project (Harvati, this volume; Karkanas et al., this volume). Two main areas of interest were defined, Area A (the findspot of Athanassiou, 2018) and Area B (to the east of Area A, including a partial *Hippopotamus* skeleton). In addition to the discovery of lithic artifacts (Karkanas et al., this volume) and the enrichment of the large mammal collection both in terms of specimens and taxa (Athanassiou et al., this volume; Konidaris et al., this volume), sampling for molluscs (Boni et al., this volume), ostracods (Papadopoulou et al., this

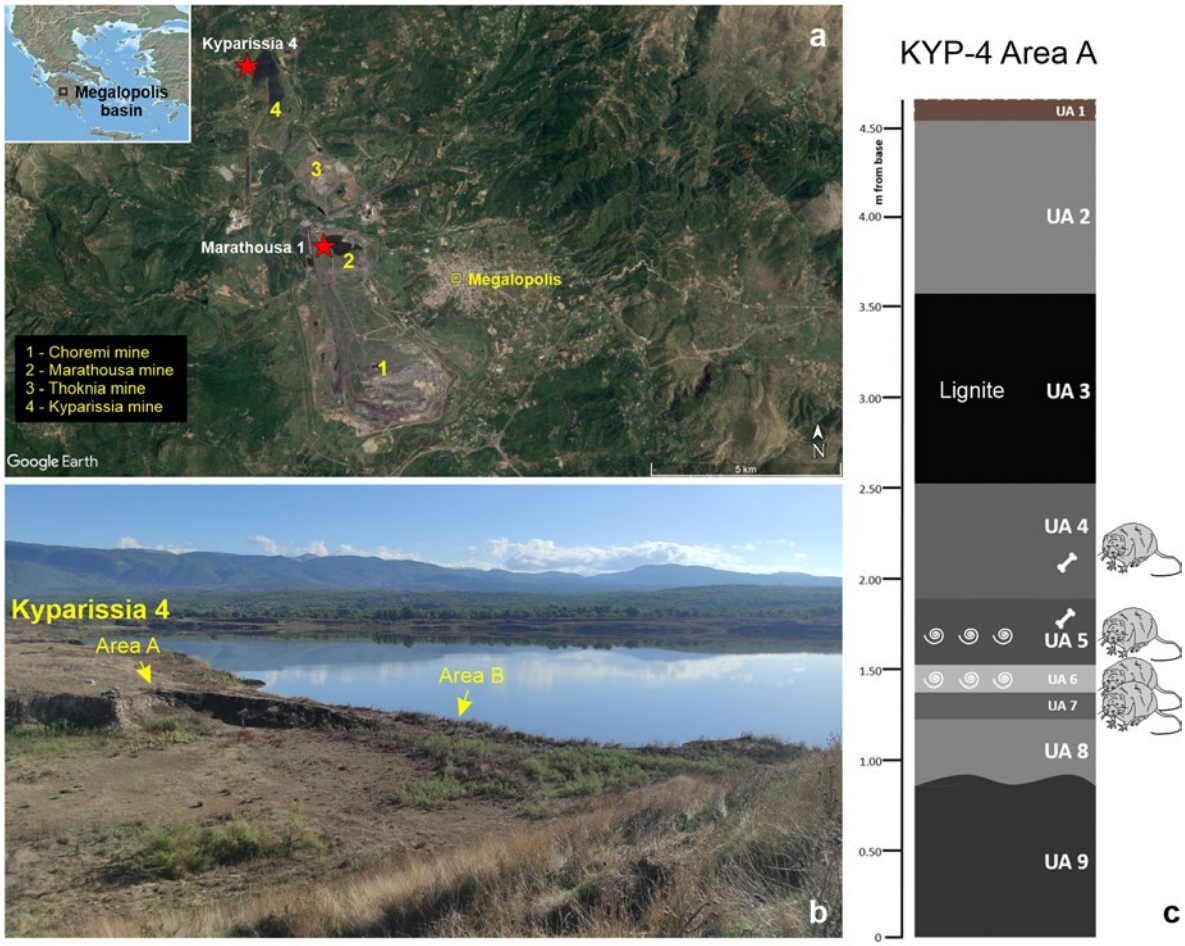

Figure 1: a, Geographic position of the Megalopolis Basin, and of the micromammal-bearing Middle Pleistocene (Lower Palaeolithic) sites Kyparissia 4 and Marathousa 1, in relation to the main lignite mines of the basin (satellite image from Google Earth); b, distant view of Kyparissia 4; c, simplified stratigraphic column of KYP-4 (Area A) showing the stratigraphic units, and the position of the samples that were taken and contain small mammals; water vole drawing redrawn and modified from https://www.drawingtutorials101.com/.

volume) and micromammals (this study) was also conducted. The KYP-4 sedimentary sequence is divided into several distinct stratigraphic units, comprising an alternation of dark grey organic rich mud layers with an intercalation of a lignite layer towards its upper part (Fig. 1b). The larger mammal fauna consists so far of the following taxa (Athanassiou, 2018; Athanassiou et al., 2018, this volume; Konidaris et al., this volume): *Castor fiber* (beaver), *Macaca sylvanus* (macaque), *Vulpes* sp. (fox), *Palaeoloxodon antiquus* (straight-tusked elephant), *Stephanorhinus* sp. (rhinoceros), *Equus* sp. (horse), *Sus scrofa* (boar), *Hippopotamus antiquus* (hippopotamus), *Dama* sp. (fallow deer), *Cervus elaphus* (red deer), *Praemegaceros verticornis* (giant deer) and *Bison* sp. (bison). The analysis of the first collection of small mammals from KYP-4 forms the primary focus of the present study.

20.3 METHODS

Sediment samples to collect small vertebrate remains were taken from the site KYP-4 during the fieldwork of 2019 and 2020. Twenty-two sediment samples, weighing ~70 kg in total, were collected. The majority of the samples originate from the main lithic/vertebrate-bearing unit UA4 (13 samples; ~40 kg) in Area A, while the rest come from UA5 (5 samples; ~15 kg) and UA6 (2 samples; ~7 kg) of the same area (Fig. 1c), as well as from the mollusc-rich *Hippopotamus*-layer in Area B (2 samples; ~6 kg). Additionally, one arvicolid hemimandible was directly collected from unit UA7 during the fieldwork. Sediment samples were air-dried and then soaked in containers filled with water and ~50 ml of 30% concentration H_2O_2. Subsequently, samples were wet sieved using a 0.5 mm mesh and then left to air-dry. Examination and sorting for vertebrate remains was conducted under a stereoscopic microscope. Complete or partly fragmented recognizable vertebrate remains were collected. Here, we focus on the more diagnostic and informative dental elements of the collected small mammals, which are identified to the lowest taxonomic level possible.

20.4 RESULTS

The Kyparissia 4 sediment samples from the units UA4, UA5 and UA6 (plus the isolated hemimandible from UA7), and the *Hippopotamus* layer in Area B, yielded in total more than 1000 small vertebrate remains; UA5 is the richest unit with ca. 700 specimens. The highly fragmented remains represent a variety of taxa: fish (Cyprinidae), frogs/toads, snakes, insectivores —shrews (to be identified)— and rodents (Fig. 2a, b). The rodent assemblage, taking into account the small number of dental remains, is very diverse. At least five different taxa could be identified: *Mimomys* sp. (cf. *Mimomys savini*) (large), *Mimomys* sp. (small), *Microtus* sp., *Apodemus* sp. and ?*Mus* cf. *spretus*. The faunal assemblage includes only seven complete molars: one shrew molar, three murid molars and three complete vole molars. Based on the characteristics of the available remains (rooted molars with cement and a *Mimomys* enamel differentiation), it is obvious that at least two taxa of the genus *Mimomys* are represented. The larger one is represented by an upper M3 (Fig. 2c) and a lower m2 (Fig. 2d); the small one is represented by a lower m3 (Fig. 2e). The small mammal assemblage also includes unrooted molars that are assigned, based on the morphological features, to the genus *Microtus*. The occlusal surface of the unrooted *Microtus* lower m1 shows the occurrence of five more or less closed triangles and an *arvalis*-type anterior cap (Fig. 2f). The morphology indicates the presence of a *Microtus* (*Microtus*) species and excludes a species of the subgenus *Microtus* (*Allophaiomys*). Species-level identification of the *Microtus* remains is not justified because of the limited number of identifiable specimens. The di-

mensions of the three murid molars indicate that we are dealing with two different species: a larger one, possibly a representative of the taxon *Apodemus sylvaticus*, and a smaller one with the size of *Mus* cf. *spretus*, a taxon that is well represented in

Figure 2: a, b, Microscope views of small vertebrate remains from Kyparissia 4; c–f, voles from Kyparissia 4, stratigraphic unit UA5: c–d, larger *Mimomys* species (cf. *Mimomys savini*): c, upper M3 sin.; d, lower m2 dext.; e, smaller *Mimomys* species: lower m3 sin.; f, *Microtus* (*Microtus*) species: lower m1 dext. (c1, d1, e1, and f1 in occlusal view; c2, d2, and e2 in lingual view; f2 in labial view).

the Choremiou 4 small mammal assemblage (van Vugt et al., 2000).

20.5 DISCUSSION – CONCLUSIONS

The occurrence of voles of the genus *Mimomys* (characteristic for Early–early Middle Pleistocene faunas) in the KYP-4 fossil assemblage, indicates that the fauna is clearly older than the one from the middle–late Middle Pleistocene site of Marathousa 1 (Doukas et al., 2018). The KYP-4 small mammal assemblage shows similarities with the Choremiou 3 and 4 mammal faunas. The presence of *Microtus* (*Microtus*) indicates that the fauna post-dates the *Allophaiomys*/*Microtus* transition that takes place roughly around the Early/Middle Pleistocene transition (Brunhes/Matuyama geomagnetic polarity boundary; 780 ka). The combination of voles with rooted molars assigned to the genus *Mimomys* and unrooted *Microtus* (*Microtus*) molars suggests an early Middle Pleistocene age for the KYP-4 small mammal assemblage. This age is in agreement with the available stratigraphic and macromammal biochronological data, and thus altogether, the current evidence indicates that KYP-4 is older than MAR-1 (500–400 ka) and is placed in the lower part of the Middle Pleistocene.

The presence of a medium-sized vole of the genus *Mimomys* is biostratigraphically important. Medium-sized *Mimomys* taxa are well represented in the European Early Pleistocene fossil record, but most of them went extinct before the end of the Early Pleistocene. Only one medium-sized vole, *Mimomys pusillus*, has a larger biostratigraphical range. A limited number of European sites, e.g., Choremiou (van Vugt et al., 2000; Doukas and Papayiannni, 2016), Kärlich, Germany (van Kolfschoten and Turner, 1996), Pakefield, UK (Parfitt et al., 2005) and Chiu-Atasova, Russia (Southern Urals; Danukalova et al., 2016) indicate the early Middle Pleistocene (predating MIS 16) occurrence of a medium-sized *Mimomys* species. The species is rare, and the remains are often assigned to *Mimomys* sp. because of the absence of diagnostic elements.

The KYP-4 small vertebrate record is small. However, if one considers the small amount of sediment that has been processed (in total ca. 70 kg; in comparison, the Choremiou sediment sample was 10 times larger), it is obvious that the deposits that have been sampled are very rich in small vertebrate remains. Remarkable is the fact that the diversity of the encountered small mammal fauna is high and that the sample includes biostratigraphically important taxa. It emphasizes the importance of the Megalopolis Basin, and in particular, the deposits exposed in the Kyparissia lignite mine, for the detailed study of the Eurasian faunal evolution. The results of these studies are of great importance to date the hominin presence in regions such as the eastern Mediterranean.

ACKNOWLEDGEMENTS

We thank all field team members and all students who participated in the washing of the sediment, and especially F. Roditi, G. Boni and D. Verrarou for its sorting in the lab. A. Ramcharan (Leiden University) collected and measured the identifiable small mammal remains. We also thank D. Kostopoulos and one anonymous reviewer for their suggestions to improve the manuscript. Field survey in the Megalopolis Basin was conducted in the framework of the Megalopolis Paleoenvironmental Project (MegaPal) under a permit granted to the Ephorate of Palaeoanthropology–Speleology, Hellenic Ministry of Culture, and the American School of Classical Studies at Athens. Fieldwork was supported by the ERC Consolidator Grant ERC-CoG-724703 (“CROSSROADS”) awarded to K.H. G.E.K., V.T. and K.H. are also supported by the Deutsche Forschungsgemeinschaft (DFG

Project no. 463225251, "MEGALOPOLIS"). K.H. is also supported by the ERC Advanced Grant ERC-AdG-101019659 ("FIRSTSTEPS").

REFERENCES

Athanassiou, A., 2018. Pleistocene vertebrates from the Kyparíssia lignite mine, Megalopolis Basin, S. Greece: Rodentia, Carnivora, Proboscidea, Perissodactyla, Ruminantia. Quaternary International, 497, pp. 198–221.

Athanassiou, A., Michailidis, D., Vlachos, E., Tourloukis, V., Thompson, N. and Harvati, K., 2018. Pleistocene vertebrates from the Kyparíssia lignite mine, Megalopolis Basin, S. Greece: Testudines, Aves, Suiformes. Quaternary International, 497, pp. 178–197.

Athanassiou, A., Konidaris G.E., Tourloukis, V., Thompson, N., Giusti, D., Karkanas, P. and Harvati, K., this volume. The Middle Pleistocene large mammal fauna from Kyparissia (Peloponnese, S. Greece): New collected material.

Benda, L., van der Meulen, A.J., Meyer, K.J. and van de Weerd, A., 1987. Biostratigraphic correlations in the Eastern Mediterranean Neogene. 8. Calibration of sporomorph- and rodent-associations from the Megalopolis Basin (Peloponnesus, Greece). Newsletters on Stratigraphy, 17(3), pp. 129–141.

Blackwell, B.A.B., Sakhrani, N., Singh, I.K., Gopalkrishna, K.K., Tourloukis, V., Panagopoulou, E., Karkanas, P., Blickstein, J.I.B., Skinner, A.R., Florentin, J.A. and Harvati, K., 2018. ESR dating ungulate teeth and molluscs from the Paleolithic site Marathousa 1, Megalopolis Basin, Greece. Quaternary, 1(3), p. 22.

Boni, G., Syrides, G., Konidaris, G.E., Athanassiou, A., Tourloukis, V., Koukousioura, O., Panagopoulou, E., Karkanas, P. and Harvati, K., this volume. Preliminary results on the taxonomy and paleoenvironmental analysis of the mollusc fauna from Marathousa 1, Marathousa 2 and Kyparissia 4 (Middle Pleistocene, Megalopolis Basin, Greece).

Danukalova, G., Yakovlev, A., Osipova, E., Kurmanov, R. and van Kolfschoten, T. 2016. Biostratigraphy of the early Middle Pleistocene of the Southern Fore-Urals. Quaternary International, 420, pp. 115–135.

Doukas, C.S., Papayianni, K., 2016. Small mammals in the Plio/Pleistocene sediments of Greece, in: Harvati, K., Roksandic, M. (Eds.), Paleoanthropology of the Balkans and Anatolia. Human evolution and its context. Springer, Dordrecht, pp. 291–302.

Doukas, C., van Kolfschoten, T., Papayianni, K., Panagopoulou, E. and Harvati, K., 2018. The small mammal fauna from the palaeolithic site Marathousa 1 (Greece). Quaternary International, 497, pp. 95–107.

Fejfar, O., and Heinrich, W.D., 1990. Muroid rodent biochronology of the Neogene and Quaternary of Europe, in: Lindsay, E.H. et al. (Eds.), European Neogene Mammal Chronology. Plenum Press, New York, pp. 91-117.

Harvati, K., this volume. Introduction to the volume.

Heinrich, W.D., 1982. Zur Evolution und Biostratigraphie von *Arvicola* (Rodentia, Mammalia) im Pleistozän Europas. Zeitschrift für geologische Wissenschaften, 10, pp. 683–735.

Jacobs, Z., Li, B., Karkanas, P., Tourloukis, V., Thompson, N., Panagopoulou, E. and Harvati, K., 2018. Optical dating of K-feldspar grains from Middle Pleistocene lacustrine sediment at Marathousa 1 (Greece). Quaternary International, 497, pp. 170–177.

Karkanas, P., Tourloukis, V., Thompson, N., Giusti, D., Tsartsidou, G., Athanassiou, A., Konidaris, G., Roditi, E., Panagopoulou, E. and Harvati, K., this volume. The Megalopolis Paleoenvironmental Project (MegaPal).

Konidaris, G.E., Athanassiou, A., Tourloukis,

V., Thompson, N., Giusti, D., Panagopoulou, E. and Harvati, K., 2018. The skeleton of a straight-tusked elephant (*Palaeoloxodon antiquus*) and other large mammals from the Middle Pleistocene butchering locality Marathousa 1 (Megalopolis Basin, Greece): preliminary results. Quaternary International, 497, pp. 65–84.

Konidaris, G.E., Athanassiou, A., Panagopoulou, E., Karkanas, P. and Harvati, K., this volume. Fossil macaques (Cercopithecidae, Primates) from the Middle Pleistocene of the Megalopolis Basin (Greece) with description of a new specimen from Kyparissia 4.

Melentis, J.K., 1961. Die Dentition der pleistozänen Proboscidier des Beckens von Megalopolis im Peloponnes (Griechenland). Annales Géologiques des Pays Helléniques, 12, pp. 153–262.

Melentis, J.K., 1965. Über *Hippopotamus antiquus* Desmarest aus dem Mittelpleistozän des Beckens von Megalopolis im Peloponnes (Griechenland). Annales Géologiques des Pays Helléniques, 16, pp. 403–435.

Panagopoulou, E., Tourloukis, V., Thompson, N., Konidaris, G., Athanassiou, A., Giusti, D., Tsartsidou, G., Karkanas, P. and Harvati, K., 2018. The Lower Palaeolithic site of Marathousa 1, Megalopolis, Greece: Overview of the evidence. Quaternary International, 497, pp. 33-46.

Papadopoulou, P., Tsoni, M., Konidaris, G.E., Tourloukis, V., Panagopoulou, E., Karkanas, P., Harvati, K. and Iliopoulos, G., this volume. Ostracod contribution to the palaeoenvironmental study of Kyparissia-4 (Megalopolis Basin, Greece).

Parfitt, S.A., Barendregt, R.W., Breda, M., Candy, I., Collins, M.J., Coope, G.R., Durbidge, P., Field, M.H., Lee, J.R., Lister, A.M., Mutch, R., Penkman, K.E.H., Preece, R.C., Rose, J., Stringer, C.B., Symmons, R., Whittaker, J.E., Wymer, J.J. and Stuart, A.J., 2005. The earliest record of human activity in northern Europe. Nature, 438, pp. 1008–1012.

Sickenberg, O., 1975. Eine Säugetierfauna des tieferen Bihariums aus dem Becken von Megalopolis (Peloponnes, Griechenland). Annales Géologiques des Pays Helléniques, 27, pp. 25–73.

Skouphos, T., 1905. Über die paläontologischen Ausgrabungen in Griechenland in Beziehung auf das Vorhandensein des Menschen. Comptes rendus du Congrès International d'Archéologie, 1re session, Athènes, pp. 231–236.

Tesakov, A.S., 1998. Voles of the Tegelen fauna. Mededelingen Nederlands Instituut voor Toegepaste Geowetenschappen TNO, 60, pp. 71–134.

Tourloukis, V., Muttoni, G., Karkanas, P., Monesi, E., Scardia, G., Panagopoulou, E. and Harvati, K., 2018. Magnetostratigraphic and chronostratigraphic constraints on the Marathousa 1 Lower Palaeolithic site and the Middle Pleistocene deposits of the Megalopolis Basin, Greece. Quaternary International, 497, pp. 154–169.

van der Meulen, A.J., van Kolfschoten, T., 1986. Review of the late Turolian to early Biharian mammal faunas from Greece and Turkey. Memorie della Società Geologica Italiana, 31, pp. 201–211.

van Kolfschoten, T., Turner, E., 1996. Early Middle Pleistocene mammalian faunas from Kärlich and Miesenheim I and their biostratigraphical implications, in: Turner, C. (Ed.), The early Middle Pleistocene in Europe, Proceedings of the SEQS Cromer Symposium. Balkema, Norwich, United Kingdom, pp. 227–253.

van Vugt, N., de Bruijn, H., van Kolfschoten, T. and Langereis, C.C., 2000. Magneto- and cyclostratigraphy and mammal-fauna's of the Pleistocene lacustrine Megalopolis Basin,

Peloponnesos, Greece, in: van Vugt, N. (Ed.), Orbital Forcing in Late Neogene Lacustrine Basins from the Mediterranean. A magneto-stratigraphic and Cyclostratigraphic Study. Utrecht University, Utrecht, pp. 69–92.

Vinken, R., 1965. Stratigraphie und Tektonik des Beckens von Megalopolis (Peloponnes, Griechenland). Geologisches Jahrbuch, 83, pp. 97–148.

21 MAGNETOSTRATIGRAPHY OF THE KYPARISSIA AND CHOREMI STRATIGRAPHIC SEQUENCES (MEGALOPOLIS BASIN): PRELIMINARY RESULTS

Serena Perini[1,*], Giovanni Muttoni[1], Vangelis Tourloukis[2,3]

[1]*Department of Earth Sciences "Ardito Desio", Università degli Studi di Milano, Milan, Italy*
[2]*Paleoanthropology, Institute of Archaeological Science, Senckenberg Centre for Human Evolution and Palaeoenvironment, Department of Geosciences, Eberhard Karls University of Tübingen, Tübingen, Germany*
[3]*Department of History and Archaeology, School of Philosophy, University of Ioannina, Ioannina, Greece*
**serena.perini@unimi.it*

http://dx.doi.org/10.15496/publikation-97640

Keywords: Magnetostratigraphy; Rock-magnetism; Pleistocene; Megalopolis; Greece

21.1 INTRODUCTION

During the 2020 research campaign of the Megalopolis Palaeoenvironmental Project, 8 oriented core samples were collected for paleomagnetism from the archeological site of KYP4. In 2021, a more extensive paleomagnetic sampling campaign was conducted across the 22 m-thick Kyparissia-4 and 28 m-thick Choremi-6 sections, located stratigraphically the former above the latter in the Kyparissia and Choremi mines, respectively (Fig. 1). Each stratigraphic section was subdivided into different sub-sections (8 subsections for Kyparissia-4 and 6 subsections for Choremi-6), in order to cover the stratigraphy homogeneously. We sampled every 20-30 cm collecting a total of 103 oriented core samples (69 at Kyparissia-4 and 34 at Choremi-6). Cores were then cut into standard-sized ~10cc cylinders to perform different magnetostratigraphic and rock-magnetic analyses from the same stratigraphic level.

The primary objective was to determine the geomagnetic polarity recorded in the sediments and perform correlations at the basin scale using primarily the Brunhes-Matuyama boundary dated to 0.773 Ma (Channell et al., 2020), which represents the most recent reversal of the Earth's magnetic field. We also aimed at identifying short reversals that could potentially improve the magnetochronology of these sections.

21.1.1. MATERIALS AND METHODS

The 8 samples from the KYP4 archeological site and the 103 samples from the Kyparissia-4 and Choremi-6 sections have undergone thermal demagnetization experiments in order to deter-

S. Perini: https://orcid.org/0000-0002-6545-2193
G. Muttoni: https://orcid.org/0000-0001-7908-1664
V. Tourloukis: https://orcid.org/0000-0002-9527-2708

Figure 1: Satellite image (source: GoogleEarth™) of the Megalopolis Basin, with the position of Kyparissia 4 and Choremi 6 sections and constituting sub-sections.

mine the characteristic remanent magnetization (ChRM) component directions, representing the registry of the magnetic polarity at the time of rock formation. The analyses were performed from room temperature up to ~450°C (for samples from Choremi-6) and 625°C (for samples from Kyparissia-4) in steps of 25°C with an ASC thermal demagnetizer, and the natural remanent magnetization (NRM) signal was measured after each temperature step with a 2G Enterprises 755 DC-SQUID cryogenic magnetometer located in a magnetically shielded room. The magnetic susceptibility was also measured with a Bartington MS2B susceptibility bridge after each step of demagnetization to monitor the mineralogic stability in function of heating. The magnetic component directions were subsequently determined through least-square analysis (Kirshvink, 1980). Samples were then subjected to thermal demagnetization of a three-component isothermal remanent magnetization-IRM (Lowrie, 1990) in fields of 0.12 T, 0.4 T, and 1.5 T using a pulse magnetizer (ASC IM-

10-30) to determine the ferromagnetic mineralogy carrying the primary paleomagnetic signal.

21.1.2. RESULTS AND FUTURE PERSPECTIVES

Thermal demagnetization analysis on the 8 samples from the KYP4 archaeological site indicates the exclusive presence of normal magnetic polarity (ChRM component directions oriented to the north with positive [downward] inclinations) attributable to the Brunhes Chron (C1n), suggesting an age of less than 0.773 Ma for this site. The 69 samples collected from the Kyparissia-4 section, extending stratigraphically above the site KYP4, yielded dominant normal magnetic polarity attributed to the Brunhes Chron interrupted by a thin ~1.2 m-thick interval of reverse magnetic polarity (ChRM component directions oriented to the south with negative [upward] inclinations) attributed to a short reversal of Earth's magnetic field occurring during the Brunhes Chron (e.g., Big Lost at 0.54 Ma), which, however, needs further investigation in light also of the lithological complexity of the section consisting of reworked silty clays and mud flows characterized by marked chromatic variations ranging from red-brownish to light blue. The thermal demagnetization of a three-component IRM performed on 8 selected samples from Kyparissia-4 shows that the magnetic mineralogy reflects these color changes whereby the IRM is carried mainly by magnetite in the light blue intervals and by hematite in the red-brown intervals. On the other hand, 2 additional samples revealed that for greyish clay of Choremi 6 the remanence is carried by sulphides.

Thermal demagnetization analysis on the 34 samples from the Choremi-6 section showed a clear change of magnetic polarity from reverse at the base to normal toward the top, indicating the presence in this section of the Brunhes-Matuyama boundary (0.773 Ma). Future analyses will focus on correlations at the basin scale using this valuable magnetochronological boundary that was previously identified in the Choremi mine area of the Megalopolis Basin by Tourloukis et al. (2018).

Future activity will involve performing detailed rock-magnetic experiments on selected samples from both Kyparissia-4 and Choremi-6, including thermomagnetic and hysteresis experiments, backfield acquisition curves of isothermal remanent magnetization (IRM), and first order reversal curves (FORC) using a Microsense EZ7 vibrating sample magnetometer. Our aim is to investigate potential links between sediment color and environmental factors, like paleoclimate variations (e.g., periods of warmer climate promoting weathering and oxidation to give red-brownish color, and periods characterized by more reducing conditions, to give the light blue color). Hysteresis loops of magnetization will be used to determine values of coercivity [Hc], saturation magnetization [Ms], and saturation remanence [Mr] after correcting for paramagnetic components, while the parameter coercivity of remanence [Hr] will be obtained from IRM backfield acquisition curves performed on the same samples. The Hc/Hr and Ms/Mr ratios will be plotted on Day diagrams (after Day et al., 1977 and subsequent modifications), allowing the identification of the domain state of the ferromagnetic grains in the sediments, as well as providing a generic indication of their size.

ACKNOWLEDGMENTS

This research was conducted under a permit granted to the Ephorate of Palaeoanthropology-Speleology, Hellenic Ministry of Culture, and the American School of Classical Studies at Athens. It was supported by the ERC Consolidator Grant ERC-CoG-724703 ("CROSSROADS") awarded to K.H. K.H. is also supported by the ERC Advanced Grant ERC-AdG-101019659 ("FIRST-

STEPS"). We thank the reviewers M. Maron and Z. Jacobs for their comments that helped improve this manuscript.

REFERENCES

Channell, J.E.T., Singer, B.S., Jicha, B.R., 2020. Timing of Quaternary geomagnetic reversals and excursions in volcanic and sedimentary archives. Quaternary Science Reviews, 228, pp. 106–114.

Day, R., Fuller, M. and Schmidt, V.A., 1977. Hysteresis properties of titanomagnetites: grain-size and compositional dependence. Physics of Earth Planetary Interiors 13 (4), pp. 260–267.

Kirshvink, J.L., 1980. The least-squares line and plane and the analysis of palaeomagnetic data. Geophysical Journal International, 62, pp. 699–718.

Lowrie, W., 1990. Identification of ferromagnetic minerals in a rock by coercivity and unblocking temperature properties. Geophysical Research Letters, 17(2), pp. 159–162.

Tourloukis, V., Muttoni, G., Karkanas, P., Monesi, E., Scardia, G., Panagopoulou, E. and Harvati, K., 2018. Magnetostratigraphic and chronostratigraphic constraints on the Marathousa1 Lower Palaeolithic site and the Middle Pleistocene deposits of the Megalopolis Basin, Greece. Quaternary International, 497, pp. 154–169.

22 PRELIMINARY RESULTS ON THE TAXONOMY AND PALEOENVIRONMENTAL ANALYSIS OF THE MOLLUSC FAUNA FROM MARATHOUSA 1, MARATHOUSA 2 AND KYPARISSIA 4 (MIDDLE PLEISTOCENE, MEGALOPOLIS BASIN, GREECE)

Georgia Boni[1*], George Syrides[1], George E. Konidaris[2], Athanassios Athanassiou[3], Vangelis Tourloukis[2,4], Olga Koukousioura[1], Eleni Panagopoulou[3], Panagiotis Karkanas[5], Katerina Harvati[2,6]

[1]*Laboratory of Geology and Palaeontology, School of Geology, Aristotle University of Thessaloniki, Thessaloniki, Greece*
[2]*Paleoanthropology, Institute for Archaeological Sciences and Senckenberg Centre for Human Evolution and Palaeoenvironment, Department of Geosciences, Eberhard Karls University of Tübingen, Tübingen, Germany*
[3]*Hellenic Ministry of Culture, Ephorate of Palaeoanthropology–Speleology, Athens, Greece*
[4]*Department of History and Archaeology, School of Philosophy, University of Ioannina, Ioannina, Greece*
[5]*M.H. Wiener Laboratory for Archaeological Science, American School of Classical Studies at Athens, Athens, Greece*
[6]*DFG Centre for Advanced Studies 'Words, Bones, Genes, Tools', Eberhard Karls University of Tübingen, Tübingen, Germany*
**georgiabonigb@gmail.com*

http://dx.doi.org/10.15496/publikation-97637

Keywords: Megalopolis; moluscs; paleoenvironment; Pleistocene

22.1 INTRODUCTION

The basin of Megalopolis, located in Arcadia (Peloponnesus, Greece), was formed during the Pliocene, and subsequently during the Pleistocene it was filled with fluvio-lacustrine sediments (van Vugt et al., 2000). Of particular importance is the Marathousa Member (Mb) of the Choremi Formation, which consists of sands, silts and clays mainly of lacustrine origin, alternating with the economically important lignite seams (Vinken, 1965). These alternations correspond to climatic fluctuations from warm and humid periods (lignites), to colder and drier ones (clastic sediments) (Okuda et al., 2002).

The basin has a long history of paleontological research, with the first systematic paleontological excavations conducted at the beginning of the 20th century. Since then, and especially during the last decades, extensive paleontological, paleoenvironmental, geological and chronological research has been conducted in the basin enriching our knowledge of the Pleistocene ecosystems of the basin and the wider region. Recently, targeted and systematic field investigations (2012–ongoing) in the basin have resulted in the discovery of several new sites and findspots, as well as in the re-investigation of previously discovered localities. Among them, Marathousa 1 (MAR-1), discovered in 2013, stands out for its wealth in paleontological and archaeological finds from well-stratified and secure paleoenvironmental contexts, and testifies homi-

G. Syrides: https://orcid.org/0000-0002-4738-5134
G. E. Konidaris: https://orcid.org/0000-0002-7041-233X
A. Athanassiou: https://orcid.org/0000-0002-9140-7011
V. Tourloukis: https://orcid.org/0000-0002-9527-2708
O. Koukousioura: https://orcid.org/0000-0001-8127-3331
E. Panagopoulou: https://orcid.org/0000-0002-4268-6157
P. Karkanas: https://orcid.org/0000-0002-7156-671X
K. Harvati: https://orcid.org/0000-0001-5998-4794

nin presence and butchering activities at the shores of the Middle Pleistocene lake during the Marine Isotope Stage 12, at ~450 ka (Panagopoulou et al., 2015; Harvati et al., 2018 and articles therein). In 2018, the nearby and almost contemporaneous site of Marathousa 2 (MAR-2) was discovered yielding fossil mammal remains, some of which preserve traces of hominin exploitation (Konidaris et al., 2019). Finally, field survey in the Kyparissia mine, including the re-investigation of the Kyparissia 4 (KYP-4) site, discovered in 2007 (Athanassiou, 2018; Athanassiou et al., 2018), enriched the vertebrate collection further and provided the opportunity for detailed paleoenvironmental reconstruction for the early part of the Middle Pleistocene (Athanassiou et al., this volume; Karkanas et al., this volume; Konidaris et al., this volume; Papadopoulou et al., this volume; van Kolfschoten et al., this volume).

Among the first faunal lists of moluscs from the Megalopolis Basin are those of Vinken (1965) and Hiltermann and Lüttig (1969); however, the first detailed study on moluscs was conducted by Schütt et al. (1985). Recently, preliminary analysis of the molusc fauna from MAR-1 was performed and provided the first taxonomic and paleoenvironmental results (Boni, 2019), while the systematic sampling carried out in 2019 and 2020 at MAR-1, MAR-2 and KYP-4 has substantially expanded the available molusc material (Boni, 2022). The present study presents the preliminary results of the taxonomy and paleoenvironmental analysis of these assemblages aiming to contribute to the reconstructions of the paleoenvironmental conditions in the Megalopolis Basin during the Middle Pleistocene. Additional molluscan material hand-collected during the excavations of 2013–2019 at MAR-1, as well as sediment samples collected from additional stratigraphic units (other than those presented herein) of the three sites, require further investigation and will be collectively analyzed in the future.

22.2 MATERIALS AND METHODS

The herein studied material includes 15 sediment samples, weighing approximately 3 kg each, and originating from three sites: MAR-1 (Areas A and B), MAR-2 (Areas A and B) and KYP-4. In MAR-1 the material comes from the stratigraphic layers UA2b, UA3a and UA3c from Area A, and layers UB2b UB3a/b, UB3c, UB4a/b, UB4c and UB5 from Area B (layers according to Karkanas et al., 2018).

Three samples were collected from MAR-2: sample 1 (Area A, layer with *Hippopotamus* fossils) and sample 2 (Area B, layer with *Hippopotamus* fossils), both corresponding to the same depositional event, and sample 3 (Area B, molusc shell-rich layer), located ~2 m bellow sample 2. From KYP-4, three samples are examined: UA2, UA5 and UA6. The analysis of the sediment samples from UA4, and UA7–UA9 is in progress.

The samples were air-dried, soaked in containers filled with ~10 L of water and ~50 mL of H_2O_2 (70%) and wet-sieved over a 0.5 mm mesh sieve. Very argillaceous and rich in organic material samples, needed re-sieving, which was not possible during the COVID-19 pandemic. However, those samples were dry-sieved in mesh sieves of 5 mm, 3.16 mm and 1.60 mm, and each fraction was examined separately; the larger fractions were handpicked with the aid of magnifying glasses and forceps, and the fine fractions were examined under a JENNA stereoscopic microscope with ×0.63, ×1.00, ×1.6, ×2.5 magnification and ×10 ocular lenses.

All recognizable molusc shells were collected and identified to the lowest possible taxonomic level, based on available literature. Afterwards, the shells per taxon were counted, and their relative frequencies were calculated. For shell numbers exceeding 100–200, their number was approximately estimated. The most representative and well-preserved larger shells were photographed using a

SONY 8-Mpixel Digital Still Camera, while the smaller shells were photographed under a ZEISS Stemi 305 trinocular stereoscopic microscope equipped with a MOTICAM S6 camera.

22.3 RESULTS

22.3.1. FAUNA

The total number of taxa identified in all studied sites is at least 28. This number is possibly larger as the bivalves of the family Sphaeriidae were not identified at species level (Fig. 1).

Class Gastropoda Cuvier, 1795

- *Bithynia candiota* Westerlund
- *Valvata cristata* Müller
- *Valvata* (*Cincinna*) *studeri* Boeters & Falkner
- *Galba truncatula* (Müller)
- *Stagnicola palustris* (Müller)
- *Lymnaea stagnalis* (Linnaeus)
- *Planorbis planorbis* (Linnaeus)
- *Anisus leucostoma* (Millet)
- *Anisus spirorbis* (Linnaeus)
- *Anisus vortex* (Linnaeus)
- *Anisus* sp.
- *Gyraulus albus* (Müller)
- *Gyraulus crista* (Linnaeus)
- *Gyraulus* cf. *acronicus* (Férrusac)
- *Segmentina nitida* (Müller)
- *Planorbarius corneus* (Linnaeus)
- *Ancylus* sp.
- *Bathyomphalus contortus* (Linnaeus)
- Planorbidae sp. 1
- Planorbidae sp. 2
- *Acroloxus lacustris* (Linnaeus)
- *Oxyloma elegans* (Risso)
- *Vertigo pygmaea* (Draparnaud)
- *Carychium tridentatum* (Risso)

Class Bivalvia Linnaeus, 1758

- *Unio* cf. *pictorum* (Linnaeus)
- *Sphaerium* aff. *corneum* (Linnaeus)
- *Pisidium amnicum* (Müller)
- *Euglesa* aff. *casertanum* (Poli)

22.3.2. MARATHOUSA-1

Area A: In UA2b the number of shells reached ~2,950 and that of gastropod operculii over ~3000. Sample UA3c was also relatively rich, with 1,200 shells, but with only 144 operculii. In contrast, UA3a is a rather shell-poor sample, with only 80 shells, but with 200 operculii.

The most abundant species are *Valvata cristata*, *Valvata studeri* and *Bithynia candiota*, which represent more than 80% of the total molluscan assemblage in each of the three samples. *Valvata cristata* is the most abundant reaching 53.1% in UA3c, 93.75% in UA3a, and 30.2% in UA2b; *Bithynia candiota* comprises 22.9% of the total shells in UA3c, 5% in UA3a, and 23.8% in UA2b, while *Valvata studeri* reaches 11.6% in UA3c, 1.25% in UA3a, and 28.8% in UA2b. In UA2b, large Unionidae fragments were also found.

Area B: The richest layer among the studied ones was UB2b (in stratigraphic correlation with UA2b) with more than 8,580 shells and ~1,300 operculii. Other shell-rich layers are UB3c, which preserves ~1,300 shells and ~500 operculii, and UB4c, being slightly less rich, with 870 shells and 65 operculii. UB3a/b and UB4a/b are somewhat poorer; UB3a/b comprises 260 shells and 200 operculii, and UB4a/b 416 shells and 400 operculii. The poorest layer of the site is UB5 with only 13 shells and 7 operculii.

The most abundant species in Area B are the same as in Area A: *Valvata studeri*, *Valvata cristata* and *Bithynia candiota*. *Valvata cristata* is the most common in UB2b, UB3a/b, UB3c, UB4a/b, and UB4c, and comprises 42–70% of the shells, while *V. studeri* presents lower values (21% in UB2b,

10.8% in UB3a/b, 11.6% in UB3c, 6.7% in UB4a/b, and 6.0% in UB4c).

In UB2b, 320 Sphaeriidae shells were found, with their total percentage reaching 3.7%, while in UB3a/b, UB3c, and UB4a/b, although the number of shells is lower, their percentage is more significant, (7.7%, 7.7%, and 6.7%, respectively).

22.3.3. MARATHOUSA-2

Area A: Sample 1 contained ~150 shells and ~100 operculii. The dominant species are *Valvata cristata* with 63 shells (44.1%), followed by *Valvata studeri* and *Bithynia candiota* with 37 (25.9%) and 32 (22.4%) shells, respectively. Besides the above,

Figure 1: Taxa of the studied samples. A: *Valvata cristata,* B: *Bithynia candiota*, C: *Valvata studeri*, D: *Planorbis plaborbis*, E: *Gyraulus albus*, F: *Planorbarius corneus*, G: *Gyraulus crista*, H: *Anisus spirorbis*, I: *Anisus leukostoma*, J: *Anisus vortex*, K: *Bathyomphalus contortus* , L: *Segmentina nitida*, M: Planorbidae sp., N: *Lymnaea stagnalis*, O: *Galba truncatula*, P: *Carychium tridentatum*, Q: *Vertigo pygmaea*, R: *Oxyloma elegans*, S: Unionidae sp., T: *Acroloxus lacustris*, U–X: Sphaeriidae spp. All the scale bars represent 1 mm, except those in E and S which represent 1 cm.

only a few Sphaeriidae valves, 5 lymnaeids and some gastropod fragments were collected.

Area B: Sample 2 contained less shells than sample 1, even though they represent the same depositional event, with only 10 *V. cristata*, 2 *B. candiota* and 30 operculii.

On the contrary, sample 3 is the most shell-rich and diversified, with ~2,550 shells and ~2,000 operculii, and 15 taxa included. The majority of the shells belong to *V. cristata*, which reaches 60.9 %, *B. candiota* and *V. studeri*, with 20.0% and 12.7%, respectively. 5 *Unio* cf. *pictorum* valves were collected, as well as some large Unionidae fragments, and 10 Lymnaeidae shells.

22.3.4. KYPARISSIA-4

The lowest studied layer, UA6 is the richest of those examined with ~6,070 shells and ~6,000 gastropod operculii. In UA5, ~760 shells and ~900 operculii were collected, and in UA2 only 2 shells and 5 operculii. In UA2, only 1 species was found (*Valvata cristata*), though the operculii indicate at least 1 more gastropod species. UA5 contains at least 12 taxa and UA6 at least 17.

In UA5, *V. studeri* is the most abundant species (39.0%), while the presence of *V. cristata* is also significant (28.8%), and *B. candiota* comprises 21.8% of the total shells. *Galba truncatula* is represented with higher values, reaching 24 shells, in addition to 28 Lymnaeidae broken shells, belonging to *G. truncatula*, *Lymnaea stagnalis* and *Stagnicola palustris*.

In UA6, *V. cristata comprises* 44.8% of the shells and *B. candiota* 26.4%, while only 79 shells of *V. studeri* were found (only 1.3%). *G. truncatula* is common in this layer, as 400 shells were found (6.6% of shells).

22.4 DISCUSSION

Approximately 25,200 molusc specimens were collected, though the true number of shells is expected to be larger. The identified taxa are at least 28, indicating quite diverse molusc faunas. However, mainly three species predominate the samples: *Valvata cristata*, *Valvata studeri* and *Bithynia candiota*, which account for ~70% or more in most studied layers, indicating that their optimal conditions, of rich vegetation and well-oxygenated waters (see Schütt et al., 1985; Okland, 1990), prevailed during the time of their occurrence. The diversity of the faunas and the abundance of the three dominant species is supported by the observations of Schütt et al. (1985), who also reported *Valvata cristata* as one of the most common taxa in shallow areas in Choremi. Similarly, *B. candiota* and *V. studeri* were very commonly found by Schütt et al. (1985).

The molusc assemblages are similar across the three sites, without many significant variations except shell richness and species diversity. The majority of the taxa are aquatic, while those characteristic of terrestrial habitats are few and statistically unimportant in most layers, with a small differentiation in KYP-4; in this site there is a slight increase of terrestrial species (*Oxyloma elegans, Vertigo pygmaea, Carychium tridentatum*; Fig. 1) and of *Galba truncatula*, which is characterized as semiterrestrial (Sparks, 1961; Welter-Schultes, 2012). Another important point is that unionids, which indicate the presence of a river or a stream in the area and which are documented at MAR-1 and MAR-2, are absent from KYP-4.

22.5 CONCLUSIONS

The Middle Pleistocene molusc fauna of the Megalopolis Basin presents an important taxonomic diversity, comprised predominantly by aquatic

species. The aquatic taxa indicate habitats with well-oxygenated waters and rich in aquatic plants, while the main components of the fauna are for the most part similar in MAR-1, MAR-2 and KYP-4. Despite the similarities, a slight difference is observed at KYP-4, which shows a somewhat increased presence of terrestrial/semi-terrestrial species. Aiming to obtain more comprehensive paleoenvironmental interpretations, future directions of the analysis will focus 1) on the detailed comparisons both within the sedimentary units of each site's sequence and among the sites, and 2) on the incorporation of the existing or in progress results from sedimentological analyses and other paleoenvironmental proxies (e.g., Karkanas et al., 2018; Bludau et al., 2021; Butiseacă et al., this volume; Papadopoulou et al., this volume). Finally, the inclusion of additional material from other sites/stratigraphic horizons of the basin will improve the resolution and expand the chronological range.

ACKNOWLEDGMENTS

Excavation at Marathousa 1 was conducted by a team from the Ephorate of Palaeoanthropology-Speleology and the University of Tübingen. Research in Marathousa 2 and Kyparissia 4 were conducted under a permit granted to the Ephorate of Palaeoanthropology-Speleology, Hellenic Ministry of Culture, and the American School of Classical Studies at Athens. The projects were supported by the ERC Consolidator Grant ERC-CoG-724703 ("CROSSROADS") and the ERC Starting Grant ERC-StG-283503 ("PaGE"), both awarded to K.H. G.E.K., V.T. and K.H. are also supported by the Deutsche Forschungsgemeinschaft (DFG Project no. 463225251, "MEGALOPOLIS"). K.H. is also supported by the ERC Advanced Grant ERC-AdG-101019659 ("FIRSTSTEPS"). The microscopic samples were photographed with the help of V. Dimou. We would like to thank the reviewers G. Iliopoulos and I. Sylvestrou for their valuable comments and suggestions.

REFERENCES

Athanassiou, A., 2018. Pleistocene vertebrates from the Kyparíssia lignite mine, Megalopolis Basin, S. Greece: Rodentia, Carnivora, Proboscidea, Perissodactyla, Ruminantia. Quaternary International, 497, pp. 198–221.

Athanassiou, A., Michailidis, D., Vlachos, E., Tourloukis, V., Thompson, N. and Harvati, K., 2018. Pleistocene vertebrates from the Kyparíssia lignite mine, Megalopolis Basin, S. Greece: Testudines, Aves, Suiformes. Quaternary International, 497, pp. 178–197.

Athanassiou, A., Konidaris G.E., Tourloukis, V., Thompson, N., Giusti, D., Panagopoulou, E., Karkanas P. and Harvati, K., this volume. The Middle Pleistocene large mammal fauna from Kyparissia (Peloponnese, S. Greece): New collected material.

Bludau, I.J.E., Papadopoulou, P., Iliopoulos, G., Weiss, M., Schnabel, E., Thompson, N., Tourloukis, V., Zachow, C., Kyrikou, S., Konidaris, G.E., Karkanas, P., Panagopoulou, E., Harvati, K. and Junginger, A., 2021. Lake-level changes and their paleo-climatic implications at the MIS12 Lower Paleolithic (Middle Pleistocene) site Marathousa 1, Greece. Frontiers of Earth Science, 9, pp. 1–26.

Boni, G., 2019. Fossil molluscs from Megalopolis Basin, Peloponnesus, Greece. Bachelor thesis, Aristotle University of Thessaloniki, Thessaloniki.

Boni, G., 2022. Paleoenvironmental reconstruction based on molusc macrofaunal analysis: A case study from the Middle Pleistocene of Megalopolis Basin (Peloponnesus, Greece). Master thesis, Interinstitutional Program of Postgraduate Studies in Palaeontology-Geo-

biology, Aristotle University of Thessaloniki, Thessaloniki.

Butiseacă, G.A. Vasiliev, I., Tourloukis, V., Junginger, A., Mulch, A., Karkanas, P., Panagopoulou, E. and Harvati, K., this volume. Preliminary biomarker/paleoclimate reconstruction results from the Marathousa 1 Lower Paleolithic site (Megalopolis Basin, Greece).

Harvati, K., Konidaris, G. and Tourloukis, E. (Eds.), 2018. Human Evolution at the Gates of Europe. Quaternary International, 497, pp. 1–240.

Hiltermann, H., Lüttig, G., 1969. Biofazies und Paläolimnologie der pliozänen und pleistozänen Seen im Megalopolis-Becken (Peloponnes). Mitteilungen der Internationalen Vereinigung für theoretische und angewandte Limnologie, 17, pp. 306–314.

Karkanas, P., Tourloukis, V., Thompson, N., Giusti, D., Panagopoulou, E. and Harvati, K., 2018. Sedimentology and micromorphology of the Lower Palaeolithic lakeshore site Marathousa 1, Megalopolis Basin, Greece. Quaternary International, 497, pp. 123–136.

Karkanas, P., Tourloukis, V., Thompson, N., Giusti, D., Tsartsidou, G., Athanassiou, A., Konidaris, G., Roditi, E., Panagopoulou, E. and Harvati, K., this volume. The Megalopolis Paleoenvironmental Project (MegaPal).

Konidaris, G.E., Tourloukis, V., Athanassiou, A., Giusti, D., Thompson, N., Panagopoulou, E., Karkanas, P. and Harvati, K., 2019. Marathousa 2: A new Middle Pleistocene locality in Megalopolis Basin (Greece) with evidence of human modifications on faunal remains, 9th Annual Meeting of the European Society for the study of Human Evolution, Liège, 82.

Konidaris, G.E., Athanassiou, A., Panagopoulou, E., Karkanas, P. and Harvati, K., this volume. Fossil macaques (Cercopithecidae, Primates) from the Middle Pleistocene of the Megalopolis Basin (Greece) with description of a new specimen from Kyparissia 4.

Okland, J., 1990. Lakes and snails. Environment and Gastropoda in 1500 Norwegian lakes, ponds and rivers. Universal Book Services / Dr W. Backhuys, Oegstgeest.

Okuda, M., van Vugt, N., Nakagawa, T., Ikeya, M., Hayashida, A., Yasuda, Y. and Setoguchi, T., 2002. Palynological evidence for the astronomical origin of lignite-detritus sequence in the Middle Pleistocene Marathousa Member, Megalopolis, SW Greece. Earth and Planetary Science Letters, 201, pp. 143–157.

Panagopoulou, E., Tourloukis, E., Thompson, N., Athanassiou, A., Tsartsidou, G., Konidaris, G., Giusti, D., Karkanas, P. and Harvati, K., 2015. Marathousa 1: a new Middle Pleistocene archaeological site from Greece. Antiquity Project Gallery, 89.

Papadopoulou, P., Tsoni, M., Konidaris, G.E., Tourloukis, V., Panagopoulou, E., Karkanas, P., Harvati, K. and Iliopoulos, G., this volume. Ostracod contribution to the palaeoenvironmental study of Kyparissia 4 (Megalopolis Basin, Greece).

Schütt, H., Velitzelos, E. and Kaouras, G., 1985. Die Quartärmollusken von Megalopolis (Griechenland). Neues Jahrbuch für Geologie und Paläontologie – Abhandlungen, 170, pp. 183–204.

Sparks, B.W., 1961. The ecological interpretation of Quarternary non-marine Mollusca. Proceedings of the Linnean Society of London, 172, pp. 71–80.

van Kolfschoten, T., Konidaris, G.E., Doukas, C., Athanassiou, A., Tourloukis, V., Panagopoulou, E., Karkanas, P. and Harvati, K., this volume. Voles (Rodentia, Mammalia) as a proxy to date the site Kyparissia 4 (Megalopolis Basin, Greece).

van Vugt, N., de Bruijn, H., van Kolfschoten, T. and Langereis, C.G., 2000. Magneto- and cyclostratigraphy and vertebrate faunas of the Pleistocene lacustrine Megalopolis Basin,

Peleponnesos, Greece. Geologica Ultrajectina, 189, pp. 69–92.

VINKEN, R., 1965. Stratigraphie und Tektonik des Beckens von Megalopolis (Peloponnes, Griechenland). Geologisches Jahrbuch, 83, pp. 97–148.

WELTER-SCHULTES, F.W., 2012. European non-marine molluscs, a guide for species identification. Planet Poster Editions, Göttingen.

23 OSTRACOD CONTRIBUTION TO THE PALAEOENVIRONMENTAL STUDY OF KYPARISSIA 4 (MEGALOPOLIS BASIN, GREECE)

Penelope Papadopoulou[1,*], Maria Tsoni[1], George E. Konidaris[2], Vangelis Tourloukis[2,3], Eleni Panagopoulou[4], Panagiotis Karkanas[5], Katerina Harvati[2], George Iliopoulos[1]

[1]*Laboratory of Palaeontology and Stratigraphy, Department of Geology, University of Patras, Rio Patras, Greece*
[2]*Paleoanthropology, Institute for Archaeological Sciences and Senckenberg Centre for Human Evolution and Palaeoenvironment, Department of Geosciences, Eberhard Karls University of Tübingen, Tübingen, Germany*
[3]*Department of History and Archaeology, School of Philosophy, University of Ioannina, Ioannina, Greece*
[4]*Hellenic Ministry of Culture, Ephorate of Palaeoanthropology–Speleology, Athens, Greece*
[5]*M.H. Wiener Laboratory for Archaeological Science, American School of Classical Studies at Athens, Athens, Greece*
**penelpapadop@upatras.gr*

http://dx.doi.org/10.15496/publikation-97593

Keywords: ostracods; Kyparissia 4; Marathousa 1; Pleistocene; Greece

23.1 INTRODUCTION

The Megalopolis Basin, situated on the central part of Peloponnese in southern Greece, is an intramontane half-graben basin, which was formed during the Pliocene and is nowadays one of the largest coal mining districts in Greece. During the Pleistocene, lacustrine and fluvial sediments were deposited, including the lignite-bearing Marathousa Member of the Choremi Formation (Vinken, 1965). The sedimentary sequence of the Marathousa member has a total thickness of ~150 m at the center of the basin, and includes alternations between clastic sediments (clay, silt and sand) and 5–30 m thick dark brown lignite seams, intercalated with thin clastic layers (van Vugt et al., 2000 and references therein).

Previous paleoenvironmental research based on ostracods focused on the Middle Pleistocene (Lower Palaeolithic) site of Marathousa 1 (MAR-1; Fig. 1a), located between the Lignites II and III of the Marathousa Member, and dated to 500–400 ka (see Harvati et al., 2018, Panagopoulou et al., 2018 and references therein; Bludau et al., 2021). In this study, we present new paleoenvironmental evidence from lower stratigraphic horizons of the Marathousa Member, based on the ostracod record from the site Kyparissia 4 (KYP-4). KYP-4, located in the Kyparissia mine (Fig. 1a), was discovered in 2007 and has yielded a rich assemblage of large mammals, including hippopotamuses, elephants and deer (Athanassiou, 2018; Athanassiou et al., 2018). The site was recently revisited during a targeted field survey in the framework of the Megalopolis Paleoenvironmental Project (MegaPal). Besides the collection of additional large mammal

P. Papadopoulou: https://orcid.org/0000-0001-8442-4115
M. Tsoni: https://orcid.org/0000-0002-1719-7634
G. E. Konidaris: https://orcid.org/0000-0002-7041-233X
V. Tourloukis: https://orcid.org/0000-0002-9527-2708
E. Panagopoulou: https://orcid.org/0000-0002-4268-6157
P. Karkanas: https://orcid.org/0000-0002-7156-671X
K. Harvati: https://orcid.org/0000-0001-5998-4794
G.Iliopoulos: https://orcid.org/0000-0002-4875-128X

fossils (Athanassiou et al., this volume; Konidaris et al., this volume), sampling for molluscs (Boni et al., this volume), micromammals (van Kolfschoten et al., this volume) and ostracods (present study) also took place. Preliminary stratigraphic and biochronological data indicate that KYP-4 is older than MAR-1, and is dated close to the lower part of the Middle Pleistocene (Athanassiou, 2018; this volume; Karkanas et al., this volume; van Kolfschoten et al., this volume). The KYP-4 sedimentary sequence has a thickness of ~4.50 m and is divided into several distinct stratigraphic units, comprised by alterations of dark grey organic rich mud layers with an intercalation of a relatively thin lignite layer (Fig. 1b).

Ostracods are one of the most frequent microfossils found in archaeological and paleontological excavations, due to their existence in a wide variety of paleoenvironments (Mazzini et al., 2015). Especially in freshwater settings, where other microfossil groups such as foraminifera, are lacking, ostracods can provide extremely detailed information about the paleoenvironment and the paleoclimate. For this reason, ostracods in the last 20 years have become a fundamental addition to multidisciplinary archaeological and paleoanthropological research (Mazzini et al., 2015). In the present study, ostracod analysis is conducted in samples deriving from different layers of KYP-4 (Fig. 1b), aiming at the paleoenvironmental reconstruction of the studied section.

23.2 MATERIALS AND METHODS

Seven sediment samples were analyzed for ostracods originating from KYP-4 Area A (the main find-bearing area; Fig. 1). 1000 g of dry sediment was treated with 10% H2O2 until reaction stopped (3 to 24 hours, depending on the sample). The residues were washed through a 2 mm and 125 μm sieve using distilled water and further dried overnight at 50°C. All ostracod valves were extracted under OPTIKA stereoscopes. Ostracods were photographed digitally with OPTICAM BS 5 Mpx stereoscope camera. Identification, ecology and distribution information of ostracod species were derived mainly from Meisch (2000), Fuhr-

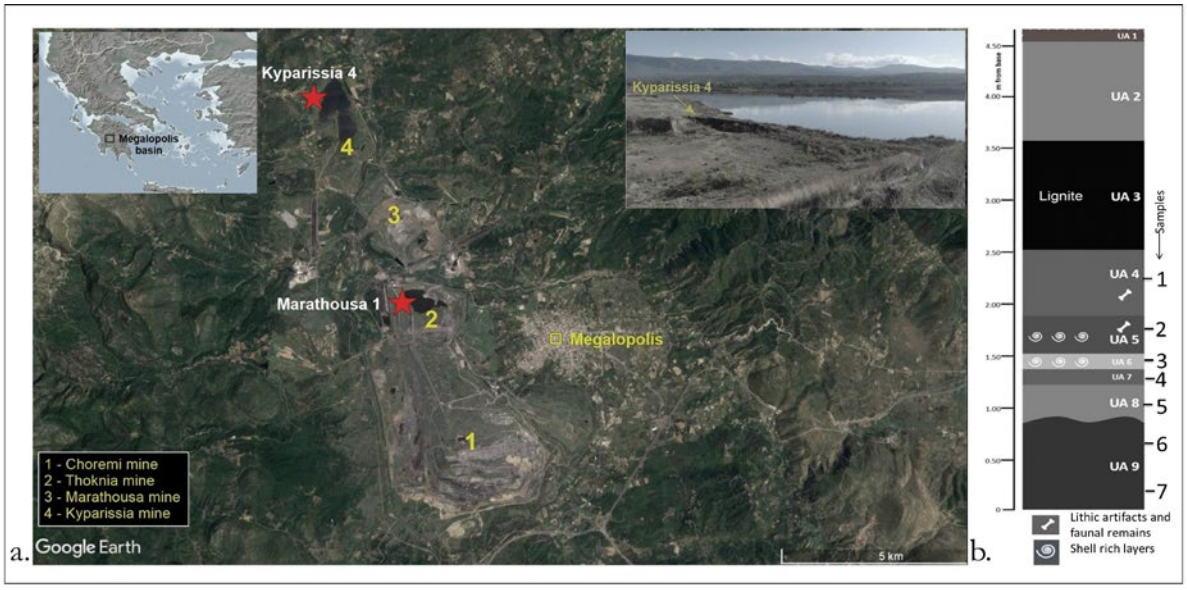

Figure 1: a, Upper left corner: geographic position of the Megalopolis Basin; center: geographic position of Kyparissia 4 and Marathousa 1 in relation to the main lignite mines of the Megalopolis Basin (satellite image from Google Earth); upper right corner: distant view of Kyparissia 4. b, simplified stratigraphic column of KYP-4 (Area A) showing the stratigraphic units and the position of the samples taken for the ostracod analysis.

mann (2012), several papers on the Stereo Atlas of Ostracod Shells (Athersuch, 1976), and other available published literature. Taphonomic indices were calculated (wherever possible) and interpreted after Schellenberg (2007) with: a) The adult to juvenile ratio (A/J) as an indirect indication for the energy of the environment. Values between 0.125–0.25 are typical for in situ death assemblages. Higher values reflect in situ death assemblages with taphonomic removal of juveniles. Significantly lower values could reflect transported juvenile valves or a mass death event (Belis et al., 1997; Schellenberg, 2007). b) The right valve/left valve ratio (RV/LV) for merely the same reason (Breman, 1980). Values significantly different from one (1) imply transportation of juvenile valves.

23.3 RESULTS AND DISCUSSION

Six out of the seven sediment samples (samples 2–7; stratigraphic units UA5–UA9) were barren of ostracods and/or contained either complete or broken molluscs, while in sample 4 (UA7), terrestrial microvertebrate bone fragments were found (Table 1). Nonetheless, a relatively rich ostracod taphocoenosis was extracted from sample 1 (UA4; 63 ostracod valves). UA4 is a crudely laminated

	Cyclocypris cf. *ovum*						*Potamocypris zschokkei*						*Fabaeformiscandona breuili*								*Candona* spp. (juveniles)						
Samples	Juveniles-Immature			Adults			Juveniles-Immature			Adults			Juveniles-Immature			Adults			A/J	RV/LV	Juveniles-Immature			%Art	RV/LV	Bone fragments (Arvicolidae)	Fragments (molluscs+ostracodes)
	LV	RV	C	LV	RV	C	LV	RV	C	LV	RV	C	LV	RV	C	LV	RV	C			LV	RV	C				
8																											
7																											
6																											
5																											
4																										*	
3																											
2																											
1		1						2			1		1			4	6		10	1,50	30	17	1		0,57		*

LV=Left valve, RV=Right valve, C=Carapace

A/J=Adult/Juvenile

C/V=Carapace/Valve

RV/LV=Right valve/Left valve

Table 1: Ostracod analysis results and taphonomy.

dark organic-rich mud with few sand clasts deposited in a low energy depositional environment. Ostracods thrive in hydrological regimes with low and moderate flow discharge but cannot withstand higher rates (Roca and Baltanas, 1993). Thus, the lack of ostracods in the other six samples could be connected to higher flow discharge.

In sample 1 (UA4), three ostracod taxa were identified down to the species level, while valves of juvenile stages were also picked (Fig. 2). Most of the identified ostracod valves (76%) belong to juvenile stages of Candoninae. However, the RV/LV ratio bears a value of 0.57, which indicates that some of them or all of them were transported from nearby freshwater environments.

Valves of the species *Fabaeformiscandona breuili* (Paris, 1920) account for 17% of the ostracod assemblage. It is a widespread species throughout central and southern Europe, present from Pleistocene to recent. It is a predominantly stygobiotic species, but it can also survive in surface environments always connected to underground waters (springs, waters flowing from springs, caves, etc.) (Meisch, 2000). As a fossil, it has been found mostly in interglacial conditions and/or in transitional conditions between the glacials-interglacials of central Germany (Fuhrmann, 2012). Only adult valves of this species were found (A/J ratio = 10), an indication of an *in situ* death assemblage with high taphonomic removal of juveniles. Relatively high transportation rates are also implied from the RV/LV ratio for the same species (RV/LV = 1.5).

Potamocypris zschokkei (Kaufmann, 1900) (5%) and *Cyclocypris* cf. *ovum* (2%) complete the taphocoenosis. *Potamocypris zschokkei* is widespread throughout Europe since the Pleistocene and it has been reported from interglacial and late glacial deposits (Fuhrmann, 2012). It is mostly found in muddy streams flowing from springs and, to a lesser extent, in stagnant waters of spring ponds (Meisch, 2000). *Cyclocypris ovum* (Jurine, 1820) prefers cool permanent water bodies, but it can survive in a wide variety of aquatic environments. Nevertheless, it seems to be reduced in high summer water temperatures and high precipitation rates (Fuhrmann, 2012). The number of valves of both species was not enough for the calculation of taphonomic indices. Actually, the *C.* cf. *ovum* valve corresponds to a juvenile individual and for this reason its identification to the species level is not ascertained. However, regarding their preservation condition (fragmentation, color, etc.), the valves of *Potamocypris zschokkei* and *Cyclocypris* cf. *ovum* do not show signs of significant transportation and were probably deposited *in situ*. It is worth noting

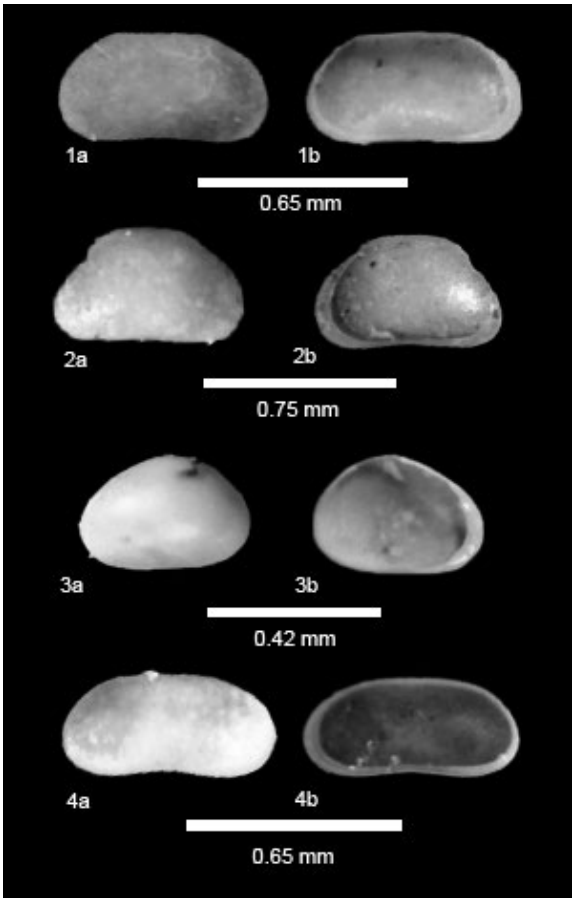

Figure 2: Digital photos of the identified ostracod taxa. 1. *Fabaeformiscandona breuili* a) left valve, external, b) left valve, internal; 2. *Potamocypris zschokkei* a) right valve, external, b) right valve internal; 3. *Cyclocypris* cf. *ovum* a) right valve, external, immature, b) right valve, internal, immature; 4. *Candona* a) right valve, external, juvenile b) right valve, internal, juvenile.

that nowadays *P. zschokkei* in combination with *C. ovum* are found in Pyrenean Bi-carbonate springs (connected to limestone basement) with relatively low temperatures (possibly lower than 15°C), low mineralization and wet climate (Mezquita et al., 1999). A significant number of widely distributed cold-water stenothermal species occurs in that area (a transitional area between northern/central European and Mediterranean regions), implying that those habitats acted as refugia for widely distributed species during the glacials (Mezquita et al., 1999), which could also be the case for the Middle Pleistocene Megalopolis Basin.

The number of species in the respective sample is apparently low which points towards stressed environmental conditions. Due to the identified species' ecological preferences, the connection of the depositional environment to a cool carbonate spring is indisputable. The limestone basement (belonging to the Pindos geotectonic zone) of the studied area is in good agreement with the inferred paleoecological data. The low number of individuals can be attributed to the low stability of the springs (Mezquita et al., 1999) or more likely to a less favorable depositional environment such as a stream flowing from the spring. This is further supported by the high transportation rates of Candoninae, implied by the respective taphonomic indices. The ostracod assemblages of such environments are not well studied, probably due to the high diversity of microhabitats.

The coexistence of *P. zschokkei* and *C. ovum* points towards a wet climate with no extreme summer temperatures. Because of the extremely low number of individuals, this paleoclimate estimation must be applied with caution. Moreover, both *F. breuili* and *P. zschokkei* are commonly found in interglacial and/or transitional stages of central Europe. Therefore, the climatic conditions during the deposition of the respective layer should have resembled those that prevailed in regions further north, during interglacial or/and transitional stages.

Samples with high numbers of juvenile Candoninae have also been noticed at MAR-1 (stratigraphic units UA2 and UA3 of Area A, and UB3 and UB4 of Area B; Bludau et al., 2021). At this site, *P. zschokkei* was also observed in low frequencies (samples from UB3 and UB7). However, some samples from MAR-1 (UA2, UA3, UB3, UB4) contained also several representatives of *Ilyocypris* spp. The paleoenvironment of MAR-1 was also interpreted as deposition in streams or ponds deriving from springs' water. However, in the sample UA4 of KYP-4, *Ilyocypris* spp. are totally absent. This can possibly be attributed to slightly higher water temperature and/or higher range difference between summer and winter temperatures at MAR-1 (Roca and Baltanas, 1993). It is worth mentioning that in the study of Lüttig (1968) on the ostracods of Megalopolis Basin, none of the identified species at KYP-4 have been mentioned, while *Fabaeformiscandona breuili* is not recorded either at MAR-1, thus it is reported for the first time from the Megalopolis Basin herein.

23.4 CONCLUSIONS

In this work, ostracod analysis shed light on the paleoenvironmental conditions that prevailed during the deposition of organic rich mud layers at the early Middle Pleistocene site of KYP-4. The different layers of the studied section must have been deposited under fluctuating flow discharge rates. The sample from the stratigraphic unit UA4 (the main lithic/vertebrate-bearing layer) was deposited in a slow to moderate flowing stream fed by a cool (constantly lower than 15 °C) carbonate spring. Even if the data presented herein are restricted, they are possibly indicative of a wet climate with relatively stable temperatures throughout the year.

The climatic conditions during the deposition of this layer could resemble the interglacial or transitional conditions of central Europe. More research is needed in order to confirm these climatic conditions.

ACKNOWLEDGMENTS

Field survey in the Megalopolis Basin was conducted in the framework of the Megalopolis Paleoenvironmental Project (MegaPal) under a permit granted to the Ephorate of Paleoanthropology–Speleology, Hellenic Ministry of Culture, and the American School of Classical Studies at Athens. Fieldwork was supported by the ERC Consolidator Grant ERC-CoG-724703 ("CROSSROADS") awarded to K.H. G.E.K., V.T. and K.H. are also supported by the Deutsche Forschungsgemeinschaft (DFG Project no. 463225251, "MEGALOPOLIS"). K.H. is also supported by the ERC Advanced Grant ERC-AdG-101019659 ("FIRSTSTEPS"). We thank A. Junginger and one anonymous reviewer for their constructive comments and suggestions.

REFERENCES

Athanassiou, A., 2018. Pleistocene vertebrates from the Kyparíssia lignite mine, Megalopolis Basin, S. Greece: Rodentia, Carnivora, Proboscidea, Perissodactyla, Ruminantia. Quaternary International, 497, pp. 198–221.

Athanassiou, A., Michailidis, D., Vlachos, E., Tourloukis, V., Thompson, N. and Harvati, K., 2018. Pleistocene vertebrates from the Kyparíssia lignite mine, Megalopolis Basin, S. Greece: Testudines, Aves, Suiformes. Quaternary International, 497, pp. 178–197.

Athanassiou, A., Konidaris, G.E., Tourloukis, V., Thompson, N., Giusti, D., Karkanas, P. and Harvati, K., this volume. The Middle Pleistocene large mammal fauna from Kyparissia (Peloponnese, S. Greece): New collected material.

Athersuch J., 1976. Stereo-Atlas Ostracod Shells, 3(21), pp. 117–124.

Belis, C. A., 1997. Palaeoenvironmental reconstruction of Lago di Albano (Central Italy) during the Late Pleistocene using fossil ostracod assemblages. Water, Air, and Soil Pollution, 99, pp. 593–600.

Bludau, I.J.E., Papadopoulou, P., Iliopoulos, G., Weiss, M., Schnabel, E., Thompson, N., Tourloukis, V., Zachow, C., Kyrikou, S., Konidaris, G.E., Karkanas, P., Panagopoulou, E., Harvati, K. and Junginger, A., 2021. Lake-level changes and their paleoclimatic implications at the MIS12 Lower Paleolithic (Middle Pleistocene) site Marathousa 1, Greece. Frontiers in Earth Science, 9, 668445.

Boni, G., Syrides, G., Konidaris, G.E., Athanassiou, A., Tourloukis, V., Koukousioura, O., Panagopoulou, E., Karkanas, P. and Harvati, K., this volume. Preliminary results on the taxonomy and paleoenvironmental analysis of the mollusc fauna from Marathousa 1, Marathousa 2 and Kyparissia 4 (Middle Pleistocene, Megalopolis Basin, Greece).

Breman, E., 1980, Differential distribution of left and right ostracode valves in the Adriatic Sea. Palaeogeography, Palaeoclimatology, Palaeoecology, 32, pp. 135–141.

Fuhrmann, R., 2012. Atlas quartärer und rezenter Ostrakoden Mitteldeutschlands. Naturkundliches Museum Mauritianum, Altenburg.

Harvati, K., Konidaris, G. and Tourloukis, V., 2018. The Gates of Europe. Quaternary International, 497, pp. 1–240.

Karkanas, P., Tourloukis, V., Thompson, N., Giusti, D., Tsartsidou, G., Athanassiou, A., Konidaris, G., Roditi, E., Panagopoulou, E. and Harvati, K., this volume. The Megalopolis

Paleoenvironmental Project (MegaPal).

KONIDARIS, G.E., Athanassiou, A., Panagopoulou, E., Karkanas, P. and Harvati, K., this volume. Fossil macaques (Cercopithecidae, Primates) from the Middle Pleistocene of the Megalopolis Basin (Greece) with description of a new specimen from Kyparissia 4.

LÜTTIG, G., 1968. Die Ostrakoden des Megalopolis-Beckens (Peloponnes) und die Grenze Tertiär/Quartär. Giornale di Geologia, 35, pp. 73–82.

MAZZINI, I., Goiran, J.P. and Carbonel, P., 2015. Ostracodological studies in archaeological settings: a review. Journal of Archaeological Science, 54, pp. 325–328.

MEISCH, C., 2000. Freshwater Ostracoda of Western and Central Europe. Spektrum Akademischer Verlag, Heidelberg

MEZQUITA, F., Tapia, G. and Roca, J.R., 1999. Ostracoda from springs on the eastern Iberian Peninsula: ecology, biogeography and palaeolimnological implications. Palaeogeography, Palaeoclimatology, Palaeoecology, 148(1–3), pp. 65–85.

PANAGOPOULOU, E., Tourloukis, V., Thompson, N., Konidaris, G., Athanassiou, A., Giusti, D., Tsartsidou, G., Karkanas, P. and Harvati, K., 2018. The Lower Palaeolithic site of Marathousa 1, Megalopolis, Greece: Overview of the evidence. Quaternary International, 497, pp. 33–46.

ROCA, R.J., Baltanas, A., 1993. Ecology and distribution of Ostracoda in Pyrenean springs. Journal of Crustacean Biology, 13(1), pp. 165–174.

SCHELLENBERG, S.A., 2007. Marine ostracods, in: Elias, S.A. (Ed.), Encyclopedia of Quaternary science. Elsevier, Amsterdam, pp. 2046–2062.

VAN KOLFSCHOTEN, T., Konidaris, G.E., Doukas, C., Athanassiou, A., Tourloukis, V., Panagopoulou, E., Karkanas, P. and Harvati, K., this volume. Voles (Rodentia, Mammalia) as a proxy to date the site Kyparissia 4 (Megalopolis Basin, Greece).

VAN VUGT, N., de Bruijn, H., van Kolfschoten, T. and Langereis, C.G., 2000. Magneto- and cyclostratigraphy and mammal-fauna's of the Pleistocene lacustrine Megalopolis Basin, Peloponnesos, Greece. Geologica Ultrajectina, 189, pp. 69–92.

VINKEN, R., 1965. Stratigraphie und Tektonik des Beckens von Megalopolis (Peloponnes, Griechenland). Geologisches Jahrbuch, 83, pp. 97–148.

24 FOSSIL MACAQUES (CERCOPITHECIDAE, PRIMATES) FROM THE MIDDLE PLEISTOCENE OF THE MEGALOPOLIS BASIN (GREECE) WITH DESCRIPTION OF A NEW SPECIMEN FROM KYPARISSIA 4

George E. Konidaris[1,*], Athanassios Athanassiou[2], Eleni Panagopoulou[2], Panagiotis Karkanas[3], Katerina Harvati[1,4]

[1]*Paleoanthropology, Institute for Archaeological Sciences and Senckenberg Centre for Human Evolution and Palaeoenvironment, Department of Geosciences, Eberhard Karls University of Tübingen, Tübingen, Germany*
[2]*Hellenic Ministry of Culture, Ephorate of Palaeoanthropology–Speleology, Athens, Greece*
[3]*M.H. Wiener Laboratory for Archaeological Science, American School of Classical Studies at Athens, Athens, Greece*
[4]*DFG Centre of Advanced Studies 'Words, Bones, Genes, Tools', Eberhard Karls University of Tübingen, Tübingen, Germany*
**georgios.konidaris@uni-tuebingen.de*

http://dx.doi.org/10.15496/publikation-97592

Keywords: *Macaca*; Marathousa 1; Kyparissia 4; southern Europe; peri-Mediterranean region; Pleistocene

24.1 INTRODUCTION

Recent fieldwork in the Megalopolis Basin (Greece) has mainly focused on two Middle Pleistocene sites, Marathousa 1 and Kyparissia 4, both of which yielded rich faunal assemblages (e.g., ostracods, molluscs, fishes, amphibians, reptiles, birds, mammals) in stratigraphic and spatial association with Lower Palaeolithic lithic artefacts, thus documenting hominin presence in the region (Harvati et al., 2018 and articles therein; Karkanas et al., this volume). Marathousa 1 (MAR-1), located in the Marathousa mine, was discovered during targeted fieldwork in 2013 and systematically excavated from 2014 to 2019 by a team from the University of Tübingen Paleoanthropology group and the Ephorate of Paleoanthropology–Speleology (see Harvati et al., 2018 and articles therein). MAR-1 is dated to ca. 450 ka and is correlated to the Marine Isotope Stage 12 (Panagopoulou et al., 2018 and references therein). The site's large mammal faunal assemblage includes (Konidaris et al., 2018): *Castor fiber* (beaver), *Mustela* sp. (weasel), *Lutra simplicidens* (otter), *Felis* sp. (wildcat), *Vulpes* sp. (fox), *Canis* sp. (medium-sized canid), *Palaeoloxodon antiquus* (straight-tusked elephant), *Hippopotamus antiquus* (hippopotamus), *Bison* sp. (bison), *Dama* sp. (fallow deer) and *Cervus elaphus* (red deer). Of particular interest are the skeletal remains of at least two elephant individuals, some of which preserve evidence of anthropogenic modifications. Kyparissia 4 (KYP-4), located in the Kypa-

G. E. Konidaris: https://orcid.org/0000-0002-7041-233X
A. Athanassiou: https://orcid.org/0000-0002-9140-7011
E. Panagopoulou: https://orcid.org/0000-0002-4268-6157
P. Karkanas: https://orcid.org/0000-0002-7156-671X
K. Harvati: https://orcid.org/0000-0001-5998-4794

rissia mine, was discovered in 2007 (Athanassiou, 2018; Athanassiou et al., 2018) and was revisited during a targeted field survey by a joint team from the University of Tübingen Paleoanthropology group, the Ephorate of Palaeoanthropology–Speleology at Athens, and the American School of Classical Studies at Athens. Preliminary stratigraphic and biochronological data indicate that KYP-4 is older than MAR-1 and is dated to the lower part of the Middle Pleistocene (Karkanas et al., this volume; van Kolfschoten et al., this volume). The site's large mammal faunal assemblage includes (Athanassiou, 2018; Athanassiou et al., 2018, this volume): *Castor fiber*, *Vulpes* sp., *Palaeoloxodon antiquus*, *Stephanorhinus* sp. (rhinoceros), *Equus* sp. (horse), *Hippopotamus antiquus*, *Bison* sp., *Sus scrofa* (boar), *Dama* sp., *Cervus elaphus* and *Praemegaceros verticornis* (giant deer).

Until recently macaques were not known from the Megalopolis Basin. During the 2019 excavation at MAR-1, an almost complete mandible (MAR-1B-9) was unearthed from the site's Area B and studied by Konidaris et al. (2022). More recently, during the 2021 field survey in the Kyparissia mine, an isolated upper first molar was found at KYP-4 (KYP4A-1075) in the sedimentary unit UA5 of Area A, which consists of dark grey sandy mud, very rich in organics and freshwater molluscs. This new macaque specimen is the primary focus of this study. Both specimens are housed at the Ephorate of Palaeoanthropology–Speleology (EPS) in Athens (Greece).

All European fossil macaque forms (except for the endemic insular *Macaca majori* Azzaroli, 1946 from Sardinia in Italy) are currently attributed to the Barbary macaque *Macaca sylvanus* (Linnaeus, 1758), a species that was geographically widely distributed in western Eurasia during the Plio-Pleistocene (Delson, 1975; Elton and O'Regan, 2014; Mecozzi et al., 2021). Three (chrono)subspecies are generally recognized (Szalay and Delson, 1979; Delson, 1980; Alba et al., 2011): *Macaca sylvanus*

Taxon	Provenance	Source
Macaca sylvanus sylvanus	extant	Alba et al. (2011), PRIMO (2021)
Macaca majori	Capo Figari (Italy)	PRIMO (2021)
Macaca sylvanus prisca	Balaruc (France)	PRIMO (2021)
	Cova Bonica (Spain)	Delson (1971)
	Gundersheim (Germany)	Rook et al. (2001)
	Montpellier (France)	PRIMO (2021)
	RDB quarry, Villafranca d'Asti (Italy)	Rook et al. (2001)
Macaca sylvanus florentina or *M. s.* cf. *florentina*	Cal Guardiola (Spain)	Alba et al. (2008)
	Estació de Vallparadís (Spain)	Alba et al. (2008)
	Monte Peglia (Italy)	PRIMO (2021)
	Quibas (Spain)	Alba et al. (2011)
	Tourkovounia-2 (Greece)	Symeonidis and Zapfe (1976)
	Upper Valdarno (Italy)	PRIMO (2021)
Macaca sylvanus pliocena or *M. s.* cf. *pliocena*	Gajtan (Albania)	PRIMO (2021)
	Heppenloch (Germany)	Adam (1975)
	Kudaro 1 (Caucasus)	PRIMO (2021)
	Quecchia Quarry (Italy)	Bona et al. (2016)

Table 1: Comparative dental sample (fossil and extant) used in the analyses of the Kyparissia 4 specimen.

prisca Gervais, 1859 from the Pliocene, *Macaca sylvanus florentina* (Cocchi, 1872) from the Early Pleistocene, and *Macaca sylvanus pliocena* Owen, 1846 from the Middle–early Late Pleistocene. The diagnosis of these subspecies relies mainly on differences in dental size and proportions; however, there is great overlap in almost all parameters among the fossil, as well as the extant, subspecies and therefore subspecific assignments are often based on (bio)chronological grounds rather than on diagnostic morphological features.

24.2 METHODS

Dental terminology follows Delson (1975). Standard dental measurements (following Alba et al., 2011) of maximum mesiodistal crown length (MD), and buccolingual crown breadth at the mesial [BLm=BL (maximum buccolingual crown breadth)] and distal (BLd) lobes, were taken with a digital caliper to the nearest 0.1 mm. A breadth/length index (BLI) was also calculated (BLI=BL/MD × 100). Comparative dental measurements (Tables 1 and 2; following in some cases the taxonomic attributions of Alba et al., 2019) were obtained from the literature and from publicly available sources [PRIMO (the New York Consortium in Evolutionary Primatology PRImate Morphometrics Online) database, accessed November 2021; http://primo.nycep.org]. Box-and-whisker plots and statistical computations were performed with the software package PAST v. 4.09 (Hammer et al., 2001; https://www.nhm.uio.no/english/research/resources/past/).

24.3 THE MARATHOUSA 1 SPECIMEN

The mandible from Marathousa 1 (Fig. 1a–c) was studied in detail in Konidaris et al. (2022), and it is only briefly presented here. The specimen originally consisted of two hemimandibles (deposited about 1.6 m apart) that fit together under the alveolus of the right P_3. The refitted complete mandible (MAR-1B-9) bears the left canine and the left P_3–M_2, and the right P_4–M_3. The mandible belonged to a male individual of advanced ontogenetic age and of estimated body mass of ~13 kg. Mandibular and dental morphology, and dental size and proportions of MAR-1B-9 fit well within the range of extinct and extant *M. sylvanus*. The dental dimensions of the MAR-1 macaque fit better within the variation of *M. s. florentina* and *M. s. pliocena* rather than with the extant representative *M. s. sylvanus*. Moreover, a principal component analysis (combining M_1 MD, M_1 BL, M_2 MD, M_2 BL, M_3 MD, and M_3 BL of complete M_1–M_3 tooth rows) shows that these two fossil subspecies differ from the modern representative in their longer and broader M_1, and the longer M_3. Although *M. s. florentina* and *M. s. pliocena* overlap greatly, the MAR-1B-9 macaque fits better with *M. s. pliocena* and does not fall within either the *M. s. florentina* or the extant *M. s. sylvanus* range (Fig. 1d).

24.4 THE KYPARISSIA 4 SPECIMEN

24.4.1. DESCRIPTION

The right M^1 KYP4A-1075 [MD = 8.3; BLm=7.9; BLd=7.2; crown height = 5.3 (at the paracone); all in mm; BLI=95] is almost unworn, and the crown is well-preserved; there is a mesial contact facet (Fig. 2a). It bears a single lingual root, a mesiobuccal one missing its tip, and a damaged distobuccal one. It displays a bilophodont occlusal pattern with a wider mesial lobe than the distal one. The lobes are separated by a relatively well-developed median lingual cleft and a less marked buccal one.

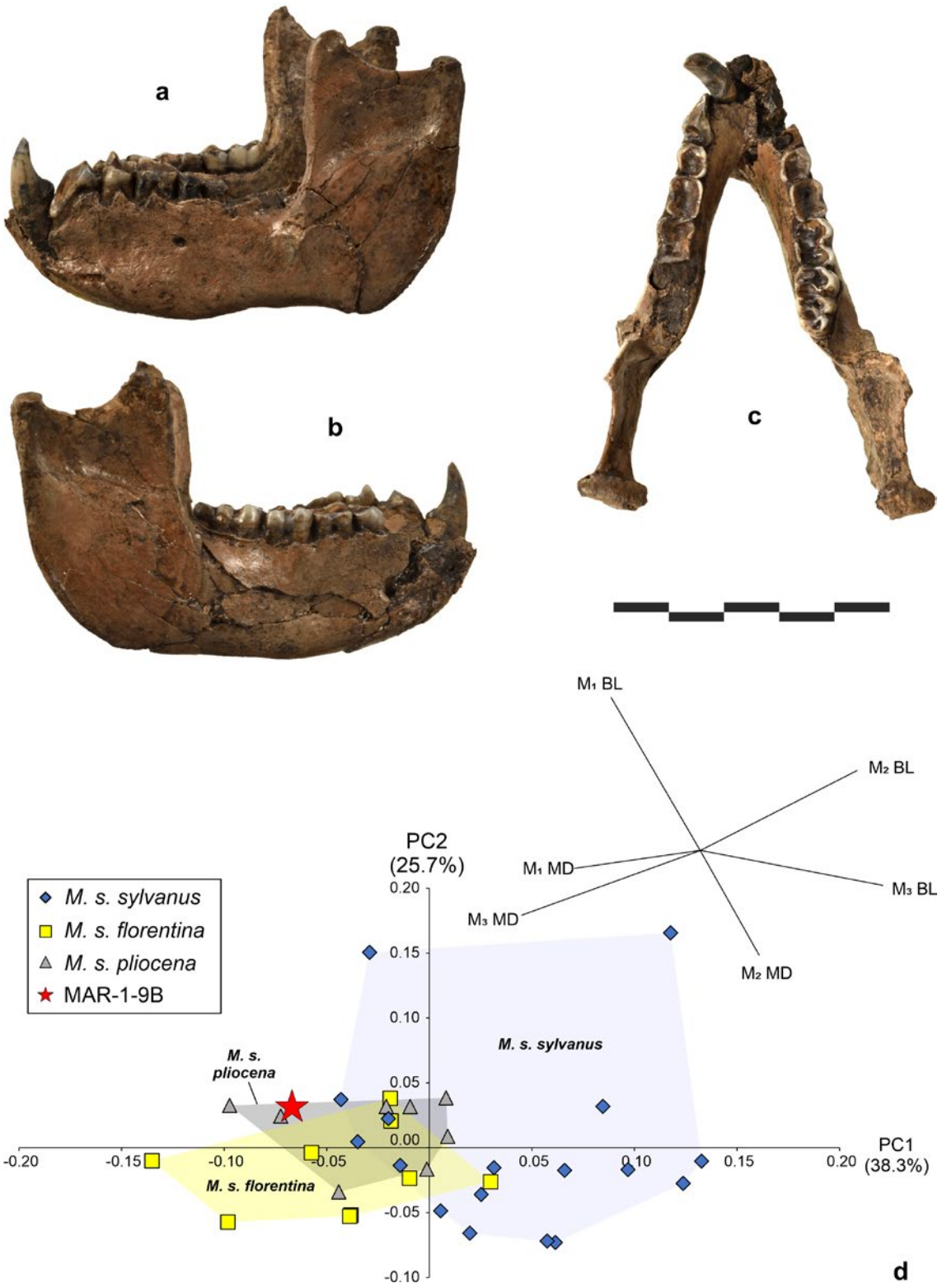

Figure 1: Mandible of *Macaca sylvanus* cf. *pliocena* (EPS-MAR-1B-9) from Marathousa 1, in a, left lateral; b, right lateral; and c, dorsal views; scale = 5 cm; d, principal component analysis of dental variables among *M. s. sylvanus* (n = 17), *M. s. florentina* (n = 9) and *M. s. pliocena* (n = 8) using Mosimann's Log-shape ratio transformation. Only complete M_1–M_3 tooth rows are included; for MAR-1B-9 the right tooth row is used. The principal component biplot depicting the projection of the original axes (variables) is also shown.

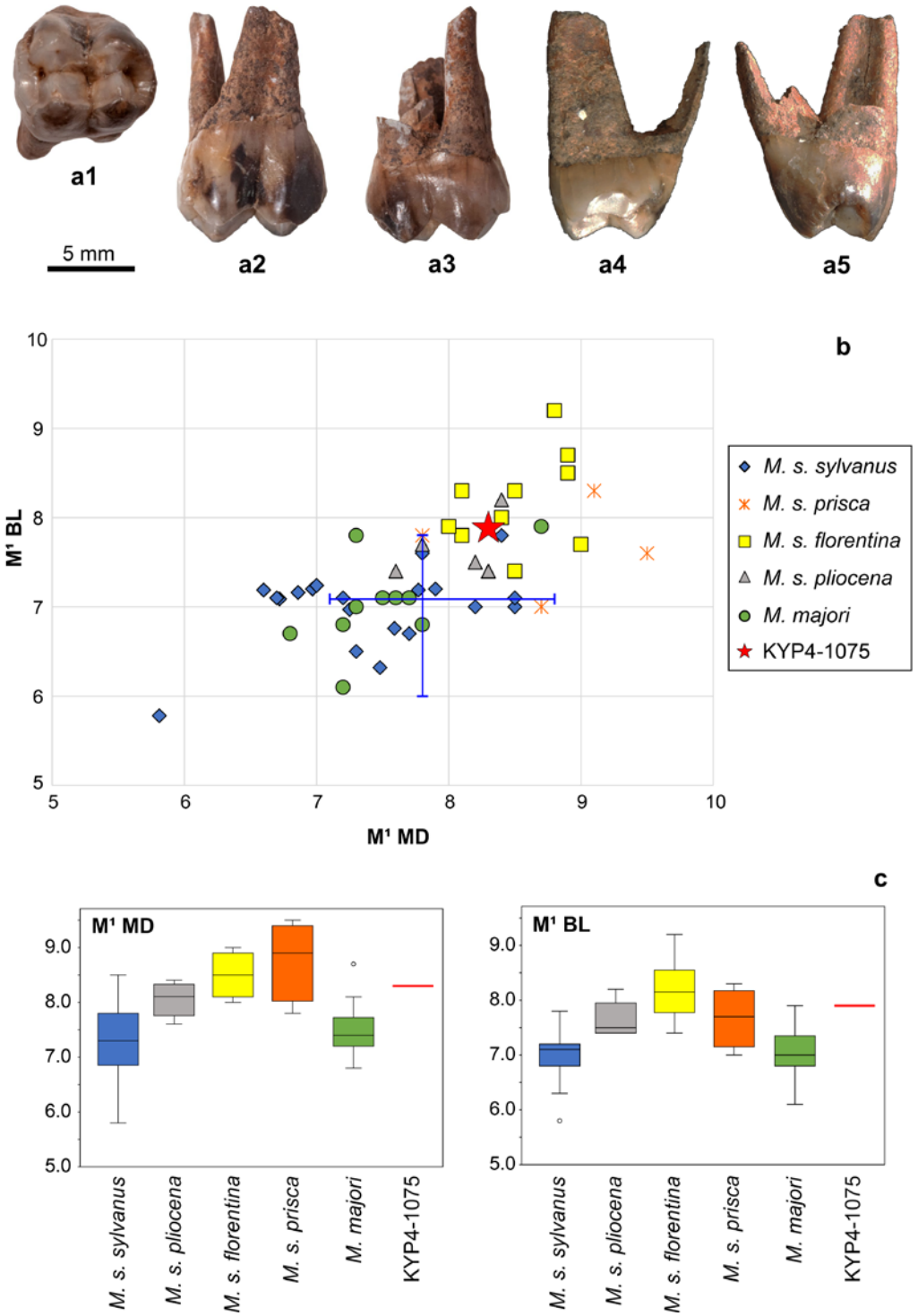

Figure 2: a, Right M^1 (EPS-KYP4A-1075) of *Macaca sylvanus* ssp. from Kyparissia 4; in a1, occlusal (mesial is to the left); a2, lingual; a3, buccal; a4, mesial; a5, distal views; b, Bivariate dental plot of BL vs. MD (in mm) for the macaque M^1 from Kyparissia 4, compared with those of modern and fossil *Macaca sylvanus* subspecies and *Macaca majori* from various localities (see Methods); the blue ranges in the plot correspond to the *M. s. sylvanus* sample (n = 35) of Alba et al. (2011); c, Box-and-Whisker plots of BL and MD (in mm) for the M^1 of extant and fossil macaques (colors correspond to those of 2b) compared with that from Kyparissia 4. Horizontal lines represent the median; boxes the 25 and 75 percentiles (interquartile range); whiskers the minimum-maximum values; circles the outliers. Comparative sample: *M. s. sylvanus* (n = 21–25), *M. s. pliocena* (n = 5–6), *M. s. florentina* (n = 10), *Macaca s. prisca* (n = 4), and *M. majori* (n = 13–14) from various localities (see Methods and Table 1).

The buccal notch is shallow relative to the height of the crown. Buccal (paracone and metacone) and lingual (protocone and hypocone) main cusps are almost aligned in each lobe. The paracone is slightly larger than the other main cusps. The mesial fovea, which is delimited by the preprotocrista, the preparacrista, and the rather strong and almost straight mesial marginal ridge, is relatively short but deep. The central fovea (trigon basin) is deeper and more expanded than the mesial and distal foveae. The distal fovea, which is delimited by the postmetacrista, the posthypocrista, and the rather strong and curved distal marginal ridge (formed by several tubercles in a row), is wide but rather shallow.

24.4.2. COMPARISONS

The generalized papionin occlusal pattern of KYP4A-1075 is compatible with an attribution to *Macaca* (e.g., Alba et al., 2008, 2011), while its dental size and proportions fit well within the range of extinct and extant *Macaca sylvanus* (Fig. 2; Table 2). On the other hand, an assignment to *Paradolichopithecus*, the other extinct European papionin also present in the Pleistocene of Greece, can be safely excluded based on the larger dental dimensions of this genus (see e.g., Kostopoulos et al., 2018).

The crown measurements of KYP4A-1075 (MD=8.3 mm; BLm=7.9 mm) are below the known metrical variation of both M^2 and M^3 of fossil *M. sylvanus* [M^2 MD=9.1–11 (*n*=26); M^2 BLm=8.0–10.9 (*n*=27); M^3 MD=8.6–10.6 (*n*=17); M^3 BLm=8.6–10.4 (*n*=17); from references cited in Table 1 plus Alba et al. (2016, 2018), Reumer et al. (2018) and van Kolfschoten (2020); see also the bivariate dental plots of M^2 and M^3 in Alba et al. (2016: Fig. 4) and Alba et al. (2018: Fig. 3b), respectively], and fit well within the size range and proportions of M^1 (Fig. 2b, c). Furthermore, in contrast to the usually moderate and marked distal tapering of the crown in the M^2 and M^3, respectively, in M^1 the tapering is rather weak (Alba et al., 2016, 2018), as it is in KYP4A-1075

		n	MEAN	SD	MINIMUM	MAXIMUM	Z-SCORE
M^1 MD	KYP4A-1075	1	8.30	-	-	-	
	*M. s. sylvanus**	25	7.33	0.69	5.80	8.50	1.40
	*M. s. sylvanus***	35	7.81	0.41	7.10	8.80	1.20
	M. s. pliocena	6	8.05	0.31	7.60	8.40	0.81
	M. s. florentina	10	8.52	0.37	8.00	9.00	-0.59
	M. s. prisca	4	8.78	0.73	7.80	9.50	-0.65
M^1 BL	KYP4A-1075	1	7.90	-	-	-	
	*M. s. sylvanus**	21	7.00	0.43	5.80	7.80	**2.12**
	*M. s. sylvanus***	35	7.09	0.41	6.00	7.80	**1.98**
	M. s. pliocena	5	7.64	0.34	7.40	8.20	0.77
	M. s. florentina	10	8.18	0.53	7.40	9.20	-0.53
	M. s. prisca	4	7.68	0.54	7.00	8.30	0.42

Table 2: Descriptive statistics and calculated z-scores for dental measurements of EPS-KYP4A-1075 compared with *Macaca sylvanus sylvanus* (*data from PRIMO, ** data from Alba et al., 2011), *Macaca sylvanus pliocena*, *Macaca sylvanus florentina* and *Macaca sylvanus prisca* (see Methods). When $z > |1.96|$, the null hypothesis that EPS-KYP4A-1075 fits within the variation of the comparative sample can be rejected at $p < 0.05$; in such cases, the z-score is typed in bold. SD = standard deviation.

(BLd=7.2 mm), while additionally the KYP-4 molar lacks any accessory cusp on the distal margin, which is frequently present in papionin last molars (Alba et al., 2018). Therefore, the KYP4A-1075 is recognized as M^1.

Morphologically, the molar does not show any substantial difference from those of extinct and extant *M. sylvanus*; therefore, we focus on dental crown dimensions. In the MD vs. BL biplot although some overlap exists, KYP4A-1075 is rather well-distinguished from *M. majori* and *M. s. sylvanus* and is comfortably placed with the fossil *M. sylvanus* subspecies (Fig. 2b). In the Box-and-Whisker plot, the MD dimension of the KYP-4 molar plots at the upper range of *M. s. sylvanus*, but outside its interquartile range; it is also distinguished from *M. majori* (Fig. 2c). The molar stands at the upper limit of the interquartile range of *M. s. pliocena*, and at the lower quartile of *M. s. florentina* and *M. s. prisca*. In terms of the BLm dimension, KYP4A-1075 is outside the range of *M. s. sylvanus* and plots at the maximum value of *M. majori*. It stands at the upper quartiles of *M. s. pliocena* and *M. s. prisca*, and at the lower quartile of *M. s. florentina*. Similar results are obtained by the statistical comparison using z-scores of KYP4A-1075 with the subspecies of *M. sylvanus* (Table 2). The analysis detects significant difference of KYP4A-1075 in terms of the M^1 BL with the extant *M. s. sylvanus*.

24.4.3. ONTOGENETIC AGE, SEX AND BODY MASS ESTIMATION

The ontogenetic age of the KYP-4 macaque individual can be estimated based on the sequence and timing of tooth eruption in primates, and on the degree of dental wear. The first permanent molar is particularly informative because it is the first of the permanent teeth to erupt in macaques and marks the end of infancy (end of weaning) and the beginning of independence (Smith, 1994; Smith et al., 1994). The presence of a mesial contact facet in the KYP4A-1075 M^1 indicates that at the time of death the tooth had been already erupted and was functional, while the absence of a distal contact facet indicates that the M^2 was unerupted, at least not completely. Available dental eruption times for extant macaques show that the M^1 and the M^2 emerge at about 17–21 months and 39–45 months of postnatal life on average, respectively (Smith et al., 1994). Therefore, KYP4A-1075 would belong to an individual of a minimum age approximately between 1.5 and 2 years old, and considering the absence of a distal contact facet, of maximum age approximately between 4 and 4.5 years old. Taking into account the almost unworn state of the molar, an age at death closer to the minimum estimate, i.e., around 2 years is more plausible. Indeed, based on its minimal wear, the KYP-4 specimen can be placed towards the end of the individual dental age stage (IDAS) 1 (infant) and the beginning of IDAS 2 (juvenile) of Anders et al. (2011). KYP4A-1075 belonged to an individual of comparable age (perhaps only slightly younger) as that of the juvenile mandible of *Macaca sylvanus* cf. *pliocena* from Gruta da Aroeira (Spain), which preserves the fully erupted dP_3, dP_4 and M_1 (the latter only slightly worn), while the P_4 and M_2 are inside their alveoli; the age at death of this individual was estimated close to 2.5 years (Alba et al., 2019). Thus overall, the KYP-4 macaque can be regarded as a (subadult) juvenile individual.

To estimate the body mass of the KYP-4 macaque, we applied the allometric regressions of Delson et al. (2000: Table 7) for cercopithecines based on M^1 MD (8.3 mm), M^1 BLm (7.9 mm) and M^1 area [MD × 0.5(BLm + BLd)]. The resulting body mass estimate was 10.6 kg. However, this value has to be regarded as corresponding to its adult stage (when the full permanent dentition would have

been erupted), and the expected body mass at the age of death of the KYP-4 macaque would be lower. Indeed, the body mass range of juveniles (with some of the permanent teeth erupted) of extant *M. s. sylvanus* is 6.2–8.6 kg (*n* = 3; Fooden, 2007: Table 2). Considering the larger dental dimensions of KYP4A-1075 than most of the comparative *M. s. sylvanus* sample (Fig. 2 b, c), a body mass at the age of death closer to the upper range (~8–9 kg) seems more plausible. On the other hand, the estimated body mass of 10.6 kg at the adult stage fits within the ranges of adult females and males, being however, very close to the mean values of females provided by Delson et al. (2000) and Fooden (2007).

24.5 DISCUSSION – CONCLUSIONS

24.5.1. TAXONOMIC ATTRIBUTION OF THE MEGALOPOLIS SPECIMENS

The metrical comparison of KYP4A-1075 separates it rather well from the extant *M. s. sylvanus* and reveals a better match with the fossil subspecies (*M. s. prisca*, *M. s. florentina* and *M. s. pliocena*); however, their great size overlap, the single specimen status, and the absence of clear-cut diagnostic criteria that may differentiate the European fossil subspecies, do not allow for a subspecific allocation at the moment. Therefore, KYP4A-1075 is attributed to a fossil European *Macaca sylvanus* ssp. Likewise, the study of the mandible MAR-1B-9 (Konidaris et al., 2022) showed that the dental dimensions fit better within the variation of *M. s. florentina* and *M. s. pliocena* rather than with the extant representative *M. s. sylvanus*, but additionally, the principal component analysis revealed a better match with *M. s. pliocena*; therefore, MAR-1B-9 was attributed to *M. s.* cf. *pliocena*, consistent also with the specimen's chronology.

24.5.2. IMPLICATIONS WITHIN THE REGIONAL AND EUROPEAN CONTEXT

The recent investigations in the Megalopolis Basin have enriched the *Macaca* record known from Greece, previously limited to the Early Pleistocene (Symeonidis and Zapfe, 1976), by adding material from secure stratigraphic, chronological and palaeoenvironmental contexts. Additionally, the Megalopolis specimens are important for several reasons:

- MAR-1B-9 represents the most complete fossil European macaque mandible known.
- The Megalopolis specimens constitute some of the very few known records of *Macaca* in the eastern sector of the peri-Mediterranean region and are among the southernmost European occurrences [see distribution maps of fossil macaques in Elton and O'Regan (2014) and Mecozzi et al. (2021)].
- They mark the first known presence of macaques during the Middle Pleistocene of Greece.
- They extend the chronological range of cercopithecids (Late Miocene to Middle Pleistocene) in the country.
- They document for the first time the coexistence of macaques and hominins in Greece.
- The exquisitely preserved, rich and well-documented assemblages of both Megalopolis Basin sites allow not only their secure chronological placement, but also a detailed reconstruction of the environmental conditions under which these individuals lived, and of the prey-predator relationships among hominins, carnivores, and macaques (Konidaris et al., 2022).
- Marathousa 1 can be added to those European sites that document the coexistence of macaques and hominins, and it has yielded evidence of elephant butchering (Konidaris and Tourloukis, 2021; Konidaris et al., 2022).
- The record of macaques in different stratigraphic levels within the Middle Pleistocene deposits of the Megalopolis Basin, including

periods of colder conditions during glacial or stadial stages (see Bludau et al., 2021; Boni et al., this volume; Butiseacă et al., this volume; Kyrikou et al., this volume; Papadopoulou et al., this volume), might point to a continuous presence in the region and suggests that this southern region could have acted as a refugium for European macaque populations. Recent paleoenvironmental reconstruction indeed points to the presence of permanent freshwater bodies throughout the year even during glacial periods (Konidaris et al., 2018; Bludau et al., 2021)

ACKNOWLEDGMENTS

Excavation at Marathousa 1 was conducted under a permit granted to the Ephorate of Palaeoanthropology–Speleology, Hellenic Ministry of Culture. Field survey in the Megalopolis Basin was conducted in the framework of the Megalopolis Paleoenvironmental Project (MegaPal) under a permit granted to the Ephorate of Palaeoanthropology–Speleology, Hellenic Ministry of Culture, and the American School of Classical Studies at Athens. All fieldwork was supported by the ERC Consolidator Grant ERC-CoG-724703 ("CROSSROADS") and the ERC Starting Grant ERC-StG-283503 ("PaGE"), both awarded to K.H. G.E.K. and K.H. are supported by the Deutsche Forschungsgemeinschaft (DFG Project no. 463225251, "MEGALOPOLIS"). K.H. is also supported by the ERC Advanced Grant ERC-AdG-101019659 ("FIRSTSTEPS"). We thank all Megalopolis field team members, and E. Delson for providing us with access to the online database PRIMO. We are grateful to the reviewers E. Delson and G. Koufos for their comments and suggestions.

REFERENCES

Adam, K.D., 1975. Die mittelpleistozäne Säugetier-Fauna aus dem Heppenloch bei Gutenberg (Württemberg). Stuttgarter Beiträge zur Naturkunde Serie B (Geologie und Paläontologie), 3, pp. 1–247.

Alba, D.M., Moyà-Solà, S., Madurell, J. and Aurell, P., 2008. Dentognathic remains of *Macaca* (Primates, Cercopithecidae) from the late Early Pleistocene of Terrassa (Catalonia, Spain). Journal of Human Evolution, 55(6), pp. 1160–1163.

Alba, D.M., Carlos Calero, J.A., Mancheño, M.Á., Montoya, P., Morales, J. and Rook, L., 2011. Fossil remains of *Macaca sylvanus florentina* (Cocchi, 1872) (Primates, Cercopithecidae) from the Early Pleistocene of Quibas (Murcia, Spain). Journal of Human Evolution, 61(6), pp. 703–718.

Alba, D.M., Madurell-Malapeira, J., Delson, E., Vinuesa, V., Susanna, I., Espigares, M.P., Ros-Montoya, S. and Martínez-Navarro, B., 2016. First record of macaques from the Early Pleistocene of Incarcal (NE Iberian Peninsula). Journal of Human Evolution, 96, pp. 139–144.

Alba, D.M., Delson, E., Morales, J., Montoya, P. and Romero, G., 2018. Macaque remains from the early Pliocene of the Iberian Peninsula. Journal of Human Evolution, 123, pp. 141–147.

Alba, D.M., Daura, J., Sanz, M., Santos, E., Yagüe, A.S., Delson, E. and Zilhão, J., 2019. New macaque remains from the Middle Pleistocene of Gruta da Aroeira (Almonda karst system, Portugal). Journal of Human Evolution, 131, pp. 40–47.

Anders, U., von Koenigswald, W., Ruf, I. and Smith, B., 2011. Generalized individual dental age stages for fossil and extant placental mammals. Paläontologische Zeitschrift, 85, pp. 321–339.

Athanassiou, A., 2018. Pleistocene vertebrates

from the Kyparíssia lignite mine, Megalopolis Basin, S. Greece: Rodentia, Carnivora, Proboscidea, Perissodactyla, Ruminantia. Quaternary International, 497, pp. 198–221.

Athanassiou, A., Michailidis, D., Vlachos, E., Tourloukis, V., Thompson, N. and Harvati, K., 2018. Pleistocene vertebrates from the Kyparíssia lignite mine, Megalopolis Basin, S. Greece: Testudines, Aves, Suiformes. Quaternary International, 497, pp. 178–197.

Athanassiou, A., Konidaris G.E., Tourloukis, V., Thompson, N., Giusti, D., Panagopoulou, E., Karkanas and P., Harvati, K., this volume. The Middle Pleistocene large mammal fauna from Kyparissia (Peloponnese, S. Greece): New collected material.

Azzaroli, A., 1946. La scimmia fossile della Sardegna. Rivista di Scienze Preistoriche, 1, pp. 68–76.

Bludau, I.J.E., Papadopoulou, P., Iliopoulos, G., Weiss, M., Schnabel, E., Thompson, N., Tourloukis, V., Zachow, C., Kyrikou, S., Konidaris, G.E., Karkanas, P., Panagopoulou, E., Harvati, K. and Junginger, A., 2021. Lake-level changes and their paleoclimatic implications at the MIS12 Lower Paleolithic (Middle Pleistocene) site Marathousa 1, Greece. Frontiers in Earth Science, 9, 668445.

Bona, F., Bellucci, L., Casali, D., Schirolli, P. and Sardella, R., 2016. *Macaca sylvanus* Linnaeus 1758 from the Middle Pleistocene of Quecchia Quarry (Brescia, Northern Italy). Hystrix, 27, pp. 158–162.

Boni, G., Syrides, G., Konidaris, G.E., Athanassiou, A., Tourloukis, V., Koukousioura, O., Panagopoulou, E., Karkanas, P. and Harvati, K., this volume. Preliminary results on the taxonomy and paleoenvironmental analysis of the mollusc fauna from Marathousa 1, Marathousa 2 and Kyparissia 4 (Middle Pleistocene, Megalopolis Basin, Greece).

Butiseacă, G.A. Vasiliev, I., Tourloukis, V., Junginger, A., Mulch, A., Karkanas, P., Panagopoulou, E. and Harvati, K., this volume. Preliminary biomarker/paleoclimate reconstruction results from the Marathousa 1 Lower Paleolithic site (Megalopolis Basin, Greece).

Cocchi, I., 1872. Su di due Scimmie fossili italiane. Bollettino del R. Comitato Geologico d'Italia, 3, pp. 59–71.

Delson, E., 1971. Estudio preliminar de unos restos de simios pliocénicos procedentes de "Cova Bonica" (Gavá) (Prov. Barcelona). Acta Geológica Hispánica, 6, pp. 54–57.

Delson, E., 1975. Evolutionary history of the Cercopithecidae, in: Szalay, F.S. (Ed.), Approaches to Primate Paleobiology. Contributions to Primatology, 5. Karger, Basel, pp. 167–217.

Delson, E., 1980. Fossil macaques, phyletic relationships and a scenario of deployment, in: Lindburg, D.E. (Ed.), The Macaques. Studies in Ecology, Behavior and Evolution. Van Nostrand, New York, pp. 10–30.

Delson, E., Terranova, C.J., Jungers, W.L., Sargis, E.J., Jablonski, N.G. and Dechow, P.C., 2000. Body mass in Cercopithecidae (Primates, Mammalia): estimation and scaling in extinct and extant taxa. Anthropological papers of the American Museum of Natural History, 83, pp. 1–159.

Elton, S., O'Regan, H.J., 2014. Macaques at the margins: the biogeography and extinction of *Macaca sylvanus* in Europe. Quaternary Science Reviews, 96, pp. 117–130.

Fooden, J., 2007. Systematic review of the Barbary macaque, *Macaca sylvanus* (Linnaeus, 1758). Fieldiana Zoology, 113, pp. 1–58.

Gervais, P., 1859. Zoologie et paléontologie Françaises (second edition). Arthus Bertrand, Paris.

Hammer, Ø., Harper, D.A.T. and Ryan, P.D., 2001. PAST: paleontological statistics software package for education and data analysis. Palaeontologia Electronica, 4, pp. 1–9.

Harvati, K., Konidaris, G. and Tourloukis, V. (Eds.), 2018. The Gates of Europe. Quaternary International, 497.

Karkanas, P., Tourloukis, V., Thompson, N., Giusti, D., Tsartsidou, G., Athanassiou, A., Konidaris, G., Roditi, E., Panagopoulou, E. and Harvati, K., this volume. The Megalopolis Paleoenvironmental Project (MegaPal).

Konidaris, G.E., Tourloukis, V., 2021. Proboscidea-*Homo* interactions in open-air localities during the Early and Middle Pleistocene of western Eurasia: a palaeontological and archaeological perspective, in: Konidaris, G.E., Barkai, R., Tourloukis, V., Harvati, K. (Eds.), Human-elephant interactions: from past to present. Tübingen University Press, Tübingen, pp. 67–104.

Konidaris, G.E., Athanassiou, A., Tourloukis, V., Thompson, N., Giusti, D., Panagopoulou, E. and Harvati, K., 2018. The skeleton of a straight-tusked elephant (*Palaeoloxodon antiquus*) and other large mammals from the Middle Pleistocene butchering locality Marathousa 1 (Megalopolis Basin, Greece): preliminary results. Quaternary International, 497, pp. 65–84.

Konidaris, G.E., Athanassiou, A., Panagopoulou, E. and Harvati, K., 2022. First record of *Macaca* (Cercopithecidae, Primates) in the Middle Pleistocene of Greece. Journal of Human Evolution 162, 103104.

Kostopoulos, D.S., Guy, F., Kynigopoulou, Z., Koufos, G.D., Valentin, X. and Merceron, G., 2018. A 2Ma old baboon-like monkey from Northern Greece and new evidence to support the *Paradolichopithecus* – *Procynocephalus* synonymy (Primates: Cercopithecidae). Journal of Human Evolution, 121, pp. 178–192.

Kyrikou, S., Marinova, E., Bludau, I.J.E., Karkanas, P., Panagopoulou, E., Tourloukis, V., Junginger, A. and Harvati, K., this volume. The Middle Pleistocene MIS12 palynological record from Marathousa palaeolake in Southern Greece: Highlighting favourable conditions in Marathousa 1 (MAR-1) refugial site during the severe glacial period.

Linnaeus, C., 1758. Systema naturae per regna tria naturae, secundum classes, ordines, genera, species, cum characteribus, differentiis, synonymis locis. Tomus 1. Laurentius Salvius, Stockholm.

Mecozzi, B., Iannucci, A., Sardella, R., Curci, A., Daujeard, C. and Moncel, M.H., 2021. *Macaca* ulna from new excavations at the Notarchirico Acheulean site (Middle Pleistocene, Venosa, southern Italy). Journal of Human Evolution, 153, 102946.

Owen, R., 1846. A history of British fossil mammals and birds. John Van Voorst, London.

Panagopoulou, E., Tourloukis, V., Thompson, N., Konidaris, G., Athanassiou, A., Giusti, D., Tsartsidou, G., Karkanas, P. and Harvati, K., 2018. The Lower Palaeolithic site of Marathousa 1, Megalopolis, Greece: Overview of the evidence. Quaternary International, 497, pp. 33–46.

Papadopoulou, P., Tsoni, M., Konidaris, G.E., Tourloukis, V., Panagopoulou, E., Karkanas, P., Harvati, K. and Iliopoulos, G., this volume. Ostracod contribution to the palaeoenvironmental study of Kyparissia 4 (Megalopolis Basin, Greece).

Reumer, J.W.F., Mol, D. and Kahlke, R.D., 2018. First finds of Pleistocene *Macaca sylvanus* (Cercopithecidae, Primates) from the North Sea. Revue de Paléobiologie, 37(2), pp. 555–560.

Rook, L., Mottura, A. and Gentili, S., 2001. Fossil *Macaca* remains from RDB quarry (Villafranca d'Asti, Italy): new data and overview. Journal of Human Evolution, 40(3), pp. 187–202.

Smith, B.H., 1994. Sequence of emergence of the permanent teeth in *Macaca*, *Pan*, *Homo*, and *Australopithecus*: its evolutionary significance. American Journal of Human Biology, 6(1), pp. 61–76.

Smith, B.H., Crummett, T.L. and Brandt, K.L., 1994. Ages of eruption of primate teeth: A compendium for aging individuals and comparing life histories. American Journal of Physical Anthropology, 37(S19), pp. 177–231.

Symeonidis, N., Zapfe, H., 1976. Primatenzähne (Cercopithecidae) aus einer plistozänen Spaltenfüllung im Steinbruch Tourkobounia, Athen. Annales Géologiques des Pays Helléniques, 28, pp. 207–214.

Szalay, F.S., Delson, E., 1979. Evolutionary History of the Primates. Academic Press, New York.

van Kolfschoten, T., 2020. Lowland monkeys. New finds from Tegelen-Maalbeek (The Netherlands), in: Bazelmans, J., Beukers, E., Brinkkemper, O., van der Jagt, I.M.M., Rensink, E., Smit, B.I., Walrecht, M. (Eds.), Tot op het bot onderzocht. Essays ter ere van archeozoöloog Roel Lauwerier. Rijksdienst voor het Cultureel Erfgoed, Amersfoort, pp. 11–17.

van Kolfschoten, T., Konidaris, G.E., Doukas, C., Athanassiou, A., Tourloukis, V., Panagopoulou, E., Karkanas, P. and Harvati, K., this volume. Voles (Rodentia, Mammalia) as a proxy to date the site Kyparissia 4 (Megalopolis Basin, Greece).

3 The late Middle and Late Pleistocene: results from Greece and beyond

25 A PRELIMINARY INVESTIGATION OF THE CRANIAL BREAKAGE PATTERNS OF THE LATE MIDDLE PLEISTOCENE CRANIA FROM APIDIMA CAVE, GREECE

Judith Beier[1,2,*], Mirsini Kouloukoussa[3,4], Konstantinos Evangelou[3,4], Vassilis G. Gorgoulis[4,5,6,7], Joachim Wahl[2], Katerina Harvati[1,2,3,8]

[1]*DFG Center for Advanced Studies 'Words, Bones, Genes, Tools', University of Tübingen, Tübingen, Germany*
[2]*Paleoanthropology, Institute for Archaeological Sciences and Senckenberg Centre for Human Evolution and Palaeoenvironment, Department of Geosciences, University of Tübingen, Tübingen, Germany*
[3]*Museum of Anthropology, Medical School, National and Kapodistrian University of Athens, Athens, Greece*
[4]*Department of Histology and Embryology, Medical School, National and Kapodistrian University of Athens, Athens, Greece*
[5]*Biomedical Research Foundation of the Academy of Athens, Athens, Greece*
[6]*Faculty of Biology, Medicine and Health, University of Manchester, Manchester, UK*
[7]*Ninewells Hospital and Medical School, University of Dundee, Dundee, UK*
[8]*Centre for Early Sapiens Behaviour (SapienCE), Department of Archaeology, History, Cultural Studies and Religion, University of Bergen, Bergen, Norway*
**judith.beier@uni-tuebingen.de*

http://dx.doi.org/10.15496/publikation-97591

Keywords: Apidima; Middle Pleistocene; cranial fractures; timing of breakage; perimortem; postmortem

25.1 THE APIDIMA SITE AND HOMININ FOSSILS

The Apidima site is located in close proximity to the village Areopolis on the coast of the Mani peninsula in the southern Peloponnese, Greece (Harvati et al., 2009; Harvati, 2016, 2022). The site consists of five caves (A, B, C, D, and E), which are located directly on the coast and can today only be reached by boat. The caves are filled with sediments from the Middle and Late Pleistocene, which are eroding out of the caves (Pitsios, 1999; Harvati et al., 2011; Bräuer et al., 2019). In the late 1970s, a team of researchers from the Museum of Anthropology of the School of Medicine, National and Kapodistrian University of Athens, unearthed two incomplete hominin crania [Apidima 1 (or LAO1/S1) and Apidima 2 (or LAO1/S2)] from the breccia of the cave wall of cave A. The remains were excavated *en bloc* and then prepared in the laboratory to free them mechanically from the surrounding breccia (Pitsios, 1999). Both crania are fragmentary, but the breccia matrix still holds the fragments in place and together.

Apidima 1 preserves a major part of the left parietal bone, the superior right parietal, as well as parts of the occipital and left temporal bones. A large piece of rock is still attached to it (cf. Figure

J. Beier: https://orcid.org/0000-0002-5375-6958
M. Kouloukoussa: https://orcid.org/0000-0003-3704-0455
K. Evangelou: https://orcid.org/0000-0002-2462-5748
V. G. Gorgoulis: https://orcid.org/0000-0001-9001-4112
J. Wahl: https://orcid.org/0000-0002-5733-8905
K. Harvati: https://orcid.org/0000-0001-5998-4794

1; Harvati et al., 2019). The second cranium, Apidima 2, is more complete and comprises large parts of the facial skeleton and a near complete cranial vault, but no mandible. The cranial base and occipital bone are not preserved (cf. Figure 1; Harvati et al., 2019). Apidima 2 represents a Neanderthal specimen and is dated to >170 thousand years ago (ka BP) (Harvati et al., 2011; Bartsiokas et al., 2017; Bräuer et al., 2019; Harvati et al., 2019), whereas Apidima 1 was classified by Harvati et al. (2019) as early *Homo sapiens*, dating to >210 ka BP (see also Harvati et al., 2020; Harvati, 2022).

25.2 OBJECTIVES AND METHODS

A previous anthropological examination of Apidima 2 has concluded that some of the fractures on the frontal bone are the result of traumatic blows (Coutselinis et al., 1991, 1995). Later, it was suggested that all fractures result from sediment pressure during deposition and thus represent taphonomic damage (Geanacos, 2001; Pitsios, 2007; Pitsios et al., 2007). The fractures of the less complete cranium, Apidima 1, have not been studied until now.

Feature (references)	Description	Fresh bone	Dry bone	Inconclusive	Criteria evaluated in this study
Outline	Course of breakage line on ectocranial surface	Curved	Stepped	Straight	Classification of each breakage line as curved, stepped, or straight
Path of least resistance (Symes et al., 2012; Fleming-Farrell et al., 2013; Galloway and Wedel, 2014; Loe, 2016)	Propagation of breakage line towards a biomechanically weaker area of the skull	Present	Absent	-	Evaluation of whether a breakage line runs towards a biomechanically weaker skull area (yes, no)
Angle (Fleming-Farrell et al., 2013; Jordana et al., 2013b; Kranioti, 2015; Sala et al., 2016)	Angulation between ectocranial cortical bone table and the breakage edge (surface of outer and inner table and diploë exposed by breakage)	Oblique (acute: <70°, or obtuse: >110°)	Right (70°-110°)	-	Measurement of the angle between the ectocranial and breakage edge surfaces at several points along one breakage line or defect in 2D cross sections
Texture (Fleming-Farrell et al., 2013; Jordana et al., 2013a; Sala et al., 2016)	Texture of breakage edge (surface of outer and inner table and diploë exposed by breakage)	Smooth	Jagged	-	Classification of the texture as smooth or jagged at the same points, where angles were measured
Plastic response (Symes et al., 2012; Fleming-Farrell et al., 2013; Kranioti, 2015)	Permanent plastic deformation (elastic capacity of bone exceeded)	Present	-	Absent	Assessment if breakage lines show signs of a plastic response (yes, no)

Table 1: Criteria used to distinguish peri- from postmortem timing of cranial breakages in the Apidima crania.

In this preliminary investigation, we examined the cranial breakage patterns of Apidima 1 and 2 to assess the timing of breakage and to evaluate whether the fractures represent postmortem taphonomic damage (dry bone breakage) or perimortem (fresh bone) fractures and, thus, could possibly be traumatic injuries.

To evaluate the timing of breakage of the two Apidima fossils, we employed virtual anthropological methods and used medical computed tomography (CT) scans of the two crania, kindly provided by the Museum of Anthropology and the First Department of Radiology of the National and Kapodistrian University of Athens. Using CT scans, the crania could be investigated in virtual cross-sections, allowing for the examination of internal structures or otherwise macroscopically inaccessible areas. This way, we were able to perform a non-destructive examination of the endo- and ectocranial morphology of the fracture lines even though most of them are still covered by breccia. For each breakage line, we evaluated five morphological breakage features: (1) breakage outline, (2) path of least resistance, (3) breakage angle (measured in CT cross sections and on several points along one breakage line), (4) texture (assessed at the same points where also angles were measured), and (5) plastic response. For details see Table 1 and references therein. We assessed these five features on 15 breakage lines in Apidima 1, and 37 breakage lines in Apidima 2 (Figure 1). In addition, we evaluated the edges of four defects (i.e., visible damages on the ectocranial surface, most of which also covered by breccia or plaster) in Apidima 2, using a reduced set of three features (breakage angle, texture, plastic response). Given the assessments of the single features, we then concluded for every breakage line whether its morphology conforms more to a fresh or a dry bone breakage, or is inconclusive regarding its timing of breakage.

25.3 RESULTS AND DISCUSSION

The evaluation of five morphological breakage features to distinguish perimortem (fresh) from postmortem (dry) bone fractures performed in this preliminary study revealed mostly inconclusive breakage lines and defects in both Apidima crania (Beier, 2021). 66.7% (10 of 15) of breakage lines in Apidima 1, and 73.0% (27 of 37) plus four defects in Apidima 2 are inconclusive regarding their timing of breakage. In Apidima 1, 26.7% (4 of 15) of the breakages exhibit a morphology that is rather in agreement with fresh bone breakage, while the morphology of 6.7% (1 of 15) of the breakages is rather in agreement with dry bone breakages. In Apidima 2, the morphology of 13.5% (5 of 37) of the breakages conforms or rather conforms with fresh bone breakage, while another 13.5% (5 of 37) of breakages are rather in agreement with a dry bone breakage morphology.

The frontal bone fractures of Apidima 2, previously assumed to result from traumatic blows (Coutselinis et al., 1991, 1995), and later assigned to a taphonomic origin (Geanacos, 2001; Pitsios, 2007; Pitsios et al., 2007), exhibit an inconclusive breakage morphology. We therefore cannot contribute additional support for any of the two previous interpretations.

Apart from the many inconclusive breakage morphologies, we found both fresh and dry bone breakage morphologies within one single breakage line in nearly half of all breakages assessed (53.3% in Apidima 1, as well as 43.2% of fractures and 25.0% of defects in Apidima 2). This is a puzzling and unexpected finding because the same fracture or defect should show a (predominantly) fresh or dry bone breakage morphology, but not a mix of both. Our findings were also inconsistent regarding the features ‘breakage angle’ and ‘texture’. Their morphology should be correlated: by definition,

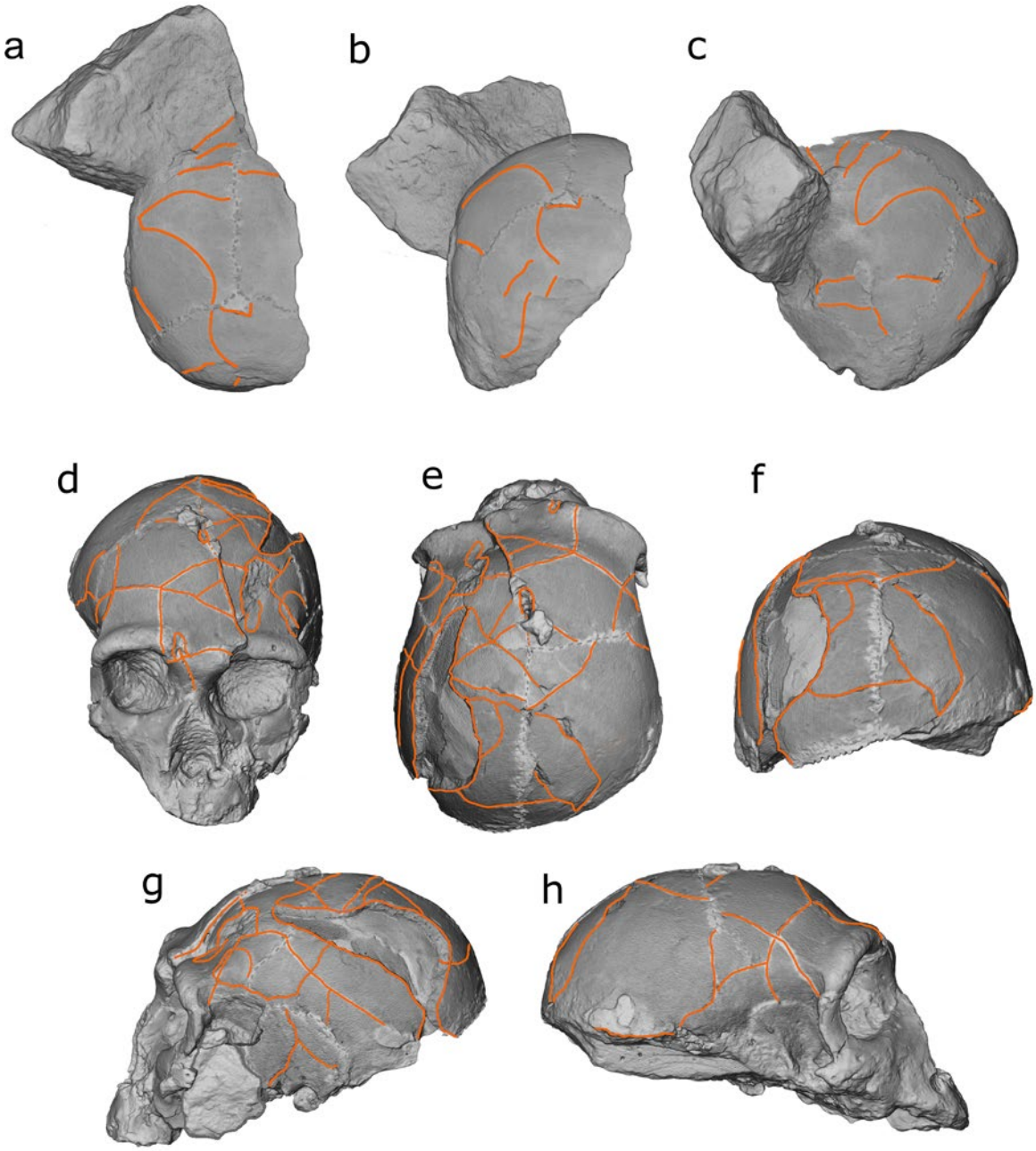

Figure 1: a-c: Overview of the 15 breakage lines examined in Apidima 1 (a: superior view, b: posterior view. c: left superolateral view). d-h: Overview of the 37 breakage lines and four defects examined in Apidima 2 (d: frontal view, e: superior view, f: posterior view, g: left lateral view, h. right lateral view)

fresh bone breakage edges should be oblique and smooth, and dry bone breakage edges should be right-angled and jagged. Here, only 53.3% of the evaluated breakages in Apidima 1, and 62.6% of the evaluated edges in Apidima 2 corresponded to the expected association between the two features 'breakage angle' and 'texture'.

At this preliminary stage of the study, we can think of different reasons that could explain these ambiguous findings. First, it is possible that the

morphological features we used to distinguish fresh from dry bone breakage were too few or too unspecific. Some additional small and subtle features suggested to be good indicators of fresh bone breakage when present could not be assessed so far because of the low resolution of the available medical CT scans. These include, for example, small osseous flake defects on the fracture edges, incomplete fractures with broken cortical layers (fissures) held in place by trabecular bone bridges, cortical bone scales resembling fish scales, and fracture hinging, i.e., broken fragments that remain partially attached to the main body of the bone (for details and additional features see Fleming-Farrell et al., 2013; Jordana et al., 2013a; Kranioti, 2015; Sala et al., 2016; Ribeiro et al., 2020). In a similar vein, very fine, possibly only superficial breakage lines observable on the original crania could often not be detected in the CT scans used here. Using high-resolution micro-CT scans of the crania instead of medical CT scans, when such might be available in the future, could have the potential to improve the analysis threefold: (1) by increasing the overall number of observable breakage lines, (2) by raising the number of successful observations of the features assessed, and (3) by enabling us to include additional features in the evaluation of the timing of breakage.

Further possible explanations for the heterogeneous and inconsistent findings of fresh and dry bone breakages between and within features could relate to the mineralized condition of the Apidima cranial remains and their depositional history. Wet depositional conditions can affect and obscure the timing of breakage through changed decomposition rates (Haglund and Sorg, 2002; Galloway et al., 2014; Augias et al., 2017; Stuart and Ueland, 2017), alterations in the breakage behavior of dry bone after rehydration (Broz et al., 1993; Moraitis and Spiliopoulou, 2006; Augias et al., 2017; King, 2017), and the increased abrasion of characteristic breakage edges in water environments (Haglund and Sorg, 2002; Moraitis and Spiliopoulou, 2006). From what we currently know about the depositional history of the Apidima crania, wet depositional conditions likely occurred on several occasions. The two crania were found only a few centimeters apart from each other, but may in fact be separated by about 40 thousand years (Harvati et al., 2019). It has been suggested that the crania were displaced from the locations where they were originally deposited at distinct times following washing out of underlying sediments, and got mixed up, perhaps by a mudflow event (Harvati et al., 2019). Moreover, sea level changes have been affecting the erosion of cave sediments in the Apidima caves, nowadays located only a few meters above sea level, since Pleistocene times (Pitsios, 1999; Harvati et al., 2011; Bräuer et al., 2019). The timing of breakage of the Apidima cranial breakages is further complicated by the possibility, that (some of) the breakages could have occurred after fossilization. If so, using fresh and dry bone breakage characteristics to determine the timing of breakage might be inadequate and could account for our inconclusive findings. Fossilized bone is assumed to break differently when impacted than both fresh and dry bone (Morlan, 1984; L'Abbé et al., 2015; Gifford-Gonzalez, 2018). To be able to identify fossilized bone breakage and distinguish it from fresh and dry bone breakage, distinct morphological characteristics would be needed, which, to our knowledge, have not been studied and described in as much detail as for dry and fresh bone breakage so far.

Our findings of the cranial breakage patterns of the Apidima fossil crania are therefore preliminary and we caution against overinterpretation of our results. Further methodological work, as well as future geoarchaeological and taphonomic investigations, will help to further clarify the breakage patterns and depositional history of the remains.

ACKNOWLEDGMENTS

This research was supported by the ERC Consolidator Grant ERC-CoG-724703 ("CROSSROADS") and the German Research Foundation (DFG FOR 2237), both awarded to K.H. K.H. is also supported by the ERC Advanced Grant ERC-AdG-101019659 ("FIRSTSTEPS"). We thank the curators and staff of the Museum of Anthropology and the First Department of Radiology of the National and Kapodistrian University of Athens for access to original specimens and for providing the CT data used in this study. We are grateful to A. Karakostis, C. Röding, and J. Kunze for technical support and assistance in this research. The authors express their gratitude to the two anonymous reviewers for their insightful comments and valuable suggestions for improving the manuscript.

REFERENCES

Augias, A., Benmoussa, N., Jacqueline, S., Boudeau, J., Femolant, J.-M., Nogel Jaeger, J., Weil, R., Muller, A.-L. and Charlier, P., 2017. Ante-, péri- ou post mortem? Profil de fracturation en contexte humide: le cas du dépôt en puits (II^{e}-III^{e} siècles apr. J.-C.) de la place du Jeu-de-Paume, Beauvais (Oise). Bulletins et Mémoires de la Société d'anthropologie de Paris, 29(1-2), pp. 112–116.

Bartsiokas, A., Arsuaga, J.L., Aubert, M. and Grün, R., 2017. U-series dating and classification of the Apidima 2 hominin from Mani Peninsula, Southern Greece. Journal of Human Evolution, 109, pp. 22–29.

Beier, J., 2021. Analyses of cranial trauma in Neanderthal and modern human fossil remains. Dissertation, University of Tübingen. http://dx.doi.org/10.15496/publikation-60423

Bräuer, G., Pitsios, T., Säring, D., Harling, M. von, Jessen, F. and Kroll, A. and Groden, C., 2019. Virtual Reconstruction and Comparative Analyses of the Middle Pleistocene Apidima 2 Cranium (Greece). The Anatomical Record, 303(5), pp. 1374–1392.

Broz, J.J., Simske, S.J., Greenberg, A.R. and Luttges, M.W., 1993. Effects of Rehydration State on the Flexural Properties of Whole Mouse Long Bones. Journal of Biomechanical Engineering, 115, pp. 447–449.

Coutselinis, A., Dritsas, C. and Pitsios, T., 1991. Expertise médico-légale du crâne Pléistocène LAO1/S2 (Apidima II), Apidima, Laconie, Grèce. L'Anthropologie (Paris), 95(2/3), pp. 401–408.

Coutselinis, A., Dritsas, C. and Pitsios, T., 1995. Forensic investigation of the Pleistocene skull LAO 1/S2 (Apidima II), Apidima, Laconia, Greece. Acta Anthropologica, 1, pp. 113–117.

Fleming-Farrell, D., Michailidis, K., Karantanas, A., Roberts, N. and Kranioti, E.F., 2013. Virtual assessment of perimortem and postmortem blunt force cranial trauma. Forensic Science International, 229(1-3), p.162.e1–162.e6.

Galloway, A., Wedel, V.L., 2014. Bones of the Skull, the Dentition, and Osseous Structures of the Throat, in: Wedel, V.L., Galloway, A. (Eds.), Broken Bones*:* Anthropological Analysis of Blunt Force Trauma. Charles C. Thomas Publisher Ltd., Springfield, Illinois, pp. 133–160.

Galloway, A., Zephro, L. and Wedel, V.L., 2014. Diagnostic Criteria for the Determination of Timing and Fracture Mechanism, in: Wedel, V.L., Galloway, A. (Eds.), Broken Bones*:* Anthropological Analysis of Blunt Force Trauma. Charles C. Thomas Publisher Ltd., Springfield, Illinois, pp. 47–58.

Geanacos, C., 2001. Report of a meeting. "*Homo (sapiens) taenarius*", the youngest or the oldest Neanderthal in Europe? Human Evolution, 16(3-4), pp. 243–244.

GIFFORD-GONZALEZ, D., 2018. An Introduction to Zooarchaeology. Springer International Publishing, Cham.

HAGLUND, W.D., Sorg, M.H., 2002. Human Remains in Water Environments, in: Haglund, W.D., Sorg, M.H. (Eds.), Advances in Forensic Taphonomy: Method, Theory, and Archaeological Perspectives. CRC Press LLC, Boca Raton, pp. 201–218.

HARVATI, K., 2016. Paleoanthropology in Greece: Recent Findings and Interpretations, in: Harvati, K., Roksandic, M. (Eds.), Paleoanthropology of the Balkans and Anatolia: Human Evolution and its Context. Springer Netherlands, Dordrecht, pp. 3–14.

HARVATI, K., 2022. The hominin fossil record from Greece, in: Vlachos, E. (Ed.), The Fossil Vertebrates of Greece: Vol. 1 - Basal vertebrates, basal tetrapods, afrotherians, glires, and primates. Springer - Nature Publishing Group, Cham, pp. 669–688.

HARVATI, K., Panagopoulou, E. and Runnels, C., 2009. The Paleoanthropology of Greece. Evolutionary Anthropology: Issues, News, and Reviews, 18(4), pp. 131–143.

HARVATI, K., Stringer, C.B. and Karkanas, P., 2011. Multivariate analysis and classification of the Apidima 2 cranium from Mani, Southern Greece. Journal of Human Evolution, 60(2), pp. 246–250.

HARVATI, K., Röding, C., Bosman, A.M., Karakostis, F.A., Grün, R., Stringer, C.B., Karkanas, P., Thompson, N.C., Koutoulidis, V., Moulopoulos, L.A., Gorgoulis, V.G. and Kouloukoussa, M., 2019. Apidima Cave fossils provide earliest evidence of *Homo sapiens* in Eurasia. Nature, 571(7766), pp. 500–504.

HARVATI, K., Röding, C., Bosman, A.M., Karakostis, F.A., Grün, R., Stringer, C.B., Karkanas, P., Thompson, N.C., Koutoulidis, V., Moulopoulos, L.A., Gorgoulis, V.G. and Kouloukoussa, M., 2020. New 3-D geometric morphometric and dating analyses of the Apidima fossil crania support early dispersal of *Homo sapiens* out of Africa [Abstract]. American Journal of Physical Anthropology, 171(S69), 116.

JORDANA, F., Colat-Parros, J. and Bénézech, M., 2013a. Breakage patterns in human cranial bones. Romanian Journal of Legal Medicine, 21(4), pp. 287–292.

JORDANA, F., Colat-Parros, J. and Bénézech, M., 2013b. Diagnosis of skull fractures according to postmortem interval: an experimental approach in a porcine model. Journal of Forensic Sciences, 58(S1), pp. 156–162.

KING, A., 2017. The Effects of Collagen Rehydration on Postmortem Fracture Morphology: Implications for the Perimortem Interval. Master Thesis, Ontario, Canada, University of Waterloo.

KRANIOTI, E.F., 2015. Forensic investigation of cranial injuries due to blunt force trauma: current best practice. Research and Reports in Forensic Medical Science, 5, pp. 25–37.

L'ABBÉ, E.N., Symes, S.A., Pokines, J.T., Cabo, L.L., Stull, K.E., Kuo, S., Raymond, D.E., Randolph-Quinney, P.S. and Berger, L.R., 2015. Evidence of fatal skeletal injuries on Malapa Hominins 1 and 2. Scientific Reports, 5, 15120.

LOE, L., 2016. Perimortem Trauma, in: Blau, S., Ubelaker, D.H. (Eds.), Handbook of Forensic Anthropology and Archaeology. Routledge Taylor & Francis Group, New York, London, pp. 346–372.

MORAITIS, K., Spiliopoulou, C., 2006. Identification and Differential Diagnosis of Perimortem Blunt Force Trauma in Tubular Long Bones. Forensic Science, Medicine and Pathology, 2(4), pp. 221–230.

MORLAN, R.E., 1984. Toward the Definition of Criteria for the Recognition of Artificial Bone Alterations. Quaternary Research, 22, pp. 160–171.

Pitsios, T., 1999. Paleoanthropological research at the cave site of Apidima and the surrounding region (South Peloponnese, Greece). Anthropologischer Anzeiger, 57(1), pp. 1–11.

Pitsios, T., 2007. Απήδημα: τα ανθρώπινα ευρήματα (Apidima: the anthropomorphic findings), in: Museum of Anthropology, University of Athens (Ed.), Proceedings of the International Scientific Symposium on Paleoanthropology of the Mani Peninsula, South Peloponnese, Greece, 25.-28. September 1998, Athens - Areopolis, Greece, pp. 33–44.

Pitsios, T., Rondoyanni, T., Mettos, A. and Georgiou, C., 2007. Paleoanthropological and Paleogeographical Research in Mani Peninsula (South Peloponnese, Greece), in: Museum of Anthropology, University of Athens (Ed.), Proceedings of the International Scientific Symposium on Paleoanthropology of the Mani Peninsula, South Peloponnese, Greece, 25.-28. September 1998, Athens - Areopolis, Greece, pp. 103–111.

Ribeiro, P., Jordana, X., Scheirs, S., Ortega-Sánchez, M., Rodriguez-Baeza, A., McGlynn, H. and Galtés, I., 2020. Distinction between perimortem and postmortem fractures in human cranial bone. International Journal of Legal Medicine, 134(5), pp. 1765–1774.

Sala, N., Pantoja-Pérez, A., Arsuaga, J.L., Pablos, A. and Martínez, I., 2016. The Sima de los Huesos Crania: Analysis of the cranial breakage patterns. Journal of Archaeological Science, 72, pp. 25–43.

Stuart, B.H., Ueland, M., 2017. Decomposition in Aquatic Environments, in: Schotsmans, E.M.J., Márquez-Grant, N. and Forbes, S.L. (Eds.), Taphonomy of Human Remains: Forensic Analysis of the Dead and the Depositional Environment. John Wiley & Sons, Ltd, Chichester, UK, pp. 235–250.

Symes, S.A., L'Abbé, E.N., Chapman, E.N., Wolff, I. and Dirkmaat, D.C., 2012. Interpreting Traumatic Injury to Bone in Medicolegal Investigations, in: Dirkmaat, D.C. (Ed.), A Companion to Forensic Anthropology. John Wiley & Sons, Ltd, Chichester, UK, pp. 340–389.

26 MUGHARET EL'ALIYA: ADAPTING THE METHOD OF SURFACE REGISTRATION TO THE HOMININ FOSSIL RECORD

Carolin Röding[1,*], Chris Stringer[2], Rodrigo S. Lacruz[3], Katerina Harvati[1,4]

[1]*Paleoanthropology, Institute for Archaeological Sciences and Senckenberg Centre for Human Evolution and Palaeoenvironment, Department of Geosciences, Eberhard Karls University of Tübingen, Tübingen, Germany*
[2]*Centre for Human Evolution Research, The Natural History Museum, London, UK*
[3]*Department of Molecular Pathobiology, New York University College of Dentistry, New York, NY, USA*
[4]*DFG Centre of Advanced Studies 'Words, Bones, Genes, Tools', Eberhard Karls University of Tübingen, Tübingen, Germany*
**carolin.roeding@uni-tuebingen.de*

http://dx.doi.org/10.15496/publikation-97590

Keywords: surface registration; iterative closest point search; fragmentary; fossil

26.1 INTRODUCTION

When hearing the words 'human fossil', most people have a few famous fossils in mind. However, besides well-known, rather complete, iconic specimens, the hominin fossil record mainly comprises fragmentary remains. Technological improvements in the last decades allow us to analyze fragmented and/or damaged fossils in a comprehensive framework and study materials that could not be analyzed in depth at the time of their discovery (e.g., Zollikofer et al., 2005; Hublin et al., 2017; Harvati et al., 2019; Bosman et al., 2019). Most of these improvements are part of the field of virtual anthropology and the toolkit of geometric morphometrics.

Geometric morphometrics relies on landmark configurations to capture shape. Landmarks are homologous points covering recognizable anatomical structures that can be extended by semi-landmarks on curves and surfaces (for discussion see e.g., Bookstein, 1997; Slice, 2007; Gunz et al., 2005; Mitteroecker and Gunz, 2009; Zelditch et al., 2012). Generalized Procrustes superimposition (GPA) enables the statistical analysis of complex shapes, which previously were difficult to quantify, in a comparative framework (e.g., Harvati, 2003; Gunz et al., 2009; Gunz and Harvati, 2007; Freidline et al., 2012). In a GPA, landmarks from all individuals within a sample are translated into a common coordinate system and the information on orientation, location, and size is removed (e.g., Zelditch et al., 2012). From a theoretical point of view, three landmarks are sufficient to capture shape differences (e.g., Zelditch et al., 2012). However, the number of landmarks considered to capture biologically meaningful shape differences is usually higher and depends mostly on the discriminating power of the landmark configuration and the complexity of the shape analyzed (for dis-

C. Röding: https://orcid.org/0000-0001-6319-2001
C. Stringer: https://orcid.org/0000-0002-9183-7337
R. Lacruz: https://orcid.org/0000-0002-0776-6143
K. Harvati: https://orcid.org/0000-0001-5998-4794

cussion see e.g., Zelditch et al., 2012; Watanabe, 2018). Fragmentary and/or damaged fossils may not preserve a biologically meaningful landmark set required for landmark-based analyses of shape, even considering well-established protocols for geometric and statistical reconstruction of missing data (e.g., Gunz et al., 2004, 2009; Zollikofer et al., 2005; Harvati et al., 2019).

Here, we aim to adapt the method of surface registration to the analysis of the fragmentary fossil hominin left maxilla from Mugharet el'Aliya (Morocco) as a case study (c.f. Röding et al., 2023). Our goal is to demonstrate the potential of the method of surface registration for the study of fragmentary fossils that preserve an insufficient number of landmarks for commonly used geometric morphometric analyses.

26.1.1. THE CASE OF MUGHARET EL'ALIYA

In 1939, a left maxillary fragment of a juvenile hominin was recovered from the cave site of Mugharet el'Aliya on the Moroccan Atlantic coast (35°45′N, 5°56′W; Coon in Şenyürek, 1940). The cave sediments have yielded archeological and anthropological material ranging from the Neolithic to the Middle Stone Age (e.g., Coon, 1957a; Hublin, 1993; Bouzouggar et al., 2002). The maxillary fragment is attributed to the Aterian lithic industry and dates to ca. 35-60 ka (e.g., Coon, 1957b; Howe, 1967; Wrinn and Rink; for discussion see Röding et al., 2023).

The Mugharet el'Aliya fossil included three unerupted teeth and a large portion of the left hemi-maxilla (Fig. 1 Step 1; Röding et al., 2023; references therein). The maxilla is characterized by a large absolute size that exceeds the size of recent modern humans of comparable dental age, lack of a deep and distinct canine fossa, a curvature along the transverse plane of the maxilla ('*incurvatio inframalaris frontalis*'), and a root of the zygomatic process that originates anterior to the first permanent molar (Şenyürek, 1940; Minugh-Purvis, 1993; Hublin, 1993, 2000; Röding et al., 2023). Some of these features deviate from the typical maxillary anatomy of adult modern humans, while others are considered to be typical of modern humans and poorly developed or absent in Neanderthals (for discussion see Röding et al., 2023; c.f. e.g., Sergi, 1947; Pope, 1991; Minugh-Puris, 1993; Lieberman et al., 2002; Weber and Krenn, 2017; Lacruz et al., 2019; Schuh et al., 2020). Because of the mixed set of traits seen in the preserved anatomy of the Mugharet el'Aliya maxilla, this enigmatic fossil has been described as showing modern human-like, unclear, or 'archaic' / 'Neanderthal-like' features (e.g., Şenyürek, 1940; Minugh-Purvis, 1993; Hublin, 1993).

The use of common linear measurements to solve Mugharet el'Aliya's enigma is hindered by the fossil's incompleteness. Further, the limited number of preserved diagnostic features provides an insufficient number of homologous points and structures for a comprehensive study using the standard toolkit of geometric morphometrics. To circumvent these shortcomings and to try to provide an unbiased description of the maxilla, we followed a recently described protocol for surface registration to enable the analysis of the entire preserved external morphology of Mugharet el'Aliya (Fig. 1; cf. Schlager and Rüdell, 2013; Röding et al., 2023).

26.2 MATERIALS AND METHODS

We evaluated the external morphology of the maxillary fragment through an ontogenetic dataset of 80 CT and surface scans comprised of Neanderthals, fossil and recent *Homo sapiens*. The resolution of the CT scans ranges from 26 to 466 µm and for meshes obtained from surface scans from 345 to 1,629 µm calculated as mean edge length. All scans were obtained by the equipment available

to the respective repositories. For further details about the sample please see Röding et al. (2023: Material & Methods).

The surface registration protocol aims to best match a reference mesh to a target mesh via an iterative closest point (ICP) algorithm (Fig. 1). A sample of triangular meshes with the identical number of corresponding vertices is created when repeating the protocol for a set of target meshes and a consistent reference mesh. Here, Mugharet el'Aliya was the consistent reference and all other individuals in the sample were considered the targets. The mesh vertices can be extracted and – after superimposition – used as coordinates during statistical analyses. Possible statistical analyses include principal component analyses (PCA), common allometric component analyses (CAC), discriminant function analyses (DFA), and the calculation of Procrustes distances (PD), all of which are frequently used in geometric morphometric studies (cf. Röding et al., 2023).

The first step is to create triangular meshes from the surfaces in question. Surface meshes can be extracted from CT scans via semi-automated segmentation (e.g., Neubauer et al., 2009) or as output from the surface scanning process. Mesh cleaning and manipulation allow the creation of a single-layered triangular mesh (Fig. 1 Step 1). In the case of samples combining surfaces from both anatomical sides, surfaces from one side have to be mirrored and their vertex orientation inverted. These preparations are essential to avoid distortions and mismatches in the following steps.

Next, a limited number of homologous landmarks are digitized on each surface. These landmarks facilitate an initial landmark-based registration via thin-plate spline (TPS) algorithm between the reference and each target and are discarded after this step (e.g., Zelditch et al., 2012). The reference is superimposed and translated into a common coordinate system with each target during the initial registration. To enable a reliable initial registration the used landmarks should be spread out over the entire surface in question as much as possible. In the case of Mugharet el'Aliya, five landmarks were sufficient during the initial registration for the analysis of the entire complex external maxillary morphology in an ontogenetic sample (Fig. 1 Step 2; c.f. Röding et al., 2023). Thereby, the optimal number of landmarks is dependent on the complexity and size of the surface region of interest. One possibility to determine the optimal number of landmarks is to compare the original meshes of a subsample with their corresponding meshes created via surface registration based on varying numbers of landmarks (cf. Results, Fig. 2). The landmark set combining as small a number of landmarks as possible with very good surface matches across the subsample can be considered optimal.

The actual step of surface registration, also called ICP-matching, includes a non-rigid ICP algorithm (Fig. 1 Step 3). Here, the elastic component is based on Gaussian displacement vectors (Moshfeghi et al., 1994). The non-rigid ICP matching is run with multiple iterations to ensure the best possible match of the reference surface onto the target. Each iteration consists of four steps (cf. Schlager and Rüdell, 2013). First, each vertex of the reference mesh is projected onto the target mesh. Then all displacement vectors for the closest points that point in the wrong direction or where the angle between the normal and the displacement vector exceeded 45° are discarded. This is followed by applying Gaussian smoothing based on the neighborhood of each vertex to the resulting displacement vectors. Then the resulting surface is smoothed to prevent mesh folding (Vollmer et al., 1999).

After the ICP-matching, the coordinates underlying the mesh vertices are extracted (Fig. 1 Step 4). GPA allows translating the coordinates of all individuals into a common coordinate system and superimposing them to allow a statistical anal-

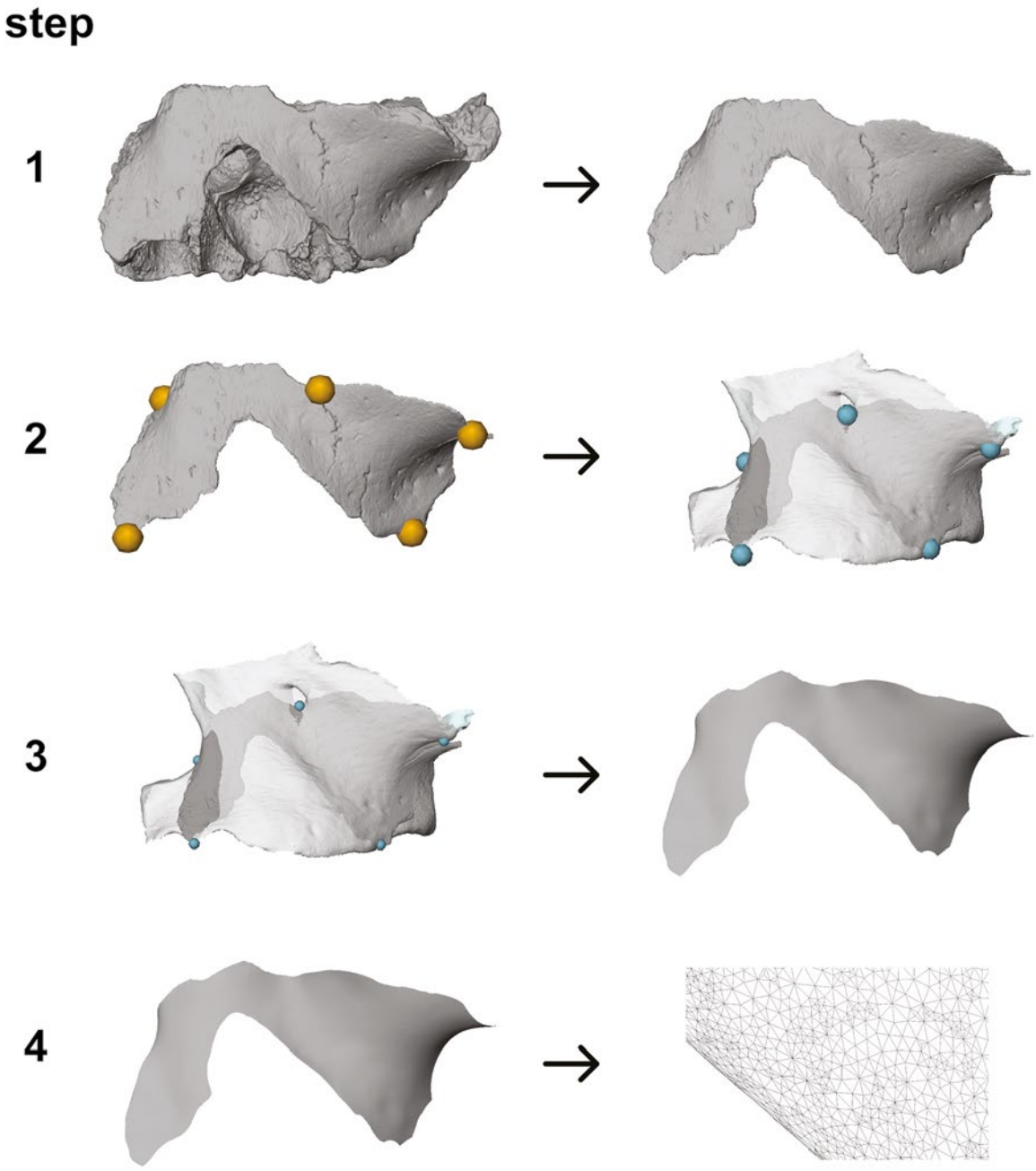

Figure 1: Visualization of the main steps for the method of surface registration. Step 1: extraction of single-layered triangular meshes from the original surfaces. Step 2: initial landmark-based TPS registration of the reference onto the target mesh. Step 3: Elastic ICP-matching of the registered reference and target meshes. Step 4: Extraction of the vertices from the resulting new single-layered triangular meshes as coordinates for further analysis. Images are not scaled. Mugharet el'Aliya is courtesy of the Peabody Museum of Archaeology and Ethnology, Harvard University, 39-69-50/N3635.0.

ysis of the resulting Procrustes shape coordinates. During GPA, information about orientation and location is removed and the coordinate configurations are scaled to centroid size (CS). CS is calculated as the square root of the summed squares of each landmark-centroid distance (e.g., Zelditch et al., 2012).

Based on the Mugharet el'Aliya dataset, the intra- and inter-observer errors of this method were evaluated via multiple measurements of the same

DISTANCE TYPE	ERROR TYPE	N	MEAN	SD	MIN	MAX
Euclidean	intraobserver 1	50	0.434	0.186	0.051	0.750
	intraobserver 2	50	0.280	0.150	0.078	0.700
	interobserver	125	0.458	0.206	0.133	1.147
mesh	intraobserver 1	349,940	0.031	0.076	0	1.343
	intraobserver 2	349,940	0.034	0.070	0	0.975
	interobserver	874,852	0.030	0.064	0	0.711

Table 1: Summary statistics of the intra- and interobserver errors. Errors at the level of landmark placement are shown as Euclidean distances between repeated measures and at the level of resulting surfaces as mesh distances between all vertex combinations. All distances are given in mm and values rounded to three decimals.

individual, which were carried out by two observers (C.R.; J.Z.). In addition, the method's inherent error was assessed by comparing each mesh created via surface registration against the corresponding original.

A combination of two different software environments made the here described measurement protocol possible. Avizo 9.2 Lite (Visualization Science Group) was used to create meshes and obtain fixed landmarks. All other steps were carried out in R (R Developmental Core Team, 2020) by using freely available R packages, mainly geomorph (version 4.0.4; Adams et al., 2022), meshR (version 0.4.200213; Schlager, 2020), Morpho (version 2.9; Schlager, 2017), Rvcg (version 0.20.2; Schlager, 2017), and shapes (version 1.2.6; Dryden, 2021). Graphics were created in R and processed in Adobe Illustrator CS5.

26.3 RESULTS

The intra- and inter-observer errors were evaluated both on the level of the landmarks placed for initial registration and the resulting surfaces (Table 1). Euclidean distances between repeated measures of the placed landmarks range from 0.05 to 1.15 mm with an overall average of 0.41 mm. This translates to an error between 0.83 and 1.755% of the Euclidean distance between each placed landmark in the configuration and the configuration centroid (for discussion see e.g., Röding et al., 2021; Singleton, 2002). In contrast, distances between all the meshes resulting from the repeated measurements show an average of 0.03 mm. Out of all vertex combinations of the error measurements (N=1,574,730) less than 0.001% (N=51) exceed a displacement of 1 mm.

Additionally, the method's inherent error was assessed via distance heat maps in which each mesh created via surface registration was compared to the corresponding original. Distance heat maps show almost no displacement within the surface area in well-preserved, complete individuals (Fig. 2a). In contrast, a smoothed mesh surface is created, and the displacement can locally exceed 1 mm in individuals showing taphonomic damage or structures absent the reference mesh (e.g., additional foramen) (Fig. 2b).

26.4 DISCUSSION

The maxillary fragment from Mugharet el'Aliya is one of many only partially published or poorly described fossil human remains. Their often-fragmented nature in combination with the lack of suitable methods available at the time of their discovery may have contributed to their limited exposure to paleoanthropological research. The method of surface registration implemented here has the potential to be a robust research alternative in the growing toolkit for the study of fragmentary specimens. Especially with respect to remains that

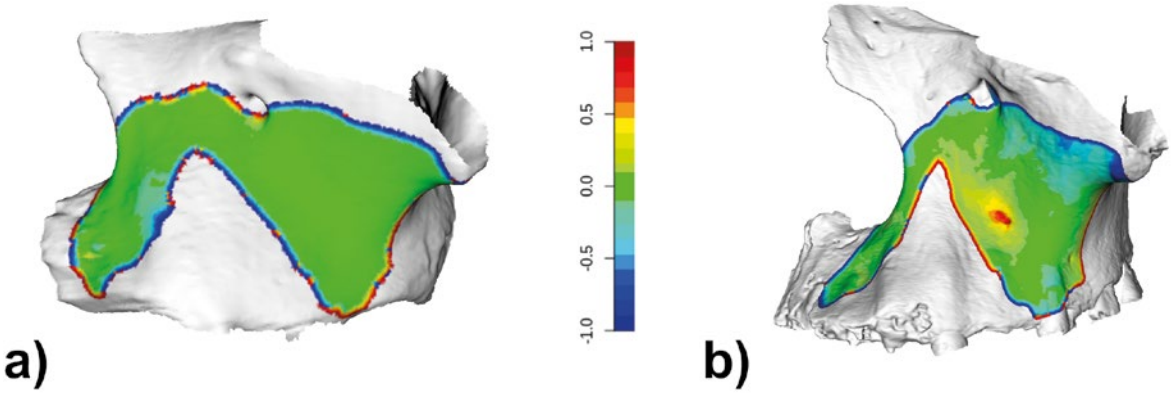

Figure 2: Illustration of the method's inherent error. a) Example distance heat map for a good match between the mesh created via surface registration and the corresponding original. b) Example distance heat map for a relatively bad match between the mesh created via surface registration and the corresponding original. Distances in the heat maps are shown in mm and translated to a color code ranging from no difference in green to ≥ 1 mm difference in dark red and to ≥ -1 mm difference in dark blue. Images are not scaled.

do not preserve enough linear measurements or homologous landmarks for a conventional linear analysis or typical geometric morphometric study, the surface registration method can potentially enable the investigation of the entire preserved morphology that was impossible to analyze quantitatively thus far. To our knowledge, the study of the maxillary fragment from Mugharet el'Aliya is among the first to use surface registration in a fossil context (cf. Röding et al., 2023).

Awareness of potential sources of error and bias is of paramount importance in the field of geometric morphometrics and especially in the study of fragmentary remains, due to potential additional sources of error such as prior reconstructions (for discussion see e.g., von Cramon-Taubadel et al., 2007; Fruciano, 2016; references therein). Our results of the error estimation for the surface registration method showed a high degree of reproducibility in a fossil dataset in due consideration of the following points. The intra- and interobserver error of the final dataset consisting of surface vertices is reduced significantly by discarding the landmark data after the initial registration (Table 1). Although landmark placement influences the error measurements at the edges of the meshes, less than 0.001% of the vertex combinations showed a displacement exceeding 1 mm on surfaces with an absolute surface area ranging from 1.2 to 5.2 cm^2. Furthermore, in our dataset, the error estimates at the level of the landmarks are on average more than 10 times greater than at the level of the vertex coordinates.

In addition to the observer error, each method possesses an inherent error. Distance heat maps between each mesh created via surface registration and the corresponding original showed a minimal method error for well-preserved, complete specimens (Fig. 2a). Here, the definition of 'well-preserved' and 'complete' is restricted to the region of interest and does not refer to the individual's overall state of preservation. The method error increases in specimens showing structures absent in the reference mesh (e.g., additional foramina) or with taphonomic damage (Fig. 2b). In such cases, the surface registration results in smoothed mesh surfaces in the areas deviating from the condition of the reference mesh. Analyses are not significantly affected by small locally confined smoothed surface areas as long as the vast majority of the original surface morphology is preserved (cf. Veneziano et al., 2018).

However, the ICP-matching and, thereby, the surface registration method are sensitive to missing data. This includes large, smoothed surface areas resulting from the above-described method error.

Individuals displaying such large, smoothed surface areas should be excluded from the samples to be analyzed (see Röding et al., 2023) to avoid artifacts and potential influence on the analyses (cf. Profico et al., 2016). In the absence of a well-established threshold, individuals were excluded on a case-by-case basis due to the amount of smoothing and distance of the smoothed surface area to the original mesh. Moreover, all individuals with missing data in crucial parts of the region of interest, or with large areas of missing data, cannot be incorporated into the surface registration protocol as described here. In the case of Mugharet el'Aliya, defining the fragmentary fossil of interest as a reference mesh proved the most efficient strategy to minimize the number of individuals excluded from the comparative sample due to missing data (Röding et al., 2023). Further research is needed to adjust the method of statistical shape models (SSM), for example, to the field of paleoanthropology to enable the statistical reconstruction of missing data. SSM's summarize the average shape and the main axis of variation of a training dataset (Sarkalkan et al., 2014). This a-priori knowledge can be applied to reconstruct missing data by completing the preserved shape components with the expected shape of the missing surface area (e.g., Semper-Hogg et al., 2017; Sarkalkan et al., 2014).

In summary, the method of surface registration has the potential to provide a robust research alternative for the study of fragmentary fossil material, which are very often represented in the human fossil record, including from the geological and chronological contexts of interest for the CROSSROADS project. Taking the above discussion into consideration, the surface registration method offers an approach with a high degree of reproducibility for fossil datasets that preserve an insufficient number of homologous points and structures for a comprehensive study using the standard toolkit of geometric morphometrics.

ACKNOWLEDGMENTS

This research was supported by the ERC Consolidator Grant ERC-CoG-724703 ("CROSSROADS") and the German Research Foundation (DFG FOR 2237), both awarded to K.H. K.H. is also supported by the ERC Advanced Grant ERC-AdG-101019659 ("FIRSTSTEPS"). C.S.'s research is supported by the Calleva Foundation and the Human Origins Research Fund and R.S.L.'s research was supported by the MA003 funding from New York University (NYU). We thank S. Schlager (University of Freiburg) for his extensive help regarding the method of surface registration. In addition, we would like to thank J. Zastrow (J.Z.) and H. Rathmann for their valuable input and assistance. We are thankful to Loring Burgess and the staff at the Peabody Museum, Harvard University, for granting access to the study of the Mugharet el'Aliya fossil and for providing its CT scans. We thank all curators and their institutions for access to original specimens or CT scans used in the comparative sample. We thank the anonymous reviewer and A. F. Karakostis for their careful reading of our manuscript and their insightful comments and suggestions.

REFERENCES

Adams, D. C., Collyer, M. L., Kaliontzopoulou, A. and Baken, E. K., 2022. Geomorph: Software for geometric morphometric analyses. R package version 4.0.4. https://cran.r-project.org/package=geomorph.

Bookstein, F. L., 1997. Morphometric tools for landmark data: geometry and biology. Cambridge University Press, Cambridge (UK).

Bosman, A. M., Buck, L. T., Reyes-Centeno, H., Mirazón Lahr, M., Stringer, C. and Harvati, K., 2019. The Kabua 1 cranium: Virtual anatomical reconstructions, in: Sahle, Y.,

Reyes-Centeno, H., Bentz, C. (Eds.), Modern Human Origins and Dispersal. Kerns Verlag, Tübingen, pp. 137–170.

Bouzouggar, A., Kozłowski, J. K. and Otte, M. 2002. Étude des ensembles lithiques atériens de la grotte d'El Aliya à Tanger (Maroc). L'Anthropologie, 106, pp. 207–248.

Coon, C.S., 1957a. The Seven Caves. Alfred A. Knopf, New York.

Coon, C.S., 1957b. Correspondence, dated 25 May 1957 to Dr. Hugh Hencken. Harvard University, Peabody Museum Archives.

Dryden, I. L., 2021. shapes: Statistical Shape Analysis. R package version 1.2.6. https://CRAN.R-project.org/package=shapes.

Freidline, S. E., Gunz, P., Harvati, K. and Hublin, J.-J., 2012. Middle Pleistocene human facial morphology in an evolutionary and developmental context. Journal of Human Evolution, 63(5), pp.723–740.

Fruciano, C., 2016. Measurement error in geometric morphometrics. Development Genes and Evolution, 226, pp. 139–158.

Gunz, P., Mitteroecker, P., Bookstein, F. and Weber, G., 2004. Computer aided reconstruction of human crania, in: Fischer-Ausserer, K., Börner, W., Goriany, M. (Eds.), Enter the Past: The E-way into the Four Dimensions of Cultural Heritage. BAR Publishing, Oxford, pp. 92–95.

Gunz, P., Mitteroecker, P. and Bookstein, F., 2005. Semilandmarks in Three Dimensions, in: Slice, D. E. (Eds.), Modern Morphometrics in Physical Anthropology. Kluwer Academic/Plenum Publisher, New York, pp. 73–98.

Gunz, P., Harvati, K., 2007. The Neanderthal 'chignon': Variation, integration and homology. Journal of Human Evolution, 52, pp. 262–274.

Gunz, P., Mitteroecker, P., Neubauer, S., Weber, G. W. and Bookstein, F. L., 2009. Principles for the virtual reconstruction of hominin crania. Journal of Human Evolution, 57(1), pp. 48–62.

Harvati, K., 2003. The Neanderthal taxonomic position: models of intra-and inter-specific craniofacial variation. Journal of Human Evolution, 44(1), pp. 107–132.

Harvati, K., Röding, C., Bosman, A. M., Karakostis, F. A., Grün, R., Stringer, C., Karkanas, P., Thompson, N. C., Koutoulidis, V., Moulopoulos, L. A., Gorgoulis, V. G. and Kouloukoussa, M., 2019. Apidima Cave fossils provide earliest evidence of *Homo sapiens* in Eurasia. Nature, 571, pp. 500–504.

Howe, B., 1967. The Palaeolithic of Tangier, Morocco. American School of Prehistoric Research Bulletin, 22, pp. 1–200.

Hublin, J. J., 1993. Recent Human Evolution in Northwestern Africa, in: Aitken, M. J., Stringer, C. B., Mellars, P. A. (Eds.), The Origin of Modern Humans and the Impact of Chronometric Dating. Princeton, New Jersey: Princeton University Press, pp. 118–131.

Hublin, J. J., 2000. Modern-nonmodern hominid interactions: a Mediterranean perspective, in: Bar-Yosef, O., Pilbeam, D. R. (Eds.), The geography of Neandertals and modern humans in Europe and the Greater Mediterranean. Peabody Museum Bulletins. Cambridge, Massachusetts: Harvard University Press, pp. 157–182.

Hublin, J. J., Ben-Ncer, A., Bailey, S. E., Freidline, S. E., Neubauer, S., Skinner, M. M., Bergmann, I., Le Cabec, A., Benazzi, S., Harvati, K. and Gunz, P., 2017. New fossils from Jebel Irhoud, Morocco and the pan-African origin of *Homo sapiens*. Nature, 546, pp. 289–292.

Lacruz, R. S., Stringer, C. B., Kimbel, W. H., Wood, B., Harvati, K., O'Higgins, P., Bromage, T. G. and Arsuaga, J. L., 2019. The evolutionary history of the human face. Nature Ecology & Evolution, 3, pp. 726–736.

Lieberman, D. E., McBratney, B. M. and Krovitz,

G., 2002. The evolution and development of cranial form in *Homo sapiens*. PNAS, 99(3), pp. 1134–1139.

Minugh-Purvis, N., 1993. Reexamination of the Immature Hominid Maxilla from Tangier, Morocco. American Journal of Physical Anthropology, 92(4), pp. 449–461.

Mitteroecker, P., Gunz, P., 2009. Advances in Geometric Morphometrics. Evolutionary Biology, 36, pp. 235–247.

Moshfeghi, M., Ranganath, S. and Nawyn, K., 1994. Three-Dimensional Elastic Matching of Volumes. IEEE Transactions on Image Processing, 3(2), pp. 128–138.

Neubauer, S., Gunz, P. and Hublin, J. J., 2009. The pattern of endocranial shape changes in humans. Journal of Anatomy, 215, pp. 240–255.

Pope, G.G., 1991. Evolution of the zygomaticomaxillary region in the genus *Homo* and its relevance to the origin of modern humans. Journal of Human Evolution, 21, pp. 189–213.

Profico, A., Veneziano, A., Lanteri, A., Piras, P., Sansalone, G. and Manzi, G., 2016. Tuning Geometric Morphometrics: an R tool to reduce information loss caused by surface smoothing. Methods in Ecology and Evolution, 7(10), pp. 1195–1200.

R Development Core Team, 2020. R: a language and environment for statistical computing; version 3.4.1. R Foundation for Statistical Computing: http://www.R-project.org.

Röding, C., Zastrow, J., Scherf, H., Doukas, C. and Harvati, K., 2021. Crown outline analysis of the hominin upper third molar from the Megalopolis Basin, Peloponnese, Greece, in: Reyes-Centeno, H., Harvati, K. (Eds.), Ancient Connections in Eurasia. Tübingen: Kerns Verlag, pp. 13–36.

Röding, C., Stringer, C., Lacruz, R. S. and Harvati, K., 2023. Mugharet el'Aliya: affinities of an enigmatic North African Aterian maxillary fragment. American Journal of Biological Anthropology, 180(2), pp. 352–369.

Sarkalkan, N., Weinans, H. and Zadpoor, A. A., 2014. Statistical shape and appearance models of bone. Bone, 60, pp. 129–140.

Schlager, S., Rüdell, A., 2013. Shape analysis of the human zygomatic bone – surface registration, 82nd Annual Meeting of the American Association for Physical Anthropology, Knoxville, Tennessee, USA, 238.

Schlager, S., 2017. Morpho and Rvcg - Shape Analysis in R: R-Packages for Geometric Morphometrics, Shape Analysis and Surface Manipulations, in: Zheng, g., Li, S., Szekely, G. (Eds.), Statistical Shape and Deformation Analysis. Academic Press, pp. 217–256.

Schlager, S., 2020. mesheR: Meshing Operations on Triangular Meshes. R package version 0.4.200213. https://github.com/zarquon42b/mesheR.

Schuh, A., Gunz, P., Villa, C., Kupczik, K., Hublin, J.-J. and Freidline, S. E., 2020. Intraspecific variability in human maxillary bone modeling patterns during ontogeny. American Journal of Physical Anthropology, 173, pp. 655–670.

Şenyürek, M. S., 1940. Fossil Man in Tangier., in: Papers of the Peabody Museum of American Archaeology and Ethnology, Vol. 16, No. 3. Harvard University Press, Cambridge (USA).

Semper-Hogg, W., Fuessinger, M. A., Schwarz, S., Ellis, E., Cornelius, C.-P., Probst, F., Metzger, M. C. and Schalger, S., 2017. Virtual reconstruction of midface defects using statistical shape models. Journal of Cranio-Maxillo-Facial Surgery, 45(4), pp. 461–466.

Sergi, S., 1947. Sulla morfologia della »facies anterior corporis maxillae« nei Paleantropi di Saccopastore e del Monte Circeo. Rivista di Anthropologia, 35, pp. 4014–08.

Singleton, M., 2002. Patterns of cranial shape variation in the Papionini (Primates: Cerco-

pitecinae). Journal of Human Evolution, 42, pp.547–578.

Slice, D. E., 2007. Geometric morphometrics. Annual Review of Anthropology, 36, pp. 261–281.

Veneziano, A., Landi, F. and Profico, A., 2018. Surface smoothing, decimation, and their effects on 3D biological specimens. American Journal of Physical Anthropology, 166(2), pp. 473–480.

Vollmer, J., Mencl, R. and Müller, H., 1999. Improved Laplacian Smoothing of Noisy Surface Meshes. Computer Graphics Forum, 18(3), pp. 131–138.

Von Cramon-Taubadel, N., Frazier, B. C. and Mirazón Lahr, M., 2007. The problem of assessing landmark error in geometric morphometrics: Theory, methods, and modifications. American Journal of Physical Anthropology, 134(1), pp. 24–35.

Watanabe, A., 2018. How many landmarks are enough to characterize shape and size variation?. PloS ONE, 13(6), e0198341.

Weber, G. W., Krenn, V. A., 2017. Zygomatic root position in recent and fossil hominids. The Anatomical Record, 300(1), pp. 160–170.

Wrinn, P. J., Rink, W. J., 2003. ESR Dating of Tooth Enamel from Aterian Levels at Mugharet el'Aliya (Tangier, Morocco). Journal of Archaeological Science, 30(1), pp. 123–133.

Zelditch, M., Swiderski, D. and Sheets, H., 2012. Geometric morphometrics for biologists: a primer (2nd ed.). Academic Press, London (UK).

Zollikofer, C. P. E., Ponce de León, M. S., Lieberman, D. E., Guy, F., Pilbeam, D., Likius, A., Mackaye, H. T., Vignaud, P. and Brunet, M., 2005. Virtual cranial reconstruction of *Sahelanthropus tchadensis*. Nature, 434(7034), pp. 755–759.

27 GEOARCHAEOLOGICAL AND GEOCHRONOLOGICAL INVESTIGATIONS OF PALAEOLITHIC OPEN-AIR SITES IN EPIRUS, GREECE

Vangelis Tourloukis[1,2,*], Georgia Kourtessi-Philippakis[3], Panagiotis Karkanas[4], Sebastien Nomade[5], Domenico Giusti[1], Nicholas Thompson[1], Aris Varis[1], Annett Junginger[6], Miriam Schaller[6], Katerina Harvati[1]

[1]*Paleoanthropology, Institute for Archaeological Sciences and Senckenberg Centre for Human Evolution and Palaeoenvironment, Department of Geosciences, Eberhard Karls University of Tübingen, Tübingen, Germany*
[2]*Department of History and Archaeology, School of Philosophy, University of Ioannina, Ioannina, Greece*
[3]*Department of History and Archaeology, National and Kapodistrian University of Athens, Athens, Greece*
[4]*M.H. Wiener Laboratory for Archaeological Science, American School of Classical Studies at Athens, Athens, Greece*
[5]*Laboratoire de Sciences du Climat et de l'Environnement, UMR 8212, CEA-UVSQ, IPSL and Université de Paris-Saclay, Gif-sur-Yvette, France*
[6]*Department of Geosciences, Eberhard Karls University of Tübingen, Tübingen, Germany*
**vangelis.tourloukis@ifu.uni-tuebingen.de*

http://dx.doi.org/10.15496/publikation-97589

Keywords: Middle Palaeolithic; geoarchaeology; open-air sites; Greece

27.1 INTRODUCTION

The province of Epirus in north-west Greece hosts the largest Middle Palaeolithic record in Greece (Elefanti and Marshall, 2015). Most of the known Palaeolithic sites in Epirus belong to a particular type of open-air sites, which consist of *terra rossa* deposits and are known as 'red-bed sites' (Fig. 1). Since the 1960's, it has been established that, wherever these red-beds occur, they are almost always associated with Palaeolithic artifacts –in fact, some of these sites are littered with thousands of chipped-stone tools (Dakaris et al., 1964; Higgs and Vita-Finzi, 1966). The interpretation of this association has generated a long and intense controversy (Bailey et al., 1992; Runnels and van Andel, 1993; King and Bailey, 1985; King et al., 1997; Papakonstantinou and Vassilopoulou, 1997; Papagianni, 2000; Runnels and van Andel, 2003; van Andel and Runnels, 2005; Tourloukis, 2009; Tourloukis et al., 2015). For a long time, those sites have been regarded as a fortuitous admixture of archaeological remains from different periods: sites with reworked deposits that essentially provide no context for the artifacts and are, therefore, of little archaeological value.

Mostly as a result of this view, extremely few of these sites have so far been examined with subsurface investigations (e.g., Dakaris et al., 1964). Recently, geoarchaeological work at the site of Kokkinopilos showed that, contrary to this old view, the red-bed sites can indeed yield artifacts from

V. Tourloukis: https://orcid.org/0000-0002-9527-2708
P. Karkanas: https://orcid.org/0000-0002-7156-671X
S. Nomade: https://orcid.org/0000-0001-7373-0571
D. Giusti: https://orcid.org/0000-0003-1438-4036
N. Thompson: https://orcid.org/0009-0003-4770-1744
A. Varis: https://orcid.org/0000-0003-2343-2087
A. Junginger: https://orcid.org/0000-0003-3486-0888
K. Harvati: https://orcid.org/0000-0001-5998-4794

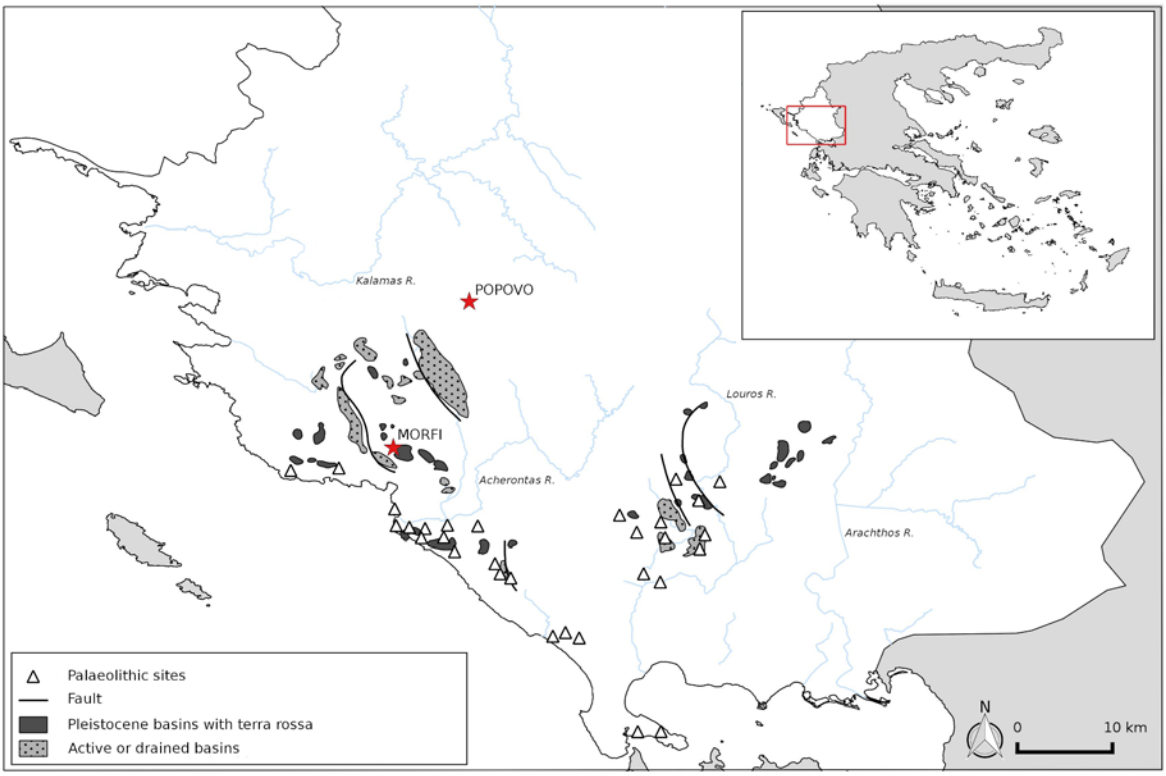

Figure 1: Map of Epirus showing the distribution of Palaeolithic sites in relation to the locations of Pleistocene basins with *terra rossa* and the active or drained poljes (modified after Runnels and van Andel, 2003). The sites of Popovo and Morfi, discussed in this study, are marked with a star.

in situ, geologically undisturbed –and hence datable– contexts (Tourloukis et al., 2015). Following on this work, we conducted a two-year geoarchaeological project (2016-2017) aimed again at red-bed sites, for two main reasons:

1) While most of the evidence from the red-beds is attributed to the Middle Palaeolithic, there are also specimens of potentially Lower and Upper Palaeolithic morphotypes. The high density of artifacts indicates an intensive and/or 'persistent' occupation during certain periods, as seems to be the case with the Middle Palaeolithic. Evidently, the lacustrine/marshy settings of those sites must have played a significant role in the Palaeolithic economy of the region (Runnels and van Andel, 2003). Yet, a focus on caves has created an unbalanced picture, biased towards Upper Palaeolithic cave contexts.

2) The collections of surface material from the red-beds comprise the bulk of the Middle Palaeolithic record of Epirus. Considering that Epirus has the largest Palaeolithic record in Greece, it becomes obvious that the investigation of those sites will have implications for our understanding of the Palaeolithic of Greece as a whole.

27.2 METHODOLOGY

Our investigations focused on the site of Morfi, which is known from the 1960s, and Popovo, which is a new site that we discovered in 2015 (Kourtessi-Philippakis et al., 2019a, b). A double intensive surface survey was conducted at both sites. At Popovo, we employed a near-total collection strategy, picking up all specimens with knapping attributes. At Morfi, however, the sheer amount of surface finds dictated a judgmental/representative collection strategy focusing mainly on cores, blanks, retouched tools and, occasionally,

knapping debris. At both sites, test trenches were opened at selected locations, with spits of 5 to 10 cm following the stratigraphy, while all finds were piece-plotted with a differential GPS device.

Designated profile sections were cleaned, logged and described following standard pedological and lithostratigraphic criteria. At geoarchaeological contexts of interest, and especially at stratigraphic boundaries, monolith-type samples of intact sediment were removed as blocks of ca. 10 x 10 x 15 cm, stabilized with plaster, for micromorphological analyses through the study of thin sections. Geological sampling included also bulk samples for isotopic, geochemical and microfossil analyses, which are still on-going.

Additionally, sediment samples were collected for radiometric dating with the methods of post infra-red infra-red stimulated luminescence (pIRIR), optically stimulated luminescence (OSL) and cosmogenic nuclides dating. Sediment samples for dating with the $^{40}Ar/^{39}Ar$ method were collected from the layer of tephra at Morfi (see below). Whether it was for geoarchaeological analyses or dating purposes, our sampling strategy sought to not only cover most of the stratigraphic sequences (vertical dimension), but also address issues of lateral variation in context (horizontal dimension).

27.3 RESULTS

27.3.1. POPOVO

The site of Popovo is located at an altitude of ~500 m in a shallow polje that is surrounded by low mountains (Fig. 2a). The geological sequence is composed of clay and silt, and is about 15 m. thick. We collected lithic artifacts from almost the entire extent of the site, but our evaluation of surface distributions showed that, rather than representing undisturbed, *in situ* concentrations, most surface aggregates essentially result from erosion and re-deposition. Small streams and gullies that run through or cut across the depression have significantly disturbed the site. The Popovo lithic assemblage includes artifact classes from all stages of the reduction sequence, namely cores, blanks, retouched tools, and waste products (Thompson et al., this volume).

The Popovo deposits have been affected by tectonic activity, but erosion and slope-washed sediments have obliterated or obscured the original geometry of the faults, some of which could be of syn-sedimentary origin. Additionally, the present-day badland landscape has been shaped by extensive recent and/or older episodes of sediment re-deposition by mass-wasting and other erosional processes, such as runoff, slope wash and colluviation. Another significant problem is the widespread presence of soft-sediment deformation structures, produced by processes such as slumping, which are triggered by seismic events or by chemical processes related to karstification; such deformations may affect the deposits at a small scale, but they also affect entire hillslopes and, in this case, have resulted in substantial slope alterations that complicate the understanding of the stratigraphy. In view of the lack of fresh geological exposures, much of our efforts focused on cleaning slope profiles at selected locations across the site, where the stratigraphic sequence was considered locally intact. Eventually, it was evident that only with heavy machinery (bulldozer) it would be possible to remove all of the slope-washed sediment and reveal intact section profiles, but this option was not covered by our research permit. The excavation of test trenches yielded only two undiagnostic artifacts; unfortunately, more stratified artifacts that were collected during the cleaning of the profiles are also typologically undiagnostic and cannot be used for attributions to specific techno-complexes. In sum, due to the combined effects of all the above-mentioned geological processes affecting

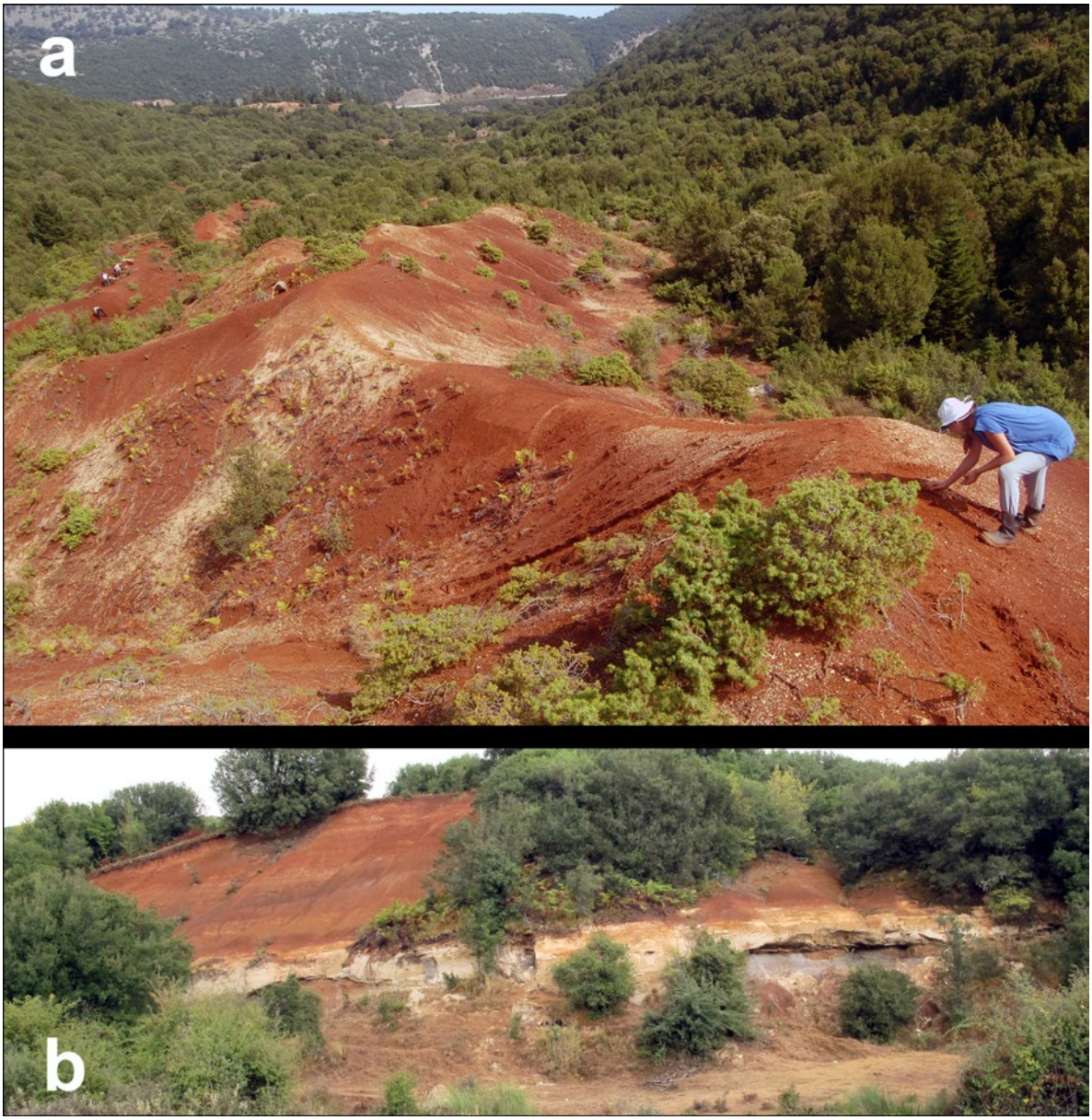

Figure 2: a) Panoramic view of the site of Popovo; b) general view of the site of Morfi, showing the layer of tephra and the overlying artifact-bearing zone of *terra rossa* deposits.

the stratigraphy, it was not possible to construct a stratigraphic scheme for the site, and the finds (stratified and/or surface) could not be placed in the local geological sequence.

27.3.2. MORFI

The raised and dissected polje near the village of Morfi (Fig. 2b) is known as a rich Palaeolithic site since the investigations of E. Higgs and S. Dakaris in the 1960s (Higgs, 1965; Higgs and Vita-Finzi, 1966). More recently, it was revisited in the framework of the Nikopolis Project (Runnels and van Andel, 2003). The site has yielded thousands of lithic artifacts, but none of the previous teams conducted test trenches, and any artifacts potentially found stratified were not documented as such or placed in a stratigraphic profile (Papayianni, 2000). Moreover, the aerial extent of the site

was never assessed or mapped. Our investigations suggest that Morfi is one of the most extensive and artifact-rich open-air sites in Epirus and includes areas with extremely dense concentrations of finds.

The geological sequence at Morfi begins with a paleosol overlying the karstic bedrock and underlying yellowish red silty clays; the latter are overlain by leached, grey clays, which are in turn overlain by a ca. 2.5-m-thick layer of tephra deposit (Pyle et al., 1998; Runnels and van Andel, 2003). The deposit of volcanic ash is exposed at three locations in the polje and so it is used as a stratigraphic marker for lithostratigraphic correlations across the site. Above the tephra layer lies a 10- to 15-m-thick zone of *terra rossa* deposits (detrital red silty clays), which includes three or four intercalated units of sand and flint gravels. The latter probably represent distal alluvial fan deposits such as debris flows, and crop out at several locations, hence they are also used for correlation purposes. This zone of *terra rossa* is currently being exposed by headward alluvial erosion, it includes artifact-rich horizons and was therefore the focus for cleaning profile sections and opening test trenches. Distinct, thin layers rich in iron and manganese oxides that form hardpan-horizons and can be followed laterally were also used as stratigraphic markers to help correlate the stratigraphy in different areas of the site.

Artifact-bearing layers occur at various levels throughout the zone of red clays (Fig. 3). This can be interpreted as indicative of repeated hominin visits during the Middle Palaeolithic. Stratified finds were retrieved from mainly three different kinds of geological contexts:

1) artifacts in gleyed sediments indicate low-energy sedimentation under wet conditions, probably related to ephemeral wetlands; drab halo root traces, mottles and iron-manganese pedo-features are redoximorphic traits, which resulted from changes in the redox conditions of the soil in response to fluctuation in water saturation (Ashley et al., 2013).

2) artifacts stratified in bedded sands and gravels; these can be considered as finds in secondary positions, associated with sheet-floods or the distal parts of dilute debris flows.

3) artifacts embedded inside paleosol horizons indicate intervals of dry conditions with subaerially exposed surfaces.

By definition, paleosols indicate breaks in the sedimentation, and in Epirus, these have been estimated to be in the order of a few to tens of thousands of years old (cf. Runnels and van Andel, 2003). Besides the paleosols, there are no major hiatuses in the sequence, as we did not observe any geological unconformities. Unfortunately, so far none of the samples from the *terra rossa* have yielded adequate quantities of mineral grains of quartz or K-feldspars for conducting the necessary measurements for luminescence dating with the methods of OSL or pIRIR. Similar problems affected the samples from Popovo, which also failed to yield any results. The overall scarcity or total lack of the desired minerals is attributed to the bedrock lithology of the area, which is dominated by limestone and evaporites (Ntokos, 2017).

In the location of Morfi, our efforts with the method of cosmogenic nuclides faced the problem that, after cleaning the samples, the remaining material was a microcrystalline quartz. This material was not suitable for cosmogenic burial dating, with *in situ*-produced ^{26}Al and ^{10}Be, most likely due to the incorporation of a substantial amount of meteoric ^{10}Be.

Nevertheless, the samples from the layer of tephra at Morfi appear to work quite well and there are already very promising first results from the on-going analyses of the $^{40}Ar/^{39}Ar$ dating method: the tephra was deposited in the polje at around 200 ka, which is considerably younger than the age obtained by Pyle and colleagues (1998). Major and minor element compositional data from the Morfi tephra are now being processed for geochemical fingerprinting and will be compared to known

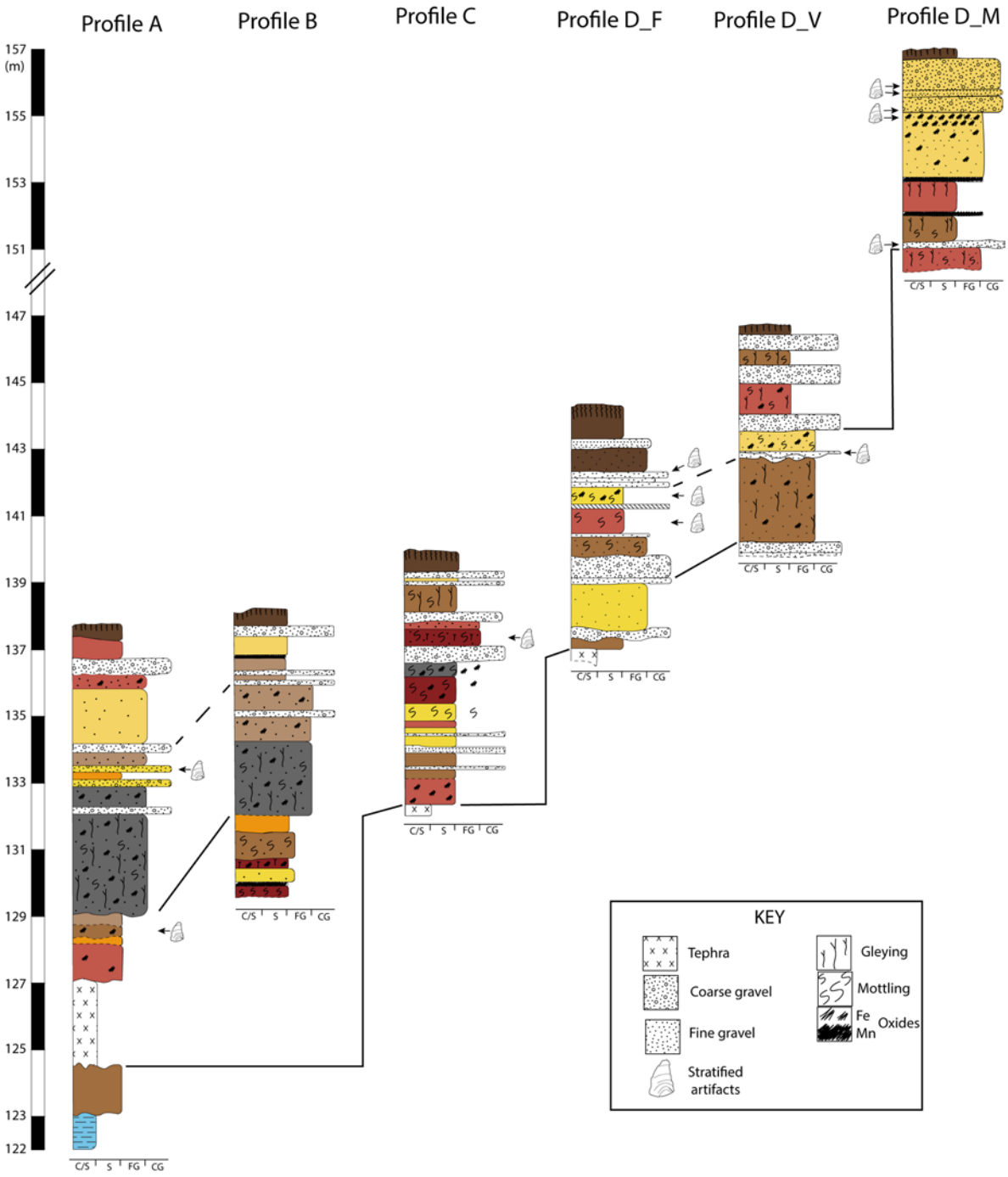

Figure 3: Preliminary stratigraphic correlations between the logged profiles at Morfi, showing the artifact-bearing horizons. Note the presence of the tephra layer at the base of the studied sequence.

late Middle/Late Pleistocene volcanic glass datasets from Mediterranean and Balkan localities, in order to determine the volcanic source.

As the tephra directly underlies the entire artifact-bearing zone of *terra rossa*, its dating provides a useful *terminus post quem* for the archaeological record of Morfi. On the grounds of macroscopic pedo-sedimentary and lithostratigraphic analyses,

there does not seem to be any considerable hiatus separating the volcanic ash from the first *terra rossa* deposits. While the final results from the micromorphological analysis are pending, if the aforementioned observation is further confirmed, then the artifacts retrieved from the lower layers just above the tephra should date to somewhere close to 200 ka.

27.4 DISCUSSION AND CONCLUSIONS

At both Popovo and Morfi, sedimentary facies with evidence of gleying and mottling attest to sedimentation under wet conditions and/or periodical waterlogging, while paleosols, bands of oxidations and desiccation surfaces mark depositional breaks and designate subaerially exposed surfaces. Stratified artifacts that have been found inside paleosols indicate the presence of hominins when the marshy setting of the poljes was mostly dry, while artifacts found in sediments deposited within the zone of water-table fluctuation, point to exploitation of the sites when the water was more abundant in localized ponds.

Both sites can be considered as including mainly cumulative but also erosional and spatial palimpsests of varying resolution (Bailey, 2007). Yet, in both cases there is a remarkable consistency in the typo-technological composition of the assemblages, the raw materials used and the intra-site range of chemical weathering; the bulk of the assemblages can be attributed to the Middle Palaeolithic, followed by an Upper Palaeolithic component. Preliminary as it may be, this assessment matches evaluations made by previous studies for Morfi and other coastal sites (e.g., Papayianni, 2000). Retouched tools diagnostic of the Neolithic or the Bronze Age occur only in extremely few numbers, pottery fragments were not observed, and ground stone-tools were not encountered at all (see also Thompson et al., this volume). As the composition of the assemblages is reported elsewhere (Thompson et al., this volume), suffice it here to note that toolkits with clear Mousterian typo-technological characteristics and the full range of Levallois flake cores are well-represented at both sites. Tool-type frequencies are overall similar, including Levallois, pseudo-Levallois, Mousterian and bifacial leaf-points. Scrapers occur in higher frequencies at Popovo than at Morfi, where there are also large single platform blade cores that are absent at Popovo, even though Middle Palaeolithic blades are similar in frequencies at both sites (Thompson et al., this volume). The study of core reduction sequences is on-going, and no particular chrono-cultural patterns can be discerned at this point.

Notwithstanding such an 'internal consistency' evident in both sites, attributing lithic assemblages to discrete chronostratigraphic units requires provenanced material as well as an adequate understanding of the stratigraphy on which this material will be eventually anchored. This was not the case at Popovo, where the combined effect of tectonics, slumping events, and contemporary erosion and re-deposition, coupled with a scarcity of stratified occurrences, altogether prevent the development of a chrono-cultural scheme framed by stratigraphy. Future investigations at this site would require a research permit for large-scale profile cleaning with heavy machinery and extensive excavation trenches. In contrast, the presence of the tephra and pedo-sedimentary features that can be used as stratigraphic markers at Morfi allow for placing different artifact-bearing deposits into a chrono-stratigraphic scheme, albeit tentative and lacking the number of radiometric dates that was originally expected. The age of the tephra at ca. 200 ka prompts us to hypothesize that the lowermost artifact-bearing layer(s) potentially date to Marine Isotope Stage 6; if confirmed, such a finding would give further support to the hypothesis that some of the red-bed sites of Epirus contain

a Middle Palaeolithic component that pre-dates the last interglacial (Tourloukis et al., 2015).

The differences in the context and preservation of finds between the two sites (e.g., frequency of stratified vs. surface occurrences) can be most likely attributed to differences in local site formation processes. The site of Morfi is located inside a basin that is larger than that of Popovo and apparently involved a more gentle, flatter terrain with low slope angles; the envisioned mass-wasting processes here include runoff, dilute debris flows and sheet-floods that may have produced archaeological palimpsests but have not altered substantially the original geomorphological configurations and the stratigraphic integrity of the site at present: geologically *in situ* artifact-bearing horizons can still be discerned and assessed. In contrast, Popovo is a relatively small, inland basin, where hominin activities occurred at places close to the mountain flanks and were likely affected by more catastrophic erosional processes (syn- and post-depositional), such as slope failures, landslides and slumping, triggered by tectonics (as faults have been identified) and accelerated by the steeper relief and the proximity to the mountain front.

The red-bed sites are known from the 1960s and they have produced thousands of artifacts, which make up the bulk of the record from Epirus, a region with probably the largest Palaeolithic record in Greece. The work presented here for the first time combined the opening of test-trenches, a dating program that included every method that could be applied on the available materials, extensive sampling for micromorphological studies and palaeoenvironmental proxies, and a stratigraphic approach in order to support chronological/cultural attributions. Our investigations led to the discovery of Popovo, a new site with a difficult stratigraphy, but still very important finds (Thompson et al., this volume). The re-dating of the volcanic ash at Morfi is expected to have major implications for research on the critical period around 200 ka in the Southern Balkans, and, in the future, it may even allow us to compare archaeological records on the two sides of the Adriatic.

ACKNOWLEDGMENTS

This research was supported by a post-doctoral research grant awarded to V.T. by the Wenner-Gren Foundation (Gr. 9271) and by the ERC Consolidator Grant ERC-CoG-724703 ("CROSSROADS") awarded to K.H. K.H. is also supported by the ERC Advanced Grant ERC-AdG-101019659 ("FIRST-STEPS"). We are grateful to the Thesprotia Ephorate of Antiquities, the Thesprotia Prefecture, as well as the National and Kapodistrian University of Athens, for all the support throughout the investigations. We would also like to thank Y. Hilbert and I. Karavanić for their comments and suggestions in reviewing the manuscript.

REFERENCES

Ashley, G.M., Deocampo, D.M., Kahmann-Robinson, J., and Driese S.G., 2013. Groundwater-fed wetland sediments and paleosols: it's all about water table. New Frontiers in Paleopedology and terrestrial paleoclimatology: paleosols and soil surface analog systems, SEPM Special Publication, 104, pp. 47–61.

Bailey, G., 2007. Time perspectives, palimpsests and the archaeology of time. Journal of Anthropological Archaeology, 26, pp. 198–223.

Bailey, G., Papakonstantinou, V., and Sturdy, D., 1992. Asprochaliko and Kokkinopilos: TL dating and reinterpretation of Middle Palaeolithic sites in Epirus, north-west Greece. Cambridge Archaeological Journal, 2, pp. 136–144.

Dakaris, S.I., Higgs, E.S., and Hey, R.W., 1964. The Climate, environment and industries of Stone Age Greece: Part I. Proceedings of the Prehistoric Society, 30, pp. 199–244.

Elefanti, P., Marshall, G., 2015. Late Pleistocene hominin adaptations in Greece, in: Coward, F., Hosfield, R., Pope, M., Wenban-Smith, F. (Eds.), Settlement, society and cognition in human evolution. Cambridge University Press, Cambridge, pp. 189–213.

Higgs, E.S., Vita-Finzi, C., 1966. The climate, environment and industries of Stone Age Greece: Part II. Proceedings of the Prehistoric Society, 32, pp. 1–29.

King, G., Bailey, G., 1985. The palaeoenvironment of some archaeological sites in Greece: the influence of accumulated uplift in a seismically active region. Proceedings of the Prehistoric Society, 51, pp. 273–82.

King, G., Sturdy, D., Bailey, G., 1997. The tectonic background to the Epirus landscape, in: Bailey, G.N. (Ed.), Klithi: Palaeolithic Settlement and Quaternary Landscapes in Northwest Greece, Klithi in its Local and Regional Setting, vol. 2., McDonald Institute for Archaeological Research, Cambridge, pp. 541–558.

Kourtessi-Philippakis, G., Pomonis, P., and Sakkas, D., 2019a. Archaeological survey research in the Middle Kalamas river basin of Thesprotia, 2011-2015: first results, in: Chouliaras, I. and Pliakou, G. (Eds.), Thesprotia I, Proceedings of the 1st Conference on the Archaeology and History of Thesprotia, Ioannina 2019, pp. 1–20 (in Greek).

Kourtessi-Philippakis, G., Tourloukis, V., Sakkas, D., and Michos-Rammos, F., 2019b. The survey research of the University of Athens in the Middle Kalamas River basin. Archaeologiko Deltio, 70, Chronika 2015, Athens, pp. 833–838 (in Greek).

Ntokos, D., 2017. Synthesis of literature and field work data leading to the compilation of a new geological map–a review of geology of northwestern Greece. International Journal of Geosciences, 8, pp. 205–236.

Papagianni, D., 2000. Middle Palaeolithic Occupation and Technology in Northwest Greece: The Evidence from Open-Air Sites. British Archaeological Reports, 882, Oxford.

Papakonstantinou V., Vassilopoulou, D., 1997. The Middle Palaeolithic industries of Epirus, in: G.N. Bailey (Ed.), Klithi: Palaeolithic Settlement and Quaternary Landscapes in Northwest Greece, vol. 2: Klithi in its local and regional setting, McDonald Institute for Archaeological Research, Cambridge, pp. 459–80.

Pyle, D.M., van Andel, T.H., Paschos P., and van den Bogaard, P., 1998. An exceptionally thick Middle Pleistocene tephra layer from Epirus, Greece. Quaternary International, 49, pp. 280–86.

Runnels, C., van Andel, T.H., 1993. A handaxe from Kokkinopilos, Epirus, and its implications for the Palaeolithic of Greece. Journal of Field Archaeology, 20, pp. 191–203.

Runnels, C., van Andel, T.H., 2003. The Early Stone Age of the Nomos of Preveza: landscape and settlement, in: J. Wiseman and K. Zachos (Eds.), Landscape Archaeology in Southern Epirus, Greece I, Hesperia Supplement, 32, American School of Classical Studies at Athens, Athens, pp. 47–133.

Thompson, N., Kourtessi-Philippakis, G., Giusti, D., Harvati, K. and Tourloukis, V., this volume. The preliminary analysis of lithic assemblages from the archaeological survey and test-trench excavations at Popovo and Morfi, Greece.

Tourloukis, V., 2009. New bifaces from the Palaeolithic site of Kokkinopilos, Greece and their stratigraphic significance. Antiquity, 83(320), Project Gallery.

Tourloukis, V., Karkanas, P. and Wallinga, J., 2015. Revisiting Kokkinopilos: Middle Pleistocene radiometric dates for stratified archaeological material in Greece. Journal of Archaeological Science, 57, pp. 355–369.

van Andel, T.H., Runnels, C., 2005. Karstic wetland dwellers of Middle Palaeolithic Epirus, Greece. Journal of Field Archaeology, 30, pp. 367–384.

28 THE PRELIMINARY ANALYSIS OF LITHIC ASSEMBLAGES FROM THE ARCHAEOLOGICAL SURVEY AND TEST TRENCH EXCAVATIONS AT POPOVO AND MORFI, GREECE

Nicholas Thompson[1*], Georgia Kourtessi-Philippakis[2], Domenico Giusti[1], Katerina Harvati[1,3], Vangelis Tourloukis[1,4]

[1]*Paleoanthropology, Institute for Archaeological Sciences and Senckenberg Centre for Human Evolution and Palaeoenvironment, Department of Geosciences, Eberhard Karls University of Tübingen, Germany*
[2]*Department of History and Archaeology, National and Kapodistrian University of Athens, Greece*
[3]*DFG Centre for Advanced Studies 'Words, Bones, Genes, Tools', Eberhard Karls University of Tübingen, Tübingen, Germany*
[4]*Department of History and Archaeology, School of Philosophy, University of Ioannina, Ioannina, Greece*
**nikothompso@yahoo.com*

http://dx.doi.org/10.15496/publikation-97588

Keywords: Middle Palaeolithic; Lithic Scatters; *Terra Rossa* badlands; bifaces; bifacial leaf points

28.1 INTRODUCTION

The two-year archaeological research program (2016-2017) conducted in Middle Kalamas, Thesprotia by the National and Kapodistrian University of Athens, in collaboration with the University of Tübingen in the framework of CROSSROADS, aimed at constructing a chrono-stratigraphic sequence for the open-air sites of Morfi and the recently discovered site of Popovo, by conducting a double-intensive targeted archaeological survey and test trench excavation of *terra rossa* Pleistocene deposits (Kourtessi-Philippakis et al., 2019a, 2019b; Tourloukis et al., this volume). Here we present the preliminary analysis of the lithic remains from the lowland locality of Morfi, and the upland locality of Popovo, Greece.

28.2 BACKGROUND

Although Epirus, northwestern Greece, is known for its rugged and wild landscape, the archaeological record (Fig. 1) from this region is dense and spans the Middle to Late Pleistocene (Tourloukis and Harvati, 2018; Tourloukis, 2021). Evidence for human activity is found in caves and rock shelters such as Asprochaliko (Bailey et al., 1992), Boila (Kotjabopoulou et al., 1999; Elefanti et al., 2021), Klithi (Bailey, 1992; 1999; Adam, 1998a; Roubet, 1999), Kastritsa (Higgs, 1968) and even more extensively at open-air sites, including the infamous red-bed *terra rossa* sites of Kokkinopilos (Dakaris et al., 1964; Bailey et al., 1992; Runnels and van Andel, 1993; Tourloukis et al., 2015), Mikro and Megalo Karvounari (Papoulia, 2011; Ligkovanlis,

 http://dx.doi.org/10.15496/publikation-97588

N. Thompson: https://orcid.org/0009-0003-4770-1744
D. Giusti: https://orcid.org/0000-0003-1438-4036
K. Harvati: https://orcid.org/0000-0001-5998-4794
V. Tourloukis: https://orcid.org/0000-0002-9527-2708

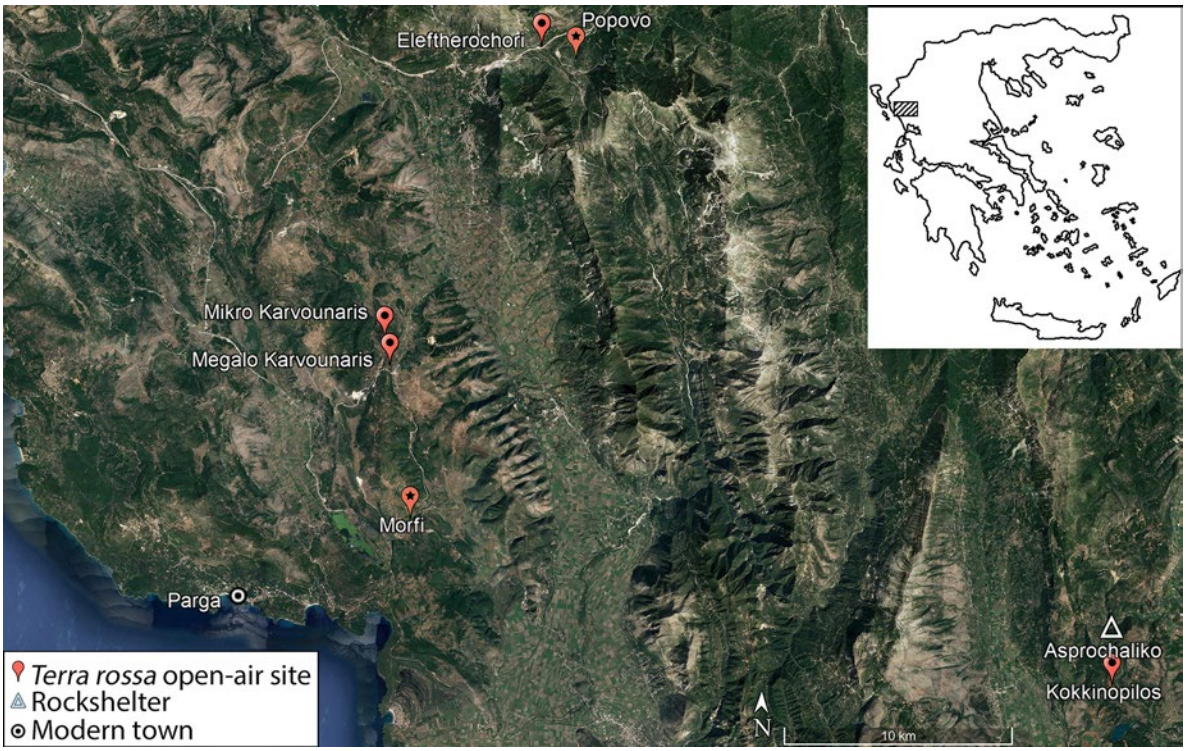

Figure 1: A satellite image with *terra rossa* red bed sites of Epirus and Asprochaliko. Popovo and Morfi are the pins with stars, while Klithi, Boila and Kastritsa are located off the map further to the north. Image, adapted from Google Earth.

2011), Morfi (Papagianni, 1999a), and Eleftherochori (Ligkovanlis, 2014; 2022) that characterize this region of Greece due to the combination of a wet humid climate, tectonics and erosion.

The *terra rossa* sites are located on the edges of rolling hills in close proximity to flood plains of both the Acherontas River for the sites of Morfi, Mikro and Megalo Karvounari, and the Louros River for Kokkinopilos. These ancient lake systems, known as raised poljes, take on their current badland form due to the combination of uplift and erosion. These sites typically occur above the coastal plains at elevations of 140 to 200 masl, protected by mountains on all sides. The exceptions to this lowland pattern are Eleftherochori and newly discovered Popovo, which are instead located in the uplands at elevations ranging from 530 to 615 masl, along the same upland drainage that joins the Acherontas flood plain further to the south.

Whereas the rock shelters of Boila, Klithi, and Kastritsa cave are younger in age, the oldest layers at Asprochaliko and the red-bed sites consist of extensive Middle Palaeolithic remains that tend to dominate the open-air lithic assemblages from this region (see Papakonstantinou and Vassilopoulou, 1997; Adam, 1999; Papagianni, 1999a; 1999b for intra-regional lithic studies). Currently, only at the open-air sites of Kokkinopilos (Bailey 1992; Adam, 2018), Megalo Karvounari and Eleftherochi (Ligkovanlis, 2011; 2014) have extensive Upper Palaeolithic remains been recovered. Of the open-air sites, only at Kokkinopilos have paleosols been dated chronometrically (Bailey et al., 1992; Runnels and van Andel, 1993; Tourloukis et al., 2015) and test trenches conducted (Dakaris et al., 1964). Therefore, the archaeological record from the remaining red bed sites is based solely on the typology of an extensive and complex surface record.

28.3 COLLECTION AREAS AND SAMPLING METHODS

At the upland locality of Popovo, lithics were recovered from five collection areas, designated as Areas 1-5. The largest *terra rossa* deposit at Area 3, provided the bulk of archaeological material, whereas the remaining collection areas with preserved sediments were patchier. The total number of lithics collected is 334, with a variability ranging from Area 1 (n=9), Area 2 (n=24), Area 3 (n=245), Area 4 (n=49) to Area 5 (n=7).

At Morfi, we collected 837 lithics from seven collection areas designated as Areas A-F and Mikro Morfi. These areas, now discontinuous on the landscape, were probably once connected and more extensive in the past. The number of finds collected from each area are: Area A (n=12), Area B (n=179), Area C (n=123), Area D (n=434), Area E (n=50), Area F (n=4), Mikro Morfi (n=35).

The lithics were collected by utilizing three separate sampling strategies: stratified lithics from 1) test trenches or 2) naturally exposed profiles; 3) surface finds. The most important is the context of test trenches, but due to the limited number of excavation units, the number of lithics recovered was insufficient to provide meaningful insights to the non-excavated remains. As such, we also collected stratified lithics from exposed section profiles in hopes of adding this data to the stratigraphy of the site, and as surface remains to help better interpret the timescale of the dense lithic scatters by use of typology (see Tourloukis et al., this volume, for the geoarchaeological results of the survey). The surveys conducted were double intensive meaning that we revisited most survey areas at least twice, but often even more times to either reinterpret the geology, or to collect more lithics.

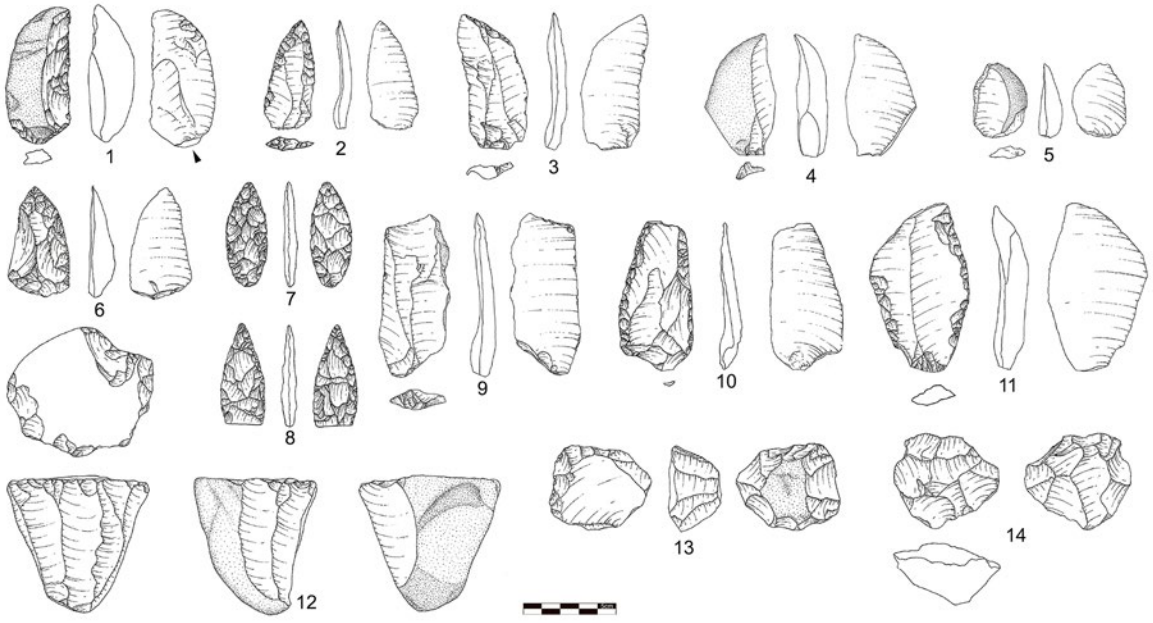

Figure 2: Sample of lithics from Popovo (2.1, 2.8, 2.9) and Morfi (2.2, 2.3-2.7, 2.10-2.14). Scrapers (2.1, 2.6, 2.11); Mousterian point (2.2); Blade (2.3); Naturally backed flakes (2.4, 2.5); Bifacial leaf points (2.7, 2.8); Backed knives on blades (2.9, 2.10); Single platform blade core (2.12); Levallois cores (2.13, 2.14).

Figure 3: Sample of lithics from Popovo (3.6,3.10-3.13, 3.15, 3.18, 3.21, 3.23, 3.24, 3.34) and Morfi (3.1-3.5, 3.7-3.9, 3.14, 3.16, 3.17, 3.19, 3.20, 3.22, 3.25-3.33, 3.35-3.41). Mousterian point (3.1); Chips (3.2, 3.3); Retouched flake (3.4); Point (3.5); Bifacial foliated leaf points (3.6, 3.7), Backed knives on blades (3.8, 3.12); Scrapers (3.9, 3.10, 3.13-3.15), Pseudo-Levallois point (3.11); Naturally backed pieces (3.12, 3.16, 3.17); Elongated flake (3.18); Bladelets (3.19, 3.20); Débordant flake (3.21); Levallois flakes (3.22, 3.25); Blades (3.23, 3.24); Plunged flake (3.26); Cores (3.27, 3.28); Levallois cores (3.29-3.35, 3.37, 3.38), Blade cores (3.36, 3.39, 3.40); Tested piece (3.41).

28.4 LITHIC PRESERVATION AND RAW MATERIALS

Because *terra rossa* sediments are acidic, organic remains like bone degrade, thus leaving lithic artifacts as the only evidence for human activities to preserve in the diachronic archaeological record from these open-air sites. Patination and freeze-thaw are common features of lithic artifacts from this region. Patination occurs when a combination of factors, such as mechanical and chemical weathering, alter the external surfaces of siliceous materials (Luedtke, 1992). The formation of patina is highly variable and is not caused by any single factor, such as the depositional age or date of manufacture of the lithic artifacts (Rottländer, 1975). In general, from the main site at Popovo, 98% of the assemblage is patinated to some extent, (compared to 91% from all the collection areas). Also, because 55% of the lithics from the main site are medium to heavily patinated, the identification of lithic raw material types is not reliable.

At Popovo, as previously mentioned, thermal frost fractures from freeze thaw are evident in the preservation of the lithic remains. After our initial sort, a total of 112 lithics from the dataset were excluded because of this post depositional process. Freeze thaw is evident when spalls randomly pop off the external surfaces like potlids from fire, but larger in scale (Luedtke, 1992). For example, when this process occurs in advanced stages, the shapes of the lithics become totally altered or even split in half making them appear as possible weathered geofacts or *vice versa*, i.e., natural pieces of flint that appear flaked.

At both sites nodular and tabular lithic raw materials are locally available. Whereas at Popovo it is more difficult to distinguish in the archaeological record, at Morfi, spherical nodules are present throughout the gravel layers of the site and were selected almost exclusively, thus partly explaining the high density of naturally backed pieces (Figs. 2.4, 2.5, 2.9; 3.12, 3.16, 3.17) from the lithic assemblage. During reduction of these cobble-sized spherical nodules, the natural backing was formed whenever a blank was removed along the lateral edges of the core. Also, of interest at Morfi is the discard of large nodular flint cores/tested pieces with a hollow geode-like center (Fig. 3.41). It seems plausible, that the ancient knappers preferred to discard these cores early in the reduction sequence instead of continuing to reduce these flawed nodules more extensively, in contrast to the more heavily reduced exhausted cores.

Even though the raw material study at Popovo is ongoing, a preliminary total of seven lithic raw material types were constructed macroscopically at Morfi using a 16x magnifying glass. The locally available flint varieties that were utilized most extensively are types 1) Gray and 2) Yellowish brown; utilized mainly in nodular form. One notable observation from this preliminary analysis was that type Gray 1 grades in color as patina forms and intensifies over time. The color changes from gray to brown to even orange or rust color. In general, artifacts produced from raw material types 1 and 2 exhibit a distinct MP character with Levallois cores, scrapers and elongated flakes and blades.

The five extra-local varieties of the less utilized flint types are 3) Dramesi brown (Pappas, 2016), 4) semi-translucent brown, 5) Drimitsa red (Pappas, 2016), 6) pink with wide circular inclusions, 7) isolated pieces with no comparable type (dusky translucent red, red radiolarite, and brownish translucent yellow). The lithic raw material types 3, 5, 6 and an isolated type 7, when utilized, are used to produce lithics that are MP in character, including a Mousterian point (Figs. 2.2, 3.1), a naturally backed blade and core. Although some pieces are typologically UP, representing only a very small percentage of the Morfi finds, such as a semi translucent brown core (Fig. 3.27), radiolarite core (Fig. 3.28) and translucent gray bladelets (Fig. 3.19, 3.20). The extra-local materials of Drimitsa

red and the Dramesi brown are located circa 30 km to the north of Morfi as the crow flies on Google Earth (for attributes and detailed descriptions of these primary nodular flint sources see Pappas, 2016; Kourtessi-Philippakis et al., 2019a).

28.5 EXCAVATION AND STRATIFIED LITHICS

At Popovo, the stratified lithics recovered from the excavation units and section profiles (n=12) are too few, undiagnostic, and occasionally too weathered or fragmentary due to freeze-thaw. Consequently, even though the majority of test trenches were sterile and devoid of stratified lithics, including a deep-test trench, the overall diversity of Middle Palaeolithic (MP) remains from Popovo makes this a promising new source of surface material, especially in contrast to the majority of the red-bed open air sites from Thesprotia that are located closer to the coast at elevations below 200 masl.

At Morfi, all test trenches were located in Areas D and E and yielded a higher number of lithics (n=59) in contrast to Popovo. The densest concentration of finds occured in a 1m x 3m test trench (n=24) from Area D north, and (n=13) from a 1m x 1m unit, Area D south. Overall, the lithics consisted of Levallois cores, tools, flakes and debris. The Levallois method of reduction dominates the lithics from not only the excavated units, but from all areas where lithics were collected, surface or stratified. Because there are no radiometric dates to support the stratigraphic context, it is currently not possible to distinguish between an older to a younger Levallois Mousterian based solely on typology and the assemblage composition of each test trench.

Furthermore, a total of 204 lithics were collected from the stratigraphic profiles at Morfi. Again, the Levallois technique for reduction dominates, with Levallois cores, flakes, blades, including double and lateral scrapers, core edge removals, plunged flakes from blade cores, and a Mousterian point. In Area B, the largest lateral scraper (Figs. 2.11, 3.9) was recovered in association with chips (Fig. 3.2, 3.3), a retouched flake (Fig. 3.4) and a Mousterian point (Figs. 2.3, 3.1) during section cleaning, a good indication of an intact paleosol with *in-situ* remains.

28.6 SURFACE LITHICS

The surface survey consisted of a double intensive targeted inspection of exposed *terra rossa* sediments, where lithics were collected over a period of two field seasons. Only Popovo, Area 5, and Mikro Morfi were surveyed once. At Popovo, a near total surface collection was conducted (n=198), whereas at Morfi, due to the higher density of surface remains, only a representative surface collection was carried out (n=571). Overall, the finds are mainly MP in character with Levallois cores (Figs. 2.13, 2.14; 3.29-3.35, 3.37, 3.38), Levallois flakes (Fig. 3.22, 3.25, elongated flakes (Fig. 3.18), débordant flakes (3.21), blades (Figs. 2.3; 3.23, 3.24), scrapers (Figs. 2.1, 2.6; 3.10, 3.13-3.15), backed knives on blades (Figs. 2.9, 2.10; 3.8, 3.12) and a pseudo-Levallois point from Popovo (Fig. 3.11). In general, at Morfi, 15% of the blanks for debitage are Levallois and at Popovo 18%, whereas facetted platforms account for 12.5% of the debitage from Morfi and 15.6% of the debitage from Popovo.

The three bifaces recovered at Popovo (Fig. 4) are possibly the main distinguishing feature of a potentially different MP facies at these red-bed sites (see Galanidou et al., 2016 for a recent summary of bifaces from Greece). Bifaces are rare and have previously only been recovered at Kokkinopilos (Runnels and van Andel, 1993; Adam, 1998b; Tourloukis et al., 2015) and Megalo Karvounari (Ligkovanlis, 2011). At Kokkinopilos two stratified bifaces have been recovered from sediments dated

to >200 ka in age (Runnels and van Andel, 1993; Tourloukis et al., 2015). Whereas at both sites, the extensive laminar blanks (Figs. 2.3; 3.18, 3.23, 3.24) and blade cores recovered (Figs. 2.12; 3.36, 3.39, 3.40) may also be part of a possibly older technocomplex dating to MIS 5. For example, at Asprochaliko the abundant laminar Levallois specimens were dated by Thermoluminescence to ~100 ka BP (Huxtable et al., 1992), while at Klissoura Cave 1, Sitlivy et al., (2007) noted that 72% of laminar blanks from the MP assemblages occur mainly in layers XVIII to XX. Layer XVIII was dated by OSL to 92.84 (7.65) ka and layer XX to 95-110 ka (Zacharias et al., 2018). Although, currently, there is no published data from other stratified Greek sites to further support this hypothesis that laminar reduction is more pronounced in the older compared to the final Mousterian.

	Popovo		Morfi		
	No.	%	No.	%	Total
Cores	29	13	93	11,5	122
Tools	56	25,2	218	26,2	274
Flakes	116	52,3	412	49,0	528
Blades	19	8,6	65	7,8	84
Chips	0	0	16	1,9	16
Debris	2	0,9	21	2,5	23
Nodules	0	0	9	1,1	9
Total	**222**	**100**	**834**	**100**	**1056**

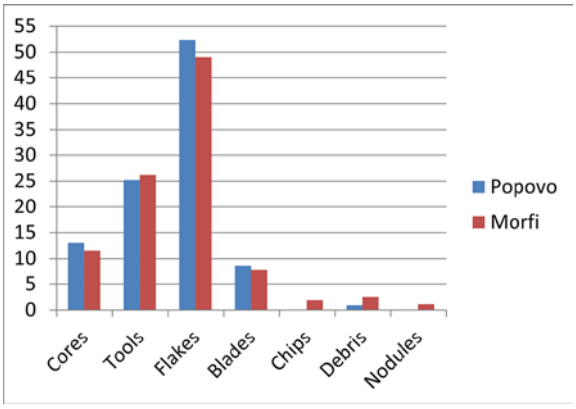

Table 1: Assemblage composition and bar graph of lithics recovered from all collection areas at Popovo and Morfi including all contexts (excavated, stratified and surface material) combined.

28.7 ASSEMBLAGE COMPOSITION

In general, the assemblage composition (Table 1) of the two sites, regardless of the differences in elevation or distance from the coast, presents some similarities. For example, flakes, tools, and cores comprise the majority of lithic finds for all the assemblages, stratified or surface.

The full range of Levallois flake cores is represented at both sites (see Figs. 2.13; 2.14; 3.29-3.38), from discoid to centripetal, whereas at Morfi there are also large blade cores (see Figs. 2.12; 3.36; 3.39; 3.40) that are absent at Popovo, even though MP blades are similar in frequencies at both sites. In general, the cores from Popovo occasionally tend to be atypical, compared to the higher density of typical Levallois cores that are found at Morfi.

28.8 TOOL TYPES

The tool-types and frequencies (Table 2) at Popovo and Morfi for the total assemblages are similar, except for bifaces at Popovo (Fig. 4), where two possible Keilmesser types and one amygdaloidal in shape were recovered as surface finds. Also, the tool-type frequencies at Popovo are much higher for scrapers, but this could be related to the shape of the raw materials because at Morfi there are higher frequencies of naturally backed pieces. In general, at both sites there are lateral, double, transverse and convergent scrapers with occasional Quina retouch (Figs. 2.1, 2.6; 3.14, 3.15), more at Popovo than Morfi. As for points, there are Levallois, Mousterian, pseudo-Levallois (Fig. 3.11), bifacial leaf points (Figs. 2.7, 2.8; 3.6, 3.7), from both sites, and a possible Gravette point (Fig. 3.5) from Morfi. Shouldered points are missing from all the red bed sites, except for a possible fragment from Megalo Karvounari (Ligkovanlis, 2011) even though there is a large assemblage of these points from Kastritsa (Adam, 1989; Adam, 2007). The

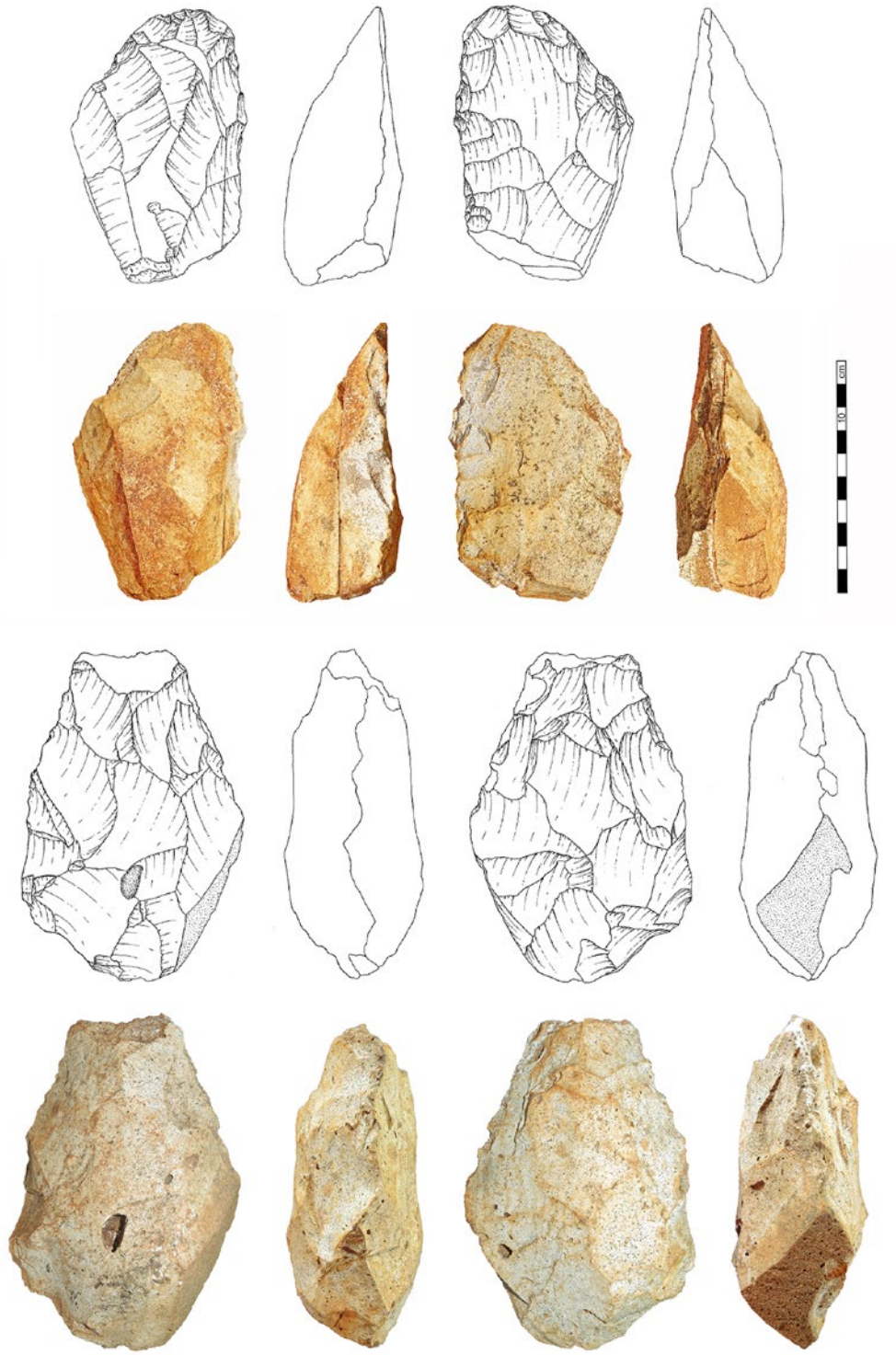

Figure 4: An amygdaloidal (bottom) and Keilmesser (top) bifaces recovered as surface finds from the initial survey at Popovo.

high frequencies of retouched pieces at Morfi compared to Popovo may reflect possible edge damage from surface material and not retouch, something that will be reinvestigated further when the material is reanalyzed. Finally, at Morfi, there are notched

	Popovo		Morfi		
	No.	%	No.	%	Total
Handaxes	3	5,4	0	0	3
Bifacial pieces	1	1,8	0	0	1
Scrapers	27	48,2	43	19,7	70
Backed knifes	5	8,9	34	15,6	39
Retouched pieces	13	23,2	76	34,8	89
Points	6	10,7	15	6,9	21
Endscra-pers	1	1,8	5	2,3	6
Notched pieces	0	0	30	13,8	30
Denticu-lates	0	0	8	3,7	8
Perfora-tors	0	0	7	3,2	7
Total	**56**	**100**	**218**	**100**	**274**

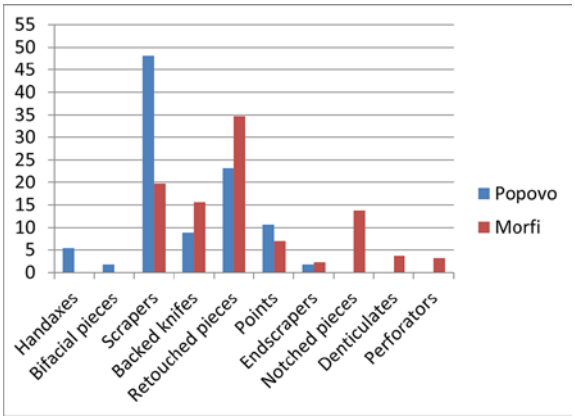

Table 2: Tool type frequencies and bar graph of Popovo and Morfi including all contexts and collection areas.

pieces, denticulates and perforators, that are absent from the Popovo assemblage.

In closing, future prospects will focus on conducting a comparative analysis with other red bed sites of the region, and to further interpret the spatial distribution of the lithic remains by constructing GIS-based inferences about intra-site and regional variability from both Popovo and Morfi, and from other red bed sites of the region.

28.9 CONCLUSIONS

In summary, the surface lithic assemblages of Popovo and Morfi are similar to other red-bed sites of Epirus that exhibit a long and rich Middle Palaeolithic history characterized by possibly an older techno-complex (with bifaces and large laminar blanks, possibly pre-MIS 5), to a younger Mousterian that is more typical to other Greek assemblages of this period. At both sites, the preferential method of reduction is dominant (on discoid and centripetal cores) and toolkits of scrapers (double, lateral and transverse), naturally backed knives and points (Mousterian, Levallois and pseudo-Levallois) with a reliance on locally available nodular flints that are more heavily patinated at Popovo in contrast to Morfi. Brown Dramesi flint and red Drimitsa flint are a few of the non-local varieties that were occasionally utilized at distances of ~30 km. At both sites, the lithic inventories also include isolated finds from the Upper Palaeolithic, such as endscrapers, bladelet cores and bladelets, whereas the majority of finds are Middle Paleolithic in character.

Consequently, because excavated sites older than MIS 3 are especially rare in Greece, the appearance of this possibly older Mousterian in Epirus reinforces the importance of trying to establish a chrono-stratigraphic framework for the conspicuous open-air red-bed sites of this region. Hence, the ambitious plan to conduct trial trenches in order to provide context to the archaeological assemblages that could be dated chronologically, and thus subsequently added to the geological sequences across the sites of Popovo and Morfi, would contribute greatly to our knowledge of not only the ages of these sites but also to identify the duration of activities and depositional histories of the archaeological remains.

As for the stratified lithics from the test trenches at Morfi, unfortunately, even though the sample of lithics recovered are typical Levallois in charac-

ter, there are currently too few in number to distinguish solely by typology if the finds are from the older or younger Mousterian. Therefore, with the exception of a characteristically Levallois debitage, with facetted platforms and dorsal scar patterns typical of centripetal flake and uni/bidirectional laminar reduction, the currently available data do not facilitate a more refined characterization. Alternatively, apart from the tephra layer located at the base of the site, there is unfortunately no other chronological marker to help remedy this situation. As a result, typology is the sole parameter for providing a provisional timescale for the archaeological record at Morfi.

At Popovo, on the other hand, the geology of the site is heavily deformed by tectonics and the stratigraphy cannot be followed horizontally across the site. Unfortunately, the lithics were even fewer in number than in Morfi, and also affected by freeze-thaw and, in many instances, the stratified lithics from the test trenches were highly fragmented and at times even more weathered than the surface finds. Nevertheless, Popovo is typologically similar to other surface scatters with lithics ranging in age from the Middle Palaeolithic to even younger periods including Upper Palaeolithic and possibly even Holocene in age at other eroded surface exposures to the north of the main site. Therefore, Popovo provides a good source of new archaeological surface material, especially for bifaces that are lacking at Morfi, but the lack of stratified remains hinders any better understanding of the timescale of activities that were conducted at the site.

Finally, in the future, with the addition of test trenches at Morfi, a more detailed picture could possibly emerge with a more rigorous approach to sampling across the site. The goals would be to locate stratified lithics, and to identify paleosols in an effort to provide a more detailed context to the remains. Increasing the density of lithic finds and constructing a more secure vertical dateable context to the overall geological sequence might provide the necessary data to make better sense of the stratified remains. However, without a chronostratigraphic sequence, critical data remains lacking to accurately describe and interpret the extensive surface scatters located where the rolling red-bed *terra rossa* sediments are preserved.

ACKNOWLEDGMENTS

This research was supported by the ERC Consolidator Grant ERC-CoG-724703 ("CROSSROADS") awarded to K.H. and by a postdoctoral research grant awarded to V.T. by the Wenner-Gren Foundation (Gr. 9271). K.H. is also supported by the ERC Advanced Grant ERC-AdG-101019659 ("FIRSTSTEPS"). We are also grateful to the Thesprotia Ephorate of Antiquities, the Thesprotia Prefecture, as well as the National and Kapodistrian University of Athens. We also thank O. Metaxas for drawing and inking a sample of lithics, V. Lekou and T. Tsirogiannis for assisting in the study of lithics, and V. Sitlivy and C. Garefalakis for providing assistance with their extensive knowledge of Middle Palaeolithic archaeology. Finally, we thank T. Tsanova and E. Adam for their critical comments during their review of this manuscript.

REFERENCES

Adam, E. 1989. A Technological and Typological Analysis of Upper Palaeolithic Stone Industries of Epirus, northwestern Greece, Oxford: British Archaeological Reports International Series 512.

Adam, E., 1998a. To know and to have: Raw material availability and Upper Palaeolithic stone assemblage structure in Epirus. In Klithi: Palaeolithic settlement and Quaternary landscapes in northwest Greece. Vol 2: Klithi in its local and regional setting, McDonald Institute

for Archaeological Research.

Adam, E., 1998b. The Work of IB EPKA in 1998, AD 53, Chronika B2, 519.

Adam, E., 1999. The Upper Palaeolithic stone industries of Epirus in their regional setting. British School at Athens Studies, pp. 137–147.

Adam, E., 2007. Looking out for the Gravettian in Greece, PALEO. Revue d'archéologie préhistorique, (19), pp.145–158.

Adam, E., 2018. A note on the Upper Palaeolithic industrial sequence in the lower Louros river valley, district of Preveza, Epirus, northwest Greece, in Nowak, P., K. Sobczyk, M. Nowak, J. Zralka (eds) Multas per gentes et multa per saecula: Amici magistro et collegae suo Ioanni Christopho Kozlowski dedicant (pp. 191-198) Jagiellonian University.

Bailey, G., 1992. The Palaeolithic of Klithi in its wider context. Annual of the British School at Athens, 87, pp. 1–28.

Bailey, G., 1999. The Palaeolithic archaeology and palaeogeography of Epirus with reference to the investigations of the Klithi rockshelter. British School at Athens Studies, pp. 159–169.

Bailey, G., Papaconstantinou, V. and Sturdy, D., 1992. Asprochaliko and Kokkinopilos: TL dating and reinterpretation of Middle Palaeolithic sites in Epirus, north-west Greece. Cambridge Archaeological Journal, 2(1), pp. 136–144.

Dakaris, S.I., Higgs, E.S., Hey, R.W., Tippett, H. and Mellars, P., 1964, December. The climate, environment and industries of Stone Age Greece: Part I. In Proceedings of the Prehistoric Society (Vol. 30, pp. 199-244). Cambridge University Press.

Elefanti, P., Marshall, G., Stergiou, C.L. and Kotjabopoulou, E., 2021. Raw material procurement at Boila Rockshelter, Epirus, as an indicator of hunter-gatherer mobility in Greece during the Late Upper Palaeolithic and Early Mesolithic. Journal of Archaeological Science: Reports, 35, 102719.

Galanidou, N., Papoulia, C. and Ligovanlis, S., 2016. The middle Palaeolithic bifacial tools from Megalo Karvounari. The Thesprotia Expedition, 3.

Higgs, E.S., 1968. Asprochaliko and Kastritsa. Antiquity, 42(167), 235.

Huxtable, J., Gowlett, J.A.J., Bailey, G.N., Carter, P.L. and Papaconstantinou, V., 1992. Thermoluminescence dates and a new analysis of the early Mousterian from Asprochaliko. Current Anthropology, 33(1), pp. 109–114.

Kotjabopoulou, E., Panagopoulou, E. and Adam, E., 1999. The Boila rockshelter: further evidence of human activity in the Voidomatis Gorge. British School at Athens Studies, pp. 197–210.

Kourtessi-Philippakis, G., Pomonis, P. and Sakkas, D., 2019a. The archaeological surface survey in the basin of Mesa Kalamas in Thesprotia, 2011–2015: first results. Thesprotia, 1, pp. 1–20.

Kourtessi-Philippakis, G., Tourloukis, V., Sakkas, D., Michos-Rammos, F. 2019b. The surface research of the University of Athens in the basin of Mesa Kalamas. Archaeological Bulletin 70, pp. 833–838, Chronicles 2015.

Luedtke, B.E., 1992. An archaeologist's guide to chert and flint. Institute of Archaeology, University of California, Los Angeles.

Ligkovanlis, S., 2011. Megalo Karvounari revisited. Thesprotia Expedition II, Environment and Settlement Patterns, 16, pp. 159–180.

Ligkovanlis, S., 2014. Human Activity and Technological Behavior during the Middle and Upper Palaeolithic in North-West Greece: the Evidence of the Lithic Assemblages from Megalo Karvounari, Molondra and Eleftherochori 7 (unpublished Doctoral dissertation, University of Crete).

Ligkovanlis, S., Iliopoulos, G., Palli, O., Tzortzatou, A. and Tsakanikou, P., 2022. Palaeolithic artifact taphonomy in terra rossa sites at north-

western Greece revisited: Two new case studies. Mediterranean Archaeology and Archaeometry, 22(3), pp. 215–229.

Papagianni, D., 1999a. Middle Palaeolithic occupation and technology in northwestern Greece: the evidence from open-air sites. Doctoral dissertation, University of Cambridge.

Papagianni, D., 1999b. Beyond 'flint scatters' and 'findspots': assessing the potential for compiling a synthesis of the Greek Middle Palaeolithic surface data. British School at Athens Studies, pp. 130–136.

Papaconstantinou, V., Vassilopoulou, D., 1997. The middle Palaeolithic industries of Epirus. Klithi: Palaeolithic Settlement and Quaternary Landscapes in Northwest Greece, 2, pp. 459–80.

Pappas, T., 2016. The lithic raw materials in the basin of Mesa Kalamas, Thesprotia: a geoarchaeological approach (MA thesis, National and Kapodistrian University of Athens/Department of History - Archaeology), Athens.

Papoulia, C., 2011. Mikro Karvounari in context: the new lithic collection and its implications for Middle Palaeolithic hunting activities. Thesprotia Expedition II. Environment and Settlement Patterns. Foundation of the Finnish Institute at Athens, Helsinki, pp. 123–158.

Rottländer, R., 1975. The formation of patina on flint. Archaeometry, 17, pp. 106–110.

Roubet, C., 1999. Expressions of an Upper Palaeolithic management of lithic resources at Klithi (Greece). British School at Athens Studies, pp. 170–178.

Runnels, C., van Andel, T.H., 1993. A handaxe from Kokkinopilos, Epirus, and its implications for the Paleolithic of Greece. Journal of Field Archaeology, 20(2), pp.191-203.

Sitlivy, V., Sobczyk, K., Karkanas, P. and Koumouzelis, M., 2007. Middle Paleolithic lithic assemblages of the Klissoura Cave, Peloponnesus, Greece: a comparative analysis. Archaeology, Ethnology and Anthropology of Eurasia, 31(1), pp. 2–15.

Tourloukis, V., 2009. New bifaces from the Palaeolithic site of Kokkinopilos, Greece and their stratigraphic significance. Antiquity, 83(320).

Tourloukis, V., 2021. Palaeolithic archaeology: a review of recent research. Archaeological Reports, 67, pp. 61–79.

Tourloukis, V., Harvati, K., 2018. The Palaeolithic record of Greece: A synthesis of the evidence and a research agenda for the future. Quaternary International, 466, pp. 48–65.

Tourloukis, V., Karkanas, P. and Wallinga, J., 2015. Revisiting Kokkinopilos: Middle Pleistocene radiometric dates for stratified archaeological remains in Greece. Journal of Archaeological Science, 57, pp. 355–369.

Tourloukis, V., Kourtessi-Philippakis, G., Karkanas, P., Nomade, S.,Giusti, D., Thompson, N., Varis, A., Junginger, A., Schaller, M., Harvati, K., this volume. Geoarchaeological and geochronological investigations of Paleolithic open-air sites in Epirus, Greece.

Zacharias, N., Polymeris, G., Koumouzelis, M., Karkanas, P., 2018. Detecting Middle Palaeolithic sequences at the Klissoura Cave 1 in Argolid, Greece using OSL dating. In: 4th ARCH_RNT Symposium Proceedings, May 2016. University of the Peloponnese Publications Series, Kalamata.

TUEBINGEN PALEOANTHROPOLOGY BOOK SERIES –
CONTRIBUTIONS IN PALEOANTHROPOLOGY 3

HUMAN EVOLUTION AT THE CROSSROADS

South East Europe has long been hypothesized as a principal Pleistocene dispersal corridor for human migrations in and out of Europe. It also comprises one of the three main European Mediterranean refugia, where plant, animal, and human populations are thought to have persisted throughout glacial intervals when they disappeared from more inhospitable regions further north. Despite the biogeographic importance of the region in human evolution, paleoanthropological research has largely been neglected there until recently, resulting in a critical gap in the puzzle of Eurasian human evolutionary history. Recent research has sparked renewed interest in the paleoanthropology of Greece, with several new discoveries indicating the importance of the region for deep prehistory.

The ERC Consolidator project 'Human Evolution at the Crossroads' (CROSSROADS), awarded to Katerina Harvati in 2016 and running from 2017 to 2022, builds on earlier work conducted by Harvati and colleagues in the framework of her previous ERC Starting project 'Paleoanthropology at the Gates of Europe' (PaGE). CROSSROADS concentrated on the earlier parts of the Paleolithic, aiming to help address hypotheses about the earliest human settlement of Europe and the evolution and adaptations of early European hominins. Several research directions were pursued: new fieldwork aimed to locate new sites dating from the Lower and Middle Paleolithic and to identify traces of early human presence and activity; a dating program was initiated to develop a chronological framework for the Paleolithic in Greece; multi-proxy paleoenvironmental reconstruction was undertaken to provide insights on the adaptations of Pleistocene humans in the region; and existing hominin fossils were re-examined with state of the art methodological approaches to shed light on their taxonomic identity and their paleobiology.

This edited volume collects twenty-eight contributions presented at the closing symposium of the ERC Consolidator project 'CROSSROADS', which took place in Tübingen in February 2022, shortly before the conclusion of the project. As such, it represents a large part of the work conducted under the 'CROSSROADS' research umbrella, showcasing the activities and results of the project.

9 783989 450028

TÜBINGEN
UNIVERSITY
PRESS